DTIC FILE COPY

NASA Conference Publication 10007
USAAVSCOM Conference Publication 88-A-001

Integrated Technology Rotor Methodology Assessment Workshop

AD-A200 007

DTIC
ELECTE
AUG 9 1988
S D
A

Proceedings of a workshop
Sponsored by NASA Ames Research Center
and the U.S. Army
June 21-22, 1983

This document has been approved for public release and sale; its distribution is unlimited.

US ARMY
AVIATION
SYSTEMS COMMAND

AVIATION RESEARCH AND
TECHNOLOGY ACTIVITY

NASA

88 8 09 05

DISCLAIMER NOTICE

THIS DOCUMENT IS BEST QUALITY PRACTICABLE. THE COPY FURNISHED TO DTIC CONTAINED A SIGNIFICANT NUMBER OF PAGES WHICH DO NOT REPRODUCE LEGIBLY.

NASA Conference Publication 10007
USAAVSCOM Conference Publication 88-A-001

Integrated Technology Rotor Methodology Assessment Workshop

Edited by
Michael J. McNulty
William G. Bousman
NASA Ames Research Center
Moffett Field, California

Proceedings of a workshop
Sponsored by NASA Ames Research Center
and the U.S. Army
June 21-22, 1983



US ARMY
AVIATION
SYSTEMS COMMAND

AVIATION RESEARCH AND
TECHNOLOGY ACTIVITY
MOFFETT FIELD CA 94305

NASA
National Aeronautics
and Space Administration

Scientific and Technical
Information Branch

1988

TABLE OF CONTENTS

Page

PREFACE.....vii

WELCOME.....ix
James A. Albers

INTRODUCTION AND BACKGROUND.....xi
William G. Bousman

SESSION ONE--METHODOLOGY ASSESSMENT COMPARISONS

1 A COMPARISON OF THE VARIOUS HELICOPTER MATHEMATICAL MODELS USED IN THE METHODOLOGY ASSESSMENT.....1
Wendell B. Stephens

2 A COMPARISON OF THEORY AND EXPERIMENT FOR AEROELASTIC STABILITY OF A HINGELESS ROTOR MODEL IN HOVER.....7
David L. Sharpe
Discussion.....24

3 A COMPARISON OF THEORY AND EXPERIMENT FOR COUPLED ROTOR-BODY STABILITY OF A HINGELESS ROTOR MODEL IN HOVER UNDER SIMULATED VACUUM CONDITIONS.....27
William G. Bousman
Discussion.....41

4 A COMPARISON OF THEORY AND EXPERIMENT FOR COUPLED ROTOR-BODY STABILITY OF A HINGELESS ROTOR MODEL IN HOVER.....43
William G. Bousman
Discussion.....66

5 A COMPARISON OF THEORY AND EXPERIMENT FOR THE AEROELASTIC STABILITY OF A BEARINGLESS MODEL ROTOR IN HOVER.....67
Seth Dawson
Discussion.....81

6 A COMPARISON OF THEORY AND EXPERIMENT FOR COUPLED ROTOR BODY STABILITY OF A BEARINGLESS ROTOR MODEL IN HOVER AND FORWARD FLIGHT.....87
Paul H. Mirick
Discussion.....102

7 A COMPARISON OF THEORY AND FLIGHT TEST OF THE BO 105/BMR IN HOVER AND FORWARD FLIGHT.....103
Paul H. Mirick
Discussion.....116

PANEL SESSION ONE--EVALUATION OF THE METHODOLOGY ASSESSMENT RESULTS.....119

INTRODUCTION.....119
Charles E. Hammond

PANELISTS' PREPARED REMARKS
Gene Sadler.....121
Dev Banerjee.....128
Frank Tarzanin.....139
Wayne Johnson.....148
Jerry Miao.....153
Dewey Hodges.....157
Richard Bielawa.....163

PANEL ONE GENERAL DISCUSSION.....171

SESSION TWO--METHODOLOGY RELATED PAPERS

8 THE IMPORTANCE OF STEADY AND DYNAMIC INFLOW ON THE STABILITY OF ROTOR-BODY SYSTEMS.....181
David A. Peters
Discussion.....202

9 EFFECTS OF STATIC EQUILIBRIUM AND HIGHER-ORDER NONLINEARITIES ON ROTOR BLADE STABILITY IN HOVER.....205
Marcelo R. M. Crespo da Silva and Dewey H. Hodges
Discussion.....216

10 AEROELASTIC MODELING OF ROTOR BLADES WITH SPANWISE VARIABLE ELASTIC AXIS OFFSET--CLASSIC ISSUES REVISITED AND NEW FORMULATIONS.....217
Richard L. Bielawa
Discussion.....229

11 COMPARISON OF EXPERIMENTAL ROTOR DAMPING DATA-REDUCTION TECHNIQUES.....231
William Warmbrodt
Discussion.....249

12 COMPARISON OF EXPERIMENTAL COUPLED HELICOPTER ROTOR/BODY STABILITY RESULTS WITH A SIMPLE ANALYTICAL MODEL.....253
P. P. Friedmann and C. Venkatesan
Discussion.....267

13 AEROMECHANICAL STABILITY ANALYSIS OF COPTER.....271
Sheng K. Yin and Jing G. Yen
Discussion.....277

14 AEROELASTIC CHARACTERISTICS OF THE AH-64 BEARINGLESS TAIL ROTOR.....279
D. Banerjee
Discussion.....298

PANEL SESSION TWO--THE PROBLEM OF MATH MODEL VALIDATION.....301

INTRODUCTION.....301
William G. Bousman

PANELISTS' PREPARED REMARKS
Jing Yen.....308
Euan Hooper.....311
Bob Wood.....318
Peter Arcidiacono.....323
Jim McCroskey.....330
Don Merkley.....336
Peretz Friedmann.....350
Bob Ormiston.....359

PANEL TWO GENERAL DISCUSSION.....365

LIST OF ATTENDEES.....377

QUALITY INSPECTED 2

Accession For
NTIS GRA&I ☒
DTIC TAB ☐
Unannounced ☐
Justification
By
Distribution/
Availability Codes
Dist | Avail and/or Special
A-1

PREFACE

The Integrated Technology Rotor (ITR) Methodology Assessment Workshop was held at Ames Research Center on June 21-22, 1983. An informal proceedings was provided to the meeting attendees that consisted of viewgraph material with some typed text for the fourteen meeting papers. The authors of the fourteen papers were asked to provide formal papers following the workshop and these papers have been combined with the transcribed panel sessions and discussion from the floor to provide the formal proceedings of the workshop that is presented here. The transcribed material presented here has had only minimal editing to maintain the informal flavor of the workshop. In those cases where slight changes have been made, it has been with the intent of keeping to the original meaning of the speakers. We apologize if any meaning has been lost in the transcribed material because of our efforts.

Prior to the workshop, the comparisons of theory and experiment that are reported in Papers 2 through 7 were circulated to seven individuals in the government active in rotorcraft dynamics research: Messrs. William G. Bousman, C. Eugene Hammond, Dewey H. Hodges, Wayne Johnson, Paul H. Mirick, David L. Sharpe, and William F. White. They were asked to judge the correlation and provide a score between 0 and 10 for each case. The average of the seven scores was obtained for each case and was converted to a verbal equivalent. For example, based on this scoring system, a rating in the good to excellent category indicates that the analysis is suitable for detail design and can be used to substitute for model test. A rating between poor-to-fair and fair-to-good indicates that the analysis may be useful for parametric studies and preliminary design, but that a model test is required to confirm the design prior to flight test. Scores of poor and below indicate an analysis that is not suitable for design or parametric use. The authors of Papers 2 to 7 have used these average scores rather than their own opinion in judging the predictive capability of these analyses.

During the period of time that has passed since the ITR Methodology Workshop and the publication of this formal proceedings, a number of organizations, both in and out of the government, have undergone name changes. No attempt has been made to treat these name changes in a consistent manner. Organizational names noted in the transcribed material are those that were in use at the time of the workshop. Author affiliations for the formal papers are those that were in use when the paper underwent final typing.

Michael J. McNulty
William G. Bousman

PRECEDING PAGE BLANK

WELCOME

James A. Albers
Deputy Director, Aeronautics and Flight Systems
Ames Research Center

Good morning. I'd like to welcome all of you to Ames Research Center on behalf of the Ames management and also the Army management for this joint Army/NASA methodology workshop on rotorcraft dynamics.

I'd like first to look at the ITR/FRR [Integrated Technology Rotor/Flight esearch Rotor] and how it relates to the overall activity within NASA and how it elates to aeronautics in general. From a simplified viewpoint, NASA has three major roles. The first major role is to provide a broad technical information base, and I'il come back to essentially what this technical information base consists of. The second major role is to retain and improve our national facilities needed to obtain this important data base. The third major role is to sustain highly trained technical personnel. The type of data base which we, NASA and the Army, want to provide is essentially a data base design of not only better airplanes, but also better space systems from the overall standpoint of the agency. Now the purpose of this data base is really to develop design tools and methodology, and that's why this methodology assessment workshop is so important; because a workshop like this is the very key to developing these design tools for the industry. It's also very important in terms of having the type of facilities to be able to take this data. It's very critical to have the most up-to-date and improved facilities available. Lastly, in terms of sustaining highly trained technical personnel, it's essential that we have the expertise, and the way we get this expertise is not only through our in-house research, but also through interchanges like this workshop. So this workshop is very important not only to all of you, but to us in terms of getting some feedback from the industry in terms of how well we do this research.

Specifically, I'd like to relate this data base and how we actually obtain it to the overall spectrum of aeronautical research. There are four basic building blocks where we obtain aeronautical research: the first is predictive analysis, essentially where we do our design methodology for aircraft; the next two blocks are ground tests, both simulation and wind tunnel; and then the last building block in aeronautical technology is flight test. It is very important that we do the best job possible in these four basic elements of aeronautical research. But the key is to do not only these four basic elements individually, but the interaction and the comparison between each one of these elements. That is one of the things that your workshop is going to do: essentially make a comparison between the predictive capability, which is your first step in aeronautical research, and some basic wind tunnel and ground tests, which is very important. Too often we do not spend enough time making detailed comparisons between experimental data and theory, and really look back and reflect on the extensive data base that we have here in terms of trying to update the previous step in the overall design process. That is why I

PRECEDING PAGE BLANK

think this workshop is vital to the industry--to be able to make a detailed comparison between the various building blocks of aeronautical research.

Now, if we look at the overall aeronautical funding here at Ames Research Center, close to 30% of the total activity at Ames, in terms of funding, is in the rotorcraft area. This also includes the facilities which support the rotorcraft systems aircraft. The total aeronautical research and technology base is concerned with all of the basic disciplines of aerodynamics, human factors, low speed and high speed research and technology. So another reason why we feel this workshop is very important to NASA is that it's a major element in terms of the overall aeronautical research. Rotorcraft is our major area of emphasis at Ames and as a result of that we think that a workshop of this type, which essentially emphasizes the first step in design methodology, is very important to us and to the Army.

With that I would once again like to welcome you to Ames Research Center and I'm sure on the basis of my remarks I would think that you will find the next two days very stimulating. Thank you.

INTRODUCTION AND BACKGROUND

William G. Bousman
ITR/FRR Project Co-Manager, Aeromechanics Laboratory

I'd like to start off this workshop by giving an introduction as to how this got started, and to do that I need to tell you a little bit about the Integrated Technology Rotor/Flight Research Rotor (ITR/FRR) program. A few years ago, the Army and NASA here at Ames Research Center were pursuing advanced rotor programs with two different objectives, but with many similarities. The Army was looking for a rotor that would apply advanced technologies and integrate them in one flight rotor, and NASA was looking at an advanced rotor that they could use to test, that is, do fundamental research to bring about advances. Both agencies were in the planning stages at that time and in this planning effort, both recognized that the similarities in objectives would give us considerable advantages in having a combined program. We began with what we saw as our user needs, both in the civilian and in the military communities, and the technology base that we had, and then through this planning exercise we went through a number of contractual steps. 1) The first one was a concept definition step in which we simply wanted to look at hub concepts that would meet our basic objectives. 2) The next step is preliminary design of an ITR/FRR system, and then 3) the third step is a detailed design, fabrication, and flight test, in which we would put the rotors on various aircraft including the RSRA and some contractor aircraft. Today we are at the beginning of preliminary design. There are three contracts: with Bell, Sikorsky, and Boeing.

To put this workshop into perspective, we have to go back to that planning phase. In NASA, as they were looking at their planning, they had funded a number of studies to look at a concept for rotors that had good research potential. In the Army's planning stage, we looked at a number of things but we felt that the methodology for aeromechanical stability prediction was probably one of the critical technologies for an ITR/FRR rotor. We were very concerned about how that would drive the program in terms of testing and so we decided, as a part of the program planning phase, to fund some studies with the companies looking at a number of experimental data sets. Essentially we wanted to contract just to run the computer programs, with no research involved or anything like that.

To do this we set out with six experimental data sets and we funded calculations with Bell, with Boeing Vertol, with Hughes, and with Sikorsky to look at the predictive capability of the analytical models. These six data sets are essentially arranged here (fig. 1) in order from simplicity to complexity. So if you look at Data Set A, it's a hingeless rotor. We're looking just at rotor stability. We don't have any body coupling with it; it's just a hover condition, and it's a model scale test. Then we started adding complexity. We had another data set [Data Set B] with a hingeless rotor in hover but with rotor-body coupling involved, and this one is a simulated vacuum case where aerodynamics are essentially eliminated. In this case [Data Set C] we add aerodynamics. In Data Set D we go to a bearingless rotor configuration which adds structural complexity, but we eliminate the body to

DATA SET	ROTOR TYPE	ISOLATED/COUPLED	FLIGHT CONDITION	SCALE	SOURCE
A	HINGELESS	ISOLATED	HOVER	MODEL	AEROMECHANICS LAB
B	HINGELESS	ROTOR-BODY	HOVER	MODEL	AEROMECHANICS LAB
C	HINGELESS	ROTOR-BODY	HOVER	MODEL	AEROMECHANICS LAB
D	BEARINGLESS	ISOLATED	HOVER	MODEL	AEROMECHANICS LAB
E	BEARINGLESS	ROTOR-BODY	HOVER/FWD FLT	MODEL	BOEING VERTOL
F	BEARINGLESS	ROTOR-BODY	HOVER/FWD FLT	FULL	BOEING VERTOL

Figure 1.- Methodology Assessment.

get some simplicity there. Then for Data Set E we go to a bearingless rotor, we now have rotor-body coupling, we have hover and forward flight, but it's a model scale test. Then for Data Set F we have a flight vehicle, so it's the whole-ball-of-wax sort of thing. We found in fact that when we tried to fund all of this we ran out of money, so we essentially cut out Data Set B; we felt that that one should be the least important. But as you will see, Hughes was able to find some funds to do some calculations there, and they are of interest.

This methodology assessment was originally envisioned as an important part of our ITR/FRR program. It has definitely met our original intent in that respect, but it's also very obvious to us that it stands by itself as a very interesting benchmark in rotorcraft stability for the industry. So, apart from the ITR/FRR program, by looking at this set of data and the correlation that has been done by industry, we see there is a lot to learn and we think that there is some progress that can be made. That is the purpose of this workshop. So in the next two days we're going to be looking at these data sets and some related calculations and try to get some answers on where we are today and what we are doing.

Basically, what we're going to do this morning is have the experimentalists who were involved with these data sets present the correlation that was made by industry, and then this afternoon we'll have a panel composed of the analysts who did the calculations, who will try to make an overall assessment. Essentially, the people talking this morning are going to be involved in a particular data set, they're really going to be looking at individual trees, and because of that they are not going to be able to give you a broad perspective. This afternoon the panel will be able to look at the whole forest and will try to bring out the most important points about these comparisons. Tomorrow, in the morning we'll have some individual papers that are related to this subject, and then in the afternoon we'll have a final panel in which we'll try to step back from the detailed correlation and address only the whole problem of math model validation: what are the problems with validating, why isn't it done more, what are the difficulties, and what are the limits to validation.

A COMPARISON OF THE VARIOUS HELICOPTER MATHEMATICAL MODELS USED IN THE METHODOLOGY ASSESSMENT

Wendell B. Stephens
U.S. Army Aeromechanics Laboratory (AVRADCOM)
NASA Ames Research Center
Moffett Field, California

Abstract

Various features of the computer codes used in the helicopter industry and by government agencies for rotorcraft aeroelastic stability analysis are compared. Mathematical rigor in modeling rotorcraft is given primarily to the rotor-system dynamic behavior; the aerodynamic modeling is still limited to strip theory and to an uneven application of corrections for stall, reversed flow, yawed flow, radial flow, and unsteady aerodynamic effects. The forward-flight regime analysis is included in five of the 11 codes surveyed. However, only two of these codes are capable of a Floquet analysis for aeroelastic stability. For the hover regime, nine of the 11 codes use eigenanalysis approach. The remaining codes perform a harmonic analysis of the transient response of system.

Nomenclature

The following abbreviations are used in Tables 1-6.

A = articulated rotor

Ae = aerodynamic center

Army-AL = Army Aeromechanics Laboratory

Ax = axial flight

B = bearingless rotor

BHT = Bell Helicopter Textron

BM = need in code for blade mode shapes

BV = Boeing Vertol

C = center of gravity

Cn = cone

CP = capability present for feature indicated

D = droop

E = elastic axis

EDT = engine/drive-train modeled

EXT = external

F = forward flight

FE = finite element

G = gimballed rotor

GDOF = gimbal degree of freedom

H = hingeless rotor

HH = Hughes Helicopter

Ho = hover

INT = internal

N = neutral axis

NA = not available in code

NHOT = no higher-order terms

PRM = pitch-roll motion

RTTrans = rotor trim from transient (20/30 REVS)

S = semiarticulated rotor

SA = Sikorsky Aircraft

SE = simple equation

Sw = sweep

T = teetering rotor

TA = transient analysis

TBA = to be added

TLU = table lookup

UTRC = United Technologies Research Corporation

Introduction

The purpose of this paper is to present comparisons of the analytical tools used by helicopter manufacturers and the government to evaluate the data sets described in the Integrated Technology Rotor (ITR) studies that were reported on in the Methodology Assessment Workshop. Although almost every technical paper describes an analytical approach the results of which are compared with theoretical, experimental, or flight data, there are few papers that try to compare all analytical tools in a particular area. In helicopter-related studies, two prominent surveys come to mind. The first was a survey conducted by Ormiston in 1974 in which he compared analytical loads results for a hypothetical helicopter rotor.[1] The loads predictions were contributed by segments of the manufacturing and government communities. Ormiston's paper revealed major shortcomings in the analyses of that period. The second survey was conducted by Johnson in 1978 (Ref. 2). That survey compared the features of a

This paper is declared a work of the U.S. Government and therefore is in the public domain.

broad range of major computer codes in areas of performance, loads and vibration, handling qualities, and aeroelastic stability. Although Johnson only tabulated features of the codes and not results, his work influenced the requirements to be set forth in the government's Second Generation Comprehensive Helicopter Analysis System (2GCHAS) Project. It also provided important guidelines for the CAMRAD (Refs. 3-5) computer code which Johnson has since developed.

The comparisons that follow are patterned after Johnson's survey, although with a narrower focus since only aeroelastic stability codes are considered. Further, only those codes used in the ITR investigations are reviewed. The analytical comparisons with the experimental data are the burden of other papers, contained in the Methodology Assessment report, that will be presented here.

Interestingly, some of the codes that were surveyed in Refs. 1 and 2 are still in use today. They have been the subjects of continual development, however, and determining their present capabilities is difficult.

Codes Surveyed

The 11 codes that are reviewed here are listed in Table 1. The organizations that developed the codes, the code identifications used in the assessment study, the flight regimes to which the codes apply, the solution methods used in the codes, and references that contain additional information about the codes are included in the table. The first eight codes in the table were developed by the major helicopter manufacturers; the last three codes were developed by government agencies. The industrial codes, as indicated earlier, have been developed over a relatively long period of time. Three versions of the E927 code are now in use as indicated in the table. The DART code is a more mature and helicopter-oriented version of the SADSAM code, and the CAMRAD code is the most recently developed and comprehensive code used in the assessment study. The last two codes, PFLT and FLAIR, were developed as research tools whose purpose it was to demonstrate modeling refinements in aeroelastic stability analysis, as such, they are applied to idealized rotorcraft models. They are predecessors to a finite-element-based code that is currently under development,[19] but it was not available for the assessment study. The first nine codes are referred to herein as applied codes and the last two as research codes.

In the tables that follow, it was necessary to make extensive use of abbreviations. Those used in a given table are defined in the footnotes to that table. For added convenience, all abbreviations are defined in the nomenclature list at the beginning of the paper.

Past Aeroelastic Stability Codes Survey

As a reference point, a comparison taken from Ref. 2 is shown in Table 2. The table includes only those codes used in the ITR study and not all the codes or features considered in Ref. 2. The code discussed in Ref. 20 is a predecessor to the CAMRAD code.

Table 2 presents a review of the code capabilities in 1978. Basically, the codes concentrated on adequately modeling the rotor and, as a result, were able to treat a variety of hub types; the mathematical models included complete blade motion. The basic disparity seemed to be in the area of the treatment of inflow dynamics. There are also restrictions built into some codes regarding the types of configurations they can analyze. The basic configuration restriction is that only one rotor system can be modeled. A note is in order concerning consistency of the code for trim and blade modes with the codes that actually perform the stability analyses: in some cases, the trim and modal analyses are performed by external programs.

Table 1 Computer codes used in methodology assessment

Code	Developer[a]	Code identification	Flight regime[b]	Solution method	References
DRAV21	BHT	BH	Ho	Eigenvalue	Not available
C81	BHT	BH	Ax,F,Ho	Time-history	6-8
C90	BV	BV	Ax,Ho	Eigenvalue	9,10
			F	Floquet	
DART	HH	HH_1	Ax,Ho	Eigenvalue	11
			F	Time-history	
E927-1	HH	HH_2	Ax,Ho	Eigenvalue	12
E927-2	SA	SA_2	Ax,Ho	Eigenvalue	12
E927-3	SA	SA_3	Ax,Ho	Eigenvalue	12
G400	SA(UTRC)	SA_1	Ax,F,Ho	Time-history	12-15
CAMRAD	NASA	NA	Ax,Ho	Eigenvalue	3-5
			F	Floquet	
PFLT	Army AL	AL	Ho	Eigenvalue	16
FLAIR	Army AL	AL	Ho	Eigenvalue	17,18

[a]Army AL = Army Aeromechanics Laboratory; BHT = Bell Helicopter Textron; BV = Boeing Vertol; HH = Hughes Helicopter; SA = Sikorsky Aircraft; SA(UTRC) = Sikorsky Aircraft (United Technologies Research Corp.).

[b]Ax = axial; F = forward; Ho = hover.

Table 2 Aeroelastic survey from Ref. 2

Feature	E927	G400	C81	Ref. 20
All helicopter configurations	NA	NA	CP	CP
All rotor types	CP	CP	CP	CP
Helicopter trimmed	NA	*a*	CP	CP
Elastic airframe motion	CP	CP	*b*	CP
Complete blade motion	CP	CP	CP	CP
Inflow dynamics	NA	CP	NA	CP
Aerodynamic interference	NA	NA	CP	CP
Programs completely coupled	NA	*c*	*c*	CP

Notes: CP = capability present; NA = not available.
[a]Partial trim.
[b]Shaft or pylon elastic motion only.
[c]Needs blade mode shapes.

Basic Features of Aeroelastic Stability Codes

Table 3 presents the same features for present codes as shown in Table 2 for 1978 codes. As in 1978, there are still only two codes that are capable of modeling more than a single rotor configuration (C81 and CAMRAD). The hub types considered by the various codes are indicated in the table. The applied codes (in the first nine columns) all show excellent capability in modeling a variety of hub conditions. There has been marked improvement in the consistency of the treatment of trim and stability models and the coupling of these models. The treatment of dynamic inflow as degrees of freedom is more of a standard today than it was in 1978. Modeling improvements in the treatment of the airframe have also advanced.

The Mathematical Model

The structural and aerodynamic modeling details for the codes are shown in Tables 4 and 5, respectively. The rotor system configuration limitations are shown in the first row of Table 4. Next, the blade modeling details are shown. Most of the codes use a modal synthesis of the blades. In the table, the solidus (/) indicates when the blade modes are uncoupled. The bending and torsion modes are uncoupled in the E927 versions and the bending flap, and lag and the torsion modes are uncoupled in G400. The number of blade modes required is often small, but the range of modes allowed by the codes is from five to 15. The use of more than five modes may be critical in detailed correlation studies. The modeling refinement in most codes is limited to 20 segments, although the CAMRAD code allows up to 50 segments. Some features that could advantageously be added to some of the codes include modeling of blade droop and sweep, noncoincident hinges, removal of small-angle restrictions on twist angles, and the capability of including fuselage aerodynamic loads. There are two codes, the G400 and CAMRAD, capable of handling rotor speed as a degree of freedom. Another modeling sophistication included by G400, DART, FLAIR, and, possibly, C90 is the ability to model redundant load paths. The codes that obtain the stability characteristics via eigenanalysis all use multiblade coordinates. This statement requires some qualification, however. As shown in Table 1, DART, G400, and C81 determine their stability characteristics via a transient response reduction analysis. The multiblade coordinates in G400 and C81 are actually used in analyses other than aeroelastic stability. All of the applied codes are capable of modeling an elastic fuselage as well as a pylon. In addition, CAMRAD is capable of including an engine/drive-train model.

In Table 5, it is seen that aerodynamic strip theory is used in all codes. It is surprising to find that some of the enhancements, most of which are simple to include, are not common to all the applied codes. Reversed flow, yawed flow, nonuniform inflow, and dynamic inflow are examples of corrections which could easily be included. The preferred treatment of determining aerodynamic coefficients remains a table-lookup procedure, and the treatment of forward flight aerodynamics is included in only five of the codes.

Related Optional Aeroelasticity Algorithms in the Codes

Table 6 summarizes the range of stability analyses available. First, it emphasizes the

Table 3 Present survey of aeroelastic stability codes

Features	DART	DRAV21	E927-2	E927-3	E927-1	G400	C90	C81	CAMRAD	FLAIR	PTLT
All helicopter configurations	NA	NA	NA	NA	NA	NA	NA	CP	CP	NA	NA
Rotor types	ABGHST	ABGHS	ABGHS	ABGHS	AGH	ABGHST	ABHS	ABGHST	AGHST	ABH	H
Helicopter trimmed	RTTrans	C81	CP	CP	CP	CP	C60	CP	CP	CP	CP
Elastic airframe motion	CP	NA	CP	CP	CP	CP	CP	CP	CP	NA	NA
Complete blade motion	CP	CP	CP	CP	NA	CP	CP	CP	CP	NA	NA
Inflow dynamics	CP	CP	CP	CP	CP	CP	NA	NA	CP	NA	NA
Dynamic stall	TA	NA	CP	CP	CP	CP	NA	CP	CP	NA	NA
Nonuniform inflow	CP	CP	CP	CP	NA	F389	NA	CP	CP	NA	NA
Aerodynamic interference	NA	NA	NA	NA	NA	NA	NA	CP	CP	NA	NA
Programs coupled	CP	BM	CP	CP	CP	CP	BM	BM	CP	CP	CP
Free wake geometry	NA	NA	NA	NA	NA	NA	NA	NA	CP	NA	NA

Notes: (1) Rotor types: A = articulated; B = bearingless; CP = capability present; G = gimballed; H = hingeless; NA = not available; S = semiarticulated; T = teetering.
(2) BM = need for blade mode shapes; RTTrans = rotor trim from transient (20/30 REVS); TA = transient analysis.

Table 4 Structural mathematical modeling details

Feature	DART	DRAV21	E927-2	E927-3	E927-1	G400	C90	C81	CAMRAD	FLAIR	PFLT
Rotors	1	1	1	1	1	1	1	2	2	1	1 Blade
Number of blades	2-5	3,4	≥3	≥3	≥3	2-5	Even No.	≥2	≥2	≥3	NA
Blade modes, bending/torsion[a]	FE	10	4/1	4/1	4/1	5-3/2	10	11	10/5	NA	15
Segments	15	20	20	20	20	20	25	20	50	26	1
Offsets	Ae,C,E,N	Ae,C,E,N	Ae,C,E,N	Ae,C,E,N	Ae,C,E,N	Ae,C,E,N	Ae,C,E,N	Ae,C,E,N	Ae,C,E,N	Ae,C,E	NA
Nonuniform mass/ stiffness matrices	CP	CP	CP	CP	CP	CP	CP	CP	CP	NA	NA
Noncoincident hinges	CP	CP	NA	NA	NA	NA	CP	CP	CP	NA	NA
Blade twist angles	CP	Nonlinear	CP	CP	CP	Nonlinear	CP	CP	CP	NA	NA
Blade orientation	Cn,D,Sw	Cn,D	Cn	Cn	Cn	Cn,D,Sw	Cn,D,Sw	Cn,D,Sw	Cn,D,Sw	NA	Cn,D,Sw
Steady-state coupling	CP	NA	NHOT	CP	CP	TA	CP	NA	CP	CP	CP
Rotor speed degrees of freedom	NA	NA	NA	NA	NA	CP	NA	NA	CP	NA	NA
Multi-blade coordination	NA	CP	CP	CP	CP	EDT	NA	CP	CP	CP	NA
Redundant bad paths	CP	NA	NA	NA	NA	CP	TBA	NA	NA	CP	NA
Fuselage	FE/HM	FE	Modal	Modal	Modal	Modal	Modal	Modal	Modal	Modal	NA
Fuselage modes, rigid body/ elastic	6/un/lm	NA	10	10	10	6/10	6/9	6/10	6/10	4/0	NA
Aerodynamics on fuselage	NA	NA	NA	NA	NA	CP	CP	CP	CP	NA	NA
Pylon	CP	PRM	GDOF	GDOF	GDOF	CP	CP	CP	EDT	NA	NA

Notes: Ae = aerodynamic center, C = center of gravity, Cn = cone, CP = capability present, D = droop, E = elastic axis; EDT = engine/drive-train modeled, FE = finite element, GDOF = gimbal degree of freedom, HM = hub modal properties, N = neutral axis; NA = not available; NHOT = no higher-order terms, PRM = pitch-roll motion, Sw = sweep, TA = transient analysis, TBA = to be added.

[a]The solidus (/) designates uncoupled.

Table 5 Aerodynamic modeling features for the codes

Feature	DART	DRAV21	E927-2	E927-3	E927-1	G400	C90	C81	CAMRAD	FLAIR	PFLT
Strip theory	CP	CP	CP	CP	CP	CP	CP	CP	CP	CP	CP
Nonuniform inflow	CP	CP	CP	CP	NA	CP	NA	CP	CP	NA	NA
Dynamic inflow	NA	CP	NA	NA	NA	CP	NA	NA	CP	NA	NA
Radial flow	TA	NA	NA	NA	NA	CP	NA	CP	CP	NA	NA
Solution method	TLU	TLU/SE	TLU	TLU	TLU	TLU/SE	TLU	TLU	TLU/SE	SE	SE
Reversed flow	NA	NA	NA	NA	NA	CP	CP	CP	CP	NA	NA
Stall	TA	CP	CP	CP	CP	CP	CP	CP	CP	NA	NA
Compressibility	TA	CP	CP	CP	CP	CP	CP	CP	CP	NA	NA
Yawed flow	NA	NA	NA	NA	NA	CP	NA	CP	CP	NA	NA
Tip correction	CP	NA	CP	CP	CP	CP	CP	CP	CP	NA	NA
Unsteady aerodynamics	CP	NA	CP	CP	CP	CP	NA	CP	CP	NA	NA
Flight regime	Ax,F,Ho	Ho	Ax,Ho	Ax,Ho	Ax,Ho	Ax,F,Ho	Ax,F,Ho	Ax,F,Ho	Ax,F,Ho	Ho	Ho

Notes: Ax = axial; CP = capability present; F = forward; Ho = hover; NA = not available; SE = simple equation; TA = transient analysis; TLU = table lookup.

Table 6 Related optional aeroelastic stability algorithms in the codes

Feature	DART	DRAV21	E927-2	E927-3	E927-1	G400	C90	C81	CAMRAD	FLAIR	PFLT
Trim	RTTrans	C81	INT	INT	INT	INT	C60	INT	INT	INT	INT
Blade modes	NA	DYNAMO6	INT/EXT	INT/EXT	INT/EXT	INT	Y-71	DYNAMO6	INT	INT	INT
Air resonance	CP	CP	CP	CP	CP	CP	CP	CP	CP	CP	NA
Ground resonance	CP	CP	CP	CP	CP	CP	CP	CP	CP	CP	NA
Time-history	CP	NA	NA	NA	NA	CP	NA	CP	NA	NA	NA
Eigenanalysis	CP	CP	CP	CP	CP	NA	CP	NA	CP	CP	CP
Floquet	NA	NA	NA	NA	NA	NA	CP	NA	CP	NA	NA
Prony's method	NA	NA	NA	NA	NA	NA	NA	CP	NA	NA	NA
Moving block	CP	NA	NA	NA	NA	CP	NA	CP	NA	NA	NA
Harmonic analysis of time-history	CP	NA	NA	NA	NA	CP	NA	CP	NA	NA	NA
Gust response	NA	NA	NA	NA	NA	CP	NA	CP	CP	NA	NA

Notes: CP = capability present; EXT = external; INT = internal; NA = not available; RTTrans = rotor trim from transient (20/30 REVS).

importance of establishing a consistent trim state from which to perturb. It shows that all codes are capable of obtaining flutter (air resonance) and ground resonance solutions. Some codes, such as DART, G400, and C81, approach the aerostability solution via a transient response and have harmonic analysis, moving block, and Prony methods for obtaining the stability solutions from these time-history analyses. Basically, the preferred approach is to rely on eigenvalue and Floquet techniques to obtain the stability data. Only C90 and CAMRAD are capable of performing the Floquet analysis, that is, the direct treatment of periodic coefficients.

Concluding Remarks

The adequacy of these aeroelastic stability codes for application to the ITR data sets will be addressed in subsequent papers to be presented at this forum. The formulation of the codes has been addressed in this paper.

The code formulations are influenced strongly by the highly interdisciplinary nature and complexity of rotorcraft dynamics and aerodynamics. This has caused code developers to make careful approximations of how much of the problem it is prudent to represent. Therefore, in most of the code architectures, the model is built into the code, leaving the analyst with limited options with which to describe the complete rotorcraft configurations in detail. Further, the codes tend to have a rather long life cycle. The disadvantage of this long development is that the older code architectures restrict unnecessarily the dimension space and, therefore, the modeling detail that can be considered. This can be seen in the number of modes and segments allowed. A further problem with the long development period is that the documentation for the codes is often far behind the code capability. These disadvantages are offset, somewhat, by a long period of validation for most capabilities in the codes.

A great amount of mathematical rigor has been placed in accurate dynamic modeling of the rotor system. The rest of the aircraft is often represented as an elastic fuselage using a modal approach. The rigor in the aerodynamic representation is somewhat lacking. The basis for the aerodynamic representation is a semiempirical strip theory. In two codes, CAMRAD and G400, an attempt is made to make this theory as consistent as possible by including reversed flow, yawed flow, radial flow, stall, tip corrections, unsteady aerodynamics, nonuniform inflow, and dynamic inflow.

The treatment of the stability algorithms varies with the flight regimes. For hover (and axial) flight all of the codes except C81 and G400 use an eigenanalysis. For forward flight, in which the coefficients are periodic, only five codes attempt to solve the problem. Of these, only CAMRAD and C90 attempt to solve the periodic coefficient equations directly using an eigenanalysis of the Floquet transition matrix. The DART system has an option which averages the coefficients over a period and then determines the eigenvalues of this "constant coefficient" approximation. The codes that can not address the periodic coefficients directly — C81, DART, and G400 — obtain a time-history solution and reduce that transient response to get the stability characteristics.

References

[1]Ormiston, R. A., "Comparison of Several Methods for Predicting Loads on a Hypothetical Helicopter Rotor," NASA SP-32, 1974.

[2]Johnson, Wayne, "Comprehensive Helicopter Analyses: A State-of-the-Art Review," NASA TM-78539 (AVRADCOM TR 78-56(AM)), 1978.

[3]Johnson, Wayne, "Comprehensive Analytical Model of Rotorcraft Aerodynamics and Dynamics. Pt. 1. Analysis Development," NASA TM-81182, 1980.

[4]Johnson, Wayne, "Comprehensive Analytical Model of Rotorcraft Aerodynamics and Dynamics. Pt. 2. User's Manual," NASA TM-81183, 1980.

[5]Johnson, Wayne, "Comprehensive Analytical Model of Rotorcraft Aerodynamics and Dynamics. Pt. 3. Program Manual," NASA TM-81184, 1980.

[6]McLarty, T. T. et al., "Rotorcraft Flight Simulation with Coupled Rotor Aeroelastic Stability Analysis. Vol. I. Engineer's Manual," USAAMRDL TR-76-41A, May 1977.

[7]Van Gaasbeck, James R., "Rotorcraft Flight Simulation Computer Program C81 with DATAMAP Interface. Vol. I. User's Manual," USAAVRADCOM-TR-80-D-38A, Oct. 1981.

[8]Hsieh, P. Y., "Rotorcraft Flight Simulation Computer Program C81 with DATAMAP Interface. Vol. II. Programmer's Manual," USAAVRADCOM-TR-80-D-38B, Oct. 1981.

[9]Lytwyn, R. T., "Aeroelastic Stability Analyses of Hingeless Rotor Helicopters in Forward Flight Using Blade and Airframe Normal Modes," Paper No. 80-24, presented at the 36th Annual National Forum of the American Helicopter Society, Washington, D.C., Mar. 1980.

[10]Gabel, Richard, "Current Loads Technology for Helicopter Rotors," Specialists Meeting on Helicopter Rotor Loads Prediction Methods, AGARD Conference Proceedings No. 122, Milan, Italy, Mar. 1973.

[11]Peterson, Leonard, "Theoretical Basis for SADSAM Computer Program," MSR-11, MacNeal-Schwendler Corp., Los Angeles, Calif., 1969.

[12]Johnston, R. A. and Cassarino, S. J., "Aeroelastic Rotor Stability Analysis," USAAMRDL TR 75-40, Jan. 1976.

[13]Bielawa, R. L., "Aeroelastic Analysis for Helicopter Rotor Blades with Time-Variable, Nonlinear Structural Twist and Multiple Structural Redundancy," NASA CR-2638, 1976.

[14]Bielawa, R. L., "Aeroelastic Analysis with Blade Appended Pendulum Vibration Absorbers — Mathematical Derivations and Program Users Manual," NASA CR-165896, 1982.

[15]Bielawa, R. L. et al., "Aeroelastic Analysis for Propellers — Mathematical Formulations and Users Manual," NASA CR 3729, Dec. 1983.

[16]Hodges, Dewey H., "Nonlinear Equations of Motion for Cantilever Rotor Blades in Hover with Pitch Link Flexibility, Twist, Precone, Droop, Sweep, Torque Offset, and Blade Root Offset," NASA TM X-73,112, 1976.

[17]Hodges, Dewey H., "Aeromechanical Stability of Helicopters with Bearingless Main Rotors. Pt. 1. Equations of Motion," NASA TM-78459, 1978.

[18]Hodges, Dewey H., "Aeromechanical Stability of Helicopters with Bearingless Main Rotors. Pt. 2. Computer Program," NASA TM-78460, 1978.

[19]Hodges, Dewey H., "General Rotorcraft Aeromechanical Stability Program (GRASP) Theoretical Manual," in preparation.

[20]Johnson, Wayne, "Aeroelastic Analysis for Rotorcraft in Flight or in a Wind Tunnel," NASA TN D-8515, 1977.

A COMPARISON OF THEORY AND EXPERIMENT FOR AEROELASTIC STABILITY OF A HINGELESS ROTOR MODEL IN HOVER

David L. Sharpe
Research Scientist
U.S. Army Aeroflightdynamics Directorate
Ames Research Center
Moffett Field, California

Abstract

Theoretical predictions of aeroelastic stability are compared with experimental, isolated, hingeless-rotor data. The six cases selected represent a torsionally soft rotor having either a stiff or soft pitch-control system in combination with zero precone and droop, 5° precone, or -5° droop. Analyses from Bell Helicopter Textron, Boeing Vertol, Hughes Helicopters, Sikorsky Aircraft, the National Aeronautics and Space Administration, and the U.S. Army Aeromechanics Laboratory were compared with the experimental data. The correlation ranged from very poor to fair.

Nomenclature

c	= blade chord, in.
E	= Young's modulus, $lb/in.^2$
c_ℓ, c_d, c_m	= blade section lift, drag, and pitching moment coefficients
G	= shear modulus, $lb/in.^2$
I_{EA}	= mass polar moment of inertia of the blade about the chordwise elastic axis, lb_m-$in.^2$
I_ζ	= blade-chord cross-sectional-area moment of inertia, $in.^4$
I_β	= blade-flap cross-sectional-area moment of inertia, $in.^4$
I_θ	= mass polar moment of inertia of hub components about centerline of flexure, lb_m-$in.^2$
J	= blade cross-sectional polar moment of inertia, $in.^4$
L	= blade length, start of uniform section to tip, in.
R_N	= Reynolds number of blade section
α	= blade section angle of attack, rad
β_d	= droop angle, deg
β_{pc}	= precone angle, deg
μ	= blade mass per unit length, $lb_m/in.$
σ	= blade lead-lag damping, sec^{-1}
θ_o	= blade pitch angle, deg
ω	= modal frequency, Hz
$\omega_{\beta NR}, \omega_{\zeta NR}, \omega_{\theta NR}$	= blade frequencies in flap, lead-lag and torsion, nonrotating model, Hz
Ω	= rotor speed, rpm

Introduction

As a part of the Methodology Assessment, six cases were selected from the experiments reported in Ref. 1. These experiments measured the lead-lag damping of a small-scale, torsionally soft hingeless rotor with uniform blade properties which was mounted on a rigid stand. The six cases included in this correlation study were chosen because they allowed a systematic study of the effects of blade precone, droop, and pitch-control stiffness on the lead-lag stability of a stiff, inplane, isolated rotor.

Eight different math models from industry and government were compared to these data. Bell Helicopter Textron used DRAV21, both with and without dynamic inflow. Boeing Vertol made the comparison with C-90. Hughes Helicopters made the comparison with the results of their time history analysis, DART. Sikorsky Aircraft used the code G400 primarily, but included some comparisons using two versions of E927. The U.S. Army Aeromechanics Laboratory made the comparisons with PFLT, and finally, NASA compared selected data points with CAMRAD.

This paper describes the experiment of Ref. 1, and compares the theoretical and experimental results. Conclusions will be made as to the quality of the correlation. Appendices are included that document the experimental model properties, tabulate the experimental data points, and show all of the correlations.

Experiment Description

A small-scale, 6.31-ft-diameter, torsionally soft, hingeless helicopter rotor was investigated in hover to determine its stability characteristics. The two-bladed, untwisted rotor was tested

on a rigid test stand at tip speeds up to 332 ft/sec. The rotor mode of interest in this investigation was the lightly damped lead-lag mode. The dimensionless lead-lag frequency of this mode was approximately 1.5/rev at 1000 rpm. The rotor was designed to allow variation in blade precone at the hub using interchangeable precone hubs, blade droop using different droop wedges, and pitch control stiffness using either a stiff or a soft pitch flexure. These features are illustrated schematically in Fig. 1. The major rotor parameters are shown in Table 1.

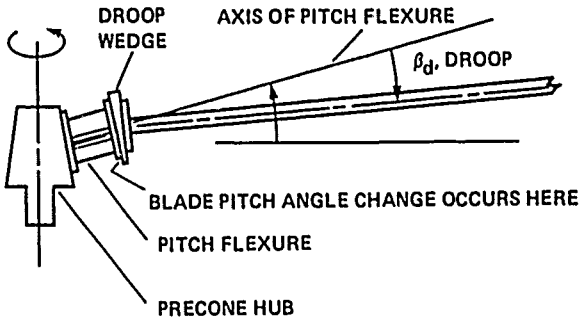


Fig. 1 Schematic of rotor hub showing precone and droop angles and location of pitch flexure.

Table 1 Experimental model properties

Variable	Value
Number of blades	2
Rotor diameter, ft	6.309
Blade length, L, ft	2.854
Blade chord, c, in.	3.4
Twist, deg	0
Nominal rotor speed, rpm	1000
R_N at tip	≈500,000
Blade frequencies at 1000 rpm, per rev	--
Flap frequency	1.15
Lead-lag frequency, stiff pitch flexure	1.50
Lead-lag frequency, soft pitch flexure	1.38
Torsional frequency, stiff pitch flexure	2.85
Torsional frequency soft pitch flexure	2.56

The model blade design is shown in Fig. 2. The blade structure was designed to minimize the blade torsional frequency while maintaining appropriate flap and lead-lag frequencies. The NACA 0012 airfoil had a unidirectional Kevlar spar, a polyurethane core, and a segmented tantalum leading edge; it was covered with fiberglass cloth. The chordwise center of gravity and the elastic axis were designed to be coincident at the blade quarter chord. The blade section stiffness and mass properties are uniform from the 9.5% radius to the tip.

An isometric view of the rotor hub components is shown in Fig. 3. The control system or pitch link flexibility is represented in the experimental model by pitch flexures mounted inboard of

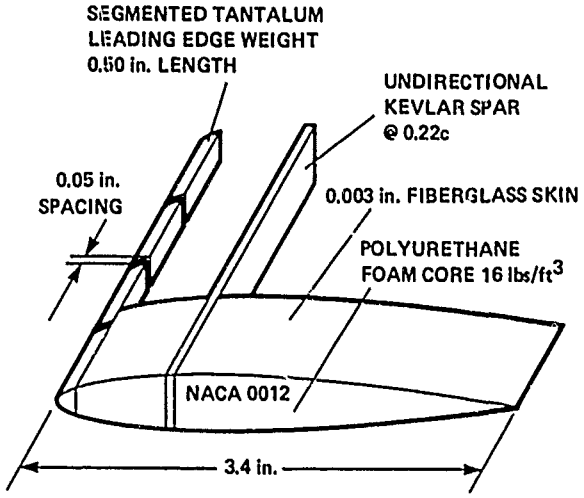


Fig. 2 Experimental-model blade design.

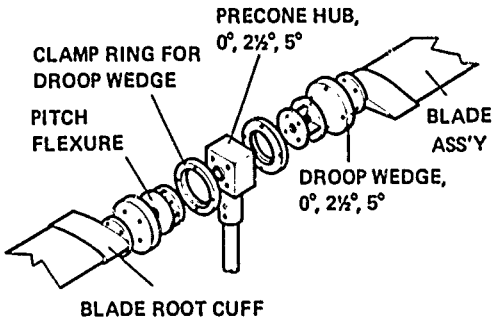


Fig. 3 Rotor hub components.

the blade. The partial cruciform cross section of these pitch flexures provides relatively high stiffness in the flap and lead-lag directions, while the torsional stiffness is controlled by the thickness of the flexure elements. Flexures of two different torsional stiffnesses were used in the experiment. Changes in precone were made with interchangeable hubs, one for each precone angle tested. Droop was varied with interchangeable droop wedges. These components were fabricated with angles of 0, ±2.5, and ±5° (positive values only for precone). In all cases the blade pitch angle was changed by rotating the blade outboard of the pitch flexure at the interface between the pitch flexure and the droop wedge. When a nonzero value of droop exists, this method of blade pitch change will introduce a small amount of blade sweep equal to the product of the blade pitch angle and the droop angle. A complete discussion of the model properties is provided in Appendix A.

The blades and associated hub components were mounted on a rigid test stand as shown in Fig. 4. Power was transmitted to the rotor shaft through a flexible belt drive. The upper truss framework which houses the drive shaft is attached to the circular mounting plate by two flexures. The lead-lag mode was excited by oscillating the upper structure about the flexures with a 50-lb electro-

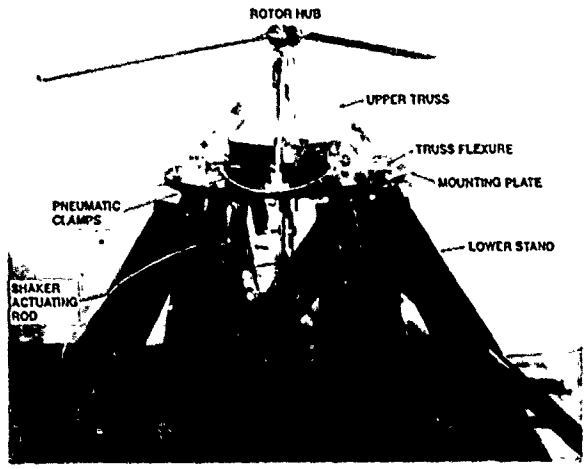


Fig. 4 Experimental rotor on test stand.

magnetic shaker. The shaker, located on the floor below the mounting plate, is attached to a forward arm of the upper truss framework by a hollow aluminum pushrod. Once sufficient lead-lag motion of the blade was obtained, the shaker excitation was shut off while a pneumatic clamp was simultaneously activated to lock the upper structure. A differential lead-lag signal was obtained by subtracting the lead-lag signal of one blade from the other to eliminate drive-system-coupling effects from the data. The lead-lag modal frequency and damping were then obtained from the differential lead-lag signal by performing a moving-block analysis on the transient decay of the blade motions.

The six experimental configurations chosen for comparison with theory in this paper are given in Table 2. The damping data shown in Fig. 5 as a function of pitch angle illustrate the wide variation in lead-lag damping that occurs for these cases. Figure 5a shows Cases 1 and 2, which are the least aeroelastically-coupled as there is neither precone nor negative droop. Both cases show similar behavior with pitch angle, except the damping increase is greater with the soft-pitch flexure (Case 2). The stiff-pitch-flexure cases with precone and negative droop compared in Fig. 5b show the same damping behavior. This figure shows that precone and negative droop are equivalent when the control system is stiff. Such is not the case for a soft control system as shown in Fig. 5c. The effect of control-system flexibility as represented here by the soft-pitch flexure is to significantly destabilize the case that includes negative droop. Figure 5d compares the cases that have 5° precone and stiff- and soft-pitch flexures. The effect of the soft-pitch flexure is to destabilize the rotor. The experimental damping data for the six cases are provided in Appendix B.

Table 2 Selected cases

Case	Pitch flexure	Precone, deg	Droop, deg
1	Stiff	0	0
2	Soft	0	0
3	Stiff	5	0
4	Soft	5	0
5	Stiff	0	-5
6	Soft	0	-5

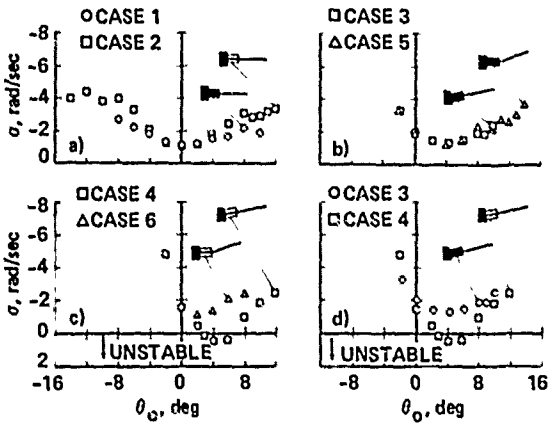


Fig. 5 Overview of experimental lead-lag damping for selected cases. a) Comparison of Cases 1 and 2 to show effects of control flexibility; b) comparison of Cases 3 and 5 to show effects of precone and droop, stiff pitch flexure; c) comparison of Cases 4 and 6 to show effects of precone and droop, soft pitch flexure; d) comparison of Cases 3 and 4 to show effects of control flexibility, 5° precone.

Correlation

The theoretical calculations were compared to the experimental results for the six cases by plotting lead-lag damping as a function of blade pitch. The experimental results including data scatter are shown in Figs. 6-11 as a stippled area. Table 3 provides the codes used on the figures for the various prediction methods. The appropriate predictions for each case are divided into two groups to increase clarity. The predictions shown in the upper group are those which

Table 3 Identification of prediction codes

ID	Prediction method	User
BH	DRAV21	Bell Helicopter Textron
BV	C-90	Boeing Vertol
HH_1	DART	Hughes Helicopters
SA_1	G400	Sikorsky Aircraft
SA_2	E927-2	Sikorsky Aircraft
SA_3	E927-3	Sikorsky Aircraft
AL	PFLT	U.S. Army Aeromechanics Laboratory
NA	CAMRAD	NASA Ames Research Center

were judged to be more accurate. The initial predictions using the code G400 were not considered adequate by Sikorsky Aircraft and the code was subsequently upgraded. Additional predictions were made with the upgraded code and are shown in the figures as triangular symbols without fairings. These modifications are described in detail in Ref. 2. Bell Helicopter Textron made the predictions using DRAV21 with both steady and dynamic inflow. Only the results from steady inflow are shown here. The complete comparison of theory and experiment for these six cases is included in Appendix C.

Case 1

The correlation shown in Fig. 6 is for the isolated rotor with 0° precone, 0° droop, and a stiff pitch flexure. The experimental lead-lag damping results cover both positive and negative pitch angles with minimum damping occurring at zero pitch angle. A distinct asymmetry is seen in the data, with the greater damping occurring at negative values of pitch angle.

The predictions with DRAV21 (BH) show good agreement over nearly the entire pitch-angle range tested. The point of minimum damping as well as the asymmetry in damping levels about that point are correctly predicted. The results of the Dynamic Analysis Research Tool (DART) (HH_1) were found to have fair correlation with the experiment. The DART damping prediction is shown to be symmetric for positive and negative pitch values and does not predict the reduced lead-lag damping at the higher positive blade pitch-angles that was found in the experiment. Agreement between the theory of CAMRAD (NA) and the experiment is fair, although calculations were not undertaken at the higher negative pitch-angle values. The Sikorsky analysis E927-2 (SA_2) shows fair agreement with the experimental data, with a slight underprediction of lead-lag damping over nearly the entire range of blade pitch angles. Since the damping predictions of this code are shown to be symmetric with positive and negative pitch angles, the underprediction is greater at high negative pitch-angles.

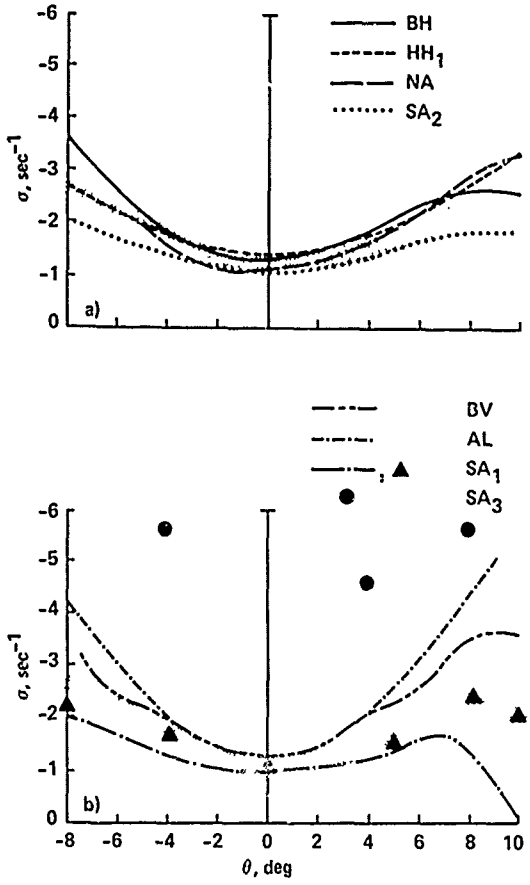


Fig. 6 Comparison of theory and experiment for Case 1; stiff pitch flexure, $\beta_{pc} = \beta_d = 0°$. a) BH, HH_1, NA, SA_2; b) BV, AL, SA_1, SA_2.

The predictions of C-90 (BV) for Case 1 are fair, showing agreement with the experimental data at negative pitch angles, but the agreement is not as good at positive pitch angles. However, the theory does show the characteristic reduction in damping at the higher positive pitch-angles. The predictions of the Aeromechanics Laboratory theory PFLT (AL) is poor-to-fair, agreeing with the test data only at low values of blade pitch angle. At pitch angles greater than 4°, agreement is poor, with the theoretically predicted increase in damping not seen in the experiment. This is probably caused by the linear representation of the aerodynamic section coefficients used in that theory. The G400 (SA_1) predictions are nearly identical to those of E927-2 (SA_2), with the exception of lead-lag damping at 10° pitch angle. The code E927-2 predicts a slight increase from the damping at 8°, whereas G400 predicts a decrease in lead-lag damping to near-neutral stability. The triangles which represent the results of the upgraded version of G400 are very good, showing a marked improvement over the original version. The theory of E927-3 (SA_3) reintroduces higher-order terms that were removed when E927-2 (SA_2) was developed from the public domain version of Ref. 3. The correlation for this code was found to be very poor. Only the lead-lag damping at zero pitch angle was predicted correctly. Damping values at blade pitch angles greater than zero were significantly overpredicted.

Case 2

The correlation shown in Fig. 7 is for a configuration having zero precone, zero droop, and a soft-pitch flexure. The increase in lead-lag damping with blade pitch angle is greater for this case than it is for Case 1. The point of minimum damping again occurs at zero pitch angle, but there is a more pronounced asymmetry about the zero point than was seen with the stiff pitch flexure.

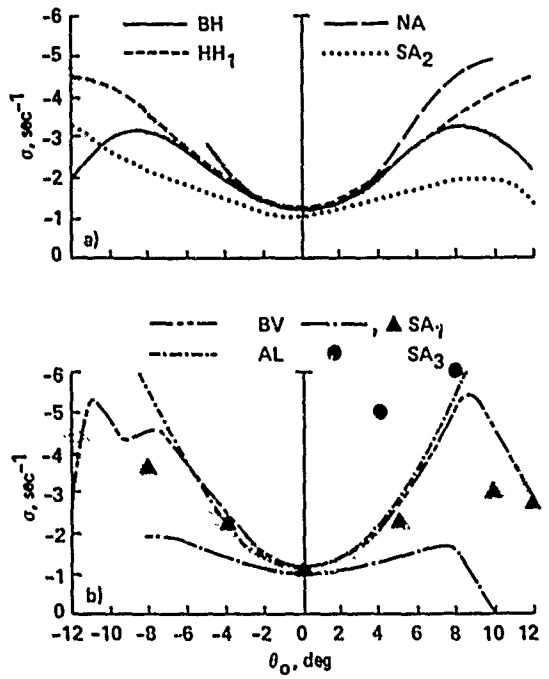


Fig. 7 Comparison of theory and experiment for Case 2; soft pitch flexure, $\beta_{pc} = \beta_d = 0°$. a) BH, HH_1, NA, SA_2; b) BV, AL, SA_1, SA_3.

The prediction of DRAV21 (BH) shows fair-to-good correlation with the experiment, but the agreement is not as good at the higher pitch angles. The theory predicts a decrease in damping due to stall above 8° which is not evident in the data. In addition, the asymmetry in damping that was correctly predicted by this theory for the stiff flexure is reversed for this case, predicting greater damping at positive blade pitch angle than at negative pitch angles. The predictions of DART (HH_1) show fair-to-good agreement with the experimental findings and show the increased lead-lag damping caused by the reduced torsional stiffness of the soft pitch flexures. The lead-lag damping predictions of CAMRAD (NA) show poor-to-fair correlation with better agreement at low pitch angles and a tendency to overpredict the damping for the higher pitch angles. The E927-2 (SA_2) code is only poor-to-fair in correlation and underpredicts the measured damping by as much as 40%. This code also shows a reduction in damping at high positive pitch angles with no change in the damping slope predicted at negative pitch angles.

The correlation of C-90 (BV) and the data are poor-to-fair, showing reasonably good agreement with the experiment at low pitch angles and an overprediction of the lead-lag damping at the higher pitch angles. This theory also predicts an asymmetry between positive and negative pitch angles, but of a different nature than was found experimentally. The weakness of the aerodynamic modeling in PFLT (AL) is again seen, with good correlation at low pitch angles and large overpredictions of lead-lag damping at high pitch angles; the overall correlation is poor-to-fair. The unmodified theory of G400 (SA_1) underpredicts the damping and again shows neutral stability at 10° pitch angle and is judged to be very poor-to-poor. The triangle symbols representing the upgraded version of G400 show greatly improved correlation. Predictions with E927-3 (SA_3) are again very poor with most lead-lag damping values being overpredicted by an order of magnitude.

Case 3

The experimental lead-lag damping results for the isolated rotor configuration having 5° of precone, 0° of droop, and the stiff pitch flexures were found to exhibit much larger changes of damping with pitch angle at low blade pitch angles than was observed for Cases 1 and 2. This is primarily due to the increased aeroelastic coupling which results from the centrifugally induced blade elastic deflection. While some of the codes were found to model this structural coupling well, others did not; this correlation is shown in Fig. 8.

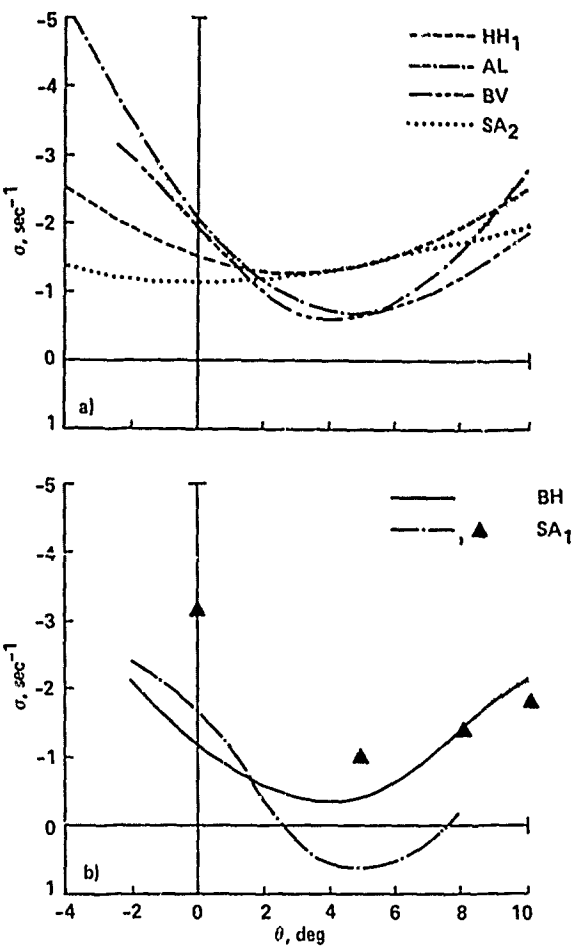


Fig. 8 Comparison of theory and experiment for Case 3; stiff pitch flexure, $\beta_{pc} = 5°$, $\beta_d = 0°$. a) HH_1, AL, BV, SA_2; b) BH, SA_1.

The lead-lag damping predictions of DART (HH_1) are good at the positive values of pitch angle where the equilibrium deflections and coupling which results are low. However, the quality of the correlation deteriorates as this equilibrium deflection and coupling grows with increasing negative pitch angle, and the overall agreement is considered fair. The theory of PFLT (AL) shows good correlation with the experiment over the negative pitch-angle range where the coupling is large, but underpredicts the damping at positive pitch angles, so overall is judged to be fair. The C-90 analysis (BV) exhibits nearly the same predictive characteristics as PFLT and also is considered to be fair. The E927-2 code (SA_2) shows agreement with the experiment at high positive pitch angles, but where the coupling is strong and the damping should show a marked increase, the predictions show little change. A comparison of Cases 1 and 3 shows that the E927-2 predictions are identical, and neither precone nor droop affect the predicted value. The correlation is judged to be poor. The DRAV21 code (BH) successfully predicts the experimental trend in lead-lag damping with pitch angle, but consistently underpredicts the experimental results, so is only considered to be poor-to-fair. The G400 analysis (SA_1) shows very poor correlation with the experimental results in the original version, predicting an instability between 2.5 and 7.5° pitch angle. The modified version of G400, shown by the triangle symbols, shows fair correlation with the experiment, with no predicted instability. The E927-3 version (SA_3) was unable to predict lead-lag stability characteristics for this case.

Case 4

The experimental lead-lag damping results for the configuration with 5° of precone and 0° of droop with soft-pitch flexures show the rotor to be dynamically unstable between 2.5 and 7° pitch angle. Nearly all the math models predict this instability but with varying degrees of accuracy. The correlation is shown in Fig. 9.

The theoretical predictions from PFLT (AL) show fair-to-good correlation with the experimental results. The pitch angle range at which the instability occurs is well predicted. The severity of the instability is slightly overpredicted and the damping at high pitch angles is also overpredicted. The correlation with DART (HH_1) shows fair agreement, with the degree of instability being somewhat underpredicted when compared to the experiment. The DRAV21 (BH) and C-90 (BV) results are nearly identical, both showing poor-to-fair correlation. The damping trend with pitch angle follows the experiment closely; however, the pitch angle range and degree of instability are substantially overpredicted. The original version of G400 (SA_1) also severely overpredicts the magnitude and range of the instability, showing nearly the same correlation as DRAV21 and C-90. The modified version of G400, shown by the triangle symbols, gives somewhat mixed

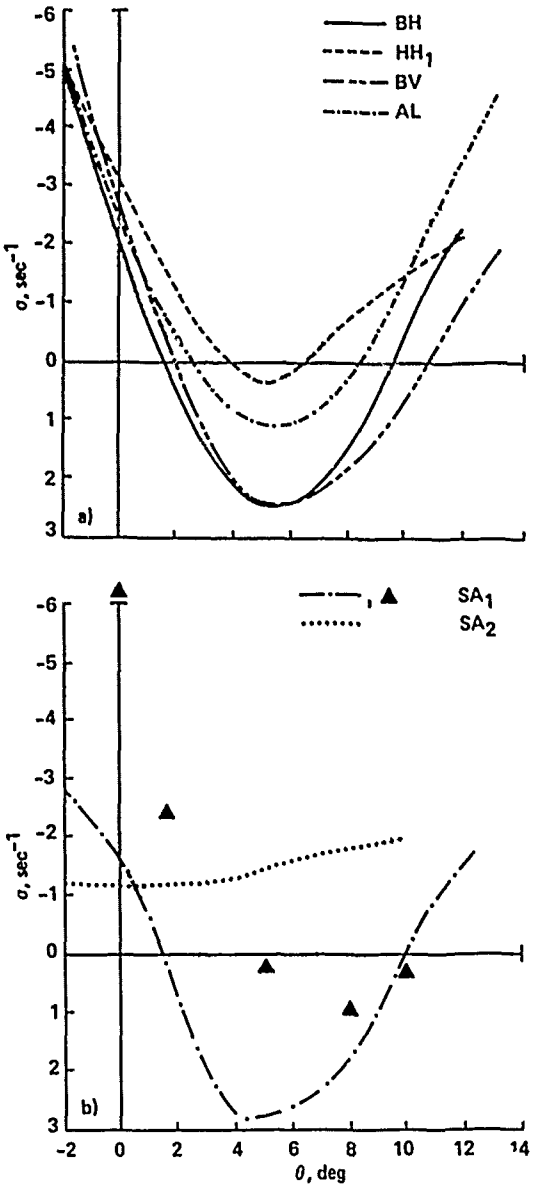


Fig. 9 Comparison of theory and experiment for Case 4; soft pitch flexure, δ_{pc} = 5°, δ_d = 0°. a) BH, HH_1, BV, AL; b) SA_1, SA_2.

results. Although the extent of the instability is reduced and is in better agreement with the experiment, the pitch-angle range where the instability occurs shows poorer correlation than with the unmodified version of G400. The E927-2 code shows very poor correlation and fails to predict the instability.

Case 5

The correlation shown in Fig. 10 is for the configuration with 0° precone, -5° droop, and stiff-pitch flexures. When the experimental results for this case are compared with Case 3 (Fig. 5b), the damping results are seen to be

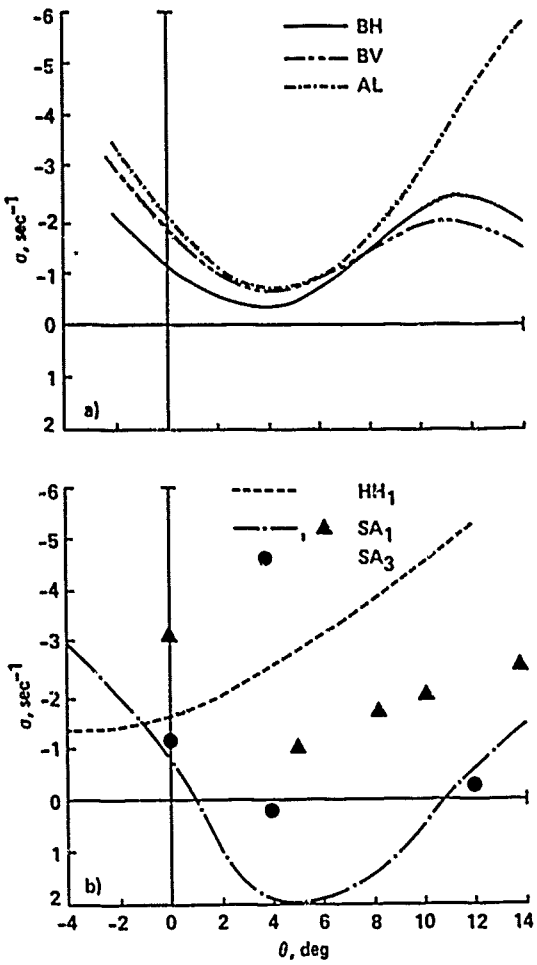


Fig. 10 Comparison of theory and experiment for Case 5; stiff pitch flexure, β_{pc} = 0°, β_d = -5°. a) BH, BV, AL; b) HH_1, SA_1, SA_3.

nearly identical. In general, the predictions of the analytical codes also show this correspondence.

The DRAV21 (BH), C-90 (BV), and PFLT (AL) codes each confirm that without control system flexibility, the 5° precone and -5° droop are dynamically the same. The correlation of these three codes is essentially the same as observed in Case 3.

The damping predictions of DART (HH_1) did not agree with the experimental results for this configuration, nor did it show any similarity to the DART prediction for Case 3 because the sign convention in the input of the droop angle was reversed. The original version version of G400 (SA_1) shows very poor correlation, with the theory predicting an instability where none existed. With modifications, the instability was no longer predicted and the overall correlation improved. Predictions with E927-3 (SA_3) were again very poor.

Case 6

The correlation for a configuration having 0° precone, -5° of droop, and soft pitch flexures is shown in Fig. 11. Although the experimental data show that the damping characteristics for this case are roughly the same as Case 5, the theoretical models show different results.

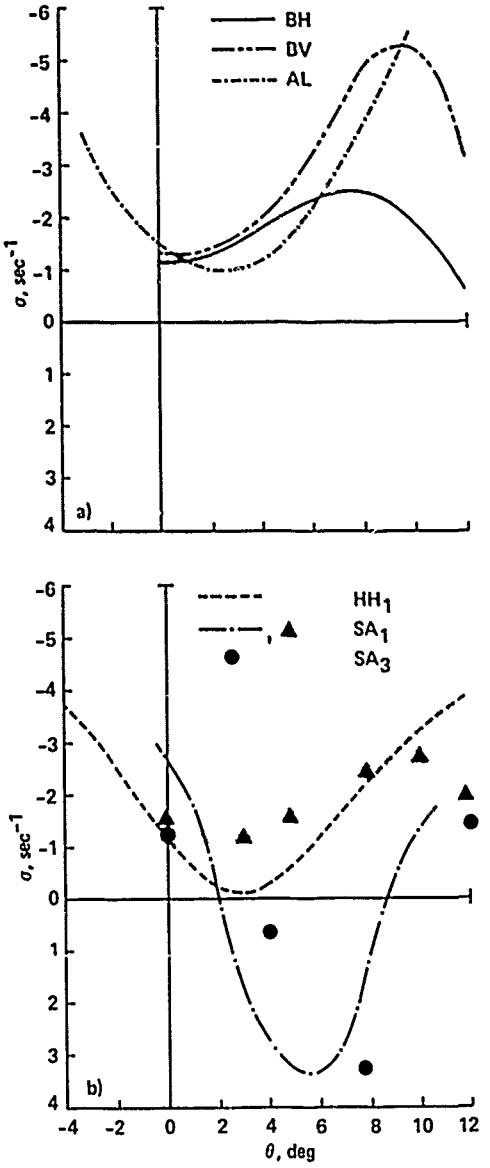


Fig. 11 Comparison of theory and experiment for Case 6; soft pitch flexure, β_{pc} = 0°, β_d = -5°. a) BH, BV, AL; b) HH_1, SA_1, SA_3.

The DRAV21 (BH), C-90 (BV), and PFLT (AL) codes show fair correlation with the experimental data at low blade-pitch angles, but the correlation becomes progressively worse as the pitch angle increases. The predicted damping for the

three codes is vastly different beyond 5°. The computer code DRAV21 (BH) agrees reasonably well with the experimental results up to about 8° blade pitch angle, at which point an abrupt decrease in damping with increasing blade pitch is predicted, with the theory substantially underpredicting the experimental results. Overall the correlation is considered to be fair. The computer code C-90 (BV) shows reasonable agreement with the experimental data for only the first 3 or 4° of blade pitch angle. At higher blade pitch angles, the correlation degrades, with the theory predicting nearly twice as much damping at about 8° pitch and a sharp reduction of damping with pitch angle beyond 10°. The correlation over the pitch-angle range is judged poor. The code PFLT (AL) shows fair agreement up to approximately 6° blade pitch angle, but increasingly overpredicts the damping beyond this value, and the overall correlation is poor-to-fair.

The correlation between the experiment and the theory for DART (HH) is poor, with the theory substantially underpredicting the experimental damping over most of the pitch-angle range and with the predictions approaching neutral stability at between 3 and 4°.

Predictions with the unmodified G400 (SA_1) were found to be very poor, showing a strong instability over much of the pitch-angle range. On the other hand, the modified version of the G400 shows very good correlation with the experimental results, with the exception of the highest pitch-angle setting where the damping is underpredicted. The E927-3 (SA_3) predictions again show very poor correlation with the experimental data.

Conclusions

Eight analyses were compared with one or more cases selected from an experiment that measured the damping of an isolated, torsionally soft rotor in hover.

1. The DRAV21 analysis used by Bell Helicopter Textron was considered to give fair correlation overall for the six cases.

2. The C-90 analysis used by Boeing Vertol was judged to have poor-to-fair correlation overall.

3. The DART analysis used by Hughes Helicopters was also considered to have poor-to-fair capability when compared to the six cases.

4. Sikorsky Aircraft used the analysis code G400 and two versions of E927: E927-2 and E927-3. Overall the G400 code was judged as very poor-to-poor, and the E927-2 and E927-3 analyses were considered poor and very poor, respectively. Subsequent to the evaluation the G400 code was upgraded and limited results are shown for the six cases. These results show that the G400 code has been substantially improved.

5. The Aeromechanics Laboratory PFLT analysis was considered to provide fair correlation.

6. The NASA Ames CAMRAD calculations were made for two cases and were judged to be fair.

References

[1]Sharpe, David L., "An Experimental Investigation of the Flap-Lag-Torsion Aeroelastic Stability of a Small Scale Hingeless Helicopter Rotor in Hover," NASA TP-2546, Jan. 1986.

[2]Bielawa, Richard L., "Considerations of Spanwise Variable Elastic Axis Offset in the Aeroelastic Modelling of Rotor Blades," NASA CP 10007, May 1988.

[3]Johnston, R. A. and Cassarino, S. J., "Aeroelastic Rotor Stability Analysis," USAAMRDL TR 75-40, Jan. 1976.

[4]Hodges, D. H. and Ormiston, R. A., "Stability of Elastic Bending and Torsion of Uniform Cantilever Rotor Blades in Hover with Variable Structural Coupling," NASA TN D-8192, April 1976.

[5]Hodges, D. H., "Nonlinear Equations of Motion for Cantilever Rotor Blades in Hover with Pitch Link Flexibility, Twist, Precone, Droop, Sweep, Torque Offset, and Blade Root Droop," NASA TM X-73,122, May 1976.

[6]Hodges, Dewey H. and Ormiston, R. A., "Stability of Hingeless Rotor Blades in Hover with Pitch-Link Flexibility," AIAA Journal, Vol. 15, No. 4, April 1977, pp. 476-482.

[7]Ormiston, R. A. and Bousman, W. G., "A Study of Stall-Induced Flap-Lag Instability of Hingeless Rotors," Preprint No. 730, American Helicopter Society 29th Annual National Forum, May 1973.

Appendix A--Model Properties

The six cases of experimental data presented in this paper are from an investigation originally reported in Ref. 1. The model properties included in this appendix have been taken from that reference. The rotor blades and associated hub hardware were specifically designed and built to match as closely as possible the theory presented in Refs. 4-6. The experimental model was built with uniform blade properties and simple hub hardware. Prior to the stability investigation, an extensive bench test program was undertaken to measure the mass and stiffness properties. In many cases more than one method was used for these measurements to assure the most accurate estimate. Where measurements were not possible, calculated values are used. A number of experimental model properties have been given in Table 1 of the main text. Additional model properties are presented in this appendix.

Rotor Mass and Stiffness Properties

The spanwise distributions of weight, stiffness, and mass polar moment of inertia of the rotor configuration having the soft pitch flexure are shown in Table 4. The radial location of the hub hardware components is shown in Fig. 12. The spanwise dimension of the soft flexure web is greater than that of the stiff flexure web to minimize its torsional stiffness. The tabulated properties in Table 4 from blade station (B.S.) 0.701 to 3.601 in. were calculated from design drawings except for the torsional stiffness of the pitch flexure (B.S. 0.726 to 1.626 in.). The pitch flexure torsional stiffness was estimated using two methods: the moment-deflection method and the frequency-inertia method. In the moment-deflection method, known moments were applied outboard of the flexure and its angular deflection was measured. In the frequency-inertia method, the frequency of the torsional spring-mass system was measured after attaching a steel bar or disk with a known polar moment of inertia to the outer flange. The torsional stiffness estimated by the moment-deflection method was 12% lower than that obtained using the frequency-inertia method. The latter method is considered more accurate so this value is used in Table 4.

The properties of the stiff-pitch-flexure rotor are the same as the soft pitch flexure except from B.S. 0.726 to 1.626 in. Over this span the properties can be determined from the pitch flexure geometry as given in Table 5.

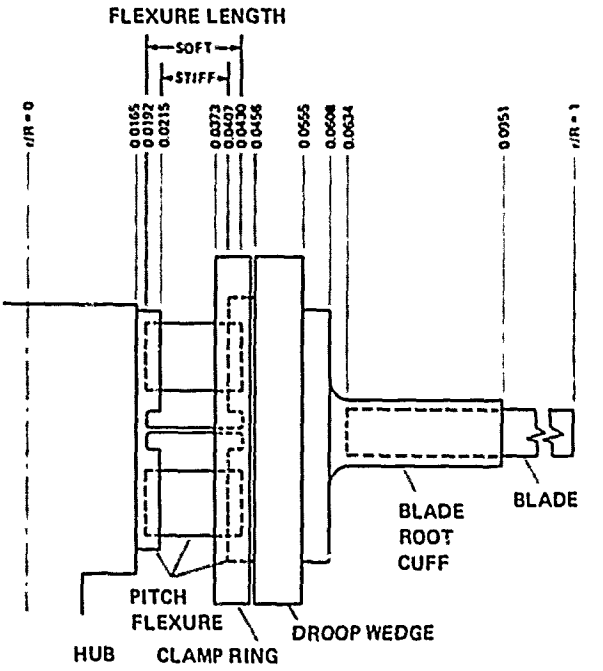


Fig. 12 Radial location of model rotor hub and blade components.

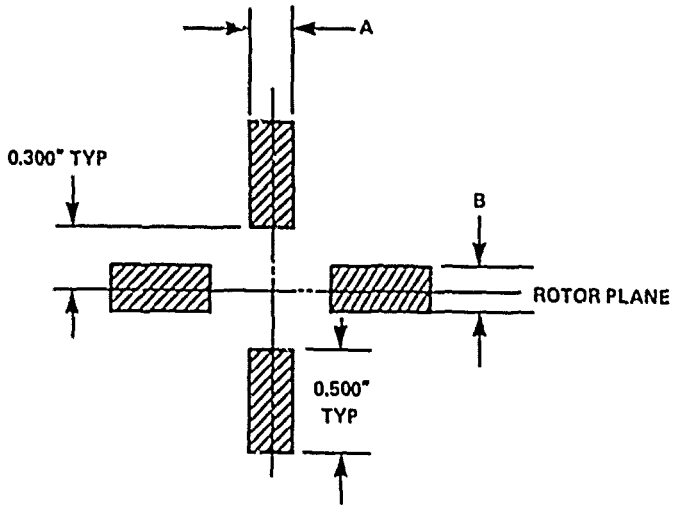
The blade mass properties outboard of B.S. 3.601 in., which is the start of the uniform section, have been determined from measurements

Table 4 Rotor mass and stiffness properties distribution for blade with soft pitch flexure

Blade station, in.	Weight, lb/in.	EI_{β}, lb-in.^{2} (10^6)	EI_{ζ}, lb-in.^{2} (10^6)	GJ, lb-in.^{2} (10^6)	I_{θ}, lb-in.^{2}/in.
0.701	0.292	20.0	20.0	19.6	
0.726	0.292	0.161	0.199	0.000327	
0.813	0.292	0.161	0.199	0.000327	
0.813	0.0115	0.161	0.199	0.000327	
1.415	0.0115	0.161	0.199	0.000327	
1.415	0.303	0.161	0.199	0.000327	
1.539	0.303	0.161	0.199	0.000327	0.543
1.539	0.560	0.161	0.199	0.000327	0.543
1.626	0.560	0.161	0.199	0.000327	0.543
1.651	0.560	21.9	21.9	19.6	0.543
1.665	0.560	21.9	21.9	19.6	0.543
1.665	0.713	21.9	21.9	19.6	0.543
1.726	0.713	21.9	21.9	19.6	0.543
1.726	0.558	27.2	27.2	19.8	0.494
2.101	0.558	27.2	27.2	19.8	0.494
2.101	0.295	18.2	18.2	7.28	0.165
2.301	0.295	18.2	18.2	7.28	0.165
2.301	0.149	0.300	30.3	1.80	0.213
2.401	0.149	0.300	30.3	1.80	0.213
2.401	0.136	0.242	21.8	1.66	0.213
3.601	0.136	0.242	21.8	1.66	0.213
3.601	0.0193	0.00589	0.120	0.00177	0.0179
37.851	0.0193	0.00589	0.120	0.00177	0.0179

Table 5 Pitch flexure dimensions

Flexure	A, in.	B, in.	Inboard blade station, in.	Outboard blade station, in.
Stiff	0.200	0.200	0.813	1.539
Soft	0.018	0.023	0.726	1.626



made on a 35.4-in. length of blade that included a 1.20-in. fiberglass cuff core. These properties were then corrected from measurements made on a separate cuff core and are given in Table 6. The values in Table 6 represent the average of two blades. The mass was determined by weighing the blades on an electronic balance. The uniform blade total-mass polar moment of inertia was measured by swinging the blades as a pendulum about the trailing edge. The blade was suspended from tape at two locations and allowed to swing freely as a pendulum. The pendular frequency was measured by an electronic counter connected to a photo cell that counted the number of interruptions of a light beam by the oscillating blade. The blade mass moment of inertia about the trailing edge was transferred to the elastic axis and is shown in Table 6.

Additional properties measured on the uniform section and given in Table 6 were the blade center of gravity and location of the elastic axis. The center of gravity was measured by using a fixture that allowed the blade to be supported between a fixed point and an electronic balance. The chord elastic axis was experimentally determined by mounting each blade vertically in a rigid fixture and applying a normal load in flapping through a slide-mounted pointer. The torsional deflection was monitored with an optical system using a mirror bonded to the blade tip and a light collimator.

Table 6 Uniform blade section properties

Property	Value
Weight, lb	0.659
Mass polar moment of inertia, lb_m-in.^{2}	0.613
Center of gravity, percent c	24.8
Elastic axis, percent c	25.3

The blade flapwise, chordwise, and torsional stiffness outboard of B.S. 3.601 in. were determined by two separate methods. The first method used force-deflection measurements for the flap and lead-lag stiffness and used moment-deflection measurements for the torsional stiffness; however, there was difficulty in measuring slight rotations of the mounting fixture. The second method used the measured frequencies and blade mass properties to calculate the stiffnesses. Frequencies were easily measured within ±1%, and blade weight was also determined within this accuracy. The stiffness was then derived from elementary beam theory as

$$EI_\beta = \frac{1}{12.4}\,\mu L^4(\omega_{\beta NR})^2$$

$$EI_\zeta = \frac{1}{12.4}\,\mu L^4(\omega_{\zeta NR})^2$$

$$GJ = 4LI_{EA}\,\frac{(\omega_{\theta NR})^2}{\pi}$$

The flapping and torsional stiffness values obtained by the two methods were within 4 and 2%, respectively. However, the value for lead-lag stiffness obtained by the force-deflection method was approximately 12% below the frequency-mass measurement. Because of the difficulty in accurately measuring fixture rotation, the frequency-mass and frequency-inertia measurements were used for the blade stiffnesses in Table 4.

The weight and mass polar of inertia for the hub components shown in Table 7 were each determined experimentally. The weights were determined by weighing each component on an electronic balance. The mass moment of inertia of each component was experimentally determined using a

Table 7 Hub component mass and inertia properties

Hub component	Weight, lb	Polar moment of inertia, I_θ, lb_m-in.^{2}
Flexure flange	0.100[a]	0.05487[a]
Clamp ring	0.065	0.1151
Droop wedge	0.207	0.206
Root cuff	0.165	0.256
Cuff core	0.071	0.061
TOTAL	0.608	0.693

[a]Calculated.

with a known spring constant. The component was mounted to the strain-gaged torsional spring. Then the frequency of the torsional spring/mass combination was measured and the mass polar moment of inertia was determined.

Nonrotating tests were conducted to determine modal frequencies and lead-lag structural damping. With the rotor stand clamped, each mode was manually excited and resulting oscillations were analyzed. The results for the first four modes for cases 1 and 2 are shown in Table 8.

Table 8 Rotor frequency and damping

	Stiff flexure		Soft flexure	
	ω, Hz	σ, sec^{-1}	ω, Hz	σ, sec^{-1}
First flap mode	5.25	--	5.19	--
Second flap mode	32.75	--	32.50	--
First lead-lag mode	23.76	-1.23	22.02	-1.03
First torsion mode	44.73	--	38.38	--

Aerodynamic Section properties

The blade profile used for the model was an NACA 0012. The Reynolds number at 0.75 R is approximately 375,000. The section aerodynamic properties are represented by the analytic functions that were used in Ref. 7.

$$C_\ell = 6\alpha - (\text{sgn } \alpha)10\alpha^2$$

$$C_d = 0.01 + 11.1|\alpha|^3$$

$$C_m = 0$$

Appendix B--Experimental Data

The experimental data for Cases 1 through 6 are tabulated in Tables 9 through 14, respectively. These data were obtained in the experiment reported in Ref. 1. The lead-lag damping and blade pitch angle are shown at 1000 rpm for all the cases. The data for the differential lead-lag mode were obtained by exciting the rotor hub with an electromagnetic shaker and the damping was obtained from the transient decay of the motions after the excitation was stopped. A moving block analysis of that transient decay was used to estimate the modal damping.

Appendix C--Correlation

The complete set of correlations between all theoretical predictions and the selected experimental results is shown in Figs. 13-34. Two formats are used for the correlation. The first format compares each individual code with the experimental data on separate plots. In this format the actual calculated points are shown as solid symbols and the fairing between points was made by the analyst. The experimental data are shown as open symbols. The second format compares all the predictions with the experimental results on a composite plot with the data shown as a stippled area. The theory of DRAV21 (Bil) is shown with and without dynamic inflow. A legend for the codes that were used is given in Table 3.

Table 9 Case 1 blade pitch angle and lead-lag damping; stiff pitch flexure, $\beta_{pc} = \beta_d = 0°$

θ_o, deg	σ, sec^{-1}	θ_o, deg	σ, sec^{-1}
-8.0	-2.81	4.0	-1.56
-8.0	-2.55	6.0	-1.87
-6.0	-2.25	6.0	-1.68
-6.0	-2.36	8.0	-2.14
-4.0	-1.88	8.0	-2.45
-2.0	-1.34	8.0	-2.11
-2.0	-1.33	10.0	-2.02
0.0	-1.19	10.0	-1.96
4.0	-1.53		

Table 10 Case 2 blade pitch angle and lead-lag damping; soft pitch flexure, $\beta_{pc} = \beta_d = 0°$

θ_o, deg	σ, sec^{-1}	θ_o, deg	σ, sec^{-1}
-12.0	-4.31	4.0	-1.86
-12.0	-4.72	4.0	-1.89
-12.0	-4.17	6.0	-2.05
-12.0	-4.44	6.0	-2.84
-12.0	-4.03	6.0	-2.51
-10.0	-3.99	8.0	-2.92
-10.0	-3.70	8.0	-3.01
-10.0	-3.71	8.0	-3.40
-10.0	-3.57	9.0	-2.68
-10.0	-3.66	9.0	-2.89
-8.0	-4.07	9.0	-2.97
-8.0	-3.74	9.0	-2.86
-8.0	-4.21	10.0	-2.75
-6.0	-3.21	10.0	-3.45
-6.0	-3.25	10.0	-2.52
-4.0	-2.10	10.0	-2.79
-4.0	-2.22	10.0	-3.17
-2.0	-1.29	11.0	-3.19
-2.0	-1.38	11.0	-3.01
0.0	-1.05	11.0	-3.76
2.0	-1.27	12.0	-3.31
2.0	-1.20	12.0	-3.32

Table 11 Case 3 blade pitch angle and lead-lag damping; stiff pitch flexure, $\beta_{pc} = 5°$, $\beta_d = 0°$

θ_o, deg	σ, sec^{-1}	θ_o, deg	σ, sec^{-1}
-2.0	-3.31	6.0	-1.53
-2.0	-3.25	8.0	-1.88
0.0	-1.92	8.0	-2.14
0.0	-1.96	8.0	-1.97
2.0	-1.44	9.0	-1.86
2.0	-1.43	9.0	-2.07
4.0	-1.35	9.0	-2.00
4.0	-1.29	10.0	-2.16
6.0	-1.48	10.0	-2.87

Table 12 Case 4 blade pitch-angle and lead-lag damping; soft pitch flexure, $\beta_{pc} = 5°$, $\beta_d = 0°$

θ_o, deg	σ, sec^{-1}	θ_o, deg	σ, sec^{-1}
-2.0	-4.92	8.0	-0.93
-2.0	-4.84	8.0	-1.44
0.0	-1.67	8.0	-0.94
0.0	-1.57	8.0	-0.97
0.0	-1.55	10.0	-1.80
2.0	-0.45	10.0	-2.16
2.0	-0.44	10.0	-1.74
2.0	-0.54	12.0	-2.76
3.0	0.10	12.0	-2.79
4.0	0.24[a]	12.0	-1.90
6.0	0.30[b]		

[a]Extrapolated; nearest test value: Ω = 993 rpm, σ = +0.13 sec^{-1}.
[b]Extrapolated; nearest test value: Ω = 997 rpm, σ = +0.23 sec^{-1}.

Table 13 Case 5 blade pitch angle and lead-lag damping; stiff pitch flexure, $\beta_{pc} = 0°$, $\beta_d = -5°$

θ_o, deg	σ, sec^{-1}	θ_o, deg	σ, sec^{-1}
-2.0	-3.29	8.0	2.30
0.0	-1.95	10.0	2.79
0.0	-1.79	10.0	2.84
0.0	-1.92	11.0	2.37
2.0	1.45	11.0	2.38
2.0	1.38	12.0	3.21
4.0	1.38	12.0	2.93
4.0	1.50	12.0	2.94
4.0	1.50	13.0	-3.47
6.0	2.71	13.0	-2.73
6.0	1.99	14.0	-4.07
8.0	2.08	14.0	-3.61
8.0	2.24	14.0	-3.48

Table 14 Case 6 blade pitch angle and lead-lag damping; soft pitch flexure, $\beta_{pc} = 0°$, $\beta_d = -5°$

θ_o, deg	σ, sec^{-1}	θ_o, deg	σ, sec^{-1}
0.0	-1.22	6.0	-2.07
0.0	-1.21	8.0	-2.37
0.0	-1.30	8.0	-2.43
2.2	-1.22	10.0	-2.51
2.2	-1.20	10.0	-3.09
2.2	-1.09	10.0	-2.52
4.0	-1.41	10.0	-2.57
4.0	-1.38	12.0	-3.45
4.0	-1.38	12.0	-3.11
6.0	-2.05	12.0	-2.82
6.0	-2.06		

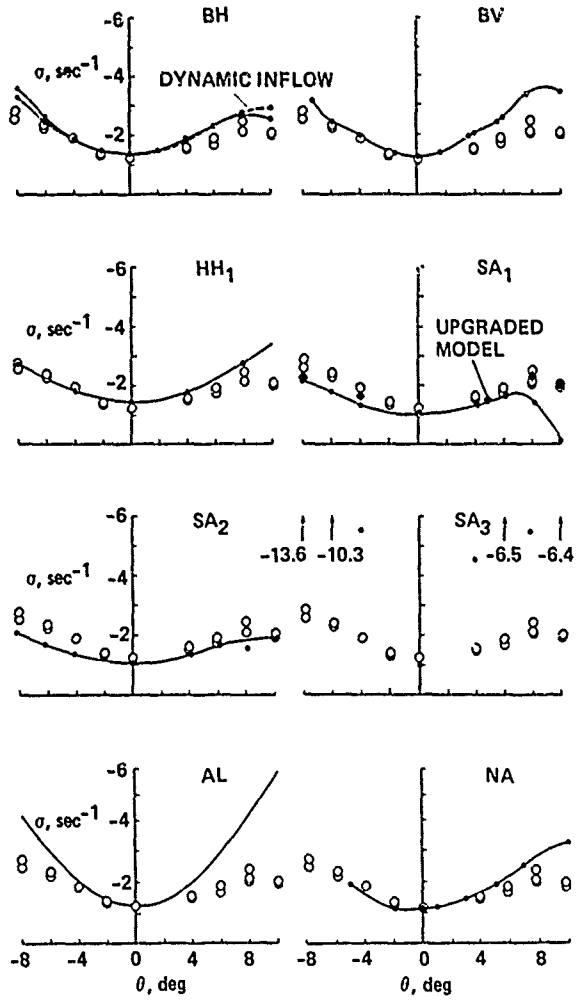


Fig. 13 Individual comparison for Case 1 lead-lag damping; stiff pitch flexure, $\beta_{pc} = \beta_d = 0°$.

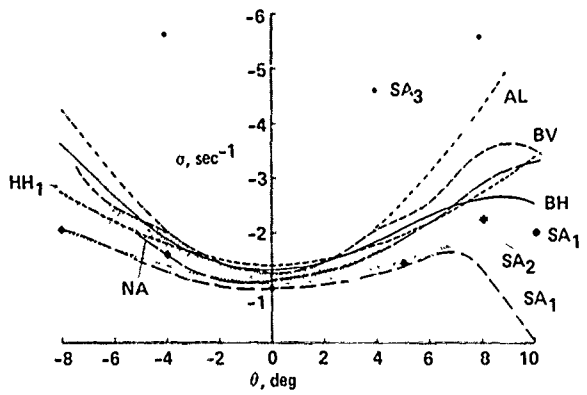


Fig. 14 Composite comparison for Case 1 lead-lag damping; stiff pitch flexure, $\beta_{pc} = \beta_d = 0°$.

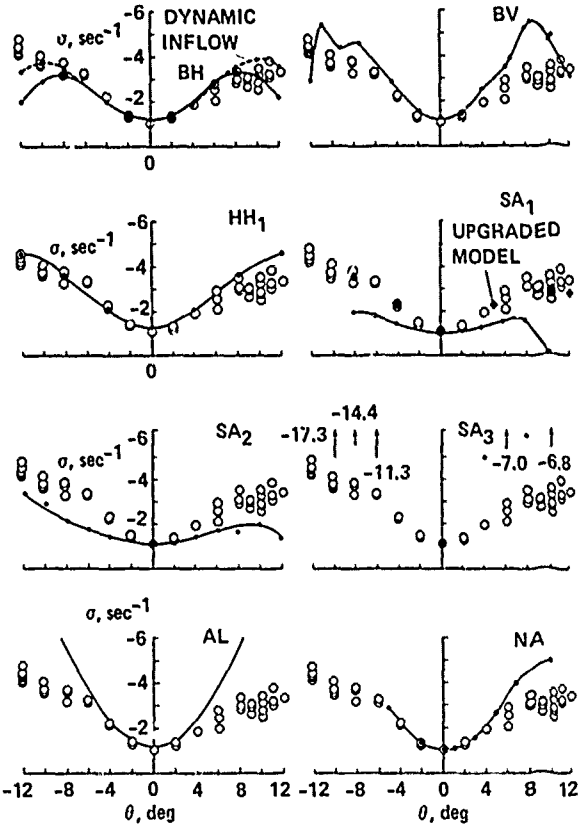


Fig. 15 Individual comparison for Case 2 lead-lag damping; stiff pitch flexure, $\beta_{pc} = \beta_d = 0°$.

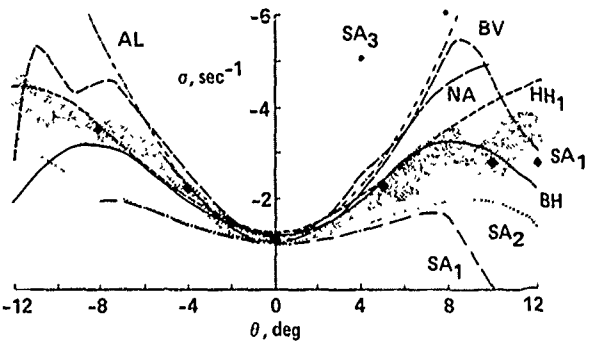


Fig. 16 Composite comparison for Case 2 lead-lag damping; soft-pitch flexure, $\beta_{pc} = \beta_d = 0°$.

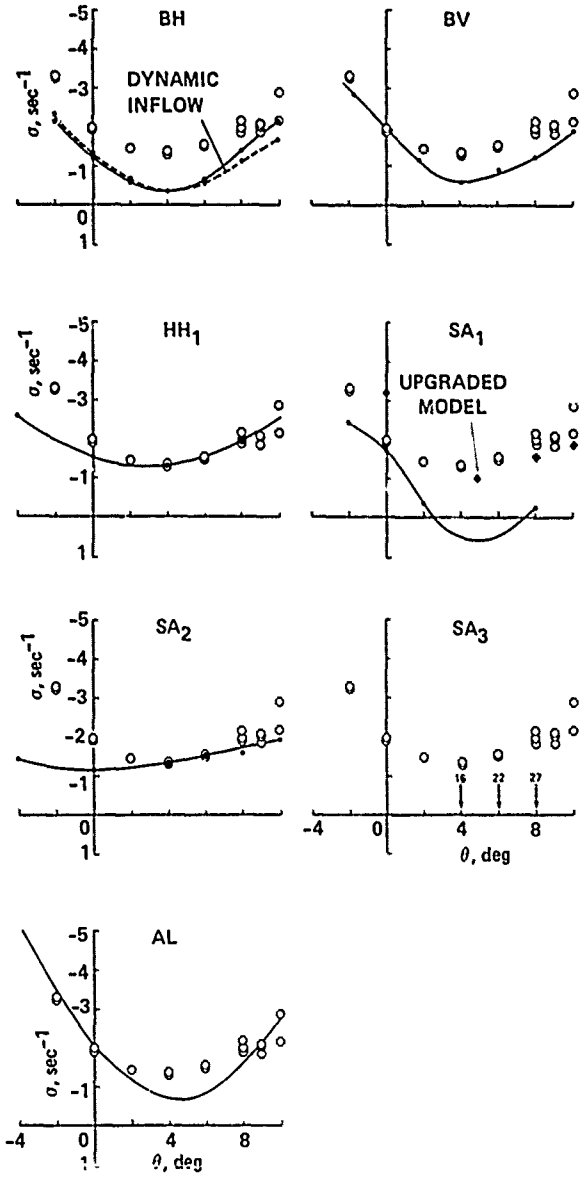


Fig. 17 Individual comparison for Case 3 lead-lag damping; stiff pitch flexure, β_{pc} = 5°, β_d = 0°.

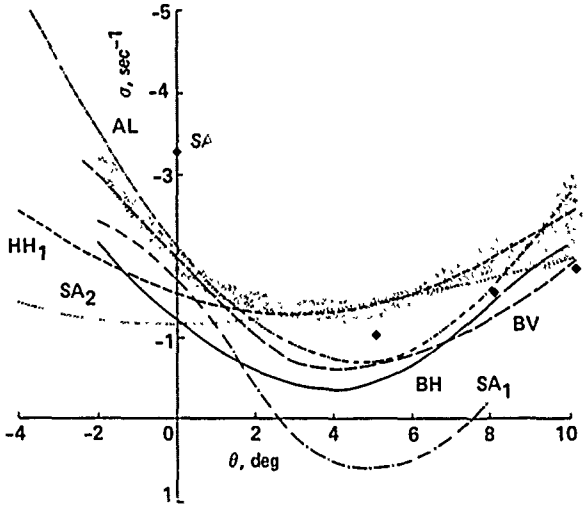


Fig. 18 Composite comparison for Case 3 lead-lag damping; stiff pitch flexure, β_{pc} = 5°, β_d = 0°.

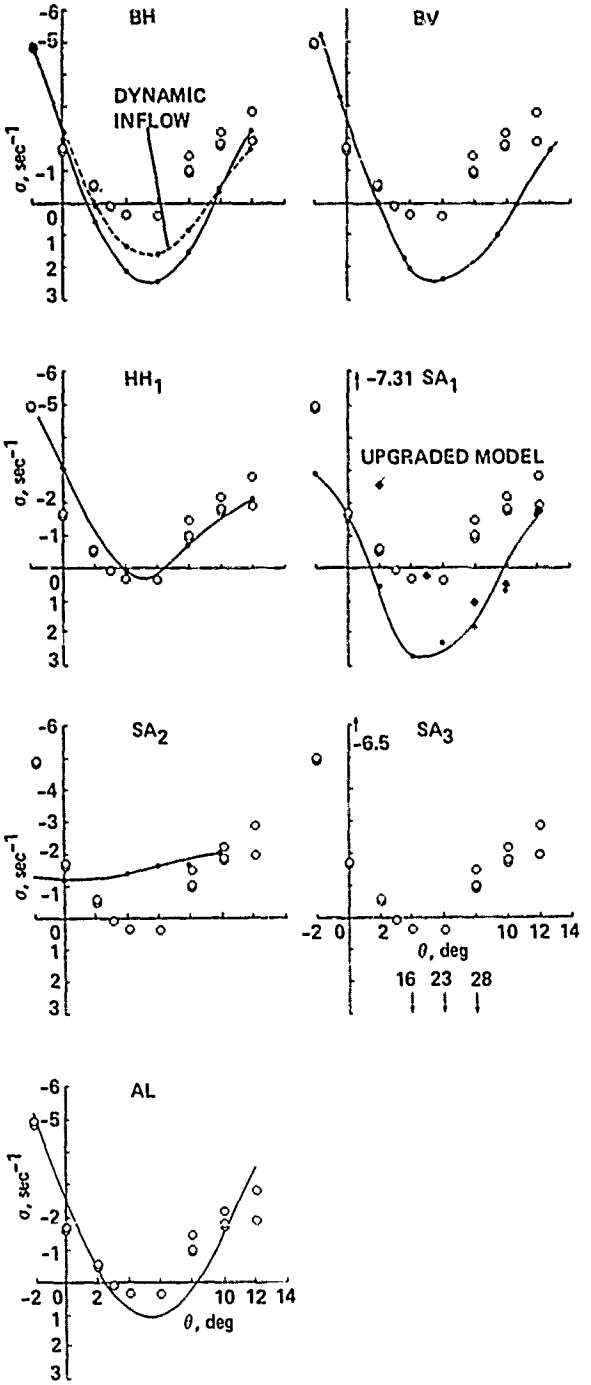


Fig. 19 Individual comparison for Case 4 lead-lag damping; soft pitch flexure, $\beta_{pc} = 5°$, $\beta_d = 0°$.

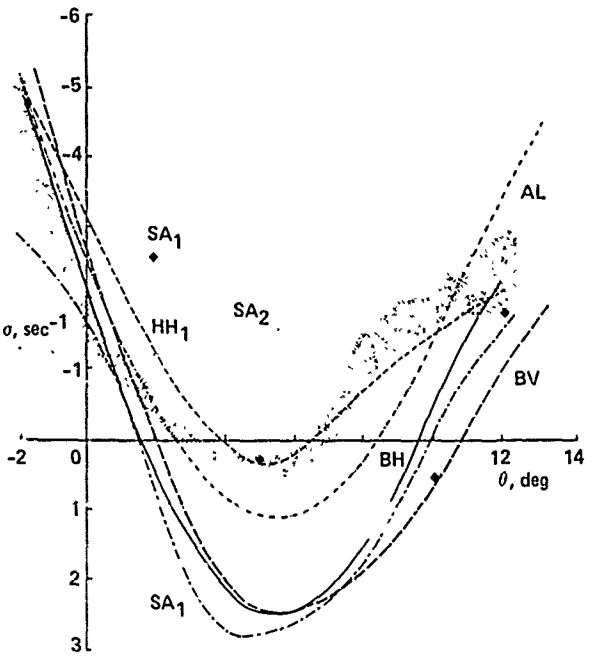


Fig. 20 Composite comparison for Case 4 lead-lag damping; soft pitch flexure, $\beta_{pc} = 5°$, $\beta_d = 0°$.

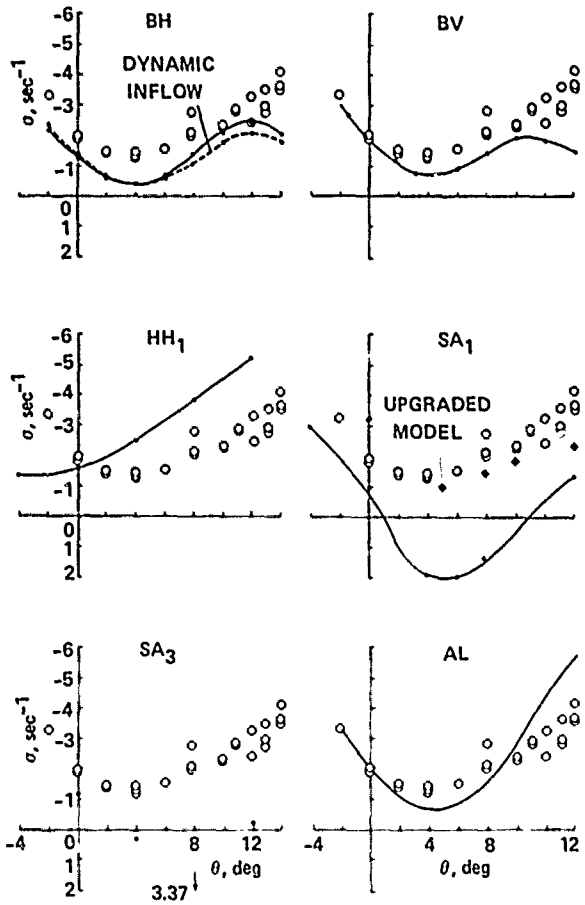


Fig. 21 Individual comparison for Case 5 lead-lag damping; stiff pitch flexure, $\beta_{pc} = 0°$, $\beta_d = -5°$.

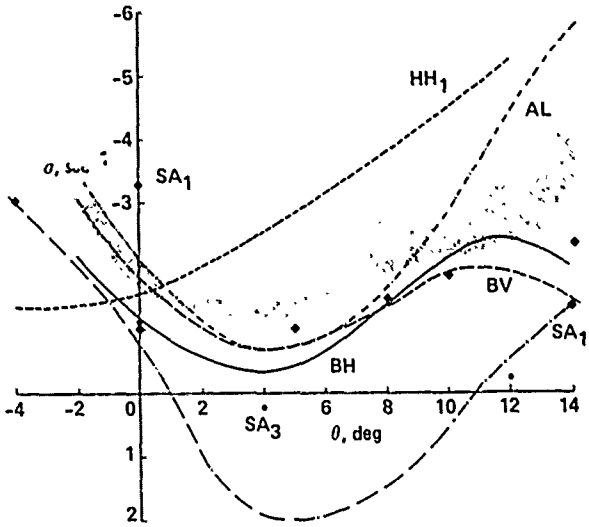


Fig. 22 Composite comparison for Case 5 lead-lag damping; stiff pitch flexure, $\beta_{pc} = 0°$, $\beta_d = -5°$.

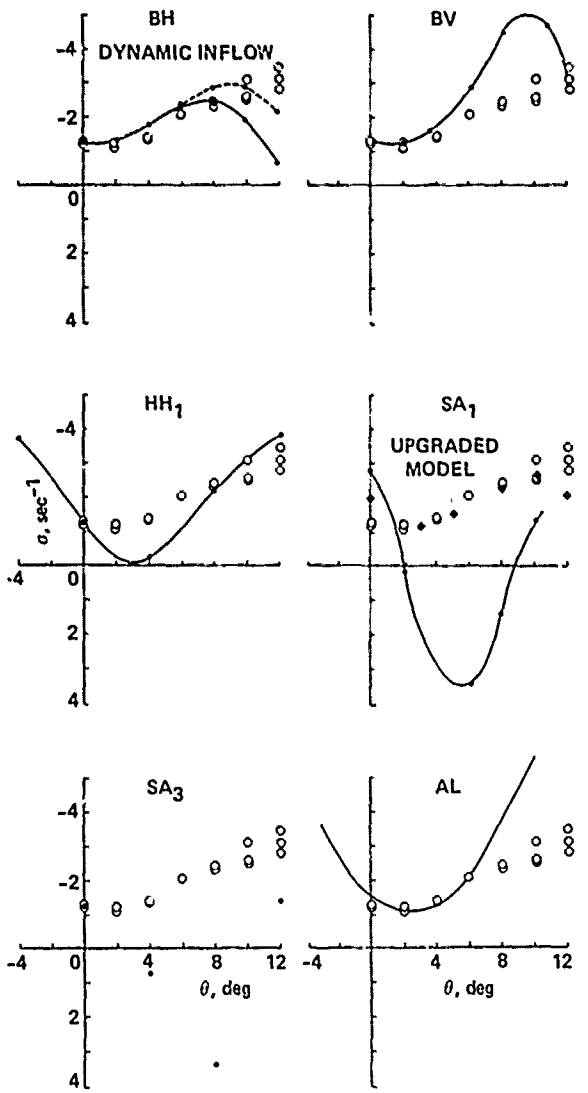


Fig. 23 Individual comparison for Case 6 lead-lag damping; soft pitch flexure, β_{pc} = 0°, β_d = -5°.

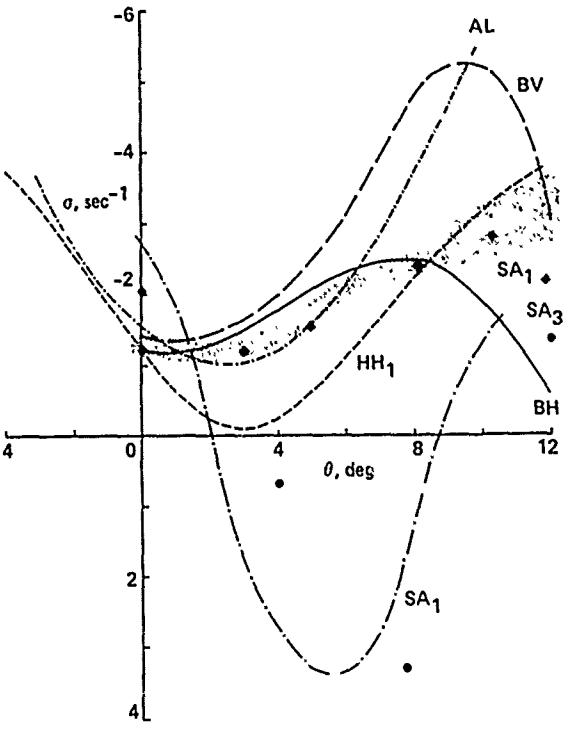


Fig. 24 Composite comparison for Case 6 lead-lag damping, soft pitch flexure, β_{pc} = 0°, β_d = -5°.

DISCUSSION

A COMPARISON OF THEORY AND EXPERIMENT FOR THE AEROELASTIC STABILITY OF A HINGELESS ROTOR MODEL IN HOVER

David L. Sharpe

Holt Ashley, Stanford University: I've got two questions. The first one has to do with dynamic stall. There are two or three places where you pointed out, in their failure in the damping predictions, that it came about as a result of stall. I believe that was with a code that is essentially quasi-steady aerodynamically, as far as stall is concerned. Would it be fair then to imply that including the dynamic stall effect is significantly important?

Sharpe: I should have pointed out in my presentation that DRAV21, the Bell Helicopter code, performed the predictions with dynamic inflow and without, I'm sorry, I guess I'm not answering the question. I should have pointed this out so I'll go ahead and say it anyway. Bell's [results with] dynamic inflow showed very close results to the predictions without the dynamic inflow, and since there was not much difference, to keep it less complex, I left out all of their predictions with the dynamic inflow.

Ashley: I have another question I'd like to ask; it has to do with the extraordinary success of what you call the modified SA_1. It really does seem to do better than the others. My question shows I am a little bit suspicious: were these data available to the guardians of that program prior to the time that they modified it?

Sharpe: The answer is yes.

Robert Ormiston, Session Chairman: I just might make a comment about that. I was thinking about that question as Dave was giving his results and I think that Bill Bousman meant to give a few remarks in the beginning about the conditions under which the data were given to the people, how they were allowed to modify it, and how the new data were incorporated in these results. I can't speak exactly as to how that was done--he may make some comments about that.

Richard Bielawa, United Technologies Research Center: I've got an answer for Holt's question. I think with regard to dynamic stall, the reduced frequency was too low for dynamic effects to have much impact. I can't quote any numbers, but the instability is essentially a low-frequency lead-lag motion.

Ashley: Below 0.02 [reduced frequency]? Does anyone have a number on that?

Dewey Hodges, Aeromechanics Lab.: I would say less than 0.1 based on . . . no that's 0.01 based on chord.

Ashley: 0.01 okay, because at 0.1 you see lots of dynamic stall. [The reduced frequency, based on the chord, was actually about 0.13. Ed.]

Hodges: Your original question had to do with stall. The stall effect that's important here is not dynamic stall as much as it is incorporating the static stall parameters because of the low-Reynolds-number effect, associated with the small size of the rotor. Since PFLT is a code that is 7 or 8 yr old now, we didn't feel it was right to go back and modify it, but some of the companies have this static stall effect already in their codes. That's the main reason for the departure of the data in the earlier cases where there was no precone or droop.

Bielawa: I have a question--have you formed any conclusions from these results?

Sharpe: No public conclusions, no.

Wayne Johnson, NASA Ames: On the dynamic stall, I should think Dave should be able to answer that since he's the one who acquired the data. If dynamic stall was really showing up in these flutter results we should be able to see that in your data. We should see a lot more participation of the torsion. So I would have expected you to notice some drastic change in torsional behavior as you went to really high pitch.

Sharpe: The answer is no.

Johnson: So I would conclude that there was no dynamic stall.

Ormiston: I'll just make a comment about that, having been very interested in these data myself. As far as I know, no rigorous correlation of the data has been made with theories which have the static stall effect and the dynamic stall effect--the typical dynamic-stall models which may be used for bending-torsion flutter and stall flutter of rotor systems. So I don't think we can answer the question rigorously unless anyone has information I don't have, but our experience is that the correlation is very good with simply the static stall models. What we're dealing with is a low-frequency instability which involves very little actual torsion motion and it's not at a torsion natural frequency.

Peretz Friedmann, UCLA: The question has been raised of dynamic stall, but what you're looking at is a precone induced flap-lag instability. That's a low-frequency instability in which the lag degree of freedom is the dominant degree of freedom and as a consequence, dynamic stall has no effect. It is exactly what Dewey says; it is static stall. You really cannot expect dynamic stall to have any effect.

Ormiston: I would say that one cannot say with certainty unless one tries both of them. It's been interesting in correlating some of this data that the effects of some of the phenomena show up unexpectedly in certain situations and places, and in other examples don't show up at all, so it's very difficult to draw those kinds of conclusions. I agree generally.

Friedmann: I just want to say that there is an added danger when you use dynamic stall because dynamic stall is based usually on semiempirical or curve-fitting types of approximations. So you are much better off with static stall because it's at least something everyone can understand. Dynamic stall is a higher degree of curve fitting which very few people understand.

Bousman: I might point out that, for these hover experiments we are talking about, we have perturbations in the degrees of freedom, but in terms of actual pitch motion there's probably extremely small pitch motions involved. In fact in most of these experiments we measured pitch motion and were not able to detect it above the noise. It did not participate in the modes of instability and it was not a measurable oscillation. So from that point of view, we infer from our measurements that dynamic stall does not contribute.

Bob Sopher, Sikorsky Aircraft: I was thinking that perhaps the most likely cause of this dropoff is the use of two-dimensional strip theory near the tip instead of three-dimensional flow. The effect would be much weaker if you had a three-dimensional theory available, and you would not get that kind of reduction in stability presented in the theories. I suspect that that may be a possibility.

Ormiston: I'd like to add one more comment about these results, and it relates to what Bob was saying. As we can see on the slides [Fig. 6], Dave has pointed out these data were heavily contaminated by stall effects because of the low Reynolds number. In fact, in the correlations which were done in experiments prior to this one, this typical dropoff shown here was an effect of the stall aerodynamics on the aeroelastic couplings, and it's a very common feature when that stall model is included. It occurs at about these angles of attack or collective pitch angles. The point is that there's an extremely wide variation in the amount of damping and the degree of falloff depending on the particular aerodynamic stall model that's used. Very small changes in two-dimensional airfoil stall characteristics make an enormous difference in the damping in this region. It's just very highly coupled aeroelastically to those aerodynamic phenomena. So that's part of the reason for the very large variation here in the theoretical results.

A COMPARISON OF THEORY AND EXPERIMENT FOR COUPLED ROTOR-BODY STABILITY OF A HINGELESS ROTOR MODEL IN HOVER UNDER SIMULATED VACUUM CONDITIONS

William G. Bousman
Research Scientist
U.S. Army Aeroflightdynamics Directorate
Ames Research Center

Abstract

Two cases were selected for correlation from an experiment that examined the aeromechanical stability of a small-scale model rotor that used tantalum rods instead of blades to simulate vacuum conditions. The first case involved body roll freedom only while the second case included body pitch and roll degrees of freedom together. Analyses from Hughes Helicopters and the U.S. Army Aeromechanics Laboratory were compared with the data and the correlation ranged from poor to good.

Introduction

As a part of the Methodology Assessment two cases were selected from the experiments reported in Ref. 1 for comparison with theoretical models. Both cases selected were of a configuration that used tantalum rods instead of conventional blades to simulate vacuum conditions for the rotor. The body has only a roll degree of freedom for the first case, but both pitch and roll degrees of freedom for the second case. The use of tantalum rods instead of blades largely removes blade aerodynamic effects and it is therefore possible to judge the adequacy of structural and inertial modeling when theory and experiment are compared.

The theoretical models compared with the data included the Dynamic Analysis Research Tool (DART) and E927-1 analyses used by Hughes Helicopters and the FLAIR analysis developed at the U.S. Army Aeromechanics Laboratory. The other company codes were not used for this data set because of funding limitations.

The paper will briefly describe the experiment from which these data were obtained and then present the correlation. Conclusions will be made as to the quality of the agreement between theory and experiment. Appendices are provided that document the experimental model properties, tabulate the experimental data points, and show all of the correlations.

Experiment Description

The model used in this experiment is shown in Fig. 1. The rotor has three tantalum rods that act as blades mounted on flap and lead-lag flexures. The flexures are mounted to a hub supported by a static mast. The rotor, static mast, transmission, and two water-cooled electric motors are supported by ball bearings in a gimbal frame that allow body pitch and roll degrees of freedom.

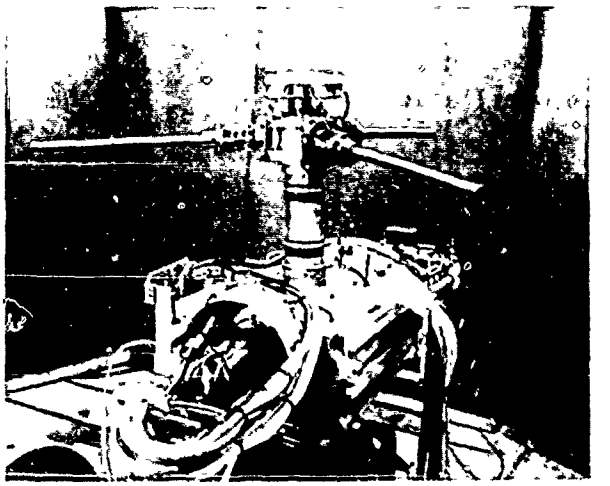


Fig. 1 Three-bladed rotor with tantalum rods mounted to gimbal with pitch and roll degrees of freedom.

The blade root flexures are shown in an exploded view in Fig. 2. Separate flap and lead-lag flexures contain essentially all of the flexibility of the rotor. The offset of both flexures is the same because of the folded-back load path. The major rotor properties are provided in Table 1.

Table 1 Tantalum Model Rotor Properties

Property	Value
Rotor radius, R, cm	38.01
Blade chord, c, cm	1.26
Solidity, σ	0.0318
Hinge offset, e/R	0.224
Lock number	0.0182

The effect of using tantalum rods of circular cross-section instead of conventional aerodynamic blades is that the lift curve slope is reduced to zero. Lock number is defined as

$$\gamma_d = \frac{\rho a c R^4}{I}\left(1 + \frac{c_{d_o}}{a}\right)$$

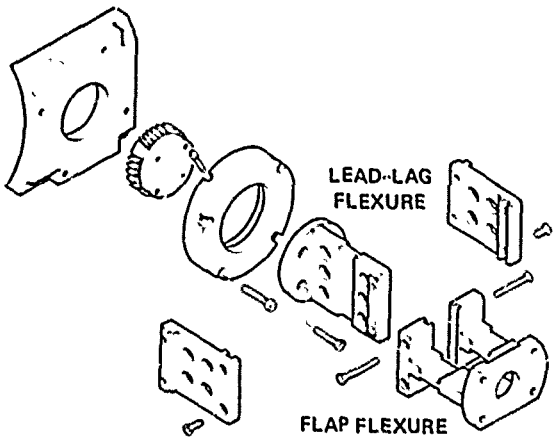


Fig. 2 Exploded view of blade root flexures.

where ρ is the density of air in g/cm^3, a is the lift curve slope, c the blade chord, R the rotor radius, I the blade flapping inertia, and c_{d_o} the blade profile drag coefficient. The term c_{d_o}/a is normally much less than 1 but as the lift curve slope approaches zero, the profile drag coefficient becomes important. To observe the rotor and body behavior for true vacuum conditions, it is necessary to reduce the density; however, this effect can be simulated by reducing the lift curve slope. For this experiment the use of tantalum rods reduced the Lock number to 0.2% of its value for conventional blades. This represents a good simulation of the vacuum condition, but the profile drag has been increased by two orders of magnitude. The mass properties of the tantalum rods were selected to match the blade nonrotating frequencies of the aerodynamic blades that were also tested in the experiment reported in Ref. 1. However, the hinge offset was effectively doubled, so rotating frequencies were not matched.

Damping and frequency data were obtained in this experiment by oscillating the rotor hub with a shaker at the modal frequency in the fixed system. When sufficient amplitude was achieved, the shaker was stopped and a pneumatic clamp on the shaker link was opened to release the model and allow the motions to freely decay. The damping and frequency were obtained using an analog equivalent of the moving-block analysis (Ref. 2). The lead-lag regressing-mode damping and frequency were measured in the fixed system following a transform to the multiblade coordinates and the quality of the data was quite good. However, body mode damping showed nonlinear behavior which was caused by Coulomb friction in the gimbal ball bearings (Ref. 3). A complete discussion of the model properties is provided as Appendix A. The experimental data used for correlation are provided in Appendix B.

Correlation

Two cases were used for correlation. These cases differed only in the body frequencies as shown in Table 2. For Case 1 the pitch degree of freedom was locked out, producing a pitch-mode frequency of 27 Hz which is well separated from the lead-lag regressing mode frequencies. Therefore, in the range of 0-10 Hz only one body mode is normally expected, but since there is no flap damping, both regressing lead-lag and flap modes should also be evident.

Table 2 Body Pitch and Roll Nonrotating Frequencies

Case	Body Pitch, Hz	Body Roll, Hz
1	27.0	2.56
2	2.58	2.55

Case 1

Modal frequency calculations are compared with the data in Fig. 3 for Case 1. The system behavior is seen most clearly by examining the predictions of the U.S. Army Aeromechanics Laboratory (Fig. 3c). The regressing lead-lag mode drops from its nonrotating value of 6.4 Hz and couples successively with the flap-progressing, body-roll, and flap-regressing modes before it reaches a zero frequency at about 500 rpm. The regressing lead-lag mode then increases in frequency and couples with the regressing flap mode, but within the test rotor speed range it does not coalesce with the body roll mode. For rotor speeds below 500 rpm the regressing lead-lag mode frequency is greater than 1/rev in the rotating system (stiff inplane), while above 500 rpm the frequency is less than 1/rev (soft inplane). It is in the latter case that rotors are susceptible to ground and air resonance.

For the Case 1 modal frequencies both the E927-1 and FLAIR codes show very good agreement with the measurements. Both codes match the data and reproduce the system behavior. However, the DART analysis shows only poor-to-fair correlation. Some reasons for this are understood and are worth discussing. The structural input for DART was derived from the tabulated mass and stiffness properties of Appendix A. The calculated nonrotating frequencies were lower than the measurements (3.3% for the lead-lag mode), which indicates errors in the documented model properties. A similar problem was noted for E927-1; in that case the input properties were adjusted to obtain a match between the calculated and measured nonrotating blade frequencies. However, this was not done for DART, and the calculated regressing lead-lag mode is shifted by approximately 50 rpm from the measurements. The disagreement between the nonrotating frequency measurements and the frequency calculations based on the tabulated mass and stiffness

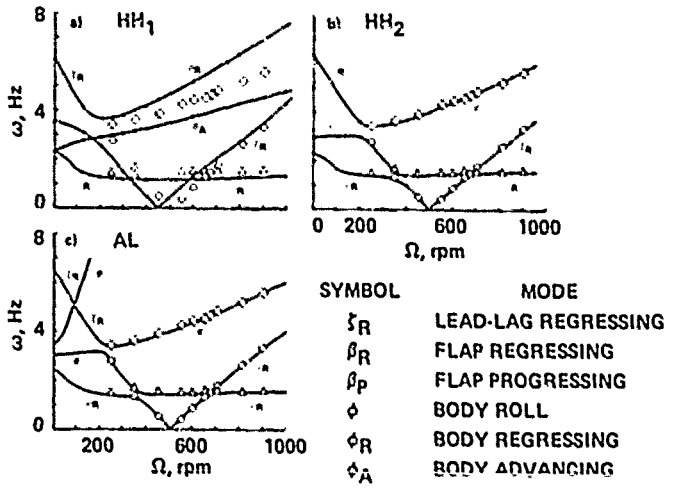


Fig. 3 Individual comparison of theory and experiment for Case 1 for modal frequencies. a) DART, Hughes Helicopters; b) E927-1, Hughes Helicopters; c) FLAIR, Aeromechanics Laboratory.

properties is probably caused by errors in the tabulated properties as these are based on calculations from design drawings rather than measurements.

A second problem with the DART prediction is that this analysis assumes an isotropic support and therefore must calculate two body modes. For a highly anisotropic support as is the case discussed here, one of the modes is an artifact of the modeling assumptions, but there is no way that coupling with this false mode can be avoided. In this case neither mode shows good agreement with the data.

A comparison of the three predictions and the data for the Case 1, regressing-lead-lag-mode damping is shown in Fig. 4. The damping measurements show a weak instability at 675 and 680 rpm which is caused by a coalescence of the regressing lead-lag and flap modes. This weak instability occurs only

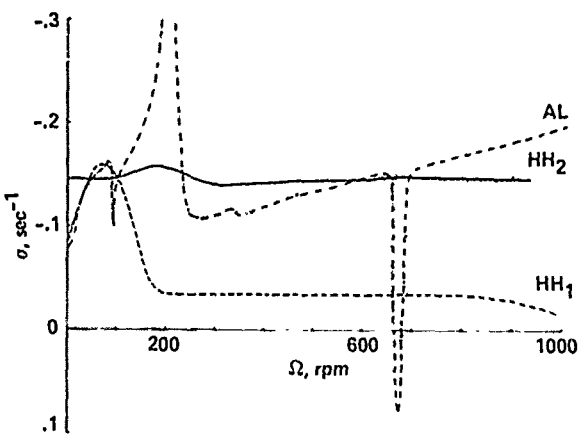


Fig. 4 Composite comparison of theory and experiment for Case 1 for regressing lead-lag mode damping. Data are shown by stippled area; analyses used are DART (HH_1), E927-1 (HH_2), and FLAIR (AL).

for the case of a single-body degree of freedom; with both body pitch and roll freedoms the instability disappears (Ref. 4). The FLAIR calculations, which used a 1- to 2-rpm grid in the vicinity of the instability, show good agreement with the data. Neither the DART nor E927-1 analyses predicted the instability, possibly because neither program calculated damping values for rotor speeds between 650 and 700 rpm.

Both E927-1 and FLAIR show about the same level of damping over most of the rotor speed range. However, DART significantly underpredicts the damping level, which is surprising considering that the damping is largely caused by the rotor structural damping and the profile drag damping.

The three analyses show very different behavior caused by coupling for rotor speeds below 300 rpm. The FLAIR analysis shows a strong effect of coupling of the regressing lead-lag and body roll modes near 200 rpm. The E927-1 program shows significantly less coupling of these two modes, while DART shows no indication of coupling. At about 90 rpm, FLAIR shows similar behavior when the lead-lag regressing and flap-progressing modes couple, but this time DART shows a similar response while E927-1 does not. Acceptable experimental data were not obtained for rotor speeds below 250 rpm so these differences cannot be resolved.

Case 2

Case 2 includes body pitch and roll degrees of freedom; the nonrotating frequencies are nearly identical as shown in Table 2. (Note, however, that the inertias and stiffnesses are not identical.) The fixed-system frequencies for this case are shown in Fig. 5. The behavior in this case is very similar to Case 1 except in Case 2 there are two body modes. At about 875 rpm, the regressing lead-lag and body pitch modes coalesce and a

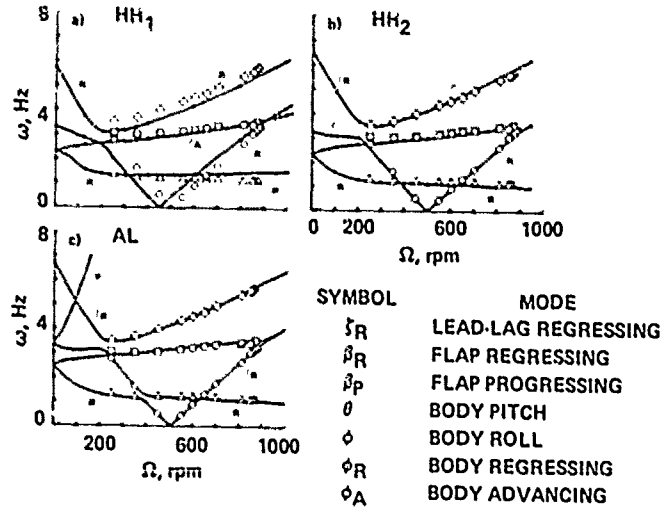


Fig. 5 Individual comparison of theory and experiment for Case 2 for modal frequencies. a) DART, Hughes Helicopters; b) E927-1, Hughes Helicopters; c) FLAIR, Aeromechanics Laboratory.

classical ground-resonance instability occurs. No instability is observed at the regressing lead-lag and flap mode crossing.

The DART analysis shows poor-to-fair correlation for this case, partly because of the frequency shift of the regressing lead-lag mode as discussed previously, and partly because the body regressing mode (body roll mode) frequencies are not well predicted. The E927-1 analysis shows good correlation and FLAIR shows very good predictive capability.

The regressing lead-lag mode damping for Case 2 is shown in Fig. 6. The damping level remains relatively constant until the regressing lead-lag and body pitch mode coalescence where an almost explosive instability occurs--a classic in vacuo ground resonance. The E927-1 and FLAIR analyses both show good to very good agreement with the data, not only in predicting the stability boundary, but also in the level of damping over the entire rotor speed range. As in Case 1 these analyses disagree as to the effect of coupling between the regressing lead-lag and body roll modes in the vicinity of 200 rpm, but no data were obtained that could resolve these differences.

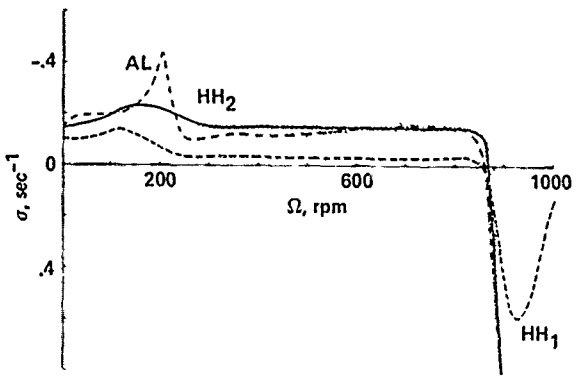


Fig. 6 Composite comparison of theory and experiment for Case 2 for regressing lead-lag mode damping. Data are shown by stippled area; analyses used are DART (HH_1), E927-1 (HH_2), and FLAIR (AL).

The DART predictive capability is fair in this case and the prediction of the neutral stability point is quite good despite the 50-rpm shift. As in Case 1, the reduction in damping away from the instability is puzzling. The damping level predicted between 300 and 800 rpm is significantly less than the structural damping measured at zero rpm.

Conclusions

The DART and E927-1 analyses used by Hughes Helicopters and the U.S. Army Aeromechanics Laboratory FLAIR analysis were compared with two cases from an experiment that measured aeromechanical stability of a model rotor and fuselage in a simulated vacuum. Overall the DART analysis showed poor correlation for this coupled rotor-body data set while the E927-1 predictions were fair-to-good. The FLAIR predictions were judged to be good.

References

[1]Bousman, William G. and Hodges, Dewey H., "An Experimental Study of Coupled Rotor-Body Aeromechanical Instability of Hingeless Rotors in Hover," Vertica, Vol. 3, 1979, pp. 221-244.

[2]Bousman, William G., "An Analog Technique for the Measurement of Damping from Transient Decay Signals," NASA TM X-73,121, June 1976.

[3]Bousman, William G., "An Experimental Investigation of Hingeless Helicopter Rotor-Body Stability in Hover," NASA TM-78489, June 1978.

[4]Ormiston, Robert A., "Aeromechanical Stability of Soft Inplane Hingeless Rotor Helicopters," Paper No. 25, Third European Rotorcraft and Powered Lift Aircraft Forum, Aix-en-Provence, France, Sept. 1977.

Appendix A--Model Properties

The two cases examined in this paper are from an experiment originally reported in Ref. 3. The experimental model properties in this appendix are taken from that reference with the exception of the tabulated mass and stiffness properties in Tables 4-7, which have not been reported before. In addition, a few errors have been found in the Ref. 3 documentation, so these are noted.

Rotor Properties

The major rotor geometric properties have been tabulated in Table 1. Additional descriptive properties are shown in Table 3. The profile drag coefficient is assumed to be approximately 1.0 based on a Reynolds number of 10,000 to 35,000 at the three-quarter span.

Table 3 Rotor Descriptive Properties

Property	Value
Blade number, b	3
Airfoil section	circular
Lift curve slope, a	0.0
Profile drag coefficient, c_{d_o}	1.0
Height above gimbal axes, h, cm	24.1

The design drawings of the hub and tantalum blade were used to calculate mass, stiffness, and pitching inertias outboard of blade station 2.034 in. This blade station is the outer face of the leftmost part in the exploded drawing of Fig. 2. Properties are tabulated separately for the lead-lag flexure, side beams, and flap flexure in Tables 4 to 6. Table 7 provides the composite properties for these components outboard of B.S. 2.034 in. Running weight and pitch inertia were assumed additive in this table and the combined stiffness was based on a series-spring representation. The calculated properties outboard of the flap flexure for B.S. 4.423 in. are also included in this table.

Measurements were made of the mass, mass centroid, and moment of inertia of one flap flexure/combination, as shown in Table 8. These measurements were adjusted to correct for the effect of that portion of the flap flexure inboard of the flap flexure centerline (B.S. 3.35 in.) and to add the contribution of the lead-lag flexure and side beams. The mass properties of the blade and hub outboard of the flap flexure centerline, shown in Table 8, were calculated from Table 7. These compare quite well with the measurements for mass and centroid, but are 3.5% too high for the flapping inertia. No measurements were made of pitch inertia or rotor polar inertia. Note that the values shown in Table 4 of Ref. 3 are in error for pitch inertia and rotor polar inertia.

The first flap- and lead-lag mode frequency and damping were measured as installed on the model with the body degrees of freedom locked out. The measured frequency values, shown in Table 9, are compared to calculated values based on

$$\omega = \sqrt{K/I_o}$$

where the stiffness is assumed to be due solely to the flexures

$$K = \frac{EI}{\ell}$$

and the EI and ℓ values are from Table 7 for B.S. 3.111 to 3.588 in. for the flap flexure and B.S. 3.225 to 3.450 in. for the lead-lag flexure. The blade inertia, I_o, is the value calculated in Table 8. As the calculated inertia was 3.5% higher than the measured value, it is expected that the calculated frequencies should be 1.7% low. As is shown in Table 9, the calculated flap frequency is 1.0% high and the lead-lag frequency is 5.5% low. The stiffnesses of the flexures are very sensitive to the thickness. The thickness specified on the design drawing of the lead-lag flexure is 0.0250 ±0.0005 in. If the frequency is calculated with the flexure assumed to be 0.0255 in. thick, then the value is 6.23 Hz which is 2.7% low. The sensitivity of the frequency to flexure dimensional data suggests that the EI values should be adjusted to match the nonrotating frequency data which represent an accurate experimental measurement. The nonrotating lead-lag damping measured on the model was 0.185% critical.

Body Properties

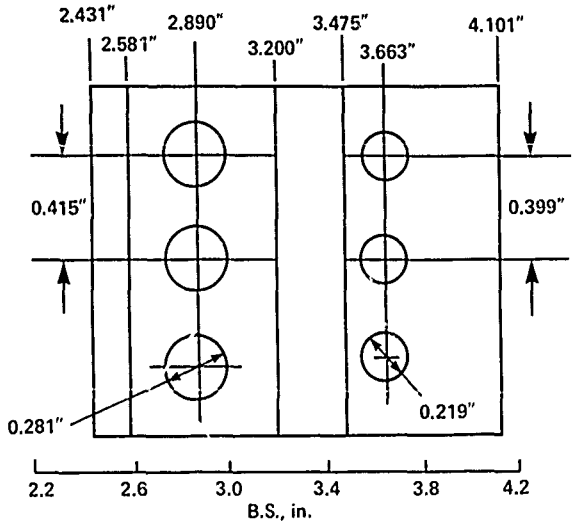
The body was weighed without the gimbal frame or hub hardware. The weight of the hub hardware inboard of the flap flexure centerline was added to the measured weight to give a value of the body mass of 42.48 lb_m. The center of gravity of the body mass was not determined, but was assumed coincident with the gimbal center.

The body pitch and roll inertias were determined for the Case-2 configuration by measuring the gimbal spring stiffnesses and the body frequencies with the rotor hardware removed. The inertias were calculated assuming a single-degree-of-freedom

Table 4 Calculated Mass and Stiffness Properties of Lead-Lag Flexure[a]

BLADE STATION in.	WEIGHT lb_m/in.	EI_f 10^6 lb·in^2	EI_c 10^6 lb·in^2	GJ 10^6 lb·in^2	I_θ lb_m·in^2/in.
2.431	0.422	5.18	5.18	3.93	0.101
2.581	0.422	5.18	5.18	3.93	0.101
2.581	0.0682	1.11	0.179	0.116	0.0110
2.750	0.0682	1.11	0.179	0.116	0.0110
2.791	0.0398	0.756	0.0102	0.116	0.0110
2.890	0.0266	0.597	0.00701	0.116	0.0110
2.989	0.0398	0.756	0.0102	0.116	0.0110
3.030	0.0682	1.11	0.0179	0.116	0.0110
3.200	0.0682	1.11	0.0179	0.116	0.0110
3.200	0.0292	0.477	0.00141	0.00139	0.00155
3.225	0.0097	0.159	0.0000521	0.00139	0.00155
3.450	0.0097	0.159	0.0000521	0.00139	0.00155
3.475	0.0292	0.477	0.00141	0.00139	0.00155
3.475	0.0682	1.11	0.0179	0.114	0.0110
3.553	0.0682	1.11	0.0179	0.114	0.0110
3.585	0.0451	0.857	0.0118	0.114	0.0110
3.663	0.0357	0.745	0.00935	0.114	0.0110
3.741	0.0451	0.857	0.0118	0.114	0.0110
3.773	0.0682	1.11	0.0179	0.114	0.0110
4.101	0.0682	1.11	0.0179	0.114	0.0110

a MAT'L – 17-4 PH STAINLESS; $\rho = 0.282\ lb_m/in^3$, $E = 29 \times 10^6\ lb/in^2$, $G = 11 \times 10^6\ lb/in^2$.
b AXIS OF SYMMETRY COINCIDENT WITH 0.25c

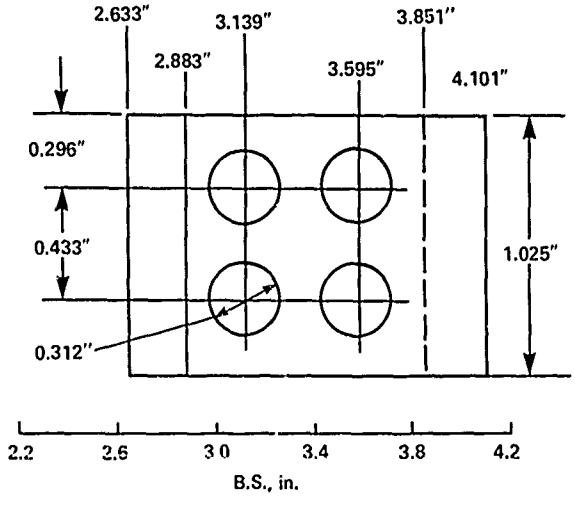


LEAD-LAG FLEXURE

Table 5 Calculated Mass and Stiffness Properties of Side Beams[a]

BLADE STATION in.	WEIGHT lb_m/in.	EI_f 10^6 lb·in^2	EI_c 10^6 lb·in^2	GJ 10^6 lb·in^2	I_θ lb_m in^2/in.
2.633	0.0535	0.468	0.298	0.0109	0.0105
2.883	0.0535	0.468	0.298	0.0109	0.0105
2.883	0.0410	0.359	0.190	0.0109	0.00493
2.983	0.0410	0.359	0.190	0.0109	0.00493
3.029	0.0234	0.269	0.109	0.0109	0.00493
3.139	0.0160	0.221	0.0745	0.0109	0.00493
3.249	0.0234	0.269	0.109	0.0109	0.00493
3.295	0.0410	0.359	0.190	0.0109	0.00493
3.439	0.0410	0.359	0.190	0.0109	0.00493
3.485	0.0234	0.269	0.109	0.0109	0.00493
3.595	0.0160	0.221	0.0745	0.0109	0.00493
3.705	0.0234	0.269	0.109	0.0109	0.00493
3.751	0.0410	0.359	0.190	0.0109	0.00493
3.851	0.0410	0.359	0.190	0.0109	0.00493
3.851	0.0613	0.537	0.220	0.0109	0.00957
4.101	0.0613	0.537	0.220	0.0109	0.00957

a MAT'L – Ti-6Al-4V ALLOY; $\rho = 0.160$ lb_m/in^3, $E = 16 \times 10^6$ lb/in^2, $G = 6.2 \times 10^6$ lb/in^2.

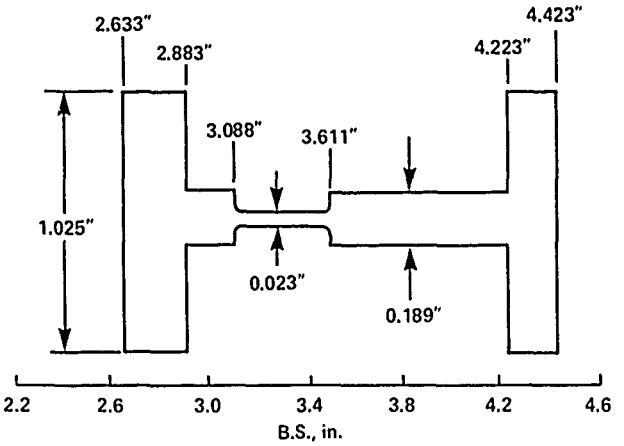


SIDE BEAMS

Table 6 Calculated Mass and Stiffness Properties of Flap Flexure[a]

BLADE STATION in.	WEIGHT $lb_m/in.$	EI_f 10^6 lb·in^2	EI_c 10^6 lb·in^2	GJ 10^6 lb·in^2	I_θ lb_m in^2/in.
2.633	0.276	2.49	9.20	9.92	0.114
2.883	0.276	2.49	9.20	9.92	0.114
2.883	0.0510	0.0156	1.70	1.46	0.0167
3.088	0.0510	0.0156	1.70	1.46	0.0167
3.088	0.0186	0.000759	0.621	0.0192	0.00106
3.111	0.0062	0.000028	0.207	0.0192	0.00106
3.588	0.0062	0.000028	0.207	0.0192	0.00106
3.611	0.0186	0.000759	0.621	0.0192	0.00106
3.611	0.510	0.0156	1.70	0.185	0.0167
4.223	0.510	0.0156	1.70	0.185	0.0167
4.223	0.242	2.00	0.763	3.98	0.0839
4.298	0.242	2.00	0.763	3.98	0.0839
4.298	0.368	3.54	6.62	3.98	0.0988
4.423	0.368	3.54	6.62	3.98	0.0988

a MAT'L – 17-4 PH STAINLESS; $\rho = 0.282\ lb_m/in^3$, $E = 29 \times 10^6\ lb/in^2$, $G = 11 \times 10^6\ lb/in^2$. AXIS OF SYMMETRY COINCIDENT WITH 0.25c.



FLAP FLEXURE

Table 7 Calculated Mass and Stiffness Properties of Hub Flexure and Tantalum Blade

Blade station, in.	Weight, lb_m/in.	EI_f, 10^6 lb-in.^{2}	EI_c, 10^6 lb-in.^{2}	GJ, 10^6 lb-in.^{2}	I_θ, lb_m in.^{2}/in.
2.034	0.573	20.1	20.1	15.6	0.403
2.431	0.573	20.1	20.1	15.6	0.403
2.431	0.422	5.18	5.18	3.93	0.101
2.581	0.422	5.18	5.18	3.93	0.101
2.581	0.0533	1.11	0.0179	3.93	0.101
2.633	0.0533	1.11	0.0179	3.93	0.101
2.633	0.398	0.291	0.0169	0.00995	0.136
2.750	0.398	0.291	0.0169	0.00995	0.136
2.791	0.369	0.259	0.00985	0.00995	0.136
2.883	0.357	0.239	0.00706	0.00995	0.136
2.883	0.120	0.0146	0.00695	0.00990	0.0326
2.890	0.119	0.0146	0.00673	0.00990	0.0326
2.983	0.131	0.0147	0.00945	0.00990	0.0326
2.989	0.131	0.0147	0.00962	0.00990	0.0326
3.030	0.143	0.0146	0.0152	0.00990	0.0326
3.088	0.139	0.0145	0.0148	0.00990	0.0326
3.088	0.106	0.000756	0.0146	0.00656	0.0170
3.111	0.0923	0.000028	0.0138	0.00656	0.0170
3.139	0.0904	0.000028	0.0135	0.00656	0.0170
3.200	0.0945	0.000028	0.0140	0.00656	0.0170
3.200	0.0555	0.000028	0.00138	0.00116	0.00754
3.225	0.0377	0.000028	0.000052	0.00116	0.00754
3.249	0.0393	0.000028	0.000052	0.00116	0.00754
3.295	0.0569	0.000028	0.000052	0.00116	0.00754
3.439	0.0569	0.000028	0.000052	0.00116	0.00754
3.450	0.0527	0.000028	0.000052	0.00116	0.00754
3.475	0.0626	0.000028	0.00139	0.00116	0.00754
3.475	0.102	0.000028	0.0146	0.00655	0.0170
3.485	0.0978	0.000028	0.0143	0.00655	0.0170
3.553	0.0932	0.000028	0.0142	0.00655	0.0170
3.585	0.0680	0.000028	0.00976	0.00655	0.0170
3.588	0.0674	0.000028	0.00968	0.00655	0.0170
3.595	0.0699	0.000250	0.00967	0.00655	0.0170
3.611	0.0777	0.000756	0.00952	0.00655	0.0170
3.611	0.110	0.0143	0.00961	0.00944	0.0326
3.663	0.107	0.0144	0.00848	0.00944	0.0326
3.705	0.115	0.0145	0.00969	0.00944	0.0326
3.741	0.133	0.0146	0.0110	0.00944	0.0326
3.751	0.144	0.0147	0.0127	0.00944	0.0326
3.773	0.160	0.0148	0.0162	0.00944	0.0326
3.851	0.160	0.0148	0.0162	0.00944	0.0326
3.851	0.181	0.0150	0.0164	0.00944	0.0373
4.101	0.181	0.0150	0.0164	0.00944	0.0373
4.101	0.051	0.0156	1.70	0.185	0.0167
4.223	0.051	0.0156	1.70	0.185	0.0167
4.223	0.242	2.00	0.763	3.98	0.0839
4.298	0.242	2.00	0.763	3.98	0.0839
4.298	0.368	3.54	6.62	3.98	0.0988
4.423	0.368	3.54	6.62	3.98	0.0988
4.423	0.615	9.18	9.18	6.74	0.175
4.573	0.615	9.18	9.18	6.74	0.175
4.573	0.222	0.761	0.761	0.558	0.0163
5.423	0.222	0.761	0.761	0.558	0.0163
5.423	0.118	0.0921	0.0921	0.0676	0.00369
14.963	0.118	0.0921	0.0921	0.0676	0.00369

Table 8 Hub and Blade Mass Properties

Quantity	Measured	Adjusted[a]	Calculated	Error[b]
Mass, lb_m	1.582	1.570	1.574	+0.3%
Centroid of mass with respect to center, in.	8.455	8.594	8.580	-0.2%
Flapping and lead-lag inertia, lb_m-in.^{2c}	60.48	59.87	61.99	+3.5%
Pitch inertia, lb_m-in.^{2}	--	--	0.116	--
Rotor polar inertia, lb-in.^{2}	--	--	414.0	--

[a]Flap flexure effect inboard of B.S. 3.35 not included (Table 6); effect of lead-lag flexure (Table 4) and side beams (Table 5) included.
[b]Based on adjusted measurement.
[c]With respect to B.S. 3.35 in.

Table 9 Rotor Modal Frequency

Modal Frequency, Hz	Measured	Calculated	Error
Flap	3.01[a]	3.04	+1.0%
Lead-lag	6.39	6.04	-5.5%

[a]Not measured directly because of flap stop restraint. Obtained from ratio of measurements made with a conventional blade installed.

oscillator and were then corrected to add the inertia of the rotor hardware inboard of the flap-flexure centerline. The measured stiffnesses and calculated inertias are shown in Table 10. The correction to the inertia for the rotor hardware is considered more accurate than the values of Ref. 3. If the rotor inertia is added to the body inertias, then uncoupled, nonrotating body frequencies can be calculated and compared to the measured coupled, nonrotating body frequencies from Table 2. Large differences between the coupled and uncoupled frequencies are not expected because the flap degree of freedom is restrained by a droop stop, and the lead-lag frequency is well separated in frequency. The calculated pitch and roll frequencies are respectively -1.6 and 5.5% apart from the measurements which suggests the inertia properties are reasonably correct.

The body damping is highly nonlinear (see Ref. 3 for a detailed discussion). Representative values of body damping of 3% have been assumed in pitch and roll.

Appendix B--Experimental Data

Tables 11 and 12 show the measured rotor speed, modal frequencies, and regressing lead-lag damping for Cases 1 and 2. These data were obtained in the experiment reported in Ref. 3. The various modes were individually excited and the modal frequency and damping were obtained from the transient decay using an analog technique described in Ref. 2. Modal damping of the body pitch and roll modes was not obtained because of nonlinear damping in the gimbal bearings. Except as noted, the regressing lead-lag mode damping was linear.

Appendix C--Correlation

All of the theoretical predictions and experimental data for the selected cases are shown in this appendix in Figs. 7-12. In some cases figures

Table 10 Body Properties

Quantity	Body Pitch	Body Roll
Gimbal stiffness, in.-lb/rad	1480	849
Inertia about gimbal, lb_m-in.^{2}	1710	603
Uncoupled body frequency, Hz[a]	2.54	2.69
Coupled body frequency, Hz[b]	2.58	2.55

[a]Includes 543 lb_m-in.^{2} for rotor inertia.
[b]From Table 2.

from the main text are repeated here for completeness. Two formats are used for the correlation. The first format compares the theoretical predictions and experimental data individually for each mathematical model used. The second format compares all the theoretical predictions on a single composite plot and the experimental data are shown as a stippled area. An exception to this format is that no composite comparison is made of modal frequencies. A code is used to identify the theoretical predictions for both the individual and composite comparisons; it is explained in Table 13.

Table 11 Modal Frequencies and Damping, Case 1

Rotor Speed, rpm	Regressing Flap Frequency, Hz	Body Roll Frequency, Hz	Regressing Lead-lag Frequency, Hz	Regressing Lead-lag Damping, sec^{-1}
250	1.44	3.44	2.75	-0.104
	1.45	--	2.75	-0.098
	1.50	--	2.77	-0.114
350	1.36	3.76	1.66	-0.115
	1.30	3.61	1.66	-0.118
	1.32	3.65	1.67	-0.131
450	1.52	3.92	0.52	-0.112
	1.44	3.92	0.52	-0.130
	1.44	3.91	0.51	-0.101
550	1.52	4.40	0.44	-0.096
	1.48	4.24	0.43	-0.114
	1.46	4.27	0.44	-0.115
	1.52	4.23	0.45	-0.111
	1.51	4.24	0.46	-0.104
	--	--	0.45	-0.117
600	1.52	4.41	0.89	-0.119
	1.46	4.48	0.90	-0.121
	1.45	4.41	0.89	-0.105
	--	4.41	0.89	-0.136
	--	4.43	0.89	-0.133
	--	4.40	--	--
	--	4.58	--	--
	--	4.58	--	--
650	1.59	4.62	1.34	-0.112
	1.57	4.60	1.35	-0.114
	--	4.58	1.35	-0.143
	--	4.61	1.35	-0.155
	--	4.62	1.34	-0.156
670	--	--	1.51	0.010
	--	--	1.51	0.005
	--	--	1.51	0.003
675	1.53	4.64	1.54	-0.013
	1.52	4.80	1.54	-0.015
	--	4.71	1.55	-0.013
	--	4.71	--	--
705	1.60	4.96	1.78	-0.120
	1.55	4.81	1.78	-0.130
	1.54	4.82	1.81	--
810	1.52	5.28	2.65	-0.159
	1.54	5.26	2.64	-0.150
	1.55	5.24	2.64	-0.140
900	1.60	5.68	3.35	-0.147
	1.57	5.65	3.34	-0.136
	1.58	5.63	3.35	-0.128

Table 12 Modal Frequencies and Damping, Case 2

Rotor Speed, rpm	Regressing Flap Frequency, Hz	Body Pitch Frequency, Hz	Body Roll Frequency, Hz	Regressing Lead-lag Frequency, Hz	Regressing Lead-lag Damping, Hz
250	1.34	3.07	3.52	2.77	-0.107
	1.32	3.04	--	2.77	-0.115
	1.28	--	--	2.77	-0.109
350	1.22	3.02	3.69	1.64	-0.125
	1.22	3.06	3.68	1.65	-0.161
	1.20	2.96	3.68	1.63	-0.130
450	1.24	3.06	3.99	0.53	-0.161
	1.24	3.07	3.93	0.52	-0.133
	1.20	3.04	4.00	0.53	-0.123
550	1.20	3.15	4.32	0.43	-0.133
	1.22	3.16	4.33	0.43	-0.139
	1.20	3.12	4.40	0.42	-0.133
600	1.20	3.19	4.52	0.88	-0.150
	1.19	3.24	4.53	0.88	-0.129
	1.20	3.20	4.56	0.88	-0.134
650	1.20	3.29	4.70	1.32	--
	1.20	3.28	4.71	1.32	--
	1.20	3.28	4.72	1.31	--
700	1.19	3.33	4.93	1.76	-0.123
	1.17	3.35	4.95	1.77	-0.155
	1.20	3.36	4.96	1.76	-0.140
810	1.13	3.45	5.40	2.68	-0.134
	1.12	3.43	5.39	2.68	-0.143
	1.12	3.44	5.40	2.70	-0.140
	--	--	--	2.68	-0.160
	--	--	--	2.68	-0.167
	--	--	--	2.69	-0.156
850	1.11	3.36	5.56	3.05	-0.097
	1.10	3.35	5.56	3.04	-0.112
	1.12	3.44	5.60	3.03	-0.103
860	1.10	3.32	5.58	3.15	-0.090
	1.10	3.30	5.62	3.17	-0.031
	--	--	--	3.14	-0.064
870	1.12	3.37	5.68	3.25	-0.022
	1.11	3.38	5.70	3.27	-0.034-0.265[a]
	1.09	3.40	5.70	3.25	-0.126[a]
880	--	--	--	3.35	0.570
	--	--	--	3.37	0.395-0.632[a]
	--	--	--	3.34	0.603

[a]Apparent nonlinearity.

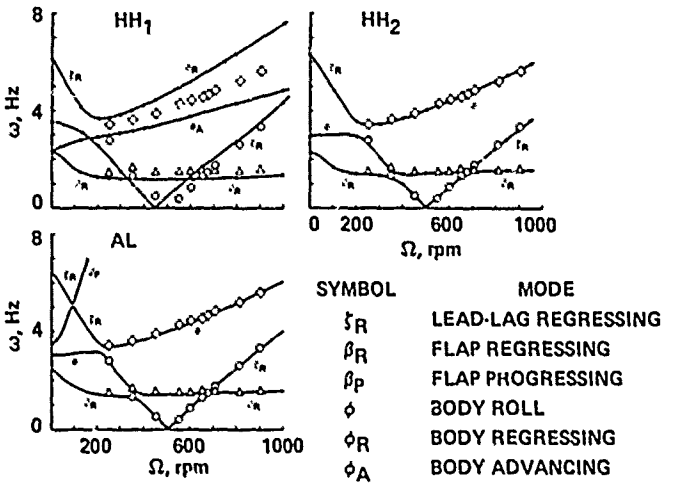


Fig. 7 Individual comparison for Case 1 modal frequencies.

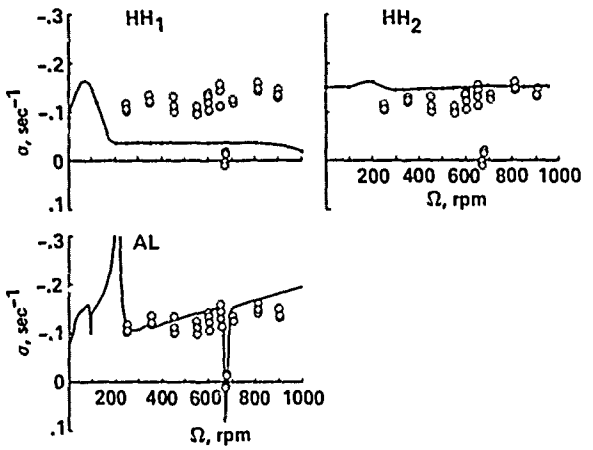


Fig. 8 Individual comparison for Case 1 regressing lead-lag mode damping.

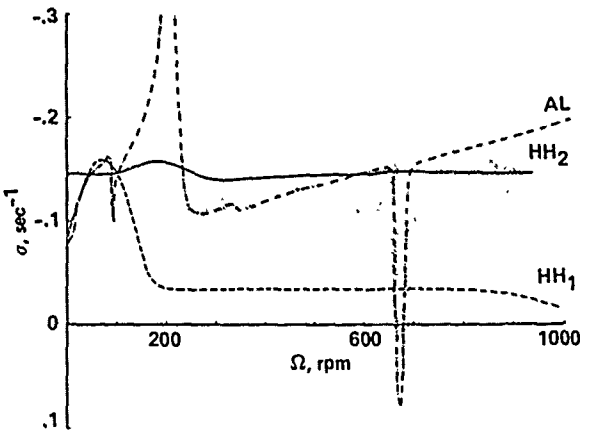


Fig. 9 Composite comparison for Case 1 regressing lead-lag mode damping.

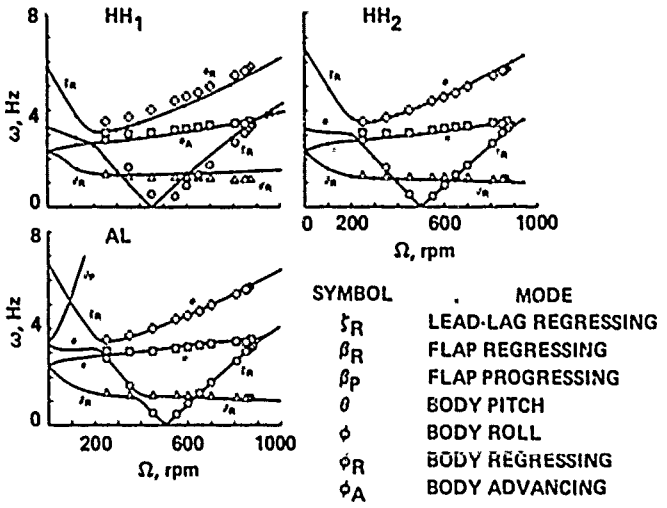


Fig. 10 Individual comparison for Case 2 modal frequencies.

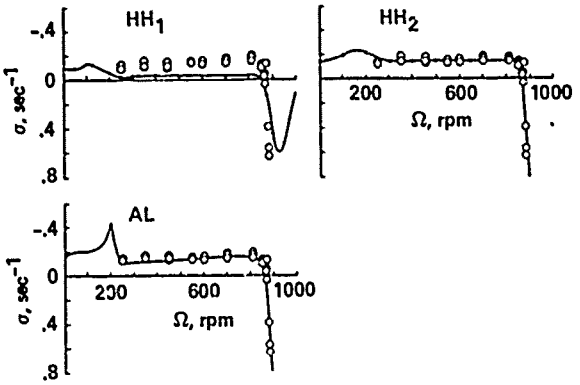


Fig. 11 Individual comparison for Case 2 regressing lead-lag mode damping.

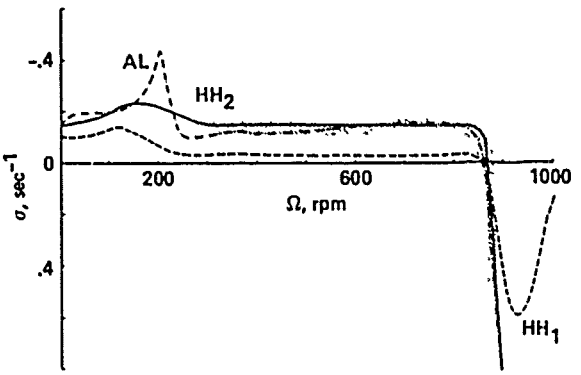


Fig. 12 Composite comparison for Case 2 regressing lead-lag mode damping.

Table 13 Explanation of Prediction Codes

Code	Prediction Method	User
HH_1	DART	Hughes Helicopters
HH_2	E927-1	Hughes Helicopters
AL	FLAIR	U.S. Army Aeromechanics Laboratory

DISCUSSION

A COMPARISON OF THEORY AND EXPERIMENT FOR COUPLED ROTOR-BODY STABILITY OF A HINGELESS ROTOR MODEL IN HOVER UNDER SIMULATED VACUUM CONDITIONS

William G. Bousman

Dev Banerjee, Hughes Helicopters: Would you care to comment on the nature of that sharp instability that we see in the previous chart [Fig. 4] where you only had, I believe, the roll degree of freedom?

Bousman: Do you mean as far as experimentally what we saw there? At one rotor speed it was neutrally damped and at the next rotor speed it was very weakly undamped. As we proceeded in rpm we tracked the frequencies of the modes and as we got close to that crossing, all of a sudden we got an instability in the lead-lag degree of freedom.

Banerjee: If you place that frequency plot over the damping plot with the same rpm-scale, you would see that coincides directly with the crossover of the flap with the lead-lag mode.

Bousman: Yes, that's correct.

Banerjee: On that crossover, as you see in this plot also, the right-hand side is when the rotor essentially is soft in-plane; that is where you have absolute crossover of the lead-lag frequency in the fixed system with the absolute value of the first flap frequency. It's not an actual crossover as you would see in the rotating system.

Bousman: I'm not sure I agree with that; we've had this discussion before. But you know that you've got conjugate modes sitting there and you can plot them in either the fixed system or rotating system. If you just plot one pair of them, yes, you'll see they're separated. But if you plot all the pairs, I think that you'll find that as you go out in some parameter, you'll find the imaginary one coming up and when you get to zero frequency, what is happening is, one is becoming imaginary and going down but its opposite pair is going up. So there is a real crossing there.

Dewey Hodges, Aeromechanics Laboratory: Also, it's an actual coalescence. It's not just a normal modal crossing. If you blow up the scale of the theoretical predictions from the flexbeam air resonance (FLAIR) analysis you'll find that the curves actually come together. If you had a big magnifying glass it would look just like a ground resonance instability, as far as the frequency crossings are concerned.

Banerjee: But it's essentially a coupling of the flap mode and the lag mode, isn't that right?

Bousman: Yes.

Hodges: That's correct, but it is a gyroscopic system and it's the same kind of instability, mathematically, as ground resonance. It's just that the numbers are different.

A COMPARISON OF THEORY AND EXPERIMENT FOR COUPLED ROTOR-BODY STABILITY OF A HINGELESS ROTOR MODEL IN HOVER

William G. Bousman
Research Scientist
U.S. Army Aeroflightdynamics Directorate
Ames Research Center

Abstract

Three cases were selected for correlation from an experiment that examined the aeromechanical stability of a small-scale model of a hingeless rotor and fuselage in hover. The first case examined the stability of a configuration with 0° blade pitch so that coupling between dynamic modes was minimized. The second case was identical to the first except the blade pitch was set to 9° which provides flap-lag coupling of the rotor modes. The third case had 9° of blade pitch and also included negative pitch-lag coupling, and therefore was the most highly coupled configuration. Analytical calculations were made by Bell Helicopter Textron, Boeing Vertol, Hughes Helicopters, Sikorsky Aircraft, the U.S. Army Aeromechanics Laboratory, and NASA Ames Research Center and compared to some or all of the experimental cases. Overall, the correlation ranged from very poor-to-poor to good.

Introduction

As a part of the Methodology Assessment, three cases were selected from the experiment reported in Ref. 1 for comparison with theoretical calculations. The three cases differ only in the type and extent of aeroelastic coupling in the rotor. Case 1 represents the simplest configuration with the blade pitch angle set to 0° to minimize coupling. Structural flap-lag coupling is incorporated in Case 2 by setting the blade pitch angle to 9°. Case 3 is the most complex configuration with flap-lag coupling combined with negative pitch-lag coupling. The three cases provide a graduated series for aeromechanical stability with increasing complexity in the rotor aeroelastic coupling. Therefore, they provide a good test of the capability of theoretical models to predict stability as the aeroelastic coupling becomes more complex.

The theoretical models that were compared with the data include the Bell Helicopter Textron DRAV21 code, the Boeing Vertol C-90, the Hughes Helicopter DART and E927-1 analyses, Sikorsky Aircraft G400 code, and the U.S. Army Aeromechanics Laboratory FLAIR analysis. The Sikorsky Aircraft E927-2 and E927-3 codes, and the NASA Ames Research Center CAMRAD, were compared with some of the data.

The paper will briefly describe the experiment from which these data were obtained and then present the correlation. The agreement between theory and experiment will be discussed. The appendices document the experimental model properties, tabulate the experimental data points, and show all of the comparisons.

Experiment Description

The model rotor and fuselage used in the experiment is shown in Fig. 1. The rotor has three blades that are mounted on root flexures that allow flap and lead-lag motion. The flexures are mounted to a hub which is supported by bearings on a static mast. The static mast is bolted to a transmission with a water-cooled electric motor at either end that represents the fuselage. The rotor and fuselage are supported in a gimbal frame with flexure pivots that allow pitch and roll motions. Springs are connected across the gimbal pivots to provide frequencies that are representative of actual helicopters; the pitch and roll inertias are appropriately scaled. The stand is stiffened below the gimbal so that the stand frequencies are higher than the body frequencies by a factor of 10.

The regressing lead-lag mode was excited with a floor-mounted 50-lb shaker that oscillates the

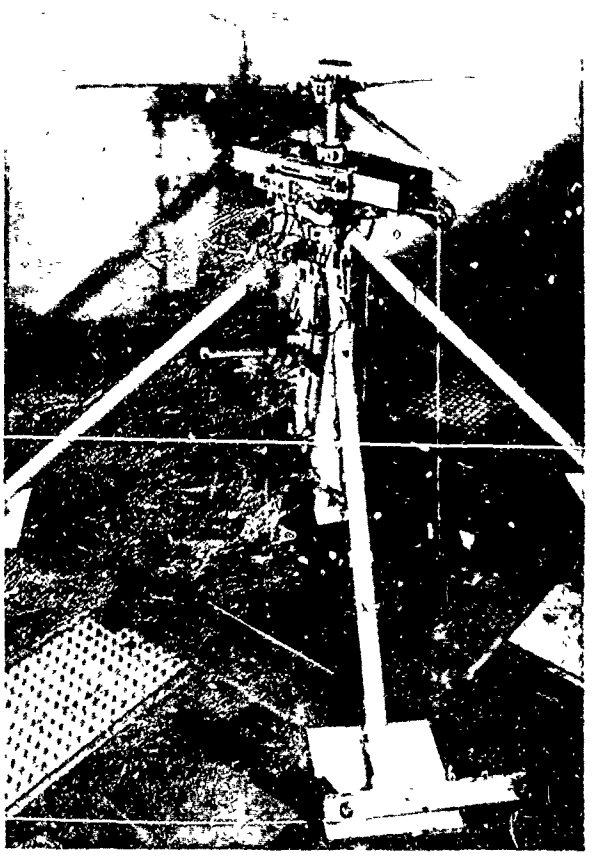


Fig. 1 Three-bladed hingeless rotor model mounted to gimbal frame and stand.

model about the roll gimbal. When a sufficient level of excitation was achieved, a pneumatic clamp was opened and the body and rotor motions were allowed to decay freely. The body pitch and roll modes were excited by deflecting the fuselage with pulley-mounted cords and then quickly releasing it.

The blade root flexures are shown in the exploded view of Fig. 2. The lead-lag flexure is fastened to a base and ring that allows the lead-lag flexure to be rotated to any pitch angle, although for the cases discussed in this paper, the lead-lag flexure was always positioned upright. The lead-lag flexure, base, and ring are firmly fastened to the rotor hub. A pair of side beams is connected to the outer part of the lead-lag flexure; these carry the load back toward the hub. The flap flexure is fastened to the inner edge of the side beams and in this way the lead-lag and flap flexure centerlines are made coincident. A blade root socket is fastened to the outer portion of the flap flexure and blade pitch angle changes are made at this point. Instead of the straight lead-lag flexure, the skewed lead-lag flexure that is shown in the inset of Fig. 2 is used to provide negative pitch-lag coupling (Case 3). The major rotor properties are shown in Table 1.

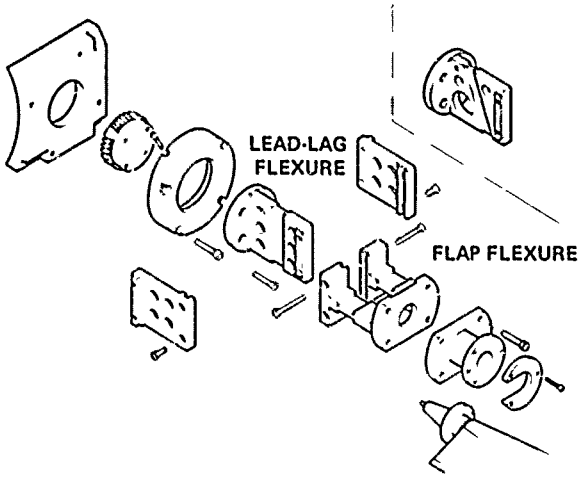


Fig. 2 Exploded view of blade root flexures.

Table 1 Model Rotor Properties

Property	Value
Rotor radius, R, in.	31.92
Blade chord, c, in.	1.65
Solidity, σ	0.0493
Hinge offset, e/R	0.105
Lock number, γ	7.37

The rotor flap and lead-lag flexures were strain-gaged as were the gimbal flexural pivots. The measured flexural strains were digitized and acquired on a digital computer. The rotating system data were transformed to the fixed system using the multiblade transform and the frequency and damping data were obtained from the rotor cyclic and body modes using the moving-block analysis.[2] A complete discussion of the model properties is provided in Appendix A. The measured modal damping and frequency used for the correlation is tabulated in Appendix B.

Correlation

Three cases were used for correlation. These cases differed only in the degree of aeroelastic coupling in the rotor as determined by blade pitch angle and pitch-lag coupling. The differences in the three cases are shown in Table 2.

Table 2 Correlation Cases

Case	Blade Pitch Angle, deg	Pitch-Lag Coupling
1	0	0
2	9	0
3	9	-0.4

Case 1

Modal Frequencies. This case examined modal damping and frequency for an uncoupled rotor configuration with the blade pitch set to zero degrees. Damping and frequency of the regressing lead-lag, body pitch, and body roll modes were obtained for rotor speeds from 0 to 950 rpm. Figure 3 shows individual comparisons of the fixed-system modal frequencies with nine different predictions. An understanding of the system behavior may be obtained by examining a typical prediction such as that done with DRAV21 as shown in Fig. 3a. The regressing lead-lag mode starts at about 6.6 Hz for nonrotating conditions and as rotor speed is increased, the fixed system modal frequency drops until it becomes zero at about 450 rpm (in the rotating system this is a 1/rev resonance). At higher rotor speeds the regressing lead-lag mode frequency increases. For rotor speeds below 450 rpm, the dimensionless regressing lead-lag frequency is greater than one (stiff inplane) and the rotor is not susceptible to aeromechanical instability. For rotor speeds above 450 rpm the dimensionless, regressing lead-lag frequency is less than one (soft inplane) and the rotor is susceptible to aeromechanical instability as the regressing lead-lag mode couples with the body pitch or roll mode. The regressing flap mode is highly damped at rotor speeds above 100 rpm and does not couple with the egressing lead-lag mode as it did for the experiment discussed in Ref. 3. The progressing flap and lead-lag modes are widely separated in frequency for rotor speeds above 200 rpm and therefore do not influence the other modes.

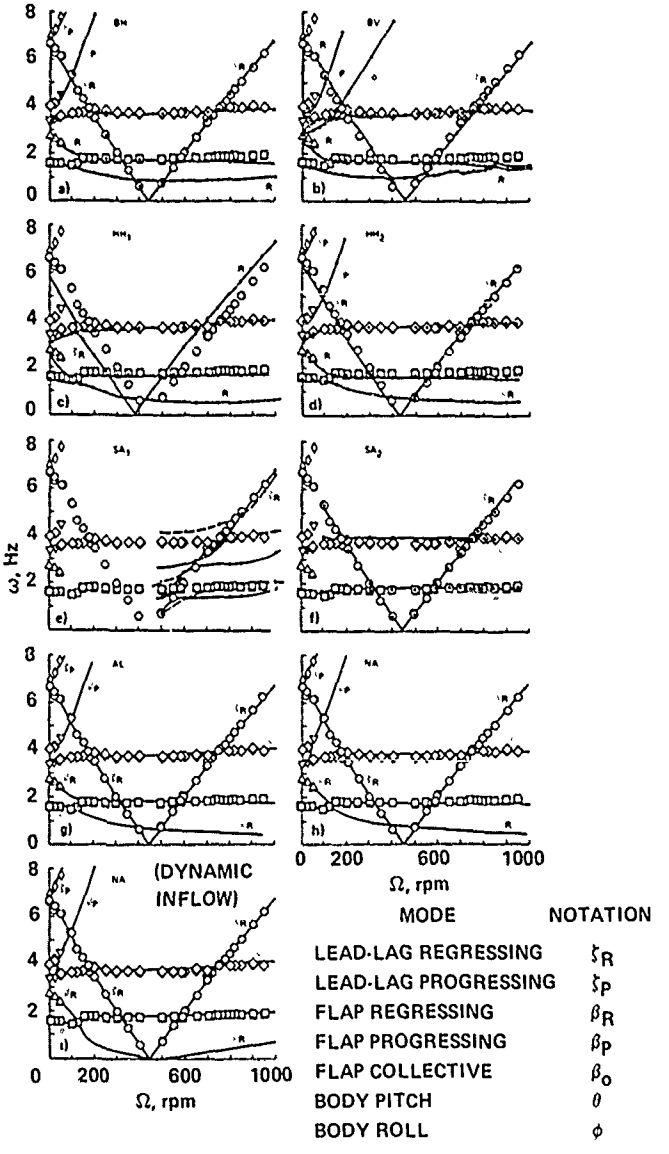


Fig. 3 Individual comparison of theory and experiment for Case 1 for fixed-system modal frequencies. a) DRAV21, Bell Helicopter Textron. b) C-90, Boeing Vertol. c) DART, Hughes Helicopters. d) E927-1, Hughes Helicopters. e) G400, Sikorsky Aircraft. Solid lines show calculations based on model properties. Dashed lines reflect change in properties to match rotating-body pitch and roll frequencies. f) E927-2, Sikorsky Aircraft. g) FLAIR, Aeromechanics Laboratory. h) CAMRAD, NASA Ames Research Center. i) CAMRAD with dynamic inflow, NASA Ames Research Center.

Most of the predictions in Fig. 3 show good to very good correlation (DRAV21, E927-1, FLAIR, and CAMRAD). The C-90 predictions show fair-to-good correlation, but exhibit some anomalous behavior. The C-90 program predicts that the collective flap mode couples with the body roll mode between 100 and 300 rpm. The mechanism for the coupling is not understood. At rotor speeds above 600 to 700 rpm, the C-90 predictions show apparent coupling between the regressing-flap and body-pitch modes (see also Fig. 5 below). This behavior appears spurious and suggests calculation problems with the code.

The DART correlation is considered to be only fair. This is largely because of the shift in lead-lag stiffness that resulted from using the mass and stiffness properties tabulated in Appendix A. These properties, which were calculated from detail drawings, predict a lower nonrotating frequency than was measured.

The G400 correlation was judged to be poor. The initial predictions using the documented model properties are shown as solid lines and do not match the measured body frequencies. Subsequently the uncoupled body pitch-and-roll frequencies were adjusted to provide a better match with the measurements; these results are shown as dashed lines. In either case the predicted frequencies indicate more coupling between the regressing lead-lag and body modes than was measured. An operational problem with G400 is the need to excite the appropriate modes in the time-history solution in order to estimate the frequency and damping from the transient decay. Considerable difficulty was encountered in exciting the body modes, particularly at the lower rotor speeds. The E927-2 correlation is considered to be fair. In general the correct behavior is shown, but the differences in the body roll mode and the absence of calculations at low rotor speeds degrade the correlation.

Regressing lead-lag mode damping. The damping of the regressing lead-lag mode for Case 1 is shown in Fig. 4. Calculations without dynamic inflow and with dynamic inflow are compared separately. The experimental measurements show a relatively constant level of damping except at the body roll mode crossing where the regressing lead-lag mode is unstable between 700 and 805 rpm. Most of the analyses show this same general behavior with the correlation ranging from fair for E927-2 and E927-3, fair-to-good for C-90, FLAIR, and CAMRAD, and good for DRAV21.

The DART analysis shows a range of instability that is much wider than the measurements and the correlation is considered to be poor. The center

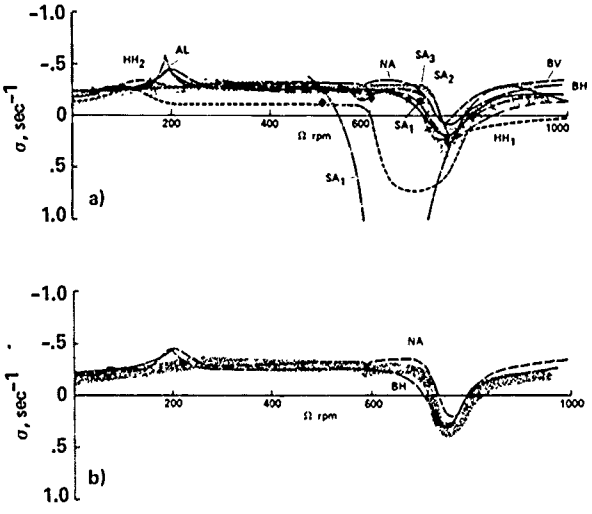


Fig. 4 Composite comparison of theory and experiment for Case 1 regressing lead-lag-mode damping. Data are shown by stippled area; analyses used are DRAV21 (BH), C-90 (BV), DART (HH_1), E927-1 (HH_2), G400 (SA_1, recalculations shown as diamond symbols), E927-2 (SA_2), E927-3 (SA_3), FLAIR (AL), and CAMRAD (NA). a) Without dynamic inflow. b) With dynamic inflow.

of instability is offset from the measured location and this is probably caused by the lead-lag frequency shift noted in Fig. 3. However, the greater range of instability that was calculated is probably caused by the inability to properly model the separate body pitch and roll frequencies with the isotropic representation used by DART. In addition, away from the body crossings DART predicts a damping level that is significantly below the rotor structural damping, and the mechanism for this destabilizing effect is unknown.

The G400 correlation is judged to be very poor and shows excessive sensitivity to body coupling effects. Following the initial Methodology Assessment, the G400 code was extensively revised. The correlation was significantly improved, as shown by the solid diamond symbols. However, the specific revisions that caused the improved predictive capability are not known.

Two of the prediction methods, DRAV21 and CAMRAD, have the option of predicting the stability with the inflow dynamics included. Although it is not completely clear from Fig. 4, the inclusion of dynamic inflow provided a minor improvement in the correlation for both of these analyses.

Body pitch mode damping. The body pitch-mode damping as a function of rotor speed is shown in Fig. 5. Theory and experiment show similar behavior with the damping rapidly increasing from its nonrotating value as the regressing flap and body pitch modes become strongly coupled between 100 and 150 rpm and then decreasing as the modes separate. Above 200 rpm there is a gradual increase in damping with rotor speed. Although similar behavior is seen in both the theoretical calculations and experimental results, the predicted level of damping from theory is significantly higher than the measurements for rotor speeds above 200 rpm. These differences are largely due to the rotor aerodynamics as the gimbal damping is very low, as can be seen by examining the zero rotor speed case. If dynamic inflow is included in the analytical model, better agreement is obtained with the experiment, as is shown in Fig. 5b.

In general, the correlation is considered poor-to-fair for the models without dynamic inflow, and fair-to-good and good for the models with dynamic inflow. The C-90 analysis is judged as poor because of the high damping level and anomalous damping increases at 675 and 850 rpm. These damping increases or bumps are not related to any frequency crossing or resonance and the lack of a physical explanation suggests that they are caused by code problems. The wobble in body pitch and flap regressing mode frequencies noted earlier appears to be related to this problem.

The G400 correlation was judged as poor. This is largely caused by the inability of the analysis to estimate the body mode damping at rotor speeds below 800 rpm. The E927-2 analysis in many ways shows the best agreement with the data, but its somewhat erratic behavior and lack of definition of

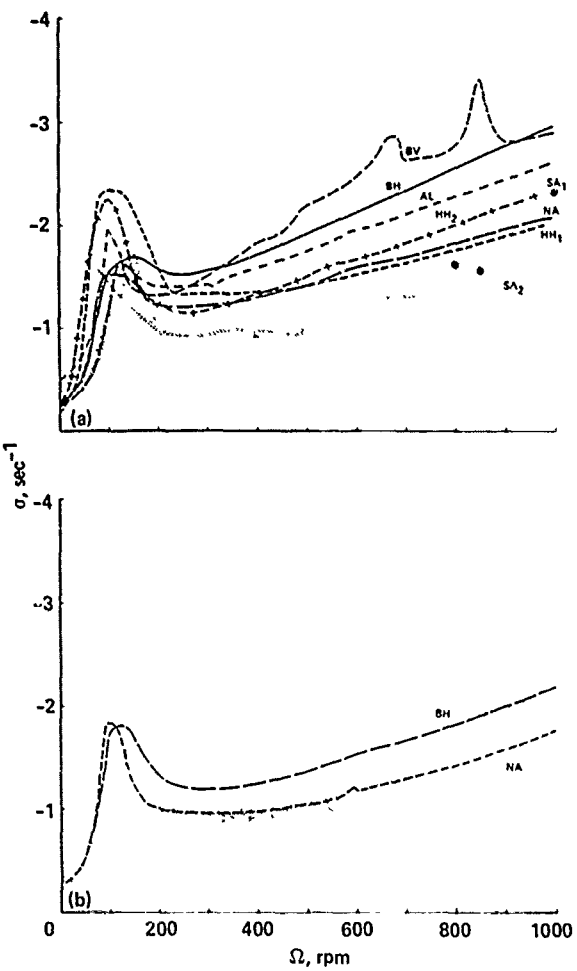


Fig. 5 Composite comparison of theory and experiment for Case 1 body pitch-mode damping. Data are shown by stippled area; analyses used are DRAV21 (BH), C-90 (BV), DART (HH_1), E927-1 (HH_2), G400 (SA_1, 3 points), E927-2 (SA_2), FLAIR (AL), and CAMRAD (NA). a) Without dynamic inflow. b) With dynamic inflow.

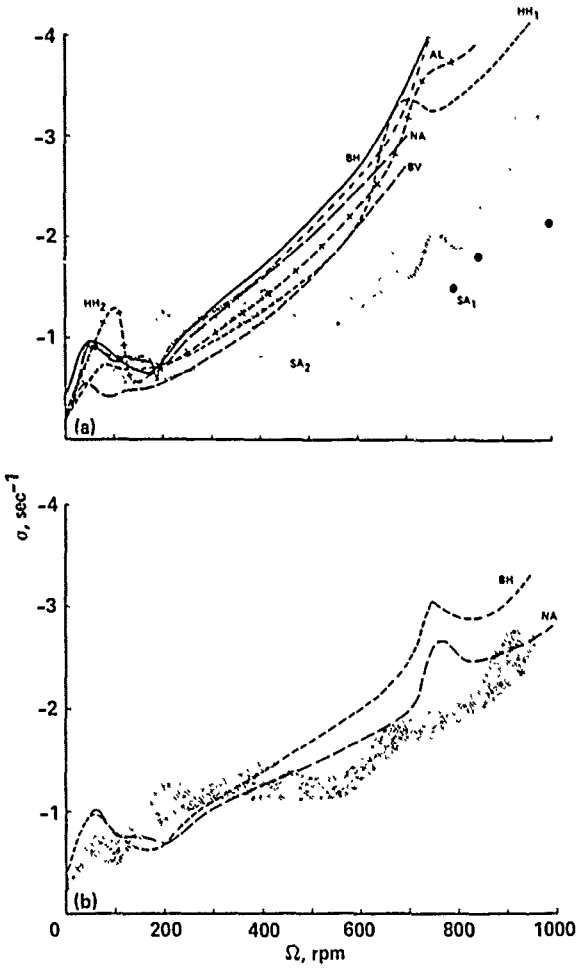


Fig. 6 Composite comparison of theory and experiment for Case 1 body roll-mode damping. Data are shown by stippled area; analyses used are DRAV21 (BH), C-90 (BV), DART (HH_1), E927-1 (HH_2), G400 (SA_1, 3 points), E927-2 (SA_2), FLAIR (AL), and CAMRAD (NA). a) Without dynamic inflow. b) With dynamic inflow.

the damping increase caused by coupling of the flap-regressing and body-pitch modes led to a judgment of poor-to-fair correlation.

Body roll-mode damping. The body roll-mode damping as a function of rotor speed is shown in Fig. 6. The experimental data show a somewhat larger increase in damping with rotor speed than in the body pitch case. However, there is no clear indication of a damping increase caused by coupling of the body roll mode with the progressing flap or regressing lead-lag modes at low rotor speeds. Note that roll-mode damping data were not obtained from 700 to 825 rpm because of the regressing lead-lag mode instability.

The theoretical predictions without dynamic inflow show a very similar increase in damping for rotor speeds above 200 rpm, and the increase is clearly greater than that seen in the experimental data. However, if dynamic inflow is included, the theory and experiment show much better agreement. The improvement in correlation that is achieved with dynamic inflow is more apparent in this case than for the body pitch mode shown in Fig. 5.

The analyses without dynamic inflow in general show only poor-to-fair correlation with the data. The damping predictions that include dynamic inflow show better agreement; the DRAV21 predictions are judged fair and the CAMRAD predictions fair-to-good. The Sikorsky E927-2 predictions are considered to be fair and would probably be judged better except for the somewhat erratic behavior that is shown. The G400 results are again considered to be poor, in part because of the inability to obtain damping estimates at lower rotor speeds.

Case 2

Individual comparisons of theory and experiment for the regressing lead-lag mode damping are shown in Fig. 7 as a function of rotor speed. The only difference between this case and Case 1 is that the blade pitch angle is set to 9° instead of 0°. The effect of this change is to couple the blade flap and lead-lag degrees of freedom and this has a strong effect upon the regressing lead-lag mode damping as can be seen by comparing this figure with Fig. 4. The destabilizing effect caused by coupling of the regressing lead-lag mode and the body pitch mode at 600 rpm is now evident, and the instability caused by coupling of the regressing lead-lag and body roll modes has deepened (0.7 sec^{-1} compared to 0.3 sec^{-1}) and broadened (150 rpm compared to 90 rpm).

The DRAV21, C-90, and FLAIR analyses all show fair correlation. The DRAV21 predictions show better agreement in the vicinity of the pitch mode, while C-90 and FLAIR show better agreement near the roll mode. However, in each case there remain areas of disagreement. Note also that for the DRAV21 calculations the effect of dynamic inflow is slight.

The E927-? predictions in Fig. 7g show fair-to-good agreement with the data, with the only discrepancy being the inability to predict the measured recovery in damping at high rotor speeds. This case and the Case 1 regressing lead-lag mode damping are the only cases in the correlation effort in which all three E927 versions were used. For Case 1 only slight differences are seen between the three versions, but in the present case significant differences are evidenced. The public domain version, E927-1, shows a frequency shift and predicts too great an instability, while E927-2 shows only a slight instability. Both show only poor or poor-to-fair correlation with the data. The major differences in coding between the three versions has to do with the representation of the torsion degree of freedom. The E927-1 version includes only a rigid torsion degree of freedom; E927-2 adds a flexible torsion degree of freedom, but deletes some of the higher-order terms; and E927-3 retains all the higher-order terms. These differing representations have a major influence on the stability predictions even though the model rotor's first-torsion degree of freedom is greater than 20/rev based on nonrotating measurements. The sensitivity of the predictive capability to the modeling assumptions in this case suggests fundamental weaknesses in the E927 family of codes.

The DART analysis shows an excessive degree of instability and the correlation is considered poor. In part, this is caused by the frequency shift in the lead-lag degree of freedom discussed previously. However, even a shift of 50 rpm would not significantly improve the correlation.

The initial G400 calculations show very poor agreement with the data. From the three calculated values provided for the updated analysis (solid

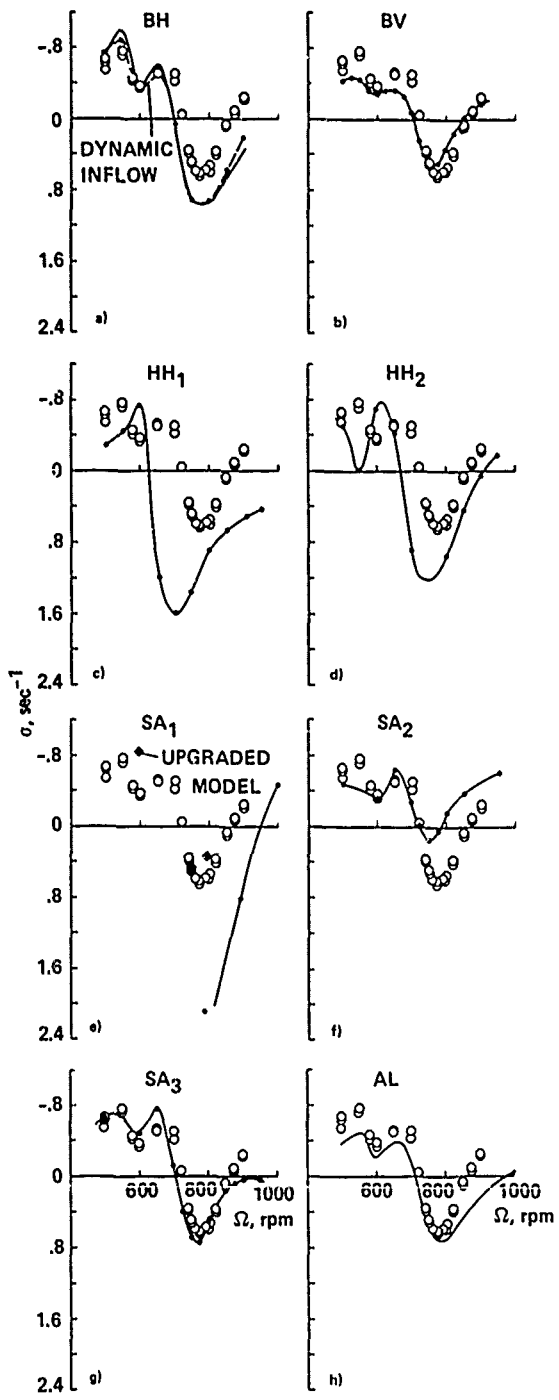


Fig. 7 Individual comparison of theory and experiment for Case 2 for regressing lead-lag-mode damping. a) DRAV21, Bell Helicopter Textron. b) C-90, Boeing Vertol. c) DART, Hughes Helicopters, d) E927-1, Hughes Helicopters. e) G400, Sikorsky Aircraft. f) E927-2, Sikorsky Aircraft. g) E927-3, Sikorsky Aircraft. h) FLAIR, Aeromechanics Laboratory.

diamonds in Fig. 7e), it appears that these problems are largely resolved. However, the number of calculated points using the updated model is too limited to adequately assess the improvement in the analysis capabilities.

Case 3

Individual comparisons of theory and experiment for the regressing lead-lag mode damping are shown in Fig. 8 as a function of the rotor speed for Case 3. The only difference between this case and Case 2 is the addition of negative pitch-lag coupling. Based on isolated blade stability theory,[4] the expected effect of the negative pitch-lag coupling would be to strongly stabilize the regressing lead-lag mode. This in fact occurs away from the body pitch- and roll-mode frequency crossings. For instance, the damping at 550 and 650 rpm is essentially doubled from Case 2 to Case 3. However, at the frequency crossings or "resonant" points, there is essentially no change in the damping.

The DRAV21 and FLAIR analyses show good agreement with the experimental measurements. The agreement for both analyses is improved over that obtained in Case 2, which is interesting in that Case 3 is considered a more difficult case to accurately analyze. As in Case 2, when dynamic inflow is included in the DRAV21 analysis, there are no significant changes in the regressing lead-lag damping.

The C-90 code shows fair agreement with the data. It correctly identifies the minimum stability points, but not the range of damping that is seen in the data. The two versions of E927 evidence difficulty in identifying the rotor speed for minimum stability. The E927-1 correlation is considered very poor-to-poor and does not predict instability, while E927-3 does show reasonably correct damping levels, but the correlation is judged poor-to-fair. The DART analysis shows excessive changes in damping, a substantial frequency shift in the minimum damping point, and an overly broad region of instability. The agreement with the measurements is considered poor.

Conservatism in Prediction of Stability

The potentially destructive nature of rotor instabilities has always been a major concern of the rotorcraft dynamics community. There is agreement that the long term goal in rotorcraft dynamics must be to obtain accurate predictions of rotorcraft stability. However, in the short term, there is a general belief that if the theoretical predictions are "conservative," that is, if they predict less stability than is measured, then they are suitable for design use. Such a feeling or belief ignores the ambiguity that exists whenever theory and experiment are compared and a difference is obtained. Is the difference due to the theory or the experiment? If it is due to some limitation of the modeling assumptions, then can any prediction be called conservative if that limitation is unknown? An example is selected from the correlation effort reported here. Figure 9 compares the

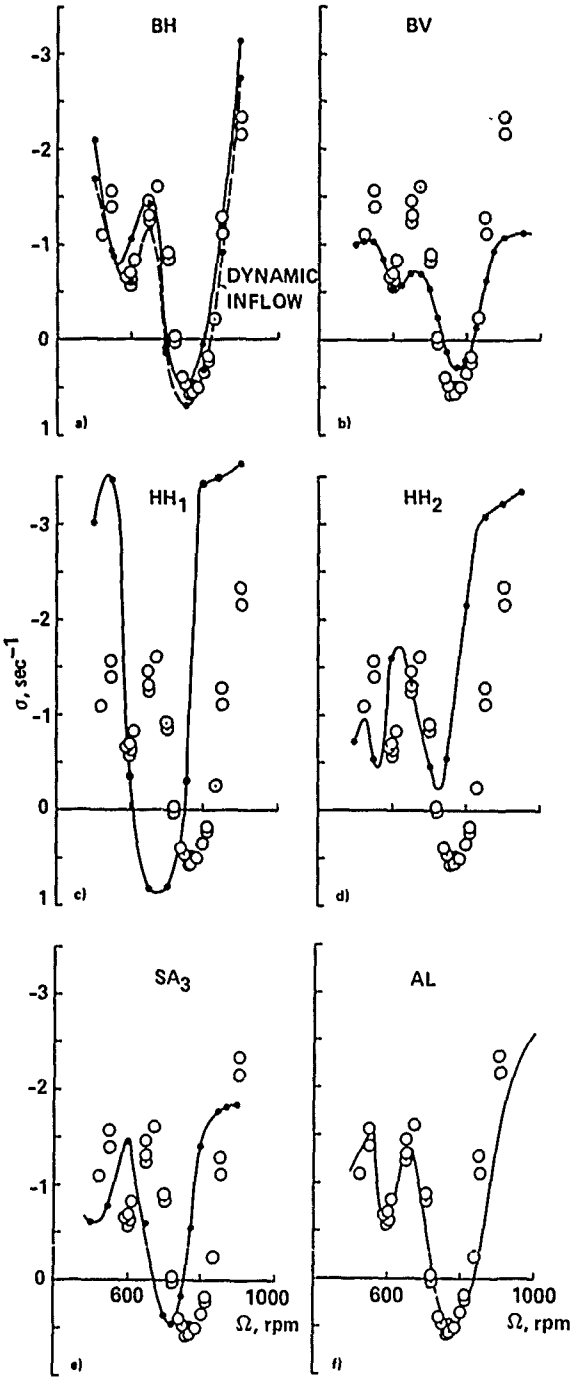


Fig. 8 Individual comparison of theory and experiment for Case 3 for regressing lead-lag mode damping. a) DRAV21, Bell Helicopter Textron. b) C-90, Boeing Vertol. c) DART, Hughes Helicopters, d) E927-1, Hughes Helicopters. e) E927-3, Sikorsky Aircraft. f) FLAIR, Aeromechanics Laboratory.

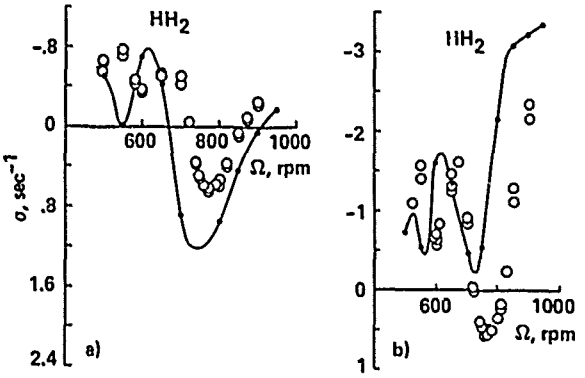


Fig. 9 Comparison of E927-1 predictions for Cases 2 and 3. a) Case 2, 9° blade pitch angle, no pitch-lag coupling. b) Case 3, 9° blade pitch angle, -0.4 pitch-lag coupling.

E927-1 predictions of regressing lead-lag mode damping for Cases 2 and 3. The only difference between the two cases is the addition of negative pitch-lag coupling in Case 3. As discussed earlier, the correlation in Case 2 is judged poor-to-fair. However, the prediction can be considered conservative in the sense that it shows less stability in general than is measured. Yet, as shown in Fig. 9b, the addition of pitch-lag coupling changes this picture. The analysis is now unconservative and predicts no instability where one was obtained in the experiment. The lack of correlation between theory and measurement represents an element of risk in the application of a theoretical model. The use of terms such as "conservative prediction" or "correct trends" unfortunately obscure this element of risk.

Conclusions

Nine analyses were compared with one or more cases selected from an experiment that measured the frequency and damping of a model rotor in hover for different conditions of rotor coupling.

1) The DRAV21 analysis used by Bell Helicopter Textron was considered to give fair-to-good correlation for the three cases.

2) The C-90 analysis used by Boeing Vertol was judged to have fair correlation overall.

3) Two analysis codes were used by Hughes Helicopter. Their DART analysis was considered to provide poor-to-fair correlation and their E927-1 code was judged fair overall.

4) Sikorsky Aircraft used the analysis code G400 and two versions of E927: E927-2 and E927-3. None of these codes was used for all cases. Overall, G400 was judged to be very poor-to-poor although a limited number of more recent calculations have shown substantial improvement. For the cases considered, E927-2 was considered poor-to-fair, while E927-3 showed better performance and was judged fair.

5) The FLAIR analysis of the U.S. Army Aeromechanics Laboratory was considered to provide fair-to-good correlation.

6) The NASA Ames CAMRAD calculations were made for one case and were judged to be good for this case.

Two of the nine analyses predicted damping and frequency with and without dynamic inflow. The effect of dynamic inflow was to significantly improve the agreement for the body mode damping of Case 1, but regressing lead-lag mode damping was only slightly affected by dynamic inflow.

References

[1]Bousman, William G., "An Experimental Investigation of the Effects of Aeroelastic Couplings on Aeromechanical Stability of a Hingeless Rotor Helicopter," Journal of the American Helicopter Society, Vol. 26, No. 1, Jan. 1981, pp. 46-54.

[2]Bousman, William G. and Winkler, Diana J., "Application of the Moving-Block Analysis," 22nd Structures, Structural Dynamics and Materials Conference Proceedings (Part 2), Apr. 1981, pp. 755-763.

[3]Bousman, William G., "A Comparison of Theory and Experiment for Coupled Rotor-Body Stability of a Hingeless Rotor Model in Hover Under Simulated Vacuum Conditions," NASA CP-10007, May 1988.

[4]Ormiston, R. A. and Hodges, D. H., "Linear Flap-Lag Dynamics of Hingeless Helicopter Rotor Blades in Hover," Journal of the American Helicopter Society, Vol. 17, No. 2, Apr. 1972, pp. 2-14.

[5]Bousman, W. G., Sharpe, D. L., and Ormiston, R. A., "An Experimental Study of Techniques for Increasing the Lead-Lag Damping of Soft Inplane Hingeless Rotors," Preprint No. 1035, American Helicopter Society 32nd Annual National Forum, May 1976.

[6]Silcox, H. F., "Analytical and Model Investigation of Hingeless Rotor Air Statility, Volume 1, Section A: Structural Analysis--Rigid Blades," Rep. No. D210-10475-1A, Boeing Company, 1972.

[7]Bousman, William G., "An Experimental Investigation of Hingeless Helicopter Rotor-Body Stability in Hover," NASA TM-78489, June 1978.

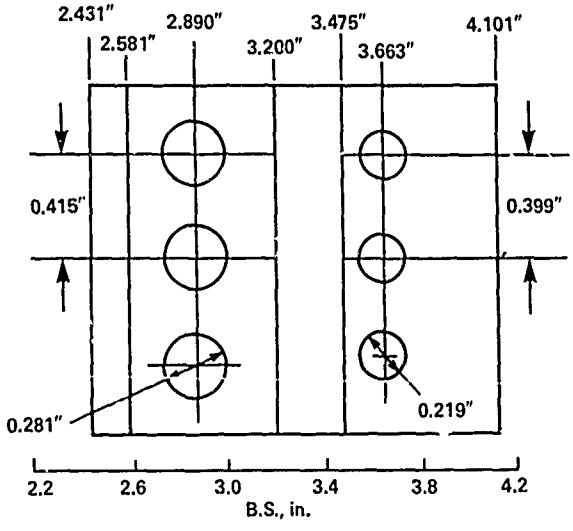
Appendix A--Model Properties

The three cases examined in this paper are from an experiment originally reported in Ref. 1. The experimental model properties in this appendix are taken from that reference with the exception of the tabulated mass and stiffness properties in Tables 3 to 6 which have not been reported

Table 3 Calculated Mass and Stiffness Properties of Lead-Lag Flexure[a]

BLADE STATION in.	WEIGHT lb_m/in.	EI_f 10^6 lb·in^2	EI_c 10^6 lb·in^2	GJ 10^6 lb·in^2	I_ρ lb_m·in^2/in.
2.431	0.422	5.18	5.18	3.93	0.101
2.581	0.422	5.18	5.18	3.93	0.101
2.581	0.0682	1.11	0.179	0.116	0.0110
2.750	0.0682	1.11	0.179	0.116	0.0110
2.791	0.0398	0.756	0.0102	0.116	0.0110
2.890	0.0266	0.597	0.00701	0.116	0.0110
2.989	0.0398	0.756	0.0102	0.116	0.0110
3.030	0.0682	1.11	0.0179	0.116	0.0110
3.200	0.0682	1.11	0.0179	0.116	0.0110
3.200	0.0292	0.477	0.00141	0.00139	0.00155
3.225	0.0097	0.159	0.0000521	0.00139	0.00155
3.450	0.0097	0.159	0.0000521	0.00139	0.00155
3.475	0.0292	0.477	0.00141	0.00139	0.00155
3.475	0.0682	1.11	0.0179	0.114	0.0110
3.553	0.0682	1.11	0.0179	0.114	0.0110
3.585	0.0451	0.857	0.0118	0.114	0.0110
3.663	0.0357	0.745	0.00935	0.114	0.0110
3.741	0.0451	0.857	0.0118	0.114	0.0110
3.773	0.0682	1.11	0.0179	0.114	0.0110
4.101	0.0682	1.11	0.0179	0.114	0.0110

a MAT'L – 17-4 PH STAINLESS; $\rho = 0.282$ lb_m/in^3, $E = 29 \times 10^6$ lb/in^2, $G = 11 \times 10^6$ lb/in^2.
b AXIS OF SYMMETRY COINCIDENT WITH 0.25c

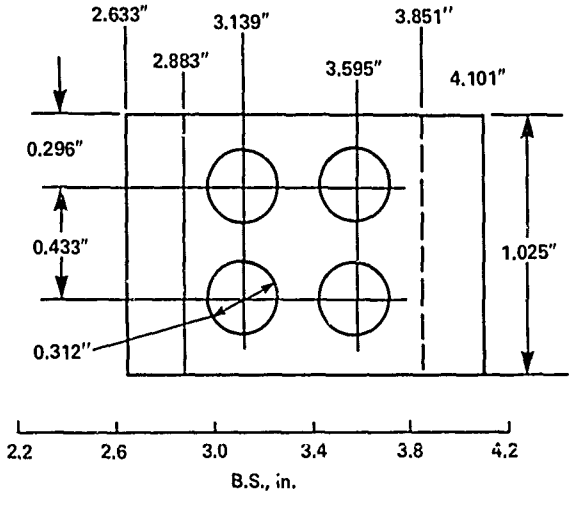


LEAD-LAG FLEXURE

Table 4 Calculated Mass and Stiffness Properties of Side Beams[a]

BLADE STATION in.	WEIGHT $lb_m/in.$	EI_f 10^6 lb·in^2	EI_c 10^6 lb·in^2	GJ 10^6 lb·in^2	I_θ lb_m in^2/in.
2.633	0.0535	0.468	0.298	0.0109	0.0105
2.883	0.0535	0.468	0.298	0.0109	0.0105
2.883	0.0410	0.359	0.190	0.0109	0.00493
2.983	0.0410	0.359	0.190	0.0109	0.00493
3.029	0.0234	0.269	0.109	0.0109	0.00493
3.139	0.0160	0.221	0.0745	0.0109	0.00493
3.249	0.0234	0.269	0.109	0.0109	0.00493
3.295	0.0410	0.359	0.190	0.0109	0.00493
3.439	0.0410	0.359	0.190	0.0109	0.00493
3.485	0.0234	0.269	0.109	0.0109	0.00493
3.595	0.0160	0.221	0.0745	0.0109	0.00493
3.705	0.0234	0.269	0.109	0.0109	0.00493
3.751	0.0410	0.359	0.190	0.0109	0.00493
3.851	0.0410	0.359	0.190	0.0109	0.00493
3.851	0.0613	0.537	0.220	0.0109	0.00957
4.101	0.0613	0.537	0.220	0.0109	0.00957

a MAT'L – Ti-6Al-4V ALLOY; $\rho = 0.160\ lb_m/in^3$, $E = 16 \times 10^6\ lb/in^2$, $G = 6.2 \times 10^6\ lb/in^2$.

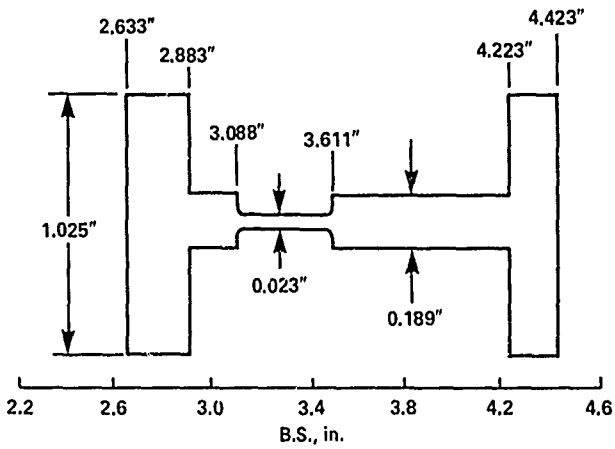


SIDE BEAMS

Table 5 Calculated Mass and Stiffness Properties of Flap Flexure[a]

BLADE STATION in.	WEIGHT lb_m/in.	EI_f 10^6 lb·in^2	EI_c 10^6 lb·in^2	GJ 10^6 lb·in^2	I_θ lb_m in^2/in.
2.633	0.276	2.49	9.20	9.92	0.114
2.883	0.276	2.49	9.20	9.92	0.114
2.883	0.0510	0.0156	1.70	1.46	0.0167
3.088	0.0510	0.0156	1.70	1.46	0.0167
3.088	0.0186	0.000759	0.621	0.0192	0.00106
3.111	0.0062	0.000028	0.207	0.0192	0.00106
3.588	0.0062	0.000028	0.207	0.0192	0.00106
3.611	0.0186	0.000759	0.621	0.0192	0.00106
3.611	0.510	0.0156	1.70	0.185	0.0167
4.223	0.510	0.0156	1.70	0.185	0.0167
4.223	0.242	2.00	0.763	3.98	0.0839
4.298	0.242	2.00	0.763	3.98	0.0839
4.298	0.368	3.54	6.62	3.98	0.0988
4.423	0.368	3.54	6.62	3.98	0.0988

a MAT'L – 17-4 pH STAINLESS: ρ = 0.282 lb/in^3, E = 29 X 10^6 lb/in^2, G = 11 X 10^6 lb_f/in^2. AXIS OF SYMMETRY COINCIDENT WITH 0.25c.



FLAP FLEXURE

Table 6 Calculated Mass and Stiffness Properties of Hub Flexure and Blade

Blade Station, in.	Weight, $lb_m/in.$	EI_f, 10^6 lb-in.^{2}	EI_c, 10^6 lb-in.^{2}	GJ, 10^6 lb-in.^{2}	I_θ, lb_m in.^{2}/in.
2.034	0.573	20.1	20.1	15.6	0.403
2.431	0.573	20.1	20.1	15.6	0.403
2.431	0.422	5.18	5.18	3.93	0.101
2.581	0.422	5.18	5.18	3.93	0.101
2.581	0.0533	1.11	0.0179	3.93	0.101
2.633	0.0533	1.11	0.0179	3.93	0.101
2.633	0.398	0.291	0.0169	0.00995	0.136
2.750	0.398	0.291	0.0169	0.00995	0.136
2.791	0.369	0.259	0.00985	0.00995	0.136
2.883	0.357	0.239	0.00706	0.00995	0.136
2.883	0.120	0.0146	0.00695	0.00990	0.0326
2.890	0.119	0.0146	0.00673	0.00990	0.0326
2.983	0.131	0.0147	0.00945	0.00990	0.0326
2.989	0.131	0.0147	0.00962	0.00990	0.0326
3.030	0.143	0.0146	0.0152	0.00990	0.0326
3.088	0.139	0.0145	0.0148	0.00990	0.0326
3.088	0.106	0.000756	0.0146	0.00656	0.0170
3.111	0.0923	0.000028	0.0138	0.00656	0.0170
3.139	0.0904	0.000028	0.0135	0.00656	0.0170
3.200	0.0945	0.000028	0.0140	0.00656	0.0170
3.200	0.0555	0.000028	0.00138	0.00116	0.00754
3.225	0.0377	0.000028	0.000052	0.00116	0.00754
3.249	0.0393	0.000028	0.000052	0.00116	0.00754
3.295	0.0569	0.000028	0.000052	0.00116	0.00754
3.439	0.0569	0.000028	0.000052	0.00116	0.00754
3.450	0.0527	0.000028	0.000052	0.00116	0.00754
3.475	0.0626	0.000028	0.00139	0.00116	0.00754
3.475	0.102	0.000028	0.0146	0.00655	0.0170
3.485	0.0978	0.000028	0.0143	0.00655	0.0170
3.553	0.0932	0.000028	0.0142	0.00655	0.0170
3.585	0.0680	0.000028	0.00976	0.00655	0.0170
3.588	0.0674	0.000028	0.00968	0.00655	0.0170
3.595	0.0699	0.000250	0.00967	0.00655	0.0170
3.611	0.0777	0.000756	0.00952	0.00655	0.0170
3.611	0.110	0.0143	0.00961	0.00944	0.0326
3.663	0.107	0.0144	0.00848	0.00944	0.0326
3.705	0.115	0.0145	0.00969	0.00944	0.0326
3.741	0.133	0.0146	0.0110	0.00944	0.0326
3.751	0.144	0.0147	0.0127	0.00944	0.0326
3.773	0.160	0.0148	0.0162	0.00944	0.0326
3.851	0.160	0.0148	0.0162	0.00944	0.0326
3.851	0.181	0.0150	0.0164	0.00944	0.0373
4.101	0.181	0.0150	0.0164	0.00944	0.0373
4.101	0.051	0.0156	1.70	0.185	0.0167
4.223	0.051	0.0156	1.70	0.185	0.0167
4.223	0.222	1.77	3.66	2.18	0.0550
4.484	0.220	1.77	3.66	2.18	0.0550
4.484	0.231	1.77	3.66	2.18	0.0550
4.613	0.231	1.77	3.66	2.18	0.0550
4.613	0.0529	1.24	1.24	0.0959	0.00247
5.078	0.0510	1.24	1.24	0.0959	0.00243
5.260	0.191	1.24	1.24	0.0959	0.0394
5.410	0.191	1.24	1.24	0.0959	0.0394
5.410	0.0243	0.0459	0.0459	0.0238	0.000728
5.469	0.0291	0.0538	0.0538	0.0288	0.000867
5.469	0.119	0.0538	0.0538	0.0288	0.0147
5.529	0.118	0.0991	0.0991	0.0616	0.0155
5.529	0.155	0.0991	0.0991	0.0616	0.0295
5.659	0.160	0.101	0.101	0.0596	0.0297
5.659	0.0447	0.101	0.101	0.0596	0.00172
5.764	0.0470	0.102	0.102	0.0568	0.00167
5.764	0.0332	0.0526	0.0526	0.0187	0.000684
5.924	0.00763	0.00228	0.0617	0.0012	0.000711
7.924	0.00758	0.00228	0.0617	0.0012	0.000869
31.924	0.00758	0.00228	0.0617	0.0012	0.000869

before. In a few cases, errors have been found in the Ref. 1 model properties, and these are corrected here.

Rotor Properties

Geometric Properties. The major rotor geometric properties have been tabulated in Table 1. Section lift and drag coefficient data for these blades have been calculated from steady bending-moment data obtained in a previous experiment.[5] Analytic functions that provide a good fit to these data are

$$c_\ell = 0.15 + 5.73\alpha$$

$$c_d = 0.0079 + 1.7\alpha^2$$

where c_ℓ is the section lift coefficient, α is the section angle of attack in radians, and c_d is the section drag coefficient. The camber of the NACA 23012 profile provides a section lift coefficient of 0.15 at zero pitch angle. A value for the section pitching moment, c_{mo}, of -0.012 is assumed.

Mass and Stiffness Properties. The design drawings of the hub were used to calculate mass, stiffness, and pitching inertias outboard of blade station 2.034 in. This blade station is the outer face of the leftmost part in the exploded view shown in Fig. 2. The mass, stiffness, and pitching inertias of the blade were obtained from Ref. 6. Properties are tabulated separately for the lead-lag flexure, side beams, and flap flexure in Tables 3 to 5. Table 6 provides the composite properties for these components as well as the blade and blade root properties outboard of B.S. 4.423 in. Running weight and pitch inertia were assumed to be additive in this table and the combined stiffness was based on a series spring representation.

Measurements were made of the mass, mass centroid, and moment of inertia for three flap-flexure blade combinations; the mean values are shown in Table 7. These measurements were adjusted or corrected to subtract the effect of the flap flexure inboard of the flap flexure centerline (B.S. 3.350 in.) and to add the contribution of the lead-lag flexure and side beams. The mass properties of the blade and hub outboard of the flap flexure centerline were calculated from Table 6 and are shown in Table 7. The difference that is seen in the blade mass is substantially greater than the differences between the three blades (±0.6%); the reasons for this are unknown. However, the calculations for the mass centroid and the moment of inertia show good agreement between the adjusted measurements, and the calculation and the difference is within the blade-to-blade variation.

There are some small differences between the mass properties of Table 7 and Table 2 of Ref. 1. In Ref. 1 the mass, centroid, and moment of inertia are defined for the blade and flap flexure outboard of the flap flexure centerline (B.S. 3.350 in.). The definition used here is based on all hub parts outboard of B.S. 3.350 in. and this includes portions of the side beams and lead-lag flexure. The calculation for rotor polar inertia used here is based on the mass properties of Table 6 and is lower than the Ref. 1 value which is considered inaccurate.

Modal Frequency and Damping. The flexure/blade combinations were removed from the model at B.S. 2.034 in. and their frequency and damping were determined individually. Mean values for three measurements are shown in Table 8. The frequencies calculated using this simple flexure and inertia representation do not account for flexibility in the blade. This flexibility will further reduce the calculated frequency, an effect that can be approximated by using the elastic coupling parameter, R.

$$\omega = \sqrt{(1 - R)}\omega_{flexure}$$

Values for R were determined in Ref. 5 from non-rotating measurements

Table 7 Hub and Blade Mass Properties

Quantity	Measured	Adjusted[a]	Calculated	Error[b]
Mass, lb_m	0.5356	0.5324	0.5199	-2.4%
Centroid of mass with respect to hub center, in.	9.562	10.01	9.984	-0.3%
Flapping and lead-lag moment of inertia with respect to B.S. 3.35 in., lb_m-in.^{2}	59.01	58.40	59.48	+1.9%
Pitch inertial, lb_m-in.^{2}	--	--	0.0898	--
Rotor polar inertia, lb_m-in.^{2}	--	--	275.3	--

[a]Flap flexure effect inboard of B.S. 3.35 in. removed (Table); effects of lead-lag flexure (Table 3) and side beams (Table 4) added.
[b]Based on adjusted measurement.

Table 8 Modal Frequency and Damping

Case	Mode	Measured Frequency, Hz	Calculated Frequency, Hz[a]	Error, %	Measured Damping, %
1,2	First flap	3.14	3.11	-1.0	--
	Second flap	32.20	--	--	0.49
	First lead-lag	6.70	6.17	-7.9	0.52
3	First flap	3.13	--	--	--
	First lead-lag	7.16	--	--	0.65

[a] $\omega = \sqrt{K/I_o}$, where $K = EI/\ell$ and is based on flexure only; I_o is from Table 7.

$R = 0.123$ for Cases 1 and 2

$R = 0.121$ for Case 3

These values produce calculated frequencies of 7.3% and 13.8% below the measurements for flap and lead-lag, respectively. This comparison suggests that the flap and chord stiffnesses tabulated in Table 6 are too low and need to be increased to properly match the measured nonrotating frequencies.

The higher blade mode-frequencies have been measured and reported in Ref. 7. The measured third flap-mode frequency was 96 Hz; the second and third lead-lag frequencies were 150 and 357 Hz, respectively; and the first torsion frequency was 342 Hz.

Body Properties

Geometric Properties. The distance from the gimbal center to the rotor plane was calculated from design drawings and is 9.470 in.

Mass and Stiffness Properties. Mass, inertia, and stiffness measurements were made on the model with the blade/flexure combinations removed leaving only the adaptor plates. The mass of the body was determined by removing the body from the stand and weighing the model with roll-axis gimbal plates attached. Separate measurements were made of the pitch-axis gimbal frame so that the measured weight could be referred to the roll axis (gimbal frame weight not included) or pitch axis (gimbal frame weight included).

The model was ballasted to locate the lateral and longitudinal c.g. positions at the gimbal center prior to weight and c.g. measurements. The vertical c.g. was determined by placing the model on its side supported by the roll flexure pivots and measuring the force required to balance the model about the gimbal center.

The model was reinstalled in the stand and connections for power, instrumentation, and so forth were made prior to making frequency measurements of the body in roll and pitch for a number of different gimbal-spring stiffnesses. The resulting frequencies are shown in Fig. 10 as a function of the square root of the effective spring stiffness. The body inertias were calculated assuming that the body acted as a single-degree-of-freedom oscillator. A linear regression fit was made to the data as shown. The spring stiffness was corrected for the offset of the model vertical c.g.

Mass and inertia measurements were adjusted to include the hub hardware inboard of B.S. 3.350 in. The measured and corrected properties are shown in Table 9 referred to both the roll and pitch axes. The data referred to the pitch axis include the effects of the gimbal frame.

Table 9 Body Mass and Inertia Properties

	Roll Axis		Pitch Axis	
	Measured	Adjusted	Measured	Adjusted
Body mass, slugs	1.26[a]	1.30	1.50[a]	1.55
Vertical c.g., in.	0.287[a]	0.574	0.241[a]	0.484
Inertia referenced to gimbal center, slug-in.^{2}	15.1	18.8	60.8	64.4

[a] Corrected for gimbal frame.

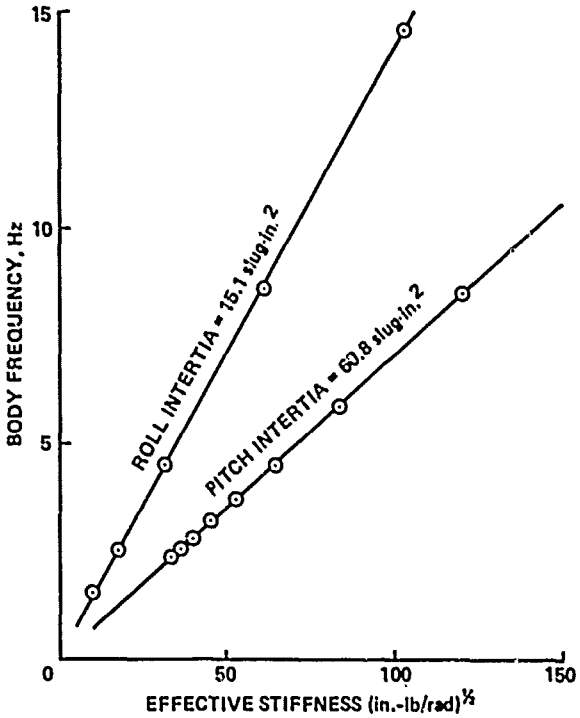


Fig. 10 Body frequency as a function of gimbal stiffness without rotor.

The stiffness of the model in roll was measured directly for the roll spring used during the experiment. The value obtained was

$$K_\phi = 985 \text{ in.-lb/rad}$$

Stiffness measurements in pitch were made with two cantilevered springs installed. However, during the experiment only one spring was used, so the stiffness may be estimated from the single-spring frequency measurements and the inertia of Table 9.

$$K_\theta = 725 \text{ in.-lb/rad}$$

Body Frequency and Damping. Measurements were made of the coupled rotor and body frequency and damping for all configurations reported in Ref. 1. Average values for body frequency and damping are

Roll: $\omega = 3.96$ Hz; $\zeta = 0.929\%$

Pitch: $\omega = 1.59$ Hz; $\zeta = 3.20\%$

Higher-mode stand frequencies were excited and measured to determine the frequency spacing with respect to the body modes. The next-higher stand frequencies were static mast--rolling and pitching at 46.0 and 45.5 Hz, respectively.

Appendix B--Experimental Data

Tables 10 through 13 give the measured rotor speed and modal frequencies and damping for Cases 1-3. For Case 1 it was possible to obtain the modal frequency and damping of the flapping modes and the progressing lead-lag mode for rotor speeds up to 50 rpm and these are given in Table 10. For Case 1 for rotor speeds above 50 rpm, modal damping and frequency were obtained for the regressing lead-lag, body pitch, and body roll modes as given in Table 11. The regressing lead-lag mode damping is shown in Tables 12 and 13 for Cases 2 and 3, respectively. These data were obtained from the experiment reported in Ref. 1. The modal frequencies and damping were measured in fixed system coordinates using the moving-block analysis[2] following a multiblade transformation from the rotating coordinates.

Appendix C--Correlation

All the theoretical predictions and experimental data for the selected cases are shown in this appendix in Figs. 11 to 21. In some cases figures from the main text are repeated here for completeness. Two formats are used for the correlation. The first format compares the theoretical predictions and experimental data individually for each mathematical model used. In this format the actual calculated points are shown as solid symbols. The curve between points was faired by the analyst involved. The data are shown as open symbols. The second format compares all the theoretical predictions on a single composite plot using the faired curve from the first format and the experimental data are shown as a stippled area. An exception to this second format is that no composite comparison is made of modal frequencies. A code is used to identify the theoretical predictions for both the individual and composite comparisons; it is explained in Table 14.

Table 10 Modal Frequencies and Damping from 0 to 50 rpm, Case 1

Ω, rpm	$\omega_{\zeta r}$, Hz	$\sigma_{\zeta r}$, sec^{-1}	$\omega_{\zeta p}$, Hz	$\sigma_{\zeta p}$, sec^{-1}	$\omega_{\beta r}$, Hz	$\sigma_{\beta r}$, sec^{-1}	$\omega_{\beta p}$, Hz	$\sigma_{\beta p}$, sec^{-1}	ω_{θ}, Hz	σ_{θ}, sec^{-1}	ω_{ϕ}, Hz	σ_{ϕ}, sec^{-1}
0	6.68	-0.184	6.94	-0.232	2.72	-0.176	3.42	-0.291	1.58	-0.323	3.95	-0.242
	6.68	-0.165	6.98	-0.152	2.72	-0.168	3.35	-0.518	1.61	-0.427	3.97	-0.284
	--	--	6.98	-0.186	--	--	3.36	-0.721	--	--	--	--
	--	--	6.94	-0.236	--	--	--	--	--	--	--	--
26	6.47	--	7.33	-0.306	2.59	-0.439	3.46	-0.756	1.58	-0.379	4.07	-0.470
	6.26	--	7.19	--	2.56	-0.426	3.37	-0.708	1.57	-0.352	4.07	-0.456
50	6.09	--	7.73	--	2.37	-0.915	4.47	--	1.56	-0.450	3.57	-0.747
	6.10	--	7.72	--	2.44	--	4.46	--	1.55	-0.443	3.53	-0.517
	--	--	7.62	--	2.47	-0.632	--	--	--	--	--	--
	--	--	--	--	2.43	-0.441	--	--	--	--	--	--

Table 11 Modal Frequencies and Damping from 100 to 950 rpm, Case 1, Continued

Ω, rpm	$\omega_{\zeta r}$, Hz	$\sigma_{\zeta r}$, sec^{-1}	ω_{θ}, Hz	σ_{θ}, sec^{-1}	ω_{ϕ}, Hz	σ_{ϕ}, sec^{-1}
100	5.30	--	1.48	-1.01	3.63	-0.498
	5.32	--	1.47	-1.11	3.64	-0.519
	5.24	--	--	--	--	--
	5.22	--	--	--	--	--
125	4.62	--	1.55	--	3.67	-0.734
	--	--	1.53	--	3.68	-0.770
150	4.28	--	1.77	-1.63	3.69	-0.780
	4.28	--	1.80	-1.69	3.67	-0.770
175	3.90	--	1.76	-1.05	3.66	--
	3.92	--	1.77	-1.07	3.66	-1.26
200	3.44	--	1.76	-1.05	3.78	--
	3.47	--	1.74	-1.02	3.79	--
	3.42	--	--	--	3.84	--
	3.45	--	--	--	3.86	--
250	2.74	-0.312	1.77	-0.890	3.73	--
	2.73	-0.311	1.74	-0.996	3.69	--
300	2.01	-0.301	1.77	-0.911	3.71	-1.20
	2.01	-0.310	1.73	-0.902	3.69	-1.22
350	1.30	-0.294	1.75	-0.881	3.70	-1.22
	1.29	-0.296	1.76	-0.958	3.67	-1.14
400	0.62	-0.273	1.76	-1.03	3.71	-1.45
	0.64	-0.295	1.74	-1.02	3.66	-1.31
500	0.75	-0.260	1.76	-0.921	3.63	-1.23
	0.74	-0.280	1.74	-0.942	3.65	-1.29
550	1.41	-0.279	1.79	-1.10	3.65	-1.26
	1.38	-0.285	1.76	-0.953	3.66	-1.31
	1.39	-0.282	1.75	-1.07	3.64	-1.20
	--	--	1.75	-1.05	3.64	-1.24
	--	--	1.76	-1.03	3.64	-1.21
580	1.77	-0.269	1.78	-0.876	3.65	-1.21
	1.80	-0.266	1.78	-0.905	3.65	-1.27
	--	--	1.78	-0.888	--	--
585	1.86	-0.227	1.82	-0.924	3.70	-1.36
	1.85	-0.239	1.81	-0.980	3.68	-1.39
	--	--	--	--	3.67	-1.34
600	2.01	-0.228	1.79	-1.27	3.71	-1.48
	2.04	-0.249	1.78	-1.22	3.69	-1.39
650	2.68	-0.249	1.81	-1.21	3.79	-1.78
	2.68	-0.255	1.82	-1.15	3.75	-1.63
700	3.31	-0.200	1.81	-1.33	3.75	-1.63
	3.33	-0.195	1.81	-1.43	3.64	--
720	3.59	-0.076	1.81	-1.52	--	--
	3.59	-0.009	1.81	-1.40	--	--
	3.59	-0.006	--	--	--	--
	3.57	-0.055	--	--	--	--
725	3.65	0.127	1.81	-1.53	--	--
740	3.80	0.325	1.87	-1.44	--	--
	3.80	0.313	1.84	-1.42	--	--
750	3.91	0.355	--	--	--	--
	3.86	0.363	--	--	--	--
	3.87	0.360	--	--	--	--
760	3.99	0.320	1.84	-1.56	--	--
	3.99	0.324	--	--	--	--
780	4.21	0.205	1.85	-1.51	--	--
	4.19	0.225	1.82	-1.59	--	--
	4.20	0.213	--	--	--	--
800	4.43	0.037	1.84	-1.73	3.94	--
	4.44	0.014	1.84	-1.73	3.93	--
	--	--	1.83	-1.77	--	--
820	4.70	-0.082	1.89	-1.52	3.95	-2.09
	4.70	-0.072	1.89	-1.52	3.95	-2.05
	4.69	-0.075	--	--	--	--
850	5.01	-0.107	1.86	-1.57	3.94	-2.06
	5.01	-0.126	1.84	-1.76	3.91	-2.20
	5.03	-0.125	--	--	--	--
	500	-0.125	--	--	--	--
900	5.64	-0.166	1.91	-2.09	4.00	-2.74
	5.64	-0.173	1.87	-2.09	3.97	-2.23
950	6.21	-0.175	1.90	-1.95	3.93	-2.71
	6.21	-0.169	1.93	-2.26	3.97	-2.52

Table 12 Regressing Lead-Lag Mode Damping, Case 2

Ω, rpm	$\sigma_{\zeta r_1}$ sec^{-1}
500	-0.666
500	-0.640
501	-0.553
549	-0.766
549	-0.721
580	-0.460
581	-0.431
600	-0.353
600	-0.373
650	-0.507
651	-0.537
700	-0.502
701	-0.425
721	-0.043
721	-0.045
740	0.378
740	0.362
748	0.486
751	0.517
760	0.580
760	0.585
770	0.611
770	0.624
779	0.636
780	0.610
790	0.585
800	0.535
800	0.539
800	0.578
801	0.591
820	0.399
820	0.374
850	0.077
850	0.088
875	-0.084
875	-0.093
899	-0.243
900	-0.231

Table 13 Regressing Lead-Lag Mode Damping, Case 3

Ω, rpm	$\sigma_{\zeta r_1}$ sec^{-1}
529	-1.10
549	-1.57
552	-1.40
591	-0.659
600	-0.710
601	-0.597
601	-0.636
610	-0.835
650	-1.25
650	-1.46
651	-1.32
673	-1.60
700	-0.819
700	-0.898
721	-0.043
721	0.005
741	0.388
750	0.462
760	0.559
770	0.542
772	0.499
781	0.480
799	0.338
809	0.205
810	0.183
830	-0.243
850	-1.12
850	-1.28
899	-1.96
900	-2.13

Table 14 Explanation of Prediction Codes

ID	Prediction Method	User
BH	DRAV21	Bell Helicopter Textron
BV	C-90	Boeing Vertol
HH_1	DART	Hughes Helicopters
HH_2	E927-1	Hughes Helicopters
SA_1	G400	Sikorsky Aircraft
SA_2	E927-2	Sikorsky Aircraft
SA_3	E927-3	Sikorsky Aircraft
AL	FLAIR	U.S. Army Aeromechanics Laboratory
NA	CAMRAD	NASA Ames Research Center

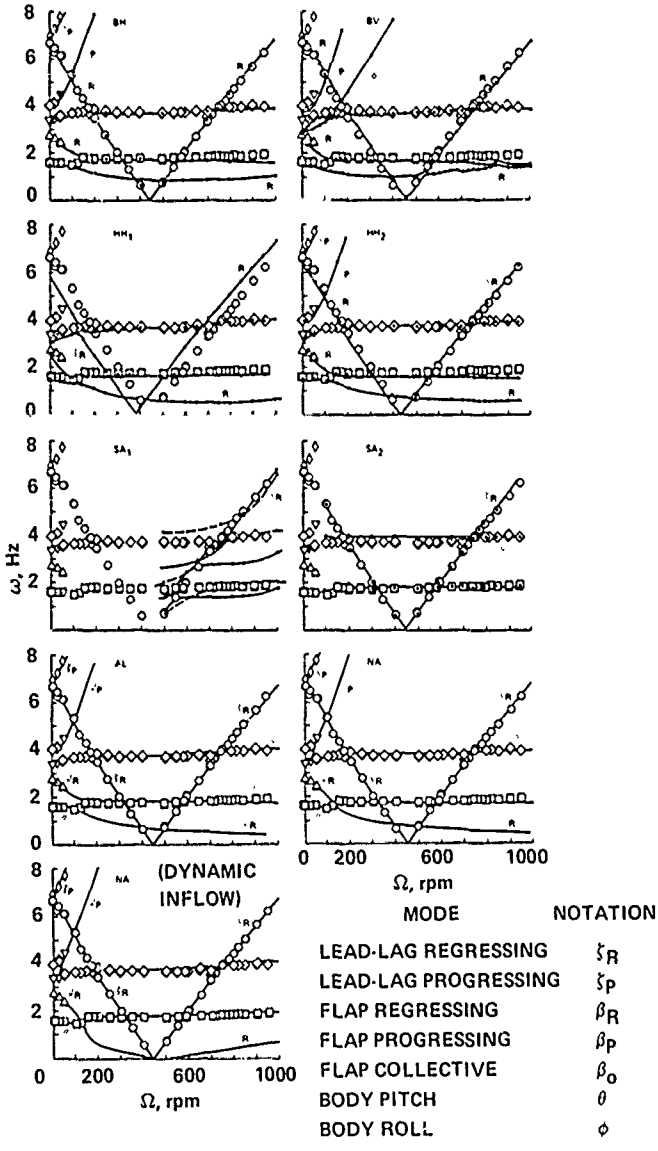


Fig. 11 Individual comparison for Case 1 modal frequencies.

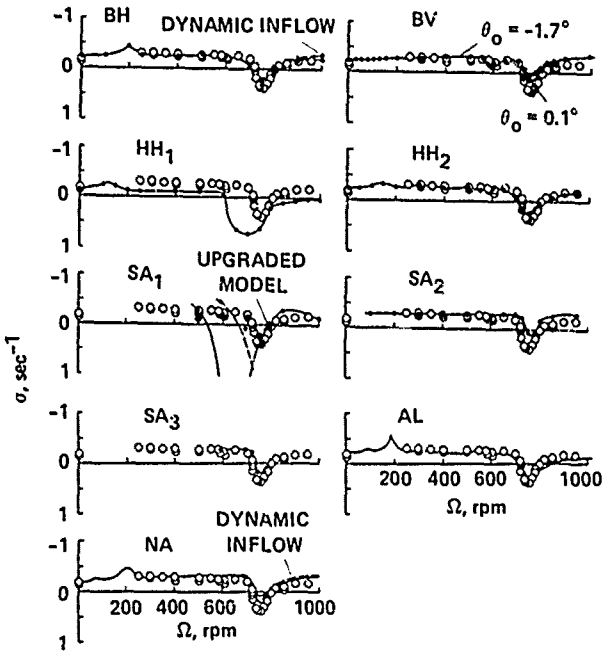


Fig. 12 Individual comparison for Case 1 regressing lead-lag damping.

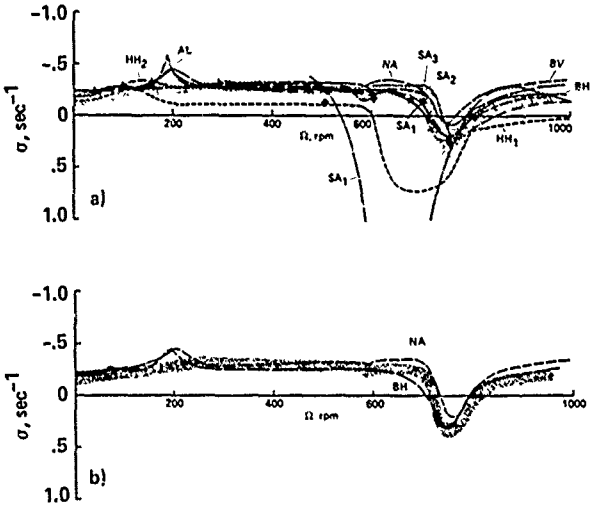


Fig. 13 Composite comparison for Case 1 regressing lead-lag damping. a) Without dynamic inflow. b) With dynamic inflow.

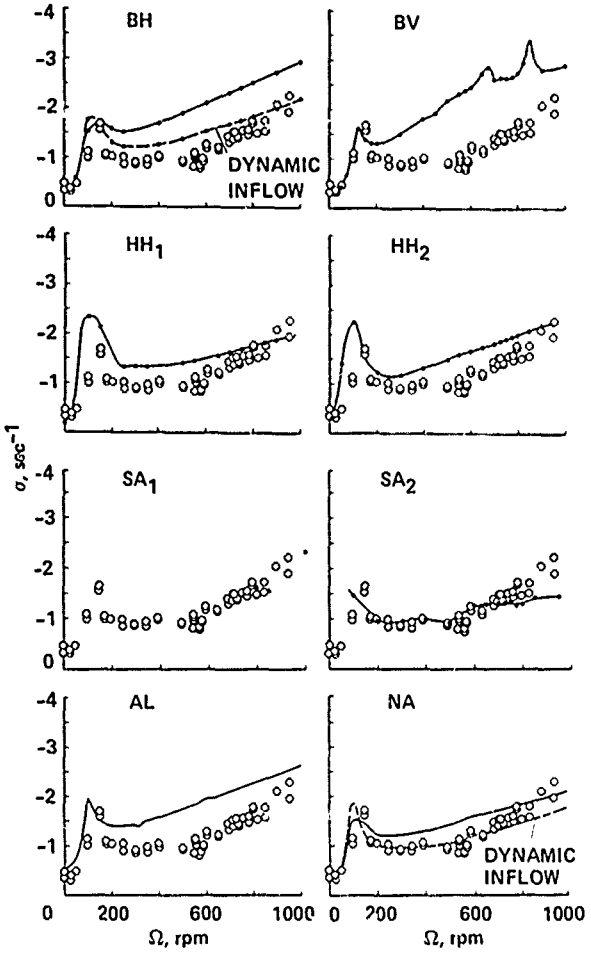


Fig. 14 Individual comparison for Case 1 body pitch-mode damping.

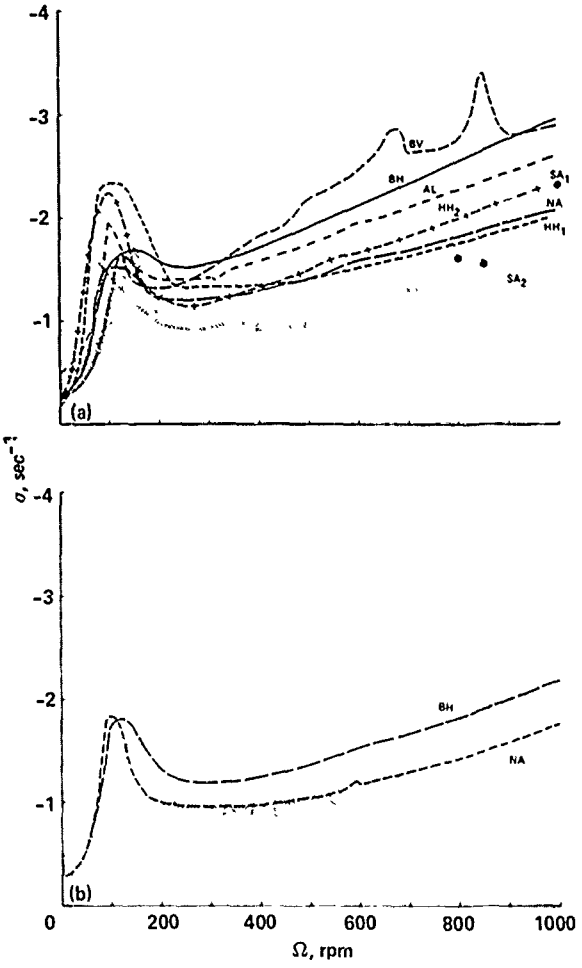


Fig. 15 Composite comparison for Case 1 body pitch-mode damping. a) Without dynamic inflow. b) With dynamic inflow.

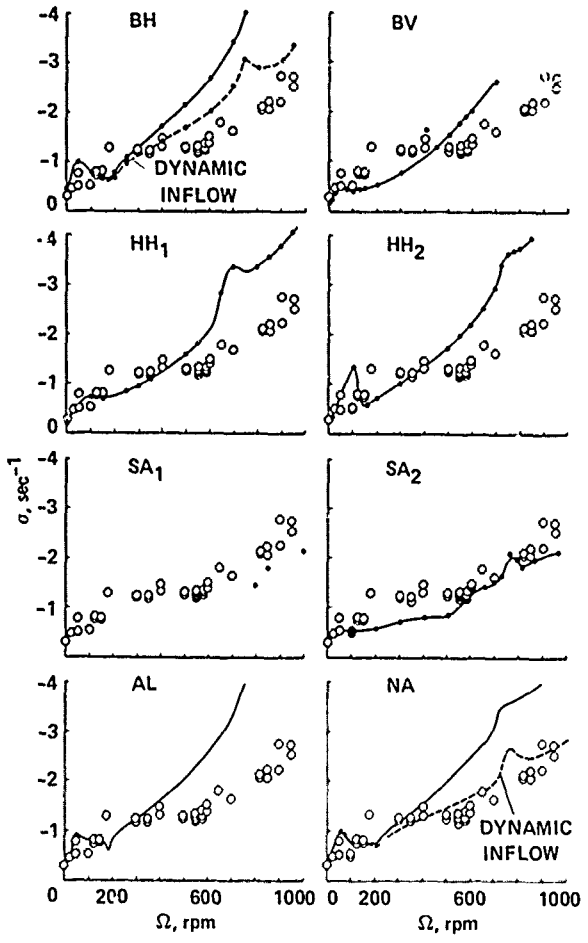


Fig. 16 Individual comparison for Case 1 body roll-mode damping.

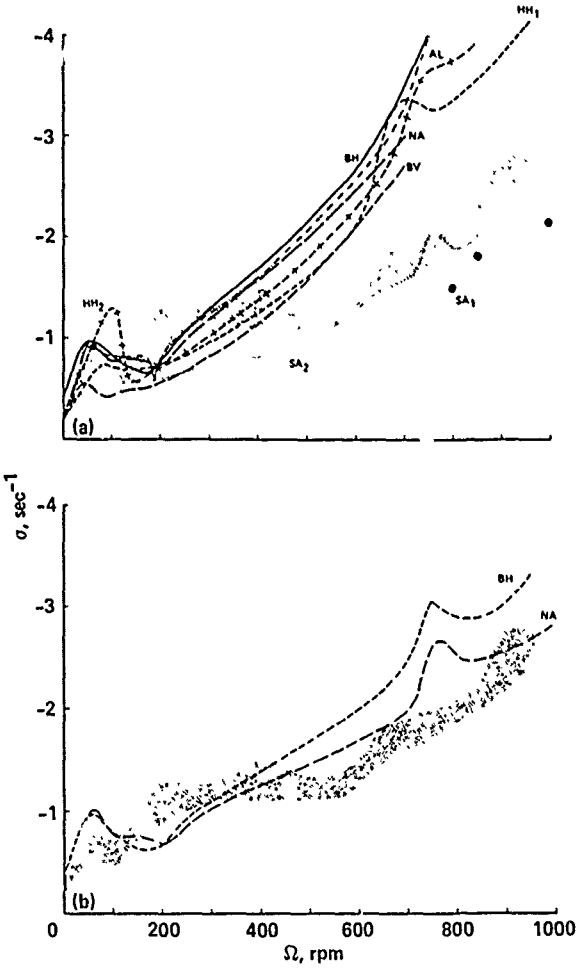


Fig. 17 Composite comparison for Case 1 body roll-mode damping. a) Without dynamic inflow. b) With dynamic inflow.

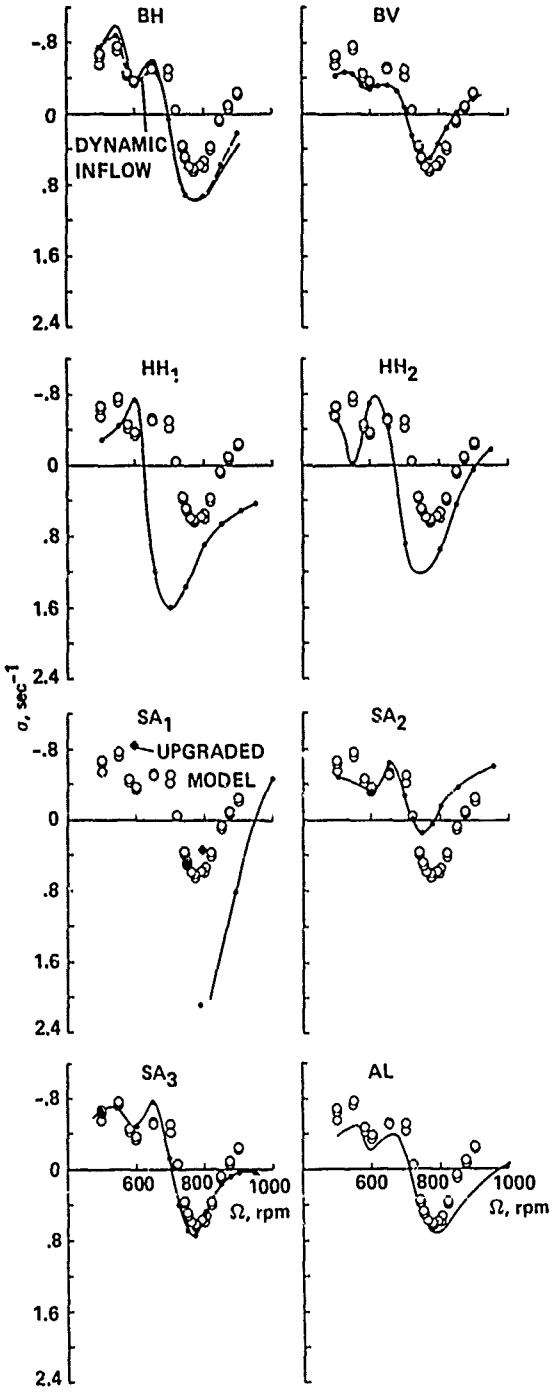


Fig. 18 Individual comparison for Case 2 regressing lead-lag damping.

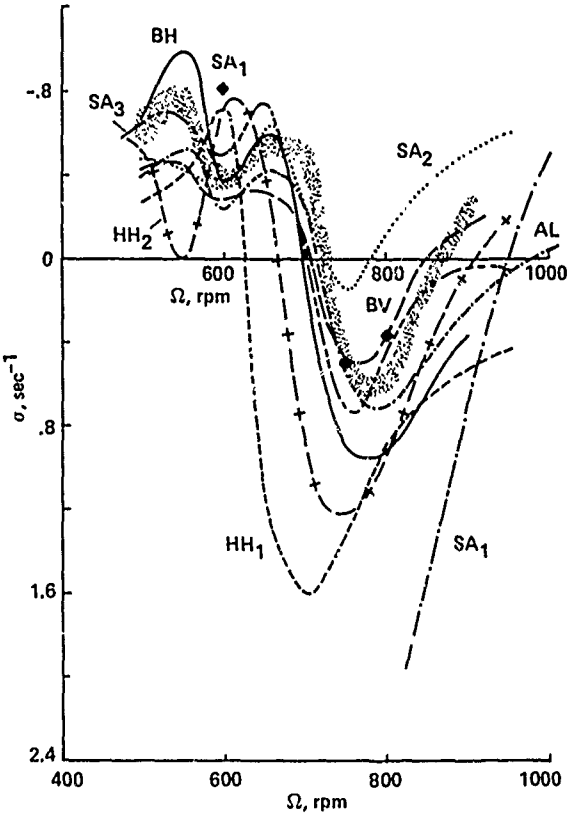


Fig. 19 Composite comparison for Case 2 regressing lead-lag damping.

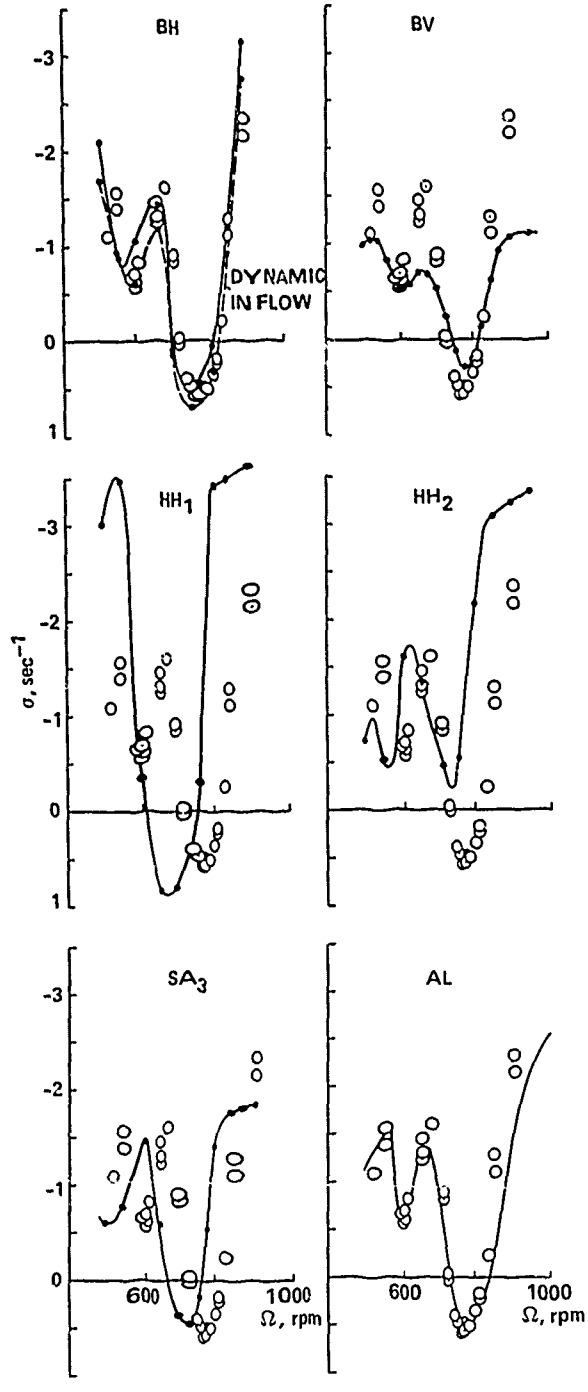


Fig. 20 Individual comparison for Case 3 regressing lead-lag damping.

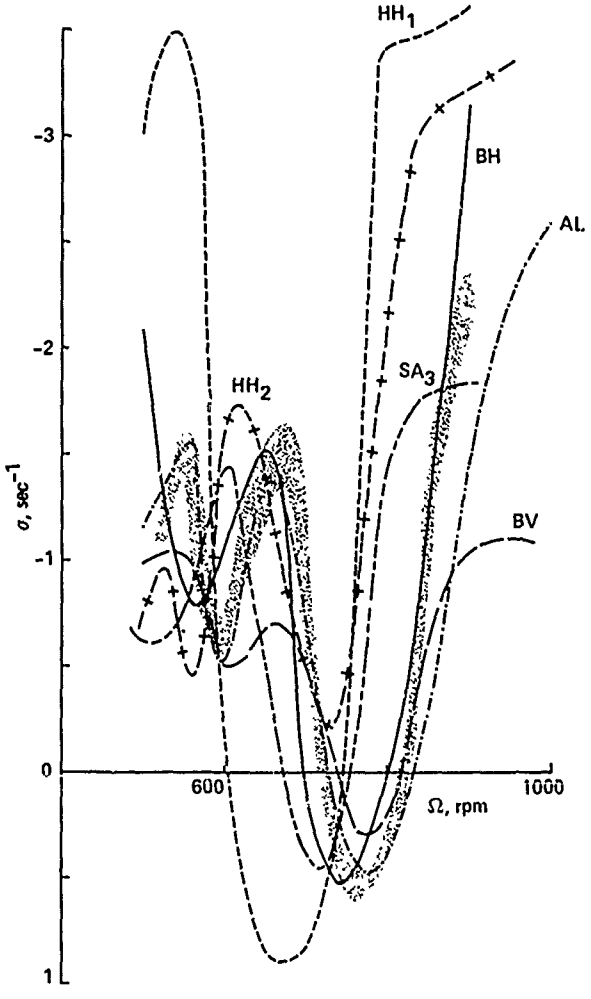


Fig. 21 Composite comparison for Case 3 regressing lead-lag damping.

DISCUSSION

A COMPARISON OF THEORY AND EXPERIMENT FOR COUPLED ROTOR-BODY STABILITY OF A HINGELESS ROTOR MODEL IN HOVER

William G. Bousman

Bob Ormiston, Session Chairman: Could you briefly go through what the conditions were for sending the data out to the members for the correlations?

Bousman: This was not a blind experiment in the sense that we did not send out just the [rotor and body] parameters and no data. By and large the data were all published in the literature. We toyed with doing something like that but we decided that, by and large, it would be too difficult. One of my conclusions is that we had so much data and we were asking for so many calculations in a relatively short period of time [and] these were so expensive to run, that there was not a lot of room to "mess up." Clearly, the results show that there was a substantial motivation to improve the correlation in many areas. I think that it would be very difficult to toy with these things. Again, we have no way of telling you whether anything was done that way or not, but it was not a double blind experiment or even a single blind experiment.

Ormiston: But you did allow recalculations to be made, and they were incorporated in this material, under certain conditions.

Bousman: Yes, the G400 calculations have been redone. Our ground rules for the original program were that we had to have the model properties that were used carefully documented; we didn't say that you couldn't change them, we just wanted it to be documented. If you said, "I made this calculation this way and it agreed with that," and "I made this calculation that way and it agreed with this," and "I think that therefore your model documentation is in error and it's preferable to use this value," that's fine as long as it was all written down. Then we asked for the computer-program input deck for all the cases run, so that we have been able to track through in a few cases, such as for Hughes where we thought that they had the droop in wrong. We went through and found out that, yes indeed, it was wrong. We wanted to have that capability.

The ground rules for new calculations were the same as the original ones and the G400 results we've seen are just points. By the way, I should make mention that all the faired curves that have been shown today and will be shown today are fairings that were done by the original analyst. Where you see points, that's because the analyst chose not to make a fairing through those points, for whatever reasons, and the G400 results are shown just as points. But they do not meet our ground rules of having been documented. We do not have the input decks for them, we have had no discussion of those analyses and I think that most of that is going to be covered by Dick [Bielawa] when he gives a paper tomorrow morning on G400. No one else has submitted new calculations, so all those are done under the original ground rules.

A COMPARISON OF THEORY AND EXPERIMENT FOR THE AEROELASTIC STABILITY OF A BEARINGLESS MODEL ROTOR IN HOVER

Seth Dawson
U.S. Army Aeroflightdynamics Directorate
Ames Research Center

Abstract

Three cases were selected for correlation from an experiment that examined the aeroelastic stability of a small-scale bearingless model rotor in hover. The 1.8-m diameter model rotor included flap, lead-lag, and torsional degrees of freedom, but no body degrees of freedom. The first case looked at a configuration with a single pitch link on the leading edge, the second case examined a configuration with a single pitch link on the trailing edge, and the third case examined a configuration with pitch links on the leading and trailing edges to simulate a pitch link with shear restraint. Analyses from Bell Helicopter Textron, Boeing Vertol, Hughes Helicopters, Sikorsky Aircraft, and the U.S. Army Aeromechanics Laboratory were compared with the data, and the correlation ranged from poor to fair.

Introduction

As a part of the Methodology Assessment, three cases were selected from the experiments reported in Ref. 1 for comparison with theoretical models. Each of the selected cases used the same blades and flexbeams; the only differences between the cases was in the pitch link configuration. Case 1 used a single pitch link on the leading edge, Case 2 used a pitch link on the trailing edge, and Case 3 had pitch links on both leading and trailing edges to simulate a pitch link with shear restraint. As the control configuration was the only variable between the three cases, it is possible to assess the capabilities of the analytical models to represent the effects of control configuration on stability, effects that are particularly important for bearingless rotor designs.

The theoretical models compared with some or all of the data included the Bell Helicopter Textron DRAV21 analysis; Boeing Vertol C-90 analysis; the Hughes Helicopters DART model; the G400 analysis and two versions of E927 used by Sikorsky Aircraft; and the U.S. Army Aeromechanics Laboratory FLAIR analysis.

The paper will briefly describe the experiment from which these data were obtained and then present the correlation. Conclusions will be made as to the quality of the agreement between theory and experiment. Appendices are provided that document the experimental model properties, tabulate the experimental data points, and show all of the correlations.

Description of Experiment

A two-bladed bearingless model rotor with a diameter of 1.8 m (5.88 ft) was tested in hover to obtain the experimental data. The experiment has been previously reported in Ref. 1. The model, which is shown in Fig. 1, was designed to match as closely as possible characteristics of the U.S. Army Aeromechanics Laboratory FLAIR program. The blades are attached to the hub using a Kevlar 49 flexbeam of rectangular cross-section that extends from an 8.7% to 19.9% radius. The exploded view of Fig. 2 shows the configuration with pitch links on the leading and trailing edge (Case 3); however, either pitch link may be removed to give a single pitch-link configuration. The pitch links are designed to minimize nonlinear structural damping by using flexural elements on either end instead of rod end bearings. Flexbeam precone and pitch angle

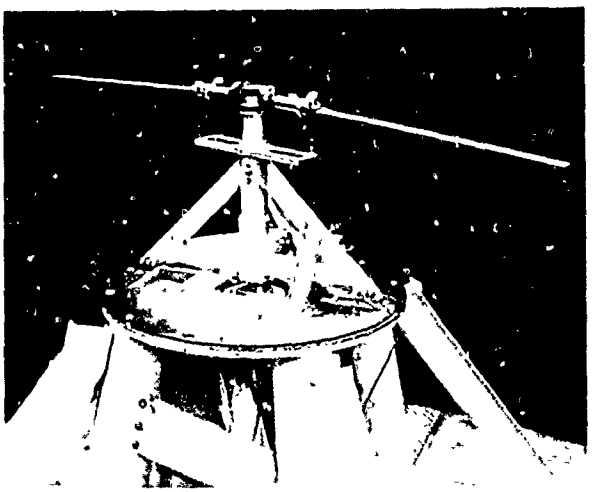


Fig. 1 Two-bladed bearingless model rotor.

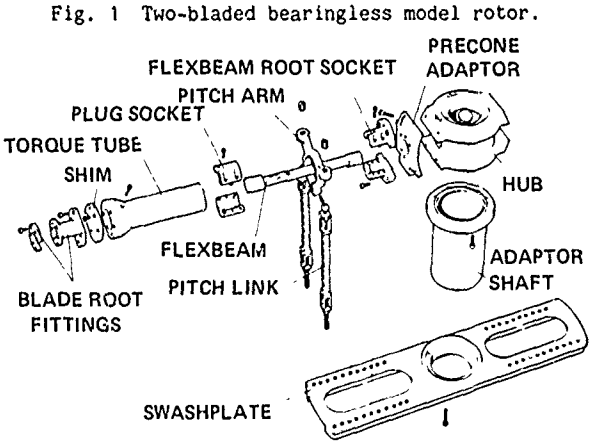


Fig. 2 Exploded view of bearingless model rotor flexbeam and hub.

with respect to the hub may be independently varied with the precone adaptor and flexbeam root socket. Blade prepitch and precone changes with respect to the flexbeam may be made independently with the blade root fittings and a shim. Pitch angle changes are made by raising or lowering the pitch links with respect to the dummy swashplate. This transmits a moment along the torque tube to the outboard end of the flexbeam, twisting the flexbeam, and introduces some flap-lag elastic coupling along with the pitch angle change. The model flexbeams on both blades are instrumented with strain-gage bridges to measure flap, lead-lag, and torsional strain. Rotor properties are given in Table 1.

Table 1 Rotor Properties

Property	Value
Radius, R, in.	35.51
Blade chord, c, in.	1.65
Solidity, σ	0.02957
Flexbeam length, in.	4.0
Flexbeam width, in.	0.32
Flexbeam thickness, in.	0.142
Flexbeam tip distance from center, in.	7.014

The rotor test stand consists of a frame that contains the driveshaft, drive sheave, and slip ring, and a lower support structure that houses the drive motor and powers the rotor through a V-belt. The upper frame is connected to the lower support structure with two flexures. A 50-lb electromagnetic shaker is used to excite the upper frame and hub at the blade lead-lag natural frequency. Two pneumatic clamps lock the upper frame following excitation of the lead-lag motion of the blades.

For each test condition the blade pitch angle was set manually by raising or lowering the pitch links. The resulting pitch angle was measured with the blade supported so that the flap bending moment on the flexbeam was zero. The rotor was then brought up to the test condition rotor speed. Transient blade lead-lag motion was induced by unlocking the pneumatic clamps to free the upper stand, oscillating the rotor hub at the fixed-system, lead-lag natural frequency ($\omega_\zeta + \Omega$) with the shaker, and once sufficient lead-lag motion was obtained, the excitation was stopped and the upper stand clamped. Frequency and damping were determined from the transient decay of the rotor differential lead-lag mode using the moving-block analysis. The blade data were recorded digitally and on analog tape. A complete discussion of the model properties is provided in Appendix A. The measured modal damping used for the correlation is tabulated in Appendix B.

Correlation

Three cases were selected from the experiment for correlation. The only difference between the cases was the location of the pitch links as shown in Fig. 3. For Case 1, a single pitch link was located on the leading edge at 10% of the flexbeam span. For Case 2, a single pitch link was located at the trailing edge and the same radial location. For Case 3, pitch links were used on the leading and trailing edges of the blade to simulate a single pitch link and vertical shear restraint. For all three configurations, the blade and flexbeam precone and pretwist angles were set to zero.

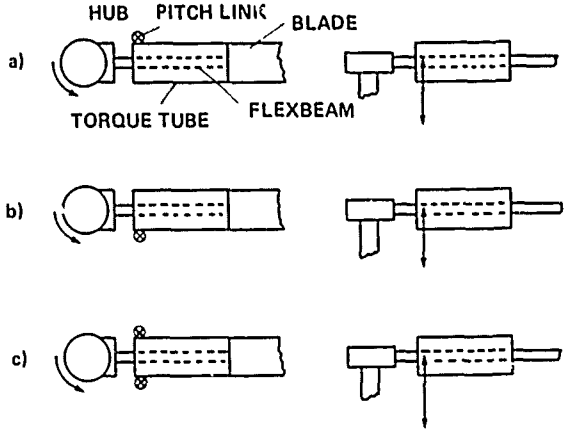


Fig. 3 Bearingless model rotor control configuration. a) Case 1--single pitch link on the leading edge. b) Case 2--single pitch line on the trailing edge. c) Case 3--pitch links on leading and trailing edges.

Two of the companies involved in the correlation effort uncovered problems with the experimental model properties documentation in setting up their analytical models. A comparison of calculated and measured nonrotating frequencies for a check case where no pitch links were mounted to the blade showed a significant underprediction of the flap and lead-lag frequencies (Table 2). It can be seen that Bell Helicopter Textron adjusted the flexbeam EI values to provide a better match of the nonrotating frequencies. However, Sikorsky changed their method of representing the flexbeam end conditions. Boeing Vertol made no change to the flexbeam properties. Hughes Helicopters did not provide nonrotating frequency calculations, and it is not known if they made any adjustments. The U.S. Army Aeromechanics Laboratory took an alternate approach in setting up the FLAIR analysis by defining the flexbeam properties for each case on the basis of a match with nonrotating frequency measurements. A comparison of nonrotating frequency measurements and calculations used for the correlation for the three cases is shown in Table 3.

Table 2 Nonrotating Modal Frequencies for a Configuration without Pitch Links

	$\omega_{\beta 1}$, Hz	$\omega_{\beta 2}$, Hz	$\omega_{\zeta 1}$, Hz	$\omega_{\theta 1}$, Hz
Measurement	4.69	24.81	10.94	19.73
Bell Helicopter Textron[a]	4.68	25.86	11.01	21.18
Sikorsky Aircraft, unadjusted[b]	4.09	22.57	8.86	19.79
Sikorsky Aircraft, adjusted[c]	4.78	25.03	10.89	19.79

[a]Flap stiffness increased 38% and chord stiffness 87% to match nonrotating frequencies.
[b]Using original tabulated stiffnesses.
[c]Adjusting tabulated stiffnesses to correct for flexbeam end effects.

Table 3 Comparison of Measured and Predicted Nonrotating Frequencies

Case		$\omega_{\beta 1}$, Hz	$\omega_{\beta 2}$, Hz	$\omega_{\zeta 1}$, Hz	$\omega_{\theta 1}$, Hz
1	Measurement	4.84	--	10.97	39.69
	Bell Helicopter Textron	4.82	25.84	11.01	45.68
	Boeing Vertol	4.38	--	8.66	--
	Sikorsky Aircraft	4.93	--	10.82	47.4
	FLAIR	4.89	--	11.03	38.76
2	Measurement	4.88	24.81	10.95	40.56
	Bell Helicopter Textron	4.83	25.84	11.01	45.73
	Boeing Vertol	4.79	--	8.99	56.34
	Sikorsky Aircraft	4.93	--	10.92	47.4
	FLAIR	4.86	--	11.10	38.57
3[a]	Measurement	6.05	24.81	10.80	173.0
	Boeing Vertol	4.22	--	8.25	--
	Sikorsky Aircraft	6.76	26.6	10.75	193.8
	FLAIR	6.02	--	11.11	179.0

[a]Bell Helicopter Textron did not predict Case 3.

Case 1

The Case 1 configuration at 1100 rpm is representative of a soft inplane rotor with a dimensionless lead-lag frequency of 0.74. The single leading edge pitch link is located radially near the root end of the flexbeam. This results in positive pitch-flap coupling (negative δ_3) and therefore the first flapping frequency is predicted to be less than 1/rev. The torsional frequency is calculated to be 2.6/rev.

Six theoretical predictions are compared with the experimental data in Fig. 4. The individual codes are keyed to the caption and the data are shown as a stippled area. Theory and data show the same behavior in general--a minimum in damping at the low pitch angles with the damping increasing with an increase in the absolute value of the pitch angle. The differences between the theoretical predictions and the data are largely seen in the change of damping with blade pitch angle and the location of the damping minimum. In this latter respect, all of the codes except Sikorsky's E927-3 predict the minimum to occur between -2° and 0° pitch, while the data show a mirror image behavior with the minimum at about +2°.

The DRAV21 predictions (BH) show a damping increase that is similar to the data, but the damping minimum occurs at about -2° instead of at +2° and the predicted minimum damping is higher than

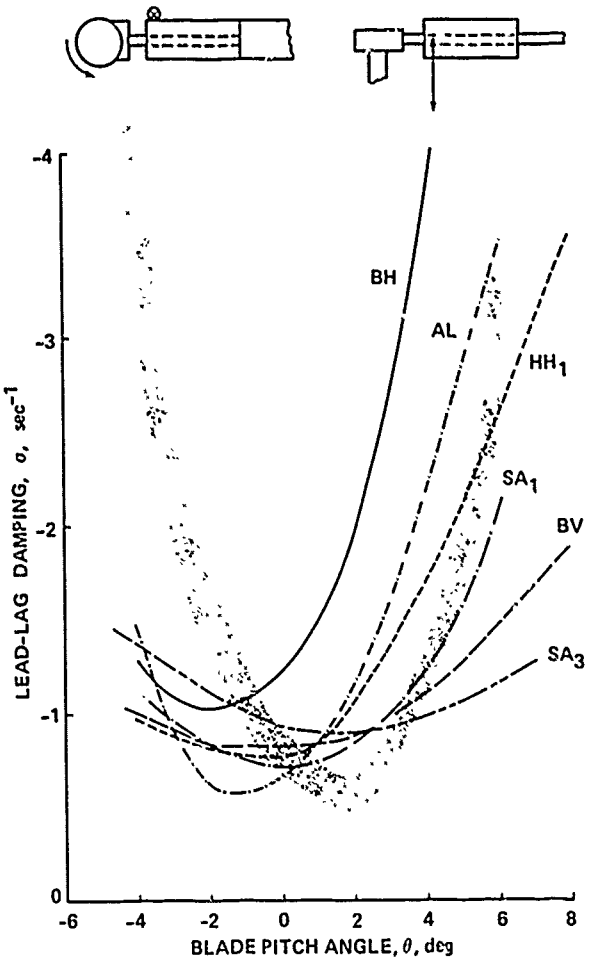


Fig. 4 Composite comparison of theory and experiment for Case 1 for lead-lag mode damping; 1100 rpm. Data are shown as stippled area; analyses used are DRAV21 (BH), C90 (BV), DART (HH_1), G400 (SA_1), E927-3 (SA_3), and FLAIR (AL).

the measurements. Overall the correlation is judged poor. The damping was also predicted using a dynamic inflow model: the results are included in Appendix C. There is perhaps a slight improvement in the agreement, but this is not considered significant.

The C-90 predictions (BV) show substantially less of an increase in damping than the measurements as pitch angle increases. The damping minimum is quite broad and occurs at about 0° rather than +2°. In general the correlation is considered to be poor.

The DART predictions (HH_1) show a reasonable agreement in the damping increase for positive pitch angles, but not at negative pitch angles. The damping minimum appears to occur at about 0° rather than +2° and the correlation is judged poor. The pitch angle shown for the DART calculations is the equilibrium or trim pitch angle that results after all steady loads have been applied. This is not directly comparable to the experimental pitch angle measurements which were made statically with the blade supported for zero flap deflection.

Sikorsky predicted the Case 1 lead-lag damping with two analyses: G400 (SA_1) and E927-3 (SA_3). In both cases NASTRAN was used to calculate the mode shapes and frequencies. The G400 code shows less of a damping increase with pitch angle than the data and predicts the minimum to occur at about 0° rather than +2°. The E927-3 predictions show relatively little variation with pitch angle; however, the damping minimum does appear to occur at about +2°. Although the G400 predictions are considered slightly better than the E927-3 calculations, the correlation for both codes is considered poor.

The Aeromechanics Laboratory FLAIR analysis (AL) shows reasonable agreement in the increase of damping with pitch angle, but as with the majority of the other codes, it shows a shift in the minimum damping to -1° or -2° rather than the measured +2°. However, unlike the other codes, FLAIR shows a fairly rapid increase in the damping at negative pitch angles and for this reason its correlation is considered poor-to-fair.

The disagreement between most of the predictions and the data in the location of the damping minimum for Case 1 is perplexing. The large variation in damping that is seen in this case allows this minimum or damping bucket to be well-defined both experimentally and theoretically. For a purely symmetric rotor it might be expected that the minimum should occur at 0°, but there are a number of asymmetries for Case 1 including blade weight, pitch-flap coupling, and the cambered 23012 airfoil that was used. For the 23012 airfoil, the zero inflow condition occurs at -1.5° although Hughes Helicopters has suggested that the damping should be symmetric about zero inflow. However, the minimum parasite drag angle occurs at a positive 1° to 2° for this airfoil and it is not clear what effect this would have on the location of the damping minimum.

Case 2

The damping as a function of blade pitch angle for Case 2 is compared with the various theoretical predictions in Fig. 5 for a rotor speed of 900 rpm. This corresponds to a measured lead-lag frequency of 0.87/rev. The single pitch link is located on the trailing edge, which results in negative pitch-flap coupling; therefore, the predicted first flap frequency is well above 1/rev. The torsional frequency is calculated to be 3.2/rev (using FLAIR). The rate of change of damping with pitch angle is much less than was seen for Case 1. Lead-lag damping data were not obtained for blade pitch angles of 0° and 2° because of a blade flutter encountered at a rotor speed of approximately 860 rpm.

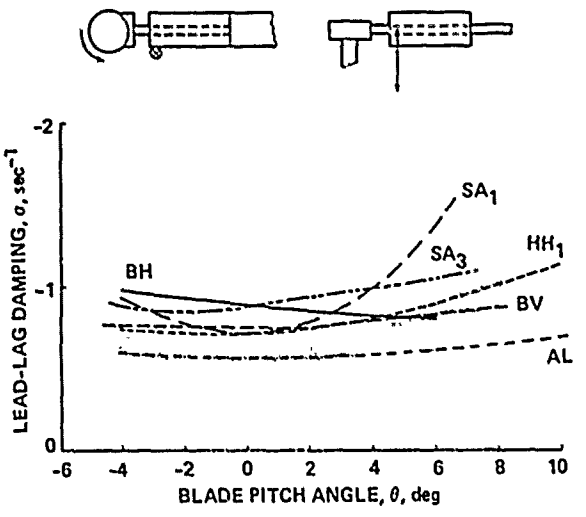


Fig. 5 Composite comparison of theory and experiment for Case 2 for lead-lag mode damping; 900 rpm. Data are shown as stippled area; analyses used are: DRAV21 (BH), C90 (BV), DART (HH_1), G400 (SA_1), E927-3 (SA_3), and FLAIR (AL).

The correlation in this case is improved over Case 1 in general. The DRAV21 analysis (BH) shows a similar damping level to the data but a different slope, and is considered poor-to-fair. The Boeing Vertol C-90 analysis (BV) shows better agreement and is judged fair. The DART analysis (HH_1) shows approximately the correct level and a similar slope and is considered fair-to-good. The DART predictions were made at 1100 rpm rather than 900 rpm and it is not known whether calculations made at the correct rotor speed would show improved agreement. The two Sikorsky analyses show a mixed effect with G400 (SA_1) showing too much effect of pitch angle and E927-3 (SA_3) showing too little variation. Both are rated poor-to-fair. The FLAIR analysis (AL) shows the best agreement at negative and low pitch angles, but does not show the damping increase at the higher pitch angles so is considered fair.

As the basis of comparison for this case was the prediction of lead-lag damping, the damping of other rotor modes was not required. However, it is interesting to note that the DART analysis showed an unstable first torsion mode at pitch angles of -4°, 0°, and +4° which is suggestive of the flutter seen on the model rotor at pitch angles of 0° and +2°. It is not known if the flutter would have been predicted if the correct rotor speed had been used for the DART calculations. In retrospect, the prediction of the experimental flutter should have been included in comparing theory and experiment for Case 2. If this had been the case, an accurate prediction of the flutter condition would result in an improved judgment of the DART analysis.

Case 3

The lead-lag damping as a function of blade angle for Case 3 is shown in Fig. 6. For this 1100-rpm condition, the measured lead-lag frequency is 0.75/rev. The location of the pitch links on the leading and trailing edges stiffens the torsional degree of freedom as compared to Cases 1 and 2 and also avoids pitch-flap coupling. This is reflected in calculated values of the first flap and torsion frequencies of 1.08/rev and 5.8/rev, respectively (using FLAIR). The damping behavior is similar to Case 2, but shows a larger variation in damping as pitch angle is changed. Bell did not provide calculations for this case as the Myklestad program, which provides blade modes for the DRAV21 analysis, is not able to properly model the double-pitch-link case.

The C-90 (BV) and DART (HH_1) analyses show very similar behavior for this case. The damping is fairly well predicted for pitch angles near zero, but neither method shows the measured damping increase for pitch angles above 4° and both are considered to be fair. The FLAIR (AL) analysis behaves very much like the C-90 and DART predictions, but is offset to a lower damping and is only considered to be poor-to-fair.

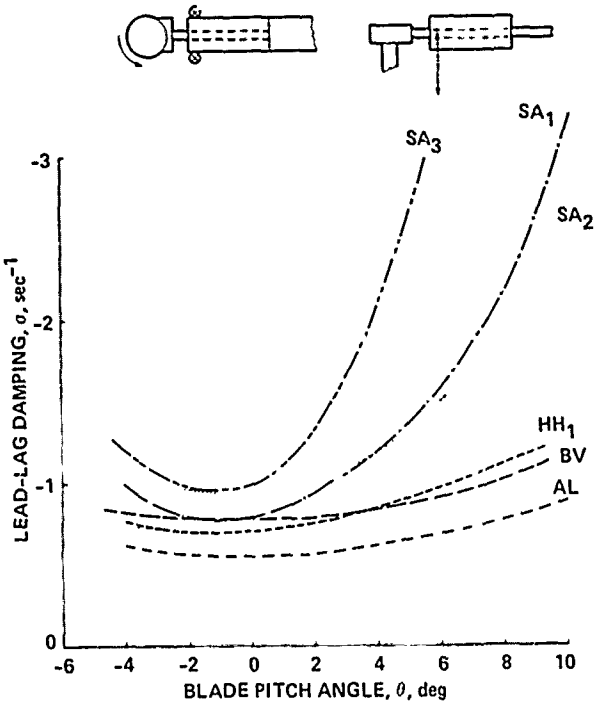


Fig. 6 Composite comparison of theory and experiment for Case 3 for lead-lag mode damping; 1100 rpm. Data are shown by stippled area; analyses used are C90 (BV), DART (HH_1), G400 (SA_1), E927-2 (SA_2), E927-3 (SA_3), and FLAIR (AL).

Sikorsky predicted the damping in this case with their G400 analysis and two versions of the E927 code. The G400 (SA_1) and E927-2 (SA_2) predictions show a behavior that is very similar to the data, but are slightly offset. The agreement in this case is judged to be fair. The E927-3 (SA_3) predictions show an excessive sensitivity to pitch angle and are considered to be poor.

Conclusions

The predictions of six analysis programs were compared with the data for three experimental data sets obtained from an experiment designed to measure the lead-lag damping of an isolated bearingless rotor in hover. Overall, the correlation varied from poor (E927-3) to fair (DART), and in this sense the use of experimental data sets did not act as a strong discriminant between the analytical methods. The fact that none of the prediction methods was able to achieve fair-to-good correlation leaves unresolved the problem of whether the major modeling difficulties lie with the theoretical or experimental efforts.

References

[1]Dawson, Seth, "An Experimental Investigation of a Bearingless Model Rotor in Hover," Journal of the American Helicopter Society, Vol. 28, No. 4, Oct. 1983, pp. 29-34.

[2]Bousman, William G., "A Comparison of Theory and Experiment for Coupled Rotor-Body Stability of a Hingeless Rotor Model in Hover," NASA CP-10007, May 1988.

[3]Silcox, H. F., "Analytical and Model Investigations of Hingeless Rotor Air Stability, Vol. 1, Section A: Structures Analysis--Rigid Blades," Report D210-10475-1A, Boeing Company, 1972.

Appendix A--Model Properties

The three cases examined in this paper are from an experiment originally reported in Ref. 1. A limited discussion of model properties was provided in that reference. The present appendix provides a substantially more detailed discussion of the model properties.

Geometric Properties

The major rotor descriptive properties are given in Table 1. The dimensional data have been obtained from design drawings. The same blade is used as in the experiment discussed in Ref. 2 and the appropriate analytic representation of the aerodynamic section properties for this NACA 23012 airfoil is:

$$C_\ell = 0.15 + 5.73\alpha$$

$$C_d = 0.0079 + 1.7\alpha^2$$

$$C_m = -0.012$$

where the angle of attack, α, is in radians.

Mass and Stiffness Properties

The design drawings of the hub, flexbeam, root hardware, and blade were used to calculate mass, stiffness, and pitching inertia outboard of blade station (B.S.) 1.400 in. This blade station corresponds to the outer edge of the cylindrical section of the hub shown in Fig. 2. The calculated properties of the flexbeam and blade are given in Table 4, and the calculated properties of the torque tube and pitch hardware are shown in Table 5. Torque tube properties are calculated inboard of B.S. 7.014 in., which corresponds to the flexbeam tip. The pitch arm is included, but not the pitch links or their ball sockets. Blade properties outboard of B.S. 8.931 in. were obtained from Ref. 3. The flexbeam and root hardware are centered on the blade quarter chord and therefore inboard of B.S. 7.994 in the center of mass and elastic axis are coincident at 0.25c. The blade outboard of B.S. 7.944 in. was designed to have the center of mass and elastic axis coincident with 0.25c as well. No measurements have been made of the blade elastic axis, but measurements of blade center of mass outboard of B.S. 7.944 in. have ranged from 0.256c to 0.266c with an average value of 0.262c.

Measurements were made of the overall mass properties of the blade and root hardware combination as shown in Table 6. The root hardware included the pitch arm but not the pitch links and a flexbeam was used that had been cut at the centerline (B.S. 5.014 in.). The mass was measured with a conventional laboratory scale and the spanwise c.g. was determined by balancing the blade on a knife edge. The moment of inertia was determined by suspending the blade from its tip and measuring its pendular frequency. These measurements were made in both the flap and chord directions; the variation was ±5.0%. The average value of the moment of inertia is shown in Table 6. Pendular measurements were also used to determine the blade/root hardware pitch inertia by suspending the blade from a point slightly behind its trailing edge. Calculations of the integrated rotor mass properties based on Tables 4 and 5 are compared to the measurements in Table 6. The agreement between calculation and measurement is excellent for the mass, but the calculated location of the blade spanwise c.g. is outboard of the measured location by a quarter of an inch (0.8% of blade radius). The calculated moment of inertia is 2.3% above the measured value, but as the measurements showed a ±5% variation, this difference is not considered

Table 4 Calculated Mass and Stiffness Properties of Flexbeam and Blade[a]

Blade Station, in.	Weight, lb_m/in.	EI_f, 10^6 lb-in.^{2}	EI_c, 10^6 lb-in.^{2}	GJ, 10^6 lb-in.^{2}	I_θ, lb_m-in.^{2}/in.
1.400	1.70	44.9	27.3	20.7	0.704
1.653	0.813	37.2	25.7	17.5	0.534
1.826	0.738	44.7	25.2	10.7	0.831
2.159	0.862	25.4	20.6	30.2	0.449
2.159	0.500	72.1	72.1	10.9	0.141
2.359	0.500	72.1	72.1	10.9	0.141
2.359	0.180	0.863	0.863	3.76	0.0169
3.014	0.180	0.863	0.863	3.76	0.0169
3.014	0.147	0.00084	0.00427	0.000066	0.0178
3.159	0.147	0.00084	0.00427	0.000066	0.0178
3.159	0.00227	0.00084	0.00427	0.000066	0.000278
7.014	0.00227	0.00084	0.00427	0.000066	0.000278
7.014	0.268	3.02	3.02	2.31	0.120
7.309	0.350	5.24	5.24	4.04	0.209
7.644	0.350	5.24	5.24	4.04	0.209
7.644	0.413	8.87	8.87	6.29	0.324
7.944	0.413	8.87	8.87	6.29	0.324
7.944	0.222	1.77	3.66	2.18	0.0550
8.005	0.220	1.77	3.66	2.18	0.0550
8.005	0.220	1.77	3.66	2.18	0.0550
8.134	0.231	1.77	3.66	2.18	0.0550
8.134	0.0529	0.124	0.124	0.0959	0.00247
8.599	0.0510	0.124	0.124	0.0959	0.00243
8.781	0.191	0.124	0.124	0.0959	0.0394
8.931	0.191	0.124	0.124	0.0959	0.0394
8.931	0.0243	0.0459	0.0459	0.0238	0.000728
8.990	0.0296	0.0538	0.0538	0.0288	0.000867
8.990	0.119	0.0538	0.0538	0.0288	0.0147
9.050	0.118	0.0991	0.0991	0.0616	0.0155
9.050	0.155	0.0991	0.0991	0.0616	0.0195
9.180	0.160	0.101	0.101	0.0596	0.0297
9.180	0.0447	0.101	0.101	0.0596	0.00172
9.285	0.0470	0.102	0.102	0.0568	0.00167
9.285	0.0332	0.0526	0.0526	0.0187	0.000684
9.445	0.00763	0.00228	0.0617	0.0012	0.000711
11.445	0.00758	0.00228	0.0617	0.0012	0.000869
35.445	0.00748	0.00228	0.0617	0.0012	0.000869

[a]Does not include torque tube, pitch arm, or pitch links.

Materials:

steel: $\rho = 0.283\ lb_m/in.^3$, $E = 29\times10^6\ lb/in.^2$, $G = 11\times10^6\ lb/in.^2$

titanium: $\rho = 0.160\ lb_m/in.^3$, $E = 16\times10^6\ lb/in.^2$, $G = 6.2\times10^6\ lb/in.^2$

Kevlar: $\rho = 0.050\ lb_m/in.^3$, $E = 11\times10^6\ lb/in.^2$, $G = 0.3\times10^6\ lb/in.^2$

Table 5 Calculated Mass and Stiffness Properties of Torque Tube[a]

Blade Station, in.	Weight, lb_m/in.	EI_f, 10^6 lb-in.^{2}	EI_c, 10^6 lb-in.^{2}	GJ, 10^6 lb-in.^{2}	I_θ, lb_m-in.^{2}/in.
3.200	0.281	12.1	26.7	3.98	0.377
3.600	0.281	12.1	26.7	3.98	0.377
3.600	0.0578	1.75	1.75	0.746	0.0193
6.872	0.0578	1.75	1.75	0.746	0.0193
6.872	0.239	2.30	2.30	0.177	0.0456
7.014	0.239	2.30	2.30	0.177	0.0456

[a]Materials:

steel: $\rho = 0.283\ lb_m/in.^3$, $E = 39\times10^6$ lb/in.^{2}, $G = 11\times10^6$ lb/in.^{2}

titanium: $\rho = 0.160\ lb_m/in.^3$, $E = 16\times10^6$ lb/in.^{2}, $G = 6.2\times10^6$ lb/in.^{2}

aluminum: $\rho = 0.101\ lb_m/in.^2$, $E = 10.5\times10^6$ lb/in.^{2}, $G = 4\times10^6$ lb/in.^{2}

Table 6 Hub and Blade Mass Properties

Quantity	Measured[a]		Calculated	Error[b]
Mass, lb_m	1.024		1.025	+0.1%
Centroid of mass, in.[c]	4.37	4.64	+6.2%	
Moment of inertia, lb_m-in.^{2}[c]	74.03		75.70	+2.3%
Pitch inertia, lb_m-in.^{2}	0.393		0.486	+23.7%

[a]Blade and root hardware including pitch arm and flexbeam outboard of B.S. 5.014 in.

[b] $\frac{\text{Calculated - Measured}}{\text{Measured}} \times 100\%$

[c]With respect to flexbeam center, B.S. 5.014 in.

significant. The calculated pitch inertia is 24% above the measurement which is a significant difference. The cause of this difference is not known.

Modal Frequency and Damping

Measurements were made of the rotor first-flap, lead-lag, and torsion-mode frequencies for each case. The measurements were made with the blades mounted on the rotor hub and average values are shown in Table 7 along with some limited measurements of damping. There is no significant effect of pitch link location between the leading edge (Case 1) and the trailing edge (Case 2). However, the addition of the second pitch link increases the first flap frequency by 25% and the torsion frequency is increased by a factor of four.

Additional nonrotating frequency measurements were made for the Case 2 configuration with the blade and root hardware cantilevered from the hub and with two pitch link configurations: a single pitch link on the trailing edge and both pitch links removed. Modal frequencies for these cases are shown in Table 8. For the case without a pitch link, it is possible to calculate approximate first-mode frequencies from beam theory:

$$\omega = \left(\frac{EI}{\ell I_\beta}\right)^{1/2} \quad \text{for flap and chord}$$

and

$$\omega = \left(\frac{GJ}{\ell I_p}\right)^{1/2} \quad \text{for torsion}$$

where the EI and GJ values from Table 4 for the flexbeam span are used to determine stiffness, I_β is the blade inertia about the flexbeam center, and I_p is the blade pitch inertia as calculated from Table 4. The calculated flap and chord frequencies in Table 8 are 11.1% and 7.3% higher than the measured values, respectively. This difference is a result of blade flexibility which is not accounted for in the frequency expressions used here and is larger in flap (blade to flexbeam ratio of EI is 2.7) than chord (ratio is 14.4) as expected. The underprediction of the torsional frequency is believed to be caused by inaccuracies in the blade pitch inertia estimate. If the measured value of pitch inertia from Table 6 is used instead of the calculated value, then the predicted frequency will be 20.25 Hz or 2.8% above the measurement.

The tabulated model properties that were originally supplied to the companies in the format of Tables 4 and 5 were based on measured elastic moduli for Kevlar rather than the standard handbook values that are shown in the tables here. The measurements of the elastic moduli were made in consideration of the sensitivity of these parameters to configuration and lay-up for composite materials. However, as discussed in the text in regard to Table 2, some of the analyses underpredicted the nonrotating frequencies, based on these original properties. Similar underpredictions were obtained using the cantilever beam formula for frequency. This difficulty led to a reexamination of the elastic moduli measurements and a rejection of them because of deflection measurement inaccuracies. The standard E and G values now used in Tables 4 and 5 are believed to provide the best estimate of the elastic moduli.

Control System Stiffness

The effective control-system stiffness was estimated from two separate measurements. The first measurement was obtained by cantilevering the torque tube at its outer end and then loading one pitch arm. The resulting value of 3840 lb/in. includes both the torsional flexibility of the torque tube and its flapwise flexibility. The second measurement was obtained by loading a single pitch link/swashplate combination vertically and then measuring its deflection. This measured value was 2690 lb/in. and is caused by both the torsional and flapwise flexibility of the swashplate. The control system stiffness is assumed to be a series-spring summation of these two measurements and, hence, is 1580 lb/in.

Appendix B--Experimental Data

Tables 9, 10, and 11 show blade pitch angle in degrees and lead-lag damping in sec^{-1} for Cases 1 to 3. These data were obtained in the experiment reported in Ref. 1. The lead-lag mode was excited and the modal frequency and damping were obtained from the transient decay using the moving-block analysis.

Appendix C--Correlation

All theoretical predictions and experimental data for the three cases are shown in this appendix as Figs. 7 to 12. Some figures from the main text are repeated here for completeness. The data and correlation with theory are presented in two formats. The first format compares the theoretical predictions and experimental data individually for each mathematical model used. In this format the actual calculated points are shown as solid symbols and the fairing between points was calculated by the experiment analysts. The data are shown as open symbols. The second format compares all the theoretical predictions and experimental data on a single composite plot. The theory is shown as the faired curve from the first format and the experimental data are shown as a stippled area.

All plots show the lead-lag damping (sec^{-1}) as a function of blade pitch angle (degrees). The sketch above each figure shows the geometry of the rotor for that particular case. A code is used to identify the theoretical predictions for both the individual and composite comparisons and is explained in Table 12.

Table 7 Flexbeam/Blade Modal Frequency and Damping

Case	Flap		Lead-lag		Torsion	
	ω, Hz	σ, sec^{-1}	ω, Hz	σ, sec^{-1}	ω, Hz	σ, sec^{-1}
1	4.84	--	10.97	0.71	39.69	--
2	4.88	--	10.95	0.70	40.56	0.50
3	6.05	--	10.80	0.75	173.0	--

Table 8 Case 2 Flexbeam/Blade Modal Frequency

Blade mode	Modal frequency with pitch link installed, Hz	Modal frequency with no pitch link installed, Hz		
	(measured)	(measured)	(calculated)	(error)
First flap	4.88	4.69	5.21	+11.1%
Second flap	24.81	24.81	--	--
First lead-lag	11.13	10.94	11.74	+7.3%
First torsion	38.28	19.73	18.24	-7.6%

Table 9 Pitch Angle and Lead-Lag Damping for Case 1 at 1100 rpm

θ, deg	σ_ζ, sec^{-1}
-4.0	-4.14
-4.0	-4.08
-4.0	-3.97
-2.0	-1.38
-2.0	-1.62
0	-0.864
0	-0.756
2.0	-0.578
2.0	-0.559
4.0	-1.19
4.0	-1.28
6.0	-3.06
6.0	-3.17
6.0	-3.32

Table 10 Pitch Angle and Lead-Lag Damping for Case 2 at 900 rpm[a]

θ, deg	σ_ζ, sec^{-1}
-4.0	-0.646
-4.0	-0.659
-2.0	-0.538
-2.0	-0.559
+4.0	-0.742
+4.0	-0.712
+6.0	-0.781
+6.0	-0.866
+8.0	-1.11
+8.0	-1.008

[a]Lead-lag damping was not measured at 0° pitch angle because of a flutter that occurred at the first torsion mode frequency.

Table 11 Pitch Angle and Lead-Lag Damping for Case 3 at 1100 rpm

θ, deg	σ_ζ, sec^{-1}
-4.0	-0.773
-4.0	-0.732
-2.0	-0.679
-2.0	-0.672
0	-0.591
0	-0.630
+2.0	-0.713
+2.0	-0.702
+4.0	-0.914
+4.0	-0.893
+6.0	-1.21
+6.0	-1.17
+8.0	-1.47
+8.0	-1.56
+8.0	-1.51

Table 12 Explanation of Prediction Codes

ID	Prediction Method	User
BH	DRAV21	Bell Helicopter Textron
BV	C-90	Boeing Vertol
HH_1	DART	Hughes Helicopters
SA_1	G400	Sikorsky Aircraft
SA_2	E927-2	Sikorsky Aircraft
SA_3	E927-3	Sikorsky Aircraft
AL	FLAIR	U.S. Army Aeromechanics Laboratory

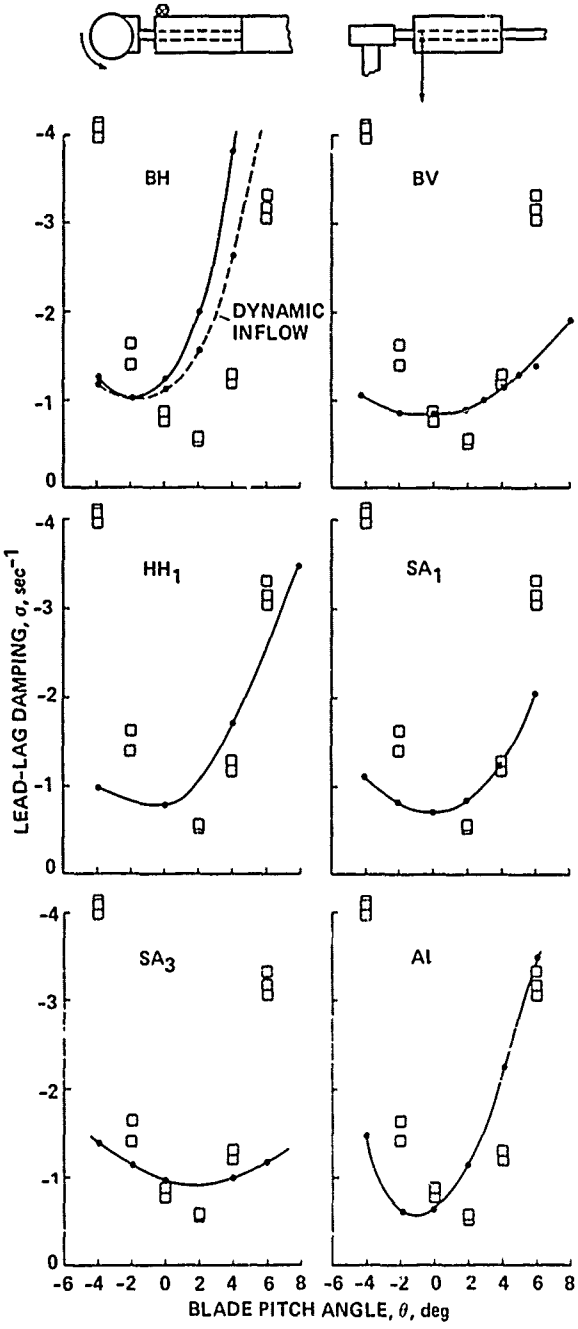


Fig. 7 Individual comparison for Case 1 lead-lag damping.

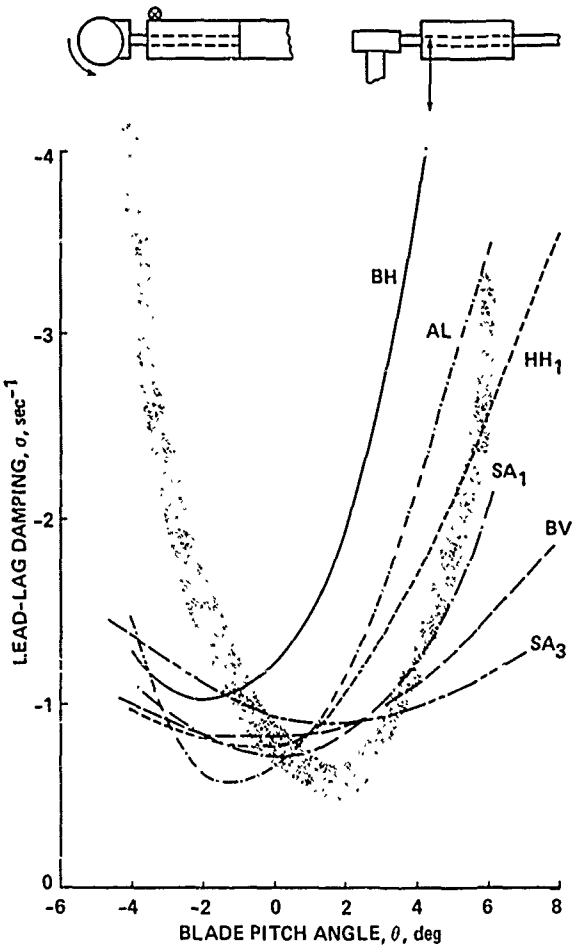


Fig. 8 Composite comparison for Case 1 lead-lag damping.

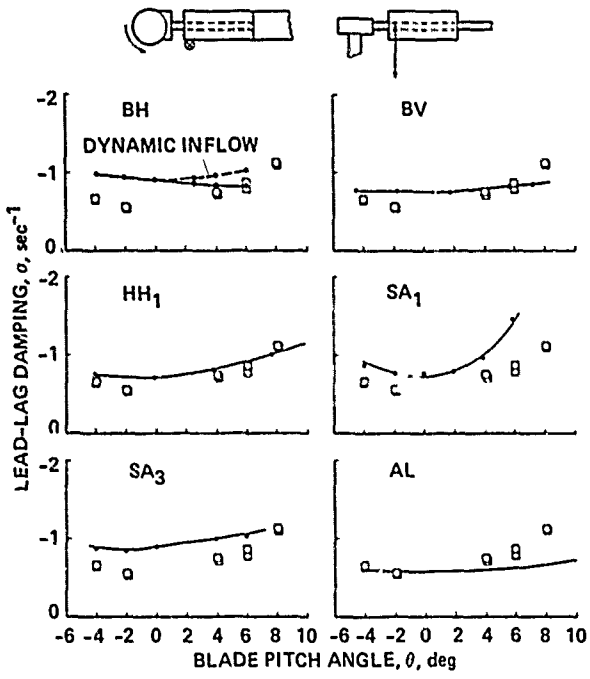


Fig. 9 Individual comparison for Case 2 lead-lag damping.

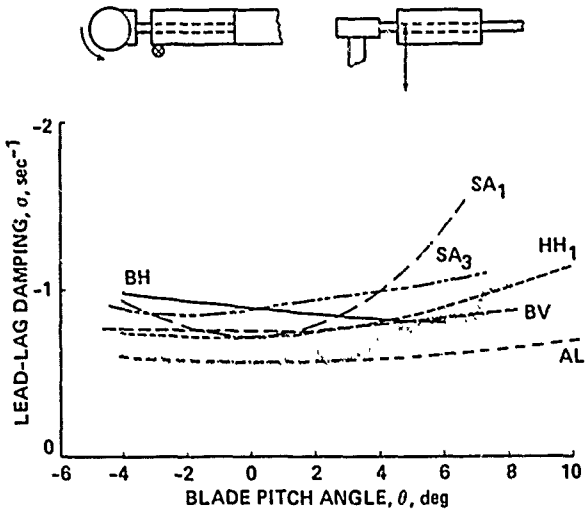


Fig. 10 Composite comparison for Case 2 lead-lag damping.

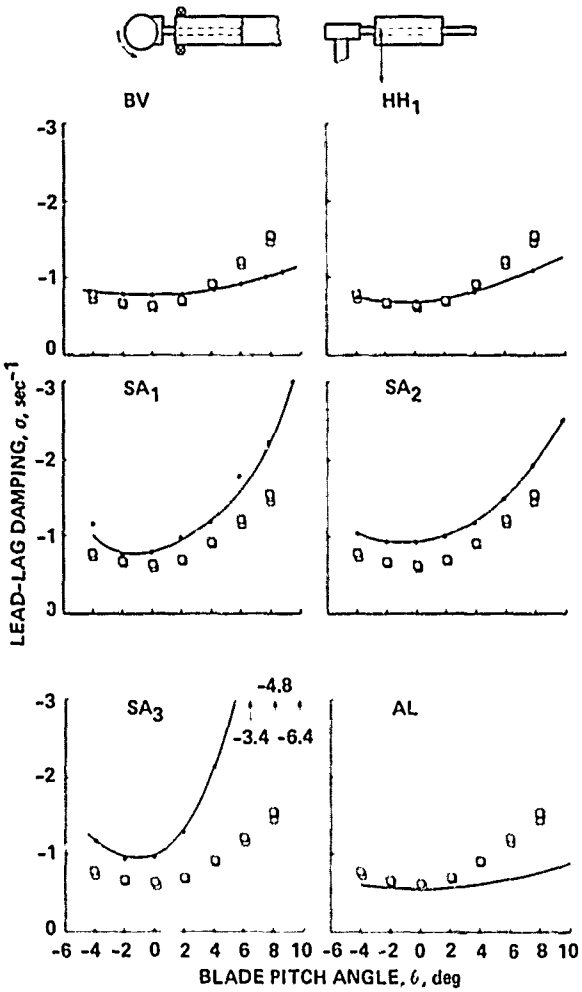


Fig. 11 Individual comparison for Case 3 lead-lag damping.

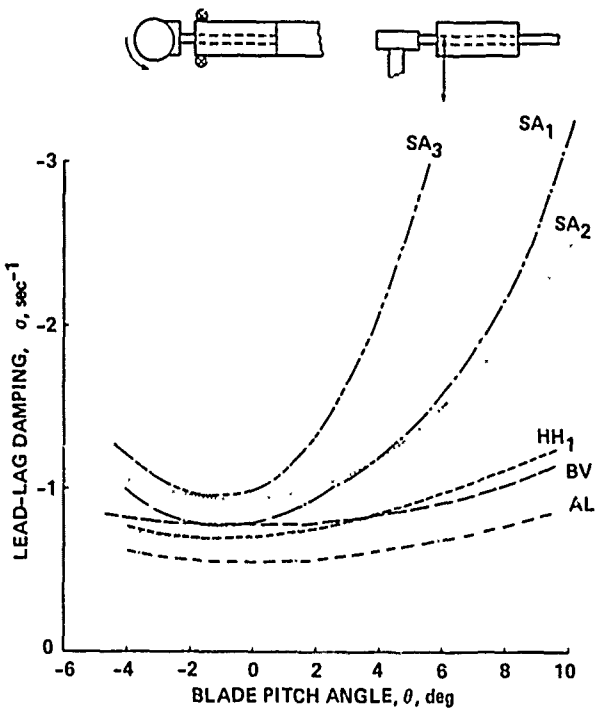


Fig. 12 Composite comparison for Case 3 lead-lag damping.

DISCUSSION

A COMPARISON OF THEORY AND EXPERIMENT FOR THE AEROELASTIC STABILITY OF A BEARINGLESS MODEL ROTOR IN HOVER

Seth Dawson

Wayne Johnson, NASA Ames: On your Case 2 that showed the flutter instability at low pitch angles, it would seem to me that your assessment of adequate correlation would not really be terribly correct. In fact, all the analyses did not predict that. Is that true? Did any of the analyses predict that instability?

Dawson: I don't know the answer to that question. I don't think so; I don't remember seeing it. For instance, Dewey Hodges' analysis doesn't predict the higher order modes which are what we think are coupling; for instance, second flap and torsion are coupling in certain places, to create these instabilities. So although they don't predict it, they don't have the higher order modes to cover that, but I'm not completely sure of the answer to your question.

Euan Hooper, Boeing Vertol: Seth, why was [Case] 2 at 900 rpm when the other two were at 1100?

Dawson: I think it had to do with the fact that we were running into a pitch-flap instability and high loads at 100 rpm for that case. I've got some test matrices that I could show you and point out where the instabilities occurred. Basically, we tried to pick the cases that were most interesting for their structural coupling rather than for the instabilities because we weren't really trying to predict the instabilities so much as just the basic damping trends here.

Gene Hammond, Applied Technology Laboratory: On the flutter type instability that you mentioned on Case 2, did you document that case in terms of the experimental data as well as you've documented the lead-lag damping cases?

Dawson: We did, [but] it's not documented as well. We made several attempts to gather as much data as we could there. They're fairly explosive instabilities, so if you're at the beginning of your test there's a natural reluctance to push yourself too far into an unstable regime because there's a considerable amount of data that you'd still like to gather with the rotor. But we do have some fairly good documentation of that and later on we could look at that.

Hammond: But with your moving block analysis you should be able to measure the subcritical damping as you approach the mode. You don't seem to be too reluctant to push the rotor into these lead-lag instabilities.

Dawson: It depends on the type of instability you're running into; some of them are obviously going rather rapidly. The torsion instabilities seem to go quite quickly and the lead-lag instabilities are spread over a wider number of rpm. If your rpm

control is only ±5 rpm and 2 rpm is enough to shoot it over the line, you really don't want to have your mechanic sitting there with his finger trembling on the rpm control because it could go rather quickly. But the pitch-flap instabilities are better documented than the torsion instabilities, I believe.

Bob Ormiston, Session Chairman: I think Bill's got a comment that may be relevant here.

Bill Bousman, Aeromechanics Lab: I want to reflect on both Wayne and Gene's comments. At the time that the assessment started we did not have any documentation at all on the flutter modes we were encountering. We knew visually that they were at the torsion mode frequency but we could not tell the analysts what they were. We could not really quantify what they were; we just knew they were a regime where we could not test for lead-lag mode stability. Although the analysts were told there was a flutter point there, none of the results indicated that they had found one. None of the theoretical results that we got indicated any kind of torsion-mode instability there.

Dawson: It's only been in the last six months that we've really started to analyze any of the flutter data, so none of that was presented at this seminar.

Bousman: Since then we have tried to quantify what actually happened there but it is not as easy as our other results, because as we approach an instability in the lead-lag mode we have a good excitation source so that we can get good subcritical mode results for lead-lag instability by oscillating the model. But for the torsion flutter, we have no way of really exciting that mode until we get to the unstable regime. So what we do is go to a slightly stable regime and just shake it as hard as we can, but we found that the scatter in those results is fairly high so it's not a really good way to do it. I think that experimentally there's a lot more work to do there in getting better experimental techniques to identify those flutters.

Ormiston: Can I get Holt's question in here?

Holt Ashley, Stanford University: It isn't a question, it's a comment. I just say I go along with about four other speakers; I'm fascinated by this lack of interest. At least all the great teachers I ever listened to told me that when you run into something unexpected in an experiment, that's where you're probably going to learn something. So I certainly hope that there are plans to understand that instability better and to attempt to predict it by appropriate methods.

Dawson: Well, it also depends on the purpose of your experiment....

Ashley: No it doesn't; that's exactly the point.

Dawson: No, if your experiment is....

Ashley: You're making an excuse, my friend.

Ormiston: Oh, we're really interested in that. We're definitely going to go back and look at it.

Dawson: I'm interested in the instabilities; I'm also interested in providing my boss with the data matrix that covers....

Ashley: I hope he's listening to the comments from the audience.

Ormiston: Speaking for myself, I'm really interested. Let's go with Gene, did you have a comment you wanted to throw out?

Hammond: I just wanted to follow up on Bill's comment with another question. Were the analysts given the torsion data for the blade that was tested?

Dawson: In terms of the inertial properties, the physical properties of the blade?

Hammond: Yes.

Dawson: Yes.

Richard Bielawa, United Technologies Research Center: I just want to underscore Holt's remarks, in that much of what we worked on was low-frequency phenomena that really didn't exercise any of our more high-powered methodology. It was not unsteady aerodynamic phenomena that we were typically looking at. I think that if we could define some instability instances where we really had to stretch the analysis to employ a lot of these new methodologies that we've worked so hard on, that in itself would be a very valuable contribution to this effort.

Ormiston: I've got to put in one comment of my own, take my prerogative here. I think we've stretched the analyses quite a bit on some very simple problems for some fairly simple configurations, and that really is surprising to a lot of us.

I've got to make a couple of comments in defense of the speaker. The boss didn't say he had to go and investigate the torsion instabilities, but we did want to get some particular data. There's a great deal of difficulty in running these kinds of experiments and making them come out right, even for a limited set of objectives. That's got to be a first concern. As far as the correlation and the interest in these kinds of instabilities and what it means for these analyses and future predictions, there's absolutely no question about it. If we can keep on with this, and we hope we can do this kind of research, we'll continue to investigate those and give you more challenges to predict with your analyses. Okay, back to you--Bill?

Bill Warmbrodt, NASA Ames: In your experiment you expressed the fact that you really didn't have a knowledge of the operating condition of the blade in terms of blade pitch under load, you only had a static measurement. In your future experiments do you intend to try and better understand what the operating condition of the rotor is?

Dawson: Yes, we've actually done a correlation where we've measured the pitch angle, basically at the end of the flex beam, by using a correlation between the steady strain-gage loads, and we've done a correlation between the operating pitch angle at the end of the flex beam, for instance, with rotor rpm. The only way you can actually pick out what the actual pitch angle of the blade at the three-quarter [radius] point is, would be to get some sort of a visual sighting technique, which we have used for blade tracking. But we are working on trying to get a better correlation. With the Hughes analysis it was simply a matter of the way their analysis measures the pitch angle versus FLAIR. I designed the model to match FLAIR; in FLAIR you put the nonrotating values into the analysis. I'm sure that to get Hughes analysis to match the data more closely we can find some sort of a way of correlating for them. But for what I was interested in, at the time the experiment was made, I was trying to match it to FLAIR.

Warmbrodt: Is there any possibility of getting a thrust measurement from your rotor?

Dawson: It would be difficult, although we've thought about it. I'd have to talk to Bill Bousman or Bob Ormiston as to how much time and effort we can put into it, but it would be a much easier way of correlating the data than measuring blade pitch angle, I think, for a number of the analyses.

Dev Banerjee, Hughes Helicopters: That was going to be my follow-up comment to Bill's question. I think we won't have any inconsistency in the representation of the x-axis if we had plotted the x-axis as a thrust measure between test data and analysis. I'd like to follow up on this flutter instability. I think if the root end structure, that is, the dual load path, the flex beam, and the pitch case, are modeled adequately structurally you would see that instability. If you go back to some of the tables we have provided you on the leading and trailing edge pitch link, you would see that approximately 3-per-rev instability of the coupled second flap-torsion mode.

That instability is basically because in your torsion mode, with the single pitch link without a snubber in the design, the torsion frequency drops to about 3 per rev and you have a strong coupling between the second flap and torsion modes.

Dawson: Oh yes, it's very low. That's where those pitch flap instabilities occurred, about 2.8 to 3.0 per rev, and it was definitely a second flap-first torsion mode because that first torsion frequency is considerably lower than for the double pitch link arrangement. Its torsion frequency is something on the order of 6 or 7 per rev for the double pitch-link arrangement, Case 3.

Ormiston: Let's take one more question. We're starting to run a little long here.

Peretz Friedmann, UCLA: I was wondering, looking at these pictures of the stand, how high the rotor is above the ground in terms of rotor diameters.

Dawson: Probably about one, one and one half [diameters].

Friedmann: Then I was wondering whether the ground effect could have any influence on the aerodynamic loading, and particularly the wakes of the rotor piling up beneath the rotor? That could cause some of these high-frequency torsional instabilities. This is just a speculative question.

Dawson: You're talking about zero-inflow-type instabilities?

Friedmann: Not necessarily.

Dawson: I don't think it does, but I think that perhaps either Bob Ormiston or Bill Bousman would be more qualified to answer. My personal opinion is that there isn't a lot of ground effect interference. Dave [Sharpe] has actually done experiments where he's tried using both a ground plane and not using a ground plane and it doesn't seem to affect the data significantly, from what I can understand.

Banerjee: I have one more question I'd like to follow up on, which is really a comment. I really think that the flutter problem is caused by the geometry and the definition of the structure at the root end where you have a low-torsion-mode coupling with the second flap mode at around 3 per rev.

Dawson: So you don't feel that the ground effect is significant then?

Banerjee: It might be, but in this particular case it's the strong coupling between the flap and torsion modes that I think is causing this.

Ormiston: I am going to shut myself off here. I'll talk about that one this afternoon if I get a chance. Thank you very much, Seth; that was very stimulating.

A COMPARISON OF THEORY AND EXPERIMENT FOR COUPLED ROTOR BODY STABILITY OF A BEARINGLESS ROTOR MODEL IN HOVER AND FORWARD FLIGHT

Paul H. Mirick*
U.S. Army Aerostructures Directorate, Hampton, Virginia

Abstract

Seven cases were selected for correlation from a 1/5.86 Froude-scale experiment that examined several rotor designs which were being considered for full-scale flight testing as part of the Bearingless Main Rotor (BMR) program. The model rotor hub used in these tests consisted of back-to-back C-beams as flexbeam elements with a torque tube for pitch control. The first four cases selected from the experiment were hover tests which examined the effects on rotor stability of variations in hub-to-flexbeam coning, hub-to-flexbeam pitch, flexbeam-to-blade coning, and flexbeam-to-blade pitch. The final three cases were selected from the forward flight tests of the optimum rotor configuration as defined during the hover test. The selected cases examined the effects of variations in forward speed, rotor speed, and shaft angle. Analytical results from Bell Helicopter Textron, Boeing Vertol, Sikorsky Aircraft, and the U.S. Army Aeromechanics Laboratory were compared with the data and the correlations ranged from poor-to-fair to fair-to-good.

Introduction

As part of the Methodology Assessment, seven cases were selected from the experiments reported in Ref. 1 for comparison with theoretical models. The experiment reported in Ref. 1 was conducted by the Boeing Vertol Company as part of the U.S. Army Applied Technology Laboratory program to design, fabricate, and demonstrate by flight test the feasibility of a Bearingless Main Rotor (BMR). This experiment included both hover and forward flight testing of a 1/5.86 Froude-scale model bearingless rotor. From the extensive data on a coupled rotor/body stability that was generated, four hover test cases and three forward flight cases were selected for comparison. The cases were chosen to determine the ability of the analyses to model a bearingless rotor with differences in precone, blade droop, and flexbeam twist in hover; and to model the effects of thrust, shaft angle, airspeed, and rotor speed in forward flight.

The theoretical models compared with the data included the Bell Helicopter Textron DRAV21 analysis in hover and C81 in forward flight, the Boeing Vertol C-90 code, two versions of the Sikorsky E-927 analysis, the Sikorsky G400 code, and the U.S. Army Aeromechanics Laboratory FLAIR analysis.

This paper briefly describes the experiment from which these data were obtained and presents the correlation. Conclusions are presented as to the quality of the agreement between theory and experiment. Appendices document the experimental model properties, tabulate the experimental data points, and show all of the correlations.

Description of Experiment

As part of the U.S. Army Applied Technology Laboratory program to design, fabricate, and demonstrate by flight test the feasibility of a Bearingless Main Rotor (BMR), the Boeing Vertol Company conducted 1/5.86 Froude-scale tests of several candidate BMR configurations (Ref. 1). The testing included both hover and forward flight conditions. The hover tests were conducted to define the optimum model configuration for maximum air-resonance-mode damping. Configuration parameters which were varied to determine the optimum rotor included precone angle, blade sweep, blade first-chord frequency, and built-in pitch orientation of the root end C-beams. The optimum configuration was then tested in the Boeing Vertol wind tunnel at forward speeds up to a scale speed of 135 knots. The conditions simulated included level flight, banked turns, and climb-and-descents. This test provided an extensive data base on coupled rotor/body stability from which four hover- and three forward-flight cases were selected for correlation.

Model Description

The model used for this test is shown in Fig. 1. It consisted of a Froude-scale model rotor mounted on a rigid fuselage having pitch and roll degrees of freedom relative to the pedestal mounting. The complete model, including the drive motor and transmission, was mounted on a two-axis gimbal with ±7° pitch and ±9° roll. The model rotor diameter was 5.5 ft. A proportional (closed loop) control system equipped with a cyclic stick provided lateral and longitudinal control to fly the model in the pitch-and-roll degrees of freedom. In addition, a shaker system was installed in the cyclic control so that excitation of the model could be applied through the swashplate actuator at desired frequencies. Blade collective pitch was remotely controlled and was set initially by means of an open loop control and a pitch angle indicator. Other controls included the pedestal-mount pitch attitude, the stick trim,

*Aerospace Engineer.

and a variable incidence horizontal stabilizer to assist the operator in trimming the model in various flight conditions. Quick-acting and slow-acting (self-centering) snubbers were installed to arrest the fuselage motion divergences or to lock out body pitch-and-roll degrees of freedom. Rotor speed was controlled by the tunnel or test cell operator.

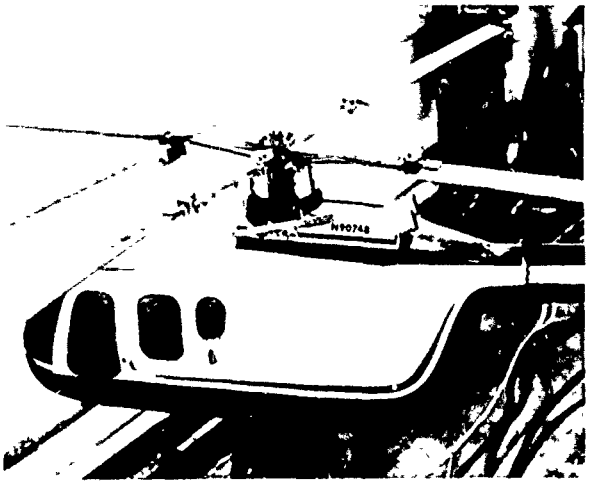


Fig. 1 1/5.86 Froude Scale Model.

Model power was supplied by a nine-horsepower water-cooled electric motor (rated at 10,000 rpm) through a 2.25:1 spur-gear reduction and then finally to the shaft through a 3:1 bevel-gear reduction.

The swashplate control system was mounted on the integral motor transmission assembly which is supported, through shear-force measuring devices, by roll pivots at the fore and aft ends of a rectangular gimbal frame. Adjustable pitch pivots on the sides of the frame provided the pitch degree of freedom and allowed variation in the center of gravity relative to the shaft axis. The model gimbal was supported through a vertical Y-frame to the pedestal base. A geometrically representative fuselage shell model of a balsa/fiberglass sandwich was suspended from the fore and aft ends of the transmission. The horizontal stabilizer was hand-adjustable in incidence.

The hub consisted of four beams made of 30% glass-filled nylon. This material was chosen to maintain geometric and aeromechanical similarity. Figure 2 shows the major components of the model hub. To study the effects of parameters variations, the hub was designed to allow beam-to-hub attachment angles of -6, 0, +6, +12° in pitch, and 0 and 2.5° in coning. The beam-to-blade juncture was designed to allow -12, -1.4, +3.6, +9.6, and +15.6° in pitch; 0 and -2.5° in blade sweep; and 0 and 2.5° in precone (negative droop).

The blade was constructed of a 1/8-in. diameter steel spar surrounded by a fiberglass-covered balsa airfoil. The blade-pitching mass moment of

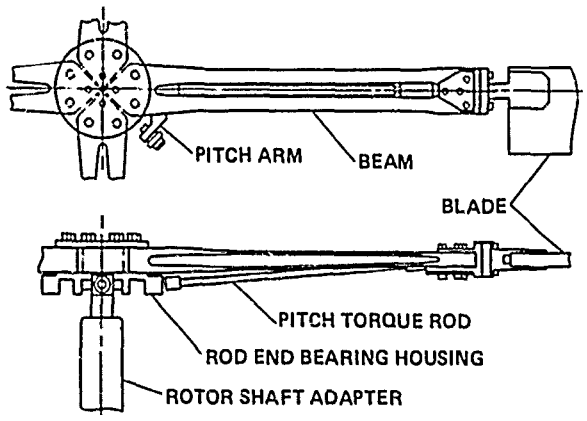


Fig. 2 Major components of BMR Froude Scale-Model Hub.

inertia together with the weight and chordwise balance was achieved through discrete distribution of tantalum wire slugs inside the balsa.

Deviations to the BO 105 blade design include exclusion of a tip overbalance weight, zero twist, and a NACA 21012 airfoil with a 1.65-in. chord and an additional trailing-edge tab of 0.17 in. over the full span of the blade. This makes a total chord of 1.82 in., which is 1/5.86-scale of the BO 105/BMR blade.

Test Procedure

The basic test procedure was to set up the desired test condition (e.g., rpm, tunnel speed, and collective pitch) and then trim the model. Trim attitude was held with the help of an SCAS system. The swashplate was oscillated in the lateral control direction for hover testing or in the longitudinal control direction for forward flight testing using a shaker set at a frequency of $(\Omega - \omega_\zeta)$. The shaker was then turned off, the transient response recorded, and the system modal damping determined by manual calculation and computer analysis.

Test Results

The model configuration was varied during the hover tests to define an optimum aeroelastically stable rotor configuration. This investigation concentrated on two aspects: 1) placing the instability boundary outside the helicopter operating rotor speed range, and 2) improving overall air resonance modal damping ratios near the normal operating rotor speed. Table 1 summarizes the configurations tested. Configuration I was selected as the baseline for the forward-flight wind tunnel testing. However, after a period of testing, it was observed that the air-resonance-damping mode had significantly increased. It was determined that the material properties of the glass-impregnated nylon had changed during testing

Table 1 BMR 1/5.86 Froude Sale Model Hover Test Configurations

Configuration	Hub-to-flexbeam pitch angle, θ_{fh}, deg[a]	Flexbeam-to-blade pitch angle, θ_{bf}, deg[a]	Flexbeam precone, β_{pc}, deg[b]	Blade droop, β_d, deg[c]	Blade sweep, Λ, deg[d]	Lead-lag dimensionless frequency @ 1028 rpm, ω_ζ
A	0	9.6	0.0	-2.5	0.0	0.68
B	-6	9.6	0.0	-2.5	0.0	0.68
C	+6	9.6	0.0	-2.5	0.0	0.68
D	-6	15.6	0.0	-2.5	0.0	0.68
E	0	9.6	2.5	0	0.0	0.68
F	+6	3.6	0.0	-2.5	0.0	0.68
G	+12	-2.4	0.0	-2.5	0.0	0.68
H	+12	-2.4	0.0	-2.5	-2.5	0.68
I	+12	-2.4	0.0	-2.5	0.0	0.65

[a]Positive, nose up.
[b]Positive, beam up.
[c]Positive, blade down.
[d]Positive, blade forward.

and therefore the Configuration I beams were replaced with the Configuration G beams.

Forward speed tests were conducted for the following conditions:

a) Airspeed sweeps in level flight at 1.0-G thrust from hover to a scaled 135 knots,

b) Thrust sweeps representing banked-turn load factors,

c) Climb and descent conditions at 1.0-G thrust,

d) Rotor speed variations, and

e) Shaft angle variations.

Selection of Test Cases

For the Methodology Assessment, seven cases from the 1/5.86 Froude-scale test were selected for correlation with the analyses. Table 2 provides the parameter varation for the cases along with the independent variables tested. Cases 1 through 4 are hover cases while 5 through 7 are for forward flight.

Case 1 was selected since it is essentially an uncoupled rotor and it should be the simplest to model mathematically. Case 2 was chosen because it has a region of neutral stability from about 900 to 1000 rpm and would provide some data on the sensitivity of the analyses in modeling this region. Case 3 was chosen to demonstrate the ability of the analyses to account for the effects of the combination of negative droop and pretwist which had shown the highest damping in the test program. Case 4 was selected to look at the effects of thrust as the independent variable. The three forward flight conditions comprise or make up the same configuration as for Cases 3 and 4. The forward flight conditions were selected to demonstrate the ability to model effects of airspeed (Case 5), shaft angle and inflow (Case 6), and rotor speed (Case 7). For Case 6, which shows the effect of climb and descent, the airspeed was selected that was the least stable for the regressing lead-lag mode. The same airspeed was used for Case 7 as well.

Correlation

The four hover cases were modeled using the Bell Helicopter Textron DRAV21 analysis, the Boeing Vertol C-90 code, the Sikorsky E927-3 Analysis, and the U.S. Army Aeromechanics Laboratory FLAIR code. The math model predictions and the experimental results for the four cases are compared in Figs. 3 through 6. Overall the DRAV21 code shows the best agreement between the experimental results and predictions.

The comparison of the predicted and measured lead-lag regressing mode damping as a function of rotor speed for Case 1 is presented in Fig. 3. The DRAV21 prediction (BH) shows fair-to-good agreement with the experimental results (shaded area). It accurately predicts the rotor speed stability boundary and closely predicts the level of damping. This analysis was performed without dynamic inflow; the same case with dynamic inflow shows only slight differences. Dynamic inflow was included in the subsequent comparisons.

The C-90 analysis (BV) closely predicts the rotor speed stability boundary and matches the trend of the experimental data, but predicts modal damping significantly higher than the test values; the agreement here is considered poor-to-fair. The reason for this is not known. However, a possible explanation is that Y-71, which provides the coupled mode shapes for the Y-71/C-60/C-90 family of programs, is not able to properly model the multiple load paths of the BMR dual-flexbeam and

Table 2 Selected Test Cases for Methodology Assessment

Case	Flexbeam precone, β_{pc}, deg	Hub-to-flexbeam pitch angle, θ_{fh}, deg	Blade droop, β_d, deg	Flexbeam-to-blade pitch angle, θ_{bf}, deg	Independent Variable
1	0	0	-2.5	-9.6	Ω varied, const thrust
2	2.5	0	0	9.6	Ω varied, const thrust
3	0	12	-2.5	-2.4	Ω varied, const thrust
4	0	12	-2.5	-2.4	thrust varied, const Ω
5	0	12	-2.5	-2.4	airspeed varied, const thrust
6	0	12	-2.5	-2.4	α_s varied, const. airspeed
7	0	12	-2.5	-2.4	Ω varied, const airspeed

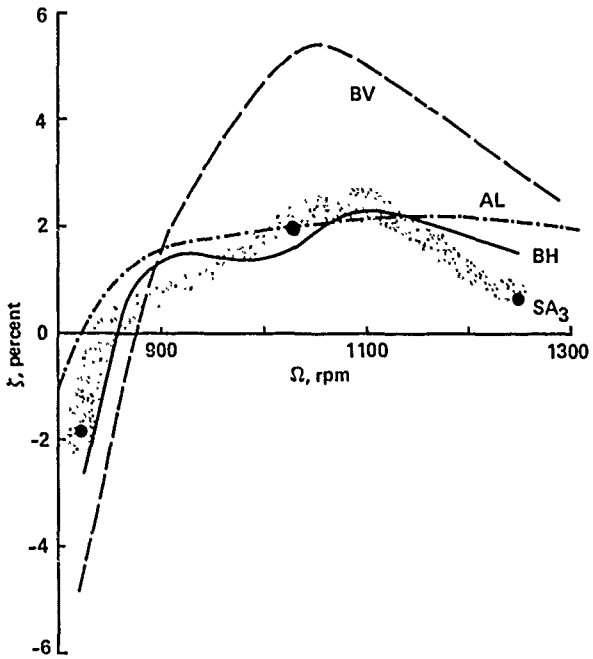


Fig. 3 Composite comparison of theory and experiment for Case 1, regressing lead-lag mode damping as a function of rotor speed for 1 g thrust; $\theta_{fh} = 0°$, $\theta_{bf} = 9.6°$, $\beta_{pc} = 0°$, $\beta_d = -2.5°$.

torque-tube design. Program Y-71 represents the dual flexbeam with a single beam approximation.

Sikorsky attempted to use both their G400 and E927-2 programs for this case, but were unable to obtain converged solutions. It was at this point that Sikorsky reintroduced torsion-bending coupling terms to the E927-2 analysis (that had been removed in the evolution of E927-1 to E927-2) to create the E927-3 version. Using this program (SA_3) three predicted values were obtained as shown by the circles. Although these three predicted points show excellent agreement with the data, the lack of additional predictions resulted in the correlation being judged as only fair.

The predictions made using the U.S. Army Aeromechanics Laboratory FLAIR model (AL) shows poor-to-fair agreement with the experimental data. The analysis slightly underpredicts the stability boundary and does not follow the decrease in stability shown in the experimental data above 1100 rpm.

Figure 4 presents the comparison of the predicted results with the experimental rotor data for Case 2. Both the DRAV21 and C-90 predicted the rotor speed stability boundary and showed good agreement with experimental data above 1050 rpm. However, these analyses fail to predict the region of neutral stability between 900 ar 1000 rpm and overall are considered to show fair-to-good correlation. The E927-3 predictions are off scale and the correlation is very poor. The FLAIR analysis fails to predict the configuration as being stable and is judged poor.

Figure 5 shows the results of the comparison of the analysis with the experimental data of Case 3. Both the C-90 and DRAV21 codes predict the stability boundary while the FLAIR analysis underpredicts this boundary by about 100 rpm. The DRAV21 analysis shows fair-to-good agreement with the experimentally measured damping while the FLAIR and C-90 codes substantially overpredict the damping, so are considered poor. There are two sets of Sikorsky data for this case. The first set, SA_3 (shown as circles), are the results obtained using the E927-3 computer program. As with Case 1, these results show good agreement with the experimental data, but were judged only fair, in part because too few points were

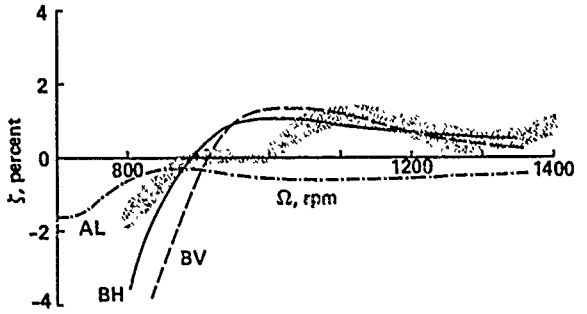


Fig. 4 Composite comparison of theory and experiment for Case 2, regressing lead-lag mode damping as a function of rotor speed for 1 g thrust; $\theta_{fh} = 0°$, $\theta_{bf} = 9.6°$, $\beta_{pc} = 0°$, $\beta_d = 0°$.

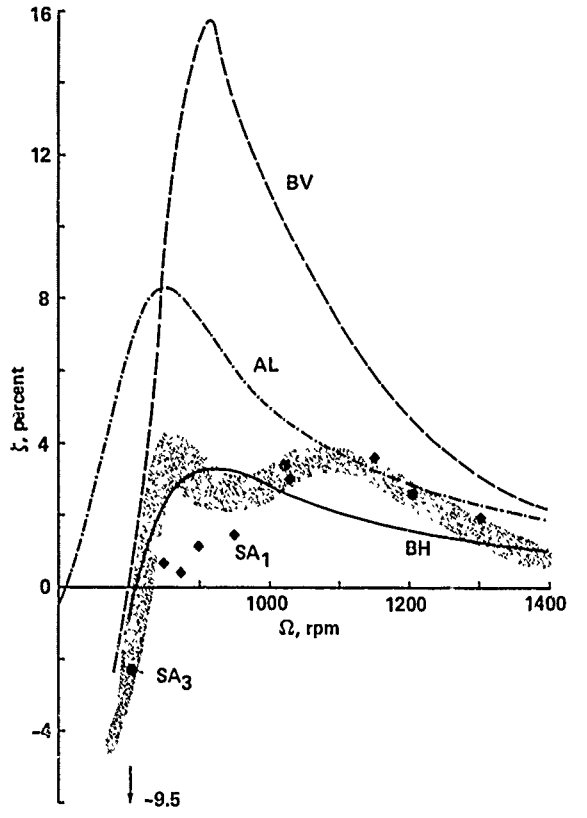


Fig. 5 Composite comparison of theory and experiment for Case 3, regressing lead-lag mode damping as a function of rotor speed for 1 g thrust; $\theta_{fh} = 12°$, $\theta_{bf} = -2.4°$, $\beta_{pc} = 0°$, $\beta_d = -2.5°$.

calculated to allow a valid assessment. The diamonds labeled SA_1 are results that were obtained by Sikorsky using the upgraded G400 analysis. When Sikorsky used their G400 analysis for this case during the contracted effort, the program would not converge. The upgraded analysis shows a substantial improvement, giving results between DRAV21 and the other codes.

The results for Case 4 are shown in Fig. 6. Unlike the other hover cases, the rotor speed was

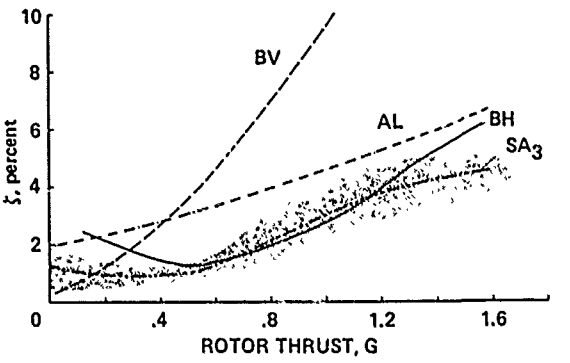


Fig. 6 Composite comparison of theory and experiment for Case 4, regressing lead-lag mode damping as a function of rotor speed for 1 g thrust; $\theta_{fh} = 12°$, $\theta_{bf} = -2.4°$, $\beta_{pc} = 0°$, $\beta_d = -2.5°$.

held constant and the rotor thrust was varied. The DRAV21 analysis shows good agreement with test data from about 0.5 to 1.2 g thrust. The lack of a proper stall representation in the aerodynamics representation is believed to be the reason for the differences seen above 1.2 g. Overall the correlation is considered to be fair to good. The C-90 analysis shows excessive sensitivity to the thrust or pitch angle and the agreement is judged as very poor to poor. The E927-3 analysis agrees quite well with the experimental results, so is considered good. The FLAIR analysis slightly overpredicts the damping level and shows similar trends, but is judged as only poor to fair.

The results of the comparison of the analyses with the three forward flight cases are shown in Figs. 7 through 9. For these cases, Bell Helicopter Textron used their C81 analysis (which was not used for the hover cases) and Boeing Vertol used their C-90 code. Sikorsky attempted to model the forward flight conditions using their E-927 analyses, but were unable to obtain stable solutions.

The results for Case 5, which show the lead-lag mode damping variation with wind tunnel speed, are shown in Fig. 7. The Bell Helicopter Textron C81 code shows good agreement with the data, both in behavior and in damping level. The Boeing Vertol C-90 analysis significantly overpredicts the damping level and the correlation is only considered to be very poor-to-poor. Sikorsky has provided a limited number of calculations with the upgraded G400 analysis. These results compare favorably with the test results.

Case 6 shows the lead-lag mode damping variation at one rotor speed and thrust as the shaft angle is varied to simulate climbs and descents. The predictions and experimental data are compared in Fig. 8. The Bell Helicopter Textron C81 prediction shows the correct damping level and damping behavior with shaft angle. The correlation is considered good. The Boeing Vertol damping is again significantly overpredicted, although the damping behavior with shaft angle is similar to the data. The correlation is judged to be poor.

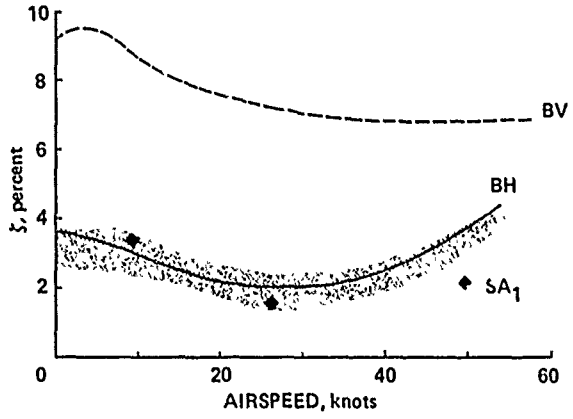


Fig. 7 Composite comparison of theory and experiment for Case 5, regressing lead-lag mode damping as a function of rotor speed for 1 g thrust; θ_{fh} = 12°, θ_{bf} = -2.4°, θ_{pc} = 0°, θ_d = -2.5°.

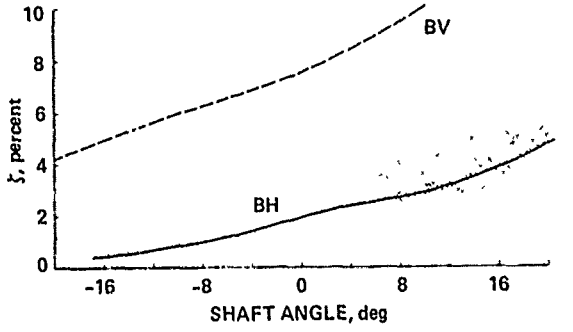


Fig. 8 Composite comparison of theory and experiment for Case 6, regressing lead-lag mode damping as a function of shaft angle for airspeed of 24.8 knots, 1 g thrust, and r = 1028 rpm; θ_{fh} = 12°, θ_{bf} = -2.4°, θ_{pc} = 0°, θ_d = -2.5°.

Figure 9 compares the measured and calculated lead-lag mode damping for Case 7 as rotor speed is varied at the minimum power speed. The damping behavior is very similar to the hover case that was shown in Fig. 5. The Bell Helicopter Textron C81 analysis shows approximately the same behavior as seen in the data, but the damping level tends to be lower and the neutral stability boundary is shifted downwards by about 40 rpm. The correlation is judged fair. The Boeing Vertol C-90 analysis also shows approximately correct behavior, but the damping level tends to be higher than the measured level. The neutral-stability rotor speed prediction is the same as for C81. Overall the correlation is considered poor-to-fair.

Conclusions

Five analyses were compared with one or more cases selected from an experiment that measured the frequency and damping of a model rotor in hover and in forward flight. The hover cases examined various couplings, while the forward flight case examined the effects of variations in

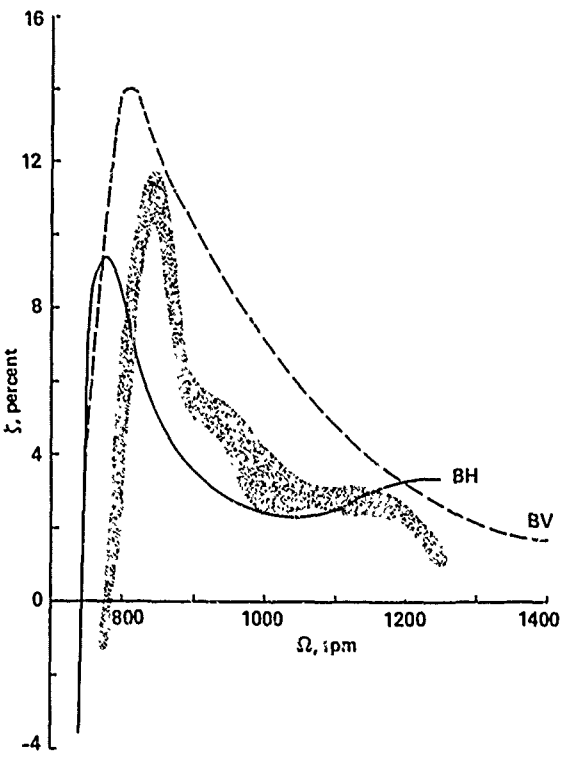


Fig. 9 Composite comparison of theory and experiment for Case 7, regressing lead-lag mode damping as a function of rotor speed for 1 g thrust and airspeed of 24.8 knots; θ_{fh} = 12°, θ_{bf} = -2.4°, θ_{pc} = 0°, θ_d = -2.5°.

forward speed, rotor speed, and shaft angle. Based on comparison of the analyses with the experimental data, the following conclusions were reached.

1) The DRAV21 analysis used by Bell Helicopter Textron gave fair-to-good correlation overall for the four hover cases. The C81 analysis used by Bell Helicopter Textron for the three forward-flight cases gave fair-to-good correlation overall.

2) The C-90 analysis used by Boeing Vertol to predict the stability for all of the cases gave poor-to-fair correlation.

3) Sikorsky Aircraft used the analysis codes G400 and E927-3 for the cases examined. The E927-3 code correlation for the hover cases shows mixed results. Limited calculations show very good agreement for two of the cases examined, but fail to adequately model precone in another hover case. Overall, the E927-3 was judged to give poor-to-fair correlation. The attempt to use the G400 analysis for the contracted effort gave unsatisfactory results. The program was upgraded later and some cases were run successfully. The calculations with the modified analysis show considerable improvement.

4) The Aeromechanics Laboratory FLAIR analysis provided poor-to-fair correlation overall.

References

[1]Chen, C., and Staley, J. A., "Aeroelastic Stability Test Results for a 1/5.86 Froude Scale Model of a Bearingless Main Rotor System on the BO 105 Helicopter," Boeing Vertol Company Rep. D210-11245-1, June 1977.

[2]Bousman, W. G., Sharpe, D. L., and Ormiston, R. A., "An Experimental Study of Techniques for Increasing the Lead-lag Damping of Soft Inplane Hingeless Rotors." Preprint No. 1035, American Helicopter Society 32nd Annual National Forum, May 1976.

Appendix A - Model Properties

The seven cases examined in this paper are from an experiment originally reported in Ref. 1. The experimental model properties in this appendix are taken from that reference.

To obtain the best representation of static and dynamic rotor aeroelastic characteristics of a full-scale helicopter, a Froude-scaled model was used. Froude scaling best maintains the proper relationship between dynamic, aerodynamic, elastic, and gravitational forces. Table 3 shows a comparison a full-scale, model-scale desired, and model-scale-actual parameters. The weight of the model was not scaled since the model had only pitch and roll degrees of freedom and only the inertias were scaled.

Rotor Properties

The rotor system tested in this experiment was a four-bladed bearingless system with a diameter of 5.5 ft which is 1/5.86 of full scale. The blades are untwisted with an NACA 23012 airfoil at the 1.65 in. chord width with an additional trailing edge tab of 0.17 in. Section lift and drag coefficient data for these blades have been calculated from steady-bending-moment data reported in a previous experiment (Ref. 2). Analytic functions that provide a good fit to these data are:

$$c_l = 0.15 + 5.73\alpha$$

$$c_d = 0.0079 + 0.17\alpha^2$$

$$c_{mo} = -0.012$$

where c_l is the section lift coefficient, α is the section angle of attack in radians, c_d is the section drag coefficient, and c_{mo} is the section moment coefficient. The camber of the NACA 23012 profile provides a section lift coefficient of 0.15 at zero pitch angle.

The beam and blade physical properties of weight, pitch inertia, flap bending EI, chord bending EI, and torsional rigidity versus blade radius are presented in Figs. 10 through 15. The

Table 3 Comparison of Full Scale and Model Properties

Parameter	Units	Model objective	Model actual	Full scale
Rotor diameter	ft	5.5	5.5	32.217
Rotor speed	rpm	1029	1029	425.0
Chord	in.	1.814	1.82	10.63
1st chord frequency	per rev	0.714	0.68	0.714
1st flap frequency	per rev	1.12	1.11	1.12
1st torsion frequency	per rev	3.66	4.45	3.66
Control system stiffness (nonrotating)	in.-lb/rad	31.9	37.8	37550.0
c.g.	% chord	25.1	24.35	25.0
a.c.	% chord	25.0	25.0	25.0
Precone (hub-beam)	deg	0	0, +2.5	0
Sweep (beam-blade)	deg	0	0, +2.5	0
Droop (beam-blade)	deg	0	0, -2.5	0
Hub and rotor weight	lbs	2.24	2.42	451.0
Pitch inertia w/rotor	lb-in.-sec^2	5.96	5.59	41174.0
Roll inertia w/rotor	lb-in.-sec^2	2.36	2.34	16304.0
Weight	lbs	22.4	38.8	4500.0

stiffness distribution of Fig. 10 is for a single beam only.

The control system stiffness of 0.664 in.-lb/deg is introduced at a blade radial station of 0.233R and includes the effects of the control system, torque tube, and flexbeam which

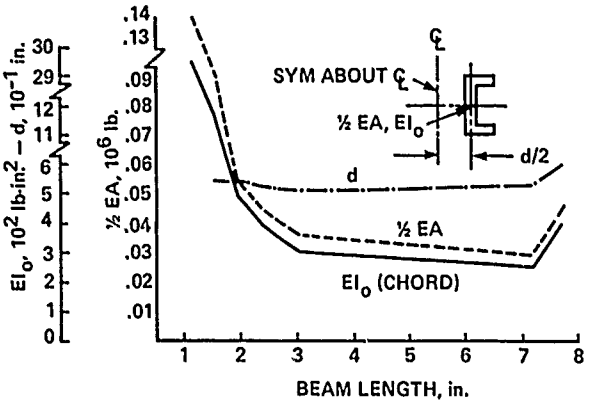


Fig. 10 Model beam chord properties; E = 0.6 × 10^6 lb/in.^{2}

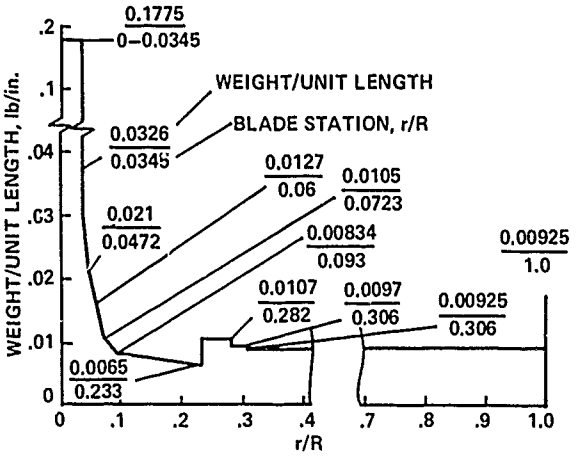


Fig. 11 Calculated model beam and blade weight/unit length (computed).

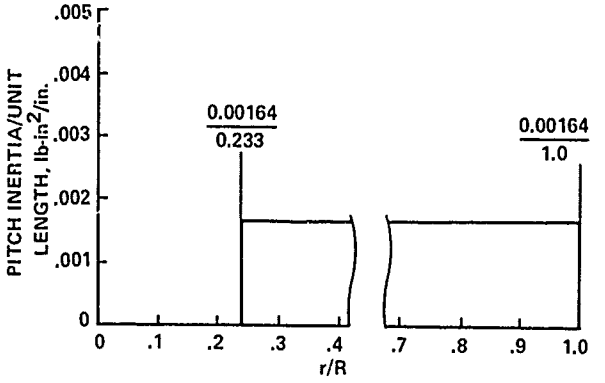


Fig. 12 Calculated model blade-pitch inertia per unit length (computed).

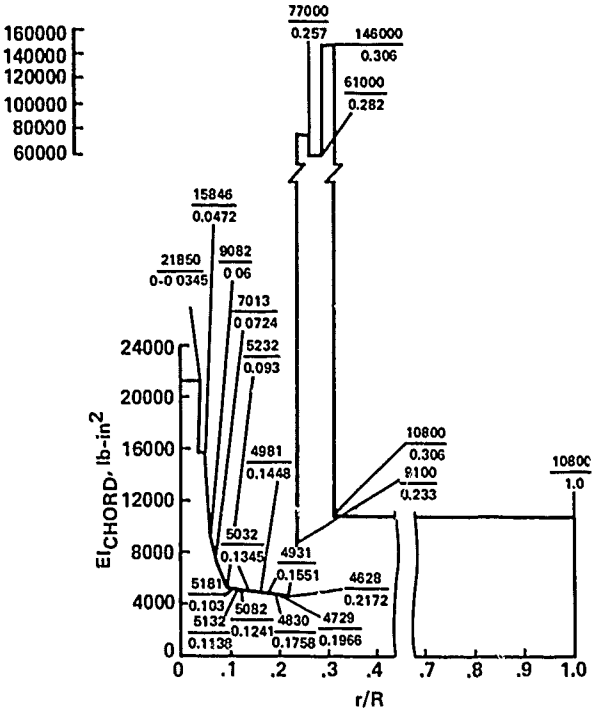


Fig. 13 Calculated model blade-chord stiffness.

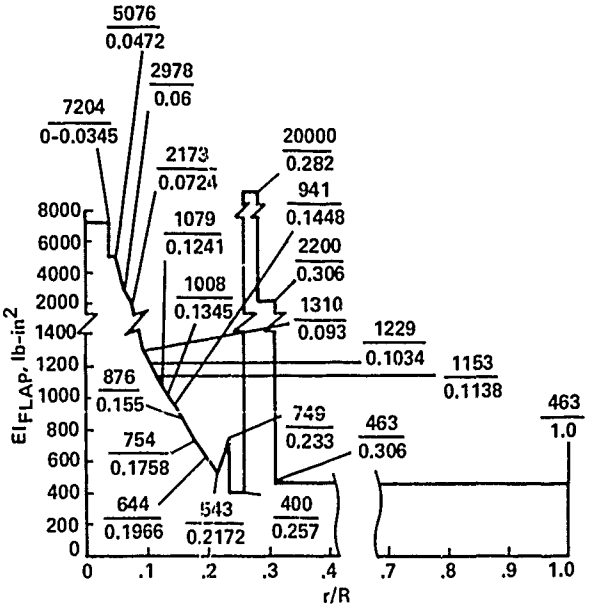


Fig. 14 Calculated model blade-flap stiffness.

were determined by twisting the blade at the flexbeam/blade attachment clevis (nonrotating). The effect of centrifugal stiffening is not included, but the calculated effect would be 0.07 in.-lb/deg at the nominal rotor speed. The torque tube is a 1/8-in. steel rod with a running mass of 0.00368 lb$_m$/in. and an EI of 360 lb-in.^{2} Its root end is pinned in flap but not chord. Figure 15 does not include the measured

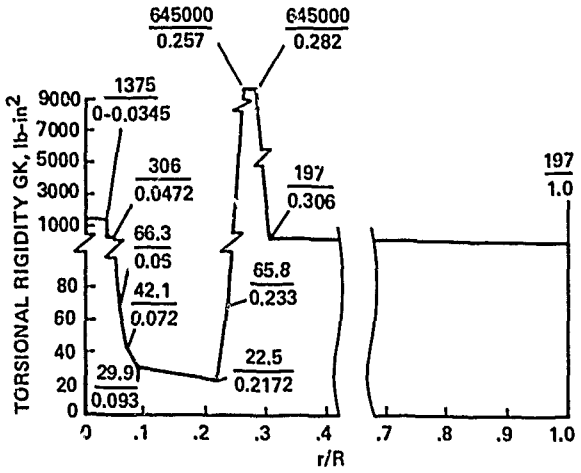


Fig. 15 Calculated model blade torsional rigidity.

model-control-system torsional stiffness of 0.664 in.-lb/deg.

Figure 16 shows a comparison between the frequencies of the 1/5.86 Froude-scaled rotor blade and the scaled-down values of the full-scale

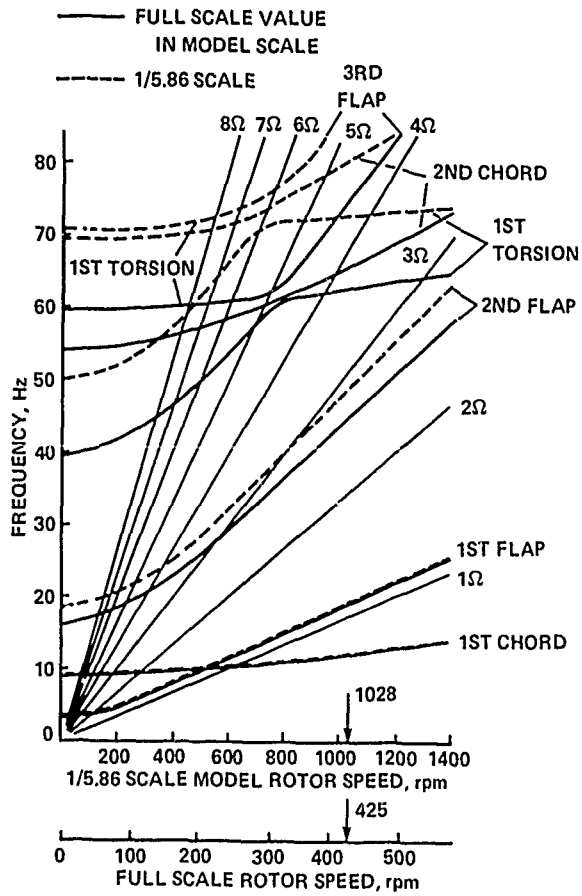


Fig. 16 Comparison of Froude Scale and corrected full-scale-model data.

BO 105 BMR. These frequencies were obtained from the Boeing Vertol Y-71 program, which is a fully coupled pitch/flap/lag analysis.

Body Properties

Prior to the aeroelastic stability testing in hover, several tests were made to determine the model fuselage inertia and damping properties. The model rigid-body inertia properties were measured with and without the rotor installed. The soft pitch and roll centering springs which center the body on the roll and pitch gimbal axes were temporarily replaced by stiffer springs so that the body roll and pitch frequencies could be determined accurately. The pitch-and-roll inertias were calculated from the nonrotating body natural frequencies and the known pitch-and-roll spring rates about the gimbal axes. The calculation for the body inertias used the following values: total rotor weight was 2.24 lb, height of the rotor above the pitch gimbal was 10.49 in., and blade flap inertia about the rotor center for one blade was 87 lb-in.^{2} Tables 4 and 5 present the results of these tests.

Appendix B - Experimental Data

The experimental data tabulated in this appendix were obtained from Ref. 1. Table 6 shows the regressing lead-lag mode damping for each test rotor speed for Case 1 at 1 g thrust in hover. This case corresponds to Fig. G-1 of Ref. 1. The data for Case 2 are shown in Table 7 and corresponds to Fig. G-18 of Ref. 1 and are also for 1 g thrust in hover. Table 8 shows the Case 3 data for 1 g thrust in hover and corresponds to Fig. G-26 of Ref. 1. The regressing lead-lag mode damping for Case 4 is shown in Table 9 for various values of thrust at a rotor speed of 1028 rpm in hover. This corresponds to Fig. G-28 of Ref. 1. Table 10 shows the lead-lag regressing damping in forward flight for various wind-tunnel-test speeds under 1 g thrust conditions for Case 5 which corresponds to Fig. G-72 of Ref. 1. The Case 6 data is shown in Table 11 which correspond to climb for positive shaft angles and descent for negative shaft angles. These data were obtained at the 24.8-knot test speed for 1-g thrust and a rotor speed of 1028 rpm. The data correspond to Fig. G-57 and G-71 of Ref. 1. Table 12 shows the lead-lag regressing mode damping as a function of rotor speed at a tunnel speed of 24.8 knots and 1 g thrust. This Case-7 condition corresponds to Fig. G-39 of Ref. 1.

Appendix C - Correlation

All of the theoretical predictions and experimental data are shown in this appendix in Figs. 17-30. In some cases figures from the main text are repeated here for completeness. Two formats are used for the correlation. The first format compares the theoretical predictions and

Table 4 Fuselage Pitch Inertia and Damping (Nonrotating)

Parameter	Model value
Pitch spring rate (stiff), in.-lb/rad	3900.0
Pitch spring rate (soft), in.-lb/rad	272.0
Body pitch frequency (without rotor--stiff spring), Hz	4.68
Body pitch frequency (with rotor--stiff spring), Hz	4.14
Body pitch frequency (with rotor--soft spring), Hz	1.11
Body pitch damping (stiff spring), percent critical	6.64
Body pitch damping (soft spring), percent critical	7.18
Body pitch inertia (without rotor, frequency = 4.68 Hz), lb-in.^{2}	1741.0
Total pitch inertia (with rotor, frequency = 6.68 Hz), lb-in.^{2}	2157.0
Total pitch inertia (with rotor, frequency = 4.14 Hz), lb-in.^{2}	2224.0

Table 5 Fuselage Roll Inertia and Damping (Nonrotating)

Parameter	Value
Roll spring rate (stiff), in.-lb/rad	1193.0
Roll spring rate (soft), in.-lb/rad	195.0
Body roll frequency (without rotor--stiff spring), Hz	4.90
Body roll frequency (with rotor--stiff spring), Hz	3.53
Body roll frequency (with rotor--soft spring), Hz	1.29
Body roll damping (stiff spring), percent critical	5.68
Body roll damping (soft spring), percent critical	2.29
Body roll inertia (without rotor, frequency = 4.9 Hz), lb-in.^{2}	486.0
Total roll inertia (with rotor, frequency = 4.9 hz), lb-in.^{2}	902.0
Total roll inertia (with rotor, frequency = 3.53 Hz), lb-in.^{2}	936.0

Table 6 Case 1 Modal Damping

Ω, rpm	ζ_r, %
825	-2.1
850	0.1
875	0.5
900	0.65
925	0.9
950	1.15
1000	1.7
1028	2.1
1050	2.1
1100	2.5
1125	2.2
1200	1.2
1250	0.8

Table 7 Case 2 Modal Damping

Ω, rpm	ζ_r, %
800	-1.7
850	0.5
900	0.0
950	0.0
975	0.0
1000	0.1
1028	0.55
1050	0.95
1100	1.1
1150	1.1
1200	0.9
1250	0.25
1250	0.65
1300	0.5
1350	0.5
1400	0.85

Table 8 Case 3 Modal Damping

Ω, rpm	ζ_r, %
775	-4.35
800	2.3
825	0.1
825	0.9
850	3.7
850	4.2
875	3.5
900	3.5
900	2.4
925	2.7
950	2.3
1000	2.7
1000	3.25
1028	3.15
1028	3.7
1100	3.75
1150	3.3
1200	2.7
1250	1.95
1300	1.90
1350	1.1
1400	0.8

Table 9 Case 4 Modal Damping

Thrust, g	ζ_r, %
0.0	0.6
0.0	1.75
0.14	0.65
0.14	1.4
0.33	0.7
0.33	0.9
0.58	0.9
0.58	1.3
0.87	1.85
0.87	3.3
1.00	3.15
1.00	3.7
1.13	2.8
1.13	4.45
1.46	3.55
1.46	4.9
1.7	4.55

Table 10 Case 5 Modal Damping

V, ft/sec	ζ_r, %
8.3	2.55
8.3	3.5
16.5	2.15
16.5	2.4
24.8	1.5
24.8	2.3
33.0	2.0
33.0	2.0
41.3	2.7
41.3	2.8
45.4	2.55
45.4	2.6
49.6	3.25
49.6	3.25
49.6	3.6
53.7	3.9
53.7	4.1

Table 11 Case 6
Modal Damping

α_s, deg	ζ_r, %
-20.5	0.45
-20.5	0.55
-20.1	0.95
-20.1	1.1
-15.1	0.9
-15.1	1.1
-15.1	0.5
-15.1	0.6
-11.1	1.15
-11.1	1.15
-9.9	0.6
-9.9	0.6
-4.9	0.85
-4.9	0.85
-4.8	1.15
-0.4	1.15
-0.4	1.0
0.3	1.1
0.3	1.7
5.0	1.7
5.0	2.9
5.0	3.1
5.0	1.75
10.0	1.9
10.0	4.55
10.0	4.7
10.0	2.3
14.5	2.45
14.5	3.1
15.1	3.3
15.1	4.85
19.4	5.15
19.4	4.25
20.0	4.4
20.0	5.1
	5.65

Table 12 Case 7
Modal Damping

Ω, rpm	ζ_r, %
775	-1.15
800	4.1
800	5.1
850	11.6
900	5.95
900	5.35
950	4.5
950	5.2
1000	2.6
1000	2.9
1028	3.4
1028	3.55
1050	2.75
1050	3.1
1100	2.6
1100	2.95
1150	2.5
1150	2.9
1200	2.3
1200	2.45
1250	1.1
1250	1.25

experimental data individually for each mathematical model used. In this format the actual calculated points are shown as solid symbols and the fairing between points calculated by the experiment analysts is indicated by open symbols. The second format compares all the theoretical predictions on a single composite plot using the faired curve from the first format and the experimental data are shown as a stippled area. A code is used to identify the theoretical predictions for both the individual and composite comparisons and is explained in Table 13.

Table 13 Explanation of Prediction Codes

ID	Prediction method	User
BH	DRAV21 (hover) C81 (forward flight)	Bell Helicopter Textron
B7	C-90	Boeing Vertol
SA_1	G400	Sikorsky Aircraft
SA_3	E927-3	Sikorsky Aircraft
AL	FLAIR	U.S. Army Aeromechanics Laboratory

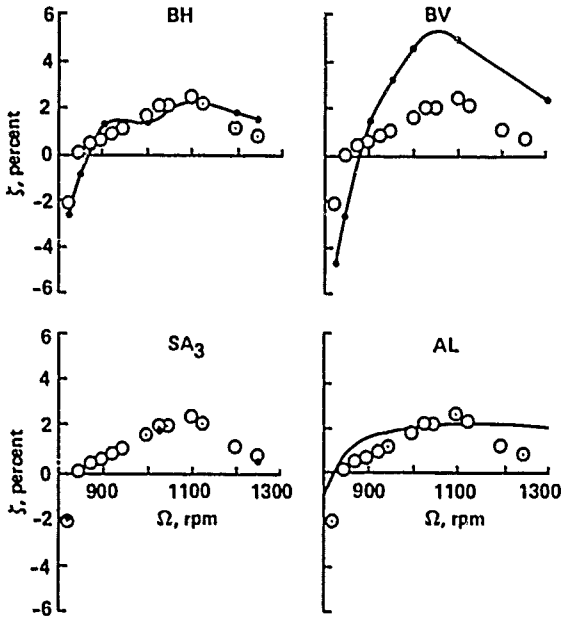


Fig. 17 Individual comparison for Case 1, regressing lead-lag mode damping as a function of rotor speed.

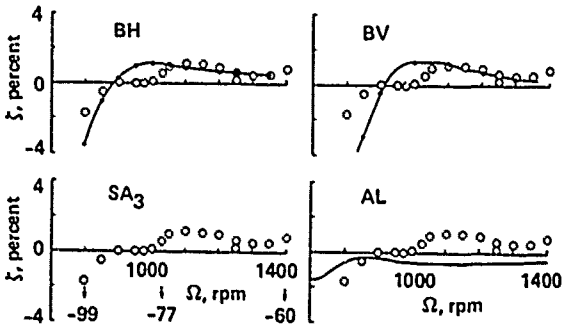


Fig. 19 Individual comparison for Case 2, regressing lead-lag mode damping as a function of rotor speed.

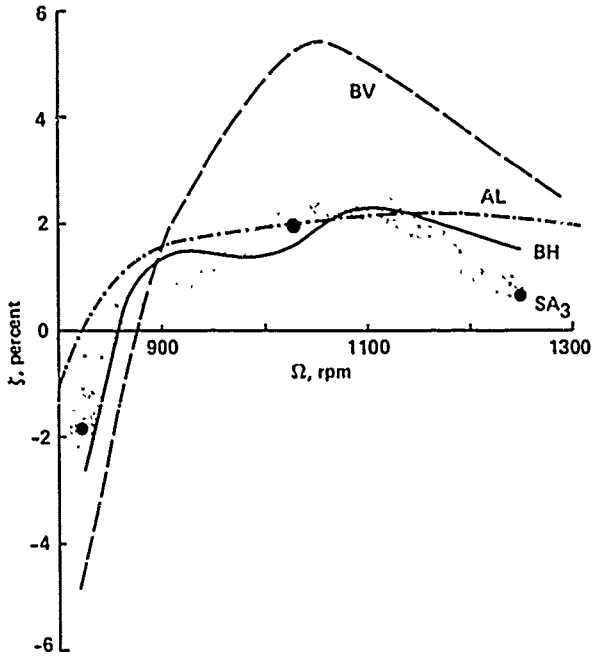


Fig. 18 Composite comparison for Case 1, regressing lead-lag mode damping as a function of rotor speed.

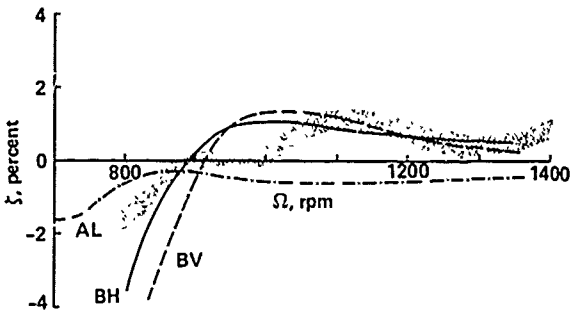


Fig. 20 Composite comparison for Case 2, regressing lead-lag mode damping as a function of rotor speed.

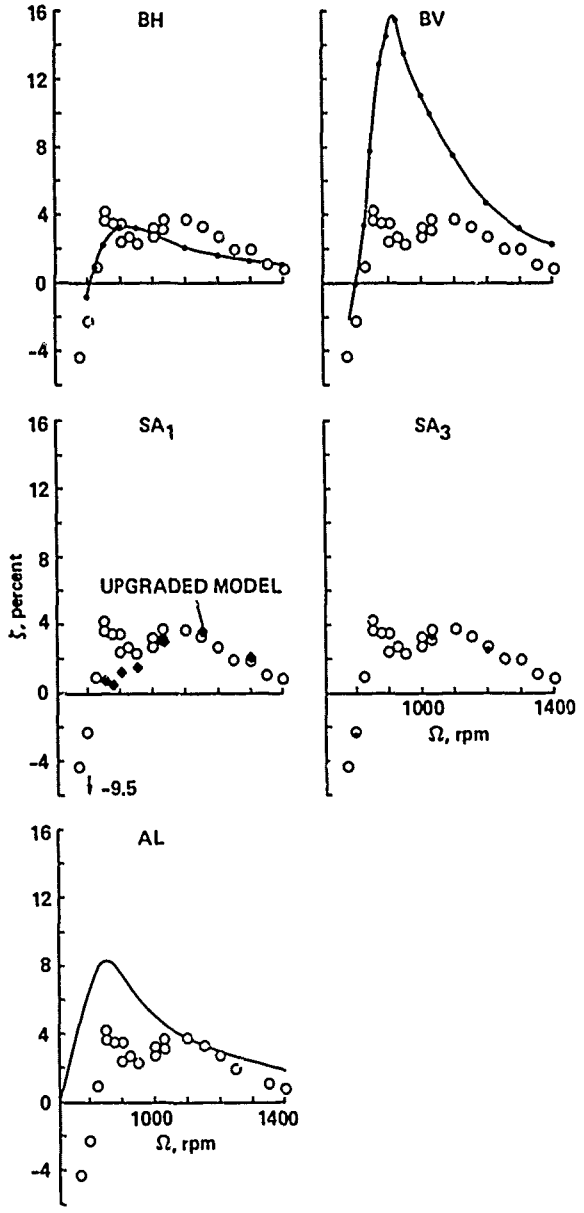


Fig. 21 Individual comparison for Case 3, regressing lead-lag mode damping as a function of rotor speed.

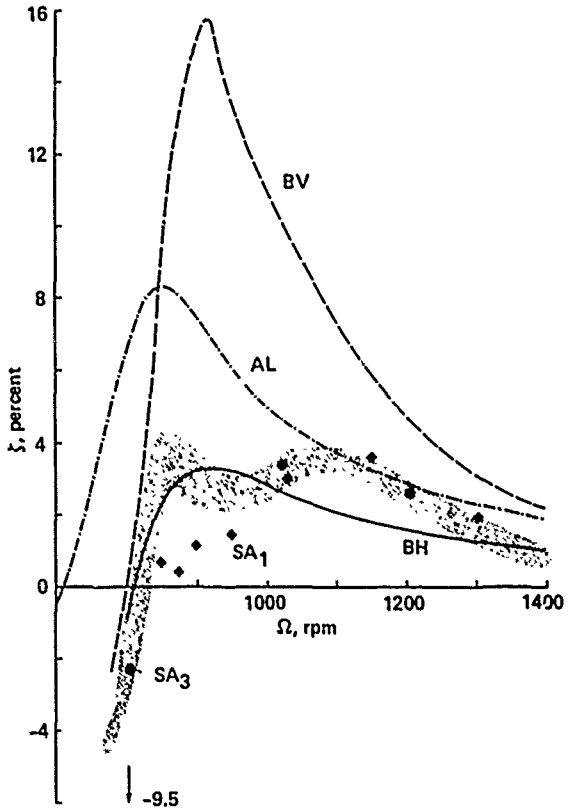


Fig. 22 Composite comparison for Case 3, regressing lead-lag mode damping as a function of rotor speed.

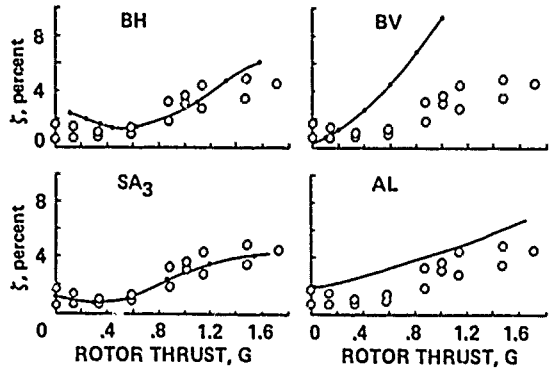


Fig. 23 Individual comparison for Case 4, regressing lead-lag mode damping as a function of rotor speed.

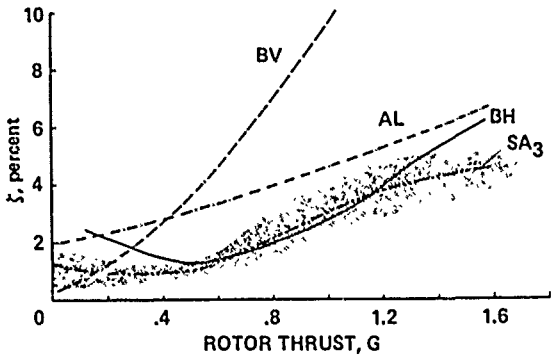


Fig. 24 Composite comparison for Case 4, regressing lead-lag mode damping as a function of rotor speed.

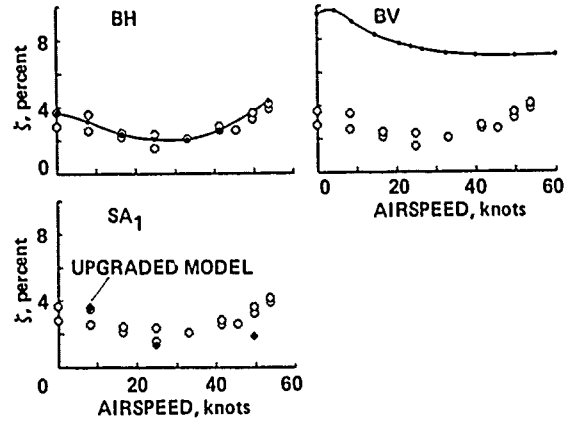


Fig. 25 Individual comparison for Case 5, regressing lead-lag mode damping as a function of rotor speed.

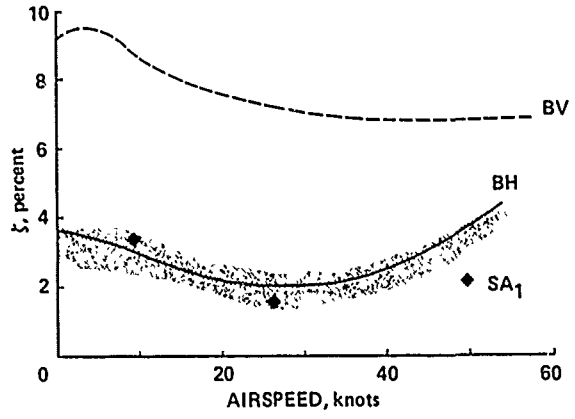


Fig. 26 Composite comparison for Case 5, regressing lead-lag mode damping as a function of rotor speed.

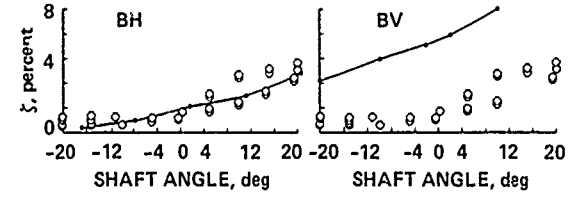


Fig. 27 Individual comparison for Case 6, regressing lead-lag mode damping as a function of shaft angle.

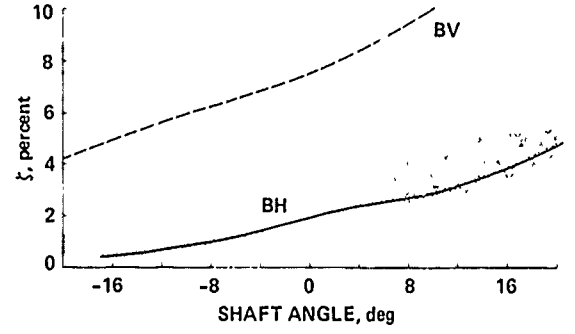


Fig. 28 Composite comparison for Case 6, regressing lead-lag mode damping as a function of shaft angle.

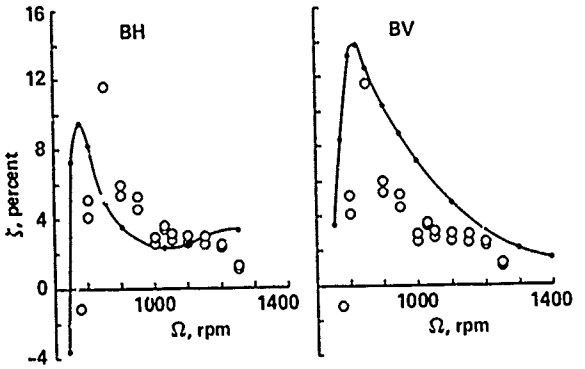


Fig. 29 Individual comparison for Case 7, regressing lead-lag mode damping as a function of rotor speed.

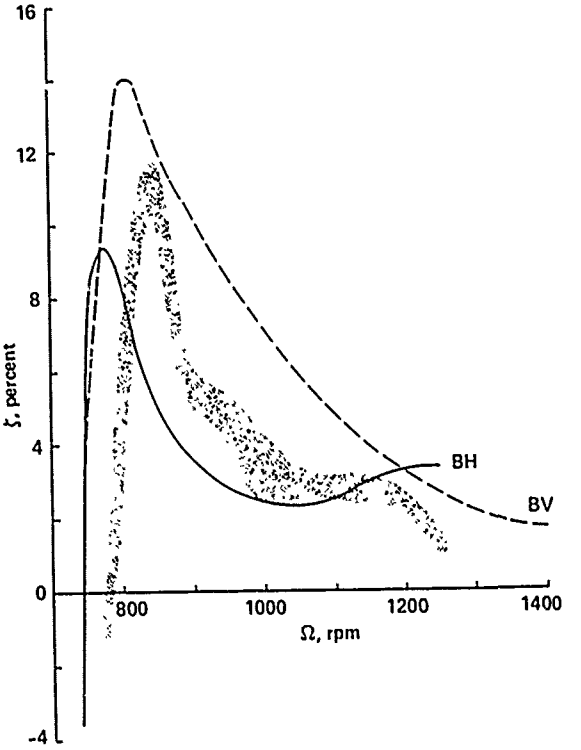


Fig. 30 Composite comparison for Case 7, regressing lead-lag mode damping as a function of rotor speed.

DISCUSSION

A COMPARISON OF THEORY AND EXPERIMENT FOR COUPLED-ROTOR-BODY STABILITY OF A BEARINGLESS ROTOR MODEL IN HOVER AND FORWARD FLIGHT

Paul H. Mirick

Bill Warmbrodt, NASA Ames: To put this paper in light of the previous papers, your percent critical damping is expressed in the fixed system?

Mirick: I believe so, yes.

Warmbrodt: Did the analysis, or the analyses, that were performed predict frequency accurately so that we could then really say that this is the decay coefficient?

Mirick: I really don't know the answer to that question. I think perhaps that might be a good one to bring up this afternoon.

Gene Hammond, Applied Technology Laboratory: You mentioned early in the presentation the method that Boeing used for computing their mode shapes. How did Bell compute mode shapes to use in the C81 analysis?

Gene Sadler, Bell Helicopter Textron: We used the rotating vacuum modes from the Myklestad program.

Hammond: Did you account for the dual load path?

Jing Yen, Bell Helicopter Textron: Yes, that's the key there.

Warmbrodt: From Wendell's paper this morning, E927-2 or -3 (I guess it is) can handle bearingless rotor configurations. Did they attempt correlation with this data set?

Mirick: The one they used here was the -3 version. The other ones I do not believe were used, unless Hughes used them.

Bill Bousman, Aeromechanics Laboratory: I think that the problem with E927-2 was with this data set, where they got the flexible torsion degree of freedom being neutrally stable rather than the regressing lead-lag mode. It was at that point that they decided that, having cut out the higher order terms, that there was some problem with the analysis. Then they returned the higher order terms and made the point calculations we've seen here.

Mirick: So that's why we show only the three points as opposed to many points.

A COMPARISON OF THEORY AND FLIGHT TEST OF THE BO 105/BMR IN HOVER AND FORWARD FLIGHT

Paul H. Mirick
Aerospace Engineer
U.S. Army Aerostructures Directorate
Hampton, Virginia

Abstract

Four cases were selected for comparison with theoretical predictions using stability data obtained during the flight test of the Bearingless Main Rotor (BMR) on a Messerschmidt-Boelkow-Blohm BO 105 helicopter. The four cases selected from the flight test include two ground resonance cases and two air resonance cases. The BMR used four modified BO 105 blades attached to a bearingless hub. The hub consisted of dual fiberglass C-channel beams attached to the hub center at 0.0238R and attached to the blade root at 0.25R with blade pitch control provided by a torque tube. Analyses from Bell Helicopter Textron, Boeing Vertol, and Sikorsky Aircraft were compared with the data and the correlation ranged from very poor-to-poor to poor-to-fair.

Introduction

As part of the Methodology Assessment, four cases were selected from the flight test reported in Ref. 1 for a comparison with theoretical predictions. The test reported in Ref. 1 was conducted by the Boeing Vertol Company as part of the U.S. Army Applied Technology Laboratory program to design, fabricate, and demonstrate by flight test, the feasibility of the Bearingless Main Rotor (BMR). The flight testing included investigation of ground resonance characteristics on both concrete and turf surfaces as well as air resonance characteristics in hover, forward flight, rearward flight, sideward flight, and climbs and descents. From the extensive stability data obtained during the BMR flight test program, two ground resonance and two air resonance cases were selected for comparison with theoretical predictions. The two ground resonance cases were selected with different landing gear configurations as this affected the body frequency and, hence, the aeromechanical stability. One air resonance case was selected with airspeed as the independent variable, and the second was selected with climb rate (inflow) as the independent variable.

The theoretical models compared with the data included the Bell Helicopter DRAV21 and C81 analyses, the Boeing Vertol C-90 code, and the Sikorsky E927-3 analysis for the hover cases. Neither Hughes Helicopters nor the U.S. Army Aeromechanics Laboratory modeled these cases.

This paper briefly describes the tests from which the data were obtained and presents the correlation. Conclusions as to the quality of the agreement between theory and test are presented. Appendices are provided that document the test aircraft and rotor system properties, tabulate the experimental data points, and show all of the correlations.

Flight-Test Program

A Messerschmidt-Boelkow-Blohm BO 105 helicopter flight-test program with a Bearingless Main Rotor (BMR) installed was conducted by Boeing Vertol as part of the U.S. Army Applied Technology Laboratory program to design, fabricate, and demonstrate by flight test the feasibility of the BMR.[1] Testing included the determination of ground resonance characteristics on both concrete and turf landing surfaces, as well as the determination of air resonance characteristics in hover, forward flight, rearward flight, sideward flight, climb, and descent. Flight loads, flying qualities, and vibration surveys were also conducted as part of this test. The results from this test provided a data base for the methodology assessment, which allowed a comparison of computer code predictions with actual flight test data.

Test Vehicle Description

The BMR installed on the BO 105 is shown in Fig. 1. The blades are modified BO 105 blades attached to a set of dual fiberglass beams at 0.25R with the beam roots attached at 0.0238R to a metal hub-plate set. All the geometric parameters of the

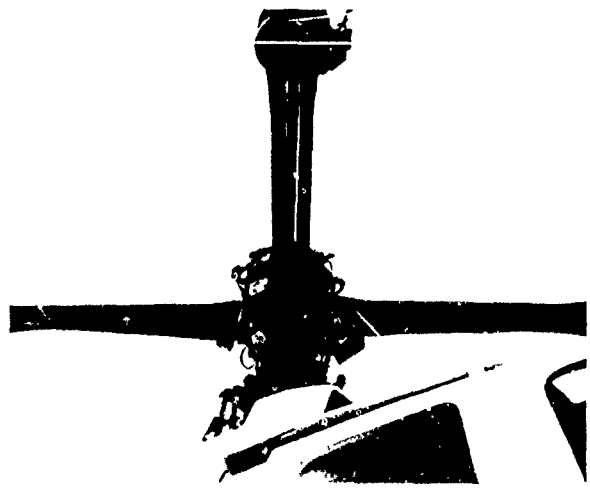


Fig. 1 BMR installed on BO 105.

individual beams, such as width, height, flange and web thickness, and spacing between the beams, vary along the length. The fiberglass beams permit flapwise bending, chordwise bending, and full torsional travel. The flap, chord, and torsional frequencies of the rotor were designed to be approximately the same as those of the BO 105 rotor system. Blade pitch is controlled by a filament-wound graphite torque tube. The outboard end of the torque tube is cantilevered at the blade-to-beam joint and supported at its inboard end by a rod end bearing. The fiberglass beams have a C-channel cross section. Detailed rotor characteristics are given in Appendix A.

The BMR hub was attached to the rotor shaft of the BO 105 helicopter through the same hole pattern as the standard hub. Because of the difference in the pitch arm attachment locations, new pitch links were fabricated. Initial ground resonance testing showed an unacceptable level of damping and, as a result, the landing gear was modified by adding two cables stretched between the left- and right-side skids as shown in Fig. 2. This resulted in an increase in the aircraft pitch and longitudinal mode frequencies and raised the critical rotor speed for ground resonance.

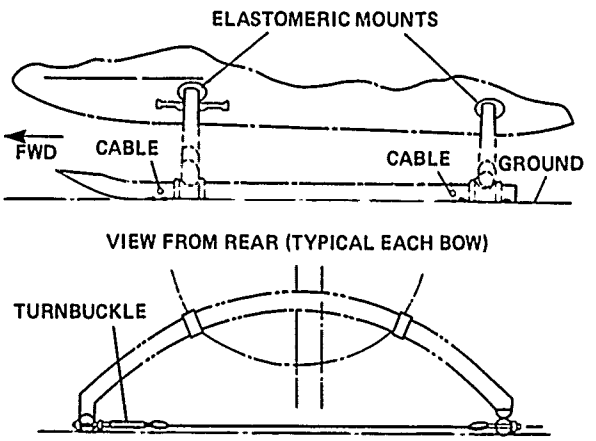


Fig. 2 Stiffening modification for BO 105 landing gear.

Test Procedure

To obtain ground or air resonance data, the aircraft was trimmed at the desired test condition. The pilot would then excite the air or ground resonance mode by moving the cyclic stick in a whirling motion at a predetermined frequency using 5% of total stick amplitude. After about eight cycles, the excitation was stopped and the blade chordwise modal decay was analyzed to determine the damping characteristics.

Two methods were used to determine air or ground resonance damping from the test data. The first method obtained the damping from the logarithmic decrement of the decay envelope as faired by hand. The second method used a computerized moving-block method to determine damping. Results obtained using both methods are contained in Ref. 1.

Test Results

Detailed results for the BMR flight tests are contained in Volumes 1 and 2 of Ref. 1 and a summary of results is contained in Ref. 2. Ground resonance data were obtained for the aircraft on concrete commencing at 75% N_R with flat pitch and incrementally building up to and including 95% N_R. Takeoffs were made at 95% N_R and landings were made on a concrete surface at rotor speeds of 95, 97.5, 100, and 102% N_R. Trimmed conditions were established at several settings between touchdown collective pitch and flat pitch. Pilot cyclic stick excitation was introduced at the appropriate frequency at each of these collective pitch settings and damping was computed from the decay of the chord bending after cyclic pitch excitation was stopped. Damping results were stable for 95, 97.5, and 100% N_R for touchdown collective pitch to flat pitch. Damping generally decreased with collective pitch, but showed a dip at a collective pitch between the touchdown and flat pitch values. This dip was different for each rotor speed. At 102% N_R, the trend below 25% collective pitch indicated a possible instability at about 15%; therefore, the test was cut off at 17% collective pitch. A possible degradation of the ground resonance mode damping was anticipated for landings on a turf surface because of the expected reduction of the body longitudinal-pitch frequency. Testing on turf was performed at 95% N_R. The damping trend indicated a possible instability at a collective pitch of about 22% and, therefore, the test was stopped at 28% N_R. To avoid this potential instability, the landing gear was stiffened by installing a wire cable between the skids (as has been shown in Fig. 2), and the ground resonance testing was repeated. Later analysis and aircraft shake testing showed that the predominant mode at the critical frequency on the ground had more longitudinal motion than pitch motion. A comparison of damping obtained for the 102% N_R case on concrete is shown in Fig. 3. Tests were then conducted on a turf surface once an acceptable damping level was demonstrated on a concrete surface.

Forward-flight testing was performed out to V_H of 109 knots for level flight and 135 knots in a maximum power descent once adequate rotor stability was demonstrated in hover and on the ground. Forward flight stability testing also included aircraft climbs/descents and autorotations.

Selection of Test Cases

Two ground resonance and two air resonance cases were selected for comparison with predictions. The first ground resonance case selected,

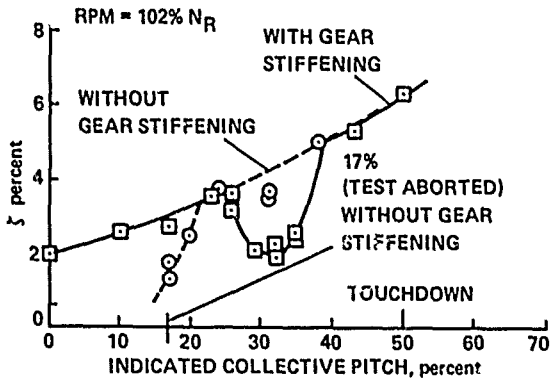


Fig. 3 BMR ground-resonance damping on concrete.

Case 1, was the BO 105/BMR on concrete, with standard gear and rotor operating at 102% of normal rotor speed. This case was selected because of the reduced stability at low collective pitch angle. The other ground resonance case selected, Case 2, was for the same conditions, but with the stiffened landing gear. The first air resonance condition selected, Case 3, was for the airspeeds from hover to 109 knots. This provided an assessment of the predictions over the full range of airspeeds. Case 4 examined the aeromechanical stability at an airspeed of 50 knots for a collective range of 0 to 6%. This case included the lowest damping that was encountered in forward flight.

Correlation

The ground resonance cases in hover were modeled by Bell Helicopter Textron with the DRAV21 analysis; Boeing Vertol used the C-90 analysis and Sikorsky used the E927-3 code. For the forward-flight air resonance cases Bell Helicopter Textron used C81 and Boeing Vertol used C-90 again. Sikorsky did not model the forward flight cases.

The comparison of the predicted and measured regressing lead-lag mode damping as a function of collective pitch is shown in Figs. 4 and 5 for the ground resonance cases. One difficult aspect of predicting ground resonance is that the aircraft body frequencies vary as the rotor thrust increases and the aircraft lifts off the ground. Bell Helicopter Textron estimated the variation of body pitch frequency with collective pitch from the known frequencies at flat pitch on the ground (3.08 Hz) and in hover (1.0 Hz). They assumed that at 7% indicated collective pitch that the body pitch frequency crossed over the lead-lag regressing mode. A curve for body frequency as a function of indicated collective pitch was generated using these values. For the cases with the stiffened landing gear, a body frequency of 3.28 Hz was used at flat pitch; 1.0 Hz for hover; and the coalescence was assumed at 32% indicated collective. A comparison of the DRAV21 results with the test data for the two ground resonance cases (Figs. 4 and 5)

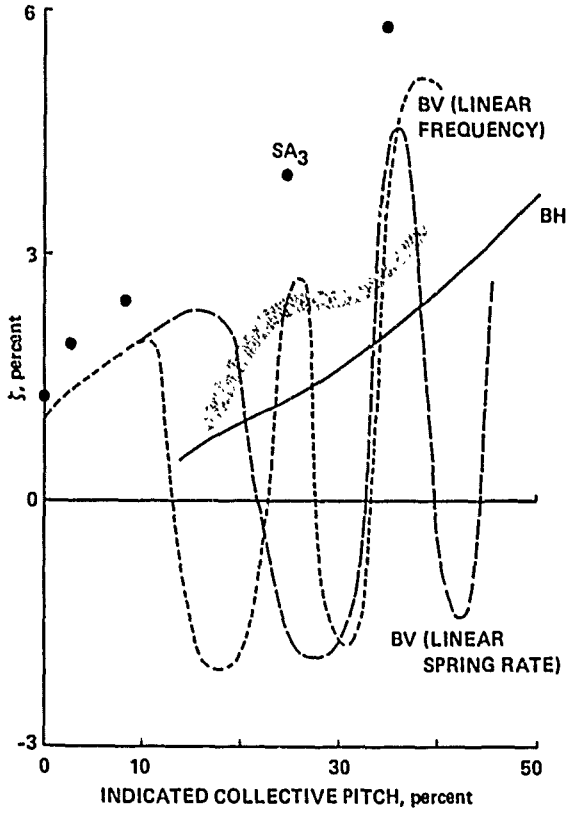


Fig. 4 Regressing lead-lag mode damping as a function of collective pitch; 102% N_R, standard gear, concrete surface.

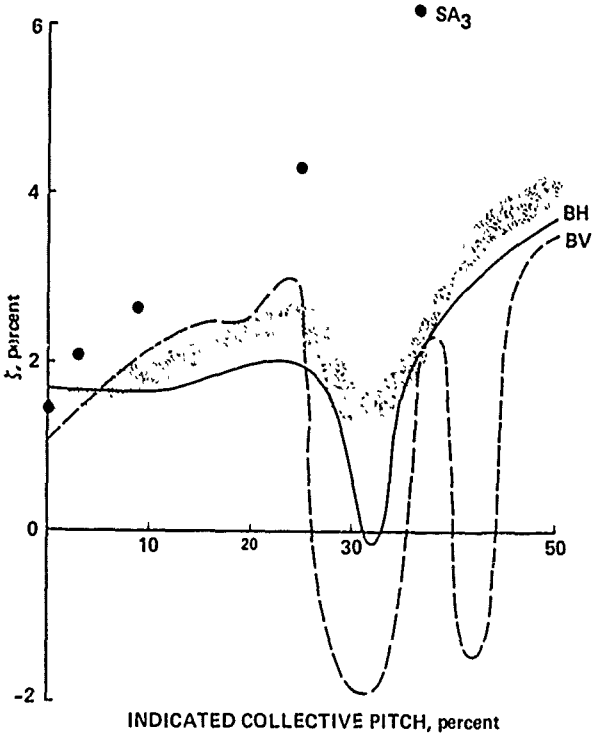


Fig. 5 Regressing lead-lag mode damping as a function of collective pitch; 102% N_R, stiffened gear, concrete surface.

shows that the analytical results follow the trend of the test data, but underpredict the level of damping. The correlation for both of these cases was judged to be poor-to-fair.

Boeing Vertol assumed that for the standard gear that either the landing-gear spring rate or the body mode frequency varied linearly with thrust; both predictions are shown in Fig. 4. For the stiffened gear, Boeing used only the linear spring rate. Both the linear frequency and the linear spring rate assumptions show two areas of instability for Case 1: a roll-lateral mode and a pitch-longitudinal mode. The first unstable region, the pitch-longitudinal mode, occurs at approximately the same collective setting at which the test data showed a large decrease in damping. The correlation for both cases is considered very poor-to-poor.

Sikorsky modeled the two ground resonance cases using the E927-3 analysis. The analysis overpredicts the damping level for all collective pitch angles except 0° in the stiffened gear case. No effect of a change in body mode frequency is observed in these predictions as the collective pitch is changed. The correlation is judged to be very poor-to-poor for both cases.

The two air resonance cases were modeled by Bell Helicopter Textron and Boeing Vertol. The data and the predictions for the two cases are compared in Figs. 6 and 7. The first air resonance case, Case 3, shows the regressing lead-lag mode damping as a function of airspeed. The C81 analysis shows a minimum in the damping at about 70 knots which is higher than the 40-knot minimum that is seen in the data. The damping level is considerably underpredicted so overall the correlation is considered to be poor-to-fair. The Boeing Vertol C-90 prediction shows the minimum in the damping at about 60 knots which is, again, higher than the minimum indicated by the data. The damping level prediction is better than seen for the C81 analysis so overall the correlation is judged fair.

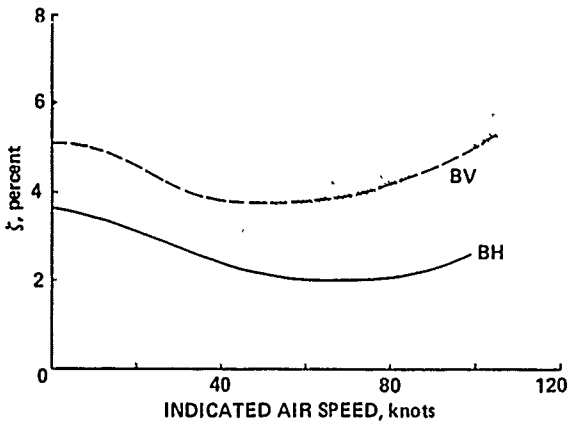


Fig. 6 Regressing lead-lag mode damping as a function of airspeed.

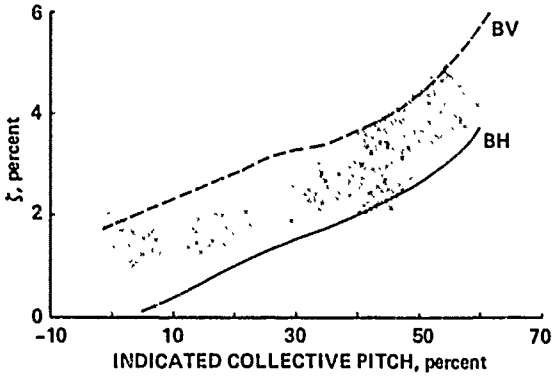


Fig. 7 Regressing lead-lag mode damping as a function of collective pitch at 50 knots.

The second air resonance case, Case 4, shown in Fig. 7, plots the regressing lead-lag mode damping as a function of indicated collective pitch as the aircraft is flown at climb and descent trim-points at 50 knots. The Bell Helicopter Textron C81 analysis shows the trend with collective pitch correctly, but the damping level is underpredicted. The correlation is judged to be poor-to-fair. The Boeing Vertol C-90 code also predicts the correct trend with collective pitch, but overpredicts the level of damping. The correlation is considered fair.

Conclusions

Four analyses were compared with one or more cases from a flight test of the BMR on a BO 105 helicopter that measured the lead-lag regressing mode frequency and damping. The four cases selected from the flight test included two ground-resonance cases and two air-resonance cases. Based on a comparison of the analyses and the experimental data, the following conclusions were reached.

1. The DRAV21 analysis used by Bell Helicopter Textron for the ground resonance cases gave poor-to-fair correlation. The C81 analysis used for the air resonance cases also gave poor-to-fair correlation.

2. The C-90 analysis used by Boeing Vertol gave very poor-to-poor correlation for the ground resonance cases and fair correlation for the air resonance cases.

3. The E927-3 analysis used by Sikorsky for the two ground resonance cases gave very poor-to-poor correlation.

References

[1]Staley, James A. and Reed, Donald A., "Aeroelastic Stability and Vibration Characteristics of a Bearingless Main Rotor," Boeing Vertol Company Report D210-11498-1, June 1979.

[2]Dixon, Peter G. C., "Design Development, and Flight Demonstration of the Loads and Stability Characteristics of a Bearingless Main Rotor," USAAVRADCOM TR-8[illegible]-D-3, June 1980.

Appendix A - Test Aircraft Properties

The four cases examined in this paper are from a flight test program originally reported in Refs. 1 and 2. The experimental properties in this appendix are taken from those references.

Rotor Description

The Bearingless Main Rotor (BMR) system is compatible in physical, dynamic and static characteristics to the current BO 105 rotor system. The BMR has no pitch bearing and no flapping or lead-lag hinges; it uses a flexible hub construction to accommodate control-system pitch inputs and normal flapping motion. The BMR assembly is shown in Fig. 8.

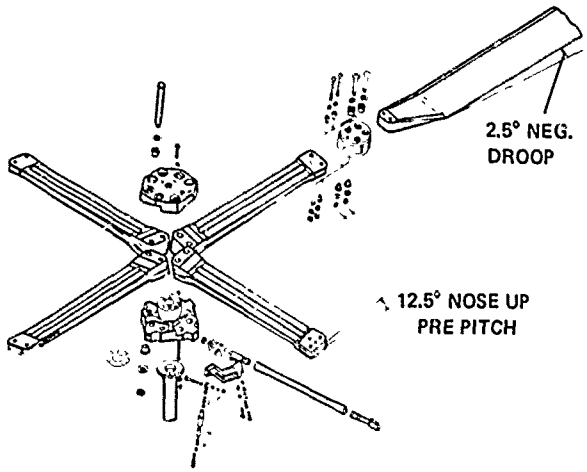


Fig. 8 BMR blade and hub arrangement.

The rotor blades used for the BMR are essentially standard BO 105 main rotor blades from the 70-in. blade station to the tip (blade station 193.37 in.). The inboard end was redesigned to replace the conventional swan-neck and single-pin wraparound retention with a double-pin wrap concept on the blade at a blade station of 52.36 in. The blades are attached to the beam flexure through a titanium clevis such that the beam is untwisted when the blade chord line at 0.70R is at a pitch angle of 9.55°. The flexbeam chord axis is at a pitch angle of 12.5° with respect to the hub. The outboard two-pin attachment of the beam to the clevis is at blade station 4.6 in. To improve the aeroelastic stability characteristics, the blade is preconed by 2.5° at the beam-to-blade clevis. The rotor blade has a constant NACA 23012 airfoil distribution and a 10.63-in. chord. The geometric twist for the blade and a comparison of the BMR blade planform with the BO 105 blade are given in Fig. 9. The spanwise mass moment can be fine-tuned with the changeable-tip weight system. The second flap and chord frequencies can be fine-tuned by adding weight to a cavity in the blade at approximately the 50% radial station. Up to four pounds

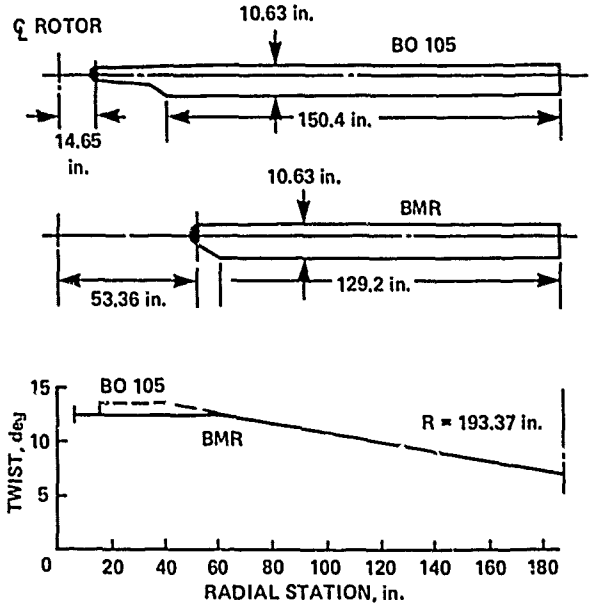


Fig. 9 BMR and BO 105 rotor blade planform and geometric twist.

of tungsten can be accommodated. Leading edge erosion protection is retained by including the standard BO 105 titanium leading-edge segments. The blade and clevis properties are summarized in Table 1.

Blade pitch-control motion is transmitted from the standard pitch link through a pitch arm attached to a filament-wound graphite torque tube. The torque tube is rigidly attached to the blade clevis at the outboard end and supported in a spherical bearing inboard.

The fiberglass beams which accommodate the flapping and lead-lag motion have a C-channel cross section, with the geometric parameters of spacing between the beams varying over the length of the beam. Data for the beams are given in Table 2. The two beams are separated by a gap to provide space for the pitch-control torque tube and are joined at the inboard and outboard ends by steel-plate shear ties. A loop at both the inboard and outboard upper and lower flange ends provides a continuous fiber load-path to retain the attached blade against centrifugal force, flap and chordwise loads. Steel bushings inside each loop provide a shear tie reinforcement between the upper and lower flanges and protect the attachment pins from the fibrous composite material. Stress concentrations in the inboard fiber wrap are relieved by an additional web-wrap reinforcement between the upper and lower flanges. The internal and external crossply

wraps provide a shear connection between the upper and lower flanges together with the required shear reinforcement to the unidirectional material. A steel hub plate accommodates the beam-to-shaft attachment and provides a prepitch angle of 12.5°. The flap-lag coupling which results from this feature improves the aeroelastic stability characteristics of the rotor system.

Aircraft Characteristics

The test aircraft used was a standard Messerschmidt-Boelkow-Blohm BO 105 helicopter with some minor modifications. Because the torisonal rigidity of the BMR beam flexures was greater than the BO 105 (141 in.-lb/deg versus 45 in.-lb/deg), the control loads were expected to be higher. In order to offset these higher control loads and provide a greater control margin, it was necessary to increase the hydraulic boost pressure from 1500 to 2000 psi. Another modification required was to fabricate shorter pitch links to accommodate the difference in the pitch arm attachment location of the BMR and the standard BO 105 rotor. A third modification was made to the aircraft when the preliminary ground resonance flight tests showed the need for stiffening the landing gear in order to increase the critical rotor speed for ground resonance.

The BO 105 properties needed to model the aircraft in the Boeing Vertol C-45 math model are summarized in Table 3. The C-45 model was used to compute the air and ground resonance characteristics for the BO 105. The sources of this data include test results, physical measurements, and computed results. A representation of the C-45 model is shown in Fig. 10. It should be realized that in determining the fuselage inertias, the C-45 model breaks the fuselage inertia into three components: fuselage, pylon, and tail. Each individual inertia is defined about its own c.g. so a calculation of complete inertia requires the appropriate transformation and summation of inertia. The rotor mass is not included in these computations.

Table 1 Blade and Clevis Properties

R, in.	r/R	Wt/in., lb/in.	EI-Flap, EI_f, 10^6 lb/in.^{2}	EI-Chord, EI_c, 10^6 lb/in.^{2}	Torsional Stiffness, GK, 10^6 lb/in.^{2}
193.37	1.0	0.71	2.38	59.4	1.36
192.02	0.993	0.71	2.38	59.4	1.36
192.02	0.993	0.511	2.38	59.4	1.36
188.92	0.997	0.511	2.38	59.4	1.36
186.99	.967	0.32	2.38	59.4	1.36
153.92	0.796	0.32	2.38	59.4	1.36
153.92	0.796	0.309	2.38	59.4	1.36
97.65	0.505	0.309	2.38	59.4	1.36
97.65	0.505	1.447	2.38	59.4	1.36
95.72	0.495	1.447	2.38	59.4	1.36
95.72	0.495	0.309	2.38	59.4	1.36
87.79	0.454	0.309	2.38	59.4	1.36
81.99	0.424	0.309	2.38	59.4	1.55
76.19	0.394	0.372	3.39	56.71	1.74
66.52	0.344	0.4762	5.084	52.21	3.02
62.85	0.325	0.5159	5.725	50.51	3.80
59.94	0.304	0.5474	6.234	49.16	4.07
53.95	0.279	0.6121	7.281	46.375	4.10
53.95	0.279	2.573	82.28	68.375	5.10
52.0	0.269	2.573	157.28	266.375	5.77
50.4	0.2607	2.573	164.4	291.38	6.32
50.4	0.2607	1.3725	164.4	521.38	41.13
49.75	0.2573	1.359	167.28	566.95	41.13

Table 2 Physical Properties of Dual Flexbeam

R, in.	Width W, in.	Height H, in.	t_{Flange} t_f, in.	t_{Web} t_w, in.	EI_f, 10^6 lb/in.^{2}	I_f, $lb_m \cdot in.^2$	EI_c, 10^6 lb/in.^{2}	I_c, $lb_m \cdot in.^2$
4.6	2.875	3.526	1.201	1.250	58.1600	15.992	380.8900	44.351
5.3	2.770	3.526	1.156	2.718	98.8550	20.223	392.3630	74.521
6.3	2.600	3.526	1.092	2.336	92.0356	18.593	350.1850	63.489
8.3	2.280	3.055	0.895	1.651	60.0551	10.617	235.5785	40.144
10.3	1.960	2.583	0.699	1.056	30.9167	5.379	151.0927	24.290
12.3	1.720	2.2756	0.593	0.676	19.5626	3.1545	104.713	15.958
14.3	1.650	2.2182	0.516	0.469	16.6151	2.673	79.639	12.358
16.3	1.650	2.1608	0.439	0.359	14.2379	2.320	60.083	10.361
18.3	1.650	2.1034	0.362	0.256	11.7275	1.949	52.548	8.401
20.3	1.650	2.0460	0.337	0.182	10.2690	1.723	46.903	7.614
22.3	1.650	1.9886	0.311	0.140	8.9609	1.520	42.021	6.934
24.3	1.650	1.9312	0.286	0.126	7.6557	1.313	38.041	6.358
26.3	1.650	1.8738	0.286	0.126	7.2890	1.249	38.014	6.349
28.3	1.650	1.8164	0.286	0.126	6.7715	1.159	37.975	6.336
30.3	1.650	1.7590	0.286	0.126	6.2735	1.072	37.935	6.332
32.3	1.650	1.7017	0.286	0.126	5.7959	0.989	37.896	6.309
34.3	1.650	1.6443	0.286	0.126	5.3369	0.909	37.857	6.296
36.3	1.650	1.5869	0.286	0.126	4.8974	0.833	37.818	6.282
38.3	1.650	1.5295	0.286	0.126	4.4774	0.761	37.778	6.269
40.8	1.650	1.4577	0.286	0.126	3.9793	0.675	37.729	6.252
42.3	1.740	1.6647	0.304	0.126	5.979	1.009	43.986	7.241
44.3	1.920	1.6970	0.410	0.126	7.7065	1.362	71.2332	11.276
46.3	2.150	1.8500	0.575	2.150	12.8540	2.269	135.6900	28.659

R, in.	$EI_{co} \times 10^6$, lb/in.^{2}	EA, 10^{-6}, lb	A, in.^{2}	GK 10^6, lb/in.^{2}	Wt/in., lb/in.	I_θ, $lb_m \cdot in.^2/in.$	Neutral axis separation, in.	EC_w 10^6, lb/in.^{4}
4.6	45.135	64.253	9.830	29.560	0.688	4.224	3.600	419.78
5.3	36.241	81.147	19.408	26.215	1.359	6.632	3.550	404.43
6.3	31.728	76.810	17.627	15.747	1.233	5.746	3.488	157.90
8.3	13.087	61.355	12.338	6.425	0.864	3.553	3.499	65.85
10.3	6.908	43.929	7.983	1.627	0.559	2.077	3.378	25.68
12.3	3.905	33.485	5.554	0.52145	0.389	1.338	3.289	11.94
14.3	3.197	27.440	4.518	0.3096	0.316	1.052	3.224	7.73
16.3	2.767	22.657	3.818	0.1936	0.267	0.888	3.221	5.75
18.3	2.235	17.716	3.095	0.1134	0.217	0.725	3.245	4.18
20.3	1.885	15.228	2.724	0.0931	0.191	0.654	3.328	3.28
22.3	1.587	13.307	2.435	0.0756	0.170	0.592	3.391	2.73
24.3	1.399	11.944	2.226	0.0611	0.156	0.537	3.414	2.40
26.3	1.394	11.926	2.216	0.0610	0.155	0.532	3.416	2.26
28.3	1.387	11.900	2.201	0.0609	0.154	0.525	3.419	2.12
30.3	1.379	11.874	2.187	0.0607	0.153	0.518	3.423	1.98
32.3	1.372	11.847	2.172	0.0606	0.152	0.511	3.426	1.85
34.3	1.364	11.821	2.158	0.0605	0.151	0.504	3.429	1.72
36.3	1.357	11.795	2.143	0.0603	0.150	0.498	3.433	1.60
38.3	1.349	11.768	2.129	0.0602	0.149	0.492	3.436	1.48
40.8	1.340	11.735	2.111	0.0601	0.148	0.485	3.440	1.34
42.3	1.638	13.127	2.358	0.0734	0.165	0.578	3.504	1.91
44.3	2.8528	18.456	3.370	0.1673	0.236	0.885	3.656	2.47
46.3	8.2719	31.577	7.955	9.7500	0.557	2.165	3.681	45.34

Table 3 C-45 Inputs for BMR on BO 105

Symbol	Definition	Value	Units
M_f	Fuselage mass	9.79	lb-sec^2/in.
I_{Fx}	Fuselage roll inertia	4218.0	lb-sec^2/in.
I_{Fy}	Fuselage pitch inertia	11790.0	lb-sec^2/in.
I_{Fxy}	Fuselage product of inertia	0	lb-sec^2/in.
M_p	Pylon mass	0	lb-sec^2/in.
I_{px}	Pylon roll inertia	343.5	lb-sec^2/in.
I_{py}	Pylon pitch inertia	1218.5	lb-sec^2/in.
I_{pxy}	Pylon product of inertia	0	lb-sec^2/in.
M_t	Tail boom mass	0.2854	lb-sec^2/in.
I_{Tx}	Tail-boom roll inertia	1040.0	lb-sec^2/in.
I_{Ty}	Tail-boom pitch inertia	1735.0	lb-sec^2/in.
I_{Tz}	Tail-boom yaw inertia	2775.0	lb-sec^2/in.
I_{Txy}	Tail-boom product of inertia	0	lb-sec^2/in.
I_{Txz}	Tail-boom product of inertia	0	lb-sec^2/in.
I_{Tyz}	Tail-boom product of inertia	0	lb-sec^2/in.
e_o	Hub offset	0	in.
e_1	Distance from hub center to first hinge	22.03	in.
e_2	Distance between first and second hinge	2.92	in.
e_3	Distance between second and third hinge	20.05	in.
l_f	Horizontal distance to M_f	14.57	in.
h_f	Vertical distance to M_f	7.28	in.
l_2	Horizontal distance from A/C Ref axis to rotor shaft	0	in.
l_3	Horizontal distance from rotor shaft to tail hinge	106.3	in.
h_3	Vertical distance from A/C Ref axis to pylon hinge	19.68	in.
h_4	Vertical distance from pylon hinge to hub center	41.77	in.
l_p	Horizontal distance from rotor shaft to M_p	0	in.
h_p	Vertical distance from pylon hinge to M_p	30.94	in.
l_t	Horizontal distance from tail hinge to M_t	110.24	in.
h_t	Vertical distance from tail hinge to M_t	23.61	in.
h_2	Vertical distance from A/C Ref axis to tail hinge	11.81	in.
f_1	Lateral distance from A/C Ref to aft landing gears	48.0	in.
f_2	Lateral distance from A/C Ref to fwd landing gears	48.0	in.
h_o	Vertical distance from A/C Ref to fwd landing gears	49.0	in.
h_1	Vertical distance from A/C Ref to aft landing gears	49.0	in.
l_1	Horizontal distance from A/C Ref axis to fwd landing gears	68.0	in.
l_3'	Horizontal distance from rotor shaft axis to aft landing gears	33.0	in.
R	Blade radius	193.37	in.
e_a	Blade cutout from hub center	52.0	in.
θ_o	Nose-up pitch at hub center	12.5	deg
θ_1	Nose-up pitch before first hinge	-2.34	deg
θ_2	Nose-up pitch before second hinge	-0.722	deg

Table 3 Concluded

Symbol	Definition	Value	Units
θ_3	Nose-up pit . before third hinge	-5.0	deg
β_o	Tip-up flap at hub center	-0.069	deg
β_1	Tip-up flap before first hinge	-0.116	deg
β_2	Tip-up flap before second hinge	-0.302	deg
β_3	Tip-up flap before third hinge	0.0213	deg
	blade Lock number	6.44	
I_a	Blade flapping inertia	1516.0	lb-sec^2/in.
	rotor speed	425.0	rpm
N	Number of blades	4	
K_{H1}	Rotational spring around first hinge	99092.0	in./lb-rad
K_{H2}	Rotational spring around second hinge	690000.0	in./lb-rad
K_{H3}	Rotational spring around third hinge	40970.0	in./lb-rad
$K\phi_x$	Pylon roll spring	12883000.0	in./lb-rad
$K\phi_y$	Pylon pitch spring	12833000.0	in./lb-rad
$K\phi_{ty}$	Tail vertical spring	5175900.0	in./lb-rad
$K\phi_{ty}$	Tail lateral spring	6563100.0	in./lb-rad
K_{x1}	Longitudinal spring rate of aft gear	2218.0	in./lb
K_{x2}	Longitudinal spring rate of fwd gear	2218.0	in./lb
K_{y1}	Lateral spring rate of aft gear	4113.0	in./lb
K_{y2}	Lateral spring rate of fwd gear	4113.0	in./lb
K_{z1}	Vertical spring rate of aft gear	4113.0	in./lb
K_{z2}	Vertical spring rate of fwd gear	4113.0	in./lb
η_{H1}	Viscous damping around first hinge	0	1. = 100%
η_{H2}	Viscous damping around second hinge	0.01	1. = 100%
η_{H3}	Viscous damping around third hinge	0	1. = 100%
β_4	Blade tip-up flap after third hinge	1.68	deg

Appendix B - Experimental Data

The experimental data tabulated in this appendix were obtained from Ref. 1. Table 4 provides the modal damping for Case 1 as a function of the collective pitch. This is the ground resonance condition with the original or unstiffened landing gear and corresponds to Fig. 41 (in part) of Ref. 1. Table 5 shows the modal damping as a function of collective pitch for Case 2, the ground resonance condition with the stiffened landing gear. These data also correspond to Fig. 41 of Ref. 1. The Case 3 data are shown in Table 6 where the modal damping data as a function of airspeed are given for 1-g flight. These data correspond to Fig. 48 of Ref. 1. The data for Case 4 correspond to Fig. 51 of Ref. 1 and are shown in Table 7. The modal data were obtained at a constant airspeed of 50 knots and the collective pitch was varied to change the rate of climb (or descent).

Table 4 Case 1 Regressing Lead-Lag Mode Damping

Collective pitch, percent	ζ_r, percent
17	0.9
17	1.033
20	1.77
24	2.36
31	2.47
31	2.48
38	3.26

Table 5 Case 2 Lead-Lag Regressing Mode Damping

Collective pitch, percent	ζ_r, percent
0	1.49
10	1.94
17	2.22
23	2.59
26	2.32
26	2.58
29	1.49
32	1.38
32	1.62
35	1.70
35	1.97
43	3.68
50	4.07

Table 6 Case 3 Regressing Lead-Lag Mode Damping

$V_{indicated}$, knots	ζ_r, percent
0	6.03
20	3.68
20	3.73
40	3.08
50	3.48
50	3.30
60	3.96
60	3.77
70	3.95
70	4.27
80	4.22
80	5.46
80	4.39
80	4.12
90	5.55
90	6.23
100	6.28
100	5.07
106	5.21

Table 7 Case 4 Regressing Lead-Lag Mode Damping

Collective pitch, percent	ζ_r, percent
-1	2.00
5	1.62
6	0.97
8	1.09
11	1.42
11	1.89
14	1.37
16	1.27
17	2.02
20	1.44
23	1.75
25	2.12
28	1.82
29	2.20
32	2.14
35	2.45
37	3.30
41	3.30
41	3.48
43	1.77
48	3.59
54	4.96
55	3.95
58	4.35
60	3.96

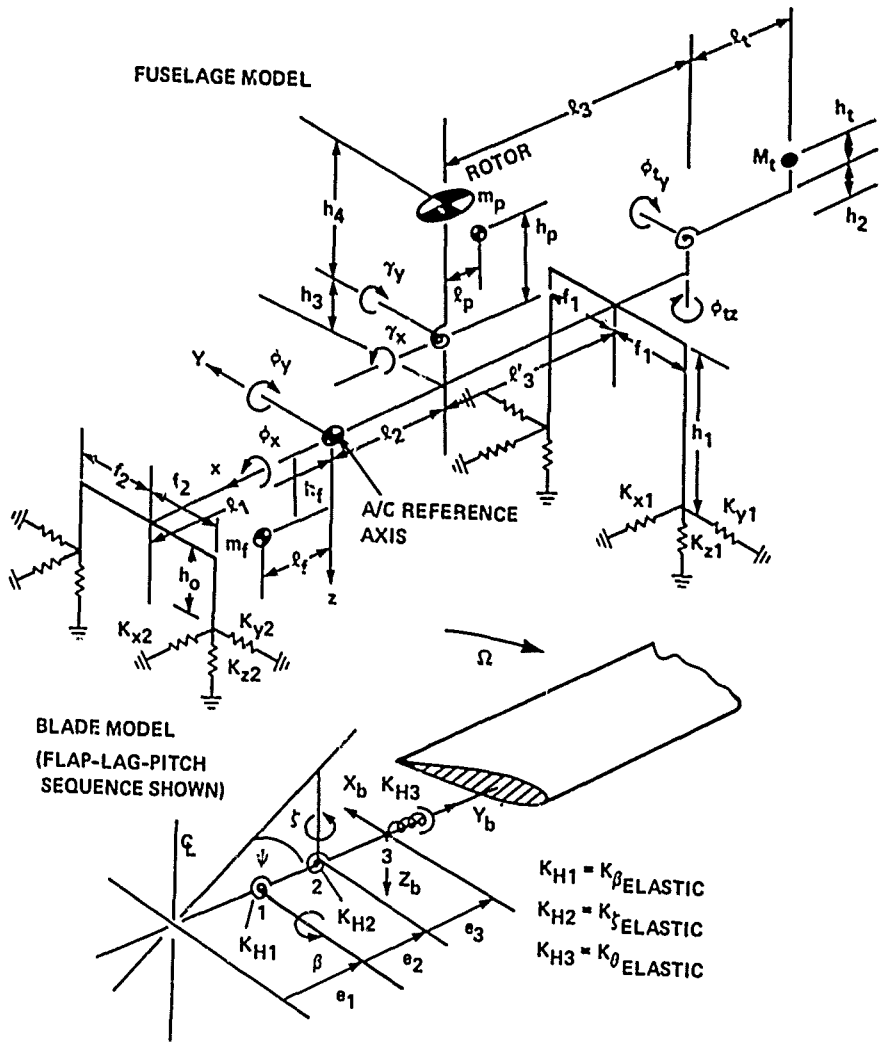


Fig. 10 Terms of reference for program C-45.

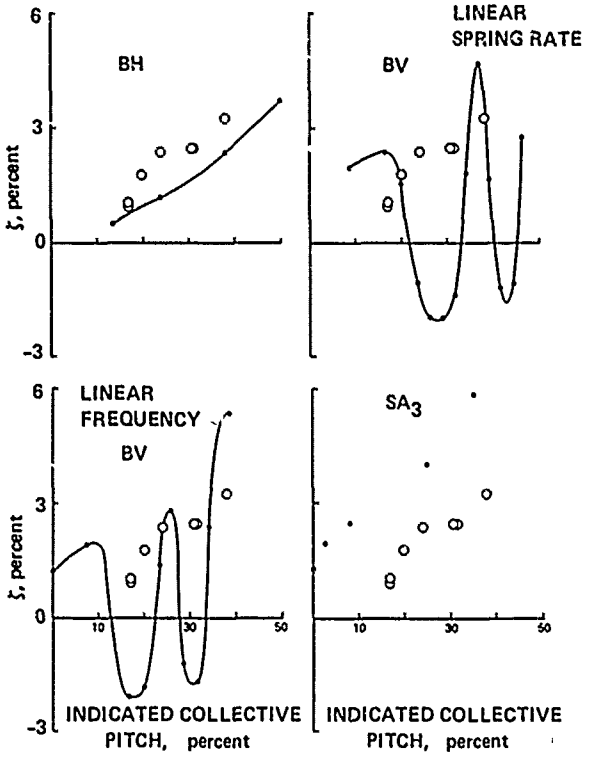


Fig. 11 Individual comparison for Case 1 modal damping as a function of collective pitch.

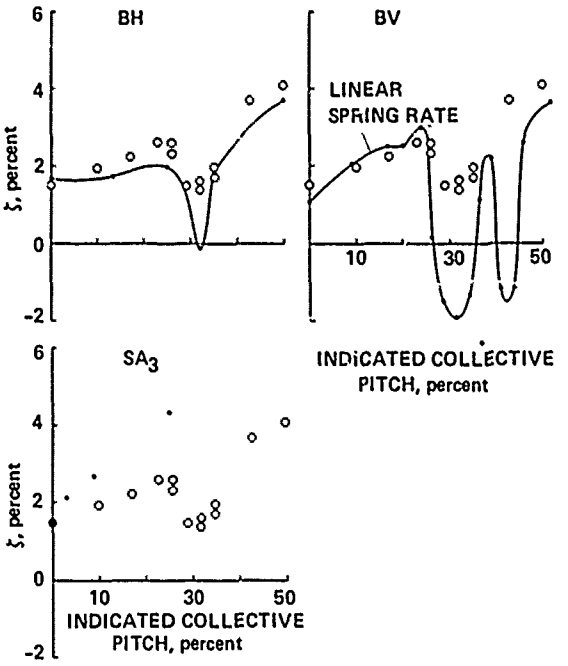


Fig. 13 Individual comparison for Case 2 modal damping as a function of collective pitch.

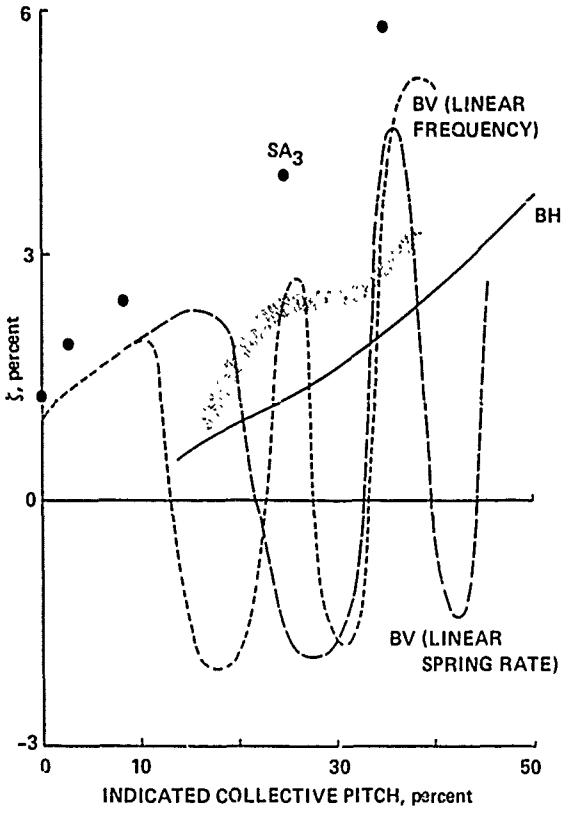


Fig. 12 Composite comparison for Case 1 modal damping as a function of collective pitch.

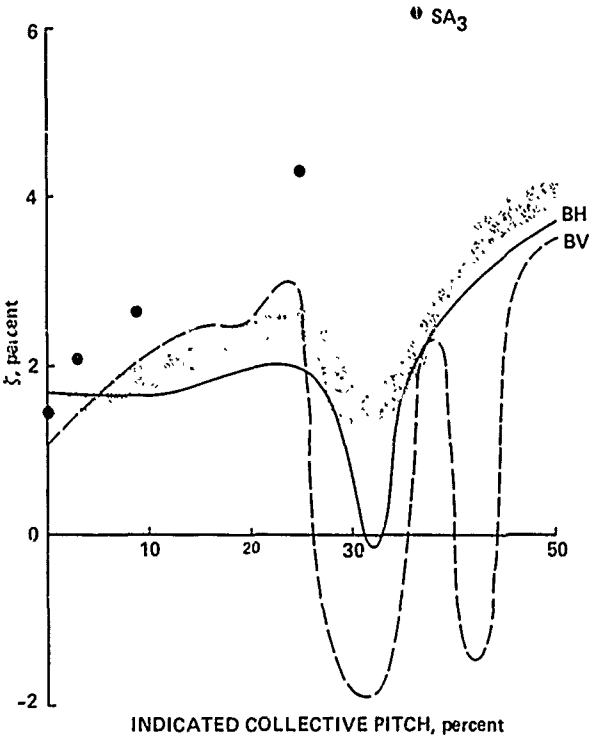


Fig. 14 Composite comparison for Case 2 modal damping as a function of collective pitch.

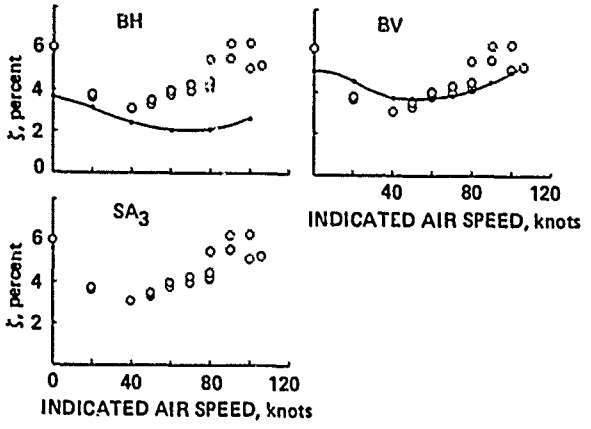


Fig. 15 Individual comparison for Case 3 modal damping as a function of indicated air speed.

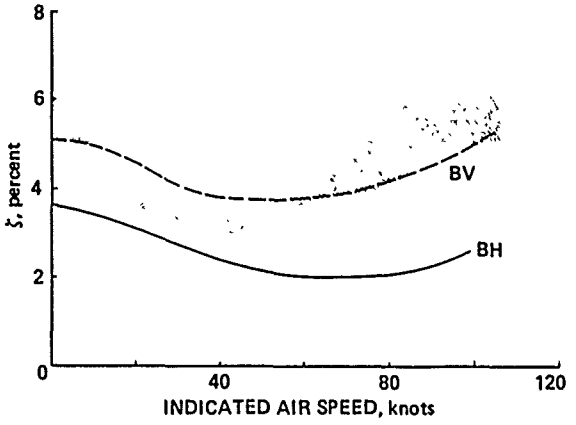


Fig. 16 Composite comparison for Case 3 modal damping as a function of indicated air speed.

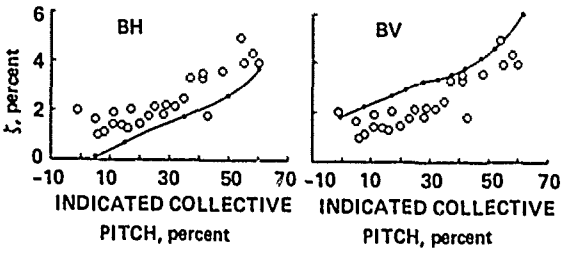


Fig. 17 Individual comparison for Case 4 modal damping as a function of collective pitch at 50 knots.

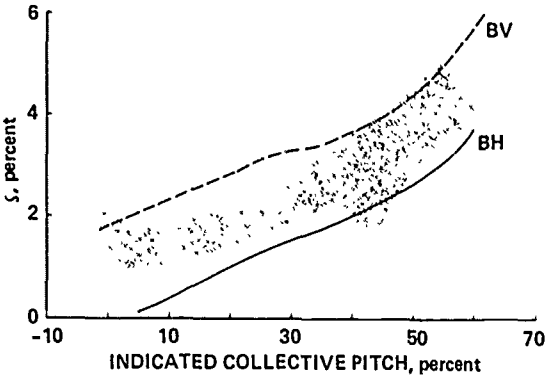


Fig. 18 Composite comparison for Case 4 modal damping as a function of collective pitch at 50 knots.

Appendix C - Correlation

All the theoretical predictions and experimental data are shown in this appendix. In some cases figures from the main text are repeated here for completeness. Two formats are used for the correlation. The first format compares the theoretical predictions and experimental data individually for each mathematical model used. In this format the actual calculated points are shown as solid symbols and the fairing between points was calculaced by the experiment analysts and are shown as open symbols. The second format compares all the theoretical predictions on a single composite plot using the faired curve from the first format; the experimental data are shown as a stippled area. A code is used to identify the theoretical predictions for both the individual and composite comparisons and is explained in Table 8.

Table 8 Explanation of Prediction Codes

ID	Prediction Method	User
BH	DRAV21 (hover) C81 (forward flight)	Bell Helicopter Textron
BV	C-90	Boeing Vertol
SA_3	E927-3	Sikorsky Aircraft

DISCUSSION

A COMPARISON OF THEORY AND FLIGHT TEST FOR COUPLED ROTOR-BODY STABILITY OF THE BO-105/BMR IN HOVER AND FORWARD FLIGHT

Paul H. Mirick

Bill White, U.S. Army AVRADCOM: I've two questions, Paul. The first one deals with your selection of the test data with the standard gear configuration. As I recall there were data measured on the aircraft that had very pronounced valeys at low collective; the measured damping was zero. It was about 3% wide in collective on either side of the minimum. Why did you not use that data since it is almost a classical textbook example from a flight aircraft? And second, would you comment on the difference in the Boeing Vertol predictions pre-first flight versus what you show up here today.

Mirick: Well, Bill Bousman made the selections of the data, so I'll let him answer that question.

Bill Bousman, Aeromechanics Laboratory: Bill, I don't recollect the case you're referring to, but very simply, the reason we chose it was that we had two configurations, one with the stiffened and one with the unstiffened gear. The stiffened gear was stable over the whole range, but it also showed the bucket where the changing body-frequency coalesced with the lead-lag regressing mode, causing instability. Whereas in the case where they aborted the condition, it seems obvious that the coalescent frequency is below....

White: That's my point, the data contradict that. They show a very distinct bucket [with] standard gear, just as you show with stiff gear. The beauty of it is they took it all the way to zero damping, so that it would have made a very good academic type of correlation effort.

Bousman: I don't see what you mean by, "they contradict that."

White: What you just said, "it didn't have a distinct coalescence," it actually did.

Bousman: Right, they aborted before they got to it. When I chose the data, I wanted two conditions, one with the two different gear frequencies. Perhaps the one that you're talking about did not have a complimentary case where they changed the gear stiffnesses and had data over the whole range. I don't know; that's the rationale I used.

Euan Hooper, Boeing Vertol: I think that's right. The case that Bill [White] is referring to, I remember it well, it went on and on and on for ten seconds or so, a long record, a very good neutral stability record, but it didn't cover the whole collective range. It stopped at that point; it was aborted. I think you probably

looked at many of the collective sweeps conducted, and I think you probably selected the one that had a complete collective range.

Mirick: I think also that that was the one that Peter [Dixon] had in his American Helicopter Society (AHS) paper, which may have also been why Bill pulled it out. Now, what was the second part of the question?

White: Could you comment on the difference in the nature of the pre-first flight versus the current correlation that you're showing here, in the Boeing Vertol results?

Mirick: Do you mean the one chart I had that showed the level of damping that was much, much higher than what was actually obtained?

Hooper: Can I make a comment on that? I think I remember reasonably well that the pre-first flight underestimated, or misestimated, the mechanism of what was going to happen. We did not appreciate the role that the flexibility of the landing gear was going to play. It wasn't until after that that it was remodeled and the prediction got closer to the fact. All these other predictions, of course, were made after the data were available, and it's much easier to get a better match.

Mirick: That's what you're really talking about, Bill, how they made the original predictions?

Bousman: If I'm correct, they're C90 calculations we're seeing now; C90 was not operational before you flew, was it? You used C45?

Hooper: That's correct. But we simply did not anticipate the role that the skid gear was going to play, and it's a very nonlinear behavior. As you lower collective pitch, there's contact first on the rear of one side and then contact on the rear on both sides and then gradually it comes down. It shows very nonlinear behavior.

Bob Ormiston, Session Chairman: I might throw in a comment of my own on that one. It was interesting to me with this set of data and these analyses and correlations, [that] the air resonance results, the model test results, and the analysis all did quite well for this configuration using the C45 analysis, which is an extremely simple representation. It's a rigid blade with three hinges, using spring elements around the hinges. That's a very surprising kind of model to be able to get good correlation for a bearingless configuration, and that worked for the coupled rotor-body configuration, the model test results, for a wide range of configurations. When the full scale rotor was first tested on a whirl tower with the isolated rotor, looking at only the lag-mode damping and comparing that with the same C45 analysis (check me here, Boeing folks) the results were quite substantially off and some very significant adjustments to the empirical, if you will, "coupling factors" required for that kind of analysis, had to be made before any kind of even reasonable correlation was obtained. That's an example of how you can really be fooled; you can get excellent correlation with the simple analysis on a very complicated problem and

then turn right around and do the simple part of it and just be out the window. That gets into this afternoon's topic, I guess.

Jerry Miao, Sikorsky Aircraft: One comment here, Bob; you just mentioned that the C45 correlates with model data very well and surprisingly that it does not correlate well with whirl tower data. Are you implying that building a model to try to reproduce the full scale is sometimes expecting too much?

Ormiston: I think a whole lot of implications might be drawn from that situation; there's a lot of food for thought there. I don't want to draw any one specific conclusion; that's certainly something to consider. Any other questions? Dev again.

Dev Banerjee, Hughes Helicopters: Paul, in the last two cases you showed correlation of damping data, but do you have corresponding correlation with frequency data? In other words, what are the coupling-parameters effects that are causing the changes of damping between the modes?

Bousman: Are you referring to the ground resonance points?

Banerjee: For the air resonance, and the ground resonance. For instance, I believe the air resonance was essentially a coupling between the lag-mode and the body pitch-mode in the air. Do you have a corresponding plot of the frequency predictions? You have test data, I'm sure, because you get the damping and frequency, but do you have any correlation with analysis?

Mirick: I don't believe we had any.

PANEL SESSION ONE

EVALUATION OF THE METHODOLOGY ASSESSMENT RESULTS

Panel Chairman: Charles E. Hammond
U.S. Army Applied Technology Laboratory

Panel Members: Stanley G. Sadler
Bell Helicopter Textron

Debashis Banerjee
Hughes Helicopters

Frank Tarzanin
Boeing Vertol Company

Wayne Johnson
NASA Ames Research Center

Wen-Liu Miao
Sikorsky Aircraft

Dewey H. Hodges
U.S. Army Aeromechanics Laboratory

Richard L. Bielawa
United Technologies Research Center

INTRODUCTION

Charles E. Hammond

This afternoon's panel is on "Evaluation of the Methodology Assessment Results," and it gives the analysts a chance to have their say. All the results were presented this morning and we had a lot of discussion back and forth, but now the analysts get their chance to talk about their particular results. I think that you know all the people who are on the panel. Rather than introducing them individually I'll go down and introduce the group momentarily and then we'll move right along. What I have asked them to do is to comment on the results from their point of view as an analyst; make any comments that they want to make about the results, about their analysis in particular and what may have been done to improve the analysis, or to go back and relook at the results. It's going to be fairly informal. What I would propose to do as far as the operation of the panel is to have each panelist take about ten minutes to make his comments and, so that we have some continuity in the overall discussion, he will entertain any specific questions of that particular panelist at that point. So we'll have some comments after each

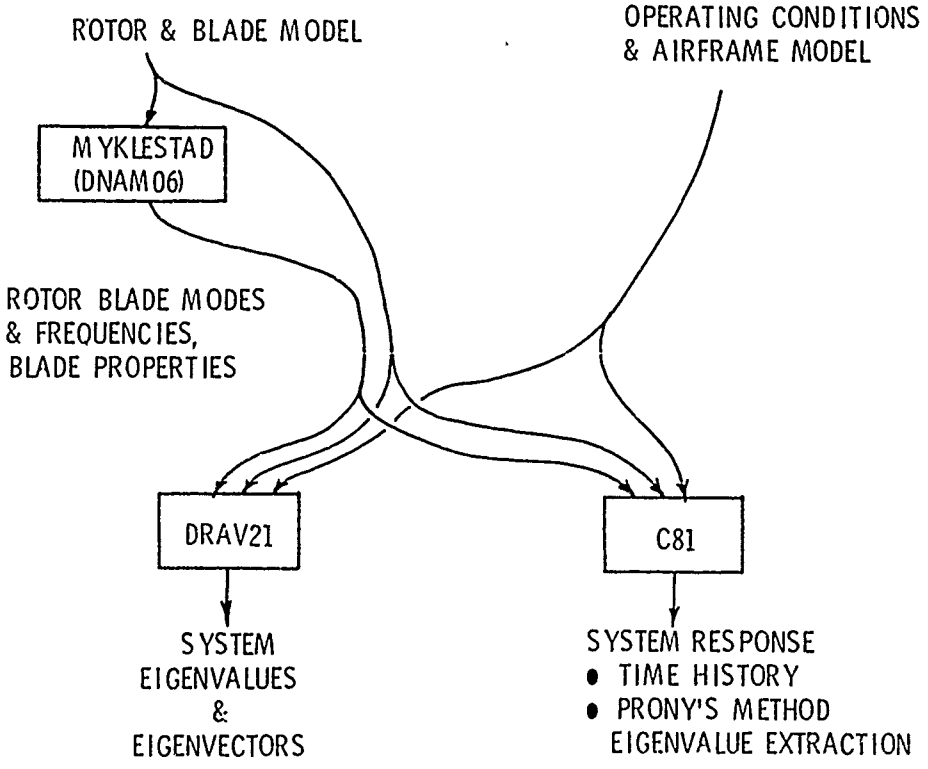
panelist. Then after all the panelists have made their comments, we'll open the floor for general discussion and you may feel free at that point to ask questions or make comments to any of the panelists, and the panelists themselves may want to make some general comments at that point.

So without further ado let me introduce the panelists and we'll go ahead and get started. On this end we have Dewey Hodges from the Aeromechanics Lab, Dev Banerjee from Hughes Helicopters, Jerry Miao from Sikorsky, Gene Sadler from Bell, Frank Tarzanin from Boeing, Wayne Johnson from NASA Ames, and Dick Bielawa from United Technologies Research Center. As far as the panelist's comments, I would like to go pretty much according to the schedule that's in your program; and according to that schedule Gene Sadler is the first one up.

PREPARED REMARKS BY GENE SADLER

I'd like to show you just a few viewgraphs. Some of the questions we had this morning, I think, will be answered by them. The analysis that we use basically uses the Myklestad program which defines blade modes and frequencies. Rotor blade properties go into Myklestad and some of those also go directly later on to DRAV21 or C81 [Slide 1]. Myklestad simply computes the coupled blade modes and frequencies. As a matter of convenience some of the blade properties are passed on, along with the modes and frequencies, to the C81 or DRAV21 programs. DRAV21 is an eigenvalue type analysis and it's good for hover or ground resonance, but not capable of doing forward flight. Out of that we get system eigenvalues and eigenvectors. Both DRAV21 and C81, of course, get some kinds of operating conditions and airframe model information that's not required or used in Myklestad. C81 is a time-history type of analysis; we have to use some of the same kind of techniques that you'd use in flight test as far as getting the thing trimmed, exciting a mode, and then analyzing the response to try to extract eigenvalues. So that's the kind of system we use for the analysis at Bell.

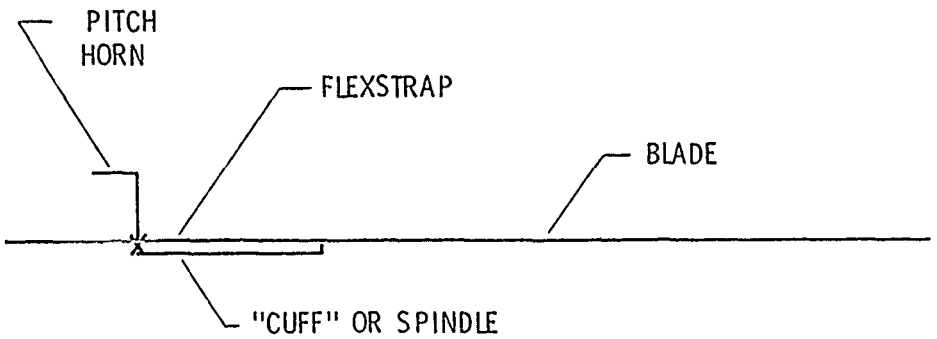
ANALYSIS SYSTEM



Slide 1

I'll show you just a couple of other viewgraphs that cover the other models in a little detail. The DNAM06 version of the Myklestad program is the one that we've been using for probably three or four years now [Slide 2]. It basically treats a blade as a single elastic axis. There is a region where, if it's necessary, we can have parallel or multiple load paths. It's limited in the kind of boundary conditions those load paths can have in that at the outboard end the so-called flexstrap and the cuff models are clamped on the blade; slopes and displacements are continuous. At the inboard end the cuff or spindle is attached to the flexstrap or, in one case, it can be attached to ground through a pin out-of-plane. In-plane, it's attached through a spring. We've done that in order to model some of the rotors that we have at Bell, for instance, the 680 rotor. From there on in, it's again a single load path. It has a single pitch-horn model; I don't know if any of you caught it, but when Case D/3 with a fore and aft, both forward and trailing edge, pitch-links was discussed, there wasn't any Bell data there. We do not have a model for the snubber-type pitch horn, so that was omitted from our analysis. The way Myklestad is usually run, in say a predesign analysis, is to take a blueprint type of blade position. If we had more information, we'd use a trim-type blade equilibrium position. That's used to define the reference coordinate axis which is, in this system, the pitch change axis. I guess, as far as weaknesses that I see with this system, part of them come in this particular area. The modes that are provided by DNAM06 are used later by C81 or DRAV21 for both trim and stability and if the trim position is not accurate enough, then you can't expect the stability to be very good. So this so-called blueprint or trim blade equilibrium position which is used to define the reference axis sometimes can be a problem.

DNAM06



"BLUEPRINT" OR "TRIMMED" BLADE EQUILIBRIUM

POSITION IS USED TO DEFINE REFERENCE AXIS (PCA)

SNUBBER PITCH HORN MODEL - NOT AVAILABLE

Slide 2

Now the DRAV21 program [Slide 3] uses modes from DNAMO6. It has a capability of using a subset. Let's say you can give it seven or eight modes. It has the capability of using a subset of them for trim and then the full set for stability, if you want to run it that way. Some of the cases were probably run that way. It does not have any true unsteady aerodynamics. The aerodynamics are quasi-steady. The representation of the airframe is with a stick model. There's one stick that represents the pylon that's connected with a rotary-type spring to the fuselage. The fuselage is connected to a platform, if you want to model it that way, or to ground with a rotary spring. If shuffle motions are important, which they are in some airframes, then that shuffle degree of freedom is modeled also. Now this particular program we use for ground resonance and hover air resonance. I think that generally speaking, for the areas where it is applicable, we've had fairly good success with the Myklestad/DRAV21 combination.

Now we do not have the capability with DRAV21 of analyzing anything in forward flight, so in that area we use C81 which is a more general representation of a helicopter [Slide 4]. It also uses modes for both trim and stability, and the stability again is done with the time history. The fuselage/pylon representation is through modal representation. So you can either have rigid-body degrees of freedom

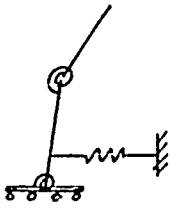
DRAV21

USES MODAL BLADE REPRESENTATION FOR

- TRIM (ITERATION)
- STABILITY (EIGENVALUE)

NO UNSTEADY AERODYNAMICS

STICK MODEL FUSELAGE & PYLON



CAPABILITIES

- GROUND RESONANCE
- HOVER AIR RESONANCE

Slide 3

C81

USES MODAL BLADE REPRESENTATION FOR

- TRIM (ITERATION)
- STABILITY (TIME HISTORY)

USES MODAL FUSELAGE / PYLON REPRESENTATION TIME

HISTORY SOLUTION FOR

- EXCITATION (CONTROL MOTIONS)
- STABILITY (PRONY'S METHOD)

CAPABILITIES

- GROUND RESONANCE (NOT USED)
- HOVER AIR RESONANCE (NOT USED)
- FORWARD FLIGHT AIR RESONANCE

Slide 4

or modal representation and those modes can really represent either pylon or airframe degrees of freedom. It uses a time history solution and the normal process is to get C81 to trim, and then to excite it with a stick stir if you're looking for, say, the regressing in-plane mode. After you've got the thing excited, you stop the excitation and look at the decay of the response. That can be, in some cases, a time consuming situation in terms of calendar time and computer time, probably for the same reason you get into some difficulties with test work. Sometimes if you excite with enough stick motion to get the blades to move the way you want them to move, you appear to be losing trim. You can start the aircraft doing strange things and you're not sure if that's kind of the tail wagging the dog or if you're really going to get what you want to get. With the stability analysis there's always a problem of having more than one frequency responding; one per rev always responds in forward flight. With C81, we have had more success with Prony's method than we have had with moving block, although that may be due to problems in the moving block analysis in C81. We usually use Prony's method for the stability analysis. I guess technically C81 would have the capability of doing ground resonance and hover air resonance but we haven't used it for that because the other program appears to be adequate and it would take a lot longer with C81. We have used it for the forward-flight air resonance cases. Any questions?

Peretz Friedmann, UCLA: I am totally ignorant and I was wondering whether you could tell me what is Prony's method?

Sadler: It's a curve fitting. It uses an exponential times a trig function and curve fits. In our case, I guess we can do up to ten or fifteen products of a damped exponential times a frequency. It's a curve fitting technique. We also basically have the same capability in the flight test data reduction area and we usually use that when we're doing, say, ground resonance shake tests.

Edward Saibel, U.S. Army Research Office: This is sort of a general question and I'd like to ask it before the other analysts speak. Is it really fair to compare the different systems that are being used without knowing how many adjustable parameters each system has used? After all, if one system is going to use a dozen adjustable ones, he may get a much better fit, but at the same time we may not be learning as much as we would from a system with fewer parameters. So, if the panelists have a chance to tell us what they can adjust, it will help us in comparing the different systems.

Sadler: Okay, let me back up to Myklestad then for a minute. The Myklestad program takes blade data; structural and inertial type information, collective pitch, twist, stuff like that. There's really nothing in that program to adjust. Yes, you can adjust the number of segments and how finely you break those segments up.

Jing Yen, Bell Helicopter Textron: I'd like to make a comment here on that question. As a result of this contract study we wrote a very comprehensive report and documented the inputs to those analyses. Most of the inputs were the input numbers or the model properties provided by the Army people. Okay, if there were any changes made, we told them the reasons why and how, and the numbers we changed them to. Those were documented in the government report.

Holt Ashley, Stanford University: You didn't say much about the aerodynamics in C81. For example, steady or unsteady, whether you've looked into things like dynamic stall, and what about the reverse flow region?

Sadler: Okay, the reverse flow region is handled; I don't believe dynamic stall was modeled.

Ashley: How do you handle the reverse flow region?

Sadler: There are tables, aerodynamic tables that go from zero to 180 degrees and cover a range of Mach numbers. Inside C81 we do a table lookup. The angle of attack and Mach number is calculated at each computation point and then it goes to the table to look up and see what the....

Ashley: That's quasi-steady for the table lookup?

Sadler: Quasi-steady, that's right.

Bill Warmbrodt, NASA Ames: Of the analyses used for the correlation effort, I believe DRAV21 is the only undocumented analysis used, at least with regard to the public domain. Does Bell have any plans of making the documentation of that program available in the future?

Sadler: I'll pass that to Jing. I don't know what the answer is there.

Yen: I think one thing, you know, that's not too good about working for Bell Helicopter is that you don't get too many chances to publish. This DRAV21 was developed back in 1975, so the program has been around for quite a few years. We've used the program to design quite a few recent Bell Helicopter soft inplane rotors such as models 412, 680, and so on. But we have not had the intentions or the time to really present it in an AHS paper format or other government report format. In-house documentation has been made available to our own guys. So to answer your question, we do not have a plan, yet, to publish it.

Friedmann: I'm going to make one comment which I guess applies to a number of people at this table. One is [that] I am somewhat surprised to hear this presentation and be told that correlation is done with a set of undocumented equations. If somebody cannot look at your equations then, in my opinion, you are not doing correlation, you are doing curve fitting. The second comment I have is that with other information which has been published since 1975 (which is eight years ago), it has been made very clear that, particularly in stability type correlation, the role of the geometrically nonlinear terms can be quite important, and how those terms are handled in a computer program is crucial. I have not seen the word "nonlinear" mentioned and that, to me, is a big danger signal. You can show me the best correlation and I will tell you, you are not doing correlation, you are doing curve fitting.

Sadler: Probably some of the nonlinear terms you are talking about are in DRAV21, but I can't show you the equations. The kind of steady bending-moment-times-curvature-type equations (at Bell we sometimes refer to them as D-cross-F-type terms), the EI-type terms, are in DRAV21. But I can't show you the equations; they are there, you know.

Hammond: That's a general sort of question that we may want to approach again during the closing general discussion.

Yen: I would like to make a comment to the comment you made there. I think those computer programs should be used as design tools. Correlation is required to build up your own confidence. We've done a lot of correlation over the years because we've done a lot of development programs, so we've built up confidence and we feel comfortable to use them. As far as the correlation shown here, whether it's good or poor, that's what came out of the program. To me the correlation is not the game. The correlation is a tool to build up your own confidence. So as long as you feel

comfortable to use it to design the ships, to me then it has really served its purpose.

Hammond: Let's move on, we'll come back and give you another chance in the wrap-up, Peretz.

Friedmann: I would like to quote Dick Bennett, who said: "Confidence, like beauty, is in the eye of the beholder."

PREPARED REMARKS BY DEV BANERJEE

This morning Wendell Stephens presented capabilities of different programs, including DART and E927, which we essentially used for our ITR methodology comparisons and correlation studies. That was a comprehensive presentation. My comments this afternoon would be on the specific correlation studies that we made and if any of you have questions regarding our analytical tools that we used please feel free to ask, but I will not be addressing it as Gene did this afternoon. Before I get started I'd also like to commend the U.S. Army personnel both here at the Aeromechanics Lab as well as the Applied Technology Labs for providing the helicopter industry this opportunity to systematically establish the strengths and weaknesses of the analytical tools to predict aeroelastic characteristics of, primarily, bearingless and hingeless rotors. The studies ranged from the simple model of a blade with a root flexure, in Case A, to correlation with flight test results of the BO 105/BMR. Within the constraints of the budget and schedule, at Hughes we opted to study Cases A through D, including Case B that Bill Bousman presented this morning, and we used aeroelastic stability analysis programs DART and E927. Both of these programs are currently being revised at Hughes to provide additional capabilities. In DART we are adding the capability of additional blade elements and Floquet analysis for studying nonisotropic support conditions as well as forward flight analysis. One of the basic limitations of the government version, E927, and I guess it's generally true, is that it doesn't have the capability of modeling bearingless rotors. It makes an approximation of bearingless and hingeless rotors to articulated models. So we are adding the capability to generate the modal characteristics of redundant load paths to model bearingless rotors. This morning a thorough presentation of correlation was given for the different tasks A through F, and essentially the findings and some of the reasons were provided for the lack of correlation. What I'd like to do is take this opportunity to make some comments on each of these correlation studies.

Task A [Slide 5], if you remember, was one of a blade with root flexures where there was precone and negative droop and variation of precone, and negative droop, and torsional flexibility of the torsion flexures and parametric studies of the damping of the lag-mode with collective pitch variation. I feel that most of our correlation predictions for all the cases were reasonably good and I'd like to point out that we neither had dynamic nor static stall in our analysis. We found that it was strictly a function of, essentially, a pitch-lag coupling. There's quite a bit of flap coupling as well due to the trim-deflected shape of the blade for each one of these cases. These couplings were amplified more for the soft flexure as compared to the stiff flexure. We could see, for instance, in the cases where we had the stiff flexure, with variation of collective pitch you found generally very little change in damping. If you look at the coupled-mode shape of the lag mode you'd find that it is predominantly a lag mode with very little pitch or flap coupling, whereas [in] a similar study with a soft flexure you would find considerable coupling. Again, if you look at the coupled mode shape, you'd find considerable coupling of torsion and flap in the lag mode, and if you look at the signs of the

TASK II A - COMMENTS

- CORRELATION GENERALLY GOOD
- COUPLING MORE SIGNIFICANT USING SOFT FLEXURE
- PRECONE (USING SOFT FLEXURE) RESULTS IN UNSTABLE LAG MODE
- ANY LACK OF CORRELATION AT HIGHER θ COULD BE ATTRIBUTED TO X-AXIS REPRESENTATION

Slide 5

coupling of the flap with the lag and the torsion with the lag you'd find that it's consistent with the trend of the damping plot; [this is] just a general observation.

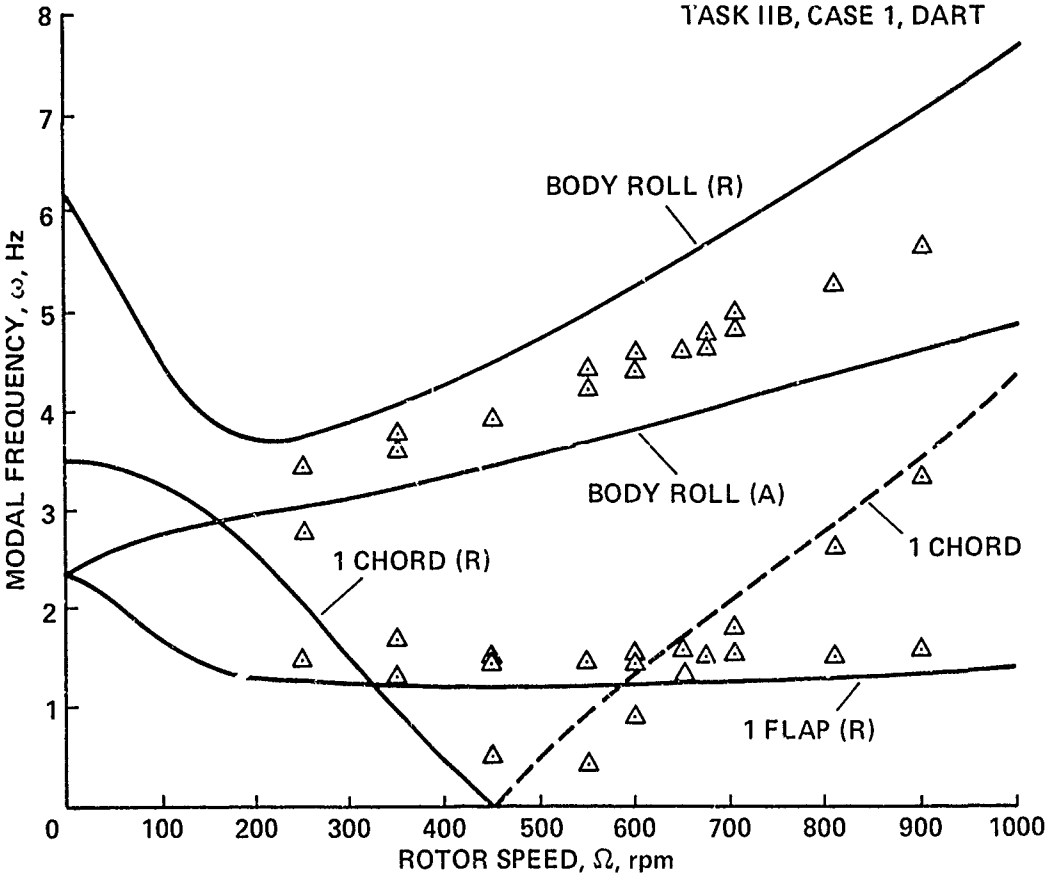
Again, this instability that we saw with the soft flexure with, I believe, three degrees of precone, essentially verified the bubble of instability that has been presented in several papers in the past by Bob Ormiston, Peretz Friedmann, and others. That essentially verifies that this instability occurs for a stiff-in-plane rotor. However, what's different between what I believe was presented in those papers as compared to what this test result shows [is] that this bubble of instability occurred for a matched stiffness rotor. My last comment on this slide is that I don't think we have a consistent basis for X-axis representation for correlation. The test data is plotted for the pitch angle that was set up in the test, whereas our analysis was based on the existing collective pitch of the blade during the test. If you have cases with soft flexures or if you have pitch-flap coupling which would change your actual pitch angle due to delta-three coupling then obviously we are comparing the wrong set of parameters. Again I could attribute some of our lack of correlation at higher collective pitch to differences between the collective pitch setting and what is actually seen in test.

Task IIB [Slide 6]--again I believe we were the only ones who did that correlation, we used both DART and E927, basically because we ran into some problems in correlating with the test data, especially the sharp instability that we saw in the test data. Again correlation of frequency and damping was generally good, I believe. One of the frustrating experiences was this matching of the lag frequency [Slide 7]. We knew it was a rigid blade, it was set up that way with a root flexure so it was essentially a blade with a root hinge, and yet we couldn't match it given the EI distribution. We went through the whole process based on the EI distribution and then when we came back, after doing all the studies, meaning to verify these results using E927, we set up the E927 model both [with] the root flexure stiffness based on frequency as well as EI distribution [Slide 8]. And there we found the difference in the calculated EI based on the test numbers and it was very obvious that the differences of our prediction with test data of the lag frequency was

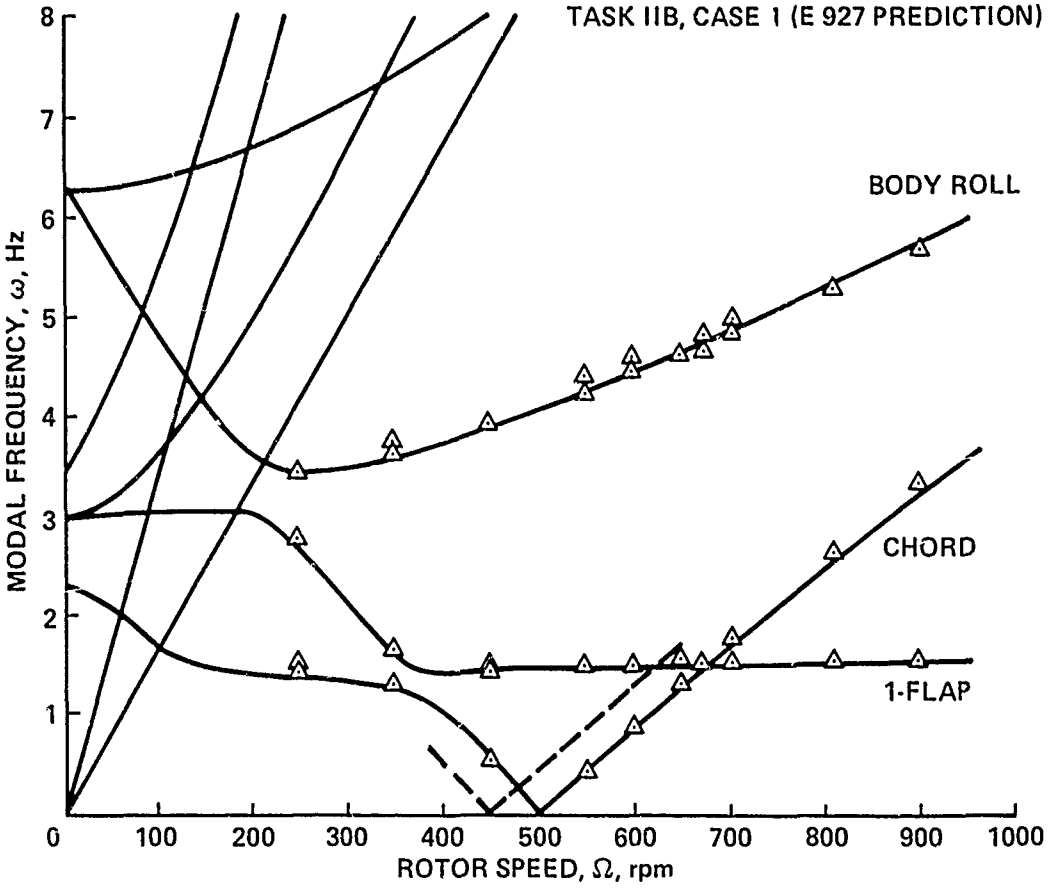
TASK IIB - COMMENTS

- CORRELATION USING DART AND E927
- CORRELATION OF FREQUENCY AND DAMPING GENERALLY GOOD
- DART PREDICTION OF LAG FREQUENCY OFFSET (3-5 PERCENT) A CONSTANT AMOUNT AT ALL RPMS
- INSTABILITY DUE TO LAG/BODY PITCH COUPLING WELL PREDICTED
- SHARP FLAP/LAG INSTABILITY NOT PREDICTED BY EITHER DART OR E927

Slide 6



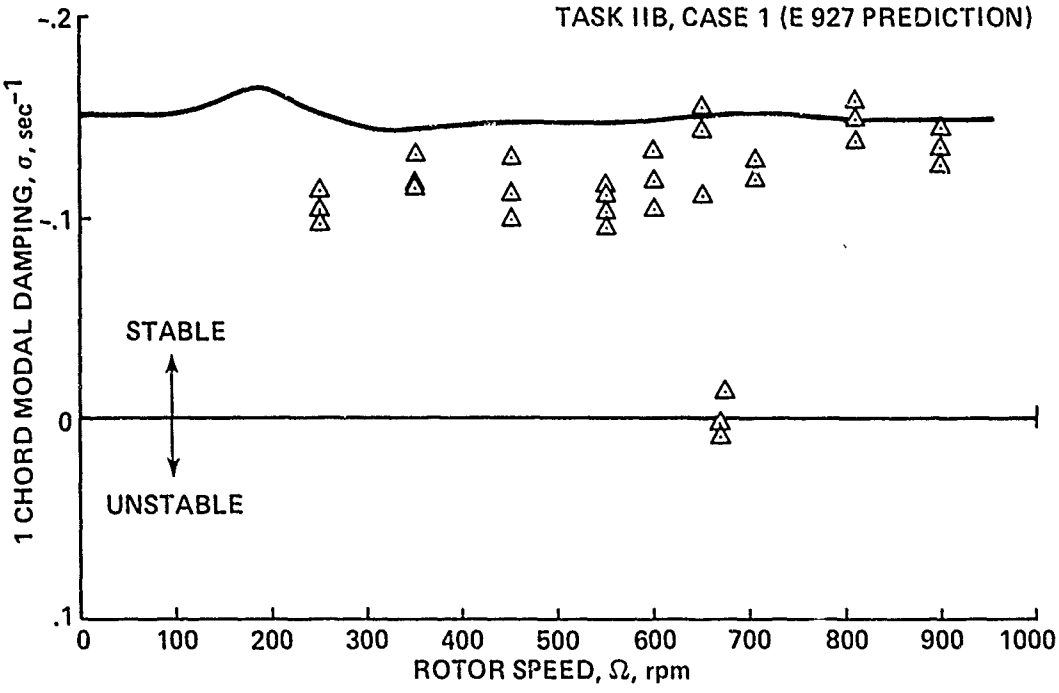
Slide 7



Slide 8

essentially this stiffness calculation of the root flexure based on EI distribution, as compared to the stiffness calculated based on test data. Again I think the instability of the lag with the body pitch coupling was generally well predicted even though, as was mentioned this morning, we do have the limitation in DART of requiring [an] isotropic support model. But we do have the flexibility of a modal representation of fuselage properties in coupling the rotor with the fuselage so we can put as many modes as we want, in any shape, for the hub modal characteristics. One last comment, again it was mentioned this morning, [but] I'd just like to throw it out. We did not see this in our correlation, in Task IIB we did not see this sharp instability [Slide 9] of the coupled flap-lag mode at around 675 RPM. Again, that's an anomaly that was our finding.

That was Task IIB; for Task IIC [Slide 10] again, correlation was done using DART and E927. Again, the delta separation of lag frequency prediction with test data [Slides 11 and 12] was the result of a wrong calculation of the stiffness, of the root flexure stiffness. I believe all the instabilities and coupling effects were well predicted, though quantitative correlation could be improved [Slide 13]. [For] these two cases, Tasks IIB and IIC, our E927 model was essentially set up as an articulated rotor with a root spring and it gave the best correlation, so I believe that's essentially how the model behaved during the test. One general

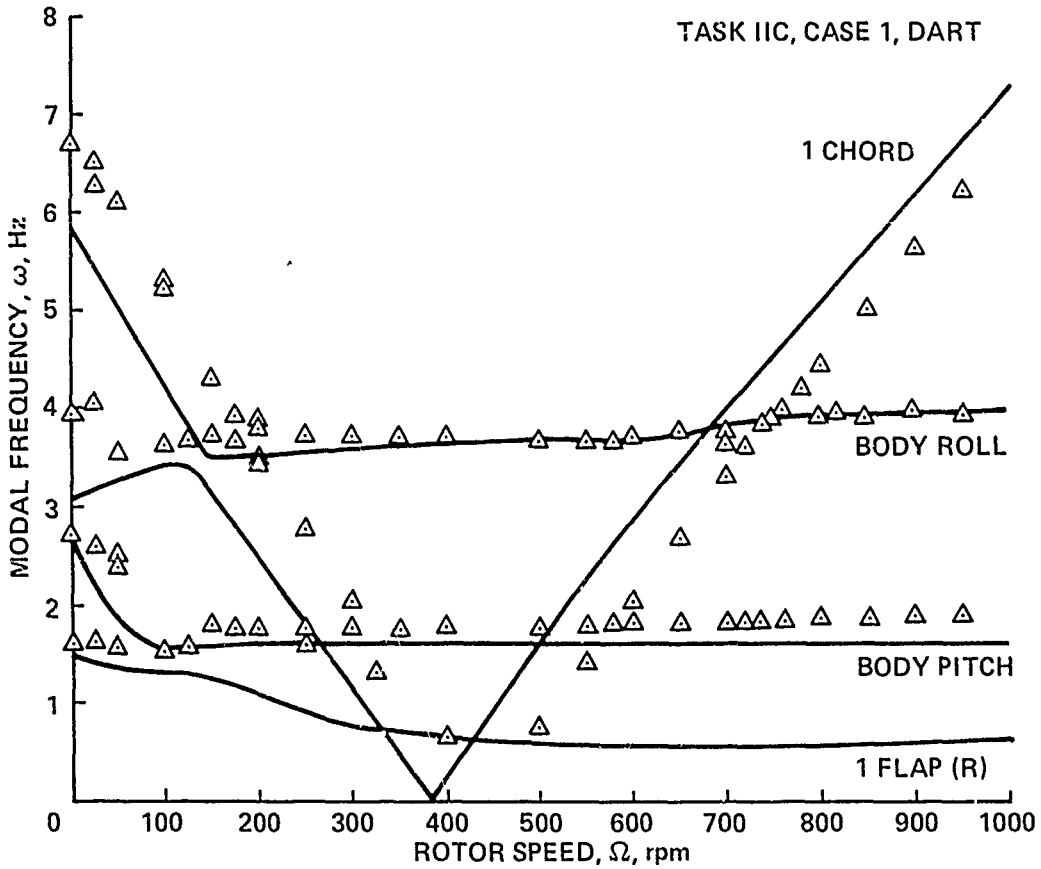


Slide 9

TASK IIC - COMMENTS

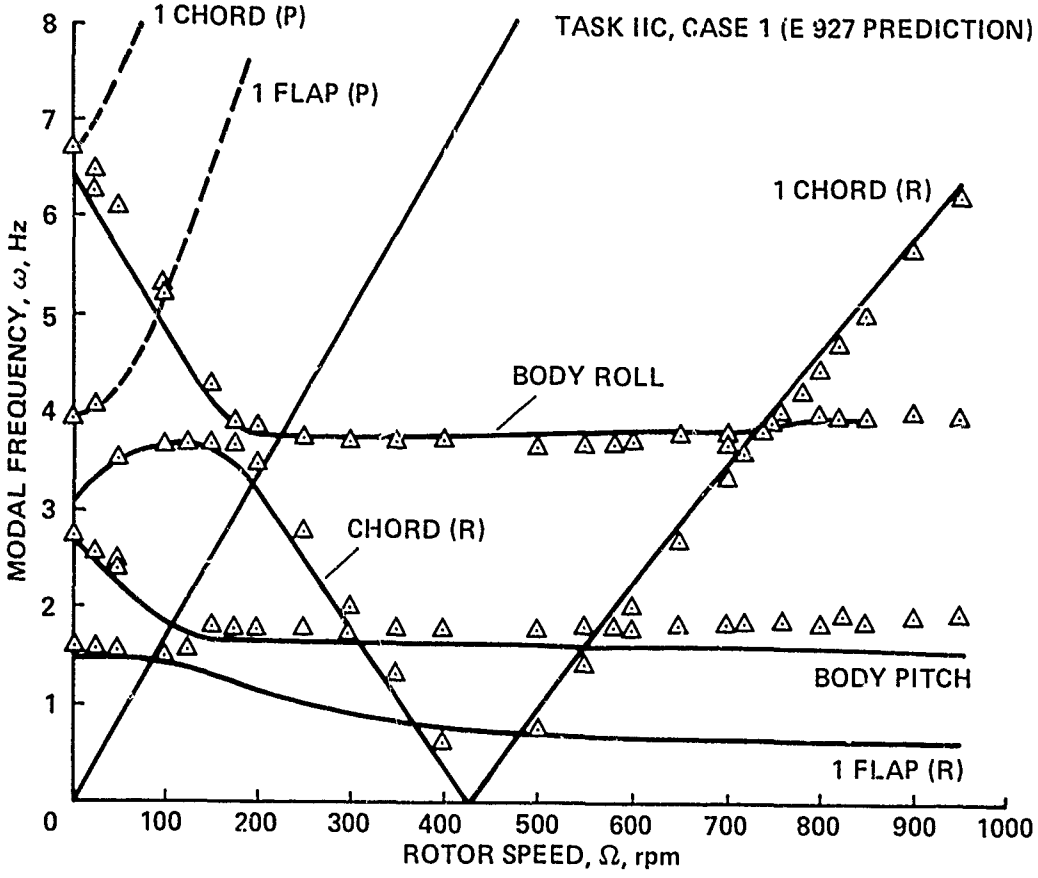
- CORRELATION USING DART AND E927
- FREQUENCY PREDICTION GOOD - Δ SEPARATION AS IN TASK IIB
- ALL INSTABILITIES AND COUPLING EFFECTS WELL PREDICTED, THOUGH QUANTITATIVE CORRELATION COULD BE IMPROVED
- TASK IIC CASE 2 - STRUCTURAL COUPLING DUE TO FLAP TRIM DEFECTION BENFITIAL FOR ISOLATED ROTOR, DETRIMENTAL TO ROTOR/FUSELAGE COUPLING
- IMPROVEMENT IN LAG DAMPING WITH NEGATIVE PITCH/LAG COUPLING PREDICTED

Slide 10

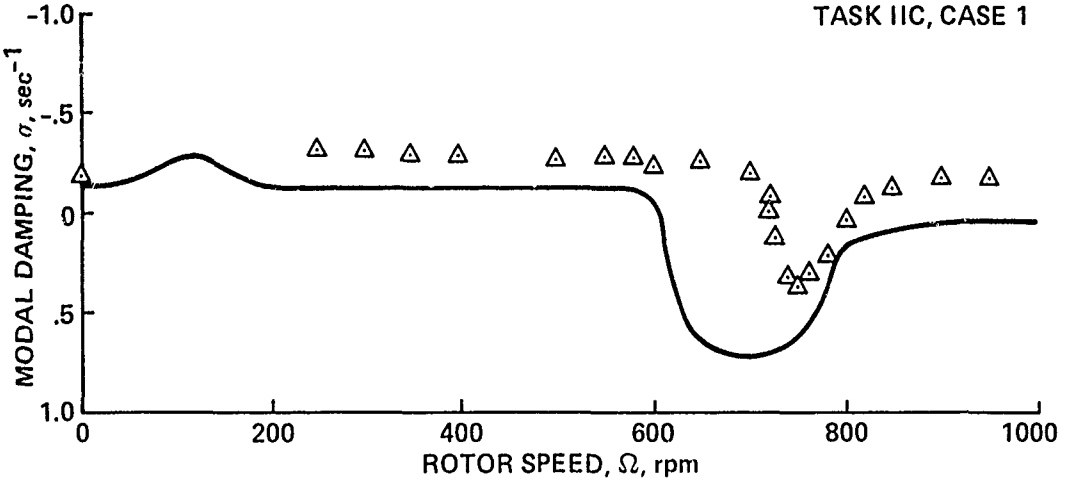


Slide 11

finding from the test cases, which I believe we've verified, is Case 2 of Task C was [that] structural coupling due to flap trim deflection was beneficial. That is, the flap-lag coupling due to the flap trim deflection was beneficial for the isolated order whereas it was, I believe, slightly detrimental to the rotor/fuselage coupling. Again I don't think that came out in most of the test studies; in other words, no effort was made to see which couplings were beneficial for isolated rotors and which were not in the coupled rotor/fuselage sense, but I think that this test result did show that. Again, improvement in lag damping with negative pitch-lag coupling, that is, kinematic coupling at the root of the blade, was predicted and the test results verified it. Task D [Slide 14] [was] the last correlation study that we made. I believe this is the first example of a truly bearingless rotor that was modeled. Again, if you set up your structural model with the dual-load path and the exact geometry of the pitch link attachment and the structural properties of the flexbeam correctly, you would get the value of the pitch-flap coupling. We find that with the leading-edge pitch link the pitch-flap coupling, delta-three, was about -35°, -37°, which resulted in the first flap frequency of about 0.68/rev, very close to the first lag frequency of about 0.67/rev. We found that there was considerable coupling between the flap and lag modes at higher collective pitch, because of the closeness of the frequencies [Slide 15]. Again, we could verify that by looking at the coupled mode shape at high collective pitch that resulted in improved damping of the lag mode, which the test results showed. Again with the



Slide 12



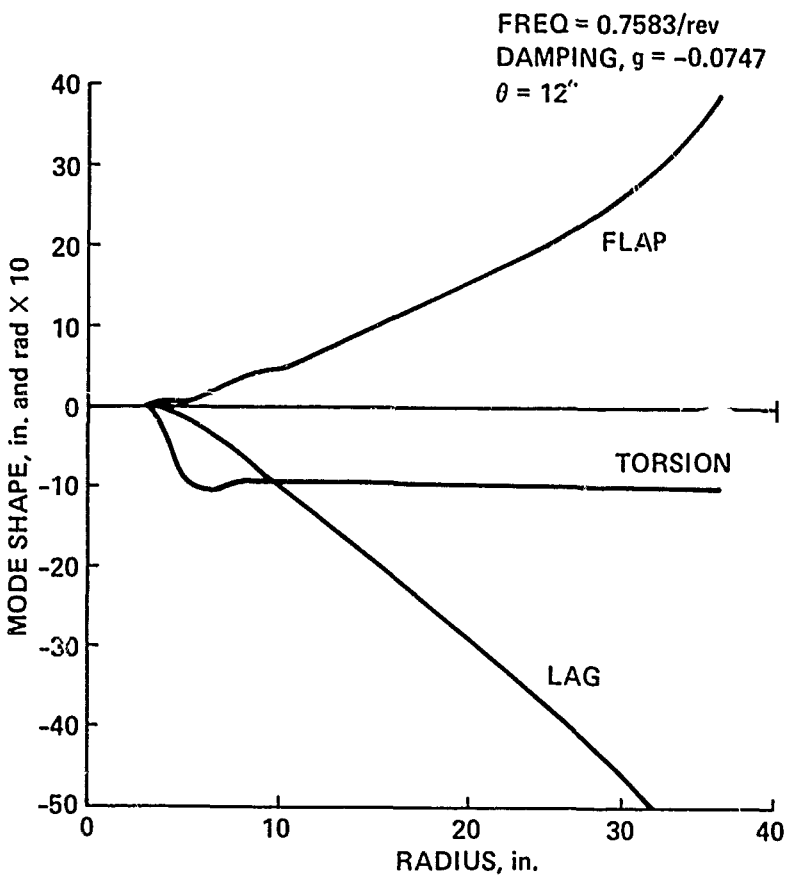
Slide 13

- L.E. PITCH LINK
  - PROXIMITY OF FLAP AND LAG FREQUENCIES (WITH NEGATIVE δ_3)
  - CONSIDERABLE COUPLING OF LAG MOTION WITH FLAP AND FEATHERING AT HIGH θ
- T.E. PITCH LINK
  - POSITIVE δ_3 ENSURES GOOD SEPARATION OF FUNDAMENTAL MODES
  - NEGLIGIBLE COUPLING FROM COUPLED MODE SHAPES
- BOTH CASES HAVE LOW TORSIONAL FREQ. (2.4/REV) AND MARGINALLY STABLE 2 FLAP/TORSION MODE AT APPROX. 3/REV
- DUAL PITCH LINK
  - NO δ_3
  - HIGH TORSION FREQUENCY (4.7/REV)
  - NEGLIGIBLE COUPLING

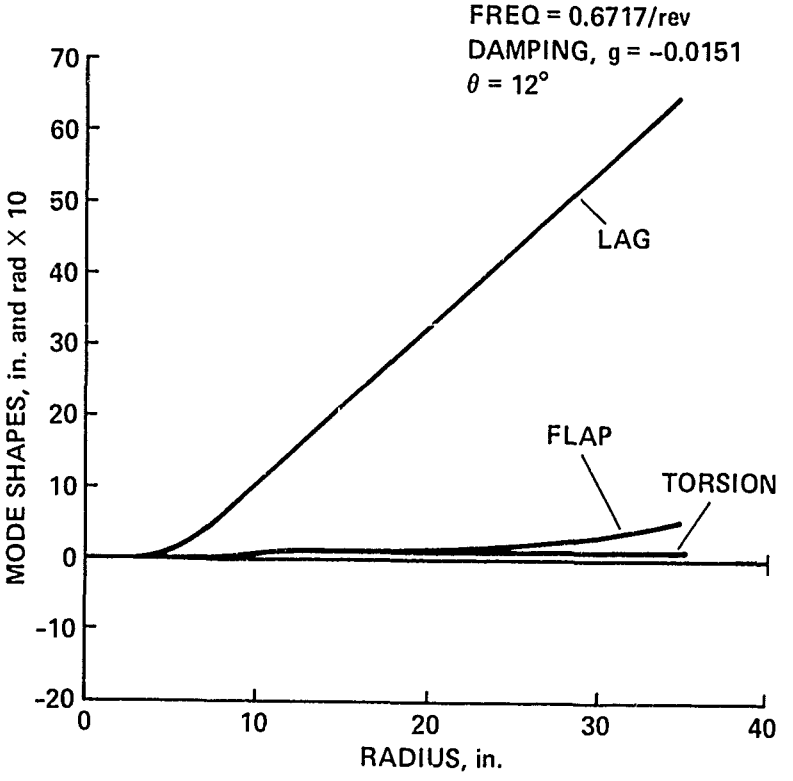
Slide 14

trailing-edge pitch link, the pitch-flap coupling reversed itself [giving] good separation between the flap and lag frequencies and relatively little coupling between the modes [Slide 16]. Hence, the trend of the damping of the lag mode with collective pitch reflects the relatively less coupling between the lag mode and the other modes. Again, for these cases we did predict a torsion mode at about 2.4/rev. Without the dual pitch link or an actual snubber, the torsion mode is extremely soft. The torsion frequency we found to be around 2.4/rev and we did essentially verify this problem of second flap/torsion flutter at around 3/rev. Again, this dual pitch-link configuration essentially eliminated delta-three coupling and also drove the first torsion frequency up, which essentially got rid of that flutter problem. We also found relatively little coupling between the lag mode and other modes with varying collective pitch.

That essentially covers my general comments on these different correlation studies. I'd like to make one comment in additon to that. I think if I were asked to choose one area in analysis that requires special attention for predicting the fundamental rotor modal characteristics, I think it would be the blade root area. I think currently a considerable emphasis is being placed on the correct structural representation of the blade root area, specifically for bearingless rotors with dual-load paths, and the [proper] geometry and kinematics of the root end structure which influence the damping of the fundamental modes, primarily the lag mode. I think considerable attention needs to be paid to that area for predicting the characteristics of the fundamental modes.



Slide 15



Slide 16

Jing Yen, Bell Helicopter Textron: I have heard you talking about this flap-torsion coupling near the frequency of, is it, 3/rev?

Banerjee: Yes.

Yen: I'm wondering what kind of aerodynamics you have in your analysis.

Banerjee: Quasi-steady aerodynamics. We have the capability of putting in different inflow values for different radial stations along the blade, essentially hover quasi-steady aerodynamics. Again, we have submitted a final report like everybody else on the methodology assessment, and I think that if you look at our report you'll find that that mode is marginally stable or unstable just because of the coupling of the second flap and torsion modes, just structural coupling.

Bill Bousman, Aeromechanics Laboratory: Did you say something about IIA being matched stiffness, or did I miss something?

Banerjee: Yes, I guess I did say that.

Bousman: I don't think it really is.

Banerjee: No.

Dewey Hodges, Aeromechanics Laboratory: What I thought he said, was that the earlier reported results for the bubble instability clustered around the matched stiffness area, and that is true. But that's not the only place where they were; they sort of fanned out from there.

Bill Warmbordt, NASA Ames: Would the MacNeal-Schwendler document on SADSAM be considered an up-to-date documentation of the program DART?

Banerjee: No. A lot of changes have been made since then and I think as far as going into the specifics of all the changes that have been made I would rather defer to Lou Silverthorn on that. It is the basic model we use but there have been considerable changes; but again the document has not been updated.

Yen: Have you ever attempted to correlate with Task IIE using DART?

Banerjee: Obviously we don't have an eigenvalue analysis in forward flight. I think the way we would go about doing it would be to do a transient response analysis--have a forced response at the frequency of interest, and [then] look at the decay and do a damping calculation study. For this program we did not venture to do the correlation for Tasks IIE and IIF. However, we did, for ourselves at a later time, correlate the air resonance characteristics of the Froude scale BO 105/BMR rotor test results, but it wasn't documented in these reports.

Gene Hammond, Panel Chairman: Other questions? I have one on the blade model that you use in DART. Is it a finite element approach or is it a modal approach?

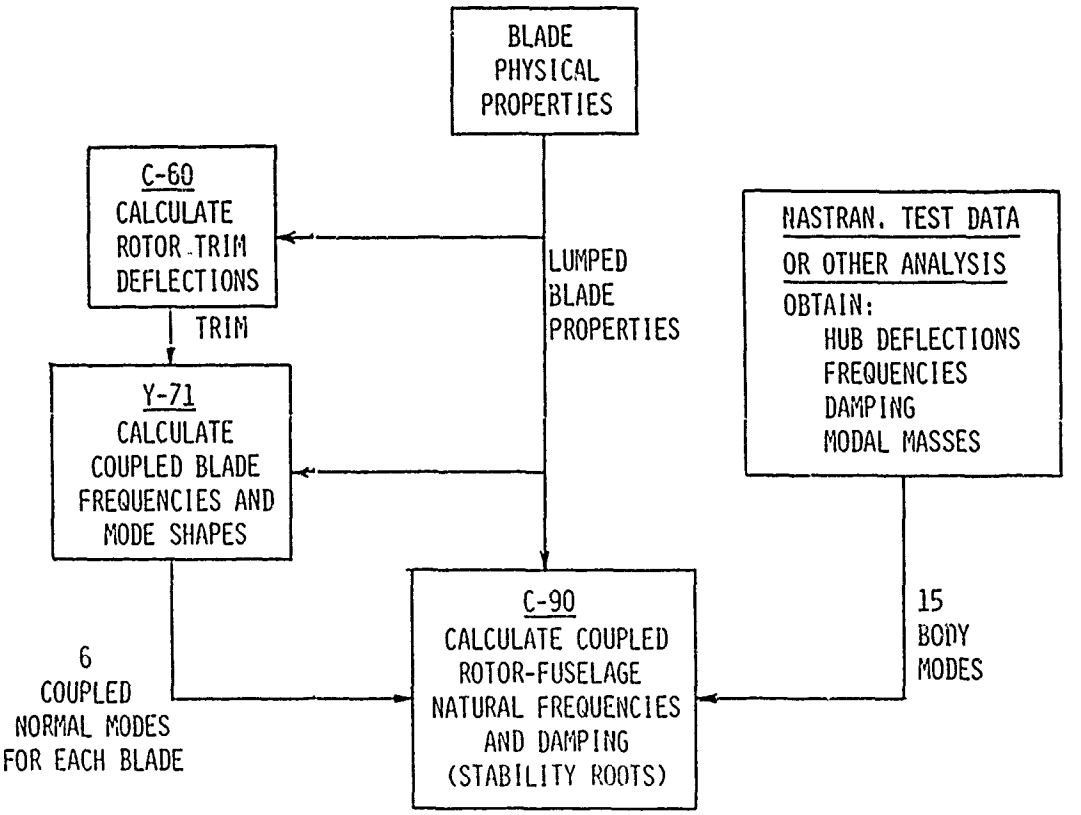
Banerjee: It's a finite element approach; again, Dewey [Hodges] might take exception to the term finite element. It's a lumped mass approach, a discrete element approach.

PREPARED REMARKS BY FRANK TARZANIN

What I will do is briefly discuss what we've learned about our stability prediction technology and what actions we've taken. However, first I'll have to quickly review what our prediction technology is. The C-90 math model allows the rotor to [have] up to four blades with each blade represented by up to six fully coupled modes. The blade modes are defined about the steady state deflections. The aerodynamics are essentially quasi-static using table look-up techniques. Reverse flow is included via the tables. The fuselage can be represented by up to 15 arbitrary fuselage modes, and the solution is the eigenvalue/eigenvector type with Floquet for forward flight.

To obtain the inputs for the C-90 program, four other computer programs must be run [Slide 17]. The first program takes the blade physical properties and discretizes them. Second, we use the discrete properties in the C-60 rotor program to calculate the steady state trim. Then we input the steady-state trim deflections to the Y-71 program and calculate the coupled blade modes about the static deflection. Then we can use NASTRAN, test data, or any number of simple analyses to obtain up to 15 body frequencies and modes.

PROCEDURE FOR PREDICTING STABILITY



Slide 17

In the correlation report we identified three deficiencies in the stability prediction procedure [Slide 18]. The first is that the C-60 program and the Y-71 program have inconsistent assumptions and it's frequently difficult to rationalize, for example, representing the root end conditions on both of these rotors with the same geometry when the level of sophistication is different in the two programs. Secondly, neither the C-60 nor the Y-71 program can analyze a rotor with a torque tube or a multiload path flexbeam. What we had to do in the case of the BMR is to define an equivalent single beam that gives you the same frequency, but obviously didn't have the right kinematics. The third deficiency was the one-per-rev cyclic motions. To obtain rotor trim you get significant one-per-rev, both cyclic and flapping motions, which could significantly change the kinematic coupling. This is true in forward flight; we recognize that.

Since the correlation was performed we've had a chance to review what everyone else did and we've identified two additional regions of suspicion. The first: we suspect that the aerodynamics may be too simplified. Generally it's been true, if you look at the C-90 correlation, that the correlation gets worse at the higher collectives. Now here's a case [Slide 19] where we have lead-lag damping versus blade pitch where it's the lowest amount of coupling. We've got no precone, no droop, no twist, and you can see that as the collective angle increases the prediction gets worse and worse and worse. In fact, I'm very appreciative that somebody mentioned this morning about the Reynolds numbers. I'm going to try that when I get home; that might really help. But if it doesn't, that certainly indicates to me a deficiency in the aerodynamic representation. The second area is a potential error in the flap coupling to the body. This shows up in poor prediction of body

PROCEDURE DEFICIENCIES

KNOWN:

- EQUATIONS AND ASSUMPTIONS FOR THE STEADY STATE DEFORMATION (C-60) AND NORMAL MODE/NATURAL FREQUENCY DEFINITION (Y-71) ARE NOT CONSISTENT
- BOTH C-60 AND Y-71 CANNOT ANALYZE A ROTOR WITH A TORQUE TUBE OR A MULTI-LOAD PATH FLEX BEAM
- ONE/REV CYCLIC MOTIONS GENERATED BY THE ROTOR TRIM ARE NOT INCLUDED IN C-90

SUSPECT:

- AERODYNAMICS TOO SIMPLIFIED
- ERROR IN FLAP COUPLING TO BODY

Slide 18

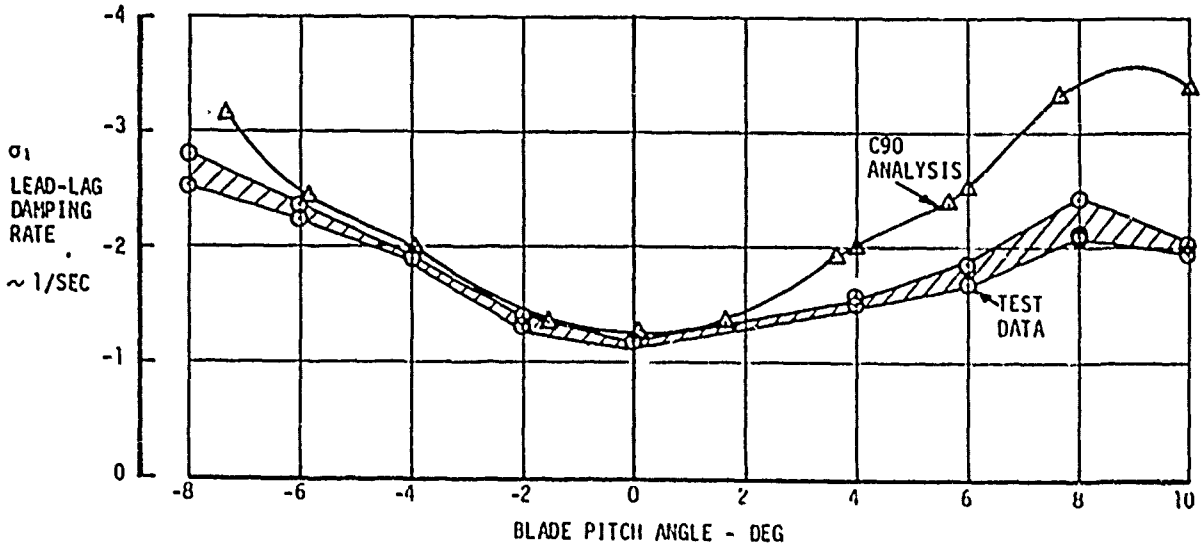


FIGURE 10. LEAD-LAG DAMPING AS A FUNCTION OF BLADE PITCH ANGLE AT 1000 RPM
STIFF FLEXURE, ZERO PRECONE AND DROOP ANGE

CONFIG. II-A, CASE 1

Slide 19

roll and body pitch damping while we find fairly good prediction of the lead-lag damping. I guess the best example of the problem is illustrated here [Slide 20]. Here we have the modal frequency versus rpm, and of particular concern is right in this region where you can see the C-90 predicting a coupling between the flap regressing mode and the body pitch mode. That clearly is not shown in the data. I suspect a straignt-out error in the code somewhere and I think this is a region we should certainly look into.

Next, I'd like to outline the actions we've taken and the actions we plan to take [Slide 21]. First, we're revising the C-60 program to include the prediction of natural frequencies and mode shapes. We're also going to include large, steady, principal axis deflections, and we're going to include a flexbeam root end with torque tube and up to four elastic beams. This will eliminate the need for Program Y-71 and will allow us to analyze any flexbeam configuration. The planned actions are [Slide 22], we'd like to investigate incorporating the one-per-rev cyclic pitch motions, we want to review the aerodynamic representation to consider including the unsteady stall and the dynamic inflow effects (but first I'm going to look at Reynolds number), and then review the body coupling equations and the code. Any questions?

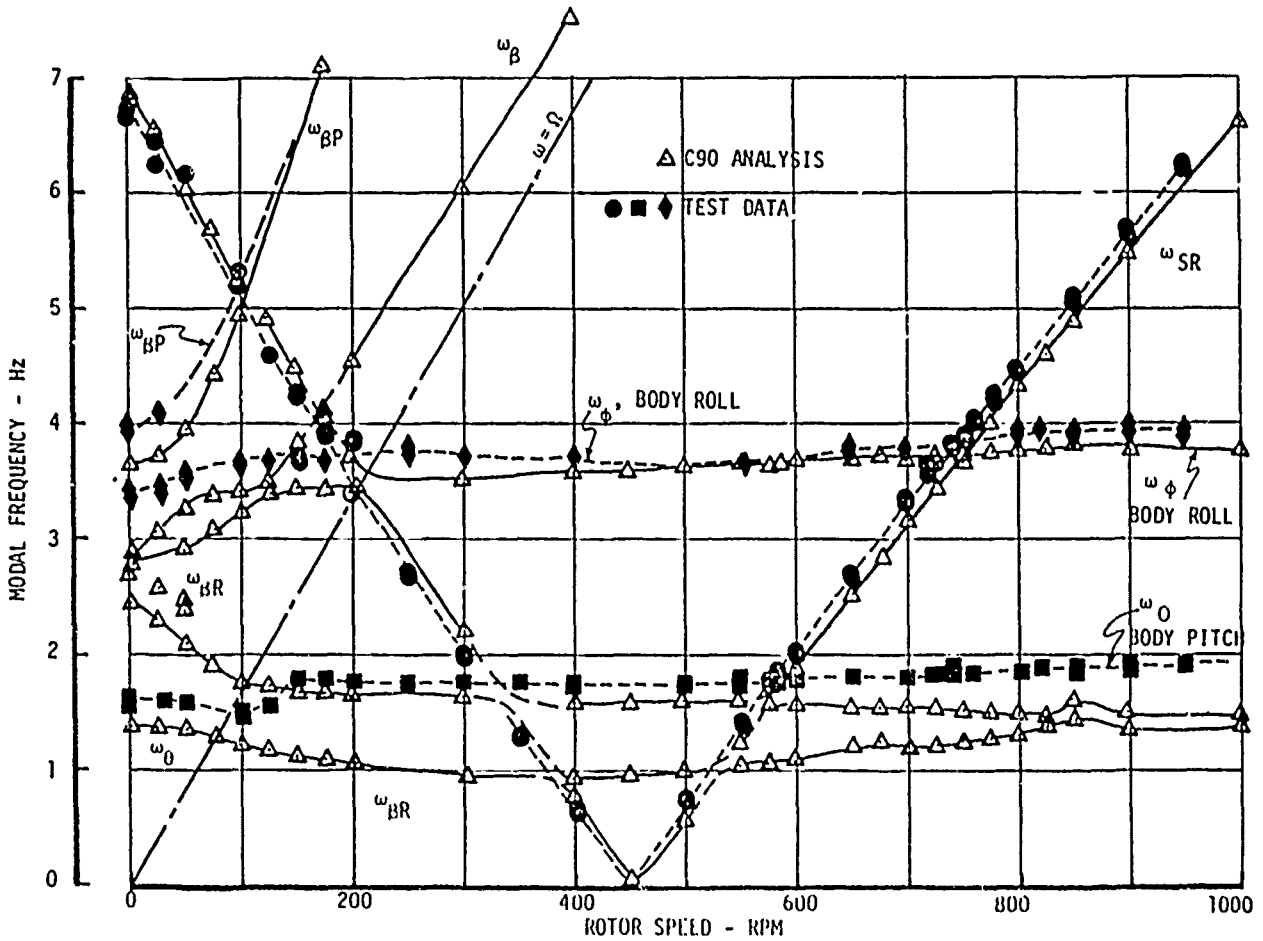


FIGURE 18 MODAL FREQUENCY VARIATION WITH ROTOR RPM

CONFIG. II-C,CASE 1: ZERO ROOT PITCH AND LEAD-LAG FLEXURE ANGLE

Slide 20

ACTION TAKEN

REVISING C-60 TO INCLUDE:

- PREDICTION OF NATURAL FREQUENCIES AND MODE SHAPES
- LARGE STEADY PRINCIPAL AXIS DEFLECTIONS
- FLEX BEAM ROOT END, WITH TORQUE TUBE AND UP TO FOUR ELASTIC BEAMS

THIS WILL:

- ELIMINATE THE NEED FOR PROGRAM Y-71
- ALLOW ANALYSIS OF ANY FLEX BEAM CONFIGURATION

Slide 21

PLANNED ACTION

- INVESTIGATE INCORPORATING ONE/REV CYCLIC MOTION GENERATED BY ROTOR TRIM
- REVIEW AERODYNAMIC REPRESENTATION AND CONSIDER INCLUDING:
  - UNSTEADY STALL
  - DYNAMIC INFLOW
- REVIEW FLAP-BODY COUPLING EQUATION AND CODE

Slide 22

Bill Bousman, Aeromechanics Laboratory: As far as the Reynolds number goes, for that experiment we took some low-Reynolds-number data that we had and fitted lift and drag coefficient terms to it. Then we gave you an analytic expression to use in your correlation in lieu of your normal tables. So you have that Reynolds number effect to within the accuracy of the expression we gave you.

Tarzanin: Then I fall back to what I have on [my slides].

Bill Warmbrodt, NASA Ames: Considering that you've identified action items relative to C-60 and Y-71, do you agree with Wendell's observation that C-90 is capable of analyzing a bearingless rotor configuration?

Tarzanin: Oh, I think it is, but I think the proof is to actually make the mods to C-60 and crank it into C-90. I think it can do it if you have the right modes. In fact it did surprisingly well considering that we used a very simple representation--we essentially fudged the EI in lag to give us the same frequency as the dual beam, and we know that the coupling is not going to be right.

Warmbrodt: So you consider that C-90 will not require any revisions?

Tarzanin: Yes, except I think the flap coupling into the body roll/pitch has a problem.

Jerry Miao, Sikorsky Aircraft: You said you fudged the EI for the dual beam to get the lag frequency right?

Tarzanin: We only had the analysis with the single load path, so how do you...?

Miao: But you use only the first edgewise bending mode for the bearingless main rotor, right?

Tarzanin: Yes.

Miao: The first edgewise mode, in the EI, if you used the dual beam, take the centroid of the composite section, EI, about its own centroid, and move it to middle of the section, that approximates the first edgewise mode very well.

Tarzanin: I think there was shear deformation in there that essentially gave you a softer effective EI.

Dev Banerjee, Hughes Helicopters: Frank, just a comment on that. I think you might be able to match your frequencies based on test data using the first lag mode but I think it would require a detailed model to determine what the kinematics are and hence its effects on the stability.

Tarzanin: Most assuredly, I totally agree, yes.

Miao: Absolutely, you're right.

Peretz Friedmann, UCLA: I'm not sure I understood what you said about having steady state trim deflections in your program and at the same time neglecting one-per-rev cyclic. Let me just see whether I understand it, even for the case of forward flight your steady state trim is a time-independent trim, is it?

Tarzanin: Yes.

Friedmann: How can that be?

Tarzanin: You take the steady deflection, perturb your modes about that deflection not considering one-per-rev cyclic and one-per-rev flapping.

Friedmann: If you look at advance ratios of like, maybe 0.3 or 0.4, you will find out that the cyclic components of pitch are equivalent to almost 10°, and you really are neglecting an imput of 10° in cyclic to the....You realize that that's somewhat absurd.

Tarzanin: That's why we said we have to put that in. I just wanted to point out we were neglecting that in forward flight, and in fact you're talking about one-per-rev deflections on the order of the steady deflection. If the steady deflection is important, certainly you would think the one-per-rev deflection is important. Now how exactly you handle that in the Flouqet technique, whether you do it for the average damping or do you look what the damping is at the worst azimuth, I'm not sure.

Friedmann: I think you should read the literature. There are some papers on this subject.

Bob Sopher, Sikorsky Aircraft: Frank, you calculate your coupled blade modes about the static deflection position, right?

Tarzanin: Yes.

Sopher: What's the major thing that you expect to get by doing this? Why could you not calculate your coupled modes about the zero deflection position?

Tarzanin: Well, to get the kinetics.

Sopher: You're talking about the pitch-lag and the flap-lag-torsion. So conceivably you could have calculated modes around a zero deflection position, but loaded into your response analysis the correct kinematics for the pitch-flap-lag coupling. Have you thought about doing that?

Tarzanin: Not really, no. I guess my thought would be that probably the easiest way to do it would be to deform the blade and then perturb from the deformation.

Sopher: Yes, I understand that you get your perturbation equations from that condition, but I'm just trying to understand what the impact of this is. What's the major impact, is it a pitch-flap-lag coupling effect, mostly the kinematics?

Tarzanin: Yes, the kinematics, that's what I get.

Warmbrodt: I'd like to comment. I'm a bit familiar with C-90 and it does have a Floquet stability analysis capability and so that sheds some light on Professor Friedmann's comment that they aren't neglecting significant effects with regards to periodicity in their stability analysis, to a degree.

Bob Ormiston, Aeromechanics Laboratory: I'm just stimulated to make a couple of comments along that line, and Bill just added some thoughts to what I'd like to say. The C-90 program does do a Floquet analysis but in fact it leaves out some of the trim terms, and as Peretz has said, some of those are known to be important in stability calculations, at least for the isolated blade calculations. There are some examples in the literature showing what happens when you throw those terms out and when you include them. The comment I was going to make was that I think we're illustrating one of the fundamental problems of analyzing these types of rotors. We're used to doing modal analyses where you calculate the modes in a vacuum for the undeformed condition, and that works fine for all kinds of linear, or mostly linear, stability calculations. Here where the couplings, the elastic couplings, the kinematic couplings and so forth, are a function of the equilibrium deflection shape, you find yourself now trying to generate so-called modes about an equilibrium solution condition. That leads to some question as to how valid or rigorous is that. Then you go to forward flight and you've got the periodic component of equilibrium [so] it gets more hazy and the more you use that approach the more questions you're going to raise for yourself. That's why a lot of people are starting to look at just plain "Let's go to finite element" methods, get away from the modal approach, and just accept the numerical consequences or burden that you have to deal with. If you're dealing with a rigid blade analysis with a few hinges, of course, no problem, it's just the physical approximation and one accepts the fact that that's simple to analyze. But of course it really doesn't work, for the bearingless configurations so it's a real dilemma. I hope people get the impression that maybe we've got to move away from the modal type analyses because they just don't form a practical basis, they leave too many questions open.

Jing Yen: I'm a little bit confused here. I've heard of the programs at Boeing-Vertol; C-90, C-45, C-60, I believe, right?

Tarzanin: Yes.

Yen: If you have seen some shortcomings with the C-90 analysis, why don't you go back to the C-60? In other words, could you comment on any math model differences between those two analyses?

Tarzanin: Oh yes, C-60 is not an eigenvalue program. It doesn't calculate stability; it calculates steady state only. We start from that to get the trim.

PREPARED REMARKS BY WAYNE JOHNSON

I'm going to start off my comments by addressing some of the cases that I didn't run calculations for, that we haven't included in the correlation efforts. Bill Bousman, in his writeup of the results, mainly just commented that I didn't do them yet. He's been constrained from speculating, I guess, by the fact he didn't pay me like he did the other guys. He didn't try. Anyway, I'll run down the cases, and I think I can give a fairly complete statement of what I think the correlation would have been if I did it.

For Case A, which is the hingeless rotor, I did two out of six. There have been a number of calculations run at Langley recently on a hingeless rotor and while I haven't seen all of them (I see their public-relations-type stuff), I hear they're getting pretty good calculations. That suggests I'd probably do fairly well. But I will add the caveat that five degrees precone and droop, which was used in the experiment, is about twice as large as you'll find on anything flying and that might be a bit too much for a real good correlation with my code. Case B, which is the simulated vacuum, I would approach not by modeling all the detailed flexures but by basically matching the nonrotating frequencies. That information is available and I feel that when you have that kind of information you should match that first and then move on to the areas to where you don't have the solid information. On that basis I would consider it a pretty straightforward problem and I wouldn't expect too many difficulties. Case C is where I did the majority of my calculations and did pretty good. The last three cases, D, E, and F, are all bearingless rotors, and the short statement shown there is simply that the code that I'm using is not intended to model bearingless rotors. It does not have multiple load paths at the root. That didn't stop us from trying to model it anyway. Three engineers actually took a try at a couple of the cases just to see what we could make it do. It would have been luck if it had worked, and it didn't. With the way the program works [we] could have just input an effective pitch-lag and pitch-flap coupling and tried to get some answers out that way, but that isn't really a proper approach. It really isn't solving it because you just get back to the question of where do you get your effective couplings. So that, in general, is an outline of what my code would do over the entire data set.

I have a couple of other comments. The presentation this morning prompts me to say that I find data set D, Seth Dawson's bearingless rotor information, to be the one that I think is most challenging, and the challenging part is not the data points they show but all these other instabilities that they found. I look forward to when they get around to actually publishing the information on all those things rather than just the lag damping which looks sort of dull. The final subject, what we were really asked to comment on, is to try and give some kind of a general assessment of the correlation we've seen. I can't really say that I see any kind of milestones being presented here in terms of analysis development. There were successes, there were failures, and there was an awful lot of inconsistency. So in that sense I don't see this effort as being something we'll look back on and say, "that's when we solved that problem." I think it is a milestone that we've taken

this opportunity to do such an extensive level of correlation, and I don't mean just the fact that you have all the companies doing it, but the fact that you have quite a few data sets. It's not uncommon to build a code and correlate it with one data set, but then to actually take existing codes and have them attack a half dozen data sets covering a wide range of parameters is definitely a milestone. I think that what we'll find coming out of this is simply some new directions. I think we'll hear, these two days, what some of those directions are, but I think also people have to think about it for a while, too, to absorb all they're learning here. That's it.

QUESTIONS FOR JOHNSON

Bob Wood, Hughes Helicopters: I guess I have just one comment, Wayne, on the fact that we see the correlation which appears to have been done objectively and we all say that there weren't milestones met in terms of actually any shaking results. I think perhaps the real measure of milestones coming from this meeting is going to be the kind of thing I'm beginning to hear from Frank and from all the others out there: the soul searching that's going on within each of the analysts as to what it was in his analysis that perhaps caused it to deviate most from the test data. And I'd just like to throw out for consideration of the panel at some point perhaps a follow-up to this meeting at some time. Maybe in a year or so, ask each of the companies, granted it is an opportunity to turn the knob if there is a knob in the analysis, but ask each of the participants to see what they've been able to do to close the loop more. I think in particular this one per rev, which apparently is not in C-90, cyclic pitch effect. Introducing those effects, if indeed the group is able to do that, it would be interesting to see what progress they can make on closing the gap.

Bob Ormiston, U.S. Army Aeromechanics Laboratory: I'd just like to throw out a general question, it's partly to reiterate a point that was made this morning as far as the data goes. One of the first data sets for one of the simplest configurations showed in the experimental results a [difference in] damping for a symmetrical configuration at positive and negative thrust conditions, or pitch angles. It isn't completely clear, even after analyzing the data, why that occurred, but if the analyses that we used to predict that didn't have any asymmetry in the input data, or there was no difference between positive and negative pitch angles in the calculations, why did the damping oftentimes appear to be different between the plus and minus pitch angles? In some cases there were known asymmetries introduced and in other cases there weren't. From my cursory look at the data and discussions with Bill Bousman, it's not clear why the calculated results showed the asymmetries and I'd like to, maybe not ask everybody at this point, but throughout the discussion if you showed an asymmetry in your case which wasn't due to an asymmetric data input, how come? Can you tell me why? Somebody ought to know somewhere.

And then a related question. Particularly for the simplified configurations, and that one in particular [Case A/1], I can understand maybe why we didn't

correlate with the data in all cases but if the configuration was simple enough to define, and these analyses all had the same input data, how come they didn't all, using F equals the same ma, come out with the same prediction even if it was different from [experiment]. I wonder if somebody would care to comment on that. It's not a simple one to answer.

Gene Hammond, Panel Chairman: Do you have any comments on that, Wayne?

Wayne Johnson: Would you repeat the question?

Ormiston: I didn't mean to throw it at him.

Johnson: I can say something about the question in the middle there that had to do directly with the asymmetries. The only one that exists physically, of course, is gravity.

Unidentified speaker: And inflow.

Johnson: Well, I'm assuming there that Dave Sharpe's exercises with the ground planes which were intended to define the effects of the inflow [were valid], and that was essentially a null result. Unless he did that wrong, then the only thing left is gravity. Now gravity I've got [in my code]. I forget whether it was for this case or whether it was when I was developing the code, I remember using that as a test case where I in fact suppressed gravity and put it in right side up and upside down and found a couple of bugs that way.

Ormiston: Well, in fact, that was checked in trying to understand the source of the asymmetry and the answer was that it's an effect, yes, but it's an extremely small effect on the lead-lag damping for that configuration.

Johnson: I still find the extent of the asymmetry that is in the data to be rather surprising. If it is only gravity then it's a surprise to me that it's so much due to gravity. Unfortunately, the results you have don't leave anything else to point to.

Ormiston: Well, there can be a question about the results, the experimental results, but the analytical results which were produced in the course of this correlation sometimes showed a very, is it coincidental, asymmetry, or did it arise from some [source]. Why did it arise in the calculations in some cases but not in others? There had to be an asymmetry in the input data presumably.

Peretz Friedmann, UCLA: I have just a comment on this asymmetry. One of them is that in calculations it's easy to get asymmetry because if you use constant inflow, and you have that square root expression, then positive and negative is not the same, and if you're not careful about it you'll get asymmetry and then you have to start thinking [about] from where it comes. But experimental asymmetry, I don't know exactly what experiments you've conducted with those planes simulating the

ground, but irrespective of my respect for the force of gravity I think the flaw in the ground effect probably is more important than gravity in generating asymmetry.

Johnson: I think, Peretz, that Dave Sharpe is about to publish all that data. What he did was he put a ceiling plane and a ground plane very near his rotor, so that the aerodynamic environment should in fact be symmetric. He still had a rotor shaft in there but the details, the lack of symmetry that was left after he got through putting his rotor in a box, were very, very small. The problem was that [between the results] without those ceiling and ground planes and with them, he found very little delta [in damping]. You would indeed expect, even if the inflow is important, you would expect that by putting those planes in you were modifying it. I still find it very puzzling. The calculations that I have made include gravity and it shows a very small effect, but the experiments show quite a bit larger effect and I don't know where it's coming from.

Pete Arcidiacono, Sikorsky Aircraft: Perhaps Wayne has answered it. If you look at the picture with the model under the rotor it certainly appears to be asymmetric and perhaps these tests with the ground plane and the plane above the rotor basically covered this situation, but it's not at all obvious that this should be symmetric.

Dave Sharpe, Aeromechanics Laboratory: What we did during this experiment, we put at the base plate there, an eight-foot-diameter plywood circle and one equidistant above. We ran the rotor with positive and negative collective pitch and found the asymmetry was still there.

Arcidiacono: It was still there? That's hard to argue with.

Bill Bousman, Aeromechanics Laboratory: I know we're more into general questions than specific, but I'd like to continue on that asymmetry question of the calculations. When we first started the calculations we asked all the analysts if the effect of gravity was included in their equilibrium solutions, because normally it may be important for a model rotor which is at very low rpm but for a full scale helicopter it would seem to be unimportant. At that time the analysts, without necessarily going back to their documentation, said, I think too quickly, "no it is not there." Then they got the results from the model and roughly half the results showed asymmetries and the other half didn't. For the ones that didn't show asymmetries then we could say, "all right, they told us there was no gravity in the equilibrium solution and they're right." For the ones that did show the [asymmetric] results there's a question there that needs to be answered, but the most perplexing question is for Bell. Because for Case A/1 they showed an asymmetric result and for Case A/2 they show a symmetric result, and that's completely perplexing because they are the same configuration except for the root flexure.

Jing Yen, Bell Helicopter: Gravity has a very important effect on your trim. I believe we've said already that gravity could change your blade trim location.

Bousman: Well, from experiments we've done with a model rotor where the analysis was very simple because it was hinged, essentially we'd show that there is a gravity

term that at very low rpms, yes, it does affect the trim and the couplings. That's why, because we had seen that, we asked everybody when we first went around, "is there gravity in your trim solution?"

Yen: The gravity is in our analysis and we found out that if you changed the angle from positive to negative, you change your trim, you change your mode shape and everything else.

Bousman: Yes, but that's why I asked you the question. If you look at your A/1 data set you'll see that you have an asymmetric result, but if you look at the A/2 data set you have a symmetric result.

Yen: That's the way it came out.

Hammond: Wayne, do you have any plans for putting a bearingless hub in your analysis?

Johnson: I have ideas, not necessarily plans. But you can never tell.

PREPARED REMARKS BY JERRY MIAO

Sikorsky's effort on this ITR methodology assessment basically is two computer programs. One is E927, the other is G400. E927 is an eigenvalue solution program and it's good for hover analysis. And G400, we rely on it extensively for forward flight analysis and it is a time history analysis. And as the data this morning shows, I think you've all seen that the G400 analysis shows a great improvement after we completed the contract. I believe everybody is dying to hear why it is so improved and I'm so happy that Dick Bielawa is here, he'll handle all that. So I will concentrate on a few things about E927. I believe that if I talk about a chronological history of E927 it will make a little more bit of sense why we went to -2 and -3 programs. As a lot of people have pointed out E927-1, the original program, is a public version. Originally, actually, it was developed for a proprotor whirl flutter analysis with coupled flap-lag blade modes in there and with pylon degrees of freedom. Then later on, we were under contract with ATL, and we added to it a pitch degree of freedom and modal fuselage. That means 6 degrees of freedom in the hub; you can input any kind modal fuselage into it. That is properly documented as E917[-1], I believe that's the version Hughes has used.

Now E927, of course, is a living program and after we had this program, we used it for a little bit and we started to add to its capabilities. One of the capabilities we put in is the six rigid bodies degrees of freedom of the airframe, to be explicit so we can study air resonance more readily. At the same time, to simplify the equations, we threw out a lot of the so-called "steady state deflection squared" terms because they appear to be extraneous calculations. That's the -2 [version]. Now we started out to correlate with these six sets of data, A through F, using -2 and as you noted when we correlated with Case 1 of configuration A, the correlation is fairly decent. That is the stiff torsional flexure and varying the collective pitch from negative to positive, and the modal damping prediction is fairly good. The next case is a soft flexure. The prime difference between these two configurations actually is the torsional frequency. The stiff flexure one is 2.8 [per rev], I believe, and the soft one is 2.5 [per rev], about. Now when we put in the soft flexure, we used E927-2 [and] we found out that the correlation is not that bad, but it didn't pick up all the increase in damping by incorporating the soft flexure, as the test data shows. So when we laid the analysis points for A/1 on top of A/2, we found out that you can hardly find any difference. It seems that E92,-2 just gives you results which are indifferent to the intricate coupling due to torsion flexure. Then we moved on to calculate the A/3 and A/4 cases; those are the ones with the stiff and soft flexure with precone. We found out that -2 again gives you the same numbers. No matter what you do to the configuration, it didn't change anything. So that gives you an inkling something is not working properly. But nevertheless simultaneously we were correlating other configurations, like configuration C, we did C/1 and C/2. Then we started on the Ds, and they're not bad. Of course, Seth Dawson is not too happy about our [correlation] there but our calculations say it's in the ballpark.

Then we started on configuration E, which is the Boeing BMR model, and this is where we ran into trouble. We found out that we got four pairs of unstable roots and if you examine the roots you find that the regressive blade torsional-mode frequency went to zero, which shouldn't be the case. That caused us to investigate the mass, stiffness, and damping matrices to find out what's causing it to go to zero. The one thing that's very apparent is that the mass ratio between the blade torsional degree of freedom, the pitching degree of freedom, versus the body pitch and roll degrees of freedom, is very, very small, meaning that if the body moves by a little bit the blade torsional degree of freedom is going to move a lot. Okay, then you say "where did that come from?" You look at that and you realize that the blade torsional inertia is increased when the blade has steady state deflection. This means, if you think of the blade pitch axis as lying in the plane of rotation and horizontal, if you have a vertical steady-state coning angle, the mass is displaced out over it and so "Md^2" is added on to the blade torsional inertia. If you look at a typical blade, the pitch inertia, the number will come out in inch-pound-second^2 units, it's about 2. If you talk about the flapping inertia, the number will come out to about 2000. This "Md^2" term, if you integrate it, comes out to be the coning angle squared times the flapping inertia. If you have a coning angle of about 3° that will come out to be a number about $2\beta_o^2 x I_\beta$ is about 2. That means the torsional inertia is doubled. If you throw out this squared term you are not getting a proper dynamic representation in the system. Because of that, all these squared terms are being put back into the program.

Also, another thing, think about it very carefully. Because we've been adding the pitch degree of freedom, the torsion degree of freedom, on the original derivation of coupled flap-lag degrees of freedom, you find out because of the way you are adding in a degree of freedom, you didn't really go back to square one to do the derivation, you're trying to add into it. So therefore the position vector definition is not exactly correct, they are a little bit...I shall say an approximation is being done there but actually if you really look at it you can say there are errors. That's one reason why, when you're putting back in those terms, you still get some kind of erroneous coupling terms.

If you remember in configuration E, that is, Boeing's BMR model data, we show three points using E927-3 for the rpm variation. These three points fall right into the test data. This is when we modified E927-2 to -3. Remember this blade is flap-lag coupled, then the torsion is added into it. Therefore, if you have pitch-lag coupling or pitch-flap coupling you have to put it in separately. We used NASTRAN to model this redundant load path and find out how much torsion is in the edgewise mode, as well as how much torsion is in the flapwise mode, putting these in as coupling terms. Then you put these into it and you run the cases, you find the modal damping comes out pretty good. Now remember this model had a blade torsional frequency of about 4.2/rev, and the torsional frequency is relatively high, compared to configuration A, [for] which both stiff and soft [flexure cases] are below 3/rev. If you look at configuration C/2, which is a coupled-rotor-body case, that blade had a torsional frequency of about 18/rev; it is practically decoupled, the torsion degree of freedom. Now you compare the -2 and -3 results for the case which has 9° of collective. The -2 shows that if you go from low rpm to high rpm, it

crosses the unstable region at the same time as the test data shows but comes back up relatively fast, the -2 version. But the -3 version picked up the depth of the instability as well as the width of the instability. The only problem is the -3 version did not give you a stable calculation when the test data, at high rpm, shows stable. Now this shows up because at the higher thrust level you probably have a lot more blade flapping motion coupled with lead-lag and torsion.

All of this ought to point out that the torsional degree of freedom is a very important thing because now you look back into configuration A, there we show a few -3 cases, the stability calculations are very poor compared to -2. That is because we still have problems in the -3 program, meaning that the torsion is not represented properly and the coupling terms are somewhat in error. Therefore configuration A, which you think is the simplest one, is the most challenging one because the torsion frequency is the lowest. None of the helicopter manufacturers make blades that soft; 4/rev is pretty soft torsional frequency [and] this is below 3/rev. It amplifies any error you have in representing the torsion degree of freedom and its coupling-to-bending deflection. My point is that this -3 version probably still can be used for analysis if my torsional degree of freedom is above, say 3.5/rev.

Now, I shall tell you that we are launching a -4 version, but because we are getting tired of E927 we're giving it a new name. Bob Sopher calls it HELSA, for Helicopter Stability and Analysis. The only problem is, I think it sounds like a girl's name. I don't know what the exact quote from Wayne Johnson is, but he said some time ago that a computer program probably should periodically should go through a "rebirth period." You have to clean it up and do the derivation again. We are starting pretty much from square one. We go back and incorporate the pitch, flap, and lag degrees of freedom, all flexible. We redefine a position vector and derive the whole set of equations of motion. I have confidence they will come out, probably give better correlation, and the program should be ready sometime in August.

To conclude the remarks, I think, number one, the steady-state-squared term cannot just be thrown out saying it is probably small. I think that as Peretz has pointed out many times too, there are ordering schemes. Some of them are first order, some second order; you have to go through these terms very carefully, finding out if it's really a compatible order or not. Especially in the torsional degree of freedom because in the torsional degree of freedom what appears to be a small term really can have a very large influence on the final outcome. Thank you.

QUESTIONS FOR MIAO

Bill Bousman, Aeromechanics Laboratory: I have something of a comment about the Task IIA being a low torsional frequency. That is exactly correct and it was chosen that way because of the very different approaches a research organization may take compared to a helicopter organization. We saw these terms, exactly the ones you are talking about that are causing trouble, we saw those in the equations from Dewey's work and we said that somenow we need to demonstrate that these are important. So

we pushed the frequencies down a little bit out of typical helicopter experience because we knew that then we would have measurable effects, the same thing with the precone being 5° rather than 2.5°. And that's the kind of stuff we've seen, but I don't think the corollary is true, that because these are not quite helicopter numbers that therefore these effects are not important. I think that's not correct.

Gene Hammond, Panel Chairman: Jerry, what sort of aerodynamics are in E927?

Miao: It's a quasi-steady aerodynamics; it uses table look up.

Euan Hooper, Boeing Vertol: What about HELSA, will that be the same?

Miao: Right now, yes. But we can incorporate more complex aerodynamics if we want to.

Dev Banerjee, Hughes Helicopters: Jerry, I have a question for you. What are your considerations for modeling bearingless rotors with the new analytical model that you're setting up?

Miao: The HELSA program that will be available by the end of August will be a typical modal approach. It will not have redundant load paths. But, we have it in the plan that about four months later, we should have a redundant load path representation in there which would take care of typical bearingless rotor types with dual flexbeams and torque-tube type of things. We're using a finite element approach which is very close to what Inderjit Chopra has been using.

PREPARED REMARKS BY DEWEY HODGES

I'd like to just take a few minutes and discuss some of the limitations of the analyses that were used from the Aeromechanics Laboratory in the correlations. On one data set the program that was called PFLT was used. That was the first data set, A, and part of the reason for the lack of correlation at higher pitch angles there, we believe, has to do with these static stall parameters as has already been brought out. The aerodynamics in that analysis are simply based on a linear C_l and a constant value for C_d, which is really crude, but it was set up originally to be a research code. We had no intention, and still don't have any intention, of putting it out as a code that other people could use, but rather we were studying the influences of various terms in the mathematical model. Now we have also determined that under certain conditions, terms of higher order than the quadratic nonlinearities that are present in PFLT may be, for some configurations, important. Marcelo Crespo da Silva will be discussing some of these ideas tomorrow morning in a paper. We feel those are the main limitations in PFLT as far as why it wasn't able to achieve the correlation that we believe it should have been able to, had we made those modifications.

The FLAIR program was used in a number of the data sets involving coupled rotor fuselage dynamics, and the FLAIR program is really based on the very simple analysis. It really doesn't deserve to be classed with some of these more general programs, nor does the first one I discussed, PFLT. The FLAIR program is also based on quasi-steady aerodynamics with linear C_l and constant C_d, but it has the additional limitation of being based on a rigid blade with a beam element at the root to represent the flexbeam of a bearingless rotor. With that kind of representation you get a quick and dirty approximation for the dynamic behavior but you miss out on any higher-order blade bending modes, and they certainly must be important for some of these cases. You also miss out on any steady state bending and torsion stresses that might be developed in the outboard portion of the blade because it is [modeled as] a rigid blade. The reason it was able to do quite well compared to most of the analyses, though, has to do with the fact that in the incorporation of geometric nonlinearity, a great deal of care was taken to include all the nonlinear terms in the flexbeam deformation. There are no small angle assumptions in FLAIR and there is no ordering scheme of any kind. It's simply a matter of writing down the exact geometric and kinematical relationships involved, and [then] the equations are solved in a numerical sense without any limitation on number of modes, or elements, or anything because they are integrated using an ordinary differential equations (ODE) solver. So along with its limitations, it does have the powerful feature of not having any limitations on angles. Now you say "well what possible difference could this make?" Well, in a bearingless rotor the flexbeam may undergo rotations in the torsional sense that violate the assumption that $\sin\theta = \theta$ and $\cos\theta = 1$, and that alone is enough of a justification to keep all the terms. Secondly, I've found that in making that derivation, it was actually simpler to include all the terms than it was to go through some kind of ordering scheme and throw terms away, because in throwing terms away one must make expansions of transcendental-type quantities. Those expansions produce a lot of terms and those terms proliferate

very quickly. Whereas if you keep all the terms you can just leave the sine or the cosine or the square root in place and not worry about expanding the term out in explicit form.

I'd like to also make some specific comments concerning the data. Just one on Data Set C. I see there, this is my own opinion now, that the NASA Ames code CAMRAD and the Aeromechanics Lab code FLAIR are virtually identical in their predictions in that particular data set, but the analyses are so totally different that such an agreement is really phenomenal, I think. I think that in light of that fact, the fact that the correlation and the predictions from FLAIR and from CAMRAD are so similar, so identical, and yet the analyses are so different, that Wayne [Johnson] then went on to include dynamic inflow and show that he had an improvement in correlation it nails down in my mind, almost with certainty, that dynamic inflow is the reason for the improvement in the correlation there and it is, for some of the modes, a necessity to include it.

Now I'd like to make some general comments. I believe that to avoid the proliferation of geometric parameters like precone, and droop, and sweep, and all these other things, we actually need a generic approach to modeling a rotor blade that talks in terms of geometric information based on, say, direction cosines of the blade elastic axis, without regard to many of these other definitions of terms which to one analyst may mean one thing and to another analyst may mean something else. Whereas if we are talking specifically in terms of direction cosines and offset vectors, then there can be no doubt as to what we are talking about as long as we're clear. I also believe that with the complexity of the rotor blades that we're modeling and with the generality that we demand and desire out of our codes, we really should be aiming in the direction of some kind of multi-level substructuring algorithms and a finite element kind of an analysis. I don't mean breaking up a straight blade into segments and calling that a finite element method. I mean a genuine finite-element method where a general structure is broken up into smaller structures, each of which is broken up into still smaller structures to some arbitrary depth until you get down to the simplest possible level where then one can identify things that are nicely modeled by beam elements, by rigid bodies, by plate elements, and by shell elements. These things should be then connected together in some kind of arbitrary fashion so that we can build the models that we need with any degree of complexity that is demanded and achieve any degree of accuracy that is demanded as well, because we should have this multilevel substructuring capability so we can have as many or as few degrees of freedom as are necessary. In doing such a thing, there are some general observations that need to be kept in mind. We want to be able to allow for hinges, and sliding mechanisms, and bearings. We cannot do that kind of problem with the traditional approach of writing the equations for a blade as if it is an individual structure. We must look at it as something that is built up from simpler components and we must incorporate some kind of constraint library that will allow us to build the model that we need as far as these features are concerned.

Furthermore, the complexity that's liable to result from such an operation is going to demand that we're very careful about the way we write down our equations

and I've found that, maybe this is something that hasn't been brought up too frequently among industry people, there are symbolic manipulation programs that are available that are ideal for checking the equations that are developed, mostly by hand in the industry I take it, and in government too. Ordering schemes are not easily made rigorous, if we are going to talk about ordering schemes. I personally have abandoned the use of ordering schemes in the work that I'm involved in right now, the development of the GRASP program, and in trying to get a "grasp" on what terms are important there, I found that the easiest approach was to simply assume that the strain was small but disregard the magnitude of rotations that were allowed due to structural deformation. That not only tended to simplify the equations but it also made for a set of equations that are much more accurate than any that I had derived in the past. When we talk about blade modes, we must be very specific about what blade modes, or condition, we're talking about, and that's sometimes something that's easy to be sloppy about, but we can't afford to do that. Also, we must talk about how the equilibrium is obtained. I've heard no one mention so far how they obtain their static equilibrium. I remember asking one person once, who was from industry, how do you get the static equilibrium about which you linearize and they said, "oh, we assume that that's given." We can't do that; we cannot assume that it's given. That's probably one of the most difficult parts of the analysis to accurately get a handle on.

I heard some mention about adding a large deflection capability to existing programs. I think such a practice is dangerous and that one must go back to first principles and incorporate nonlinearities as part of the derivation. Otherwise one must recognize that he's going to be faced with inconsistencies and there is virtually no way of getting rid of those inconsistencies other than going back and starting from scratch. The correct kinematics must be in the equations. The modes used, whether they're coupled and about what equilibrium they're calculated, can only serve to increase or decrease the computational burden. I think that's all the general overview comments I have.

QUESTIONS FOR HODGES

Euan Hooper, Boeing Vertol: At any time in this workshop is anybody going to say anything about GRASP? About where it stands, when it will come into action, what it will comprise?

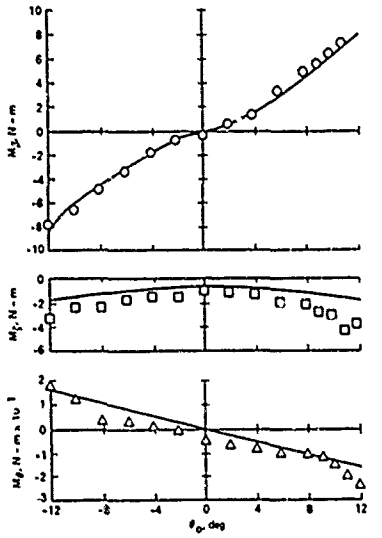
Hodges: I'll say something right now if I have a couple more minutes here. The GRASP program is designed to be a multielastic-body type of a program that is completely generic in that when one is analyzing a particular element of the structure, the algorithm in GRASP is set up in such a way, and the equations are derived in such a way, that one doesn't care whether we're talking about a helicopter or spacecraft or whatever; it's simply a collection of substructures, and [GRASP] has the multilevel capability of substructuring that I mentioned. It also has the generic approach in that the equations are derived for a general frame of reference which has some specified motion with respect to an inertial frame. To get away from this

definition of precone, and droop, and sweep and all the other things, we simply allow the analyst to put in direction cosines and offsets between elements and define his elements as he would for something like a NASTRAN input, although ours is probably more general.

The GRASP development effort has turned out to be about a three-year effort, of which we are in the process now of wrapping up the last few months. We estimate that between four and five months from now, we will have a code that is at least finished from the development point of view, but that does not mean at that point it will be available for the industry. It will have to be checked out much more extensively, even though we are doing check out as we go. The kind of validation that I believe in is likely to require months and months and even years of checking. We might release a version, of course, before we finish totally checking it out. I believe in doing calculations using a program like GRASP, even if it is as large a program as it is, because I believe in doing calculations for problems for which you know the answer. If your program doesn't get the answer for those kinds of problems then it's certainly fortuitous if it seems to get any correlation with anything else. I believe that one of the things that this workshop has provided, and I hope that most of us recognize this, is a set of data for problems that we have a lot of confidence about the answer. We should now have some benchmarks to validate our codes by this data.

In addition to the subtask A data that Dave Sharpe reported this morning, he also measured static root bending and torsion moments. He did not report this in the ITR Methodology Assessment, but it is going to come out in a TP that's about to be published. One of the things that we've done with GRASP is to use GRASP to correlate with these static-root bending moments and torsion moments for a hingeless rotor rotating about an axis which is, for all intents and purposes fixed in space, with varying degrees of precone, and droop, and pitch, and flexure stiffness, et cetera, in the hovering flight condition. We then took the numbers for the properties of that structure and ran them in the GRASP program [Slide 23]. The top curve here is flap bending moment near the root of the blade, the middle curve is lead-lag bending, and the bottom curve represents the torsional moment. The stripes on there are not fairings of the experimental data but are the calculations from the GRASP analysis. This is one set of data that we've correlated with a preliminary version of GRASP. There are others too but this is typical of the correlation that was obtained through a wide range of parameters. Again, I might say that this was done with one finite element; GRASP is a finite element analysis. It was done with one finite element and [for] that element the number of degrees of freedom was jacked up until we converged. That took 27 degrees of freedom in that element, which is not too bad. I could show you more, but I guess some comment about the status of GRASP is probably in order.

We have identified nine levels of capability that we want to achieve with GRASP, each of which takes from three to five weeks of effort to program. We have finished two of them and we're just about to start the third one, probably tomorrow, of those nine. So for that reason I'm sure that we're under six months, maybe down close to four months, away from achieving operational capability. At least that's



Steady blade moments versus blade pitch angle, no precone or droop, soft pitch flexure

Slide 23

our current estimate. As you know, with software development it's very, very difficult to estimate, especially with a program like GRASP where such a large portion of the code, as with any finite element code, has to do with shoving data around from place to place rather than actually being equations. If we only had to program the equations it would be a trivial exercise and we would have been done a long time ago, but building the kind of generality that we wanted to achieve in this analysis, that is, the capability of analyzing any kind of rotor system that your head can conceive of, required that we incorporate some of these features that heretofore had not been included in any kind of analysis that we had seen.

Pete Arcidiacono, Sikorsky Aircraft: I'd like to follow up on that, Dewey; I still didn't hear when you'd be ready to release at least a preliminary version of the program.

Hodges: Preliminary version release? I would say between six and nine months from now we might be ready to release some kind of preliminary version. I anticipate though as time goes on we'll be having additional releases. You know we'll be updating it, enhancing it, adding elements, this sort of thing.

Arcidiacono: Will there be documentation on the program available?

Hodges: Absolutely. The documentation is being developed along with the program and we're taking a lot of pains to go into great detail in the documentation, as painful as it is. You know, I've come to the conclusion that it's much harder to describe something like this than it is to do it and if it's taking us three years to do it, then to adequately describe it may take a great deal of time. So the documentation may be something that is evolutionary in nature and it will grow as time goes on.

Bill White, U.S. Army AVRADCOM: Dewey, would you briefly describe your aerodynamic representation?

Hodges: Okay, the aerodynamic representation is one that's pretty much standard with a lot of these codes that we've been talking about for hovering flight aeroelastic stability. It is a quasi-steady aerodynamics, two-dimensional strip theory kind of an approach with table look-up for C_l and C_d and C_m versus angle of attack. It is sort of a takeoff on the Greenberg approach, although we correct one of the glitches that has been identified in the Greenberg approach, but it's more or less along that line. It is believed to be adequate in hover for the [problems] that the program is designed to deal with, and those are basically isolated blade-stability problems, coupled rotor-fuselage aeromechanical stability, ground resonance, air resonance, and axial flight kinds of problems. We intend to deal with all of these areas but we do not intend at this time to get into forward flight because of the expected appearance of the 2GCHAS program on the horizon.

Bill Bousman, U.S. Army Aeromechanics Laboratory: Will it predict the [Case] D/2, Seth Dawson's, flutters?

Hodges: Not with the present aerodynamics in there. We would have to have some kind of lift deficiency function, truly unsteady aerodynamics, in order to predict that and we do not have any plans at this point to incorporate anything like that, although it's certainly not something that is impossible to do. It's just not something that we set out to do in the original specifications for the program.

PREPARED REMARKS BY RICHARD BIELAWA

My prepared remarks are going to be a little different from everybody else's in that, I guess, when Gene said that he wanted to hear some words on correlation from the analyst's point of view, I interpreted that to mean that we were going to compare scars, and I've got a few scars I want to talk about. They consist of the five issues that I've identified there [Slide 24], some of them are more important than others but let's take them in turn. The chronology of G400's contributions to this ITR effort are twofold. Initially, the first set of G400 results were calculated with me standing off in the wings and the analysis being run cold at Sikorsky by analysts there. Frankly, it was disastrous. The results were, as you know, quite bad and I came into the picture in an active role, and I became the digger and searcher of needles in haystacks. The issues I want to talk about now are some of the things that became important to me as issues.

First, there was the proper use of the program [Slide 25]. Being the author of the program I know exactly what to do and others may not know the right switches to turn on and which things to deem important with regard to the input data. This is

CORRELATION FROM ANALYSTS' POINT OF VIEW

ITR Methodology Assessment Workshop
Richard L. Bielawa, UTRC

- Proper usage of the analysis
- Reliability of the input data
- Use of time-history solutions for stability assessment
- Interpretation of a bad calculation
- Recommendations

Slide 24

PROPER USAGE OF PROGRAM

- Selection of input data and options
- Need for user transparency
- Need for internal diagnostics of input data and internal calculations

Slide 25

something that I had to learn and a lot of things got flushed out. The crying need here, of course, is the need for user transparency. Anybody should be able to use any code and get the same answer that somebody else would get. I don't feel that we're really there with G400, but we're working on it. I think one of the things that might be needed would be to have some system of internal diagnostics in the program wnere if you select a set of switches, [currently] the program will say, "fine, I'll get you an answer" where in fact they are nonsensical. The program should be able to interrogate the data and say "whoops you made a mistake, you might want to reconsider this selection of parameters."

The issue of reliability of the input data is one that probably is universal with analysts [Slide 26]. It's always somebody else's problem. You know, I'm doing my job perfectly and, well, the truth is probably somewhere in between. There is an issue with regards to the accuracy of the model data, not so much maybe what we get from the experimentalist, but how we interpret it and how we use it. The one thing in the results that we saw this morning were variations with regard to pitch angle. Personally, I would have been more comfortable trying to generate variations with regard to thrust, because this is what you design to. You design a ship to have a certain C_T/σ; that's what you design to and that's what the designer wants to know. Perhaps we would have better or worse correlation if we used that as the parameter rather than pitch angle. There were some problems with regard to interpreting the model data that we got from Bill Bousman, and these things had to be resolved. With regard to required approximations, any code is only as good as the data that you put into it and getting the data for a big comprehensive code like G400 or any of the other codes is a problem. You have to have a feel for how you break the blade up. Do you put fine segments in the root? Do you make it uniform? Do you assume only two flatwise modes and one edgewise mode knowing that you're going after that kind of a problem, or do you want to include other modes because you might want to pick up a flutter instability? You have the problem of how do you put in the effective structural damping, which we typically can only measure in a nonrotating condition. By and large, there is an attention to details that has to be followed and it requires a certain amount of user lore with the programming. This is a problem because it impacts on user transparency.

Now the one thing that I always get asked is "what did you do to the code?" It's a very difficult question to answer because there are a lot of things that I did with the code, but tnere are other things that make the G400 application of ITR

RELIABILITY OF INPUT DATA

- Accuracy of model data
- Required approximations
- Attention to details

Slide 26

rather unique. G400 has a very basic beam bending-torsion basis. It does not use coupled modes; it uses uncoupled modes--probably the simplest kind of representation you can use. However, the distinction I think with the G400 is it was the only one that used time history solutions of essentially the full body of nonlinear differential equations [Slide 27]. By that I mean they were not equations which were linearized and then a time history solution obtained from them. They were the full nonlinear equations without any expansions, and solved in a manner that kept all the terms. Then use of time history solutions has advantages and disadvantages. Very clearly the disadvantages are that they take a lot more computing time, typically talking about at least one and possibly two orders of magnitude more time and money than eigensolutions. You have the further disadvantage that you have the forced response buried in with all the transients that you want to use to get your stability answers. You've got to address them somehow [to] get them out or be able to look beyond them, which means that you have to have some kind of post-processing to obtain the conventional stability descriptors. We use two methods. One is just plotting the results and using a log decrement, and we also use the moving block.

Now the advantages of using a time history solution are that the accuracy is not a function of the degree of linearization. By that, I mean, you take things in step, you make sure your equations are correct first, make sure that the equations themselves are functioning to get the right stability level, then the next step, in my view, is to linearize them so that your linearized equations give the same stability information as your nonlinear ones. So this is an advantage. We can get a better handle on the accuracy of the equations themselves using a time history solution. The problem that has been raised several times with regard to obtaining the equilibrium responses which you need to linearize about, is not required, it is inherent. The time history solution simulates the blade as you would test it. Lastly, the item that was a real payoff as far as improving the correlation and

USE OF TIME-HISTORY SOLUTIONS

- Disadvantages:
  - Calculations require more time (and $)
  - Inherently includes forced responses
  - Postprocessing required to obtain conventional stability descriptors
- Advantages:
  - Accuracy not a function of degree of linearization
  - Equilibrium responses (for linearization) not required
  - Enables rapid modifications to equations of motion

Slide 27

getting it where it's starting to work was that it enabled very rapid modifications to the equations. I could get in, overhaul the equations, and add new terms very quickly, very efficiently with the time history solution, as opposed to a linearization where if you added a new term you'd have to linearize it, expand it out, which typically takes a lot of time. So this, I feel, was the big advantage in obtaining the improved correlation with G400. Generally, the details I will try to answer tomorrow.

The real problem with my involvement with ITR was what do you do when you've got a really bad correlation, a bad calculation [Slide 28]. I felt that without the body of data that was put together on this program, I would not have been successful. The overlapping of complexities, the spectrum of complexities, was extremely valuable. I think this is one of the real contributions that was made under this program. I spent a lot of time just on two cases, IIA Case 3 and IIA Case 5, that were supposed to give the same answer. They were tested, they gave the same stability level. Yet the analysis had to be corrected so that it was consistent and would give the same answer for Cases 3 and 5. This was extremely useful in dealing with a bad calculation.

I want to spend a little time now with some ideas that I just offer for another tool, another set of ideas that you could use for detailed diagnostics of an unstable motion. You get an answer and it's bad, fine. What do you do about it? I want to talk a little bit about two ideas, or actually one idea with two faces, and that is the idea of the force phasing matrix which can be used for eigensolutions, and then an analogous method for the time history solutions. The force phasing matrix is an idea that I evolved a number of years ago, but I'm not sure it has gotten much use and I thought I'd just throw it out on the table now for your consideration. I think it has some merit as far as being able to look at your equations and say, where are the drivers, where are the terms that are making this go unstable? The basic idea [Slide 29] is where you take your eigensolution problem:

INTERPRETATION OF A BAD CALCULATION

- Usefulness of overlapping configurations and a spectrum of complexities
- Need for detailed diagnostics of unstable motion
  - Force phasing matrices method for eigensolutions
  - Analogous method for time-history solutions

Slide 28

FORCE PHASING MATRICES

- Equation form:

$$\left[[A]\lambda_i^2 + [B]\lambda_i + [C]\right]\{\phi^{(i)}\} = \{0\}$$

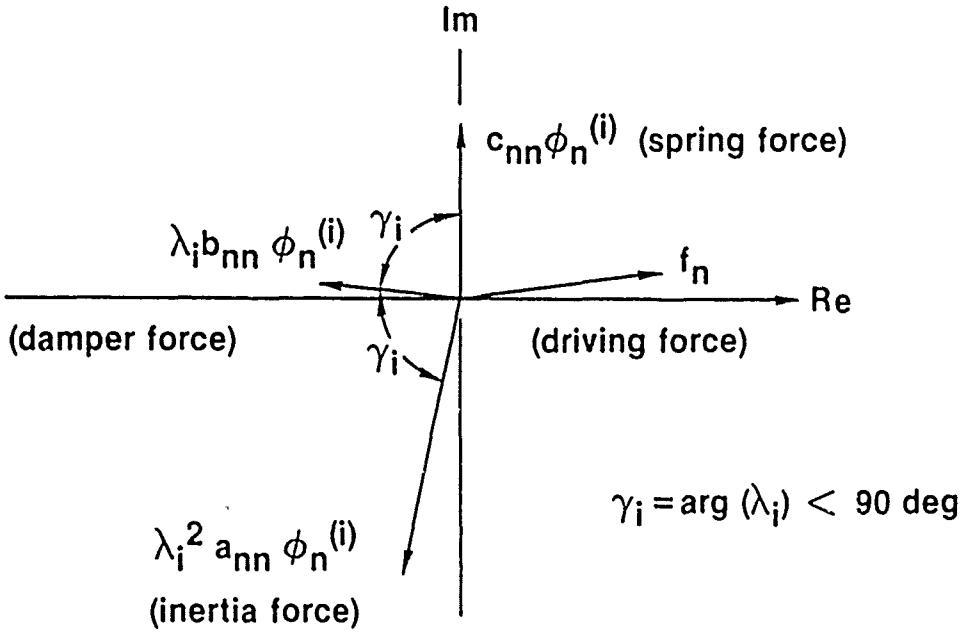
- For nth degree-of-freedom

$$a_{nn}\lambda_i^2\,\phi_n^{(i)} + b_{nn}\lambda_i\,\phi_n^{(i)} + c_{nn}\,\phi_n^{(i)} + \underbrace{\sum_{j\neq n}(a_{nj}\lambda_i^2 + b_{nj}\lambda_i + c_{nj})\,\phi_j^{(i)}}_{f_n} = 0$$

Slide 29

you have an A inertia matrix, you have a B damping matrix, and a C stiffness matrix, and if you take any one of those equations you can write it in terms of the diagonal terms, the a_{nn} and b_{nn} and c_{nn} terms, these are the terms on the diagonal for any one degree of freedom, and then you lump all the other terms together and you call it f_n. So we have four quantities, and for an eigensolution they are all complex numbers, but we know that they have to add up to be equal to zero all the time, forever. Now, how do we interpret these four vectors? If you plot them in a phase plane [Slide 30] such that your spring force is pure imaginary, and then plot your damper force and your inertia force, they're separated by this angle, γ_i, and for unstable motion that angle always has to be less than 90°. So generally they will fall in the phase plane in that general orientation, such that the driving force, f_n, for unstable motion always has to have a positive real part. So for an unstable motion we know that all of the components that go into building up that f_n, if they are a driver for the instability, they have to have a positive real part, and this is the basic idea for the force phasing matrix. The next slide [Slide 31] has a definition for how to construct these matrices P_A, P_B, P_C. These are matrices that have the same size as the A, B, and C matrices and they're kind of companion matrices. The way you use them, and you construct them from that formula, is that wherever you find a positive term in the force phasing matrix, that term, say it's a (3,4) element in the phasing matrix, that says that that term in the original equation is a driver. It's contributing to your instability, it's a coupling term that's driving that instability. There's an η term there, η is either equal to i for oscillatory motion or -1 for a pure divergence. It's a tool and I'm throwing it out because I think it has some merit as far as an analyst is

FORCE PHASING MATRICES (CONT)



Slide 30

FORCE PHASING MATRICES

- Formal definition of F-P matrices

$$[P_{A_i}] = Re[\eta/\phi^{(i)}]\lambda_i^2[A][\phi^{(i)}]$$

$$[P_{B_i}] = Re[\eta/\phi^{(i)}]\lambda_i[B][\phi^{(i)}]$$

$$[P_{C_i}] = Re[\eta/\phi^{(i)}][C][\phi^{(i)}]$$

$$\eta = i \text{ or } -1$$

- Usage:
  - Destabilizing terms in original equation are (+) in F-P matrices

Slide 31

concerned where he's faced with the problem, "where do I go from here, how do I improve my understanding of an instability?"

Now I think you can extend the same idea to time history as well. This is a page of a typical G400 azimuthal printout [Slide 32] and this is one point in an oscillation for the IIA Case 4, which was the unstable one. In each page of the printout the aerodynamic descriptors are given and then SAZ5, SAY5, MAX5 are the actual air load distributions, the instantaneous air load distributions. The other ones, SDY5, SDZ5, and MDX5, are the dynamic loads. These are the descriptors that go on the right hand side of the equation. Now I purposely selected an azimuth, a ψ value, where the first edgewise mode, QV1, has a pure velocity, pretty much a pure velocity. I selected a point where the acceleration was changing sign so the edgewise mode has a pure velocity. Now you look at what loads are acting on that degree of freedom when it has a pure plus velocity. If you look at the airload distribution, the SAY5 is negative; it is acting as a damper as you would expect. Drag loads on the airfoil should be retarding the motion. Now if you look at SDY5, the dynamic loads in the edgewise direction are positive. What this is saying is that you ve got inertia loads that are driving that edgewise degree of freedom and they're acting as a negative damper. So this is a time history analogy to the force phasing matrix where you attempt to say "okay, you've got something going with velocity, what's in phase with it, what are the terms that are contributing to your instability."

The last slide [Slide 33] is my viewgraph of recommendations. This is where I hope we generate some controversy. First I think that we should start defining guidelines for assumptions that are needed to insure reasonably accurate analysis. We've identified lots of things implicitly, but I think that we ought to somehow get it out on the table and identify [that] we need this kind of term if we are going to make an accurate analysis of this kind of instability and so on. Secondly, I listened to Bill Bousman's words this morning, and I hear you, Bill. There is no such thing as a conservative analysis. On the other hand we need something that we can hold on to and I really think that we ought to have a "Bousman number," some kind of parameter that varies from zero to ten and gives a quantitative, not qualitative but quantitative, evaluation of stability correlation. I think that if you can somehow define for us what that number is so we can apply our analysis to it and say, "aha, we got a Bousman number of 4, we got a Bousman number of 10," then we can say that we're gaining on it. Lastly, with regard to some of the problems that I encountered in trying to match up model data with input data for the computer code, I think that we ought to somehow define some standards that we need for experimental testing procedures with regard to instability/flutter testing. I've tried to correlate in some things within some body of data where there was no measurement of [the structural] damping, and how do you do something like that? I think that if there were some well-defined industry standards for what you have to measure when you run a test like this, it would be extremely useful. So, that's the end of my remarks. Can we take a vote on some of those recommendations?

PSI (1) = 340.0 DEG REV = 12 TIME = .72 SEC LAMBDA 0 = -.0389 LAMBDA 1C = .0000 LAMBDA 1S = .0000

N	XCEN	LAMBDAS	GAMMA	PHI	ALPHA	A	ALPHAW	MACH	CL	CD	CM	SA75	SAY5	MAX5	MAY5
1	.0100	.00	.00	-75.57	-75.61	.000	.000	.012	.000	.000	.000	.00	.00	.00	.000
2	.0300	.00	.00	-52.33	-52.89	.000	.000	.014	.000	.000	.000	.00	.00	.00	.000
3	.0500	.00	.00	-37.84	-30.89	.000	.000	.018	.000	.000	.000	.00	.00	.00	.000
4	.0700	.00	.00	-29.01	-22.11	.000	.000	.024	-.535	.122	.000	.00	.00	.00	.000
5	.0900	.00	.00	-23.32	-16.43	.000	.000	.028	-.633	.097	.000	.00	.00	.00	.000
6	.1100	.00	.00	-17.94	-11.12	.000	.000	.034	-.724	.075	.000	-.03	.01	-.01	.000
7	.1850	.00	.00	-11.12	-4.81	.000	.000	.056	-.435	.017	.000	-.05	.01	.00	.000
8	.3150	.00	.00	-6.30	-.68	.000	.000	.095	-.069	.011	.000	-.02	.00	.00	.000
9	.4400	.00	.00	-4.16	.83	.000	.000	.132	.085	.011	.000	.05	-.01	.00	.000
10	.5600	.00	.00	-2.93	1.55	.000	.000	.165	.154	.011	.000	.15	-.02	.01	.000
11	.6800	.00	.00	-2.10	1.98	.000	.000	.206	.195	.012	.000	.28	-.03	.01	.000
12	.8000	.00	.00	-1.49	2.30	.000	.000	.243	.224	.012	.000	.45	-.04	.01	.000
13	.9000	.00	.00	-1.10	2.56	.000	.000	.277	.248	.012	.000	.64	-.04	.01	.000
14	.9550	.00	.00	-.92	2.63	.000	.000	.290	.245	.012	.000	.71	-.05	.01	.000
15	.9850	.00	.00	-.83	1.85	.000	.000	.299	.121	.012	.000	.37	-.04	.01	.000

N	XCEN	VERT. DEFL.	INPLANE DEFL.	TORSION DEFL.	SDZ5	SDY5	MDX5	MEX9	FLATWISE STRESS	EDGEWISE STRESS	CORNER STRESS	TORSION STRESS	TORSION MOMENT
1	.0100	.00	.00	-.04	-.27	.00	.00	.00	-225.	-61.	285.	-11.	-11.13
2	.0300	.00	.00	-.56	-.20	.00	.00	.00	-197.	-59.	257.	-11.	-10.97
3	.0500	.00	.00	-1.05	-2.30	.00	.00	.00	-161.	-82.	242.	-11.	-10.57
4	.0700	.00	.00	-1.10	-.93	.00	.00	.00	-135.	-79.	213.	-10.	-9.93
5	.0900	.00	.00	-1.11	-.69	.00	.01	.00	-117.	-76.	186.	-9.	-9.18
6	.1100	-.01	.00	-1.18	-.26	.00	-.06	-.11	-86.	-69.	156.	-8.	-8.33
7	.1850	-.11	.01	-1.64	-.34	.01	-.06	-.05	-34.	-60.	94.	-5.	-5.22
8	.3150	-.44	.05	-2.38	-.58	.02	-.06	-.01	-7.	-45.	52.	-4.	-3.53
9	.4400	-.80	.09	-3.01	-.81	.05	-.06	.00	1.	-32.	33.	-3.	-2.80
10	.5600	-1.15	.12	-3.52	-1.04	.07	-.06	.00	0.	-22.	22.	-2.	-2.24
11	.6800	-1.49	.16	-3.92	-1.27	.09	-.06	.00	0.	-13.	13.	-2.	-1.68
12	.8000	-1.82	.20	-4.20	-1.57	.11	-.07	.00	-1.	-6.	6.	-1.	-1.07
13	.9000	-2.09	.23	-4.33	-1.70	.12	-.07	.00	-1.	-2.	3.	-1.	-.54
14	.9550	-2.23	.24	-4.36	-1.80	.13	-.07	.00	0.	-1.	1.	0.	-.25
15	.9850	-2.31	.25	-4.37	-1.86	.14	-.07	.00	0.	0.	0.	0.	-.08

	QW1	QW2	QW3	QW4	QW5	QV1	QV2	QV3	QT1	QT2	BETA	DELTA
	-.649-001	.260-002	.000	.000	.000	-.262-003	.000	.000	-.763-001	.000	.873-001	.175-007
(*)	-.264-001	-.130-002	.000	.000	.000	.264-001	.000	.000	-.269-001	.000	.000	.000
(**)	.145-001	-.244-002	.000	.000	.000	-.813-002	.000	.000	.216+000	.000	.000	.000
XI	.724-003	-.112-003	.000	.000	.000	-.148-003	.000	.000	.146-004	-.241-004	.000	.000

	QPRM1	QPRM2	QPRM3	QPRM4	QPRM5	QPRM6
	.000	.000	.000	.000	.000	.000
(*)	.000	.000	.000	.000	.000	.000
(**)	.000	.000	.000	.000	.000	.000
XI	.000	.000	.000	.000	.000	.000

	QVXH	QVYH	QWX4	QWYH	QYZH	QWZH	DPSIH	PHIF	THETAF	PSIF
	.000	.000	.000	.000	.000	.000	.000	.000	.000	.000
(*)	.000	.000	.000	.000	.000	.000	.000			
(**)	.000	.000	.000	.000	.000	.000	.000			
XI	.000	.000	.000	.000	.000	.000	.000			

Slide 32

RECOMMENDATIONS

- Define guidelines for assumptions needed to insure reasonably accurate analysis
- Define industry standards for *quantitative* evaluation of stability correlation
- Define industry standards for experimental stability testing procedures

Slide 33

GENERAL DISCUSSION

Larry Lehman, Neilsen Engineering and Research: I have some general comments, I guess, to make which relate to what you said and what a number of the panelists have said and this is just some notes that I have written down through the process of the day. A couple of things really come to mind again. One is [that] there are clearly several classes of things that we've seen here. There are cases where all the programs tend to agree between themselves but not with the data, clearly there are questions there. Others in which the programs don't really agree with anything or the data or themselves, which are some other questions. We've sort of tended to focus a little bit on those situations where the analytical results do not necessarily agree with the test results, but we shouldn't lose sight of the fact that there are probably some very interesting questions associated with the cases that do agree, and try to set a consensus, as to why they really do agree. That will be more and more the case as we develop more and more accurate codes, because I suspect that we could go through the cases that have been considered today, and clearly there are cases where there's agreement, where everyone is certain as to why it agreed, it's a well known fact, it's been tested [and] proved long ago; but interestingly enough I'd bet you'd find quite a few cases where everyone had his own opinion as to why it agreed. Some fundamental agreement needs to be put together as to why they even agree, which I think is very useful in addition to determining what does not agree and why.

A couple of other things related to developing new classes of codes and something which I have not seen mentioned today but which I'm sure that a number of different analysts use in one sense or another, and that is really the technique of sensitivity analysis. No one has really mentioned that, but it can be a very

crucial tool in really sorting out some of these difficulties as to why an analysis does what it does, whether it's too sensitive, whether it's not sensitive enough, or whether it's entirely wrong; it's not affected by certain parameters and we sort of hinted at that in one sense or another. Unfortunately, I think a lot of the large analysis codes we have now are not really geared to being able to easily or readily do sensitivity analyses and [for] any new codes that are developed some thought should be given to easier ways of actually doing a sensitivity analysis, because it can be a very important tool in design, not just analysis. We've talked pretty much about analysis but when you start thinking a little more along design lines or use with optimization codes or other techniques, then you begin to ask this question about sensitivity and what it means and some very interesting questions come out of just analyzing the sensitivity.

Again, related to that, there are a number of what I would call estimation techniques, some people call them identification although I don't want to label them necessarily as such. There are some rather interesting tools being developed in other areas which really look into solving inverse problems. And that is, given an answer can you really figure out what are the missing fundamentals or physical facts that are not in your current models. That's not necessarily taking a parameter fitting where you begin with a known model because sometimes your results there are only as good as the model that you assume. Maybe some more work needs to be thought about along the lines of actually taking good results that are known to be good, and examining what are the missing fundamentals, and [developing] techniques for automating that practice; that's a mouthful because that's not a simple thing to do at all. That is again related to this sensitivity approach because when you start using any estimation or identification techniques one very crucial thing that comes up is that you cannot expect, necessarily, to take any given experimental test and be able to get the results that you want out of it, partly because of this sensitivity issue. So that sometimes if you wish to get certain things out of a test, you have to design the original test and the combinations of parameters, their sizes and so forth, with that in mind; that you wish to use a technique to get additional information or identification from. Because if any of you...I'm sure some of you have probably tried this in different areas and you can try to apply identification to just any problem on an ad hoc basis and not get anything worthwhile at all and you conclude, well, it just can't be done. It's partly because of the fact that you have to combine your test and your analysis together. give some pre-thought to your test.

Another thing which comes up is in the areas of nonlinearities, some of which have been mentioned in various aspects. That is, including them, or for example which, if you wish to simplify at all, which techniques are really acceptable for handling nonlinearities short of just doing the full thing, or whether the full nonlinear analysis is really the way to go.

If it is the way to go, then there is one other interesting area there that clearly could use some work, and that is if you are getting full nonlinear solutions. We're getting a lot of results out of that; they're expensive but there's a lot more information hidden in those results that we don't know how to get out of

it. It would be worthwhile looking at some other techniques, some of which are currently being used but others that need to be developed, that can extract some more useful information in a ready fashion from these rather complicated nonlinear analyses. Because they are becoming more accurate and much more realistic in certain cases of real systems, and we all know that with a lot of data processing techniques, sometimes that you can take results from real nonlinear systems and extract some useful information from that that you did not even think was there initially.

Hammond, Session Chairman: Thank you very much. It was very interesting, very useful.

Alex Berman, Kaman Aerospace Corp: Well, I just have some general comments I'd like to make. I've been rather disturbed all afternoon by observing the state of the software that's used in the manufacturing companies in the designing and analyzing of helicopters. We've been talking for years about structured programming, structured design, and documentation. The programs that we have today are the same programs that we had five years ago or ten years ago, except that they've been modified haphazardly. They probably contain more errors today than they did five or ten years ago, and I don't think that anyone has any confidence that their predictions have any physical meaning at all. The fact that they all not only disagree with the test data but disagree with each other is probably more serious than not matching the test. The comment was made at this AHS meeting, a year ago, that when the helicopter industry first started using computers that we had to simplify the analysis to fit on the computers so we could get calculations. Now things have changed and computers are better than the methods that we had implemented, so it's really important that we upgrade our theories to the level of our understanding of the problem, because the computers can handle it. It seems to me none of the programs that we have have been proved over the past number of years. The duplication of effort is a tremendous waste of resources. The plans for improvement are really not reasoned, no one has gone through and looked at the theories, and looked at what we have and decided what the important things are to add there. They're just done on a haphazard basis; somebody thinks of something and they implement it and somebody thinks of something else and they implement that, but there is nothing structured or planned about the whole process. Of course, I can talk because I'm not up on the panel; I'm not saying that our programs are any better than the rest of the industry. The whole industry is, I think, in a very sorry condition when you compare what we really know about the phenomena with what we have implemented in our computer programs.

Gene Hammond: Does anyone on the panel want to respond to any of those comments?

Bielawa: Yes, I want to make one comment that as an analyst I enjoy this kind of work, making sure that the codes correlate really well and that the points fit right on the middle of the experimental data bands, but the world needs helicopters, not helicopter analyses, and somewhere along the way we have to say, "this is good enough, we can build a good helicopter with it." I think getting very accurate

stability answers has to be put in the context of what the industry is trying to do. Maybe we don't need as much accuracy as we think we do.

Euan Hooper, Boeing Vertol: Yes, I was about to come up with the same thought because the whole emphasis here is on achieving great correlation and I was going to ask, and I thought Wendell Stephens might have illustrated it this morning, what's the cost of running each of these programs? Some of them are probably rather short, some of them are very long, some are not only long in computer running but they're long to set up, long to get familiar with, long to train new people to use, a great investment in time and activity. There's some trade there, you don't need all that much accuracy. It's nice, it gives you a warm feeling when you get great correlation, but there's a value to it. I'm not calibrated on the whole range of programs but one program I like very much is FLAIR. I think that's a good trade. It's a simple program and I think it's not too long running, it's been well checked out, and it's got simplifications which even Dewey feels a bit apologetic for when he explains it to other people. But I think it's probably a very good balance between what's needed by the industry for a useful program which can steer designs along. I'd appreciate somebody else's comments on that. For instance, the other extreme is by chasing after more and more accuracy, better and better representation, the programs grow and grow in size and I suspect GRASP is in danger of sinking under its own weight. By the time it becomes available, the whole ITR program may be over and done with. It may have just grown too much and may not in fact be as useful as FLAIR.

Hammond: Would anyone on the panel like to comment on computer running time and complexity?

Gene Sadler, Bell Helicopter Textron: I think it makes a difference on how the analyst uses the tool, and especially if you're in a time crunch. If you've got an analysis that doesn't take too much input, that runs fast, and that you can get a lot of turnaround on, you have a tendency to use that rather than one that's going to take a long time to generate the input and maybe a long time to get computer turnaround. And let's face it, most of us work at places where the bean counters get priority over the scientific stuff and if you go down and ask for priority too many times they start to look at you funny. Turnaround time really is important. If we can get jobs done in under one minute of CPU time we don't have any fuss, if it goes between one and five it's a problem, and if it's over five it's a big problem.

Frank Tarzanin, Boeing Vertol: I don't know if there's any answer to this because I understand what you're saying and I agree in one sense, but if you miss one instability, that happens to wreck your whole program. How do you know? You don't know. Where do you draw the line? I don't know, but I guess you have to keep trying.

Hooper: Well, the difference in accuracy in stability prediction between CAMRAD, for instance, which seems to have every bell and whistle possible, if you look down

Wendell's list it's black all the way down, it's got everything, and FLAIR, which has practically nothing, the difference in accuracy is very small in effectiveness.

Bielawa: I think you have to temper that. Your remarks are true with regard to the class of problems we've identified for ITR. For other classes, flutter problems and so on, it may be different.

Banerjee: I think that's true. I'd like to make one comment. For instance Dewey mentioned about his correlation between CAMRAD and FLAIR for Task IIC. Again the experiment, I believe, was set up such that the blade could be represented as a rigid element and we did essentially an analytical model using E927 which was set up as a rigid blade with a root spring, and it gave very good correlation. Hence, there is no surprise that FLAIR would give pretty good results, because the experiment was set up that way. However, you have the situation of [Data Set] A where the elastic deflection, flapwise trim deflection of the blade, is the main impetus to the lag damping and the coupling. There, I would think, a blade element model would be essential for good correlation.

Bob Wood, Hughes Helicopters: I think I'd just like to comment. It seems like prior to the onset of the computer, we go back to the 19th century where we had all the classical fluid mechanicians, classical elasticians, and then with Dr. Theodorsen in 1935, classical flutter. Here were a group of people, that had no computers, and they applied purely brain power to solving [these problems]. Once the computer came in we began to spoil all the good problems for them. We could take the computer and no matter what problem it was we didn't need a classical solution. We could just grind that thing to death if we went to enough detail. It seems to me that in the solutions we're looking for in rotary wing that what we're really asking for, what we need and what we require here, is a combination of both. We require the capability in the right areas to model in great detail, but we also require the insight to know where not to model in great detail, I'd say, a combination of what the classical theoretician did combined with taking advantage of the computer as a tool. But I think that [if we] go to the infinite detail of just modeling everything with the computer right down to microscopic extent we'll be at it forever.

Hammond: That's a very good comment. Pete?

Pete Arcidiacono, Sikorsky Aircraft: I'd like to echo what Bob Wood just said. At Sikorsky we keep a list of stability problems that we have known and loved, or hated, and they include classical flutter, or pitch-lag, or ground resonance, the list is probably at least 15 or 20. What you need is a simple analysis that you know handles that specific problem and it's fast and you know you've got, hopefully, the classical problem under control. And then we try to combine that with a global analysis that hopefully will surface any new combination of degrees of freedom that produces a problem. So I agree that we need a combination of approaches.

Inderjit Chopra, University of Maryland: Is there any comparative study of the computer time for these various methods?

Hammond: I don't know; Bill, do you have an answer for that?

Bill Bousman, Aeromechanics Laboratory: Yes, we did ask for the average run time per case but they were for different machines. Just glancing over the numbers briefly, it looked like it would take me a lot more time to try to figure it out in any reportable form. So I'd say as of now, no, we haven't done a comparison of it. Whether those numbers are good enough to compare, I'm not sure at this time.

Chopra: Another question is that we didn't consider compressibility. Is it that the tip Mach number is low? Any other reason?

Bousman: Yes, in all the model tests the tip Mach number is very low.

Chopra: Low means what? Any number?

Bousman: Oh, like 200 or 300 feet per second.

Marcelo Crespo da Silva, University of Cincinnati: I've heard a little bit about modeling with computers. The way I see the problem it has very little to do with computers. If we could get someone who could work as fast as a computer that would be good enough. The basic problem to me is in modeling. It is "how do you describe?" It is "are the equations representative?" Now if you all have the same equations, you should all get the same results. Now because you don't have the same results, my guess is that you have differences in the equations, unfortunately I cannot comment on the differences because I have no idea what kind of terms [are there], what you have done to the equations. But after you have the equations and you are satisfied that the equations are modeling the helicopter behavior in an appropriate way, after that it is just taking our modern slide rule, which is the computer, and doing all sorts of number crunching.

Arcidiacono: That's a good point. I know during the agony we went through using E927 I often asked, "well, let me see the torsion equation and how does it compare with Dewey Hodges' equation, et cetera, et cetera, and it's been very, very difficult, if not impossible, to get the torsion equation laid out from the various groups, G400 included. It might be a very instructive exercise to get the torsion equations in the same symbols and get all the definitions down and make a comparison.

Al Pierce, Georgia Tech: I'd like to allude to a point which I feel is a bit of a deficiency. Wendell Stephens presented some tables this morning and one of these tables had in it aerodynamic considerations. It is my understanding that the originators of the programs supplied the information for the tables and I believe that they're on the panel. Now one item is listed as unsteady aerodynamics and seven of the eleven programs said "yes, there is unsteady aerodynamics in the program." I'd like to address the panel as a whole or individually to see what these unsteady aerodynamics are that a e in the program. I haven't heard the word used today.

Hammond: Who would like to be the first on the panel to address that? Dick Bielawa.

Bielawa: First off, I think that the results that we are trying to correlate with probably didn't need unsteady aerodynamics. Again, we're talking about very low reduced-frequency phenomena. As far as the G400 program is concerned, we have more than one type of unsteady aerodynamics. We have the unsteady stall methodology, which is a semi-analytic method based upon measured unsteady stall loops. We also have two different forms of the linear Pade-type aerodynamics, both in time history and eigensolution.

Pierce: That would be table lookup on the stall?

Bielawa: The unsteady stall?

Pierce: Yes.

Bielawa: Not quite. It's a methodology that generates semi-analytic functions from a small collection of parameters which then is used with the static data to incorporate the unsteady effects of stall. One way of describing it might be to take the unsteady stall signature and apply it to the static data.

Pierce: In the Pade approximation, I presume what this does is just simply introduce a lag, is that correct?

Bielawa: More than one lag. The one parameter that's used in the unsteady stall modeling is what we call lift decay function which is based upon a form of the Wagner function; it's a parameter, it's an unsteady parameter. This parameter by itself is capable of generating a time-history representation of the Wagner function. In addition, we have developed for the propeller version G400 a Pade unsteady representation which is both in the time history and the eigensolution.

Johnson: In the analysis that I use the unsteady aerodynamics that are relevant to these problems are simply the noncirculatory parts of classical incompressible unsteady aerodynamics, plus for the wake effects using what amounts to an augmented state model, which is the dynamic inflow model. All the other aerodynamics that were addressed in the table and that I have the code are not really relevant to the problems that are in this survey.

Tarzanin: We didn't claim that we had any unsteady aerodynamics; we just use the static airfoil tables.

Sadler: I guess the only unsteady aerodynamics really, if you want to think of it that way, in DRAV21 is the unsteady inflow. It's not really unsteady aerodynamics. The C81 program has two or three unsteady aerodynamic models but I don't think they were used in this study.

Jing Yen, Bell Helicopter Textron: No, they were not used in this correlation effort.

Hammond: What unsteady models are in C81?

Sadler: Carta type, the α, A, B method.

Jing Yen: We have two there, one is Carta's and the other was developed by an Army employee who was working for Boeing Vertol at the time, Bob Gormont.

Sadler: Yes.

Jerry Miao: I have to emphasize that in this aeromechanical stability there is no need for this unsteady aerodynamics.

Hooper: Yes, it's totally unnecessary.

Miao: It's unnecessary, but in E927 it's really a very simple kind of thing. I think that if you are talking about loads analysis you probably really need it, here it's really beside the point, though.

Pierce: I'm afraid I can't agree. I mean for many years the entire fixed wing industry has been going up and down the wall trying to perfect the unsteady aerodynamic representations, and has proven beyond a doubt that it's important from the standpoint of flutter. Now is there any proof currently available that this is not true for the helicopter rotor system?

Johnson: Well, I disagree with that too. I think you went a little bit too far there. The pitch damping is primarily aerodynamic; if you didn't have that in these pitch-flap-lag problems you wouldn't get anywhere close to the answer. There are particular problems where the wake effects are also important and that's unsteady aerodynamics and that's not to be ignored. I think we're confusing things a little bit if you mean dynamic stall, if you're trying to include that in unsteady aerodynamics. I think that that has nothing to do with any of the problems in this data set. But that's only one part of unsteady aerodynamics.

Miao: When I say that it's very simple unsteady aerodynamics, I mean that it's a Theodorsen type of pitch damping term that we do have in E927; that's providing a lot of pitch damping. I think in a helicopter company, normally we don't worry about the fixed wing type of flutters so much because, I think, a helicopter blade is not subjected to such high speed flight. Really, it's a different problem.

Pierce: With the placement of the elastic axis and the c.g. you're not as susceptible to flutter.

Johnson: Well, that instability that Dawson found is probably unsteady aerodynamics. It's not irrelevant.

Pierce: Well, we're saying we are not worried about flutter here?

Miao: No, we're not saying that.

Bousman: I'd like to comment on that question about flutter and what Dawson found out. I think that in bearingless rotors there are potentials for very simple designs in which we will drive frequencies down and force pitch-flap couplings which would make us susceptible to flutter. What, in fact, I believe that the industry has concluded is that they will avoid all of those configurations because they cannot analyze them, not because they're bad. And the simplicity that is there might be worth investigating if we had the tools, but we have not made an effort to get those kinds of flutter analyses. I think that's the problem there.

Peretz Friedmann, UCLA: I just wanted to comment on Pierce's comment and to say that I have been faced with the same problem for a long time and I have my own brand of answer to his question. It's not true that unsteady aerodynamics is not important for rotary wing aeroelasticity, but by the same token it's very true that rotary wing aeroelasticity is very, very different from fixed wing aeroelasticity. Therefore, it's probably true to say that unsteady aerodynamics is important for a few limited cases, which rotary wing aeroelasticians are sometimes aware of and maybe sometimes not quite aware of, but it's in a different context from the fixed wing context.

Bielawa: What you say is true; however, the difference between a helicopter rotor and a fixed wing is that, even putting stability considerations aside, the rotor operates in an unsteady environment. I think that as we get into the other problem, the vibration problem, the vibratory loads problem, we are going to have to look at unsteady aerodynamics because there we're talking about reduced frequencies that are not small; blade passage frequencies which yield significant reduced frequencies. And there there's no question, we're going to have to use unsteady aerodynamics to improve our accuracy.

Hammond: Those of us who are interested in higher harmonic control are interested in unsteady aerodynamics. We'd like for some of you to have those in your analyses so that maybe we could predict the effects of higher harmonic control.

Tarzanin: But that's not a stability analysis, right? You're talking about a loads analysis.

Hammond: One more comment, then we're going to have to wrap it up. Yes, Bob?

Wood: This is just brief. I think, Al, perhaps this is the context of what many of the other companies have done. [The] DART analysis has Theodorsen unsteady aero in it, and that has been used and flutter problems have been identified. They normally begin at frequencies up around 8/rev. I think for this particular study that option was not implemented by Dev and his group when they were operating, in other words they used quasi-steady. It also has the dynamic stall in the α, A, B sense, those options are in there, but I guess the question is whether people turned that switch

on when they did this particular study. I would say that in our case we did not. Do you want to comment, Dev?

Banerjee: We had a closed form expression for the Theodorsen lag function, but we did not use a time history solution to determine the damping characteristics and neither did we use a dynamic stall analysis. But we did have a closed form expression for the Theodorsen lag function which we did utilize for this analysis. I don't know how much of a difference it made but we did use it for DART.

Hammond: Okay, with that what I'd like to do is have us continue this dialogue at the wine and cheese tasting. But before we do, I'd like to thank the panelists for their comments and also the audience for all the very nice discussion, and I'd like to give the panelists a hand for their efforts.

THE IMPORTANCE OF STEADY AND DYNAMIC INFLOW ON THE STABILITY OF ROTOR-BODY SYSTEMS

David A. Peters
Professor and Chairman
Department of Mechanical Engineering
Washington University
St. Louis, Missouri 63130

Abstract

The induced flow field of a rotor responds in a dynamic fashion to oscillations in rotor lift. This has long been known to affect the stability and control derivatives of the rotor. More recently, however, it has also been shown that this dynamic inflow also affects rotor and rotor-body aeroelastic stability. Thus, both the steady and unsteady inflow have pronounced effects on air resonance. Recent theoretical developments have been made in the modeling of dynamic inflow, and these have been verified experimentally. Thus, there is now a simple, verified dynamic inflow model for use in dynamic analyses.

Notation

a = slope of lift curve, per radian

B = tip loss factor

C_{do} = drag coefficient

C_{do}^* = equivalent drag coefficient

C_L = roll moment coefficient

C_M = pitch moment coefficient

C_Q = torque (or power) coefficient

C_T = thrust coefficient

e_{pc} = pocket cut-out divided by radius

$\{F\}$ = vector of loadings

$\bar{f}$ = flat plate drag area over rotor area

k = reduced frequency based on free stream, $= \omega/v$

K_I = apparent inertia coefficient

K_M = apparent mass coefficient

$[L]$ = matrix of inflow gains

$[L']$ = normalized L matrix

$[M]$ = inflow apparent mass matrix

p = nondimensional flapping frequency

r = nondimensional distance from rotor center, $0 < r < 1$

R_e = elastic coupling parameter

v = mass flow parameter

$\bar{v}$ = nondimensional free stream

V_I = total nondimensional flow at rotor, Table 3

α = pitch angle, angle of incidence, positive nose down

α^* = pitch angle at rotor, $\alpha^* = \sin^{-1}[(\lambda + \nu)/\mu)]$

γ = Lock number

γ^* = equivalent Lock number

υ = nondimensional free-stream velocity

υ^* = free-stream velocity at rotor, $\upsilon^* = \sqrt{\mu^2 + (\lambda + \nu)^2}$

ζ = axis of minimum damping

η = inplane damping

θ = total pitch angle

θ_o = collective pitch

θ_s, θ_c = cyclic pitch

λ = normal freestream component, $\lambda = \upsilon\sin\alpha$

λ_o = total uniform inflow, $\lambda_o = \lambda + \bar{\nu}$

λ_c = fore-to-aft steady gradient

μ = advance ratio, $\mu = \upsilon\cos\alpha$

ν = total induced flow

ν_o = uniform induced flow

ν_s = side-to-side induced flow gradient

ν_c = fore-to-aft induced flow gradient

ζ = axis along free stream

σ = rotor solidity, real part of eigenvalue

$[\tau]$ = matrix of inflow time constants

λ = inflow angle

λ_s = side-to-side gradient in inflow angle

ω = excitation frequency, imaginary part of eigenvalue, per rev

ω_ζ = inplane frequency, per rev

Ω = rotor speed, rpm

$(\bar{\ })$ = average value

$(\tilde{\ })$ = perturbation value

Introduction

Almost everyone would agree that the induced flow field of a rotor is an important contributor to the performance and vibrational characteristics of that rotor. What is less well known, however, is that the induced flow field of a rotor is also an important contributor to the aeromechanical stability of that rotor. The contribution of induced flow to stability is manifested in two ways. First, the steady induced-flow field affects the equilibrium flapping angles, the cyclic pitch, and the inflow angles of the rotor. These, in turn, impact directly upon aeromechanical stability. Second, the induced flow field responds (in a dynamic fashion) to oscillations of the rotor; and this inflow response can fundamentally change the damping of the rotor oscillation. Because of the important influence of unsteady induced flow, a good deal of effort has gone into the modeling of dynamic inflow for helicopter applications. This paper examines the history of this modeling effort including the latest developments and experimental verification.

Steady Inflow

The major contribution of steady inflow to rotor damping can be understood in terms of the axis of minimum damping, as shown in Figure 1. In the top figure, we see an airfoil pitched at an angle θ with the relative air flow impinging at an angle λ. The vertical direction is flap and the inplane direction is lead-lag. It turns out that the least stable direction of motion is at $(\theta + \lambda)/2$, Reference 1. In other words, a coupled flap-lag mode with a principle direction of motion at $(\theta + \lambda)/2$ will have the least damping of all modes. The physical basis for this "minimum damping" is illustrated in the lower part of the figure. The blade lift is always perpendicular to the direction of air flow. Thus, a blade motion directed along an axis ϕ creates an increased lift which is opposite to the direction of motion-damping. However, if ϕ is larger than λ, then lift is in the same direction as the motion and can create negative damping. The maximum negative contribution occurs at $\phi = (\theta + \lambda)/2$.

Now, it is clear that the induced flow directly affects the angle λ. Thus, induced flow can either move the axis of minimum damping closer to the modal axis (which is destabilizing) or further from the modal axis (which is stabilizing).

The mathematical description of this phenomenon is given by

$$\eta = \eta_o + \left[\frac{\theta + \lambda}{2} - \frac{R_e(\omega_\zeta^2 - p^2 + 1)}{(\omega_\zeta^2 - p^2)}\right]^2 \quad (1)$$

The negative real portion of the inplane eigenvalue is η and is a measure of inplane damping. Here, we see that there is a contribution to this damping that is minimum when $(\theta + \lambda)/2$ is equal to the direction of blade motion. The modal direction depends upon the elastic coupling (R_e) and upon the difference between the inplane and flapping stiffnesses ($\omega_\zeta^2 - p^2$). For a stiff inplane rotor, $\omega_\zeta^2 > p^2$, the worst case is at a positive $\theta + \lambda$. For soft inplane rotors, $p^2 - 1 < \omega_\zeta^2 < p^2$ (including those with matched-stiffness $\omega_\zeta^2 = p^2 - 1$), the worst case is for $\theta + \lambda$ negative. This occurs during autorotational descent and partially accounts for the fact that autorotation is often the most critical air-resonance condition.

The effect of induced flow on inplane damping turns out to be the most powerful effect that forward flight exerts on inplane damping. To be more specific, the decrease in induced flow (that accompanies forward speed) and the tip-path tilt (that is used for propulsive force) both combine to significantly change the inflow as a function of μ. Figure 2, taken from Reference 2, depicts inplane damping as a function of advance ratio. The figure shows a sharp drop in damping with μ. When the μ-related changes in induced flow are ignored, however, as shown in the top curve, this loss of damping is not predicted. Therefore, we conclude that the major effect of advance ratio is the drop in λ (and hence the movement of the axis of minimum damping). In fact, up to $\mu = .25$, most of the effect of forward flight can be included by a hover analysis with inflow appropriately changed to account for forward flight. When propulsive trim is included (the short-dashed curve), the rotor shaft tilts forward with advance ratio to overcome fuselage drag. This tends to increase inflow and, therefore, to cancel the lower induced flow. Thus, for $\mu > .25$ the damping again increases.

A similar phenomenon is manifested in wind turbine (or autorotatinal) damping, as shown in Figure 3, taken from Reference 3. Here, the wind-speed ratio directly affects ϕ, which results in minimum damping at a particular velocity. The same can be said of wind-turbine damping versus power coefficient, as seen in Figure 4. At a particular value of C_Q, the induced flow is such as to make the damping a minimum.

Thus far, we have considered only the uniform (or average) value of induced flow. It is also interesting to investigate the effect of gradients in the induced flow field. The Figure 5 compares inplane damping for the case of no gradients ($\lambda_c = 0$) with that for the case of a full gradient ($\lambda_c = \lambda_o$), which implies zero induced flow at the leading edge of the rotor disc and maximum induced flow at the trailing edge. One can see that there is only a minor variation in damping between the two cases. Even in hover (for which no gradient physically exists), the effect is small. Thus, fore-to-aft gradients are not important in the context of the effect of steady induced flow on inplane damping.

In Figure 6, we see the effect of a side-to-side gradient on inplane damping. A wind turbine is chosen, for which such gradients occur due to the earth's boundary layer. Here, there is some effect on stability at moderate μ. The reason for this is straight-forward. Changes in ν from fore-to-aft generally cancel in terms of damping. Side-to-side gradients, on the other hand, tend not to cancel due to the large changes in relative free-stream velocity in forward flight. Thus, induced flow gradients are more important in the lateral direction than in the longitudinal; but neither effect is very large.

Early Work In Dynamic Inflow

In the preceding development, we have seen that the steady induced-flow field has a significant effect on blade damping. We now turn our attention to the effect of unsteady fluctuations in the flow field (dynamic inflow). To begin, it might be good to review the past developments in this area. In 1950, Ken Amer noted that the pitch-rate damping of a helicopter depends upon the thrust coefficient in a repeatable, quantitative fashion, Reference 4. In 1952, G. J. Sissingh successfully showed that this measured effect is due to a transient behavior of the induced flow, Reference 5. That is, a roll-rate of a helicopter causes a side-to-side gradient in lift which creates roll damping. However, the formation of this lift gradient also creates an induced-flow gradient that partially negates the lift gradient that finally develops. (This is the effect of dynamic inflow.) Since the induced flow depends greatly upon the mass flow through the rotor, there is a strong C_T dependence, as measured by Amer. In related work, Reference 6, Carpenter and Fridovitch developed experimental and theoretical results that related to how quickly induced flow follows a change in lift (i.e., a time constant). They found that the time delay could be modeled satisfactorily by the apparent mass of an impermeable disk, as developed in Reference 7. Therefore, by 1953, researchers had identified both the effect of transient inflow and the effect of apparent mass. These two pieces (the induced flow due to lift perturbations and the related time constants) form the kernel of all subsequent work in dynamic inflow.

The early work of these researchers was picked up by several investigators in the early 1970's. This later work concentrates on stability and control derivatives as well as forced response (both of which are dramatically affected by the dynamic inflow phenomenon identified by Sissingh). In 1970, Pat Curtiss and Norm Shupe included the Sissingh model in their helicopter flight equations, References 8-9. (This was a quasi-steady model, and no time constants were used.) The work of Curtiss and Shupe points out that the quasi-steady effect of induced flow in pitch and roll can be accounted for by a simple reduction in the lift coefficient (i.e., by an equivalent Lock number). In other words, changes in lift produce changes in inflow which lower the expected change in lift. Thus, we have an equivalently lower lift-curve slope and lower gamma.

In 1972, Ormiston and Peters took the Sissingh-Shupe model and extended it to include plunge, pitch, and roll for combinations of lift, climb, and forward flight, Reference 10. Calculations of control derivatives with this model were then compared with experimental data taken by Dave Sharpe and Bill Kusczynski with a 7-1/2 ft diameter model rotor. The results show that the Sissingh-Shupe dynamic inflow model (based on momentum theory) gives excellent correlation in hover but not in forward flight. Alternative models for forward flight were then suggested, including an empirical model based on curve fitting the measured data.

By 1974, Peters and Ormiston had extended the dynamic inflow models to the unsteady condition (time constants, etc), Reference 11. Sharpe and Kuczynski had obtained experimental frequency-response data both in hover and forward flight, Reference 12; and this data was compared to the theory in Reference 11. At the same time, Hohenemser and Crews were obtaining similar frequency-response data for a very small-scale rotor, Reference 13; and they also compared with theory. Both studies showed a dramatic effect of dynamic inflow. Furthermore, these two independent studies revealed a completely consistent picture of the gains and time constants of dynamic inflow. In hover, they found that momentum theory (combined with the apparent mass of an impermeable disc) captured all of the experimental features. Thus, when these theoretical gains and time constants were combined with the theory, amazing correlation was obtained.

Figure 7 shows an example of this correlation. Here we have the roll moment (on the left) and the pitch moment (on the right) due to an oscillation in θ_s (longitudinal cyclic). Both the amplitude and the phase of the response are given. The circles are experimental data from the 7-1/2 ft rotor. The solid line is the normal theory in which only steady induced flow is taken (no dynamic inflow). The results are preserted for frequencies of swashplate oscillation from 0 to 1.2 per revolution and for 4° of steady collective pitch. One notices large, qualitative deviations between the solid, theoretical curve and the experiment, especially in the phase of C_L and in the amplitude of C_M. The discrepancies are largest at small values of ω and decrease for larger values of ω. Perhaps the most significant aspect of the comparison (between the solid line and the data) is the fact that none of our standard analytic excuses could explain the difference. Collective pitch is only 4°, so there is no stall; and the analysis includes several elastic modes in flapping, so that the dynamics are well represented. Thus, the only candidate to improve correlation is dynamic inflow.

The short-dashed curve gives results for a simple, quasi-steady momentum-theory model of dynamic inflow. That is, the dynamic inflow is assumed to follow changes in lift immediately according to simple momentum theory. The result is dramatic. Every single detail of the data is matched for $\omega < .4$ per rev. At larger ω, however, the theory with quasi-steady theory begins to deviate from the experimental result. The reason for this is that inflow actually responds with a time delay. When this unsteady effect is added, however, (the long dashed curve) the new analysis agress at both low and high ω. The time constants used in this amazing correlation are the apparent mass and inertia of an impermeable disc. This yields the nondimensional inertia and mass terms ($K_I = .1132$, $K_m = .8488$). This simple theory leads to the correlation shown in both magnitude and phase.

It seems impossible that anyone could study these results and not be convinced that: a) dynamic inflow is an important, physically-based effect, and b) it can be modeled in hover by simple momentum theory with simple apparent mass terms. In general, one would not always admit that a theory is good simply because in improves correlation. In many cases, improvement might simply be luck; because there can be so <u>many</u> unknown effects that one error might coincidentally cancel another. In this case, however, all reasonable errors have been accounted for. Furthermore, the details of the response are so well simulated that coincidence is out of the question. These results establish dynamic inflow as a fundamental cornerstone of rotor analysis.

We now turn from the response of cyclic pitch oscillations and study the response due to shaft oscillations, as shown in Figure 8. Here, we look at the amplitude and phase of roll moment and pitch moment as a result of pitch oscillations. Because of the symmetry in hover, roll oscillations should create responses identical to those due to pitch (except for a 90° phase shift). Thus, both pitch and roll data are plotted together on this figure (circles and dots). Where the two sets of data begin to deviate ($\omega = .25$), a stand resonance is contaminating the results. Below $\omega = .25$, however, the pitch and roll data are consistent. The solid curve represents conventional theory with no dynamic inflow. One is impressed with how poorly it models the response. (C_L with α is in error by several hundred percent.) When either quasi-steady or unsteady dynamic inflow is included, however, the amplitude and the phase are completely captured. This data correlation leads one to believe that an air resonance mode could be very sensitive to dynamic inflow, since such modes occur from 0.2 to 0.5 per rev.

In forward flight, there is also a large effect of dynamic inflow; but it is not well modeled by simple momentum theory. Figure 9 shows response of the same rotor as that of the previous figures, but with $\mu = .51$. C_L due to all three controls is given. Momentum theory (shown by the dashed line) does not at all correlate with the data. The long dashed curve in the figure is a calculation based on an empirically identified model. This model is identified at <u>$\omega = 0$ only</u>. The effect of ω is included by the same apparent mass terms used in hover. Thus, we see an excellent correlation which includes the presence of an anti-resonance (zero amplitude and phase discontinuity) predicted and measured for the θ_s derivative at $\omega = .4$. Thus, dynamic inflow is important even at high advance ratios.

The effect of dynamic inflow and the satisfying correlation shown above are not flukes of one rotor in one wind tunnel. Figure 10 shows data taken by Kurt Hohenemser and Sam Crews with a 20-inch diameter rotor at Washington University, Reference 13. Here, harmonic excitation is applied in the rotating system by a rotating eccentric. The magnitude of flapping angle due to θ is plotted versus the excitation frequency in the rotating system, ω. The squares are the test data, the solid curve is the analysis with no dynamic inflow, and the dashed curve is the analysis including dynamic inflow. The parameters L and τ are chosen to give the best fit of the data, and yet they agree with the values from momentum theory within a few percent. For example, $K_I = .113$ (momentum), $K_I = .112$ (Reference 13). Therefore, dynamic inflow is established as an effect independent of rotor site or wind-tunnel characteristics.

In summary, the early work in dynamic inflow concentrates on forced response of rotors. It shows beyond reasonable doubt that dynamic inflow is an important effect. In hover, the quasi-steady inflow is well modeled by momentum theory; but, in forward flight, momentum theory is completely inadequate. In both hover and forward flight, however, the apparent mass of an impermeable disc provides the correct time constants.

Effect On Stability

The superb data correlations given thus far were developed for the forced response of rotors. It was not long, however, before researchers began studying the effect that dynamic inflow might have on the stability and damping of rotor systems. We now mention a few of the developments in this area. In 1976, Bob Ormiston studied the effect on flapping eigenvalues, Reference 14. He discovered the importance of mode type (collective, progressing, regressing) on the effect of dynamic inflow. In 1979, Peters and Gaonkar studied the effect on lead-lag eigenvalues, Reference 15. One of the more interesting aspects of that paper was the introduction of an equivalent drag coefficient. In other words, just as the lowered lift (due to dynamic inflow) can be modeled by a loss in lift-curve slope, even so, the corresponding increase in induced drag (also caused by dynamic inflow) can be modeled by an equivalent increase in C_{d_o}.

In 1982, Gaonkar and several co-authors extended this work to include aeromechanical stability, Reference 16. That same year, Wayne Johnson also used dynamic inflow theory to correlate Bill Bousman's test data, Reference 17. At this point, it might be good to briefly review the findings of each of these papers with respect to the stability and damping of rotors.

First we look, in Figure 11, at the calculation from Reference 14 of the negative real part of the flapping eigenvalue as a function of collective pitch for $p = 1.02$ and 1.15. With no dynamic inflow, there is a constant value of damping equal to $\gamma/16$, independent of θ_o. When dynamic inflow is included in the analysis, however, one finds two distinct damping values depending upon the mode, progressing or regressing (collective is not included). The difference in damping of the two modes is attributed to the fact that each mode has a different frequency and therefore affects the inflow in a different way. The quasi-steady approximation (shown by the dashed curve) is closer to the regressing mode because that mode is of lower frequency. The results show clearly the large effect of dynamic inflow. The effect is most pronounced for the regressing mode at low collective pitch. Such a plot indicates that one cannot count on flap damping to stabilize ground resonance at low θ_o.

Another interesting aspect is that even the progressing mode, with a relatively high frequency, is affected by dynamic inflow.

Figure 12 shows the real part of the inplane eigenvalue as a function of advance ratio, Reference 15. The solid curve is the theory without dynamic inflow, and the broken curves are the modes with dynamic inflow. We notice that the higher-frequency progressing and collective modes are only moderately affected. The lower-frequency, regressing mode, however, shows a substantial alteration due to dynamic inflow. Thus, we conclude that dynamic inflow has a potentially large effect on inplane damping, and thus on rotor-body damping.

Next we look at calculations of coupled rotor-body modes from Reference 16, as shown in Figure 13. Here we have body roll-mode damping both for an RPM sweep and for a collective-pitch sweep. The dashed-dot curves are quasi-steady theory; and the dashed-only curves are conventional, unsteady theory. The rotor is matched stiffness. The figure on the left shows a fairly uniform effect of dynamic inflow within the RPM range of interest. This effect is about 30%. The right-hand figure gives a collective sweep. As might be expected, the effect of dynamic inflow increases with decreased lift. Again, the theoretical predictions are that dynamic inflow should play a major role in rotor-body damping; and this effect comes from equivalent changes in both flap damping and inplane damping, as we understand from Reference 16.

It fell to Wayne Johnson to finally compare these predictions with experimental data, as shown in Figure 14. This figure presents the real part of the eigenvalue for the pitch-mode damping. The dashed curve is the theory without inflow dynamics, and the solid curve is the theory with inflow dynamics. Dynamic inflow successfully predicts the peak in damping at low μ and the 25-30% loss of damping at higher values of μ. Figure 15 shows a similar comparison for roll. Again, the dynamic inflow provides a substantial improvement in correlation.

The previous two figures show that the NASA analytic model does reasonably well in correlation and that dynamic inflow is an important part of that correlation. Therefore, an analysis without dynamic inflow, but that correlated with experimental data, would be suspect, since dynamic inflow is well-documented and damping analyses are not, and since we know that dynamic inflow has an important effect.

For those who might still be skeptical, we present Figure 16, also from Reference 17. This figure compares measured and calculated frequencies as a function of RPM. The astounding part of the comparison is that one of the branches, labeled λ, is the frequency of a mode that is predominantly dynamic inflow. This branch does not even exist when dynamic inflow is not included. With dynamic inflow, however, the branch appears and matches the experimental data nearly perfectly. Thus, we are looking not just at the effect of dynamic inflow on some mode; we are looking at

the measured dynamic-inflow mode, itself, as seen for the first time.

A final comparison with data is given in Figure 17, which represents two of the correlation studies presented at this workshop. One is Wayne Johnson's correlation with the NASA program, and the other is Sheng Yin's correlation with the Bell Helicopter program. In either case, dynamic inflow represents a significant contribution and improves the correlation of the analysis.

Before leaving the stability correlation, we need to make an important point about the role of these correlations in verifying dynamic inflow theories. The point is this. The validity of a particular dynamic inflow theory (or of dynamic inflow as a phenomenon) cannot presently be made on the basis of comparisons with inplane damping or rotor-body stability data. The reason for this is clear. Stability calculations are not yet accurate enough to uniquely distinguish dynamic inflow from other effects. The role of dynamic inflow in such calculations is, however, important. The reason for this is straightforward. First, we know from flapping response that dynamic inflow exists as a phenomenon and that it is important. The accuracy of any dynamic inflow theory can be determined by comparisons with low-lift flapping response data, which is accurate and relatively unhindered by unknown structural or aerodynamic effects. It is this exact same theory that is applied to inplane stability analyses. (There is not one "flapping" dynamic inflow and one "inplane" dynamic inflow.) Therefore, the comparison with stability data does not test the inflow theory. Instead, the dynamic inflow theory is included in the analysis in order to see the effect of dynamic inflow and to verify the analysis package. This is why we said earlier that a theory that correlates without dynamic inflow would be suspect. Such a theory must have two errors that are cancelling. One error is the omission of dynamic inflow, and the other error is the unknown omission that is somehow cancelling the inflow effect.

Momentum-Theory Formulation

In the early portions of this paper, we briefly reviewed the early work in dynamic inflow; but we did not go into detail as to the exact mathematical formulations used. In this section, we consider these formulations in more detail. The vast majority of the work in this area has been based on simple momentum theory. In hover, this implies that each elemental section of rotor area is treated independently. Then, for each section, the thrust is set equal to the product of the mass flow through the element and the total change in velocity in the associated stream tube. The next step in the analysis (and this is crucial to the theory) is to average the loads and induced flow over the rotor disc. In other words, the theory of dynamic inflow does not concern itself with details of either load distribution or induced flow distribution. It concerns itself, rather, with global averages. This further implies that the induced flow is treated more as a large mass of air rather than as individual vortices.

As a simple example, we consider the average induced flow ν due to the total thrust coefficient, C_T

$$C_T = 2\nu^2 \tag{2}$$

Equation (2) is nonlinear in ν. Usually, however, we consider perturbations about a steady condition ($\bar{C}_T$, $\bar{\nu}$). Thus, we have for the quasi-steady case

$$C_T = \bar{C}_T + \tilde{C}_T \tag{3a}$$

$$\nu = \bar{\nu} + \nu_o \tag{3b}$$

$$\bar{C}_T = 2\bar{\nu}^2 \tag{4a}$$

$$\tilde{C}_T = 4\bar{\nu}\nu_o \tag{4b}$$

Equation (4b) is the typical perturbation relation between charges in thrust, C_T, and charges in uniform inflow, ν_o. In a more general formulation, we may add cyclic variations in lift (i.e. roll and pitch moments) and cyclic variations in induced flow

$$\nu = \bar{\nu} + \tilde{\nu} \tag{5a}$$

$$\tilde{\nu} = \nu_o + \nu_s r\sin\psi + \nu_c r\cos\psi \tag{5b}$$

where ν_s and ν_c are induced flow gradients. Simple momentum theory gives

$$\tilde{C}_T = 4\bar{\nu}\nu_o \tag{6a}$$

$$\tilde{C}_L = -\bar{\nu}\nu_s \tag{6b}$$

$$\tilde{C}_M = -\bar{\nu}\nu_c \tag{6c}$$

Equations (6a-c) represent the momentum theory model in hover used in References 5, 8, 9, 10, 11, 14, 15, and 16.

Although equation (6) works well for hover, it is natural to try to extend the formulation to combinations of thrust, climb, and forward flight. To do this, $\bar{\nu}$ in equations (6a-c) is replaced by $v/2$ where v is a mass-flow parameter. In climb,

v is given by

$$v = \lambda + 2\bar{v} = \lambda_o + \bar{v} \tag{7}$$

where λ is the inflow due to climb, and λ_o is the total inflow, Reference 8. In forward flight with perfectly edgewise flow and no lift, we have

$$v = \mu \tag{8}$$

as given in Reference 9 and 10, (although forward flight certainly stretches the assumptions of momentum theory to the extreme).

Most investigators agree on the formulations of equations (7) and (8), but a more difficult problem is the transition from hover to edgewise flow. If we consider a freestream velocity v and a rotor incidence α, then the relative flow is given by

$$\mu = v \cos \alpha \tag{9a}$$

$$\lambda = v \sin \alpha \tag{9b}$$

$$v = \sqrt{\mu^2 + \lambda^2} \tag{9c}$$

If we then add the induced flow, we obtain for the flow at the rotor disc

$$\lambda_o = v\sin\alpha + \bar{v} = \lambda + \bar{v} \tag{10a}$$

$$v^* = \sqrt{\mu^2 + (\lambda + \bar{v})^2} = \sqrt{\mu^2 + \lambda_o^2} \tag{10b}$$

$$\alpha^* = \tan^{-1}\left(\frac{\lambda + \bar{v}}{\mu}\right) = \tan^{-1}\left(\frac{\lambda_o}{\mu}\right) \tag{10c}$$

The real problem is to relate v to μ, λ, and $\bar{v}$.

In References 9 and 18, this is accomplished by the following ad hoc formula

$$v = v + 2\bar{v} \sin \alpha = \frac{\mu^2 + \lambda^2 + 2\bar{v}}{\sqrt{\mu^2 + \lambda^2}} \tag{11}$$

Equation (11) gives the correct value of v in hover ($\mu = 0$, $v = \lambda + 2\bar{v}$); but for edgewise flow, equation (11) gives an inconsistent result ($\lambda = 0$, $v = \mu$). Now, $v = \mu$ is correct for edgewise flow with no lift; but the inconsistency is that, for $\lambda = 0$, equation (11) gives no effect of thrust (i.e. of $\bar{v}$) in the formula. Thus, in the limit as ($\lambda = 0, \mu \to 0$) we obtain a different value of v than we do for ($\mu = 0$, $\lambda \to 0$). There is a discontinuity in the function at ($\mu = 0$, $\lambda = 0$), and this is unacceptable.

A more reasonable formulation of v is given in Reference 11 from basic principles

$$v = v^* + \bar{v} \sin \alpha^* = \frac{\mu^2 + (\lambda + \bar{v})(\lambda + 2\bar{v})}{\sqrt{\mu^2 + (\lambda + \bar{v})^2}} \tag{12}$$

where v^* and α^* are the total flow and angle at the rotor including induced flow. Equation (12) is derived from momentum principles (not on an ad hoc basis) and provides a much more reasonable formulation of the transition between hover and forward flight. When v is represented by equation (12), it is always positive (with no singularities) except at the vortex-ring boundary, where $v = 0$, Reference 19.

In more recent work by Johnson, Reference 20, equation (12) is obtained for the C_T relation, equation (6a); but a different formulation is derived for the C_L and C_M relations, equations (6b) and (6c). In particular, Reference 20 uses for C_L and C_M

$$v = v^* = \sqrt{\mu^2 + (\lambda + \bar{v})^2} \tag{13}$$

This is in direct contrast to equation (12). Furthermore, in Reference (20), the v for the C_T relation is altered by use of an "approximation" of equation (12)

$$v = v^* + v\sin\alpha^* \approx v^* + \lambda + \bar{v} = \sqrt{\mu^2 + (\lambda + \bar{v})^2} + (\lambda + \bar{v}) \tag{14}$$

It is not at all clear why the approximation in equation (14) should be valid. Although Reference (20) states that it is valid "for low inflow ratio," this claim is actually not correct.

Table 1 provides a comparison of equations (11)-(14) at critical flight conditions. There are several interesting comparisons in the table. First, in the hover results, we note the Johnson model for roll and pitch differs by a factor of 2 from all previous work (including Sissingh, Curtiss, Shupe, Ormiston, Peters, and Azuma), even in hover. Since these previous results show such an excellent correlation with flapping data, there can be little doubt that Reference 20 is in error. The source of the error can be quickly traced to a failure to include v_s and v_c in the mass flow term of each generic element. Along this same line, Reference 20 mentions agreement with the results of Loewy, Reference 21, as confirmation of the accuracy of the formulation. Reference 21, however, is for a zero-lift climb (no wake contraction). The second row of Table 1 shows that for a climb, equation (13) is acceptable for roll and pitch, giving the correct answer $v = \lambda$. With lift, however, the formulation is incorrect.

The second row of Table 1 also reveals an error in the C_T formulation of Reference 20. Whereas all other formulations (including Reference 21) result in $v = \lambda$, the approximation of equation (14) (from Reference 20) gives $v = 2\lambda$. Here, the error lies in the approximation and not in the original formulation. When the conditions of climb and lift are combined, the third row of Table 1, the error in the formulation of Reference 20 is more clear. The correct value, $\lambda + 2\bar{v}$, is the flow speed downstream from the rotor. The two incorrect formulas $(\lambda + \bar{v})$ and $2(\lambda + \bar{v})$ do not provide any effect of wake contraction, for they treat thrust and climb equally.

Going on with Table 1, we see that all formulations give the same value, $v = \mu$, for zero lift edgewise flow; but when lift is added, row 5, there is a wide range of answers. Only the results of Reference 11 and Reference 20 (C_T) are consistent in the sense that they reduce both to μ as $\bar{v} \to 0$ and to $2\bar{v}$ as $\mu \to 0$. When we further consider the case of zero lift but with incidence, row 6, the results of Reference 20 (C_T) also fail, which leaves the result of Reference 11 as the only viable choice. (For no lift, only $\sqrt{\mu^2 + \lambda^2}$ makes physical sense.) Finally, the last row of Table 1 gives results for zero normal flow, which can occur in a descent. Here, another failure of Reference 8 is noticed. Thus, the v parameter from Reference 11 is the most logical choice of transition between hover and forward flight in momentum theory. To summarize, its attributes are:

1) Correct limiting behavior in climb, hover, and edgewise flow

2) No singularities

3) Foundation in momentum theory

4) Prediction of vortex-ring boundary

The above discussion has considered only the quasi-steady effect of inflow. (Induced flow is assumed to follow immediately any change in loads.) The concept of momentum theory can also be extended, however, to include the time lag between lift and induced flow. In general, equations (6a-c) can be extended as follows.

$$K_M \dot{v}_o + 2v v_o = \tilde{C}_T \tag{15a}$$

$$K_I \dot{v}_s + v/2\, v_s = -\tilde{C}_L \tag{15b}$$

$$K_I \dot{v}_c + v/2\, v_c = -\tilde{C}_M \tag{15c}$$

Here K_M and K_I are time constants associated with the rotor air mass. These can be taken as completely general and identified experimentally, as in References 6 and 13. On the other hand, they can be obtained from first principles by potential flow theory. K_M is developed (in Reference 7) and K_I is found (in Reference 11) in this way.

$$K_M = \frac{8}{3\pi} = .8488 \tag{16a}$$

$$K_I = \frac{16}{45\pi} = .1132 \tag{16b}$$

In each case, the parameters are based on the apparent mass (or inertia) of an impermeable disc. Equations (15) and (16) form a complete unsteady dynamic inflow theory. With $K_M = K_I = 0$, we recover quasi-steady theory.

One of the most valuable results of momentum-theory inflow dynamics has been the discovery that the quasi-steady theory is tantamount to the use of an equivalent Lock number and drag coefficient, References 9 and 15. The formulation is as follows

$$\gamma^* = \frac{\gamma}{1 + \frac{\sigma a}{8v}} \tag{17a}$$

$$\left(\gamma \frac{C_{do}}{a}\right)^* = \gamma\left[\frac{C_{do}}{a} + \frac{(\theta - \phi)^2}{1 + 8v/\sigma a}\right] \tag{17b}$$

$$\left(\frac{C_{do}}{a}\right)^* = \frac{C_{do}}{a}\left(1 + \frac{\sigma a}{8v}\right) + \frac{\sigma a}{8v}(\theta - \phi)^2 \qquad (17c)$$

Although equation (17a) was originally derived for rigid flapping only, Reference 22 shows that the formulation is quite general. Therefore, a simplified estimate of the effect of dynamic inflow can be obtained from a simple change of γ and C_{do} in any analysis package.

Another interesting aspect of the γ^* approximation is that it can also be used in unsteady, harmonic response analyses, Reference 11 and 13. In particular,

$$\frac{\gamma^*}{\gamma} = 1 - \frac{1}{1 + \frac{8v}{\sigma a} + \frac{16K_I i\omega}{\sigma a}} \qquad (18a)$$

The crucial parameter may be rewritten as

$$\frac{8v}{\sigma a} + \frac{16K_I i}{\sigma a} = \frac{8v}{\sigma a}\left(1 + \frac{2i\omega K_I}{v}\right) \qquad (18b)$$

Equation (18b) shows that there is a reduced frequency, $k = \omega/v$, associated with dynamic inflow. Therefore, the effect of mass flow, v, can be very complicated since it changes both gain and reduced frequency.

More Advanced Formulations

The formulation of equations (15a-c), while being excellent in hover, has proven very poor in forward flight. (For example, it does not allow for a fore-to-aft gradient due to C_T.) For this reason, several attempts have been made to extend the theory. Up to now, all such attempts have been based on a matrix formulation of equation (15).

$$[\tau]\begin{Bmatrix}\dot{\nu}_o\\ \dot{\nu}_s\\ \dot{\nu}_c\end{Bmatrix} + \begin{Bmatrix}\nu_o\\ \nu_s\\ \nu_c\end{Bmatrix} = [L]\begin{Bmatrix}\tilde{C}_T\\ \tilde{C}_L\\ \tilde{C}_M\end{Bmatrix} \qquad (19a)$$

$$[M]\begin{Bmatrix}\dot{\nu}_o\\ \dot{\nu}_s\\ \dot{\nu}_c\end{Bmatrix} + [L]^{-1}\begin{Bmatrix}\nu_o\\ \nu_s\\ \nu_c\end{Bmatrix} = \begin{Bmatrix}\tilde{C}_T\\ \tilde{C}_L\\ \tilde{C}_M\end{Bmatrix} \qquad (19b)$$

$$[M]\{\dot{\nu}\} + [L]^{-1}\{\nu\} = \{F\} \qquad (19c)$$

If we look at equation (19a) and temporarily ignore the "dot" term, we see a quasi-steady inflow law. The various harmonics of inflow (described by a vector, $\{\nu\}$) are assumed to be linearly proportional to the aerodynamic loads on the blade (such as thrust, roll moment, and pitch moment). These loads are represented by the vector, F. The matrix L is the dynamic inflow matrix and expresses the coupling relationships between inflow and loads. Generally, we consider $\{\nu\}$ and $\{F\}$ in this equation to be perturbation quantities about some steady inflow and loading distributions.

The term, $[\tau]\{\dot{\nu}\}$, then represents time constants of the system. These imply that the induced flow does not instantaneously follow perturbations to the loads. The τ-terms imply "unsteady" as opposed to "quasi-steady" inflow theory. In an equivalent form of the general theory, given by the second matrix equation, the system is premultiplied by L-inverse. In this alternative version, the $L^{-1}\tau$ matrix takes on the roll of apparent mass terms, [M]. The crux of all dynamic inflow theories is to find the elements of L and [M]. In the early momentum theory (Sissingh, Curtis, Shupe, and Peters), the M-matrix and the L-matrix were diagonal, 3 x 3 matrices, as given by equation (15). In later work, Reference 10, other [L] matrices were considered based on empirical considerations. These were very successful, but lacked physical foundation. Thus, a need was recognized to find [L] and [M] from more basic theories.

In principle, any induced flow theory that keeps track of the three-dimensional, unsteady vorticity automatically includes dynamic inflow, eg., Reference 21. In practice, however, few present-day programs provide a transient rotor wake analysis. Furthermore, even the steady wake programs are much too cumbersome for use in a dynamics analysis, Reference 23. What is needed, therefore, is some analysis that can be used to obtain [M] and [L] in a simple, usable form. The prime candidate for this analysis is actuator-disc theory. In Reference 24, the first attempt was made to extract dynamic inflow data from an actuator-disc theory. It should be pointed out that many people had used actuator-disc theories to obtain induced flow, but no one had exercised them in the context of obtaining dynamic-inflow derivatives.

Although Reference 23 came a long way toward the desired answer, the analysis became so involved that no definitive results could be obtained. The problem is illustrated by Figure 18. The dynamic inflow theory is just one part of an overall rotor analysis. However, if one tries to identify the inflow law in the presence of blade dynamics and airfoil theories, the problem becomes too complicated for a fundamental solution. What is needed is a look at the open-loop transfer function of dynamic inflow without the complications of blade theory.

The ideal theory for attempting such a derivation is the actuator-disc theory of Mangler and Squire, as applied by Joglekar and Loewy in Reference 25. This theory is based on the Kinner closed-form pressure potentials for an actuator disc. Figure 19 gives a schematic of such a disc in an ellipsoidal coordinate system (ν,η,ψ). The free-stream enters at an angle α, and positive lift is taken in the negative Z direction. Kinner was able to obtain a closed-form potential function to describe an arbitrary pressure discontinuity across the disc. This function is expressed in terms of Legendre functions and can be used to find the induced-flow field for any given loading. Although the theory is successfully applied (in Reference 25) to give a specific inflow distribution, it is not used to find the dynamic inflow matrices.

In Reference 27, Dale Pitt extends the Kinner theory to include unsteady effects and uses it to find the elements of [L] and [M]. Two different radial lift distributions are used to verify that the matrices are not sensitive to the details of blade loading. Table 2 provides the final forms of the matrices as suggested in Reference 26, where [L] takes the form

$$[L] = \frac{1}{v} [\mathcal{L}] \qquad (20)$$

The $[\mathcal{L}]$ matrix is symmetric with elements that depend only upon the angle of incidence, α. The entire matrix is divided by the free-stream velocity, v. For forward flight with lift, v becomes the mass flow parameter of equation (12) and α becomes the local angle, α^*, equation (10c). In axial flow ($\alpha = \alpha^* = 90°$), the [L] matrix reduces to that of momentum theory, a very satisfying result of the theory. Similarly, the M-matrix also agrees with momentum theory for the roll and pitch inertias, although the apparent mass for thrust is different than that of momentum theory when the loading is zero at the rotor center.

In Reference 27, the formulation of Table 2 has been verified by two independent means. First, for the quasi-steady terms, the [L] matrix has been checked against a free-vortex wake analysis written by Landgrebe. The prescribed wake model of Landgrebe is exercised in numerical experiments in which changes in cyclic and collective pitch create changes in induced flow patterns, and these are interpreted in terms of the wake coupling matrix, L. Figure 20 presents the first column of L, inflow due to thrust. The horizontal line is the theoretical value of $L_{11} = 1/2$ that relates thrust to uniform inflow; it is completely independent of lift distribution. The open triangles are results from the wake program and agree within 10%. The long dashed and dash-dot lines provide the L_{31} term, which is zero in hover ($\alpha = 90°$) and maximum at $\alpha = 0°$. Two different loading distributions are used, labelled "corrected" and "uncorrected." The results from Landgrebe's program are given by squares. (Solid squares indicate convergence problems.) The corrected curve, which enforces zero lift at the center, is very close to the Landgrebe results, and is the formulation used in Table 2. The two solid squares are suspect because no data has ever shown the fore-to-aft gradient decreasing as incidence goes to zero. The L_{21} term is zero for both the theory and the Landgrebe model.

Figure 21 provides a comparison of the second column of L, induced flow due to roll moment. In theory, the only term should be L_{22}, given by the two curves and the triangles. One can see that there is little difference in L_{22} for the two possible lift distributions. Furthermore, the prescribed-wake results agree to within a few percent for $\alpha > 30°$. Therefore, the simpler uncorrected curve is used in Table 2. L_{32} on the other hand (fore-to-aft inflow due to roll moment, shown by squares) is theoretically zero but exhibits a non-zero value from the prescribed wake. The explanation of this is the wake rotation (which is not included in the actuator-disc theory). Fortunately, the effect is not large. L_{12} is zero for both theory and numerical experiment.

When we look at the third column of L, Figure 22, we again see the wake rotation effect $L_{23} = -L_{32} = .2$, ideally zero from actuator-disc theory. The L_{33} term, shown as diamonds, displays an excellent correlation between actuator-disc and vortex models, as does the L_{13} term, shown in triangles. Again, the corrected versus uncorrected pressure distributions do not show an appreciable effect on L, and uncorrected is used in Table 2.

Reference 27 also provides a verification of the unsteady part of dynamic inflow, the M-matrix. In particular, an exact solution of the unsteady, potential flow equations is compared to the simpler approach of a direct superposition of $[L]^{-1}\{v\}$ and $[M]\{\dot{v}\}$ terms. The result is given in Figure 23 for $L_{22} = L_{33}$ ($\alpha = 90°$) as a function of reduced frequency, $k = \omega/v$. For both magnitude and phase, the simple model of equation (19) gives excellent agreement with a more rigorous, Theodersen-type, unsteady theory.

It should also be mentioned here that References 26 and 27 discuss the possibility of using additional radial and azimuthal degrees of freedom in the inflow model, and an expanded 5 x 5 model is explicitly given. In Reference 28, this 5 x 5 model is compared to the 3 x 3 model with respect to its effect on inplane damping. The results show two

things. First of all, the 5 x 5 model gives extraneous answers for rotors with less than 5 blades (as a result of a mathematical indeterminancy). Second, for rotors with 5 or more blades (or for constant-coefficient analyses), the 5 x 5 results are essentially the same as the 3 x 3 results. Therefore, Reference 28 concludes that the 3 x 3 model is adequate and is probably the most sophisticated model that is possible for dynamic inflow in matrix formulation.

With dynamic inflow verified by both experimental and computational data, it is presently ready to be used in dynamics analyses. The theory as it now stands is a perturbation theory and thus applicable to linearized analysis packages. It is easily extended, however, to a nonlinear version for use in time history solutions. Table 3 shows the nonlinear version of L. Here, v_o represents the total uniform induced flow (steady plus perturbation). You may recall that the linear version of L is divided by v, the mass-flow parameter, equation (20). In the nonlinear version, the first column of L is divided instead by the total mass flow V_T. The mass flow parameter v is simply related to V_T through a derivative as shown. Consequently, the nonlinear L-matrix has perturbation equations identical to those of the linearized dynamic-inflow theory.

Summary

The following statements summarize our present understanding of the importance of inflow to rotor and rotor-body damping.

1. Steady inflow (mostly uniform) is important for inplane damping in that it changes the axis of minimum damping.

2. The largest effect of advance ratio on inplane damping is the associate change in inflow.

3. Dynamic inflow is an important effect on rotor damping, and its importance has been physically verified many times.

4. The effect of dynamic inflow is largest for the low-frequency, regressing rotor-body modes.

5. Presently, the best dynamic-inflow theory is a 3 x 3 closed-form model based on actuator-disc theory. It's accuracy has been verified by comparisons with more sophisticated models.

References

1. Peters, David A., "An Approximate Closed-Form Solution for Lead-Lag Damping of Rotor Blades in Hover," NASA TM X-62,425, April 1975.

2. Peters, David A., "Flap-Lag Stability of Helicopter Rotor Blades in Forward Flight, "Journal of the American Helicopter Society, Vol. 20, No. 4, October 1975, pp. 2-13.

3. Wei, F-S and Peters, D. A., "Lag Damping in Autorotation by a Perturbation Method," Proceedings of the 34th Annual National Forum of the American Helicopter Society, Washington, D.C., May 1978, Paper 78-25.

4. Amer, K. B., "Theory of Helicopter Damping in Pitch or Roll and a Comparison with Flight Measurements," NACA TN-2136, October 1950.

5. Sissingh, G. J., "The Effect of Induced Velocity Variation on Helicopter Rotor Damping in Pitch or Roll," Aeronautical Research Council Paper No. 101, Technical Note No. Aero 2132, November 1952.

6. Carpenter, P. J. and Fridovitch, B., "Effect of Rapid Blade Pitch Increase on the Thrust and Induced Velocity Response of a Full Scale Helicopter Rotor," NACA TN-3044, November 1953.

7. Tuckerman, L. B., "Inertia Factors of Ellipsoids for Use in Airship Design," NACA Report No. 210, 1925.

8. Shupe, N. K., A Study of the Dynamic Motions of Hingeless Rotored Helicopters, Ph.D. Thesis, Princeton, September 1970.

9. Curtiss, H. C., Jr. and Shupe, N. K., "A Stability and Control Theory for Hingeless Rotors," Proceedings of the 27th Annual National Forum of the American Helicopter Society, May 1971, Paper No. 541.

10. Ormiston, Robert A. and Peters, David A., "Hingeless Rotor Response with Nonuniform Inflow and Elastic Blade Bending," Journal of Aircraft, Vol. 9, No. 10, October 1972, pp 730-736.

11. Peters, David A., "Hingeless Rotor Frequency Response with Unsteady Inflow," Rotorcraft Dynamics, NASA SP-352, February 1974I pp 1-13.

12. Kuczynski, W. A. and Sissingh, G. J., "Characteristics of Hingeless Rotors with Hub Moment Feedback Controls Including Experimental Rotor Frequency Response," NASA CR 114427, January 1972.

13. Crews, S. T., Hohenemser, K. H., and Ormiston, R. A., "An Unsteady Wake Model for a Hingeless Rotor," Journal of Aircraft, Vol. 10, No. 12, December 1973, pp 758-760.

14. Ormiston, Robert A., "Application of Simplified Inflow Models to Rotorcraft Dynamic Analysis," Journal of the American Helicopter Society, Vol. 21, No. 3, July 1976, pp 34-39.

15. Peters, David A. and Gaonkar, Gopal H., "Theoretical Flap-Lag Damping with Various Dynamic Inflow Models," Journal of the American Helicopter Society, Vol. 25, No. 3, July 1980, pp 29-36.

16. Gaonkar, G. H., Mitra, A. K., Reddy, T.S.R., and Peters, D. A., "Sensitivity of Helicopter Aeromechanical Stability to Dynamic Inflow," Vertica, Vol. 6, No. 1, January 1982, pp 59-75.

17. Johnson, Wayne, "Influence of Unsteady Aerodynamics on Hingeless Rotor Ground Resonance," Journal of Aircraft, Vol. 19, No. 8, August 1982, pp 668-673.

18. Azuma, Akira and Nakamura, Yoshiya, "Pitch Damping of Helicopter Rotor with Nonuniform Inflow," Journal of Aircraft, Vol. 11, No. 10, October 1974, pp 639-646.

19. Peters, D. A. and Chen, S. K., "Momentum Theory, Dynamic Inflow, and the Vortex Ring State," Journal of the American Helicopter Society, Vol. 27, No. 3, July 1982, pp 18-24.

20. Johnson, Wayne, Helicopter Theory, Princeton University Press, 1980, pp 520-526.

21. Loewy, R. G., "A Two-Dimensional Approximation to the Unsteady Aerodynamics of Rotary Wings," Journal of Aeronautical Sciences, Vol. 24, 1957.

22. Gaonkar, Mitra, and Reddy, "Feasibility of a Rotor Flight Dynamics Model with First-Order Cyclic Inflow and Multi-Blade Modes," proceedings of the AIAA Dynamics Specialists' Meeting, Atlanta, Georgia, April 9-10, 1981, p 15.

23. Landgrebe, A. J., "An Analytical Method for Predicting Rotor Wake Geometry," Journal of the American Helicopter Society, Vol. 14, No. 4, October 1969.

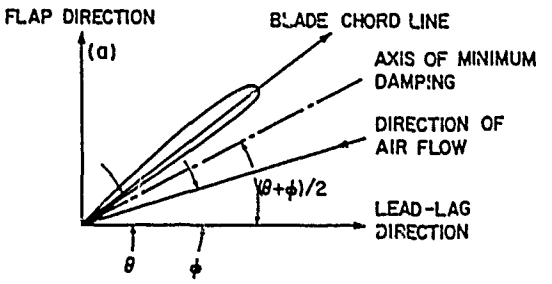
24. Ormiston, Robert A., "An Actuator Disc Theory for Rotor Wake Induced Velocities," AGARD Specialists Meeting on the Aerodynamics of Rotary Wings, Marseille, France, September 13-15, 1972.

25. Joglekar, M. and Loewy, R., "An Actuator-Disc Analysis of Helicopter Wake Geometry and the Corresponding Blade Response," USAAVLABLS Technical Report 09-66, 1970.

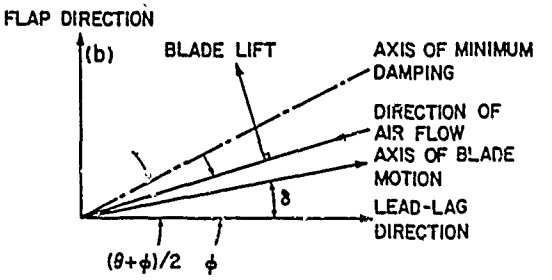
26. Pitt, Dale M. and Peters, David A., "Theoretical Predictions of Dynamic Inflow Derivatives," Vertica, Vol 5, No. 1, March 1981.

27. Pitt, Dale M. and Peters, David A., "Rotor Dynamic-Inflow Derivatives and Time Constants from Various Inflow Models, "9th European Rotorcraft Conference, Stresa, Italy, September 13-15, 1983, Paper No. 55.

28. Gaonkar, et. al., "The Use of Actuator-Disc Dynamic Inflow for Helicopter Flap-Lag Stability," Journal of the American Helicopter Society, Vol. 28, No. 3, July 1983, pp 79-88.



(a) Motion geometry.



(b) Force geometry.

Figure 1. The Axis of Minimum Damping.

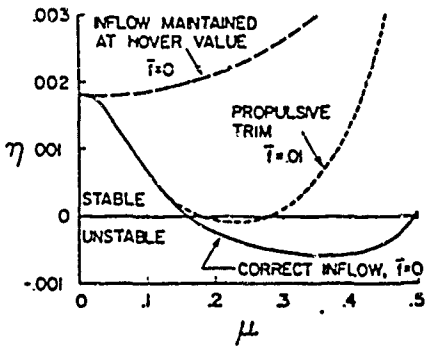


Figure 2. Effect of Inflow on Inplane Damping, p=1.15, ω_ζ=1.4, R_e=0, γ=5, σ =.05, C_{d_o}=0.., C_T/σ =0.2, trimmed.

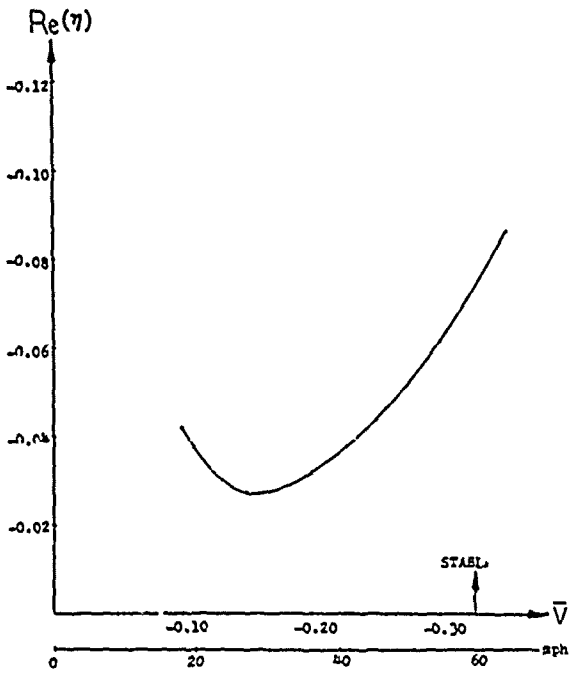


Figure 3. Wind Turbine Inplane Damping Versus Wind Speed, $\gamma'=12.3$, $p=2.76$, $\omega_f=3.62$, $C_{d_o}=.01$, $C_Q/\sigma=.007$, $\sigma=.0255$, $R_e=1.0$, $\mu=0.0$.

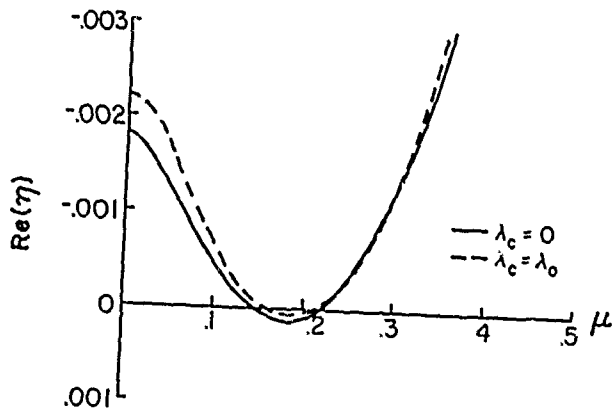


Figure 5. Effect of Fore-to-Aft Inflow Gradients on Inplane Damping, $p=1.15$, $\omega_f=1.4$, $R_e=0$, $\gamma'=5$, $\sigma=.05$, $C_{d_o}=.01$, $\epsilon_o=0.3$, $\epsilon_s=\epsilon_c=0$.

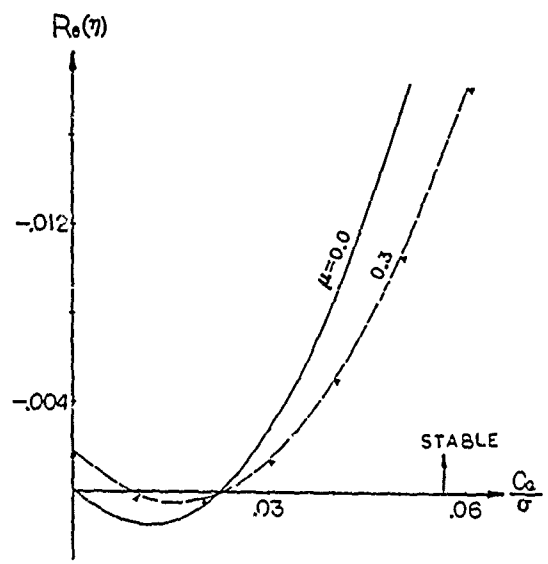


Figure 4. Wind Turbine Inplane Damping Versus Power Coefficients, $C_T=.01$, $\omega_f=0.7$, $R_e=0.0$, $\sigma=.05$, $p=1.15$, $\gamma'=5.0$, $C_{d_o}=.01$.

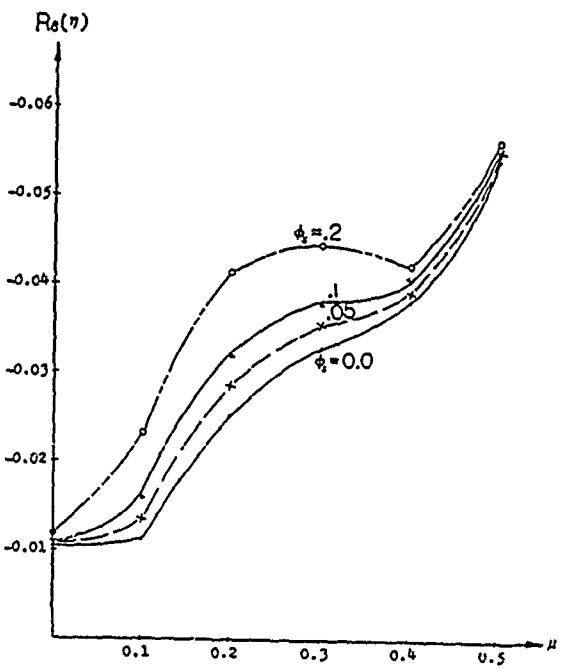


Figure 6. Effect of Lateral Gradients on Inplane Damping of Wind Turbine, $C_T=.01$, $C_Q/\sigma=.06$, $\sigma=.05$, $p=1.15$, $\omega_f=1.4$, $C_{d_o}=.01$, $\gamma'=5.0$.

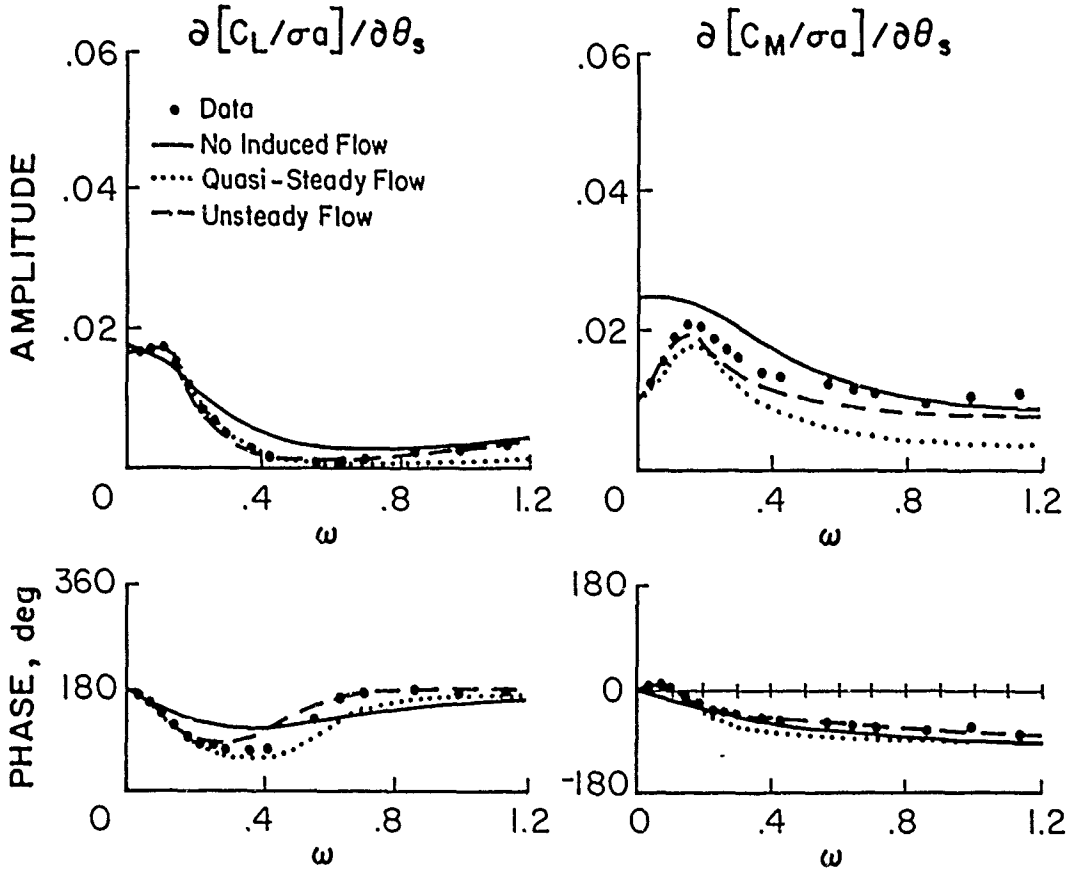


Figure 7. Rotor Response to Cyclic Pitch in Hover, p=1.15, γ=4.25, B=.97, e_{pc}=.25, μ=0, σa=.7294, $\bar{\nu}=\bar{\lambda}$=.03, θ_0=4°, momentum theory, single rotating mode.

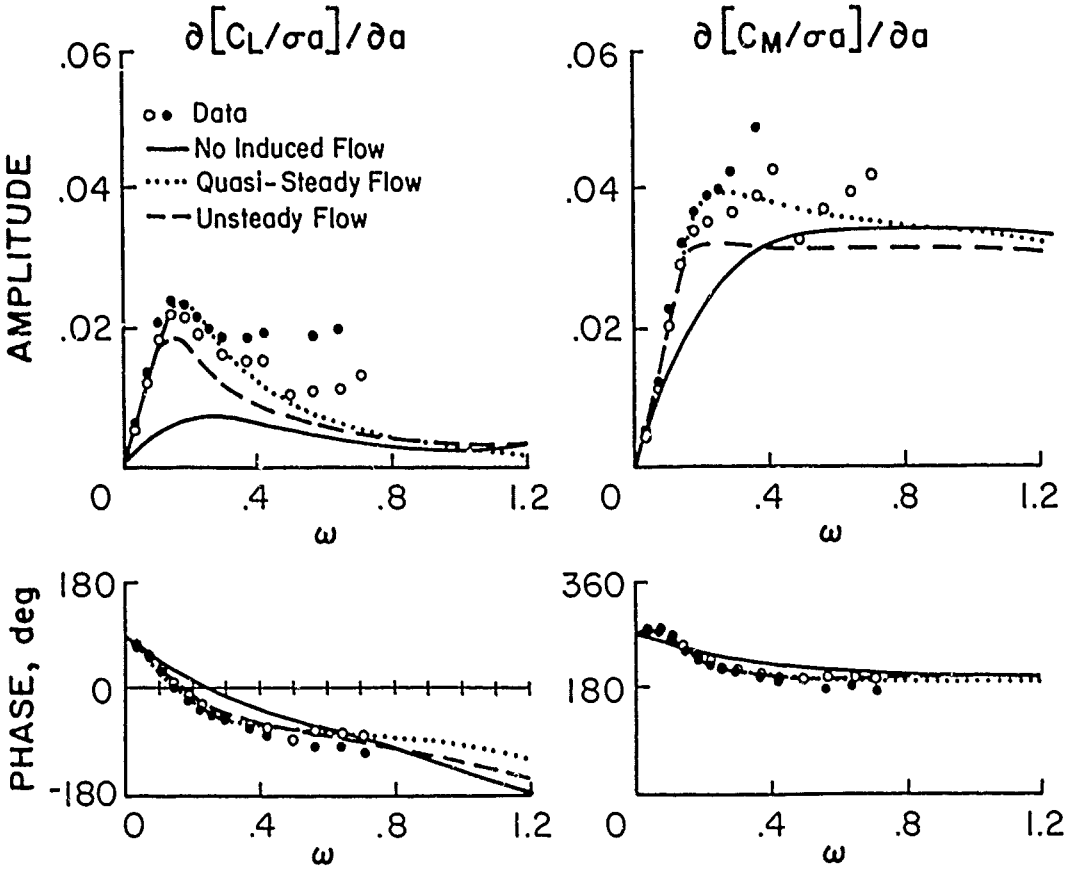


Figure 8. Rotor Response to Hub Motions in Hover, p=1.15, γ^{*}=4.25, B=.97, e_{pc}=.25, μ=0, σa=.7294, $\bar{\nu}=\bar{\lambda}$=.03, θ_o=4°, momentum theory, single rotating mode.

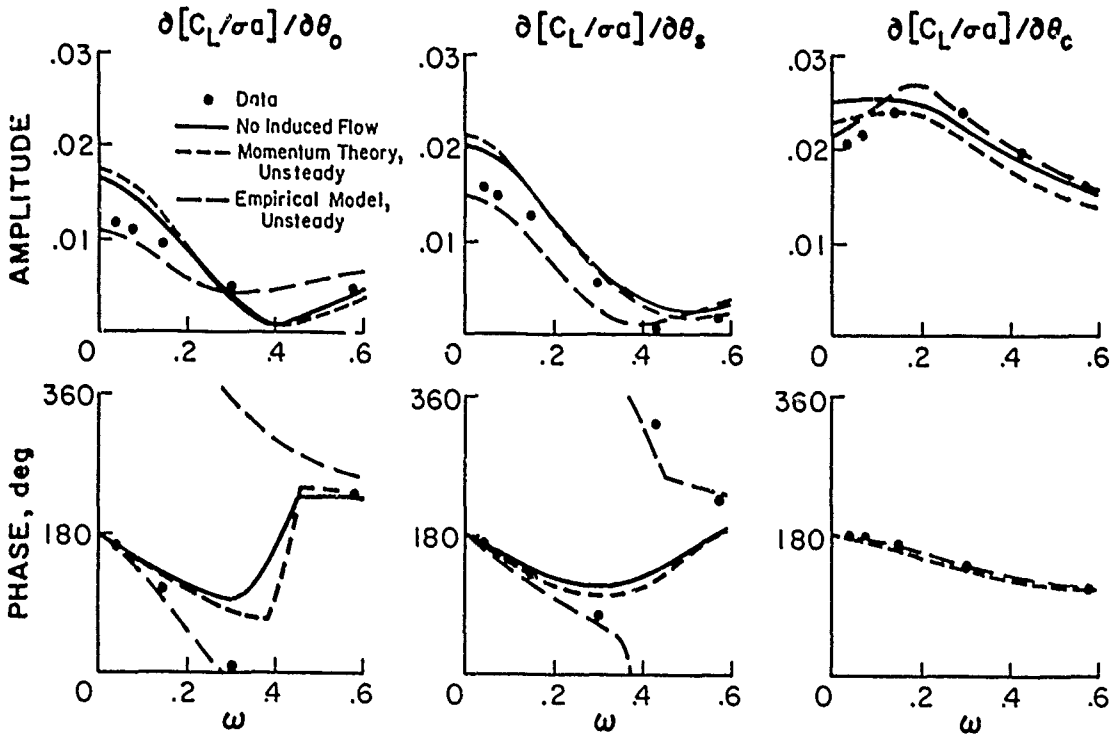


Figure 9. Rotor Response to Cyclic Pitch in Forward Flight, p=1.15, γ=4.25, B=.97, e_{pc}=.25, μ=.51, σa=.7294, $\bar{\nu}=\bar{\lambda}=0$, θ_0=1/2", single rotating mode.

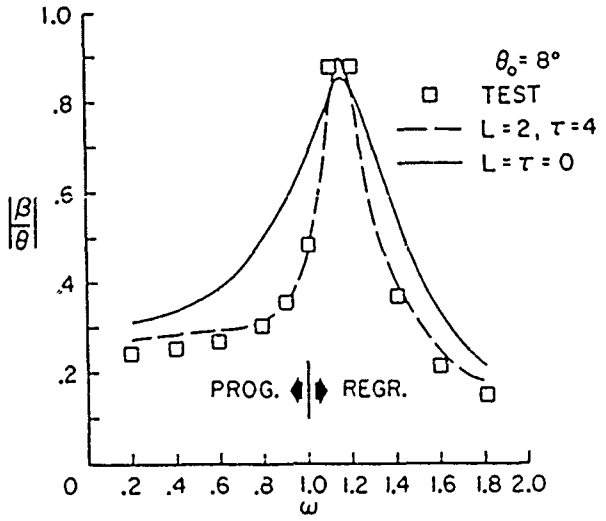


Figure 10. Rotor Response to Pitch Stirring, p=1.21, γ=4.0, ν=0, B=.97.

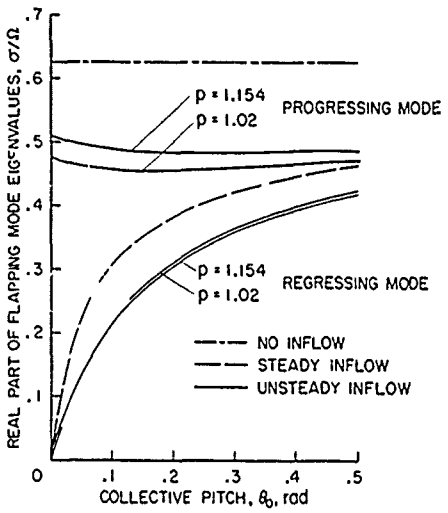


Figure 11. The Effect of Different Induced Flow Models on Flap Mode Damping, γ=10, σ=.15.

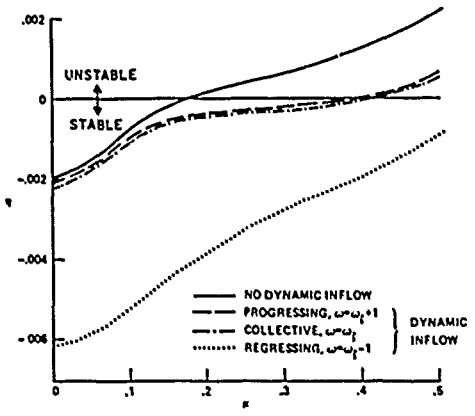


Figure 12. Effect of Dynamic Inflow on Lead-Lag Mode, ω_ζ=1.4, p=1.15, γ=5, C_T=0.1, σ=.05, C_{d_0}=.01.

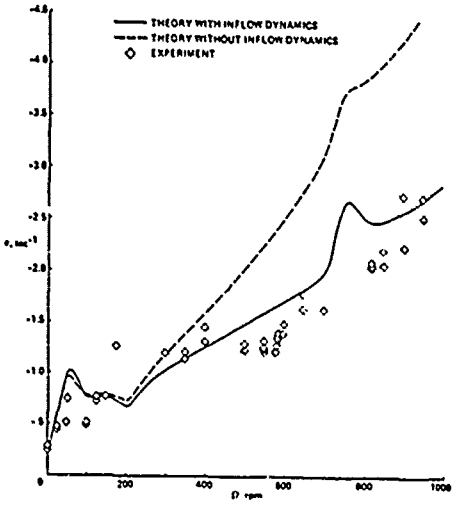


Figure 15.

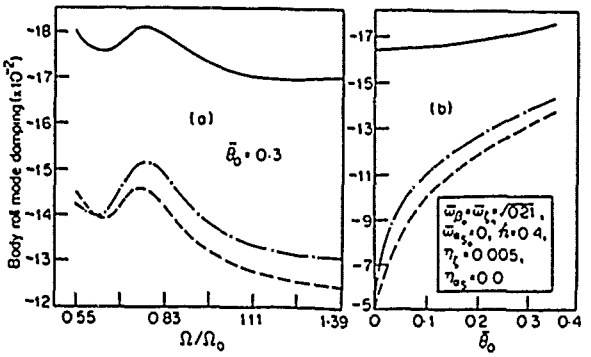


Figure 13.

Body Role Mode Damping of a Matched-Stiffness Rotor with: No Dynamic Inflow (—), Quasi-steady Inflow (—·—), and Unsteady Inflow (- - -); μ=.1, γ=5, σ=.05, p=1.1.

Body Roll Mode Damping as a Function of Rotor Speed, σ=.05, γ=8.4, Hover.

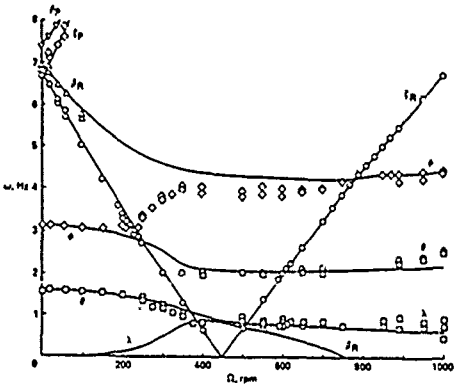


Figure 16.

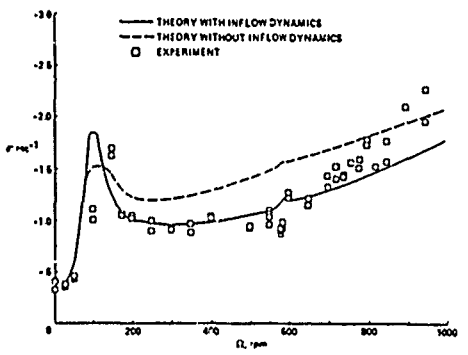


Figure 14.

Modal Frequencies as a Function of Rotor Speed: Comparison, Theory (—) and Data (○, ◇, □), σ=.05, γ=8.4, Hover.

Body Pitch Mode Damping as a Function of Rotor Speed, σ=.05, γ=8.4, Hover.

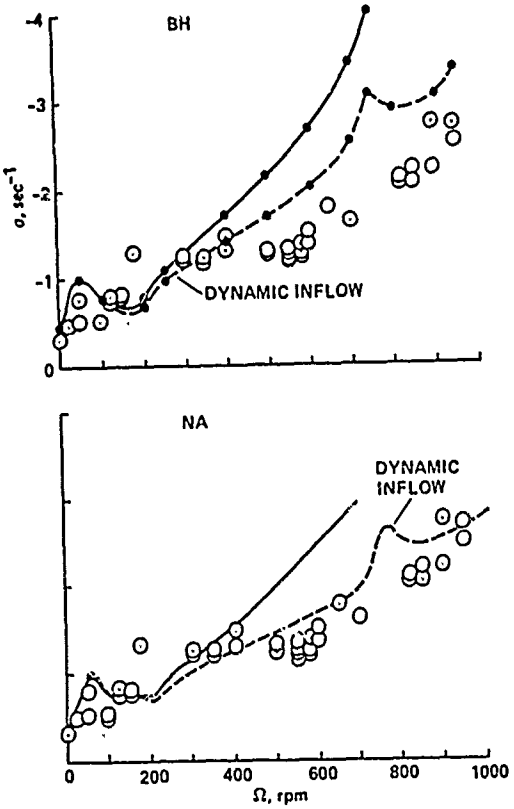


Figure 17. Comparison of Roll Mode Damping, Bell and NASA Ames Models.

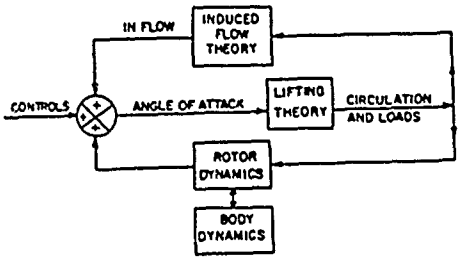
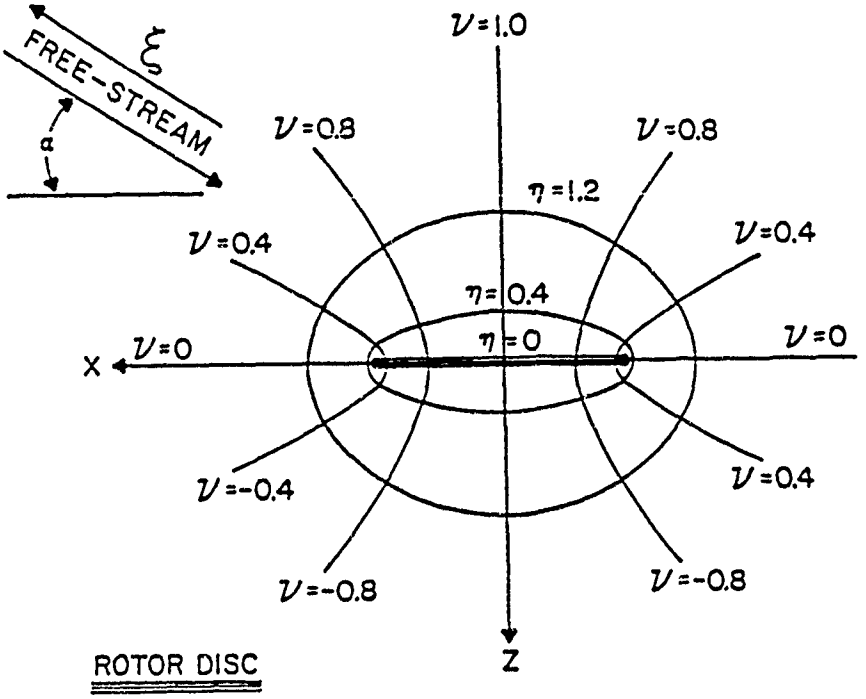


Figure 18. Block Diagram of Inflow Dynamics.

Figure 19.

Ellipsoidal Coordinates.



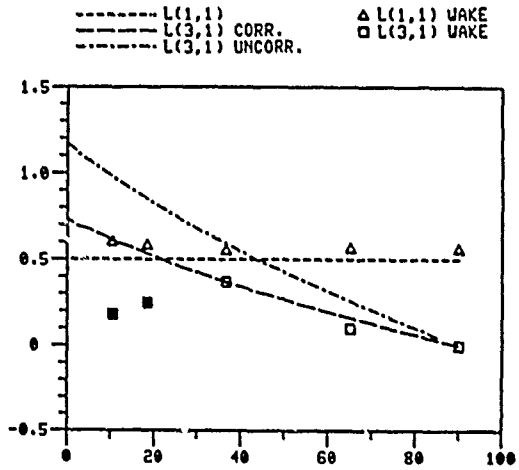


Figure 20. Verification of First Column of L.

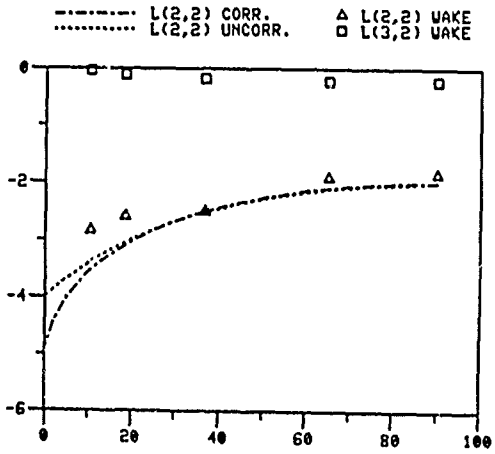


Figure 21. Verification of Second Column of L.

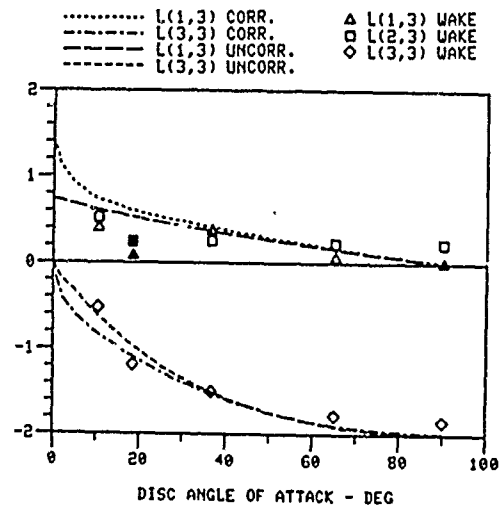


Figure 22. Verification of Third Column of L.

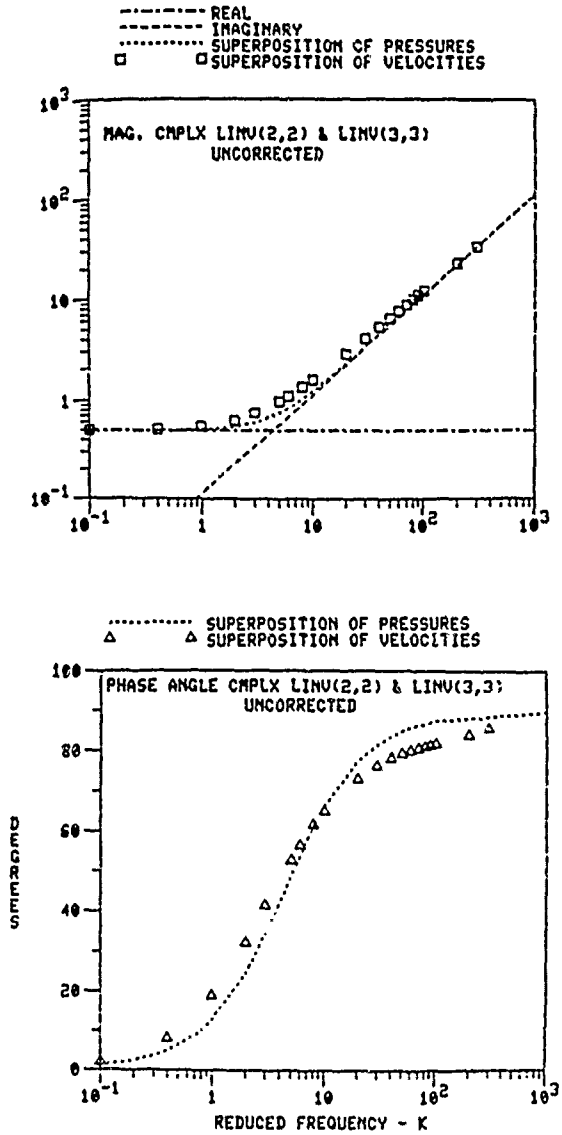


Figure 23.

Comparison of Unsteady Pressure Distribution with Superposition of Apparent Mass Terms.

Table 1. Comparison of Mass Flow Parameters

Condition	$v^* + \bar{v} \sin\alpha^*$ Ref. 11	$v + \bar{v} \sin\alpha$ Ref. 8	$v^* + \lambda + \bar{v}$ Ref. 20, C_T	v^* Ref. 20, C_L and C_M
Hover, $\mu = \lambda = 0$	$2\bar{v}$	$2\bar{v}$	$2\bar{v}$	$\bar{v}$
Zero lift, climb $\bar{v} = 0$, $\mu = 0$	λ	λ	2λ	λ
Climb, $\mu = v$	$\lambda + 2\bar{v}$	$\lambda + 2\bar{v}$	$2\lambda + 2\bar{v}$	$\lambda + \bar{v}$
Zero lift, edgewise $\bar{v} = 0$, $\lambda = 0$	μ	μ	μ	μ
Lifting, edgewise $\lambda = 0$	$\dfrac{\mu^2 + 2\bar{v}^2}{\sqrt{\mu^2 + \bar{v}^2}}$	μ	$\sqrt{\mu^2 + \bar{v}^2} + \bar{v}$	$\sqrt{\mu^2 + \bar{v}^2}$
Zero lift $\bar{v} = 0$	$\sqrt{\mu^2 + \lambda^2}$	$\sqrt{\mu^2 + \lambda^2}$	$\sqrt{\mu^2 + \lambda^2} + \lambda$	$\sqrt{\mu^2 + \lambda^2}$
No normal flow, $\lambda = -\bar{v}$ (descent)	μ	$\dfrac{\mu^2 - \lambda^2}{\sqrt{\mu^2 + \lambda^2}}$	μ	μ

$$[L] = \frac{1}{v}\begin{bmatrix} \frac{1}{2} & 0 & \frac{15\pi}{64}\sqrt{\frac{1-\sin\alpha}{1+\sin\alpha}} \\ 0 & \frac{-4}{1+\sin\alpha} & 0 \\ \frac{15\pi}{64}\sqrt{\frac{1-\sin\alpha}{1+\sin\alpha}} & 0 & \frac{-4\sin\alpha}{1+\sin\alpha} \end{bmatrix}$$

$$[M] = \begin{bmatrix} \frac{128}{75\pi} & 0 & 0 \\ 0 & \frac{-16}{45\pi} & 0 \\ 0 & 0 & \frac{-16}{45\pi} \end{bmatrix}$$

Table 2. Analytic Forms of L-matrix and M-matrix

$$[L] = [\mathcal{L}]\begin{bmatrix} 1/V_T & 0 & 0 \\ 0 & 1/V & 0 \\ 0 & 0 & 1/V \end{bmatrix}$$

$$V_T = \sqrt{(\lambda+v_0)^2+\mu^2} \qquad V = \frac{d}{dv_0}(v_0 V_T)$$

$$V = \left[(\lambda+v_0)(\lambda+2v_0)+\mu^2\right]/V_T$$

Table 3. Nonlinear Version of Dynamic Inflow Theory

DISCUSSION

THE IMPORTANCE OF STEADY AND DYNAMIC INFLOW ON THE STABILITY OF ROTOR-BODY SYSTEMS

David A. Peters

Presented by Donald L. Kunz

Kunz: I'll entertain questions, but I reserve the right to refer them to Wayne [Johnson] or Bob [Ormiston] if he's in the audience. Yes, Wayne, you've got me.

Wayne Johnson, Session Chairman: Bob can handle this one. I'll start out with more of a comment, I guess. I think it's pretty clear from your summary that dynamic inflow for helicopters has, for the last decade, essentially been the work of dynamicists, and so one wonders what the theory might have looked like if, in fact, the aerodynamicists had been the ones giving the attention to it for a while. I think that at the very least we'd find more formulation in terms of a lift-deficiency function, which I personally prefer because it does help you make the connection between these models and other unsteady aerodynamic models. If there's a question here, it's just to find out whether anybody disagrees. It's my feeling that this has to be done eventually, that we do need to get a little bit more fundamental aerodynamics into it. The main reason is that, as useful as it is, it is an approximate model and we can't really expect to push an actuator disk model too far. So at some point you're going to have to get closer to more classical aerodynamic approaches.

Kunz: I don't see Bob here, but I would agree with you that this is an approximate approach and I think that the way that I would like to see aerodynamics go is in the direction of a lift deficiency function.

Actually I have a question for Bill Bousman about the correlation that Wayne did with your data, the slide that Dave had here [Fig. 16] that showed the dynamic inflow mode. From your experimental data were you able to determine that that's what that mode was? Did it look like something else? Was it a mystery?

Bill Bousman, Aeromechanics Laboratory: The answer is, it was a mystery at the time and perhaps still is. We measured the various modes that we label on the graph as pitch, roll, and lead-lag regressing. When we did the experiment, we were making measurements in the various physical coordinates and so when we took a moving-block damping measurement at the same time we would also get the amplitude and phase of that frequency in all of the coordinates. We could then plot phase vectors to try to identify the modes. What we found was that that mode that in the slide was labeled as the body pitch mode and the mode that was labeled as an inflow mode both had substantial body pitch motion, substantial body roll motion, and limited rotor motion in them. Although we could usually characterize the differences between a roll and a pitch mode by the proportional amounts of roll and pitch motion and their

phasing, for the mystery mode or inflow mode it was very similar to the body pitch mode, but very distinct. I think the most convincing evidence that it is indeed an inflow mode is in Wayne's TM [81302]; after showing the plot we've seen here, he presents a calculation of what the pitch-mode coordinate fast Fourier transform (FFT) would look like. That calculation looks essentially identical to the pitch-mode we measured. So exactly how you name the mode I'm not sure, but the resemblance between theory and experiment is quite substantial.

Johnson: I think I'd like to echo that a little bit. I think we shouldn't get too hung up on the labels that you put on eigenvalues. When they're very highly coupled that can be subjective at best. The point is that the theory predicts that this is a mode that has a lot of pitch motion and so it predicts the measurability of that mode as well as the existence of it, and perhaps we should leave it at that.

Euan Hooper, Boeing Vertol: What about the damping of that mode, do you have any measure of the damping of it?

Johnson: Yes, the damping was measured for both those modes, and again there are essentially two modes that show up in the pitch measurement and again you can label them however you like, but you have two frequencies and two damping values. If you don't have the unsteady aerodynamics in the model, you simply can't predict two, you're stuck.

Hooper: What does the damping come out to be, of that mode?

Johnson: It's about the same in both modes. I'd have to look at the details.

Hooper: It's not a heavily damped mode, is it?

Johnson: Well, he showed the pitch mode. Well, actually that's for the other case, but the ITR case is the same. No, it's not a heavily damped mode, that's the point. Otherwise it wouldn't be measurable. There is a third mode that I tend to label the regressing flap mode that is heavily damped, and you just never can measure that one whatever the circumstances.

EFFECTS OF STATIC EQUILIBRIUM AND HIGHER-ORDER NONLINEARITIES ON ROTOR BLADE STABILITY IN HOVER

Marcelo R.M. Crespo da Silva*
and
Dewey H. Hodges**

Aeromechanics Laboratory
U.S. Army Research and Technology Laboratories (AVRADCOM)
Ames Research Center
Moffett Field, California

Abstract

The equilibrium and stability of the coupled elastic lead/lag, flap, and torsion motion of a cantilever rotor blade in hover are addressed, and the influence of several higher-order terms in the equations of motion of the blade is determined for a range of values of collective pitch. The blade is assumed to be untwisted and to have uniform properties along its span. In addition, chordwise offsets between its elastic, tension, mass, and aerodynamic centers are assumed to be negligible for simplicity. The aerodynamic forces acting on the blade are modeled using a quasi-steady, strip-theory approximation.

1. Introduction

An important problem in helicopter dynamics is the determination of the dynamic response and aeroelastic stability associated with the rotor blades. Considerable attention has been directed to rotary-wing aeroelasticity problems, and it is now widely recognized that such problems are inherently nonlinear. Hodges and Dowell[1] developed a comprehensive set of differential equations of motion, with quadratic nonlinearities, describing the flap-lead/lag-torsional dynamics of slender, rotating extensional rotor blades undergoing moderately large elastic deformations. An ordering scheme based on a small parameter ϵ was introduced in Ref. 1 to systematically neglect higher-order terms in the equations. Some important linear terms of order ϵ^3 were kept in the equations such as aerodynamic damping terms in the lead/lag and torsional differential equations and inertia terms in the torsional differential equation. Nonlinear terms of $O(\epsilon^3)$ were systematically neglected. The equations of motion developed in Ref. 1 were used in Ref. 2 to investigate the stability of the elastic motion of a uniform cantilever rotor blade in the hover flight condition.

A set of $O(\epsilon^3)$ nonlinear differential equations describing the flexural-flexural-torsional motion of inextensional beams undergoing moderately large deformations was derived by Crespo da Silva and Glynn and used by the same authors to analyze the response of the system[3] They have considered nonrotating beams, and determined the effect of these nonlinearities on the response of the system for the cases in which the torsional frequencies of the beam are much larger than its bending frequencies. For such cases, the nonlinearities present in the differential equations of motion are $O(\epsilon^3)$ rather than $O(\epsilon^2)$.

The question that immediately arises for the rotating rotor-blade problem is whether cubic nonlinearities can also play a significant role in the equilibrium and stability of the elastic motion of the blade. To address this question, the differential equations, and their boundary conditions, describing the flap-lead/lag-torsional elastic motion of a rotor blade were derived in Ref. 4 with the objective of retaining in the equations all the nonlinear terms up to $O(\epsilon^3)$ in a small parameter ϵ. The equations developed in Ref. 4 extend those developed in Ref. 1 to include not only all linear $O(\epsilon^3)$ terms but all nonlinear terms to this same order.

In this paper, the $O(\epsilon^3)$ differential equations developed in Ref. 4 are used to investigate the influence of these higher-order terms in the elastic response and stability of a rotor blade in the hover flight condition. First, a brief review of the derivation of the equations is given. A small arbitrary ordering-parameter ϵ is then introduced and the equations are simplified by expanding their nonlinearities into a power series in ϵ. The resulting equations are more amenable to analysis, and Galerkin's method is applied to them. After the equilibrium solution to the equations is determined, the blade's elastic deflections are then perturbed about their equilibrium to yield a set of variational equations that are linearized and used to determine the eigenvalues associated with the perturbed motion. The influence of a number of $O(\epsilon^3)$ terms on the blade's response is determined for a range of values of collective pitch.

2. Equations of Motion

2.1 Basic Assumptions and Outline of Derivation

Consider an initially straight rotor blade of closed cross section. Its maximum cross-sectional dimension is assumed to be much smaller than its undeformed length R, so that it may be approximated as a beam. A blade segment, both in its undeformed and deformed states, is shown in Fig. 1. The (η, ς, ξ) axes shown in the figure, with unit vectors indicated by a *hat* as $\hat{()}$, are the principal axes of the cross section at the shear center C_e of the deformed blade cross section. It is assumed that the cross section is symmetric about the η-axis. The ξ-axis is tangent at all times to the elastic axis of the blade. When the blade is undeformed, the

* Professor, Aerospace Engineering and Applied Mechanics Dept., University of Cincinnati, Cincinnati, Ohio (on academic leave).

** Research Scientist

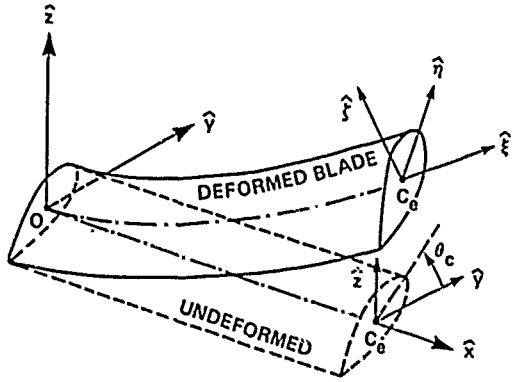


Fig. 1 Undeformed and deformed blade segment with coordinate systems and unit vectors.

principal (η, ς) axes make an angle θ_c–the collective pitch angle–with the y-axis. The (x, y, z) axes, with unit vectors also indicated by a *hat*, are a set of rotating reference axes as shown in Fig. 2. The x-axis is coincident with the elastic axis of the blade when it is undeformed. These axes are assumed to rotate in space with constant angular velocity Ω about the vertical, which is taken to be perpendicular to the rotor hub. The (X, Y, Z) axes shown in Fig. 2 are a set of inertial axes. The absolute orientation of (x, y, z) may be described by first aligning (x, y, z) with (X, Y, Z) and then performing two successive rotations. The first rotation $\tau = \Omega t$, where t denotes dimensional time, about Z brings the (x, y, z) triad to its new orientation $(X_1, Y_1, Z_1 = Z)$; a second rotation β—the blade's pre-cone angle—about the negative Y_1 direction brings (X_1, Y_1, Z_1) to its "final" orientation (x, y, z). For simplicity, the blade-root offset e_1 shown in Fig. 2 is assumed to be zero.

Because of the elastic deformations, point C_e in Fig. 1 moves from location $(Rx,\ y{=}0,\ z{=}0)$ to $[Rx + Ru(x,\tau), Rv(x,\tau), Rw(x,\tau)]$ relative to the (x, y, z) rotating axes shown in Figs. 1 and 2. Here, (u, v, w) are the components of the elastic displacement vector for C_e, normalized by R. They are functions of the nondimensional variable x–the distance along the x-direction, normalized by R–and of the nondimensional time τ. The orientation of the cross-sectional principal axes (η, ς, ξ) centered at C_e may be described by a sequence of three-axes Euler angles $(\theta_x = \arctan v'/(1+u'),\ \theta_y = \arcsin w'\partial x/\partial r, \theta_z)$, as described in Refs. 1–4. Here, primes are used to denote partial differentiation with respect to x, and

$$\frac{\partial x}{\partial r} = \left[(1+u')^2 + v'^2 + w'^2\right]^{-\frac{1}{2}} \tag{2.1}$$

The elastic angle of twist of the blade, $\phi(x,\tau)$, is obtained by integrating the torsion of the blade and is related to the Euler angle $\theta_x(x,\tau)$ as[1-4]

$$\phi = \theta_x + \int_0^x \theta_y' \sin\theta_y \, dx \tag{2.2}$$

To obtain the differential equations of motion, and their boundary conditions, use is made of Hamilton's extended principle[5]. These equations were developed in Ref. 4 in terms of the elastic deformations $u(x,\tau)$, $v(x,\tau)$, and $w(x,\tau)$,and of the angle $\theta_x(x,\tau)$. If the blade's mass centroid offset from its elastic axis is neglected, for simplicity, the equations associated with the virtual displacements δu, δv, and δw are of the form

$$G_u'(x,\tau) = \ddot{u} - 2\,\dot{v}\cos\beta + w(\sin 2\beta)/2 - (x+u)\cos^2\beta - Q_u \tag{2.3}$$

$$G_v'(x,\tau) = \ddot{v} + 2\,\dot{u}\cos\beta - 2\,\dot{w}\sin\beta - v - Q_v \tag{2.4}$$

$$G_w'(x,\tau) = \ddot{w} + 2\,\dot{v}\sin\beta + (x+u)(\sin 2\beta)/2 - w\sin^2\beta - Q_w \tag{2.5}$$

with the cantilever boundary conditions

$$u(0,\tau) = v(0,\tau) = w(0,\tau) = \theta_x(0,\tau) = v'(0,\tau) = w'(0,\tau) = 0 \tag{2.6}$$

$$G_u(1,\tau) = G_v(1,\tau) = G_w(1,\tau) = \phi'(1,\tau) = 0 \tag{2.7}$$

In the above equations, dots denote differentiation with respect to τ. The G_u, G_v, G_w and G_{θ_x} terms are nonlinear functions of the elastic deformations and of their spatial and temporal derivatives[4]. The Q_u, Q_v, Q_w terms are the distributed forces (normalized by $mR\Omega^2$, where m is the blade's mass per unit length, which is assumed to be constant) associated with the virtual displacements $R\,\delta u$, $R\,\delta v$, and $R\,\delta w$, respectively; and Q_{θ_x} is the distributed moment, normalized by $mR^2\Omega^2$, associated with

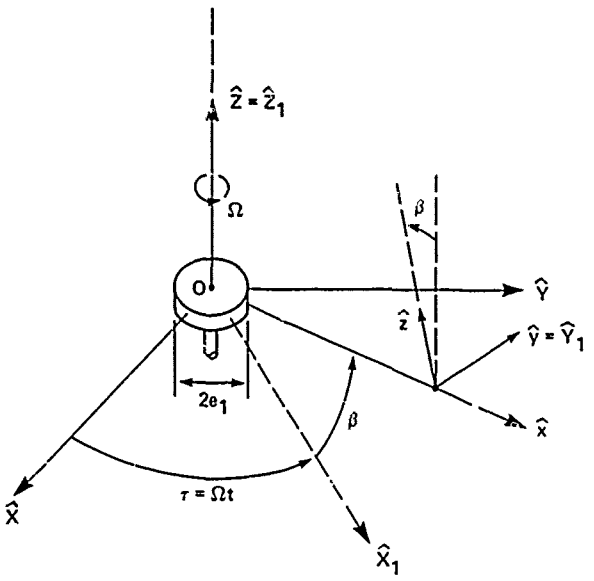


Fig. 2 Nonrotating and rotating coordinate systems with unit vectors.

the virtual rotation $\delta\theta_x$. The normalized virtual work due to these generalized forces is expressed in the form $Q_u\,\delta u + Q_v\,\delta v + Q_w\,\delta w + Q_{\theta_x}\,\delta\theta_x$. The boundary conditions $G_v(1,\tau) = G_w(1,\tau) = 0$ imply $v''(1,\tau) = w''(1,\tau) = v'''(1,\tau) = w'''(1,\tau) = 0$.

For compactness, the fourth differential equation obtained from Hamilton's principle, namely, the equation associated with the virtual rotation $\delta\theta_x$, is presented in the next section in its simplified expanded form only. For its complete form, the reader is referred to Ref. 4.

The aerodynamic forces and moments acting on the blade are modeled using quasi-steady strip theory based on Greenberg's extension of Theodorsen's theory in which only the (η,ζ) components of the blade's elastic axis velocity relative to the air are assumed to affect the aerodynamic loading[2,4,6-8]. These components, normalized by the blade's tip speed ΩR, are given as[4]

$$U_\eta = T_{22}\left[\dot v + (x+v)\cos\beta - w\sin\beta\right] + T_{23}\left[\dot w + v\sin\beta + \lambda\cos\beta\right] \tag{2.8}$$

$$U_\zeta = T_{32}\left[\dot v + (x+u)\cos\beta - w\sin\beta\right] + T_{33}\left[\dot w + v\sin\beta + \lambda\cos\beta\right] \tag{2.9}$$

where,

$$T_{22} = \cos\theta_z\cos\theta_x - \sin\theta_x\sin\theta_y\sin\theta_z \tag{2.10-a}$$

$$T_{23} = \sin\theta_z\cos\theta_y \tag{2.10-b}$$

$$T_{32} = -(\sin\theta_z\cos\theta_x + \cos\theta_z\sin\theta_y\sin\theta_x) \tag{2.10-c}$$

$$T_{33} = \cos\theta_z\cos\theta_y \tag{2.10-d}$$

and λ is the induced inflow velocity normalized by ΩR.

As shown in Ref. 4, the generalized forces Q_u, Q_v, Q_w, and Q_{θ_x} due to the aerodynamic loading are determined as

$$Q_u = T_{21}F_\eta + T_{31}F_\zeta - Q_{\theta_x}w'\frac{\partial\theta_x}{\partial u'}\frac{\partial x'}{\partial r} \tag{2.11-a}$$

$$Q_v = T_{22}F_\eta + T_{32}F_\zeta - Q_{\theta_x}w'\frac{\partial\theta_x}{\partial u'}\frac{\partial x'}{\partial r} \tag{2.11-b}$$

$$Q_w = T_{23}F_\eta + T_{33}F_\zeta \tag{2.11-c}$$

$$Q_{\theta_x} = -\frac{\gamma}{6}\left[\frac{c^2}{16}(\omega_\xi\sqrt{U_\eta^2+U_\zeta^2} - \dot U_\zeta) + 3\frac{c^3}{128}\dot\omega_\xi\right] \tag{2.11-d}$$

with,

$$T_{21} = -(\cos\theta_z\sin\theta_z + \sin\theta_x\sin\theta_y\cos\theta_z) \tag{2.12-a}$$

$$T_{31} = (\sin\theta_x\sin\theta_z - \cos\theta_x\sin\theta_y\cos\theta_z) \tag{2.12-b}$$

$$F_\eta = \frac{\gamma}{6}\left[U_\zeta^2 - \frac{c}{2}U_\zeta\omega_\xi - \frac{c_{d0}}{2\pi}U_\eta\sqrt{U_\eta^2+U_\zeta^2}\right] \tag{2.12-c}$$

$$F_\zeta = \frac{\gamma}{6}\left[-U_\eta U_\zeta + \frac{c}{2}U_\eta\omega_\xi - \frac{c}{4}\dot U_\zeta + \frac{c^2}{16}\dot\omega_\xi - \frac{c_{d0}}{2\pi}U_\zeta\sqrt{U_\eta^2+U_\zeta^2}\right] \tag{2.12-d}$$

In the above equations, c denotes the blade's chord, normalized by R, γ is the Lock number, c_{d0} is the airfoil profile drag coefficient, and ω_ξ is the $\hat\xi$ component of the absolute angular velocity of the principal axis system (η,ζ,ξ). It is given as

$$\omega_\xi = \dot\theta_x + (\dot\theta_z + \cos\beta)\sin\theta_y + \sin\beta\cos\theta_y\cos\theta_x \tag{2.13}$$

In order to compare results with those obtained via the equations developed in Ref. 2, the normalized induced inflow λ is modeled as being uniform along the blade radius and is given as

$$\lambda = \mathrm{sgn}\left[\theta_c + \phi_c(0.75)\right]\frac{bc}{8}\left[\sqrt{1+\frac{12}{bc}\left|\theta_c + \phi_c(0.75)\right|} - 1\right] \tag{2.14}$$

where b is the number of blades, and $\phi_c(0.75)$ is the equilibrium value of the elastic angle of twist at $x = 0.75$.

2.2 Ordering Scheme and Expansion of the Equations to $O(\epsilon^3)$

Because of the complexity of the differential equations presented in the previous section, they will now be restricted to *moderately large* deflections by expanding their nonlinear terms in a Taylor series in a small ordering parameter ϵ, and truncating the result to $O(\epsilon^3)$. Our objective here is to evaluate the influence of these higher-order terms on the motion of the system. We then let $v(x,\tau) = O(\epsilon)$, $w(x,\tau) = O(\epsilon)$ and $\theta_x(x,\tau) = O(\epsilon)$. In addition, $u(x,\tau) = O(\epsilon^2)$. As an example, the expanded form of $\theta_y = \arcsin w'\partial x/\partial r$ is

$$\theta_y = w'(1 - u' - v'^2/2) - w'^3/3 + O(\epsilon^5) \tag{2.15}$$

By making use of the boundary condition $G_u(1,\tau) = 0$, Eq. (2.3) may be integrated over x to obtain an expression for u' in terms of the remaining variables. With $u(0,\tau) = 0$, the following expression is obtained for $u(x,\tau)$ (Ref. 4)

$$u(x,r) = -\frac{1}{2}\int_0^x [v'^2 + w'^2 - \frac{1}{EA}(1-x^2)\cos^2\beta]\,dx - \frac{1}{EA}\int_0^x \int_1^x [2\,\dot{v}\cos\beta + Q_u]\,dx\,dx + O(\epsilon^4)$$
$$\frac{1}{EA} = O(\epsilon^2) \qquad (2.16)$$

where E is the Young's modulus of the material, normalized by $m\Omega^2$, and A is the blade's cross sectional area, normalized by R^2. Both of these quantities are assumed here to be constant.

With u as given by Eq. (2.16), the $O(\epsilon^3)$ expansions for the quantities $G_v(x,r)$ and $G_w(x,r)$ in the δv and δw equations, Eqs. (2.4) and (2.5), respectively, are now in integro-differential form. Furthermore, since $G_v(1,r) = G_w(1,r) = 0$, it is convenient to reduce these equations further by integrating them in x from $x = 1$ to $x = x$ and applying the Galerkin procedure to the latter equations. For simplicity, it is also assumed that $\sin\beta = O(\epsilon)$ (with $\cos\beta$ left as an $O(1)$ quantity in the equations), and that $c = O(\epsilon)$, $\lambda = O(\epsilon)$, and $c_{d0} = O(\epsilon^2)$ in the generalized aerodynamic forces.

The expanded $O(\epsilon^3)$ form of the fourth differential equation obtained from Hamilton's principle namely, the equation associated with the virtual rotation $\delta\theta_x$, becomes, after some higher-order cross-sectional integrals are neglected, as is commonly done in the literature (e.g., Refs. 1–4),

$$\begin{aligned}
&\jmath_\xi\left(\ddot{\theta}_x + \underline{\ddot{w}'\cos\beta}\right) + (\jmath_\zeta - \jmath_\eta)\{\underline{\dot{v}'\sin(2\theta_c) - \dot{w}'\cos(2\theta_c)} \\
&\quad + [\theta_x\cos(2\theta_c) + \sin\theta_c\cos\theta_c]\cos\beta\}\cos\beta \\
&\quad - \left\{D_\xi\left[\theta_x' + v''w' - \theta_x'\frac{\cos^2\beta}{EA}(1-x^2)\right] + EI_\xi\theta_x'\frac{\cos^2\beta}{EA}(1-x^2)\right\}' \\
&\quad + (D_\eta - D_\zeta)[\frac{1}{2}\left(v''^2 - w''^2\right)\sin 2(\theta_c + \theta_x) - v''w''\cos 2(\theta_c + \theta_x)] \\
&\quad + \frac{\gamma c^2}{96}[x\left(2\,\dot{\theta}_x + \underline{\underline{w'\cos\beta}} + \underline{\underline{\sin\beta}}\right)\cos\beta\cos\theta_c \\
&\quad + \underline{\underline{\bar{v}\sin\theta_c - \bar{w}\cos\theta_c}}] + O(\epsilon^4) = 0
\end{aligned} \qquad (2.17)$$

All quantities in the above equation are nondimensional. The blade's distributed mass moments of inertia $(\jmath_\eta, \jmath_\zeta, \jmath_\xi)$ are determined in terms of its material density $\rho(\eta,\zeta)$ as

$$m\jmath_\eta = R^2\int\int \rho\zeta^2 d\eta\,d\zeta \qquad (2.18-a)$$

$$m\jmath_\zeta = R^2\int\int \rho\eta^2 d\eta\,d\zeta \qquad (2.18-b)$$

$$\jmath_\xi = \jmath_\eta + \jmath_\zeta \qquad (2.18-c)$$

The blade's normalized area moment, I_ξ, is

$$I_\xi = \int\int (\eta^2 + \zeta^2)d\eta\,d\zeta \qquad (2.18-d)$$

and (D_η, D_ζ, D_ξ) are the blade's flexural and torsional normalized stiffnesses determined as

$$D_\eta = E\int\int \zeta^2 d_\eta\,d\zeta \qquad (2.18-d)$$

$$D_\zeta = E\int\int \eta^2 d_\eta\,d\zeta \qquad (2.18-e)$$

$$D_\xi = G\int\int [\,(\zeta + \frac{\partial\psi}{\partial\eta})^2 + (\eta - \frac{\partial\psi}{\partial\zeta})^2\,]d\eta\,d\zeta \qquad (2.18-f)$$

where G is the normalized shear modulus of the blade's material and $\psi(\eta,\zeta)$ is the warp function (normalized by R^2) for the blade's cross section. It is assumed that ψ is anti-symmetric in (η,ζ).

For compactness in presentation, two terms in $\sin 2(\theta_c + \theta_x)$ and $\cos 2(\theta_c + \theta_x)$ are shown in Eq. (2.17), but they were actually approximated by their respective expansions to $O(\epsilon^3)$ about $\theta_x = 0$ by writing $\sin 2(\theta_c + \theta_x) = \sin 2\theta_c + 2\theta_x\cos(2\theta_c) + O(\epsilon^2)$ and $\cos 2(\theta_c + \theta_x) = \cos 2\theta_c - 2\theta_x\sin(2\theta_c) + O(\epsilon^2)$. The nonlinear $O(\epsilon^3)$ terms associated with these expansions, namely, the terms in $v''^2\theta_x$, $w''^2\theta_x$ and $v''w''\theta_x$, will henceforth be referred to as the *ijkl terms in the $\delta\theta_x$ equation* in the next figures. The $O(\epsilon^3)$ terms underlined in Eq. (2.17) are not included in the equations developed in Ref. 2. The single underlined terms are linear pitch-flap and pitch-lead/lag coupling terms, and the remaining underlined terms are $O(\epsilon^3)$ linear terms in the aerodynamic pitch moment that are kept for consistency in the formulation. Until a better understanding and more accurate modeling of aerodynamic phenomena is achieved, the validity of terms such as these may be questionable. The $1/(EA)$, $O(\epsilon^3)$, terms in Eq. (2.17) were also neglected in Ref. 2. Again, these terms are kept here for mathematical consistency. For values of EA greater than about 200, we found that the influence of these terms in the results presented later is so small that they may actually be neglected in practice.

2.3 Application of Galerkin's Method

We approximate the solution to Eq. (2.17) and to the integrated form of Eqs. (2.4) and (2.5) as a series of the form

$$v(x,\tau) = \sum_{j=1}^{N} v_{tj}(\tau)\,f_j(x) \qquad (2.19-a)$$

$$w(x,\tau) = \sum_{j=1}^{N} w_{tj}(\tau)\,f_j(x) \qquad (2.19-b)$$

$$\theta_x(x,\tau) = \sum_{j=1}^{N} \theta_{tj}(\tau)\,g_j(x) \qquad (2.19-c)$$

and then reduce the integro-differential equations to ordinary differential equations by making use of Galerkin's method Ref. 5. The functions $f_j(x)$ and $g_j(x)$ are chosen here as the orthogonal eigenfunctions for a nonrotating clamped/free beam,

$$f_j(x) = \cosh(\beta_j x) - \cos(\beta_j x) - \alpha_j[\sinh(\beta_j x) - \sin(\beta_j x)] \qquad (2.20-a)$$

$$g_j(x) = \sqrt{2}\sin[\pi(j-\tfrac{1}{2})x] \qquad (2.20-b)$$

where

$$\alpha_j = \frac{\cos\beta_j + \cosh\beta_j}{\sin\beta_j + \sinh\beta_j} \qquad (2.20-c)$$

and β_j is the j^{th} $(j = 1,2,...,N)$ root of the characteristic equation

$$1 + (\cosh\beta_j)\cos\beta_j = 0 \qquad (2.20-d)$$

All the *Galerkin coefficients* obtained by the procedure described above were evaluated numerically, stored in a computer file, and then used to generate the results presented in Sections 3 and 4. The ordinary differential equation obtained by applying Galerkin's method to the $\delta\theta_z$ equation is obtained as

$$\begin{aligned}
&\tfrac{1}{2}(\mathcal{I}_\zeta - \mathcal{I}_\eta)Q_i(\sin 2\theta_c)\cos^2\beta + \frac{\gamma c^2}{192}(\sin 2\beta)(\cos\theta_c)\underline{\underline{\underline{S_i}}} \\
&+ \sum_{j=1}^{N}\Big([\mathcal{I}_\xi\ddot{\theta}_{tj} + (\mathcal{I}_\zeta - \mathcal{I}_\eta)\theta_{tj}(\cos 2\theta_c)\cos^2\beta]\delta_{ij} \\
&- [\mathcal{I}_\xi\dot{w}_{tj} + (\mathcal{I}_\zeta - \mathcal{I}_\eta)(\dot{v}_{tj}\sin 2\theta_c - \dot{w}_{tj}\cos 2\theta_c)]\underline{L_{3,ji}}\cos\beta \\
&- \Big[D_\xi(P_{ij} + \frac{2\cos^2\beta}{EA}N_{ij}) - \frac{EI_\xi}{EA}N_{ij}\cos^2\beta\Big]\theta_{tj} \\
&+ \frac{\gamma c^2}{96}\Big\{(\cos\beta)(\cos\theta_c)\ [2\dot{\theta}_{tj}M_{ij} \\
&+ (\cos\beta)w_{tj}\underline{\underline{R_{ij}}}] + (\ddot{v}_{tj}\sin\theta_c - \ddot{w}_{tj}\cos\theta_c)\underline{\underline{\underline{O_{4,ji}}}}\Big\}\Big) \\
&+ \sum_{j=1}^{N}\sum_{k=1}^{N}\Big\{D_\xi A_{3,jik}v_{tj}w_{tk} \\
&+ (D_\eta - D_\zeta)\big[\tfrac{1}{2}(v_{tj}v_{tk} - w_{tj}w_{tk})\sin 2\theta_c \\
&- v_{tj}w_{tk}\cos 2\theta_c\big]K_{ijk}\Big\} \\
&+ (D_\eta - D_\zeta)\sum_{j=1}^{N}\sum_{k=1}^{N}\sum_{l=1}^{N}[(v_{tj}v_{tk} - w_{tj}w_{tk})\cos 2\theta_c \\
&+ 2v_{tj}w_{tk}\sin 2\theta_c]\theta_{tl}B_{3,jilk} \\
&+ O(\epsilon^4) = 0 \qquad (i = 1,2,...,N)
\end{aligned} \qquad (2.21)$$

where

$$S_i = \int_0^1 x g_i\,dx \qquad (2.22-a)$$

$$R_{ij} = \int_0^1 x g_i f_j'\,dx \qquad (2.22-b)$$

$$L_{3,ij} = -\int_0^1 f_i' g_j\,dx \qquad (2.22-c)$$

$$O_{4,ij} = \int_0^1 f_i g_j\,dx \qquad (2.22-d)$$

$$B_{3,ijkl} = \int_0^1 f_i'' g_j g_k f_l''\,dx \qquad (2.22-e)$$

The terms that are underlined in Eq. (2.21) correspond to those similarly underlined in Eq. (2.17). The $L_{3,ij}$, $O_{4,ij}$, and $B_{3,ijkl}$ Galerkin coefficients also appear in the δv and in the δw equations, with the $L_{3,ij}$ coefficient in the form of a $\dot{\theta}_{tj}$ term. The S_i and R_{ij} coefficients appear only in Eq. (2.21).

3. Equilibrium Solution

3.1 Numerical Method

The differential equations outlined in Section 2 admit the equilibrium solution $v_{tj}(\tau) = \text{constant} = v_{ej}$, $w_{tj}(\tau) = \text{constant} = w_{ej}$, and $\theta_{tj}(\tau) = \text{constant} = \theta_{ej}$. The $3N$ quantities v_{ej}, w_{ej} and θ_{ej}, $j = 1,2,...,N$, were determined numerically by solving the algebraic equations obtained from the differential equations in Section 2 using a minimization program[9].

The equilibrium solutions were obtained for a four-bladed rotor with $c = \pi/40$, and using a Lock number $\gamma = 5$, a profile drag coefficient $c_{d0} = 0.01$, and $EA = 200$. The equilibrium deformations at the blade tip, $v_e(x=1)$, $w_e(x=1)$ and $\phi_e(x=1)$ are plotted in Figs. 3 and 4 versus θ_c for $\beta = 0$. The quantities ω_v^*, ω_w^*, and ω_ϕ^* shown in these and in the subsequent figures denote, respectively, the first rotating uncoupled blade natural frequencies normalized by Ω as obtained in Ref. 10. The results shown in these figures were obtained by using $N = 5$ nonrotating beam normal modes in the Galerkin procedure. Greater values of N did not significantly affect the results obtained. The dashed lines shown in Figs. 3 and 4 and in subsequent figures represent the results obtained using the equations in Ref. 2, while the solid lines represent the results obtained when the additional $O(\epsilon^3)$ terms presented here are included in the differential equations of motion. These lines are marked a, b, c and d and they represent the following cases:

a the full $O(\epsilon^3)$ equations;

b the $O(\epsilon^3)$ equations, but with $B_{3,ijkl} = 0$;

c the $O(\epsilon^3)$ equations, but with all the $O_{4,ij}$, R_{ij} and $L_{3,ij}$ terms removed, and $B_{3,ijkl} = 0$;

d the $O(\epsilon^3)$ equations, with all the $O_{4,ij}$ and R_{ij} terms removed.

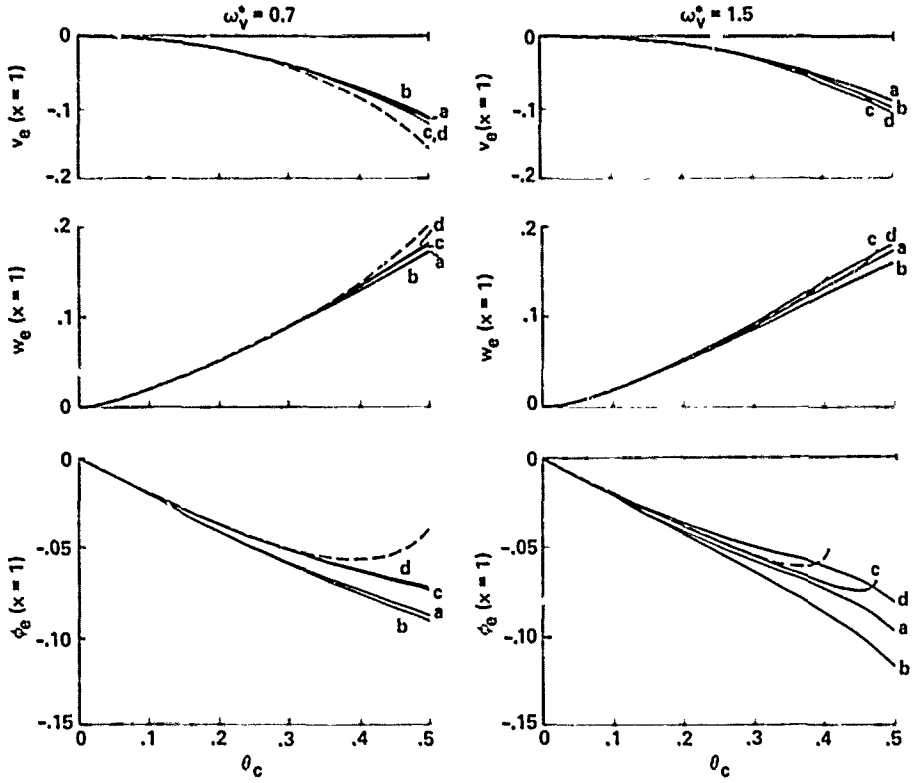


Fig. 3 Chordwise deflection (v_e), flapwise deflection (w_e), and angle of twist (ϕ_e) at $x = 1$ versus collective pitch (θ_c) for $\omega_w^* = 1.06$, $\beta = 0$, $\omega_\phi^* = 2.5$, (N = 5).

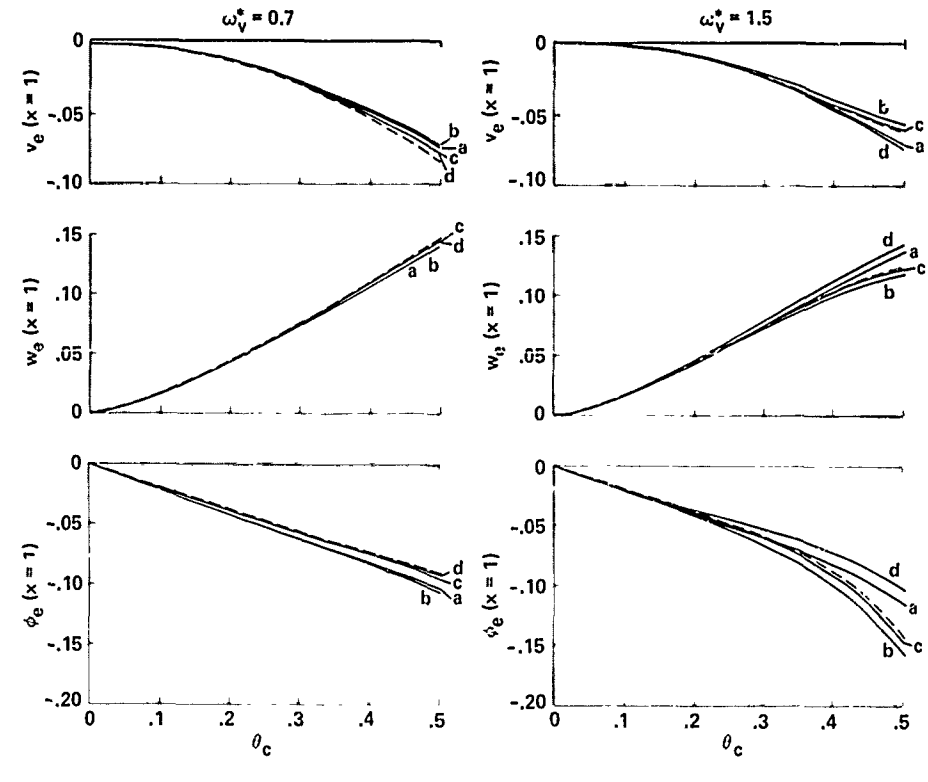


Fig. 4 Chordwise deflection (v_e), flapwise deflection (w_e), and angle of twist (ϕ_e) at $x = 1$ versus collective pitch (θ_c) for $\omega_w^* = 1.15$, $\beta = 0$, $\omega_\phi^* = 2.5$, (N = 5).

3.2 Discussion of Results

Figs. 3 and 4 illustrate the importance of the $O(\epsilon^3)$ terms of the type underlined in Eq. (2.21) in the equilibrium solution of the blade. Their effect is particularly reflected in the equilibrium value of the blade's angle of twist, $\phi_e(x = 1)$, especially for the lower value of the uncoupled flap frequency $\omega_w^* = 1.06$. Several of the nonlinear terms may have only a minor influence on the blade's equilibrium deflections. For soft in-plane blades with $\omega_v^* = 0.7$, for example, it is seen that the equilibrium curves a and b are nearly identical; the same is true of curves c and d. This indicates that for such blades, the additional aerodynamic $O(\epsilon^3)$ terms of the type indicated in Eq. (2.21) are essentially responsible for the difference between curve a and the remaining curves. For these blades, the nonlinear $B_{3,ijkl}$ terms in Eq. (2.21) could have been neglected without causing any significant change in the blade's equilibrium deflections. For high values of collective pitch, however, those terms exert a significant influence on the blade's equilibrium, affecting especially its elastic angle of twist.

Another characteristic of the full $O(\epsilon^3)$ equations is disclosed by examining the equilibrium response of a stiff in-plane blade with $\omega_w^* = 1.06$. The numerical determination of the equilibrium deflections based on the equations developed in Ref. 2 fails to converge when θ_c is about 0.4. This *singularity* is shifted to a higher value of θ_c when additional $O(\epsilon^3)$ terms are included in the equations. For the full $O(\epsilon^3)$ nonlinear equations, no singularity is exhibited in the range of θ_c shown in Figs. 3 and 4. If the aerodynamic $O_{4,ij}$ and R_{ij} terms and the $B_{3,ijkl}$ terms are neglected, but if all other additional terms in the equations are kept, the singularity now appears near $\theta_c = 0.5$.

It was verified that the $O(\epsilon^3)$ *ijkl terms in the* δv and δw *equations*, did not contribute significantly to the determination of the blade's equilibrium response and, therefore, could have been neglected for practical purposes.

4. Stability Analysis

4.1 Numerical Method

To analyze the stability of the motion about the equilibrium determined in Section 3, we let

$$v_{tj}(\tau) = v_{ej} + v_j(\tau) \qquad (4.1-a)$$

$$w_{tj}(\tau) = w_{ej} + w_j(\tau) \qquad (4.1-b)$$

$$\theta_{tj}(\tau) = \theta_{ej} + \theta_j(\tau) \qquad (4.1-c)$$

and then linearize the $3N$ differential equations of motion in the variables $v_j(\tau)$, $w_j(\tau)$, and $\theta_j(\tau)$ to obtain a matrix equation of the form

$$M\underline{\ddot{q}} + C\,\underline{\dot{q}} + K\underline{q} = \underline{0} \qquad (4.2)$$

where $\underline{q}$ is a $3N \times 1$ column vector whose components are $v_1(\tau)$, ... , $v_N(\tau)$, $w_1(\tau)$, ... , $w_N(\tau)$, $\theta_1(\tau)$, ... , $\theta_N(\tau)$. The matrix M is symmetric, and the matrices K and C are non-symmetric.

The stability of the perturbed motion $\underline{q}(\tau)$ is determined by the eigenvalues associated with Eq. (4.2). To determine such eigenvalues, Eq. (4.2) is first rewritten in a first-order form. After introduction of a column vector $\underline{z}$ with components $\underline{q}$ and $\underline{\dot{q}}$, Eq. (4.2) may be written as

$$B\,\underline{\dot{z}} = A\underline{z} \qquad (4.3)$$

with $B_{11} = I$, a $3N \times 3N$ identity matrix; $B_{12} = B_{21} = [0]$; a $3N \times 3N$ null matrix; $B_{22} = M$; $A_{11} = [0]$; $A_{12} = I$; $A_{21} = -K$; and $A_{22} = -C$. The eigenvalues associated with the $6N \times 6N$ matrix in Eq. (4.3) were determined numerically by making use of the IMSL routine EIGZF[9].

The real and imaginary parts of the first lead/lag (σ_v and ω_v), first flap (σ_w and ω_w), and first torsion (σ_ϕ and ω_ϕ) eigenvalues determined as indicated above are plotted versus collective pitch (θ_c) in Figs. 5 to 10 using the same parameter values and labeling convention indicated in Section 3.1.

4.2 Discussion of Results

Figs. 5 and 6 show the first lead/lag eigenvalue associated with Eq. (4.3) for the rotating blade as a function of the pitch angle θ_c. It is seen that for a soft in-plane blade with uncoupled rotating natural frequency $\omega_v^* = 0.7$ the nonlinear $O(\epsilon^3)$ $B_{3,ijkl}$ term that appear in Eq. (2.21) has no substantial influence on either σ_v or ω_v. For such blades, the influence of the remaining higher-order terms underlined in Eq. (2.21) is reflected in the difference between curve d (i.e., with the aerodynamic terms $O_{4,ij}$ and R_{ij} removed from the equations) and that obtained with the full $O(\epsilon^3)$ equations (curve a), and curves a and c (i.e., with the $L_{3,ij}$ torsion-bending coupling terms, and the $O_{4,ij}$ and R_{ij} aerodynamic terms removed from the full $O(\epsilon^3)$ equations). The additional $O(\epsilon^3)$ terms included in the δv and δw equations account for the difference between the results obtained by using the equations developed in Ref. 2—represented by the dashed line—and those represented by curves a in Figs. 5 and 6.

As ω_v^* is increased, however, the situation described above changes. For a stiff in-plane blade with $\omega_v^* = 1.5$, the nonlinear $B_{3,ijkl}$ term that appears in Eq. (2.21) now exerts a major influence on the real part σ_v of the first rotating lead/lag eigenvalue, whereas the terms in the underlined coefficients in Eq. (2.21) do not. The effect of the $O(\epsilon^3)$ nonlinearities that appear in the δv and δw equations is seen by comparing curve c with the dashed curve obtained by using the equations in Ref. 2. For values of θ_c as high as about 0.4, the latter equations yield, for this stiff in-plane blade, practically the same values for ω_v as the full $O(\epsilon^3)$ equations used in this paper. At about $\theta_c = 0.4$, the numerical calculation of the eigenvalues based on the equations in Ref. 2 fail to converge.

The first flap eigenvalue obtained from Eq. (4.3) is shown in Figs. 7 and 8. Again, the effect of $B_{3,ijkl}$ on both σ_w and ω_w is negligible for a soft in-plane blade with $\omega_v^* = 0.7$, but significant for a stiff in-plane blade with $\omega_v^* = 1.5$ for higher values of collective pitch. The effect of the apparent inertia, $O_{4,ij}$, and of the R_{ij} aerodynamic terms, generally neglected in the literature, is reflected in

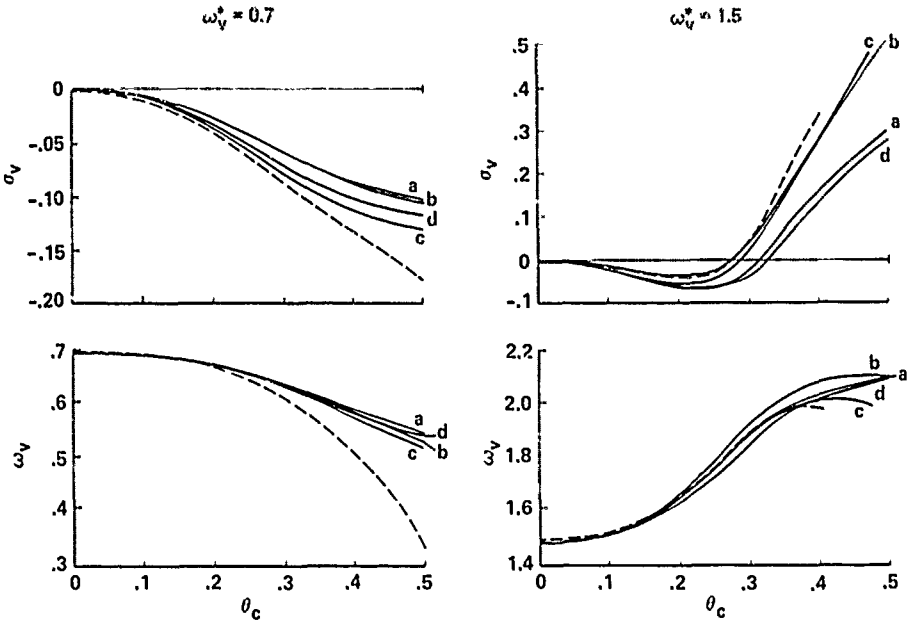


Fig. 5 First lead/lag eigenvalues (real part, σ_v, and imaginary part, ω_v) versus collective pitch (θ_C) for $\omega_w^* = 1.06, \beta = 0, \omega_\phi^* = 2.5$, (N = 5).

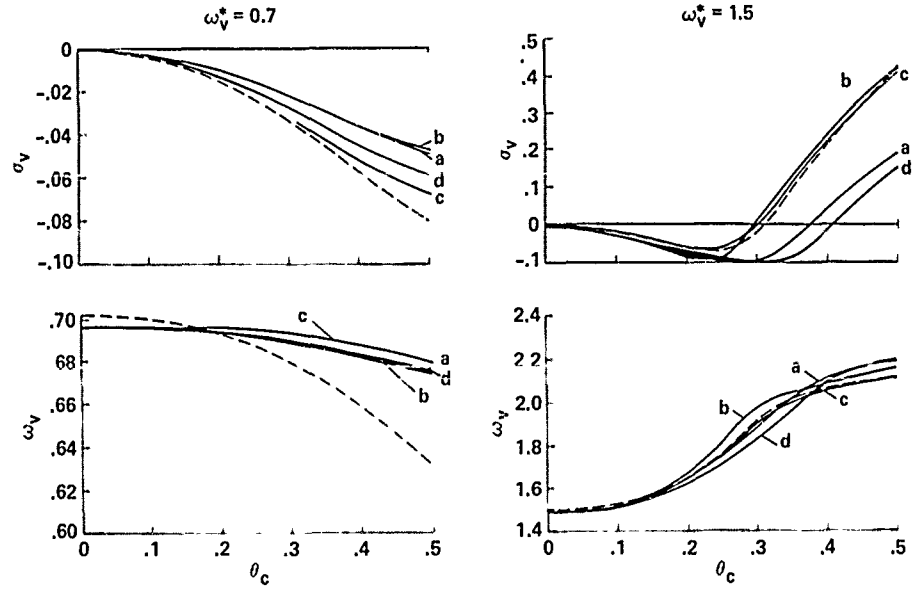


Fig. 6 First lead/lag eigenvalues (real part, σ_v, and imaginary part, ω_v) versus collective pitch (θ_C) for $\omega_w^* = 1.15, \beta = 0, \omega_\phi^* = 2.5$, (N = 5).

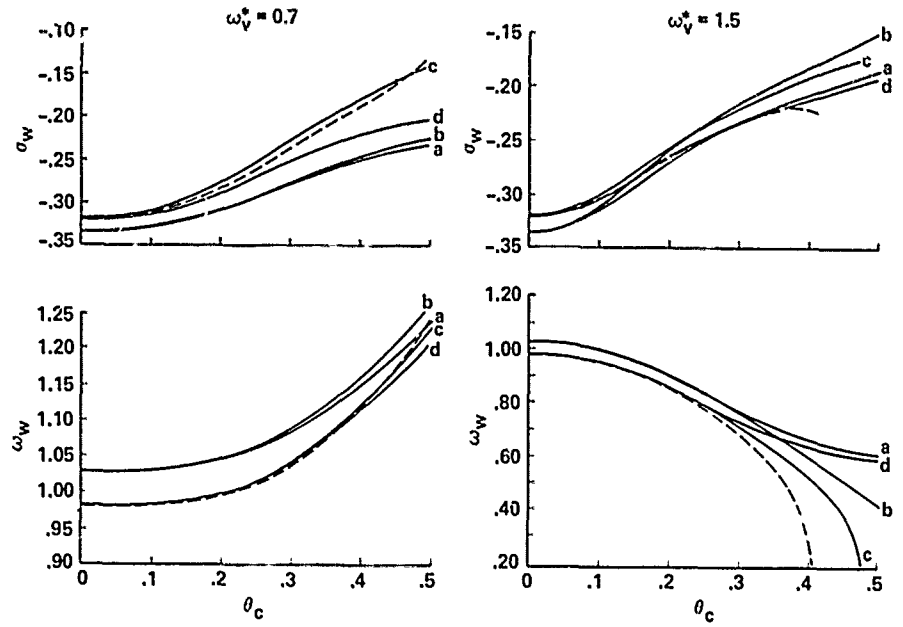


Fig. 7 First flap eigenvalues (real part, σ_w, and imaginary part, ω_w) versus collective pitch (θ_c) for $\omega_w^* = 1.06, \beta = 0, \omega_\phi^* = 2.5$, (N = 5).

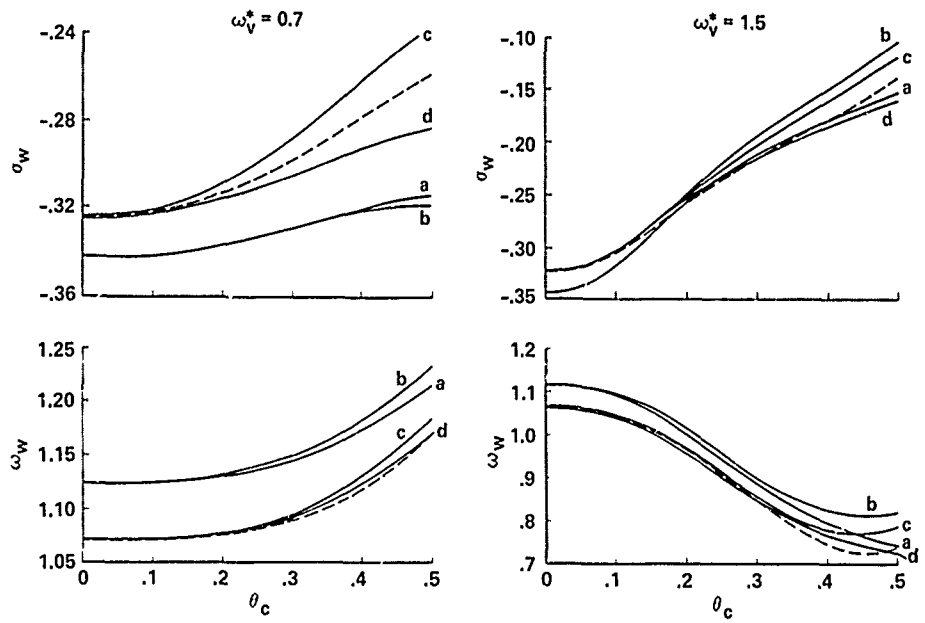


Fig. 8 First flap eigenvalues (real part, σ_w, and imaginary part, ω_w) versus collective pitch (θ_c) for $\omega_w^* = 1.15$, $\beta = 0, \omega_\phi^* = 2.5$, (N = 5).

the eigenvalue (σ_w, ω_w) even for $\theta_c = 0$. It was verified numerically that the $L_{3,v}$ torsion-bending coupling term that appears in Eq. (2.21)—and also in the δv and δw variational equations as a $\dot{\theta}_y$ term—has no practical influence on ω_w. Its influence on σ_w was found to be negligible for $\omega_v^* = 1.5$, but significant when $\omega_v^* = 0.7$. As indicated by Figs. 7 and 8, the damping for the perturbed flap motion for a soft in-plane blade can be significantly affected by the additional $O(\epsilon^3)$ terms included in the equations used here.

Figs. 9 and 10 show the real and imaginary parts of the first rotating torsion eigenvalues of Eq. (4.3). The values of the torsional frequency ω_ϕ are relatively large, and, as seen from these figures, there is little difference between the results obtained here and those obtained by using the equations in Ref. 2 for small values of θ_c. For larger values of collective pitch θ_c, however, the full $O(\epsilon^3)$ equations used here and those in Ref. 2 predict a different trend for ω_ϕ as θ_c is increased further. However, this trend difference is

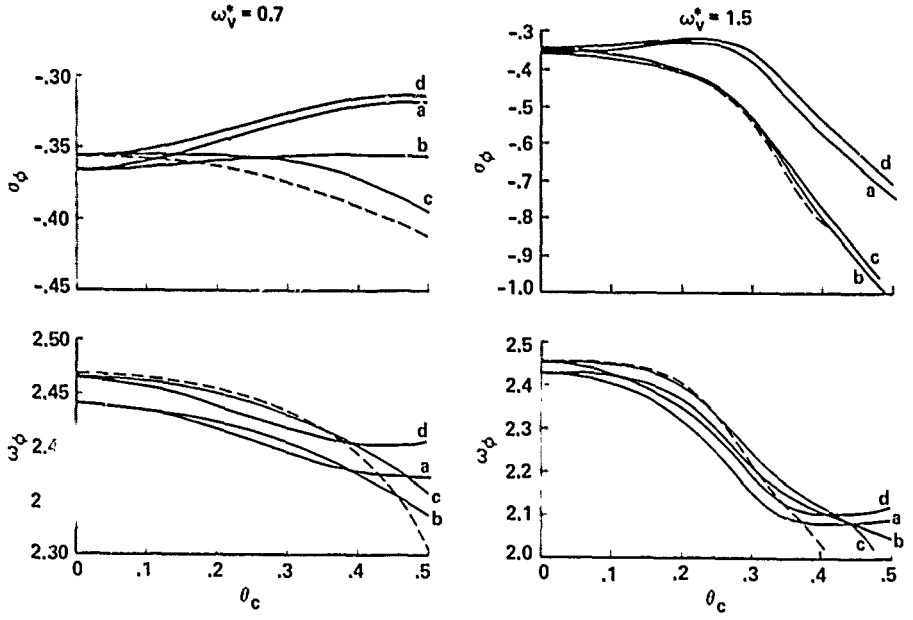


Fig. 9 First torsion eigenvalues (real part, σ_ϕ, and imaginary part, ω_ϕ) versus collective pitch (θ_c) for $\omega_w^* = 1.06, \beta = 0, \omega_\phi^* = 2.5$, (N = 5).

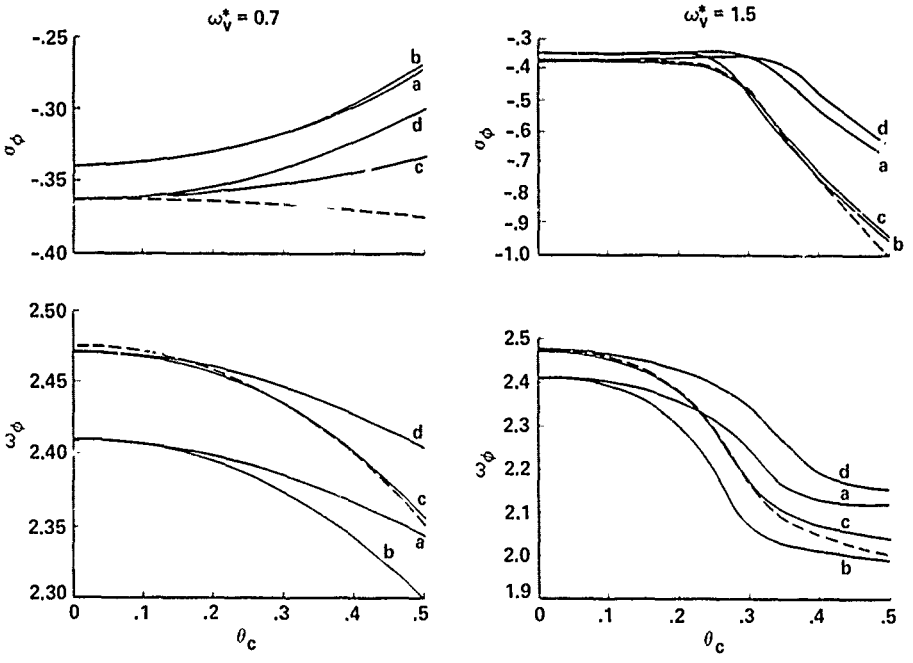


Fig. 10 First torsion eigenvalues (real part, σ_ϕ, and imaginary part, ω_ϕ) versus collective pitch (θ_c) for $\omega_w^* = 1.15, \beta = 0, \omega_\phi^* = 2.5$, (N = 5).

exhibited at such high values of θ_c that it may not be of practical significance.

The torsion damping is significantly affected by the $O(\epsilon^3)$ terms included in the equations used in this paper. Particularly noticeable in Figs. 9 and 10 is the opposing torsion damping trends for a soft in-plane blade with $\omega_\zeta^* = 0.7$ for increasing values of θ_c. This is observed by comparing the results given by curve a, obtained with the full $O(\epsilon^3)$ equations, and by the dashed curve obtained by using the equations in Ref. 2.

It is worth mentioning that all the results shown in Figs. 3 to 10 were essentially unaffected by the $O(\epsilon^3)$ *ijkl terms in the* δv and δw *equations.* These are terms in $v_{tj}w_{tk}\theta_{tl}$, $v_{tj}\dot{w}_k\theta_{tl}$, etc.

5. Concluding Remarks

Numerical results obtained from nonlinear rotor blade equations for the hovering flight condition, with terms retained up through $O(\epsilon^3)$, are presented and compared with results from a simpler $O(\epsilon^2)$ model obtained by previous investigators[2]. In order to facilitate an understanding of which terms are important in the present model that were absent in the previous, simpler model, the present model was exercised with several different classes of terms systematically omitted. Present results, a subset of all the results obtained, indicate that both linear and nonlinear terms of $O(\epsilon^3)$ can significantly affect results for both nonlinear static equilibrium and linear aeroelastic stability. For the results presented here, the most significant cubic nonlinear terms are those associated with structural geometric nonlinearity in the torsion equation. It would appear that such terms should be present in any general-purpose rotor dynamics analysis. The corresponding terms in the equations for bending, although not practically significant in the present results, do make the structural terms in the equations symmetric. The most significant linear terms in the present model but absent in Ref. 2 are associated with an approximate aerodynamics model, the accuracy of which has not been rigorously ascertained. For completeness, it is recommended that a similar investigation be undertaken for the forward flight condition to determine if similar trends hold.

6. References

1. Hodges, D. H. and Dowell, E. H., "Nonlinear Equations of Motion for the Elastic Bending and Torsion of Twisted Nonuniform Blades," NASA TN D-7818, December 1974.

2. Hodges, D. H. and Ormiston, R. A., "Stability of Elastic Bending and Torsion of Uniform Cantilever Rotor Blades in Hover with Variable Structural Coupling," NASA TN D-8192, April 1976.

3. Crespo da Silva, M. R. M. and Glynn, C. C., "Nonlinear Flexural-Flexural-Torsional Dynamics of Inextensional Beams. I. : Equations of Motion; and II. Forced Motion," *J. Structural Mech.*, Vol. 6, No. 4, 1978, pp. 437-448; 449-461.

4. Crespo da Silva, M. R. M., "Flap-Lag-Torsional Dynamic Modeling of Rotor Blades in Hover and in Forward Flight, Including the Effect of Cubic Non-linearities," NASA CR-166194, July 1981.

5. Meirovitch, L., *Analytical Methods in Vibrations.* McGraw Hill, New York, N.Y., 1967.

6. Bisplinghoff, R. L., Ashley, H., and Halfman, R. L., *Aeroelasticity.* Addison-Wesley, 1955.

7. Greenberg, J. M., "Airfoil in Sinusoidal Motion in a Pulsating Stream," NASA TN-1326, 1946.

8. Theodorsen, T., "General Theory of Aerodynamic Instabilities and the Mechanism of Flutter," NACA Report No. 496, 1935.

9. *The International Mathematical and Statistical Library,* Vol. 4, Chapter Z, IMSL Inc., Houston, Texas, 1982.

10. Peters, D. A., "An Approximate Solution for the Free Vibrations of Rotating Uniform Cantilever Beams," NASA TM X-62,299, 1973.

DISCUSSION

EFFECTS OF STATIC EQUILIBRIUM AND HIGHER-ORDER NONLINEARITIES ON ROTOR BLADE STABILITY IN HOVER

Marcelo R. M. Crespo da Silva
Dewey H. Hodges

[Editors' note: The only question asked was by Jing Yen of Bell Helicopter and it was answered by Crespo da Silva and Hodges. It had to do with the meanings of his various curves in terms of the terms in his equations. He answered by pointing out terms on his slide, so the text of the discussion is not very enlightening. Their paper provides the same information at the end of section 3.1.]

Aeroelastic Modeling of Rotor Blades with Spanwise Variable Elastic Axis Offset - Classic Issues Revisited and New Formulations

by

Richard L. Bielawa
Senior Research Scientist
United Technologies Research Center
East Hartford, CT
06108

Abstract

In response to a systematic methodology assessment program directed to the aeroelastic stability of hingeless helicopter rotor blades, improved basic aeroelastic reformulations and new formulations relating to structural sweep have been achieved. Correlational results are presented showing the substantially improved performance of the G400 aeroelastic analysis incorporating these new formulations. The formulations pertain partly to sundry new solutions to classic problem areas, relating to dynamic inflow with vortex-ring state operation and basic blade kinematics, but mostly to improved physical modeling of elastic axis offset (structural sweep) in the presence of nonlinear structural twist. Specific issues addressed are an alternate modeling of the ΔEI torsional excitation due to compound bending using a force integration approach, and the detailed kinematic representation of an elastically deflected point mass of a beam with both structural sweep and nonlinear twist.

Nomenclature

B	Tip loss factor
C_L, C_M	Rotor roll and pitch moment coefficients, respectively, (moment/$\rho\pi R^5$), ND
C_I	Rotor thrust coefficient ($T/\rho\pi R^4$), ND
EI_y, EI_z	Section bending stiffness in flatwise and edgewise directions, respectively, lb-in^2 or ND, ($\Delta EI = EI_z - EI_y$)
$\mathcal{F}$	Induced velocity function, ND
F_T	Tension cosine resolution function, ND
K	Induced velocity gradient factor, ND
P_{x_5}, P_{y_5}, P_{z_5}	Section shear load distributions in directions of "5" coordinate system, ND
q_{v_k}	Blade k'th edgewise modal response variable
q_{w_i}	Blade i'th flatwise modal response variable
q_{x_5}, q_{y_5}, q_{z_5}	Section moment load distributions about axes in the "5" coordinate system, ND
q_{θ_j}	Blade j'th torsion modal response variable
R	Rotor radius, ft.
r	Blade spanwise coordinate, measured from offset in x_5 direction, ND
S_{x_2}	Component of load distribution in radial (x_2) direction, ND
T	Tension at blade section, or rotor thrust, as appropriate, lbf.
$[TAS]$	Coordinate transformation matrix relating "5" and "6" coordinate systems, due to structural sweep, ND
u_e	Inward radial (x_5) foreshortening of blade element point due to combination of built-in sweep and elastic deformation, ND
v	inflow parameter
v_e, w_e	Elastic deflections in the edgewise and flatwise directions, respectively, ND
v_o	Uniform component of momentum induced velocity, ND
v_{1_c}, v_{1_s}	Cosine and sine components, respectively, of momentum induced velocity, ND
Δv, Δw	Deflection correction functions due to first order twist effects, ND
ΔV, ΔW	Deflection correction terms due to second order twist effects, ND
x_5, y_5, z_5	Components of position vector in the "5" system (rotating, coned and lagged), ND
$y_{5_{EA}}$, $z_{5_{EA}}$	Built-in offset distances of elastic axis from x_5 axis in inplane and out-of-plane directions, respectively, ND
$y_{10_{EA}}$, $z_{10_{EA}}$	Built-in offset distances of elastic axis from x_5 axis, in edgewise and flatwise directions, respectively, ND
θ_B	Built-in blade precone, deg.
$\Delta\theta$	Built-in precone outboard of pitch bearing (negative droop), deg.
$\bar{\Gamma}_{y_{\epsilon_j}}$, $\bar{\Gamma}_{z_{\epsilon_j}}$	Nonlinear j'th torsion modal weighting functions for torsion excitation due to edgewise and flatwise force loadings, respectively, ND
$\bar{\bar{\Gamma}}_{y_{\epsilon_j}}$, $\bar{\bar{\Gamma}}_{z_{\epsilon_j}}$	Nonlinear j'th torsion modal weighting functions for torsion excitation due to flatwise and edgewise moment loadings, respectively, ND
γ_E γ_F	Inplane and out-of-plane slope projection angles, respectively, defining blade element orientation, rad.
γ_{v_k}	Deflection mode shape for the k'th edgewise normal mode, ND
γ_{w_i}	Deflection mode shape for the i'th flatwise normal mode, ND
γ_{ϵ_j}	Deflection mode shape for the j'th torsion normal mode, ND
θ	Total local blade pitch angle, radians
θ_e	Elastic torsion deflection angle, radians
θ_o	Collective pitch angle, deg.
Λ_{e_5}	Structural sweep angle projection onto x_5-y_5 plane, rad.
Λ_{f_5}	Structural sweep angle projection onto x_5-z_5 plane, rad.

Presented at the ITR Methodology Assessment Workshop at Ames Research Center, Moffett Field, California, June 1983.

$\lambda(r,\psi)$	Inflow ratio with spanwise and azimuthal variability, ND
λ	Normalized rotor through flow parameter, ND
λ_{RAM}	Part of uniform inflow arising from rotor forward flight, ND
λ_0	Uniform component of variable inflow, ND
μ	Rotor advance ratio, ND
ρ	Air density, lb-sec^2/ft^4
σ	Alternately, rotor solidity, and real part of eigenvalue, ND
ψ	Blade azimuth angle, rad.
Ω	Rotor rotation speed, rpm.

Subscripts and Superscripts

$(\ )_e$	Due to elastic deformation
$(\ )_{EA}$	Defined at the elastic axis
$(\ ^{\bullet})$	Differentiation with respect to ψ
$(\ )'$	Differentiation with respect to (r/R)
$(\ ^{A})$	Denotes evaluation at zero collective angle as applied to deflections

Introduction

For most production helicopter design applications, the principal role of contemporary comprehensive rotor aeroelastic analyses has been that of providing calculations of forced structural responses and, in particular, of blade dynamic stresses. The United Technologies Corporation family of G400 rotor aeroelastic analyses comprises such a comprehensive analysis technology and has undergone extensive development in the last ten years with this principal role as a prime objective. The present G400 technology has evolved from an analysis originally formulated for the unique aeroelastic characteristics of the composite bearingless rotor. That analysis represented an advancement in the state-of-the-art with regard to the modeling of rotors with time-variable, nonlinear structural twist and multiple structural redundancy, as described in Reference 1. The G400 technology which has evolved now includes a family of four actively used versions with a completely general range of applicability in rotor type (articulared, hingeless, teetered and gimballed) and vehicle application (helicopters, propellers and wind turbines). The mathematical modeling capabilities of the G400 analyses are summarized in Figure 1.

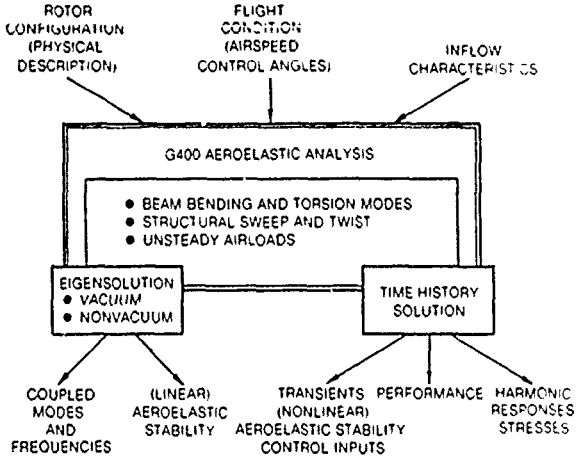


Fig. 1 - Basic capabilities of G400 Aeroelastic Analyses.

Of the two major solution types, eigensolution and time-history solution, the latter contains the most complete physical modeling of the blade aeroelasticity. This includes the dynamics, airloads, excitations and kinematic couplings with the full retention of all nonlinearities which have been identified as being potentially germaine to the aeroelastics. Thus, no nonlinearities have been deleted from the time-history solution for reasons of mathematical convenience. Prior to 1983, the major documentation of the G400 technology was available only in References 1 through 3. Since completion of the work reported herein, another major documentation source has become available (Reference 4).

Within the context of only forced response calculations, limited harmonic response correlation studies have been performed. These have been conducted principally under corporate and contractual funding; References 5 and 6 are the available documentations of this type of correlation study. Detailed aeroelastic stability correlation studies, however, had not been performed prior to the performance of the Integrated Technology Rotor/Flight Research Rotor (ITR/FRR) Methodology Assessment study (Reference 7). One reason for the lack of G400 stability correlation calculations is clearly the emphasis placed on forced response loads calculations by the principal users of the code. Another more logistical reason, however, is that over most of its development life the G400 analysis has been principally a time-history solution analysis. As a result, the eigensolution capability had not kept pace with the increased sophistication of this time-history solution capability. Consequently, accurate stability calculations have typically required the use of transient time-history calculations. Such calculations are generally both time and cost intensive and, hence, had been eschewed. Despite the cost disadvantage, however, time-history solutions present a distinct advantage in the calculation of transient stability, as is discussed in greater detail in a subsequent section.

Under contract NAS2-10864, the in-house helicopter version of G400 was exercised for stability correlation as part of this methodology assessment study. Initial results of this study were generally poor. The G400 stability predictions were deemed unacceptably inaccurate and a concerted corporate-sponsored methodology improvement project was initiated. The general results of this improvement project were completely successful. The stability predictive capability of G400 was definitely raised to an acceptably accurate level (giving good to excellent correlation results) while retaining a valid, mathematically consistent formulation. Over and above this immediate positive result, however, this methodology improvement study produced new formulations and revised existing ones; these formulations are of interest in their own right.

The nature of the detailed reformulations were of three main types: The first consisted of the detection and correction of outright errors in the programmed implementations of the existing derived equations. The second consisted of a sundry class of modifications wherein established aeroelastic methodology was extended from the generally accepted norm. And the third consisted of an improved representation of structural sweep. A discussion of the first type of reformulation is clearly inappropriate for publication and is omitted from further discussion. The second and third types of reformulation, however, constitute new knowledge and form the basis of this paper. The remainder of this paper is divided into three main sections: (1) a review of the pertinent G400/ITR correlation results, (2) a description of the sundry modifications arising from enhanced reformulations of existing theory, and (3) a description of the new formulations relating to structural sweep.

Review of Pertinent ITR Correlation Results

The ITR Methodology Assessment Study, as defined in Reference 7, concentrated on the aeroelastic stability characteristics of hingeless and/or bearingless rotors both in hub-fixed and hub-flexible configurations. Particular emphasis was placed on the stability of the already lightly damped blade edgewise (inplane) mode as affected by couplings with the blade flatwise (out-of-plane) and torsion modes, and with the flexible hub degrees-of-freedom. In all cases, the pertinent mode, whose stability characteristics were to be calculated, was characterized by relatively low reduced frequencies along the blade and for most conditions by an absence of stall. Hence, the stability phenomena could be assumed to be reasonably well-governed by conventional quasi-static airloads.

The original results from applying G400 to the experimental correlational data were generally poor for most of the configurations defined in the study. Of particular significance were the poor correlations achieved with the simplest configuration: that of an isolated hingeless model rotor with no twist or cyclic pitch (configuration IIA, as described in detail in Reference 8). Although the other configurations were equally, if not more, important to the ITR study as a whole, only this configuration will be addressed in this paper because it was the primary vehicle which led to the enhancements to be discussed herein.

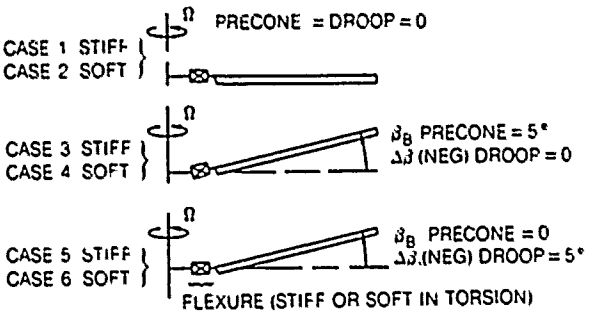


Fig. 2 Correlation cases for ITR configuration IIA, isolated hingeless rotor.

The configuration IIA rotor stability data consisted of 6 distinct cases involving simple parameter variations in precone, β_B, droop, $(-)\Delta\beta$, and torsional flexure stiffness, as shown in Figure 2. A measure of the torsional stiffness of the two flexures is afforded by the first torsional mode amplitudes near the blade root. For the stiff and soft flexures, the calculated torsion modal amplitudes (at the 3% spanwise location) were, respectively, .00013 and 0.12754. For each of these parameter variations, the damping constant, σ, was obtained as a function of blade collective angle, θ_0, as shown in Figures 3a thru 3f. These figures present the experimentally obtained values together with the initial (12/81) G400 calculations and the updated (5/83) ones. The improved correlation of the updated G400 results is apparent and is generally representative of all the results obtained by including the three types of reformulations. These figures will be referred to in the subsequent sections to illustrate the impact of the various specific reformulations.

(a) Case 1 - stiff flexure, $\beta_B = \Delta\beta = 0$.

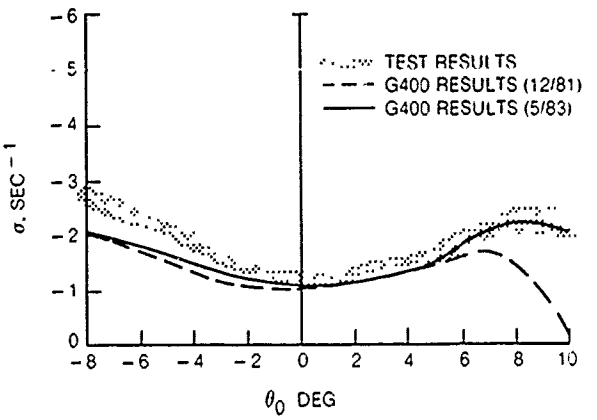
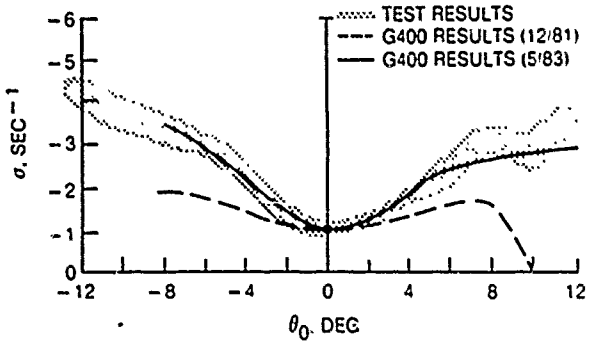
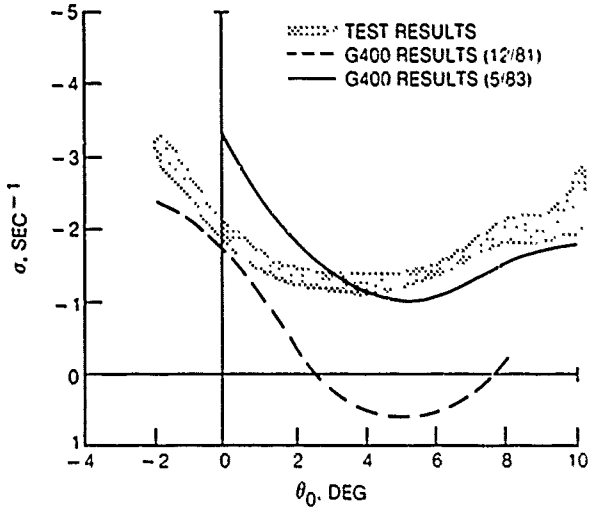


Fig. 3 - Comparison of experimental results with initial and revised G400 calculations-configuration IIA.

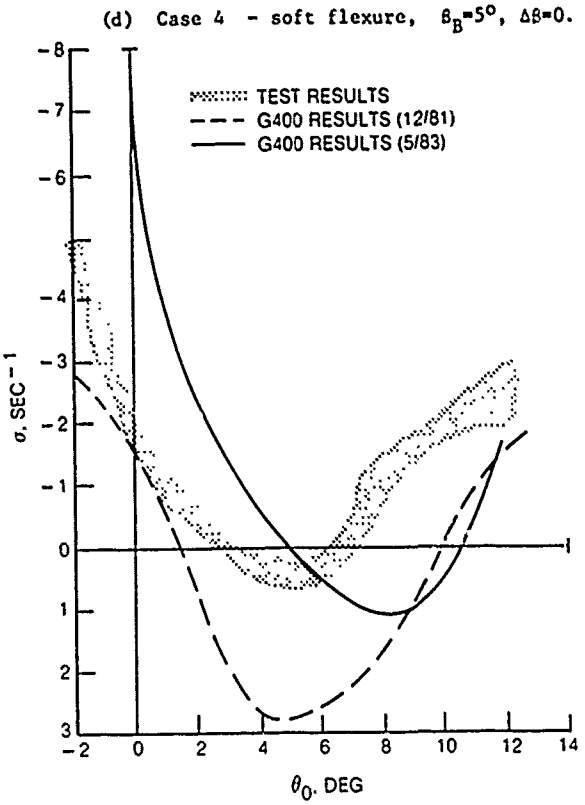
(b) Case 2 - soft flexure, $\beta_B = \Delta\beta = 0$.



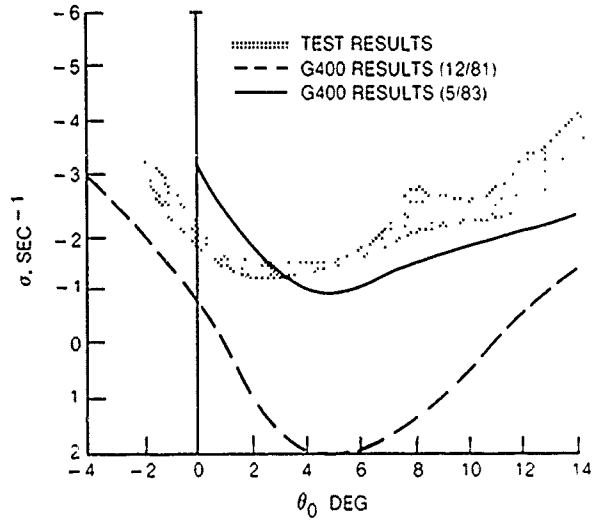
(c) Case 3 - stiff flexure, $\beta_B = 5^\circ$, $\Delta\beta = 0$.



(d) Case 4 - soft flexure, $\beta_B = 5^\circ$, $\Delta\beta = 0$.



(e) Case 5 - stiff flexure, $\beta_B = 0$, $\Delta\beta = -5^\circ$.



(f) Case 6 - soft flexure, $\beta_B = 0$, $\Delta\beta = -5^\circ$.

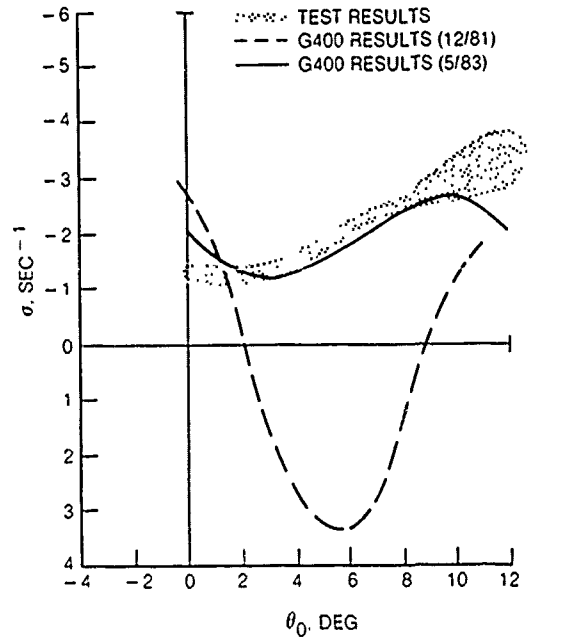


Fig. 3 continued - Comparison of experimental results with initial and revised G400 calculations-configuration IIA.

Sundry Reformulations Relating to Existing Theory

Air Mass Dynamics

Examination of Figures 3a and 3b shows an experimentally observable falloff of rotor stability at sufficiently high values of collective angle. The most obvious inaccuracy of the initial G400 calculations is the premature falling off of the damping constant with increasing collective angle. The physics governing this attenuation of damping is twofold: First, increases in collective will necessarily increase the blade loading and, thereby, the static out-of-plane blade bending. This increase in static bending will significantly impact on the effective pitch-edge coupling which, in large measure, defines the pitch-flap-lag stability. Secondly, increases in collective will also increase the penetration of the blade section angles-of-attack into the near stall, high drag rise coefficient regime of airfoil operation. As shown in Reference 8, this regime of rotor operation is generally destabilizing. The basic parameter common to and controlling each of these effects is the local blade section angle-of-attack. The angle-of-attack, however, is determined from both geometric and inflow contributions. From inspection of the initial G400 results it appeared that the section angle-of-attack vs. pitch angle relationship might be incorrect and such in fact was the case.

The G400 technology incorporates a representation of air mass dynamics which closely conforms to the established state-of-the art (e.g. Reference 9). The major departure of the G400 technology from that typified by Reference 9 is twofold. First, the technology employs a nonperturbational, totally nonlinear form of the momentum equations. Second, in order to accommodate the high thrust loadings at which a wind turbine is capable of operating, the G400 technology employs an empirical correction procedure for simulating operation in or near the vortex-ring state. These ideas are summarized in the following development. The total (nonperturbational) form of momentum variable inflow is assumed to be as follows:

$$\lambda(r,\psi) = \lambda_{RAM} - v_0 - r\left[(v_{1_C} + Kv_0)\cos\psi + v_{1_S}\sin\psi\right] \qquad (1)$$

where the Glauert factor, K, is approximated[10] by the following simple expression:

$$K = \frac{4}{3}\,\frac{(\mu/\lambda_0)}{1.2 + (\mu/\lambda_0)} \qquad (2a)$$

, where:

$$\lambda_0 = \lambda_{RAM} - v_0 \qquad (2b)$$

and where v_1, v_{1_C} and v_{1_S} are the uniform (zeroth harmonic), and first harmonic components of induced velocity, respectively. These components of induced velocity are governed by appropriate first order differential equations:

$$\overset{*}{v}_0 = \frac{3\pi}{4}\left[\frac{C_T}{2B^2} - \frac{v_0}{\mathcal{T}}\right] \qquad (3)$$

$$\begin{Bmatrix} \overset{*}{v}_{1_C} \\ \overset{*}{v}_{1_S} \end{Bmatrix} = \frac{45\pi}{16}\left\{\frac{1}{B^3}\begin{bmatrix} -C_M \\ C_L \end{bmatrix} - v\begin{Bmatrix} v_{1_C} \\ v_{1_S} \end{Bmatrix}\right\} \qquad (4)$$

where $\mathcal{T}$ is a newly-defined rotor induced velocity function whose independent variable is taken to be the normalized through-flow parameter defined as follows:

$$\hat{\lambda} = \mathrm{sgn}(\lambda_0 C_T)\sqrt{\mu^2+\lambda_0^2}\,\Big/\sqrt{|C_T|/2B^2} \qquad (5)$$

and the usual inflow parameter, v, is defined as:

$$v = \frac{\mu^2 + \lambda_0(\lambda_0 - v_0)}{\sqrt{\mu^2+\lambda_0^2}} \qquad (6)$$

For rotor operation well removed from the vortex ring state ($|\hat{\lambda}|\geq 1.4$) the rotor induced velocity function, $\mathcal{T}$, consists of two branches and is directly obtainable from standard momentum theory as given simply by $1/|\hat{\lambda}|$. For values of $|\hat{\lambda}|$ less than 1.4 and especially approaching zero, the momentum representation breaks down (and eventually goes singular). Alternate empirical correction curves which connect the two valid momentum branches for values of $\hat{\lambda}$ between -1.4 and +1.4 are suggested by material presented both by Gessow and Myers [11] and by Lissaman, as shown in Figure 4.

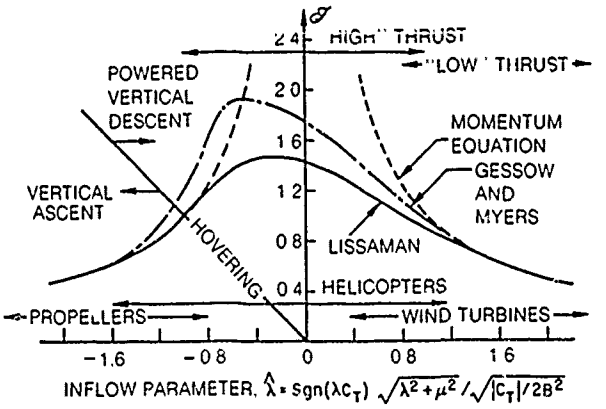


Fig. 4 Rotor induced velocity function.

Essentially the reformulations pertaining to air mass dynamics which were included in the updated G400 technology were to include the signum function factor in the definition for $\hat{\lambda}$, as given in Equation (5) (in order to accommodate negative values of inflow, λ), and to abandon the Lissaman data in favor of the Gessow and Myers data. For the configuration IIA correlation cases, these changes resulted in values of $\mathcal{T}$ which were above the momentum values compared with ones which were initially below, at the high thrust (high collective angle) conditions. This correction to the formulation of the induced velocity function accounted for the difference in steady section angles-of-attack needed to bring the high collective pitch angle results into agreement with experiment.

Basic Considerations of Blade Kinematics

The high relative torsional stiffness of the "stiff" flexure, cases 3 and 5 of configuration IIA (see Figure 2), result in these cases taking on especially useful significance. For these two cases, the rotor blade is essentially rigid in torsion up to the point just outboard of the flexure. Thus, they are aeroelastically equivalent and should have the same stability characteristics. The experimental results shown in Figures 3c and 3e do confirm this supposition.

Within the context of the G400 technology, however, cases IIA-3 and IIA-5 must be respectively modeled as a blade with a straight elastic axis preconed at a 5 degree angle, and as a blade without precone, but with a 5 degree bend in the elastic axis. The effective equivalency of cases IIA-3 and IIA-5 thus forms the basis for validating the consistency of formulations especially with regard to elastic axis offset (structural sweep).

The aeroelastic significance of both radial foreshortening and spanwise tension (treated in the subsequent subsections) is that they are each an important source of coupling between flatwise bending and edgewise bending. Because of the contributions of flatwise bending to radial foreshortening, flatwise rate terms appear in the Coriolis force dependent terms in the edgewise equation. Similarly, because of the contribution of edgewise rate to the centrifugal force, edgewise rate terms appear in the tension terms in the flatwise equation. Because of the evident significance of these terms, a useful test for assessing the accuracy and self-consistency of the improved formulations was that the stability predictions for cases IIA-3 and IIA-5 be the same.

Kinematics of Radial Foreshortening

The original G400 development [1] invoked various principal assumptions which were intended to allow for advancement of the art of modeling nonlinear structural twist while avoiding unnecessary obfuscation caused by the inclusion of numerous nonlinear terms. Accordingly, the radial foreshortening of a mass element due to elastic bending, u_e, was kept simplistic and assumed to be limited to that accruing from flatwise bending only. It was accordingly represented by a quadratic function in flatwise bending:

$$u_e = \frac{1}{2} \sum_{i,m} \left[\int_0^r \gamma'_{w_i} \gamma'_{w_m} dr_i \right] q_{w_i} q_{w_m} \qquad (7)$$

In the reformulated G400 technology[4], this restrictive assumption was relaxed. The two basic assumptions which were retained, expanded upon and utilized as an alternative basis are as follows:

1) The elastic (torsion axis is defined to be the spanwise locus of shear centers of the two-dimensional blade (beam) sections taken perpendicular to this spanwise locus. Note that this definition treats the elastic axis as an abstracted section property, as contrasted with what one would measure in a bench test of an actual curved beam. The built-in structural sweep (elastic axis offset), together with the elastic bending deflections, define an elastic axis which is generally a space-curve about which the local torsion deflection must take place.

2) The arc length of the so-defined elastic axis is invariant both in toto and per blade segment. Radial foreshortening accrue entirely from the kinematics of bending and distributed torsion along the space-curve elastic axis.

3) Local radial foreshortening is defined relative to the total extended arc length of the elastic axis. A hypothetical beam formed by the straightening out of the arc length of the elastic axis and the elimination of all pitch and twist is herein defined to be the "equivalent beam."

Contributions to radial foreshortening then accrue from (a) the built-in structural sweep, i.e. that which restores the equivalent beam to the original swept planform (b) first order (linear) functions of bending, arising from built-in structural sweep, (c) second order (nonlinear) functions of bending each with elastic torsion arising from built-in structural sweep, and (d) second order functions each of both flatwise and edgewise bending. These contributions are pictorially indicated in Figure 5.

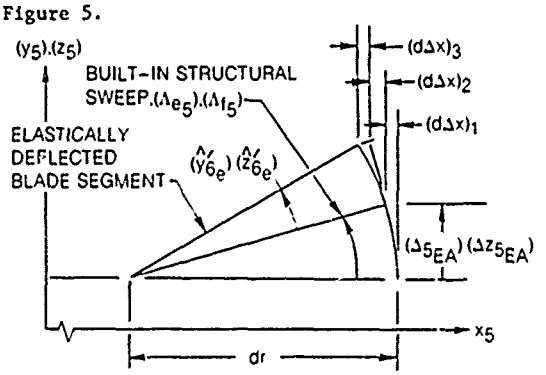


Fig. 5 Contributions to incremental radial foreshortening due to structural sweep and elastic deformations.

Each of these contributions can be modeled in a straightforward manner, and in lieu of the detailed development given in Reference 4, are simply stated as follows:

$$(d\Delta x)_1 = dr - dx = dr - \sqrt{dr^2 - \Delta y_{5_{EA}}^2 - \Delta z_{5_{EA}}^2} \tag{8}$$

$$= dr\left[1 - \sqrt{1 - (\Delta y_{10_{EA}}/\Delta r)^2 - (\Delta z_{10_{EA}}/\Delta r)^2}\right]$$

$$(d\Delta x)_2 = dr\left[\sin\Lambda_{f_5}\cos\Lambda_{e_5}\hat{z}_{6_e}' - \sin\Lambda_{e_5}\cos\Lambda_{f_5}\hat{y}_{6_e}'\right] \tag{9}$$

$$(d\Delta x)_3 = \cos\Lambda_{e_{5_0}}\cos\Lambda_{f_{5_0}}\left[1 - \sqrt{1 - v_e'^2 - w_e'^2}\right] dr$$

$$\cong \cos\Lambda_{e_{5_0}}\cos\Lambda_{f_{5_0}}\cdot\frac{1}{2}(v_e'^2 + w_e'^2)\,dr \tag{10}$$

where $\Delta y10_{EA}$ and $\Delta z10_{EA}$ are, respectively, the built-in changes per segment length of the chordwise and flatwise distances of the elastic axis from the reference, x_5, axis. And where Λ_{e5} and Λ_{f5} are, respectively, the structural sweep angle projections onto the x_5-y_5 and x_5-z_5 reference planes.

The total elastic radial foreshortening at the center of the nth segment is then determined by the following integral:

$$u_{e_n} = \int_0^{r_n}\left[(d\Delta x)_1 + (d\Delta x)_2 + (d\Delta x)_3\right] \tag{11}$$

The details of this integration are straightforward but sufficiently tedious to be beyond the intent and usefulness of this paper. Symbolically, u_e is finally given by:

$$u_e = (DUEAO) + (DUEAF_i)q_{w_i} + (DUEAE_k)\,q_{v_k}$$

$$+ (UELSET_{k_j})\,q_{v_k}q_{\theta_j} + (UELSFT_{i_j})\,q_{w_i}q_{\theta_j}$$

$$+ \frac{1}{2}(UELASE_{km})q_{v_k}q_{v_m} + \frac{1}{2}(UELASF_{in})q_{w_i}q_{w_n} \tag{12}$$

This formulation thus contains Equation 7 as a contributing term.

Spanwise Tension Distribution

Of all the terms appearing in the blade dynamic equations, the tension force is by far the greatest in magnitude and, by definition, qualifies as a "zeroth order" term. The difficulty in accurately modeling tension is that although it is a zeroth order term, the zeroth order component is equilibrated by other zeroth order effects (e.g. the steady blade airloads). Indeed, it can be well appreciated that the significant dynamics of rotor blades are determined by the higher order terms. Thus, even though tension is principally a zeroth order quantity, it still becomes important to model it with sufficient detail to capture the salient higher order effects.

Tension has been typically calculated as the direct spanwise integration of the radial force loading, S_{x_2}, outboard of the blade field point (center of blade segment). The radial force loading is, in turn, taken to be that due to centrifugal force and is thus dependent on the mass element radial position and inplane velocity, both of which include higher order terms. The formulations of the previous subsection, therefore, clearly impact on the calculation of centrifugal force. In addition to these reformulations, an additional higher order effect relating to tension was identified which subsequently led to the required self-consistency. In the reformulated G400 technology, account has been taken of the fact that tension is a vector whose local direction is determined by the orientation of the beam element (blade segment). The centrifugal force on the other hand is a vector always oriented radially in the rotor rotation plane. Hence, tension and centrifugal force are not generally codirectional. Upon defining the out-of-plane and inplane projections of the skew angle, γ, between these two vectors, as γ_F and γ_E, respectively, the effect of non-codirectionality on tension can be written as:

$$T(r) = F_T(r)\int_r^l S_{x_2}\,dr_l \tag{13}$$

where:

$$F_T(r) = \cos\gamma(r) = \sqrt{1 - \sin^2\gamma_E - \sin^2\gamma_F} \tag{14}$$

Reformulations Relating to Variable Elastic Axis Offset

As originally formulated, the G400 technology assumed the elastic axis to define a space-curve as a result of combined flatwise and edgewise bending. In this case, the blade curvature is directly proportional to the elastic modal degrees-of-freedom. This situation consequently allowed for considerable simplicity in structural modeling especially with regard to the nonlinear torsion excitation resulting from combined flatwise and edgewise bending (the ΔEI term). For the case of built-in variable elastic offset (structural sweep) the accurate definition of such sweep in terms of its curvature becomes impractical. Also, while an approximation to the blade kinematics resulting from "small sweep" could be obtained heuristically by considering the structural sweep to consist of "pre-bends" in the elastic axis, this procedure becomes suspect at moderate to large structural sweep. These issues become important in cases IIA-1 and IIA-2 wherein large bending deflections occur at the high collective angles, and in case IIA-6 where the effects of structural sweep are most pronounced. The following subsections address these two issues.

Torsion Excitation due to Compound Bending

As given in Reference 1, and as recognized elsewhere in the literature, the torsion differential equation is comprised of three basic parts. The first part consists of the usual elastic stiffening terms, and the second consists of combinations of distributed moment loadings. The third part is comprised of the wholly nonlinear torsion loadings accruing from distributed force loadings acting on moment arms provided by curvature in the elastic axis. As given in Reference 1, the torsion equation is given by:

$$\underbrace{\left[GJ\theta_e' + \Theta k_A^2 T + \frac{1}{2}EB_1(\Theta'^2 - \theta_B'^2)\Theta' - EB_2\theta_B' v_e''\right]'_{(I)}}_{\text{elastic stiffening}} = \underbrace{\left[-q_{x_5} - y_5' q_{y_5} - z_5' q_{z_5}\right]_{(II)}}_{\text{moment loadings}}$$

$$+ \underbrace{\left\{y_5'' \int_r^l \left[z_5' \int_{r_1}^l p_{x_5}(r_2)\,dr_2 - \int_{r_1}^l p_{z_5}(r_2)\,dr_2 + q_{y_5}(r_1)\right]dr_1 - z_5'' \int_r^l \left[y_5' \int_{r_1}^l p_{x_5}(r_2)\,dr_2 - \int_{r_1}^l p_{y_5}(r_2)\,dr_2 - q_{z_5}(r_1)\right]dr_1\right\}_{(III)}}_{\text{curvatures} \qquad \text{functions of force loadings}} \tag{15}$$

In Reference 1, the curvatures used in the (nonlinear) third portion of the torsion equation were assumed to arise entirely from the elastic bending deflections, v_e'' and w_e''. As such, it can be shown that the nonlinear excitation term in Equation (37) can be reduced to a compact expression which includes the familiar difference of bending stiffness term, ΔEI ($= EI_z - EI_y$):

$$\{\cdots\}_{(III)} = \left[(EI_z - EI_y)v_e'' w_e'' - (e_A T + EB_2(\theta_B' + \tfrac{1}{2}\theta_e')\theta_e')w_e''\right] \tag{16}$$

This method for including the effect is attractive principally because of its simplicity and has been used to good advantage by numerous investigators. Three difficulties exist with this method of implementation, however. The first difficulty relates to the fact that the implementation of Equation (16) is based on a "mode deflection" description of internal bending moment. The difficulty with a mode deflection formulation per se is two-fold. Studies of the characteristics of mode deflection formulations (References 12 and 13) have established that convergence to accurate representations of internal bending moment is often not assured with a small number of modes. This accuracy problem is then compounded by the fact that the two components of this nonlinear excitation are subtractive. This is evidenced by the differencing of the section bending stiffnesses as indicated above.

A second difficulty with using the ΔEI method relates to the assumed space curve character of the elastic axis. As such, torsion deflections are seen to contribute to inplane and out-of-plane deflections in the presence of bending. Thus, an analogous nonlinear excitation exists in both the flatwise and edgewise bending equations. In the framework of the G400 technology, these nonlinear excitations in the bending equations are most practically implemented using a "force integration" approach. Consequently, the use of a ΔEI mode deflection implementation in the torsion equation together with a force integration implementation in the bending equations results in a (coupled) modal mass matrix which is generally nonsymmetric. A nonsymmetric mass matrix is not intrinsically a weakness for isolated rotor simulation and has been successfully used for years in that mode. However, the potential exists for spurious divergent response conditions caused by an inertia matrix becoming nonpositive-definite due to this deflection dependent nonsymmetry.

The third difficulty with the Equation 16 formulation is that it is difficult to include the built-in curvature due to structural sweep. Equation (16) requires curvature information which is not generally available for the built-in geometry.

Because of these difficulties, the conventional ΔEI approach of Equation (16) was abandoned in favor of a "force integration" approach. Accordingly, the Galerkin approach is first applied to the nonlinear excitation term and then integration by parts is used to achieve an intermediary step needed to eliminate the explicit curvature terms:

$$\int_0^l \gamma_{\theta_j}\{\cdots\}_{(III)}\,dr = \int_0^l \Big\{-p_{z_5}\int_0^{\bar r}\int_0^{\bar r_1}\gamma_{\theta_j} y_5''\,dr_2\,dr_1 + p_{y_5}\int_0^r\int_0^{r_1}\gamma_{\theta_j} z_5''\,dr_2\,dr_1 + (z_5'T + q_{y_5})\int_0^{\bar r}\gamma_{\theta_j} y_5''\,dr_1 - (y_5'T - q_{z_5})\int_0^{\bar r}\gamma_{\theta_j} z_5''\,dr_1\Big\}\,d\bar r \tag{17}$$

Since this term represents the nonlinear effects, it is reasonable to use a zeroth order approximation to the curvature terms wherein the structural sweep is assumed to be "small". With this assumption, all the integrals in Equation (17) can be evaluated using the deflection correction functions defined in Reference 1.

Thus, Equation (17) becomes:

$$\int_0^1 \gamma_{\theta_j}\{\cdots\}_{\textcircled{III}}\,dr = \int_0^1 \{\Gamma_{y\theta_j}[p_{y_5}\cos\Theta + p_{z_5}\sin\Theta] - \Gamma_{z\theta_j}[p_{z_5}\cos\Theta - p_{y_5}\sin\Theta] + \tilde{\Gamma}_{z\theta_j}[T(w_e' + z_{IO_{EA}}' - \Delta w^{(2)\prime} - \Delta w^{(2)\prime}) + q_{y_5}\cos\Theta + q_{z_5}\sin\Theta] - \tilde{\Gamma}_{y\theta_j}[T(v_e' + y_{IO_{EA}}' + \Delta v^{(2)\prime} - \Delta v^{(2)\prime}) - q_{z_5}\cos\Theta + q_{y_5}\sin\Theta]\}\,dr \tag{18}$$

where:

$$\Gamma_{y\theta_j} = \gamma_{\theta_j}(w_e + z_{IO_{EA}} - \Delta w - \Delta w) - (\Delta v_{EA_j} - \Delta v_{EA_j}) \tag{19a}$$

$$\Gamma_{z\theta_j} = \gamma_{\theta_j}(v_e + y_{IO_{EA}} + \Delta v - \Delta v) - (\Delta w_{EA_j} + \Delta w_{EA_j}) \tag{19b}$$

$$\tilde{\Gamma}_{y\theta_j} = \gamma_{\theta_j}(w_e' + z_{IO_{EA}}' - \Delta w^{(2)\prime} - \Delta w^{(2)\prime}) - (\Delta v_{EA_j}^{(2)\prime} - \Delta v_{EA_j}^{(2)\prime}) \tag{19c}$$

$$\tilde{\Gamma}_{z\theta_j} = \gamma_{\theta_j}(v_e' + y_{IO_{EA}}' + \Delta v^{(2)\prime} - \Delta v^{(2)\prime}) - (\Delta w_{EA_j}^{(2)\prime} + \Delta w_{EA_j}^{(2)\prime}) \tag{19d}$$

Equation (18) represents the required form of the "force integration" implementation of the nonlinear torsion excitation term. Upon recognizing and utilizing various cancellations arising in Equation (18) itself and in combination with similar terms contained in the (II) moment loadings term, the final most useful form of the torsion equation can then be written as:

$$\int_0^1 \gamma_{\theta_j}'\left[GJ\theta_e' + \cdots\right]'dr = \int_0^1 \{\gamma_{\theta_j} q_{x_5} - \Gamma_{y\theta_j}[p_{y_5}\cos\Theta + p_{z_5}\sin\Theta] + \Gamma_{z\theta_j}[p_{z_5}\cos\Theta - p_{y_5}\sin\Theta] + (\Delta w_{EA_j}^{(2)\prime} + \Delta w_{EA_j}^{(2)\prime})[T(w_e' + \cdots + q_{z_5}\sin\Theta] - (\Delta v_{EA_j}^{(2)\prime} - \Delta v_{EA_j}^{(2)\prime})[T(v_e' + \cdots + q_{y_5}\cos\Theta]\}\,dr \tag{20}$$

To conclude this subsection, three observations can be made of the above formulations:

1. Equations (19) all reduce to zero for zero structural sweep and zero elastic deflection, as would be expected from the behaviour of Equation (16).

2. In Equation (18), the terms multiplying the nonlinear torsion weighting functions ($\Gamma_{y\theta_j}$,...) are actually the force and moment loadings defined for the linear excitations of the bending equations. The nonlinear torsion weighting functions, Equations (19), thus serve in effect, as the virtual deflection functions arising from <u>torsion</u> deflections appropriate to the <u>bending</u> generalized loads.

3. The validity of the force integration approach is enhanced by the fact that the resulting terms in the torsion equation which represent rows of the inertia matrix (reflecting the integration of inertia forces) produce complete mass matrix symmetry and consequently insure positive-definiteness.

<u>Kinematic Representation for Structural Sweep</u>

The selected general approach to modeling structural sweep is to use the simple well established concepts for bending and torsion of straight beams as a departure point. Accordingly, blade elastic bending is defined by conventional beam bending differential equations wherein the usual independent spanwise variable is taken to be the arc length along the elastic axis. Furthermore, these bending differential equations are defined locally using the loadings normal to the built-in elastic axis. Within this context, explicit elastic bending-torsion coupling due to structural sweep is omitted in favor of implicit coupling due to inertial, aerodynamic and gravitational loadings taken with appropriate sweep related kinematics. Within this context, the major necessary task in modeling structural sweep is to define the kinematics of the blade element mass centers and aerodynamic centers as explicit functions of the blade modal response variables. This subsection addresses this major task, from which the formulations of inertial aerodynamic and gravity loads follow in a straightforward manner. These subsequent formulations for loadings are thus omitted herein for clarity.

Structural sweep is defined in a general sense wherein both inplane and out-of-plane offsets of the built-in elastic axis, $y_{5_{EA}}$ and $z_{5_{EA}}$, respectively, are admitted (see Figure 6). The basic objectives of the structural sweep related reformulations are: (1) to define a coordinate system rotation transformation from the "5" pitch axis system to the swept "6" system (which is locally attached to the elastic axis), and (2) to define the deflections in the "5" system as functions of the built-in structural sweep and the elastic bending and torsion motions, which are measured in the "6" system. These two objectives must also be met while including the previous G400 formulations with regard to structural twist. The procedure formulated for including these two structural elements (sweep and twist) is summarized in the material which follows; the reader is directed to Reference 4 for a more detailed description.

The general modeling of the blade y_5 and z_5 kinematics due to combined structural twist and sweep is accomplished in the following steps:

1. The elastic axis of the "equivalent beam" described in an above subsection is "distorted" back to the original planform defined by the built-in structural sweep and segment arc length distributions (but without pitch or twist). This step essentially defines the position in space of the elastic axis space curve. This positioning requires the x_5, y_5 and z_5 offset distances of the centers of the segments as well as projections onto the x_5-y_5 and x_5-z_5 planes of the swept elastic axis line segments. These projections define the sweep angle distributions, Λ_{e_5} and Λ_{f_5}.

2. As shown in Figure 6, the orientations of the elastic axis line segments define the local "6" coordinate system. x_6 is defined parallel to the axis of the elastic axis line segment; y_6 is defined parallel to the x_5-y_5 plane, (+) in leading edge direction; z_6 is orthogonal to x_6 and y_6, (+) in the normally positive thrusting motion. It should be stressed that the result of step 1 is to produce, in addition to the inplane and out-of-plane offsets (Δy_5 and Δz_5) of the elastic axis from the (reference) x_5 pitch axis, a radial foreshortening (x_5) due to the constancy of the total arc length of the elastic axis. This Δx_5 foreshortening is given by the negative of u_e, as developed in the previous section.

3. The blade segments of the blade configuration resulting from steps 1 and 2 are then pitched and twisted about their respective elastic axis line segments (x_6 axis) to restore the blade back to its original built-in, but elastically undeflected position. The pitch and twist angles for each segment are defined relative to the y_6 axis.

4. The blade is then elastically deflected in torsion ($\theta_e = \sum_j \theta_j q_{\theta_j}$) about the built-in space curve elastic axis as defined by $y_{10_{EA}}$ and $z_{10_{EA}}$ to define a first set of "small" incremental y_5 and z_5 deflections.

5. The blade is then elastically deflected in flatwise and edgewise bending (w and v, respectively in the presence of the torsion deflection) to define a second set of small incremental deflections. This second set of incremental deflections is measured in the "6" coordinate system and is governed by the basic G400 deflection correction transformations defined in Reference 1.

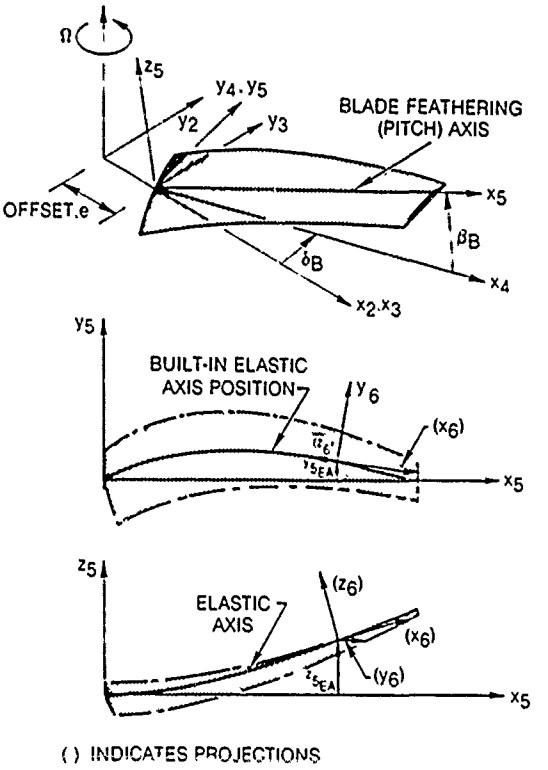


Fig. 6 Schematics of the "5" and "6" coordinate systems.

6. The second set of small incremental "6" coordinate system deflections defined in step 5 is transformed to the "5" coordinate system using an Euler angle transformation derived from sweep angle projections, Λ_{e_5} and Λ_{f_5}, as discussed in above step 1.

7. The results of steps 1, 4 and 6 are then combined to define the total y_5 and z_5 position vector components. These procedures are mathematically described by the following material.

First, the sweep angle projection distributions are defined using the built-in elastic axis line segment changes per segment length, the (invariant) segment arc lengths Δr, together with changes to the projection angles caused by elastic torsion deflection:

$$\Lambda_{e_5} = \sin^{-1}\left\{-\frac{\Delta y_{5_{EA}}}{\Delta r} - \left[\left(\Delta v_{EA_j}^{(2)'} - \Delta V_{EA_j}^{(2)'}\right)\cos\circledast + \left(\Delta w_{EA_j}^{(2)'} + \Delta W_{EA_j}^{(2)'}\right)\sin\circledast\right] q_{\theta_j}\right\} \quad (21)$$

$$\Lambda_{f_5} = \sin^{-1}\left\{\frac{\Delta z_{5_{EA}}}{\Delta r} + \left[-\left(\Delta w_{EA_j}^{(2)'} + \Delta W_{EA_j}^{(2)'}\right)\cos\circledast + \left(\Delta v_{EA_j}^{(2)'} - \Delta V_{EA_j}^{(2)'}\right)\sin\circledast\right] q_{\theta_j}\right\} \quad (22)$$

where $y_{5_{EA}}$ and $z_{5_{EA}}$ are the built-in elastic axis offset changes per segment length. For consistency with the definitions used for other previously defined radial distributions, these spanwise variable quantities are considered to be "derived" quantities calculated from the corresponding quantities defined in the chordwise and thicknesswise directions, $y_{10_{EA}}$ and $z_{10_{EA}}$, respectively. In practice, however, the "5" coordinate system quantities are the more accurately known and the "10" coordinate system quantities are derived using trigonometric resolution with the local built-in pitch angle.

The coordinate system transformation relating the pitch axis ("5") coordinate system with the swept ("6") coordinate system makes use of the sweep angle projections given in Equations (21) and (22):

$$\left\{\Delta X_6\right\} = \left[TAS\right]\left\{\Delta X_5\right\} \tag{23}$$

$$\left\{\Delta X_5\right\} = \left[TAS^{-1}\right]\left\{\Delta X_6\right\} = \left[TAS^{T}\right]\left\{\Delta X_6\right\} \tag{24}$$

where:

$$\left[TAS\right] = \begin{bmatrix} X & -\sin\Lambda_{e_5} & \sin\Lambda_{f_5} \\ \dfrac{\sin\Lambda_{e_5}}{\cos\Lambda_{f_5}} & \dfrac{X}{\cos\Lambda_{f_5}} & 0 \\ \dfrac{-X\sin\Lambda_{f_5}}{\cos\Lambda_{f_5}} & \dfrac{\sin\Lambda_{f_5}\sin\Lambda_{e_5}}{\cos\Lambda_{f_5}} & \cos\Lambda_{f_5} \end{bmatrix} \tag{25}$$

and where:

$$X = \sqrt{1 - \sin^2\Lambda_{e_5} - \sin^2\Lambda_{f_5}} \tag{26}$$

The above development can then be combined to yield the required expressions for inplane and out-of-plane displacement:

$$\begin{Bmatrix} y_5 \\ z_5 \end{Bmatrix} = \begin{Bmatrix} y_{10_{EA}}\cos\theta_B - z_{10_{EA}}\sin\theta_B \\ y_{10_{EA}}\sin\theta_B + z_{10_{EA}}\cos\theta_B \end{Bmatrix}$$

$$+ \sum_{j=1}^{NTM} \begin{Bmatrix} (\Delta v_{EA_j} - \Delta V_{EA_j})\cos\Theta + (\Delta w_{EA_j} + \Delta W_{EA_j})\sin\Theta \\ (\Delta v_{EA_j} - \Delta V_{EA_j})\sin\Theta - (\Delta w_{EA_j} + \Delta W_{EA_j})\cos\Theta \end{Bmatrix} q_{\theta_j}$$

$$+ \left[E\right]\left[TAS^{-1}\right]\begin{Bmatrix} 0 \\ (v_e + \Delta v - \Delta V)\cos\Theta - (w_e - \Delta w - \Delta W)\sin\Theta \\ (v_e + \Delta v - \Delta V)\sin\Theta + (w_e - \Delta w - \Delta W)\cos\Theta \end{Bmatrix} \tag{27}$$

where:

$$\left[E\right] = \begin{bmatrix} 0 & 1 & 0 \\ 0 & 0 & 1 \end{bmatrix} \tag{28}$$

and where v_e, w_e, Δv, Δw, ΔV, ΔW are linear and nonlinear combinations of q_{w_i}, q_{v_k}, and q_{θ_j}, as per the original G400 structural twist formulations (1). Thus, the objectives defined above have been met; the addition of structural sweep is accomplished while retaining the structural twist formulation. The formulation given by Equation (27) together with that for radial foreshortening, Equation (11), extends the kinematic modeling to applications with large structural sweep and moderate structural twist. Note that these formulations are generally quite nonlinear in the elastic modal response variables, q_{w_i}, q_{v_k} and q_{θ_j}.

Eigensolutions vs. Time-History Solutions

As shown in Figure 1, the basic G400 mathematical capability includes both an eigensolution and a time-history solution. Yet, despite the known advantages of eigensolutions, the time-history solution capability was used exclusively and produced results which were probably unattainable using the conventional eigensolution approach. The generally well-identified disadvantages of time-history solutions relative to eigensolutions (for stability calculations) are: (1) The calculation (CPU) time, and hence cost, is at least one order of magnitude greater; (2) the calculations inherently include the integral order forced responses which obscure assessment of the transients, and (3) postprocessing is required to obtain conventional stability descriptors.

The time-history solution, as formulated and implemented in the G400 technology, does not solve essentially linearized equations using an appropriate quadrature algorithm. Rather, the dynamic equations are retained in their nonlinear (implicit) form without recourse to the explicit expansion of loadings (as is typically required for eigensolutions). For the present study, this compact implementation presented clear advantages which outweighed the above identified disadvantages: (1) the accuracy of the basic physical modeling is separated from the issue of selected linearization scheme (mathematical modeling); (2) there is no need to calculate accurate equilibrium trimmed responses (as required for eigensolution linearization schemes), and, most significantly, (3) the compact implicit modeling scheme allows physical modeling modifications to be made easily to the coding and then quickly evaluated. It should be stressed that these advantages are related mostly to research and methodology development issues. For routine production calculations, the cost-effectiveness of eigensolutions is not to be denied. Thus, a synergistic relationship is implied between time-history solution and eigensolution development. The former is the superior physics modeling tool needed by the

latter before the mathematical modeling processes of linearization should occur. Clearly, the former provides an excellent alternate basis for validating the latter, whereas, the latter, once validated provides superior computational resources to the analyst.

Concluding Remarks

The challenge posed by the ITR/FRR Methodology Assessment study to correlate analyses with detailed experimental stability data has borne fruitful advances in the development of aeroelastic methodology. The United Technologies G400 analysis after being upgraded as a result of this study now appears to be well validated. Whereas, some of the reformulations constituting this upgrading are indigenous only to the G400 technology base, others appears to have general applicability to the field of rotor aeroelastics. These reformulations constitute, in part, some new solution techniques for some old problems: the inclusion of vortex-ring state effects into air mass dynamics, the kinematics of radial foreshortening, and a more accurate modeling of tension. More significantly, these reformulations constitute solution techniques for the relatively new problem area posed by combined variable structural sweep and structural twist. These latter reformulations should find useful application to a wide range of advanced rotor craft, such as aeroelastically conformable helicopter rotor blades, advanced technology propellers and propfans.

Rererences

1. Bielawa, R. L., "Aeroelastic Analysis for Helicopter Rotor Blades with Time-Variable, Nonlinear Structural Twist and Multiple Structural Redundancy-Mathematical Derivation and Program User's Manual," NASA CR-2638, February 1976.

2. Bielawa, R. L., "A Second Order Nonlinear Theory of the Aeroelastic Properties of Helicopter Rotor Blades in Forward Flight," Ph.D. Thesis, Massachusetts Institute of Technology, June 1965.

3. Bielawa, R. L., "Aeroelastic Analysis for Helicopter Rotors with Blade Appended Vibration Absorbers - Mathematical Derivations and Program User's Manual," NASA CR-165896, June 1982.

4. Bielawa, R. L., Chi, R. M., Johnson, S. A., and Gangwani, S. T., "Aeroelastic Analysis for Propellers - Mathematical Formulations and Program User's Manual," NASA CR-3729, June 1983.

5. Bielawa, R. L., Cheney, M. C. Jr., Novak, R. C., "Investigation of a Bearingless Helicopter Rotor Concept Having a Composite Primary Structure," NASA CR-2637, October 1976.

6. Sopher, R., and Kottapalli, S.B.R., "Correlation of Predicted Vibrations and Test Data for a Wind Tunnel Helicopter Model," 38th Annual National Forum Proceedings, May 1982.

7. Anonymous, "Integrated Technology Rotor Methodology Assessment - Request for Proposal," NASA Ames Research Center, FRP 2-30221 (BR), September 1980.

8. Ormiston, R. A., and Bousman, W. G., "A Study of Stall-Induced Flap-Lag Instability of Hingeless Rotors," American Helicopter Society 29th Annual National Forum Proceedings, May 1973.

9. Peters, D. A., and Gaonkar, G. H., "Theoretical Flap-Lag Damping with Various Dynamic Inflow Models," Journal of the American Helicopter Society, Vol. 25, No. 3., July 1980.

10. Payne, P. R., Helicopter Dynamics and Aerodynamics, Pitman & Sons, Ltd., London, 1959.

11. Gessow, A., and Myers, G., Aeordynamics of the Helicopter, MacMillan Co., 1952, Republished by Frederick Ungar Publishing Company, New York, 1967.

12. Bisplinghoff, R. H., Ashley, H., and Halfman, R L., Aeroelasticity, Addison-Wesley Publishing Co., Inc. 1957.

13. Bielawa, R. L., "Blade Stress Calculations Mode Deflection vs. Force Integration," Journal of the American Helicopter Society, Vol. 24, No. 3, July 1978.

DISCUSSION

AEROELASTIC MODELING OF ROTOR BLADES WITH SPANWISE VARIABLE ELASTIC AXIS OFFSET--CLASSIC ISSUES REVISED AND NEW FORMULATIONS

Richard L. Bielawa

Bob Ormiston, Aeromechanics Laboratory: Basically to repeat the question I had yesterday, the new results shown there [Figs. 3(a) and 3(b)] presumably have symmetrical airfoil data and symmetrical inflow data, but they show an asymmetry in the results. I presume you've got the gravity term in that calculation.

Bielawa: Yes, it is a time-history analysis so it's automatically there.

Ormiston: But is that the total reason for the asymmetry in the results?

Bielawa: I believe so.

Ormiston: It never appeared anywhere near that large in the calculations we did. It's not a major effect but it's still there. If all these terms are all straightened out, then what's going on?

Bielawa: As you can see, the effect I described was very powerful in raising this up.

Ormiston: Forget about the dotted line [just consider the solid one].

Bielawa: Well, the point I'm trying to make is that this curve was raised because of what would appear to be a rather subtle modification to the inflow.

Ormiston: That's the next question. Is that change totally due to the inflow formulation change?

Bielawa: This aspect of it, I think, was.

Ormiston: You didn't run a case that showed just the effect of the inflow change?

Bielawa: No. The point I was trying to make is that what would appear to be a rather subtle effect had a big effect on the steady bending.

Ormiston: How many percent on the steady bending?

Bielawa: I can't give you an answer for that. Yes, Wayne?

Wayne Johnson, Session Chairman: Could you say a little bit more about what you did to track down what needed to be changed? How did you identify the candidates?

Bielawa: Yes I spent a lot of time with Case [A/3] and Case [A/5]. I knew that they had to give the same answer and a lot of the things I did with trial and error were to make those two cases honestly the same, without putting in any fudge factors. I learned a lot from those cases. I learned a lot from Case [A/6].

Peretz Friedmann, UCLA: I just wanted to mention that I believe that that dynamic torsional-excitation term, which you have massaged using the integration by parts to get that relatively long expression, is a consequence of the fact that you are patching an old formulation. You don't have a basically inherently nonlinear formulation where you distinguish between the undeformed and deformed coordinates, because if you had such a formulation this patching or correlation would not be required. Is that true or am I wrong?

Bielawa: Well, as I interpret your question, it's a separating out of the nonlinear terms in the torsion equation. In conversation we have identified some other deficiencies in the elastic representation of the torsion. The nonlinear terms I'm alluding to here are the ones that people typically associate with the ΔEI; bending out-of-plane with in-plane loads and bending in-plane with out-of-plane loads.

COMPARISON OF EXPERIMENTAL ROTOR DAMPING DATA-REDUCTION TECHNIQUES

William Warmbrodt
NASA Ames Research Center, Moffett Field, CA

Abstract

The ability of existing data reduction techniques to determine frequency and damping from transient time-history records was evaluated. Analog data records representative of small-scale helicopter aeroelastic stability tests were analyzed. The data records were selected to provide information on the accuracy of reduced frequency and decay coefficients as a function of modal damping level, modal frequency, number of modes present in the time history record, proximity to other modes with different frequencies, steady offset in the time history, and signal-to noise ratio. The study utilized the results from each of the major U.S. helicopter manufacturers, the U.S. Army Aeroflightdynamics Directorate, and NASA Ames Research Center using their inhouse data reduction and analysis techniques. Consequently, the accuracy of different data analysis techniques and the manner in which they were implemented were also evaluated. It was found that modal frequencies can be accurately determined even in the presence of significant random and periodic noise. Identified decay coefficients do, however, show considerable variation, particularly for highly damped modes. The manner in which the data are reduced and the role of the data analyst was shown to be important. Although several different damping determination methods were used, no clear trends were evident for the observed differences between the individual analysis techniques. From this study, it is concluded that the data reduction of modal-damping characteristics from transient time histories results in a range of damping values. This degree of uncertainty should be considered in interpreting experimental data trends, and when performing correlation with analytical predictions.

Notation

$\|F(\omega)\|$	Fourier transform magnitude at frequency
t	time, sec
ζ	critical damping coefficient (rotating system)
ζ_k	inplane motion measurement signal for kth blade
ζ_{1c}	cosine multiblade inplane measurement
σ	modal decay coefficient, 1/sec
Ω	rotor rotation speed, rad/sec
ω	modal frequency, rad/sec

Introduction

The ability of the helicopter designer to develop new rotor systems with acceptable aeroelastic stability characteristics is dependent on the use of accurate analyses to predict rotor dynamic behavior. For new bearingless-rotor-system configurations, these analyses have yet to demonstrate an ability to accurately predict rotor stability for configurations that are major departures from the previous designs. To evaluate the accuracy of these prediction methods, carefully obtained experimental data are required to provide a database for correlating and validating these analyses. In other cases, when rotor designs are proposed that go beyond the current analysis capability, experimental programs are sometimes the only means for evaluating the design concept. In light of these considerations, the use of experimental data obtained from model rotor systems is important to the understanding and prediction of rotor system dynamic behavior.

Although numerous experiments have been performed to provide aeroelastic stability data on advanced rotor-system designs and to establish a database for validating analytical prediction methods, little work has been performed to quantify the capability of the experimental process to acquire accurate aeroelastic stability data. A number of factors contribute to the experimental process: design and fabrication of the models; verification of the system's design parameters (stiffnesses, inertias, dampings); model operation; instrumentation and quality of data signals; data acquisition; data reduction and analysis. This entire process must be carefully carried out to ensure the reduced data from the test program adequately establish system stability levels, allow for accurate determination of stability trends with operating condition and parametric variations in the test configuration, and can be used for correlation with analysis.

It is widely recognized that the experimental determination of aeroelastic stability from model and full-scale helicopter rotor dynamic systems is statistical in nature. Even when given the most carefully controlled experiment, the determination of aeroelastic stability characteristics (modal frequency and damping) is not exact. Different data records taken at the same operating conditions typically yield repeatable modal

Presented: ITR Methodology Workshop, NASA Ames Research Center, Moffett Field, CA June 1983.

frequencies yet give different modal damping values. Many researchers acknowledge this variability by reporting the results from several different data records, each obtained at the same operating conditions. Such an approach establishes the inherent variability in the data resulting from the entire experimental process (model operation, data acquisition, data reduction, and data analysis). However, such an approach does not provide any indication from where this variation comes. If the sources could be identified, it is possible that appropriate steps could be taken to ensure minimal impact of these factors in the final results.

In addition, this approach also implies that, for each data record being analyzed, there is only one corresponding frequency and damping value. This concept of uniqueness is shown in this study to be incorrect.

This study attempts to evaluate the importance of the data reduction and analysis steps in establishing the variability (or the confidence limits) in rotor aeroelastic stability determinations. This study is limited to the specific applications of data reduction and analysis techniques used within the helicopter technical community. Some of the factors that influence the statistical aspects of experimental stability data are identified and evaluated.

Objectives of Study

This study concentrates exclusively on the techniques currently being used within the rotorcraft community to reduce and analyze small-scale helicopter rotor stability data from transient time histories. The approach used removed the uncertainty associated with the model design and fabrication, the definition of its physical parameters, or its operation since the starting point of this study was analog data records which were taken from various experiments. Each analyst was provided the same information. Consequently, this study considers only the data reduction and analysis steps and their impact on the final, reduced aeroelastic stability parameters. The objectives of the current study are:

1. Evaluate various data reduction techniques used to determine aeroelastic stability characteristics.

2. Determine the importance of the analyst and his techniques in reducing experimental data records.

3. Investigate and attempt to quantify the effects of different test variables on the data reductions and analysis process, including

   a) rotor-system damping level

   b) type of measurement signal analyzed

   c) proximity of other modes to the mode of interest

   d) signal-to-noise levels

4. Establish a degree of confidence in identified stability characteristics for aid in interpreting level of correlation with analytical predictions.

This study was undertaken in support of the Integrated Technology Rotor (ITR) Methodology Assessment program. The results of this study establish a perspective regarding the conclusions of the ITR correlation activity and, in fact, any aeroelastic stability correlation activity. This study also yields a better engineering appreciation of the inherent statistical nature of experimental aeroelastic stability data. In doing so, it establishes the degree of correlation that one can expect from the use of these and similar experimental data when comparing with analytical predictions.

Approach

The approach used in this evaluation of experimental helicopter rotor inplane stability characteristics was to have several organizations, each using their own data reduction and analysis techniques, determine the inplane modal frequency and damping values from 30 experimental data records. The data were provided to each analyst on an FM analog tape (tape speed 7.5 ips; carrier frequency of 13.5 KHz). Data records were between 6 and 15 sec in length. All data records were from resistance-type strain gages installed at the rotor-blade root. Maximum half peak-to-peak voltage was approximately 2 volts for each record. The data time histories were on only one data track, with a second track used as a voice channel to aid in data reduction. The documentation provided with the analog tape identified the location on the tape of each data record, its length, and the approximate modal frequency of interest for analysis.

All of the transient time history data records were acquired in small-scale helicopter rotor tests. Model rotor operation was between 550 and 1100 rpm for the cases selected. The data records were inplane (lead-lag or chordwise) strain-gage measurements. Data were used from soft inplane ($\omega < \Omega$) and stiff inplane ($\omega > \Omega$)

rotor configurations. Single-blade measurements, as well as combined or multiblade measurements, were included in this study. Data from both isolated rotor and rotor/body models were also included in the study. Therefore, the analyst had to analyze modal characteristics from approximately 1 to 23 Hz.

The 30 data records provided each analyst were not identified with any particular rotor system, test configuration, or experiment. No information was provided on the dynamic characteristics of the rotor model used for the data records. The data records were put in random order to further reduce attempts by the analyst to assume information regarding each data record. No information was given on the type of data channel or measurement signal being analyzed. In addition, neither the type of transient excitation used nor the rotor operating condition were specified so the analyst could not a priori eliminate signal components exclusively caused by rotor excitation, rotation effects, or other modes.

The experimental data used were taken from several model helicopter rotor tests reported previously.[1-5] These data sets are listed in Table 1. Three of the data sets included data from rotor configurations used in the ITR Methodology Assessment program.[6] The last two were chosen as representative of a current, advanced bearingless-rotor configuration with a full-scale counterpart (unlike the other three rotors which were designed, in part, to acquire data on idealized rotor hub configurations). The test conditions at which the data were obtained are given in Table 2. These test conditions are considered representative of the data acquired in each test program.

Each data set was chosen for several reasons which are summarized in Table 3. These rotors and the operating conditions allowed the study to consider a range of rotor modal frequencies and damping levels, and signal background noise levels (both random and periodic). The sources of signal contamination shown in Table 3 are other modes (coupled rotor/body configurations versus isolated rotor configurations), random noise superimposed on individual signals in addition to the background noise in the baseline signal (data set 4), and periodic noise due to excitation of the rotor system in forward flight. The use of different signals in data set one was evaluated when time histories for ζ_1, ζ_2 and $(\zeta_1 - \zeta_2)$ were analyzed for the same test condition. Variable frequency refers to evaluating the modal frequency and damping parameters with a variation in the rotor-rotation rate which results in changing modal frequencies. The data acquired near resonant conditions for these systems provided the opportunity to investigate the influence of modal frequency proximity in the time history. Only one data set (number 3) had a mean offset in each analog record of approximately -1 volt. All other data records had steady offsets less than ±0.2 volt.

Analysis

Each organization participating in this study was encouraged to use the data reduction and analysis techniques that would provide their best determination of identified frequency and damping levels from the analog time histories. The techniques used by each organization are listed in Table 4. Only two digital transient time history data analysis techniques were used: the moving block analysis and Prony's method. Although both analyses assume sinusoidal exponential decay of linear, second order systems, the Prony method can specifically account for several degrees of freedom in the time history, each at its own frequency with its level of damping. The moving-block analysis uses the identified modal frequency and then analyzes the decaying time history for the single degree-of-freedom mode at that frequency.

The moving-block analysis technique[7] assumes that the decaying transient time history is a viscous and lightly damped, single degree-of-freedom sinusoidal signal. The modal frequency, ω, is first identified within the decay portion of the record typically using an FFT. Using this frequency, a discrete Fourier transform of the decay signal is calculated using only a portion, or block, of the sample record. This calculation is performed for a number of blocks moving through the decay record with each block having the same number of discrete data points. The natural logarithm of the Fourier coefficient magnitude at the analysis frequency, $|F(\omega)|$ is then plotted versus time where the time is given by the location in the original record where the analyzed block of data begins. This yields

$$\begin{aligned} \text{Slope} &= \ell n|F(\omega)|/dt \\ &= \sigma \\ &= -\zeta\omega \end{aligned}$$

From this definition, the decay coefficient σ is negative and the critical damping coefficient ζ is positive for a stable mode.

It should be noted that, although five organizations used the moving-block analysis, because of the hardware systems and the preferences of the individual analysts, each implementation of the moving-block process was different. These differences in implementation, as well as the role of the analyst in the data analysis process, are the sources of disagreement between the organizations

that used the moving-block approach in the resultant identified modal parameters. One objective of this study is to quantify these differences in the final identified frequency and modal decay coefficients.

Bell Helicopter used the Prony method to analyze the transient time histories.[8] This method treats the time history as a sum of complex exponential functions. The roots and coefficients of a difference equation are solved directly for an m-order model from a set of 2*m equations using 2*m discrete data points; approximate coefficients and roots can be determined using more that 2*m data points via the method of least squares. For this study, the model order was chosen to be 20.

A third analysis technique was employed in this study, a nondigital data analysis using a measurement of the time-to-half amplitude from a hard copy of the time history. This hand analysis of the data records is similar to the data analysis approach used prior to 1970 and the advent of digital data analysis for aeroelastic stability determinations.

Further detail on the specific implementation of the data reduction and analysis steps from each participating organization is presented below. One organization used analog prefiltering prior to digitization; no organization utilized digital filtering subsequent to digitization.

U.S. Army Aeroflightdynamics Directorate: The moving-block program analyzed up to 5 sec of data digitized at 100 Hz. A fine resolution of the modal frequency for analysis was determined using Goertzel's algorithm. Typically, the block size was set to approximately one-fourth the edited signal length.

NASA Ames Research Center: The moving-block program analyzed 1024 samples of digitized data. In general, a sampling frequency of 128 Hz and a record length of 8 sec were used. In cases where the transient data record was greater than 8 sec, a sampling frequency of 64 Hz with a 16 sec record length was used.

Hughes Helicopters, Inc.: Approximately 15-sec data records were acquired at a 1000 Hz sampling rate. The modal frequency was determined by choosing an appropriate harmonic number for the Fourier transform, and then slightly varying the edited time segment length. For the moving block, block size was chosen to yield about 50 blocks for the edited time segment, and typically, only every other point within the block was used.

Bell Helicopter Co.: In the Prony method, a maximum of 20 individual modes were used in the analysis to represent the time history. The calculated time history was visually compared to the actual data record for satisfactory agreement. The sampling rate was 256 samples per sec. Typically, only a few seconds of data were analyzed.

Boeing Vertol Co.: Digitized data records were acquired at a sampling rate of 500 Hz. Typically a 4-sec portion of the transient decay record was utilized in the moving block analysis. Usually a one-half block size was used without neglecting any data points within the block.

Sikorsky Aircraft: The data reduction and analysis was performed at the West Palm Beach flight test facility. The analog data were low-pass filtered with a cut-off frequency of 30 Hz. The data were then sampled at 250 Hz. The moving block program allowed for 512 digitized samples. In general, only every other point was used in the analysis.

General Discussion

There are a number of factors which should be considered in interpreting the results of this study. These factors were identified prior to and during the conduct of the program. They are summarized below.

(1) Data records were of varying quality. This is representative of virtually any aeroelastic stability test program. The length of each individual data record was between 6 to 15 sec long. This required selection of various record lengths for data analysis. The level of excitation and modal damping resulted in a range of transient decay time histories from clear, several-second-long exponential decay records to relatively rapid signal reductions to the baseline level. The signal-to-noise levels were different for each record and were, in fact, deliberately increased in several records to evaluate the influence of background noise on the analysis process.

(2) The data records did not explicitly provide information on when forced excitation was terminated. Although the time histories were intended for transient decay analysis, several records did include portions of forced response at the beginning of the time history. The forced response was obtained by either fixed system excitation or with sudden changes in blade pitch. It was left to the data analyst to select that portion representing exponential decay of the data record for analysis. Incorrect selection of a portion of the record (which included forced response) would result in incorrect damping determinations. This could have been overcome by providing the analyst a second data track which

indicated both the nature of the system excitation and when it was terminated. However, each record was carefully chosen to allow for a reasonable portion of the data record to be easily observed as the decaying transient time history portion. Consequently, this should not have impacted the reduced damping determinations when appropriate care was taken.

(3) The analyst had no familiarity with how the data were obtained. This meant that the analyst could not use his familiarity with the rotor model, how the data were acquired, or the anticipated modal characteristics to guide him in his analysis. Consequently, the analyst could rely only on his analysis techniques and experience in obtaining the modal characteristics from these records. To avoid making the modal identification process too difficult, the analyst was provided the approximate modal frequency for the analysis for each data record.

(4) The dynamic system being tested was not a linear single degree-of-freedom system. Like most aeroelastic systems, the models tested could not be fully characterized as a linear system. As such, the transient time history decay records could not be perfectly modeled as a linear system exponential decay over the entire transient record. This is an inherent problem of helicopter aeroelasticity. However, in implementing the data analysis, the analyst must recognize the limitations of the process and obtain the best estimate of the equivalent linear system. This often requires evaluating the data record where the transient amplitudes are likely to have only linear damping characteristics. Likewise the presence of many modes in the data record must be best addressed through the data reduction and analysis process. For this study, each analyst attempted to identify the equivalent linear system frequency and damping characteristics of the fundamental rotor inplane bending mode.

(5) The data record used were not necessarily those analyzed in prior publications documenting that specific test. The first three data sets identified in Table 1 were taken from the data tapes acquired in the experiments used for the ITR Methodology Assessment program. Data sets 1, 2, and 3 correspond to configurations A/4, C/3, and D/1, respectively. During the test programs, numerous data records were acquired at each test condition, and only a portion of those were reduced and analyzed to document the systems behavior. Consequently, the individual data records for data sets 1, 2, and 3 may or may not have been analyzed and are included in the results presented in Refs. 1-3. However, each record that was analyzed as part of this study from data sets 1, 2 and 3 should be considered to be fully representative of these data, and can be used for direct comparison with published results.

In interpreting the results from this study, the variability in the identified damping from one single data record was not accounted for in the published results of Refs. 1-3. Rather, the variability, or scatter, in these references are due exclusively to the range of individually determined damping levels obtained through the analysis of several different time history data records. Each of these tests used the U.S. Army Aeroflightdynamics moving- block analysis described above for data reduction and analysis. The data records used for data sets 4 and 5, in this study were, in fact, those analyzed and reported in Refs. 4 and 5 respectively. The reduced modal damping levels given in Ref. 4 were obtained from hand analysis of strip-chart records. Reference 5 used the Prony method described above.

Results

The results from this study are the determinations of the modal frequencies and damping values of the time history data records. The legends on each frequency and damping figure identify the organization providing this result (see Table 4 for the key). Every organization provided results for each data record except where noted. No identified modal frequency results are presented for the hand analysis NASA(H).

The first results are presented in Figs. 1, 2, and 3 for data set number one, isolated hingeless rotor experiment (Table 1). The operating condition is 1000 rpm. Collective pitch is varied between 0° and 8°. The measurement signals analyzed were obtained by subtracting the inplane bending moment signal of blade 2, ζ_2, from the inplane bending moment signal from blade 1, ζ_1. The identified inplane modal frequency is shown in Fig. 1. Because of the relatively low background noise levels for this two-bladed rotor in hover, frequency determinations are very consistent with less than 2% variation from the mean identified frequency. These small variations are, in part, due to frequency resolution of the particular data reduction technique. The corresponding damping determinations from each analysis is shown in Fig. 2a. For the 4° collective pitch operating condition, only three analyses were able to identify the modal damping level for the mode at 21.4 Hz. There is little scatter in the reduced results. However, variability in the decay coefficient σ of 0.3 to 0.4 sec^{-1} for the records with $\sigma < 0.5$ sec^{-1} exists. For these records, a unique damping value does not exist. In general, there was less variation in the identified damping for the lower damped cases. When the system is slightly stable (collective pitch of 4°) there is

virtually no variation in the identified damping. However, when the system is determined to be slightly unstable at a collective pitch of 6°, there is greater variation in the identified decay coefficient. Consequently, the observation that damping can be most accurately determined for lower damped systems does not apply for small negatively damped systems.

Comparing the results of this study with those of Ref. 1 (in Fig. 2b) show the same trend with increasing collective pitch. The thin band shows the range of all the identified decay coefficients for that data record; the heavy band is obtained by neglecting the smallest and largest identified decay coefficient. Eliminating the extreme values results in a significant reduction in the scatter of the reduced data, particularly for highly damped conditions. However, this is not justifiable given that each analysis is indeed correct. It is important to note that, for this data set as well as for the others in this study, it is not possible a priori to identify which analysis will yield an extreme value. Neglecting the largest and smallest values is an attempt to reduce the scatter from the decay coefficient values identified in this study, and to provide smaller ranges of estimates of the decay coefficient for comparison with published results. Also shown in Fig. 2b are the identified decay coefficients AA which represent a second attempt at evaluating damping with the same data reduction technique used in Ref. 1. The data analyzed in this study were not necessarily those actually analyzed and reported in Ref. 1, and yet should be considered to be representative. The AA results from this study agree very well with the previously published results. From these comparisons, damping determinations in this study are generally greater than those published, except at 8° collective pitch. Data scatter is representative of the range of published data. In this study, the inplane mode was found to be stable at 4° collective pitch unlike Ref. 1.

Data set number one, which has been studied in Figs. 1 and 2, is from a stiff-inplane, two-bladed rotor with a dimensionless lead-lag frequency approximately 1.5 times the rotor rotation rate. Although the data presented in Figs. 1 and 2 used a signal which was obtained by subtracting the inplane motion of the second blade from the motion of the first blade ($\zeta_1 - \zeta_2$) to provide accurate isolated blade behavior, this study also evaluated the use of the individual inplane motions of each blade (ζ_1 and ζ_2) for comparison to determine sensitivity to the measurement signal. The results of this comparison for one data point is shown in Fig. 3. This comparison is for the operating condition shown in Figs. 1 and 2 at a 2° collective pitch and 1000 rpm. The scale of the vertical axis is expanded from that in Fig. 2 to show more detail. From these results, it is noted that less scatter is obtained when using the inplane motion measurement from a single blade then for the ($\zeta_1 - \zeta_2$) measurement. The results also indicate that the signal quality from blade number 2 was perhaps better than that from blade number one. It is not surprising then that a signal composed by combining the two signals results in a signal yielding at least as much scatter as the poorest quality signal. In this case, the variation in the identified decay coefficient from the combined signal is approximately 100% greater than that using the number one blade measurement directly.

The results for data set number two are shown in Figs. 4 and 5. This data set is for a coupled hingeless rotor/body system with the rotor operating at 9° collective pitch. The measurement signal is the multiblade coordinate signal ζ_{1c} which is obtained by appropriately combining the inplane measurement signal from each of the three rotor blades. Figure 4 shows the identified modal frequency from the time history record. This data set has very low modal frequency values ($\omega/2\pi < 6$ Hz) , significantly different than the modal frequency values of data set number one ($\omega/2\pi > 21$ Hz) . The ability to determine the modal frequency as a function of rotor rotation rate is satisfactory. The greatest scatter is at the lowest modal frequency.

Figure 5a shows the variability in the identified decay coefficient for the results from this study. Again, the higher damped conditions show greater scatter. This is evident from a comparison of 550 rpm (0.7 sec^{-1} scatter) and 900 rpm (1.5 sec^{-1} scatter) operation. The reason for the data scatter at 600 rpm is due to one single high damping estimate. The identified decay coefficient at 600 rpm without this one high value would be more reasonable since it would then be comparable to the data scatter at 650 and 700 rpm (which has the same level of damping). Similar to the results from data set one, the scatter for small, negatively damped decay coefficients is relatively large. From this data set, for the majority of data records, a unique, single value for the decay coefficient cannot be determined. This characteristic is present in all the data sets. The results of this study are compared with published results in Fig. 5b. Once again, the heavy band shows the range of identified decay coefficients with the smallest and largest estimates neglected. Only for operation at 600 and 900 rpm do the decay coefficient extreme values significantly increase the data scatter. In general, highly damped cases show significantly more scatter than the published results. Yet, for all conditions where the decay coefficient is

≥ -1.0 sec^{-1} good correlation is shown, except for operation at 650 rpm. Here, the results of this study, although showing very little variation between each analysis, are less damped than are the published results. The results AA are also plotted on the figure which represent a second analysis of the data from this test using the same data reduction technique as that used in Ref. 2. The AA analysis is consistent with the other analyses of this study, and significantly deviate from the published results only at 650 rpm.

The results for data set number three are shown in Figs. 6 and 7. The three-bladed rotor is operating at 1100 rpm in hover and collective pitch is varied from -4° to +4°. For this data set the measurement signal is the inplane bending moment of one blade. Since these results are also for an isolated inplane rotor blade model, the variability in the reduced modal parameters for this data set are somewhat similar to those obtained from data set one. As seen from Fig. 6 there is very little discrepancy in the identified modal frequencies between each separate analysis. Even when differences exist, the variability is only about 2% of the mean value. The identified modal decay coefficients (Fig. 7a) show scatter, again, particularly for the highest damped operating conditions. Note the extreme variation at -4° collective pitch. This degree of variability is easily the largest from this study, and occurs for the highest damped operating condition used. It is a bit surprising that the variability is relatively small for -2° collective pitch, yet this is not unlike the results from data set number two.

The results of this study are compared with published results in Fig. 7b. Again, the thin band shows the range of all the identified decay coefficients for that data record, and the heavy band is obtained by neglecting the smallest and largest identified decay coefficient. Also shown are the AA results which again represent a second analysis of the data record (using the same analysis technique as in Ref. 3). Except for the larger amount of variability of the identified damping from this study, the correlation with the published results is good. The trend with increasing collective pitch is obtained. For each operating condition, the extreme identified decay coefficients do increase the range of identified values. Basically, the results from this study would seem to indicate a greater degree of scatter than that given from Ref. 3 for numerous, repeated stability, data records. The agreement between AA and the published results of Ref. 3 is very good.

The results for data set four are shown in Figs. 8, 9, and 10. This data set is for a one-fifth scale model of the Model 680 bearingless rotor system with representative body degrees of freedom. Data records for constant thrust operation (222 N) in hover were analyzed and the identified frequencies are shown in Fig. 8. These results are completely consistent with the frequency determinations of each of the previous data sets. The modal decay coefficients shown in Fig. 9a, however, show somewhat more scatter than do the previous three. If the one single high decay determination for 780 rpm is excluded, the amount of variability in the identified damping for operation at 700, 780, 850, and 950 rpm is almost constant. For this data set, very low damping values ($\sigma > -0.5$ sec^{-1}) still, surprisingly, yield considerable scatter unlike the previous three data sets. This may be due to the overall quality of the analog data records obtained during this experiment. Figure 9b shows the correlation between this study and the published results of Ref. 4. These results were obtained using hand analysis of hard copy records. In general, reasonable correlation is obtained although the higher damped operating conditions seem to have their damping underestimated in Ref. 4, and the extreme identified damping values significantly increase data scatter at 780 and 950 rpm. Figure 9c shows the comparison of hand analyzed results[4] with the digitally reduced values using the Prony method (BELL) from the same organization, and the hand analyzed results from this study. It is clear that, although the general trends are the same, the use of the two different analysis techniques can result in different identified damping levels. This is consistent with the results of this study. Also, the good agreement (except at 850 rpm) between the two hand analyses indicate less variability between non-digital techniques than between digital techniques.

An investigation of the influence of signal-to-noise ratio was done in this study by superimposing random noise on the baseline time history record of data set four for 850-rpm rotor operation. For this study, the baseline data record was analyzed, then records with first 0.1 volt RMS noise, and then with 0.2 volt RMS noise superimposed on the original baseline data record were analyzed. In both instances, the RMS noise had 0.1 to 50 Hz frequency content. The three time history data records are shown in Fig. 10 with each record's frequency spectra. The vertical scales of the time history plots (Fig. 10a) are arbitrary. The inplane modal frequency was approximately 10 Hz for this operating condition. The 0.2 volt RMS noise masks much of the transient decay record. The noise reduces the transient

time history decay noticeably, yet the digital data analysis techniques easily extracted the proper frequency information (not shown). The identified decay coefficient results shown in Fig. 11, on the other hand, show considerable variability which significantly increases with greater noise level. A five-fold increase in data scatter owing to the introduction of the broadband noise is noted for the 0.2 volt RMS noise case. This noise level has virtually no affect on four of the data analyses, including the nondigital analysis and the analysis where the analog data were low pass filtered below 30 Hz prior to digitization. (It is not understood why the BELL or HHI analysis showed particular sensitivity to the noise level.) These results are sufficient to demonstrate the sensitivity of the data reduction and analysis programs to background noise levels.

The results for data set number five are presented in Figs. 12 and 13. Data set number five is for the same fifth-scale Model 680 system used in data set number four, however, the transient time histories were acquired for forward flight operating conditions at 750 rpm. This results in significant periodic noise (1P frequency spectra amplitude up to three times the modal frequency amplitude) present at the rotor rotation rate (12.5 Hz) in the data record which do not decay with the transient fundamental inplane mode motion. Again, the measurement signal is for the inplane motion of one blade. The ability to determine modal frequency is evaluated in Fig. 12. Although the hover condition shows significant scatter (poor quality data record), the inplane frequencies were easily determined with little variability for forward flight.

The identified decay coefficient from this study are shown in Fig. 13a. Except for the exceptionally large data scatter in hover (perhaps owing to poor excitation of the rotor inplane motion which also resulted in poor modal frequency determination), the variability in the damping is somewhat greater than that obtained in the hover results of Fig. 9. The variability itself does not seem to increase with forward speed. The hand analysis results are, once again, as accurate as the digital data analysis techniques, even for forward flight. This is a general observation from each data set. However, it should be noted the use of digital analysis techniques has the advantage of accurate modal frequency determination, a consistent step-by-step procedure for analysis of various data records, and is anticipated to have less dependence on the experience level of the analyst.

In Fig. 13b comparison with the results presented in Ref. 5 are made with the results in the present study (again, the range of identified values with the extreme data points removed is the heavy band). In general, the correlation is good, except this study would seem to indicate the rotor system is slightly less damped. The same trends with forward flight were observed in this study as in Ref. 5. Lastly, an interesting comparison is made in Fig. 13b between the results of this study and those taken from Ref. 5. Since the data reduction process in Ref. 5 used the same identical data record as was used in this study, it is interesting to compare the published results with this study using the values obtained with the same Prony method for data reduction. Here the differences would be related to the manner in which the two analysts (using the same digital analysis) performed the data reduction and analysis steps. Although for each set of results, the same gross trends are obtained with operating condition, the results of this study show a much greater degree of stability in hover, and do not show a stabilizing effect at high advance ratio. It is clear that the role of the analyst is important in determining the reduced damping parameters, even when identical data reduction techniques are employed.

Conclusions

This study has attempted to quantify the degree of variability in analyzing transient time history data records. The inherent variability in this analysis process establishes a guideline for the degree of correlation one can expect in comparing analytical predictions with experimental data. For a single data record there is no one correct decay coefficient. Although modal frequency can often be established for good signal-to-noise data records, identified modal damping values are inherently statistical and nonunique. The specific conclusions from this study are:

1. Identified modal frequencies showed very little variation except for poor quality data records.

2. Identified decay coefficients do show considerable variation, particularly for highly damped modes with the decay coefficient magnitude greater than 1.0 sec^{-1}.

3. Variability in the identified decay coefficients is dependent on the damping level:
   a) Lightly damped modes ($\sigma > -0.5$ sec^{-1}) have approximately 20% scatter band (±10%).
   b) Heavily damped modes can have greater than 50% scatter band (±25%).

4. No clear trends were evident for observed differences between the individual techniques.

5. The quality or signal-to-noise level of the data record is critical to accurate determination of the modal decay coefficient.

Acknowledgment

The author is indebted to many individuals for their contributions to this study: W. Bousman, D. Sharpe, and S. Dawson of the U.S. Army Aeroflightdynamics Directorate; R. Peterson and W. Johnson, NASA Ames Research Center; F. Straub of Hughes Helicopters, Inc.; P. Teare and F. Tarazanin of Boeing Vertol; J. Yen of Bell Helicopter Company; and R. Sopher and J. Milgram of Sikorsky Aircraft. Special acknowledgment is given to Mr. John Davis, U.S. Army Aviation Research and Technology Activity, and Dr. Robert Ormiston, U.S. Army Aeroflightdynamics Directorate, for their assistance in implementing this study.

Reference

[1]Sharpe, D. L., "An Experimental Investigation of the Flap-Lag-Torsion Aeroelastic Stability of a Small-Scale Hingeless Helicopter Rotor in Hover," NASA TP 2546, Jan. 1986.

[2]Bousman, W. G., "An Experimental Investigation of the Effects of Aeroelastic Couplings on Aeromechanical Stability of a Hingeless Rotor Helicopter," Journal of the American Helicopter Society, Vol. 26, No. 1, Jan. 1981, pp. 46-54.

[3]Dawson, S., "An Experimental Investigation of a Bearingless Model Rotor in Hover," Journal of the american Helicopter Society, Vol. 28, No. 4, Oct. 1983, pp. 29-34.

[4]Weller, W. H., "Correlating Measured and Predicted Inplane Stability Characteristics for an Advanced Bearingless Main Rotor," NASA CR166280, Jan. 1982.

[5]Weller, W. H., "Correlation and Evaluation of Inplane Stability Characteristics for an Advanced Bearingless Rotor," NASA CR166448, May 1983.

[6]Proceedings of the Integrated Technology Rotor Methodology Workshop, Ames Research Center, Moffett Field, CA June 21-22, 1983.

[7]Hammond, C. E. and Doggett, R., "Demonstration of Subcritical Damping by Moving Block/Randomdec Applications," NASA SP-415, Oct. 1975, pp. 59-76.

[8]Hildebrand, F. B. Introduction to Numerical Analysis, McGraw Hill, New York, 1974, pp. 457-462.

Table 1 Data set identification used in study

Data Set Number (Ref. no.)	Rotor Config.	ITR Config.	Body Modes	Number of Blades	Measurement Signal
1	Hingeless Rotor	A4	No	2	$\zeta_1 - \zeta_2$, ζ_1, ζ_2
2	Hingeless Rotor	C3	Yes	3	ζ_{1c}
3	Bearingless Rotor	D1	No	3	ζ_1
4	Bearingless Rotor	--	Yes	4	ζ_1
5	Bearingless Rotor	--	Yes	4	ζ_1

Table 2 Test conditions for each data set in study

Data Set Number	Rotor Config.	RPM	Collective Pitch, deg	Advance Ratio	Shaft Angle, deg
1	Hingeless Rotor	1000	0 2* 4 6 8	0	0
2	Hingeless Rotor	550 660 650 700 770 810 850 900	9	0	0
3	Bearingless Rotor	1100	-4 -2 0 4	0	0
4	Bearingless Rotor	650 700 780 850** 950	Set to provide 222 N lift	0	0
5	Bearingless Rotor	750	Set to provide 222 N lift	0 .05 .15 .24	0 -1 -3 -5

* Three different signal used.
** Two different levels of superimposed noise used.

Table 3 Summary of characteristics of each data set

Data Set	Signal Contamination			Different Signals	Freq. Variable
	Other Modes	Random Noise	Periodic Noise		
1	No	No	No	Yes	No
2	Yes	No	No	No	Yes
3	No	No	No	No	No
4	Yes	Yes	No	No	Yes
5	Yes	No	Yes	No	No

Table 4 Summary of analysis techniques used

Organization	ID	Type of Analysis
U.S. Army Aeroflightdynamics Directorate	AA	Moving Block
NASA Ames Research Center	NASA(MB) NASA(H)	Moving Block Hand Analysis
Hughes Helicopters, Inc.	HHI	Moving Block
Bell Helicopter Company	BELL	Prony Method
Boeing Vertol	BV	Moving Block
Sikorsky Aircraft	SA	Moving Block

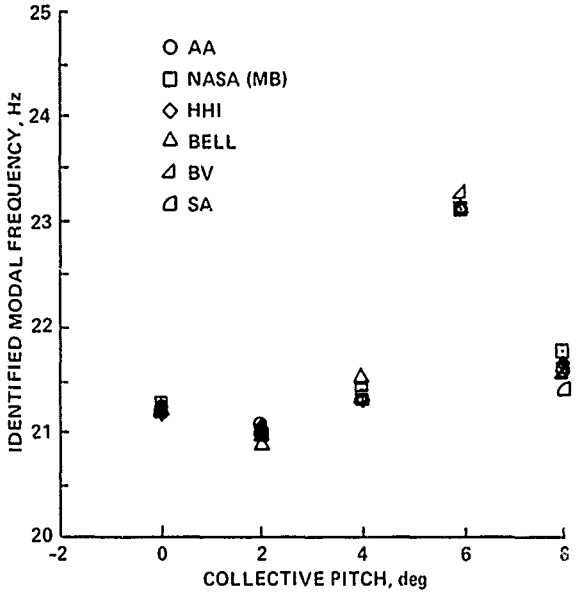
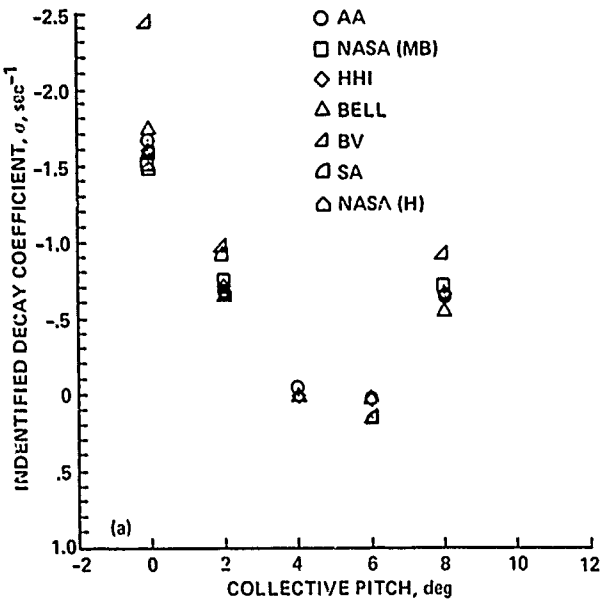
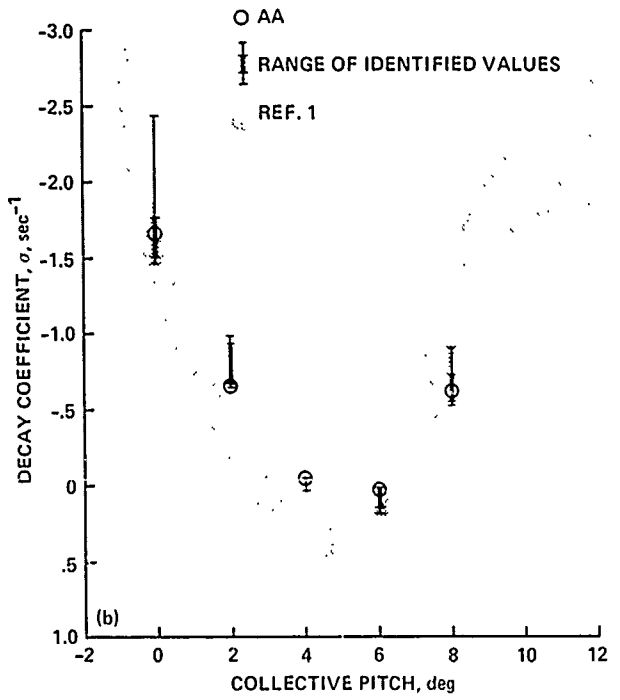


Fig. 1 Identified modal frequency for data set number one; 1000 rpm.



a) Identified modal decay coefficient



b) Comparison with published results

Fig. 2 Modal damping for data set number one; 1000 rpm.

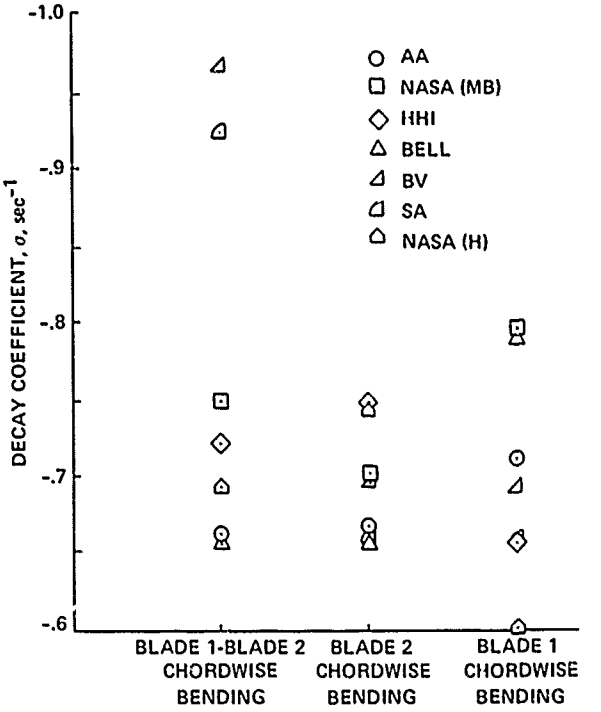


Fig. 3 Comparison between different measurement signals: Data set number one; 1000 rpm, 2° collective pitch.

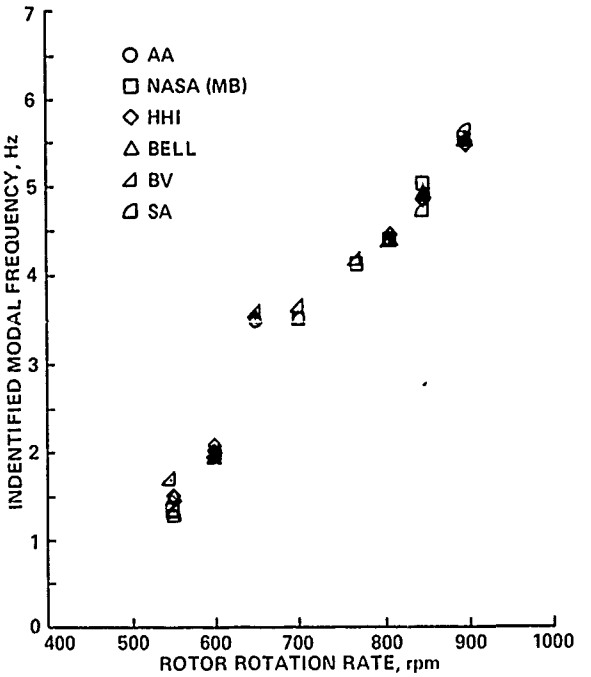
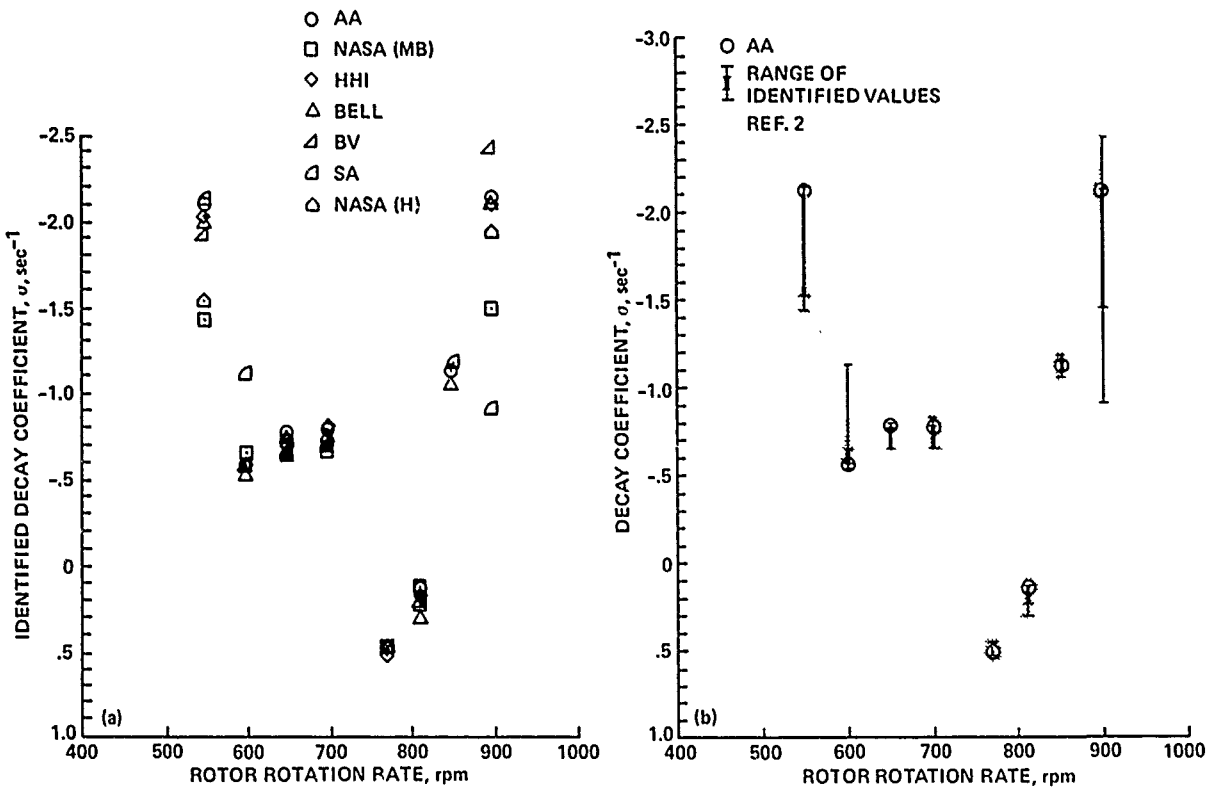


Fig. 4 Identified modal frequency for data set number two; 9° collective pitch.



a) Identified modal decay coefficient.

b) Comparison with published results.

Fig. 5 Modal damping for data set number two; 9° collective pitch.

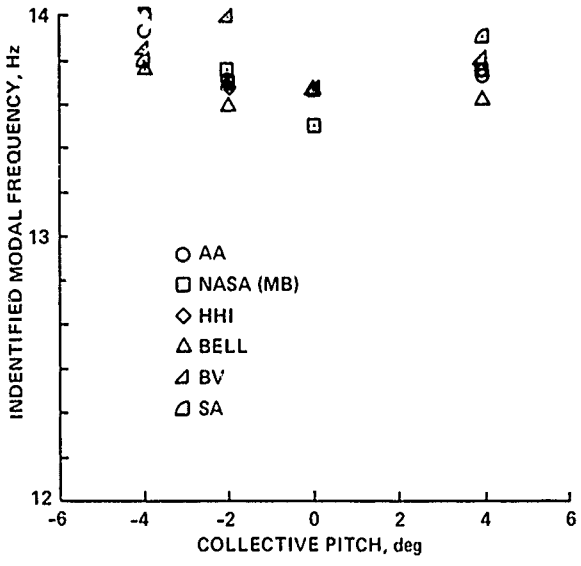
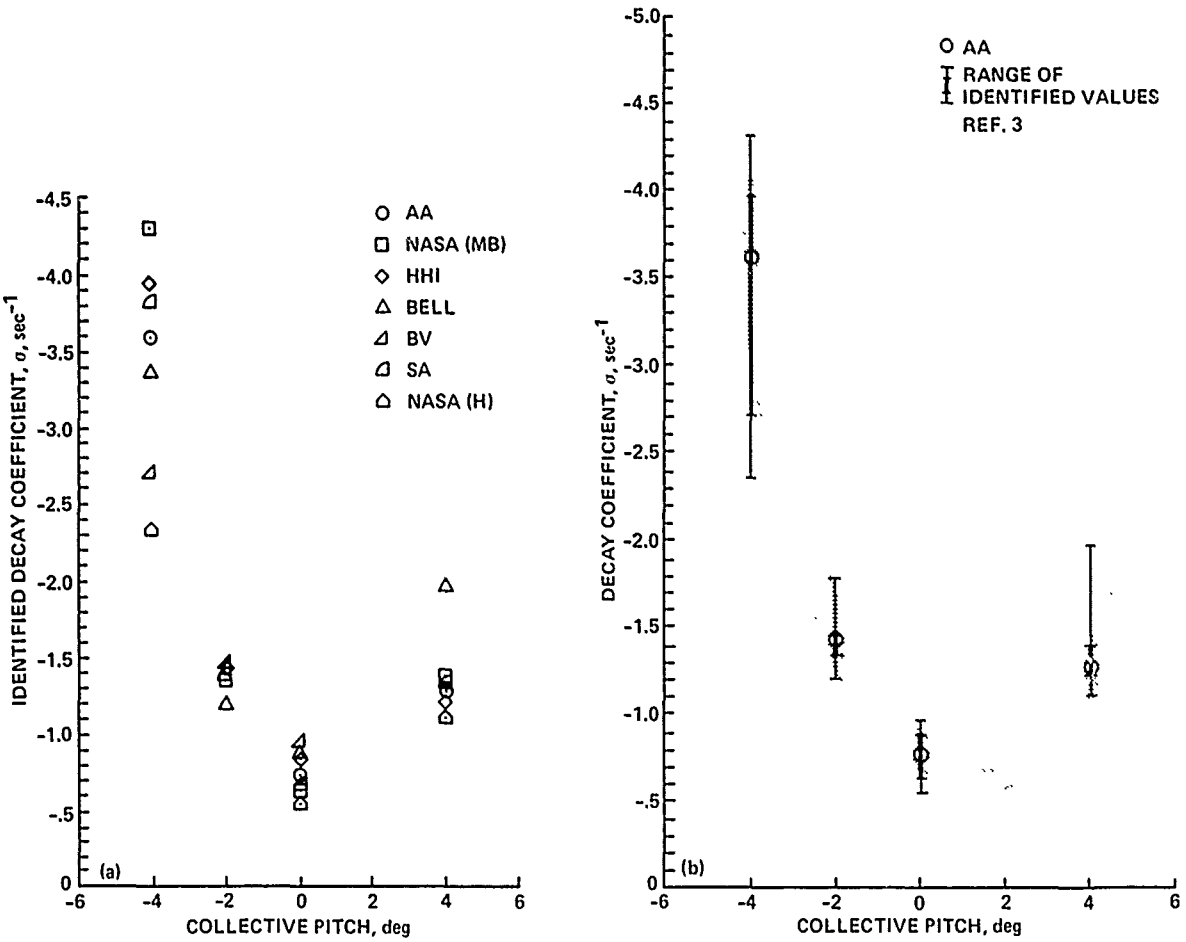


Fig. 6 Identified modal frequency for data set number three; 1100 rpm.



a) Identified modal decay coefficient

b) Comparison with published results

Fig. 7 Modal damping for data set number three; 1100 rpm.

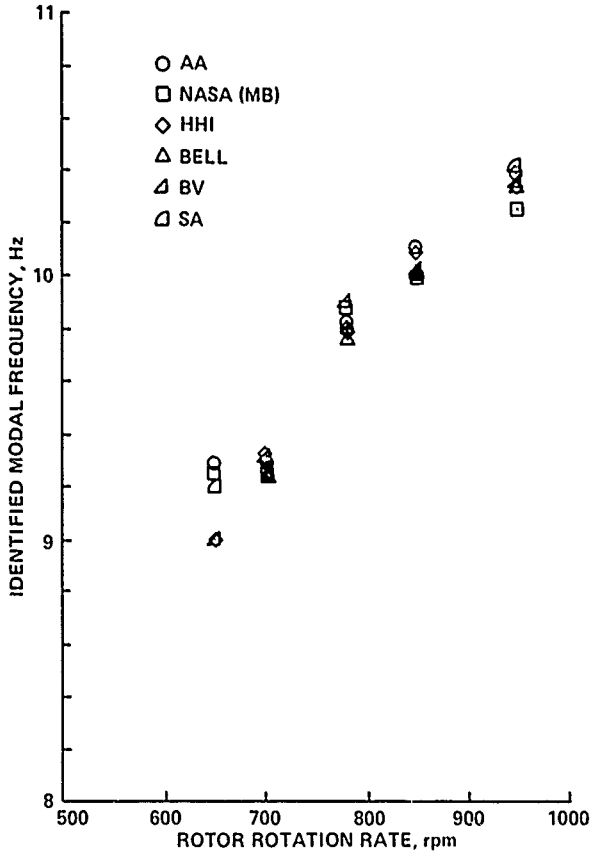
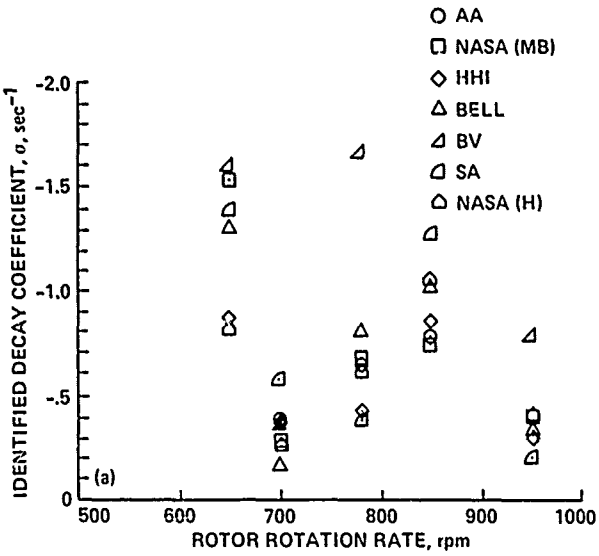
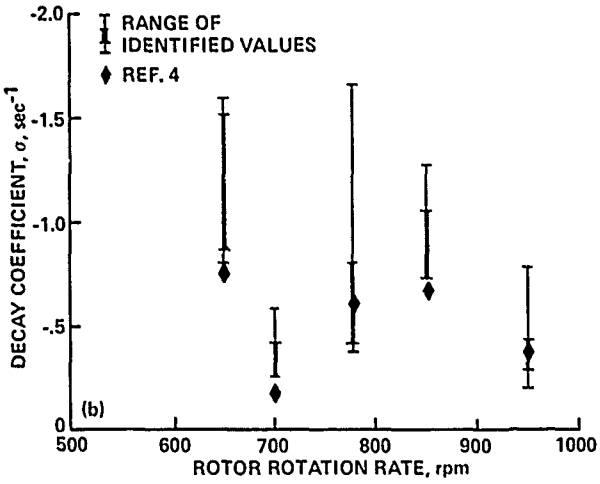


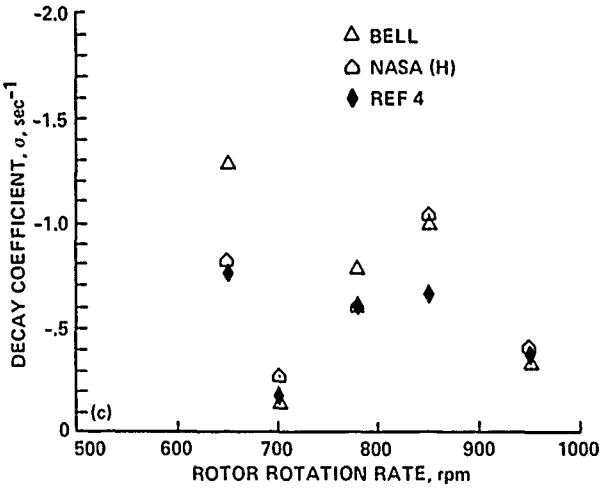
Fig. 8 Modal frequency for data set number four; 222 N lift, hover.



a) Identified modal decay coefficient.

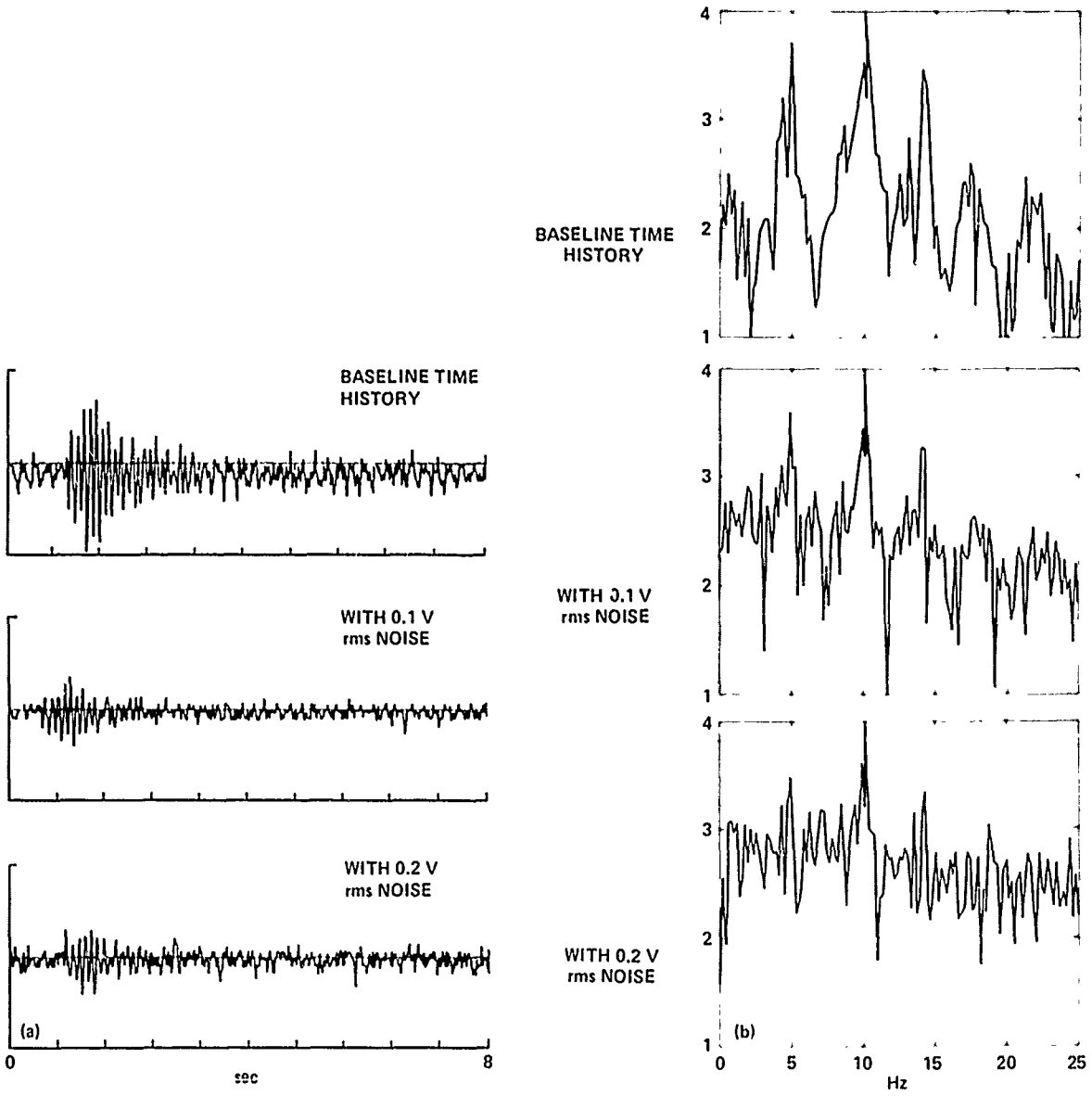


b) Comparison with published results.



c) Comparison with specific analyses.

Fig. 9 Modal damping for data set number four; 222 N lift, hover.



a) Time history records.

b) Frequency spectra.

Fig. 10 Data records with superimposed random noise; 0.1 to 50 Hz, data set number four, 850 rpm, 222 N lift.

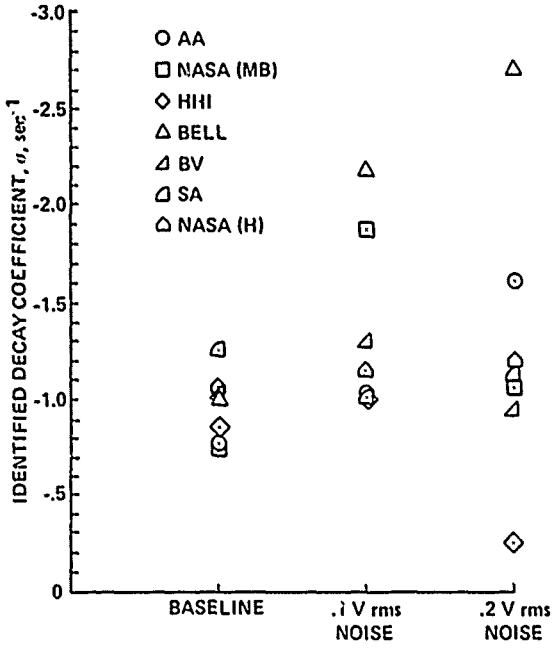


Fig. 11 Influence of background noise on modal damping: data set four.

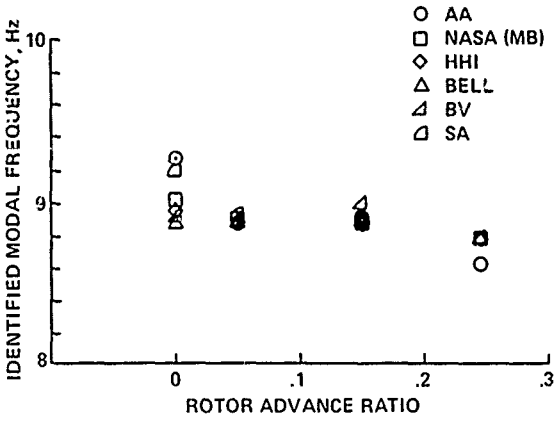
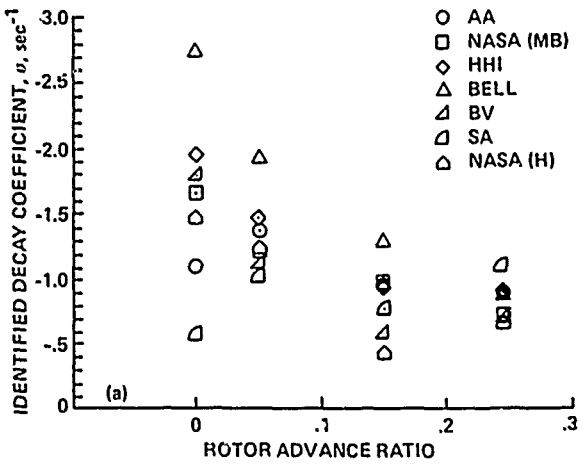
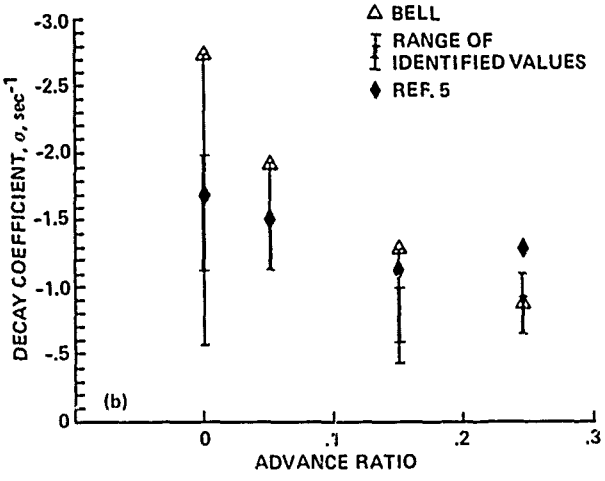


Fig. 12 Identified modal frequency for data set number five; 750 rpm, 222 N lift.



a) Identified modal decay coefficient



b) Comparison with published results

Fig. 13 Modal damping for data set number five; 750 rpm, 222 N lift.

DISCUSSION

COMPARISON OF EXPERIMENTAL ROTOR DAMPING ANALYSES

William Warmbrodt

Bill Bousman, Aeromechanics Laboratory: If you go back to A/4 [Figs. 1 and 2], I think most of the problem you described can be explained from the experimental point of view. Just to remind us from yesterday how that experiment was done: the upper truss of that stand is unlocked and is oscillated, and then when you're ready to take the measurement you lock the stand and let the motions decay. When you're oscillating the stand, you, in fact, have a separate dynamic system. It's a very soft system and is a coupled system where you get a different frequency of the blades during excitation. Then when you lock it up, there is a frequency shift because you have a much more rigid system; you have a very rigid stand instead of a highly coupled stand with a shaker. The 23-Hz frequency is roughly the frequency you get during that initial oscillation and I think that when Bill originally looked over the data, he saw two modes because he took a record length that overlapped excitation and decay. So the 23-Hz mode was in fact during excitation and the 21-Hz mode was during decay. So the case for 6° pitch angle in fact is not a decay record (you see the damping is zero), it is an excitation record.

Warmbrodt: That's incorrect.

Bousman: I don't believe it is incorrect.

Warmbrodt: Okay, for that data record the audio voice on the tape says that the system is not being excited.

Bousman: Taking that audio record, perhaps the system was not excited but not locked up yet.

Warmbrodt: Okay, that could be.

Bousman: Because if the system were not locked up, that frequency would be at 23 Hz. I don't know for the case at 4° why there are two modes there, but if you looked at the FFT I would guess that one is a very predominant mode and one is a very small mode.

Fort Felker, NASA Ames: The fact that the damping is zero doesn't indicate that it's being excited, because that agrees with the published experimental results for that figure.

Bousman: No, but that's a case of zero damping. What I'm saying is that if it were a case of excitation, you would expect very low damping because a system that is being excited appears to have neutral damping during the forced response. So it's

very difficult to tell. But in that case, because it is the excitation frequency, it's either unlocked or being excited.

Dave Sharpe, Aeromechanics Laboratory: One other comment on our test techniques. When we're in an unstable region, when we lock the stand and watch the transient decay, it it starts to go unstable we have to reduce the rotor speed quickly. A lot of times when you're taking that transient response, that transient record, you have to be very careful because the rpm may be changing there, too. There is a possibility that the analyst who looks at that is not taking a look at it before we change the rpm.

Wayne Johnson, Session Chairman: Does anybody have questions other than about this particular case?

Richard Bielawa, United Technologies Research Center: Had you considered providing an artificial trace for which you did know the answer?

Warmbrodt: I had considered that; unfortunately our digital-to-analog converter was inoperational. I considered generating a digital signal and then providing it in an analog form, so that I'd know exactly what it was, [but was unable to].

Bielawa: Do you have any guess what the result would have been?

Warmbrodt: No.

Gene Hammond, Applied Technology Laboratory: I'd think you would see the same sort of scatter you see in those; we've done that internally.

Johnson: If there was no noise, I think everyone would get the same result, but as soon as you start adding noise you'd start seeing scatter.

Jing Yen, Bell Helicopter Textron: Would you please put the C/3 comparison up [Fig. 5(b)]? I would assume the data band you show here includes the inputs from the government so therefore I would expect that your zone, your band, should at least hit the shaded area because the government should be able to repeat the result they had before. At that point, around 650 rpm, why does the band never come close?

Warmbrodt: Now recall that I took their data records that they had acquired during the test. I don't know if that point, that record, was reduced and used for the correlation effort. They do show four points in this area so it is well defined. Now perhaps this is a poor data point. Maybe we should give this one a "Bousman number."

[Unidentified]: I just wonder if anyone who participated in this analysis reconstructed the time histories from the frequency and damping values and then attempted to analyze the residuals for randomness and things like that. Was that a part of [this effort]?

Warmbrodt: I'm not aware of any of the approaches doing that, reconstructing the time histories.

Hammond: I have a comment and a question. The comment pertains to the two different Bell analyses on the last slide that you showed [Fig. 14]. In all of these data reduction techniques there are enough knobs in there that the analyst can turn, [for example] sampling rate; in the Prony's method it depends on the number of damped exponentials that you use to fit the data. Because of all those knobs, unless all of them are set exactly the same way, I don't think you should expect two analysts from the same company to get the same result.

Warmbrodt: If you're looking at one unique time history, hopefully, your physical system has one unique level of damping.

Hammond: That may be true for the physical system but the analyst looking at it sees a different thing depending on who's looking at it, and what knobs they're turning.

Johnson: I think you're right as a characterization of where we are now. But where we would like to be, certainly, is that if you took the same data reduction program and only had two operators, you would like a lot less scatter. Also, all these techniques, all the moving block techniques, are very close [to each other in implementation]. I think you'd like to have a lot less scatter. In fact there is more work to be done. There has been work on techniques that are, in fact, more powerful than moving block for dealing with transients. The problem is that transients are a very fast way to get your data; people haven't wanted more accuracy badly enough to acquire more data in order to get better repeatability.

Hammond: Yes, I would agree and I think that it's desirable to move in that direction. But because of the variability in all the parameters for the current methods, I don't think that you should be too surprised to see two analysts get two different results.

Johnson: We're not surprised, Gene.

Hammond: A question about the moving block analyses. There were a lot of them used there. Can you tell me how the moving block is applied to all these methods, because I suspect that it's different in all of them? Are they used blind or are they interactive?

Warmbrodt: I would say that all of them are interactive to the extent that the operator is able to edit his time history. Individual details on the techniques as they were applied will appear in the published paper.

Bob Wood, Hughes Helicopters: Just one added comment on what Gene said. I think just one parameter alone in Jing's study with Bill Weller is this question of record length and where the analyst sets those two indicators. The [frequency resolution] is one over the record length, and just where you set those two, I mean if you do

move back into the stable region at all. The fact that there's that much spread, it seems to me [with] the Prony thing is not a great surprise. I'm like Gene; I'm not overwhelmed.

Warmbrodt: Well, what we've identified here is a weakness in our capability.

Wood: No, it's the analyst; it's the individuality of the analyst. There will be differences.

Sam Crews, U.S. Army AVRADCOM: [It can be] one guy knowing where the excitation stops and the other guy not knowing.

Warmbrodt: I don't think that you can identify [all] the scatter that we've seen here from the same excuse that they were analyzing part of the forced response.

Wood: No, I'm not saying that. I'm just saying that where they set that will cause a difference. The fact is that probably all of them did their very best and we still got this much scatter. The fact two people using the same method get different answers doesn't knock me out of my seat.

Warmbrodt: Last question.

Holt Ashley, Stanford University: Let me transfer a little experience from the flutter business. As I'm sure you know there have been a lot of efforts to get accurate damping information out of both flight flutter test results, which follow excitation, and also model test work such as what's done in the Transonic Dynamics Tunnel (TDT) at Langley. There's a very interesting paper, I think it was a year ago at the Structures, Dynamics, and Materials (SDM) Conference that someone from the TDT used four different methods essentially on the same record, and they are pretty sophisticated identification methods. Perhaps one suggestion is that you might want to take a look at some of those other methods, but the bottom line of that investigation, which was using a pretty good data record, was that the sort of scatter that they got from the various methods was of the same order as what you're showing here. So I think that the message is that it's just very hard to get very accurate damping off of a record and you've got to keep trying.

Jing Yen: You've got to analyze the same block of data, otherwise you will not get the same thing; someone will take one second and someone else will take one and one half seconds.

Bousman: Let me make one last comment to try to sum it up. I think that we probably cannot, in an experiment, estimate the scatter due to different analysts without going to great expense, but we can estimate the scatter by at least taking multiple data points. So I think that probably a minimum step we have to take is to get beyond taking single data points, despite the cost.

COMPARISON OF EXPERIMENTAL COUPLED HELICOPTER ROTOR/BODY STABILITY RESULTS WITH A SIMPLE ANALYTICAL MODEL*

P. P. Friedmann+ and C. Venkatesan++
Mechanics and Structures Department
University of California
Los Angeles, CA 90024

Summary

This paper presents the results of an analytical study aimed at predicting the aeromechanical stability of a helicopter in ground resonance, with the inclusion of aerodynamic forces. The theoretical results are found to be in good agreement with the experimental results, available in the literature, indicating that the coupled rotor/fuselage system can be represented by a resonably simple mathematical model.

Nomenclature

a	= lift curve slope
$C(k)$	= Theodorsen's lift deficiency function
c_{d0}	= profile drag coefficient of the blade
e	= hinge offset
f	= rotating natural frequency
h_2	= height of rotor hub above the gimbal
$I_{xx}, I_{xy}, I_{yy}, I_{yx}$	= rotary inertia of the model about the gimbal axes
K_β, K_ζ	= stiffness of the root springs of the blade in flap and lag respectively
m	= mass/unit length of the blade
R	= rotor radius
s	= complex eigenvalue
t	= time
β_{nc}, β_{ns}	= n - cosine, n-sine flap coordinates
β_p	= blade precone, in the equations
β_p	= progressing flap mode (high frequency) in the figures only
β_R	= regressing flap mode (low frequency)
β_o	= rotor blade equilibrium angle in flap
β_{1c}, β_{1s}	= cyclic flap coordinates
$\Delta\beta_k$	= time dependent perturbations of the k^{th} blade in flap
ϵ	= order of magnitude used for ordering various quantities
ζ_p	= progressing lag mode (high frequency)
ζ_R	= regressing lag mode (low frequency)
ζ_{1c}, ζ_{1s}	= cyclic lag coordinates
ζ_o	= rotor blade equilibrium angle in lag
$\Delta\zeta_k$	= time dependent perturbations of the k^{th} blade in lag
ζ_{nc}, ζ_{ns}	= n - cosine, n - sine lag coordinates
θ	= body pitch
θ_c	= collective pitch setting of the blade
θ_{eff}, θ_o	= effective angle of attack
θ_{ZL}	= zero lift angle of attack
λ	= inflow ratio
σ	= model damping (real part of s)
$\bar{\sigma}$	= solidity ratio
ϕ	= body roll
ψ	= nondimensional time (Ωt)
ω	= modal frequency (imaginary part of s)
Ω	= rotor R.P.M.

Presented at the Integrated Technology Rotor (ITR) Methodology Assessment Workshop, NASA Ames Research Center, Moffett Field, CA., June 21-22, 1983.

*This work was supported by NASA Ames Research Center under Grant NAG 2-116.

+Professor of Engineering and Applied Science

++Assistant Research Engineer

$(\bar{\ })$ = nondimensionalized quantity, with respect to R when involving length, and with respect to Ω when involving frequency

$(')$ = $\frac{d}{d\psi}$

I. Introduction

The aeromechanical instability of a helicopter, on the ground and in flight, is caused by coupling between the rotor and the body degrees of freedom. This instability is commonly denoted air resonance when the helicopter is in flight and ground resonance when the helicopter is on the ground. The physical phenomenon involved during this instability is quite complex, the rotor lead-lag regressing mode usually couples with the body pitch or roll to cause the instability. The nature of the coupling which is both aerodynamic and inertial is introduced in the rotor due to body or support motion. Development of a mathematically consistent model capable of representing the coupled rotor/fuselage dynamic system is of fundamental importance for the study of these type of problems. The mathematical model should be consistent because the geometrically nonlinear terms associated with moderate blade deflections are known to have a significant role in rotary wing aeroelasticity[1]. Thus various terms having the same order of magnitude must be retained throughout the derivation of the equations of motion. A consistent mathematical model has been developed[2,3], by the authors, to study the aeroelastic, structural dynamic and aeromechanical effects in multi-rotor systems.

Bousman[4] has obtained excellent experimental data for aeromechanical stability of a hingeless rotor on a special gimbaled support simulating body pitch and roll degrees of freedom. The availability of this high quality experimental data provides an opportunity for comparing the results obtained from the analytical model with this experimental data. Bousman attributed some of the discrepancies found between the theoretical results presented in his paper and experimental results to dynamic inflow. This conclusion was also examined by Johnson[5], in a recent study, where unsteady aerodynamic effects on the rotor was represented by a perturbation inflow model[6]. Johnson showed that theoretical results based on his model[7], with dynamic inflow provided results which showed better agreement with the experimental results than the results based on a quasi-steady aerodynamic model without dynamic inflow. He concluded from his study that unsteady aerodynamic effects are represented quite well by a dynamic inflow model.

Using the mathematical model developed by the authors[2,3], it is shown that the theoretical results, based on the quasi-steady aerodynamic model, are for most cases in better agreement with the experimental results than the agreement noted by Bousman[4]. The agreement with the experimental data is also comparable to that obtained by Johnson[5], except that the quasi steady model is incapable of predicting the "dynamic inflow mode" found by Johnson[5], which is a result of the augmented state due to inflow dynamics.

The good agreement between the analytical and experimental results indicates that the relatively simple analytical model is accurate for this case. Furthermore it also implies that only part of the discrepancy between theory and experiment, found by Bousman, may be attributed to dynamic inflow.

II. A Brief Summary of the Experiment

A clear description of the experimental set up, used for simulating the fundamental aspects of the aeromechanical stability of a hingeless rotor helicopter, is presented in Ref. 4. The rotor consisted of three blades and five different configurations were tested. The different configurations represent different blade parameters characterized by the nonrotating natural frequencies of the blade in flap and lag, pitch-lag coupling and flap-lag coupling. The rotor was designed such that most of the blade flexibility is concentrated at the root by building in root flexures. The rotor assembly was supported on a gimbal which had pitch and roll degrees of freedom. In this paper the analytical results obtained were compared with the experimental results, presented by Bousman, for rotor configurations 1 and 4, where the designation of these configurations is consistent with those in Bousman's paper[4].

A brief description of these configurations is presented for the sake of completeness. Configuration 1 had different stiffnesses in flap and lag respectively, the corresponding nonrotating flap frequency was 3.13 Hz and that for lead-lag was 6.70 Hz. Configuration 4 was a matched stiffness case where the nonrotating flap frequency was 6.63 Hz and that for lead-lag was 6.73 Hz. The airfoil cross-section of the blade was cambered and had a zero lift angle of attack equal to -1.5 degrees. Thus a substantial part of the experimental data was obtained for zero pitch setting, however, due to the presence of camber the rotor produces a small amount of thrust at this pitch setting. The rotor blades were rigid outboard of the flap and lag flexures which were located at a radial station 0.105R. There was no flap-pitch or pitch-lag couplings for these two configurations (configurations 1 and 4). Furthermore, the blade was very stiff in torsion. In the case of the experiments conducted for pitch angles other than zero, the experimental set up was so designed as to introduce the changes in pitch angle outboard of the flexures and hence there was no flap-lag structural coupling for these cases. The structural damping in body roll was very small in comparison with that for body pitch. The body pitch and roll frequencies were controlled by cantilever springs on which the gimbal was mounted. It is stated in Ref. 4 that the body pitch spring was selected to provide a dimensionless body pitch frequency of about 0.12 at the nominal rotor speed of 720 R.P.M. and the roll spring was selected to give a dimensionless

roll frequency of about 0.28. (The frequencies are nondimensionalized by dividing by rotor speed.) Based on these values, the dimensional frequencies in pitch and roll are 1.44 Hz and 3.36 Hz respectively. It was also mentioned in Ref. 4 that the dimensional values of the body pitch and roll frequencies are about 2 Hz and 4 Hz respectively. So the difference, noted between the two sets of body frequencies, raises a question as to what are the exact values for the pitch and roll frequencies. However the experimental results presented in Ref. 4 showed that over a wide range of Ω (200 ~ 1000 R.P.M.) the pitch and roll frequencies are very close to 2 Hz and 4 Hz respectively. Hence, for the present analysis, the pitch and roll frequencies are selected to be 2 Hz and 4 Hz. The reason for choosing 2 Hz and 4 Hz for body frequencies was that at approximately 750 R.P.M., the lead-lag regressing mode of the rotor was close to the body roll frequency causing an aeromechanical instability. The data used in our calculations, is presented in the Appendix B.

III. Description of the Analytical Model

The analytical model used to study this aeromechanical stability problem is based on the equations developed for a multi-rotor system presented in Ref. 2 and 3. Those equations represent the dynamics of the coupled rotor/vehicle system consisting of two rotors interconnected by a flexible structure. The various degrees of freedom considered, in deriving the equations, are flap, lag, torsion for each blade, rigid body translation and rotation of the complete vehicle and also the degrees of freedom representing the normal modes of vibration of the supporting structure. From this multi-rotor analytical model, only those degrees of freedom and the corresponding equations of motion that are relevant for the present study have been retained. The most important assumptions upon which the formulation is based on are: (1) the rotor consists of 3 or more number of blades, (2) the rotor is lightly loaded, (3) the rotor is in uniform inflow, and (4) the rotor blade is modelled as a rigid blade with orthogonal springs located at the root of the blade (Fig. 1), where K_β and K_ζ represent the stiffness of the blade in flap and lag motions.

The aerodynamic model is based on Greenberg's[8] derivation of unsteady aerodynamic loads on an oscillating airfoil in a pulsating flow. This theory is basically a modified form of Theodorsen's unsteady aerodynamic theory. By assuming the Theodorsen's lift deficiency function $C(k) = 1$ and neglecting the torsional motion of the blade, the aerodynamic model becomes a simple quasi-steady model with apparent mass terms. In the present calculations, only this quasi-steady aerodynamic model with apparent mass terms is used. It was found from our calculations that neglecting the apparent mass terms from the aerodynamic model affects the results only by 2 ~ 4%.

The inflow ratio λ, used in the calculation of the aerodynamic loads was evaluated from[6]

$$\lambda = \frac{\bar{\sigma}a}{16}\left[\sqrt{1 + \frac{24\,\theta_{eff}}{\bar{\sigma}a}} - 1\right] \qquad (1)$$

where $\bar{\sigma}$ is the solidity ratio

a is the lift curve slope

and θ_{eff} is the effective angle of attack of the blade.

As indicated in Ref. 4, a cambered airfoil was used in the model rotor tested, thus

$$\theta_{eff} = \theta_c - \theta_{ZL} \qquad (2)$$

where θ_c is the collective pitch setting of the blade

θ_{ZL} is the zero lift angle of attack.

The zero lift angle of attack, for the airfoil employed[4] (NACA 23012), was $\theta_{ZL} = -1.5$ degrees.

As mentioned earlier, the equations of motion are nonlinear, because geometrical nonlinearities due to moderate deflection of the blade are included. Retention of the nonlinear terms is based upon an ordering scheme[1,2]. The blade degrees of freedom, representing blade slopes are assigned an order of magnitude represented by a symbolic quantity ε, and are denoted to be of order $0(\varepsilon)$, where $0.1 < \varepsilon < 0.15$. The fuselage degrees of freedom are assumed to be of a slightly smaller magnitude $0(\varepsilon^{3/2})$. As indicated in Ref. 1, this assumption is quite important for obtaining equations which are manageable from an algebraic point of view. The ordering scheme consists of neglecting terms of order $0(\varepsilon^2)$ when compared to order one, thus $1 + 0(\varepsilon^2) \simeq 1$.

The degrees of freedom considered in this aeromechanical stability analysis are: the fundamental flap and lag modes for each blade and the pitch and roll degrees of freedom of the body. In this class of problems, it has been established that the collective flap and lag modes do not couple with the body motion and thus, these modes are not considered. Therefore, the total number of degrees of freedom governing the aeromechanical problem are six. These consist of: cyclic flap (β_{1c},β_{1s}), cyclic lead-lag (ζ_{1c},ζ_{1s}), body pitch (θ) and body roll (ϕ).

IV. Method of Solution and Discussion of Results

The method of solution for coupled rotor/fuselage problem follows essentially the procedure explained in Ref. 1 and 3. A brief outline of the procedure is given in the following few paragraphs.

The equations of motion, for coupled rotor/fuselage problem, are usually nonlinear

differential equations with periodic coefficients. These differential equations can be either ordinary or partial depending on the type of model used for the representation of the rotor blade. If the blade is modelled as a rigid blade with root springs, the resulting equations will be nonlinear ordinary differential equations. On the other hand, if the blade is modelled as a flexible beam, the final equations will be nonlinear partial differential equations. In this case, the partial differential equations are first transformed into ordinary differential equations using Galerkin's method. Thereafter the method of solution is the same regardless which of these two blade models is used. In the present case, because the blade is modelled as rigid blade with root springs (Fig. 1), the equations of motion are nonlinear ordinary differential equations with periodic coefficients. The steps involved, in solving these equations to obtain the stability information, are as follows.

1. Evaluation of the equilibrium position for the blade.

2. Linearization of the nonlinear ordinary differential equations about the equilibrium position. (Linearized equations will have periodic coefficients.)

3. Transformation of the linearized equations with periodic coefficients to linearized equations with constant coefficients, by applying multiblade coordinate transformation.

4. Evaluation of the eigenvalues of the linearized system with constant coefficients to obtain the information about the stability.

For the case of hover, the equations which represent the static equilibrium of the blade are obtained by imposing the requirement that all time derivatives of the blade degrees of freedom and the fuselage perturbations vanish in the equations. The resulting equations are nonlinear algebraic equations and they are identical for all the blades in the rotor indicating that the static equilibrium is same for all blades. This static equilibrium position is obtained by solving the nonlinear algebraic equations using a numberical method, namely the Newton-Raphson technique. Then the blade degrees of freedom are expressed as time varying perturbations about the static equilibrium position, β_0 and ζ_0 for flap and lag respectively.

$$\beta_k(\psi) = \beta_0 + \Delta\beta_k(\psi)$$

$$\zeta_k(\psi) = \zeta_0 + \Delta\zeta_k(\psi)$$

Substituting these into the nonlinear ordinary differential equations of motion and neglecting terms which contain the product of the perturbation terms, yields the linearized equations of motion. The linearized equations for the k-th blade will have periodic coefficients, since the k-th blade equations are written in the blade fixed rotating coordinate system Transformation of the perturbations equations to a nonrotating system will result in equations with constant coefficients. This transformation is performed using the multiblade coordinate transformation[6]. During this transformation, the individual blade degrees of freedom will transform to a new se of rotor degrees of freedom. In the past, these rotor degrees of freedom have been referred to as multiblade coordinates or Coleman coordinates or Fourier coordinates or rotor-plane coordinates. These coordinates are basically representative of the behavior of the rotor as a whole when viewed from a nonrotating frame. For the sake of completeness the equations of blade equilibrium, the linearized perturbational blade equations (in the multiblade or rotor plane coordinate system) and the perturbational equations for the pitch and roll degrees of freedom are presented in Appendix A.

Stability of the linearized system is determined by performing an eigen-analysis on the linearized constant coefficient perturbation equations. The eigen-values appear as complex pairs $s = \sigma \pm i\omega$. The complex part of the eigen value (ω) refers the modal frequency and the real part (σ) refers the modal damping. The mode is stable if σ is negative and it is unstable if σ is positive.

For the present problem, there are six pairs of complex eigen-values each one representing one of the six degrees of freedom, namely, β_{1c}, β_{1s}, ζ_{1c}, ζ_{1s}, θ and ϕ. The modes corresponding to the rotor degrees of freedom (β_{1c}, β_{1s}, ζ_{1c}, ζ_{1s}) are referred to either progressing mode or regressing mode. The designation of progressing or regressing to a particular mode is based on the numerical value of the rotating natural frequency of the rotor. Suppose the rotating natural frequency, say in lead-lag, is f/rev. Then the two frequencies corresponding to the cyclic lag modes (ζ_{1c}, ζ_{1s}) will be (f+1)/rev and (f-1)/rev, where f+1 is the high frequency lag mode and f-1 is the low frequency lag mode. If f is greater than 1/rev, the high frequency lag mode (f+1) is a progressing mode and the low frequency lag mode (f-1) is a regressing mode. On the other hand, if f is less than 1/rev, the high frequency lag mode is a progressing mode and the low frequency lag mode is also a progressing mode. These designations are also applicable for the flap modes of the rotor. A clear description of these is given in Ref. 6. For a stiff-in-plane rotor, the rotating natural frequency in lead-lag greater than 1/rev. Hence the high frequency lead-lag mode is a progressing mode and the low frequency lead-lag mode is a regressing mode. For a soft inplane rotor since the rotating natural frequency is less than 1/rev, both high frequency and low frequency lag modes are progressing modes.

In the present study, aimed at the aeromechanical stability of a model helicopter, the behavior of the model is studied at various Ω's of the rotor. Thus due to the variation in Ω, a stiff inplane rotor at low Ω's will become a soft inplane rotor at high Ω's. In the experiment performed by Bousman[4], the flexibility of the blade in lead-lag is such that the rotor becomes a soft inplane rotor beyond Ω = 445 R.P.M. Hence, for Ω < 445 R.P.M., the lead-lag modes will have one progressing mode and one regressing mode and for Ω > 445 R.P.M., both the lag modes will be progressing modes. In Refs. 4 and 5, even for Ω > 445 R.P.M., the low-frequency lag mode is referred as regressing mode instead of progressing mode. The reason could be to avoid any confusion while referring to various modes. So, for the sake of consistency, during the discussion of our results, the low frequency lag mode is always referred as lag regressing mode.

The results for configuration 1 are presented in Figs. 2-7, while the results for configuration 4 are presented in Figs. 8-12. The variation of the various modal frequencies with Ω are presented in Fig. 2, together with the experimental data obtained in Ref. 4. The progressing flap and progressing lead-lag frequencies increase very rapidly with Ω. The lead-lag regressing mode frequency evaluated from the analytical model is in excellent agreement with the experimental results. The body pitch and roll frequencies have slightly higher values than the experimental results. The damping in pitch as a function Ω is shown in Fig. 3. The analytical results are in relatively good agreement with the experimental data. The variation of the damping in roll as a function of Ω is shown in Fig. 4. It is evident that for this case the analytical results yield values which are somewhat higher than the experimental data. The differences observed between our analytical results and the experimental points, for the frequency and damping in body modes, could be explained as follows. In our calculations, the numerical values used for the stiffness and structural damping in body pitch and roll modes are evaluated based on pitch frequency equal to 2 Hz and roll frequency equal to 4 Hz. As pointed out in Sec. II of this paper, there is some doubt about the correctness of the body frequencies (2 and 4 Hz) because in Ref. 4, there are two different sets of frequencies for pitch and roll, namely 1.44 and 3.36 Hz, and 2 and 4 Hz respectively.

Figure 5 represents the variation of damping in lead-lag regressing mode with Ω. As indicated before, Johnson's results[5] show that the theory with inflow dynamics shows better agreement with experimental data than the theory with quasi-steady aerodynamics. However, even with quasi-steady aerodynamics, the results of the present analysis show slightly better agreement than the results obtained in Ref. 5 with inflow dynamics. It is also important to note that in the region, beyond 800 R.P.M., our results are in excellent agreement with the experimental data, while the theory with inflow dynamics predicts higher values.

Results from the calculations performed indicated that the progressing and regressing flap modes are always stable and the damping in these modes increases monotonically with Ω for configuration 1 as well as for configuration 4. Since these modes are always stable, the results are not presented in this paper.

Changes in the damping of the lead-lag regressing mode as a function of the collective pitch setting of the blade are presented in Fig. 6. Since Johnson[5] has not presented a corresponding set of results, it was not possible to compare these results with an analysis based on the dynamic inflow model. At Ω = 650 R.P.M., the results shown in Fig. 6a indicate that the theoretical analysis used by Bousman[4] predicts a much lower value for the damping than the experimental results. The present analysis shows considerably better agreement. It should be noted however that for larger values of pitch setting the difference between the predicted results and the experimental results increases. This difference could be attributed to the simple quasi-steady aerodynamic model used in our analysis. This difference however is much smaller than the one exhibited by Bousman's results. Even more interesting are the results presented in Fig. 6b, corresponding to Ω=900 R.P.M. For this case experimental results indicate a lead-lag regressing mode which is always stable, but the theoretical results shown by Bousman[4] imply an instability which becomes stronger beyond a collective pitch setting of 2 degrees. As evident from Fig. 6b, the results of our analysis predict the correct trend and the predicted damping levels are much closer to the experimental results. It should be noted again that the agreement between the predicted and experimental results diminishes with increasing collective pitch setting. An item to be noted in these figures (6a, 6b) is that the curve representing our analytical results starts from an angle θ_c = -1.5 degrees. Although Fig. 6 contains an experimental data point corresponding to θ_c = -3 degrees, we have not computed the results for this pitch setting because for θ_c = -3 degrees, the relation between inflow ratio and the collective pitch of the blade (Eq. 1) becomes indeterminate.

The variations in pitch damping as a function of collective pitch setting are shown in Fig. 7a, and similar variations for roll damping are shown in Fig. 7b. As evident from 7b, the damping in roll is predicted quite well. However the damping in pitch predicted by the present analysis is much lower than the experimental results. One can only speculate on the possible cause for this discrepancy. One possible reason could be the slight nonlinearity present in the structural damping in pitch mentioned in Ref. 4.

At Ω = 650 R.P.M., the lead-lag regressing mode frequency is close to the body pitch frequency (Fig. 2) and therefore the amplitudes in pitch could be higher. Thus nonlinearity in structural damping in pitch could manifest itself by increasing the total damping in pitch.

The results for configuration 4 are presented next. The variation of modal frequencies with Ω are shown in Fig. 8. The lead-lag regressing mode frequency is in excellent agreement with our analytical predictions. The pitch and roll frequencies are predicted well. Bousman's[4] experiments showed the presence of a frequency of about 0.8 Hz beyond Ω = 350 R.P.M., whereas the present analysis has not predicted any frequency close to this value. Note that the regressing flap mode frequency is close to the pitch mode over a wide range of Ω($400 < \Omega < 1000$ R.P.M.). Thus it is possible that the pitch mode can be excited by the proximity of the regressing flap mode. The explanation for the presence of the 0.8Hz frequency, measured in the test, posed a problem since the theoretical results presented by Bousman[4] as well as those obtained by Johnson[5], with the quasi-steady aerodynamics, were incapable of predicting a 0.8Hz frequency. It is quite relevant to quote Bousman on this matter, Ref. 4, p. 53. In Bousman's words, "However in the experimental case, measurements in the pitch coordinate show two modes of comparable damping at rotor speeds beyond 350 R.P.M., one mode at about 0.8 Hz and the other at 2.0 Hz". Bousman refers one as pitch mode (0.8 Hz) and the other as flap regressing mode (2.0 Hz). However, in identifying these modes Bousman states, "To call one mode the body mode, and the other flap regressing mode is somewhat arbitrary; the rationale used here is that as the blade pitch angle increases only one of these modes remains, and it is assumed to be the body pitch mode". But Johnson[5], using the inflow dynamics model, was able to predict theoretically a frequency close to 0.8 Hz and he called it as the inflow mode and he identified the other frequency (2.0 Hz) as the pitch mode. Quoting Johnson, Ref. 5, p. 672, "That it is measurable (i.e., 0.8 Hz inflow mode) is surprising, since in fact the inflow variables λ_x and λ_y do not correspond to real physical states of the system". He proceeds to interpret this behavior as "the unsteady aerodynamics introduces behavior of the system, as observed in either time or frequency domain, that can be approximated by an additional oscillatory mode with low or moderate damping. Approximating the behavior by an additional mode implies then the existence of additional states or degrees of freedom of the system". Johnson also states that this behavior is observed only for matched stiffness case because "the flap regressing mode will be more coupled with the body motion". But examination of Fig. 6 in Ref. 5 (the results based on the theory with inflow dynamics) reveals that the flap regressing mode frequency is not near the body pitch frequency, so it is questionable whether coupling could occur between these two modes. In our analysis, however the results show that the flap regressing mode is close to the body pitch mode, as indicated in Fig. 8. Thus it appears that the interpretation offered by Johnson for the presence of the 0.8 Hz frequency mode and its designation as the inflow mode frequency is possible, albeit speculative.

The variation of lead-lag regressing mode damping with Ω is presented in Fig. 9. Again, the present analytical results are in closer agreement with the experimental results than those predicted by the theory with inflow dynamics. Figure 10 and 11 show the variation of damping in roll and pitch modes with Ω. The pitch damping is predicted well. The roll damping is overestimated.

The variation in damping levels of the lead-lag regressing mode with collective pitch angle, of the blade are shown in Fig. 12, for two different values of angular speed. It is evident from Fig. 12b that for the case of Ω=1000 R.P.M., the theory used by Bousman predicts an unstable region beyond θ_c = 3 degrees, however the experiment indicates a stable configuration. The results of the present analysis are in good agreement with the experimental results. The agreement noted in Figs. 6 and 12, between the analytical results of our study and the experimental data, for nonzero values of collective pitch, seems to indicate that the discrepancy between theory and experiment for these cases, evident in Ref. 4, could be associated with the details of the mathematical model and is not related to unsteady aerodynamic effects such as dynamic inflow.

V. Concluding Remarks

In this paper, the results of a theoretical analysis, of the aeromechanical stability of a hingeless rotor helicopter, are compared with the experimental results. Using a quasi-steady aerodynamic model, it was found that the results of the present analysis compare quite well with the experimental results. It is interesting to note that this correlation with experimental data appears to hold in both the region of zero collective pitch angles considered by Johnson[5] as well as in the nonzero range of collective pitch angles which was considered by Bousman[4], but not by Johnson. Obviously the quasi steady aerodynamic model is incapable of predicting the "dynamic inflow mode" which is caused by the augmented state of the system, when the dynamic inflow model is used. In an extension of this study which will include dynamic inflow, the physical meaning of the dynamic inflow mode will be reexamined.

This study also indicates that the discrepancy between the predicted values of regressing mode lag damping and the experimental measurements, noted in Ref. 4, for configurations 1 and 4, do not seem to be associated with dynamic inflow and are more likely to be related to the details of the mathematical model.

Furthermore the analytical model used in this study has the capability of simulating the experiment, with good accuracy, because it is based on the same blade model which was actually tested.

Finally, it should be noted that the analytical model was based on an ordering scheme where blade slopes were assumed to be of order ϵ and the fuselage rotations in pitch and roll were assumed to be of order $\epsilon^{3/2}$, which leads to simplification in the equations of motion. The cases considered in the present study (both experimental and theoretical) were restricted so that only the linear first order terms in fuselage rotations were important. Thus other classes of problems, in which nonlinear terms in fuselage rotations are also exercised, have to be considered to determine the overall reliability of this particular ordering scheme.

Acknowledgment

The authors would like to express their gratitude to W. Bousman, W. Johnson and H. Miura for the constructive comments they have made on the draft version of this paper.

References

1. Friedmann, P.P., "Formulation and Solution of Rotary-Wing Aeroelastic Stability and Response Problems", Presented at the Eighth European Rotorcraft Forum at Aix-En-Provence, France, Aug. 31-Sep. 3, 1982, Published in Vertica, Vol. 7, No. 2, 1983, pp. 101-141.

2. Venkatesan, C. and Friedmann, P.P., "Aeroelastic Effects in Multirotor Vehicles with Application to Hybrid Heavy Lift System, Part I: Formulation of Equations of Motion", Submitted to NASA for publication as a Contractor Report, Dec. 1982.

3. Venkatesan, C. and Friedmann, P.P., "Aeroelastic Effects in Multirotor Vehicles, Part II: Method of Solution and Results Illustrating Coupled Rotor/Body Aeromechanical Stability", NASA CR Report in preparation.

4. Bousman, W.G., "An Experimental Investigation of the Effects of Aeroelastic Couplings on Aeromechanical Stability of a Hingeless Rotor Helicopter", Journal of the American Helicopter Society, Vol. 26, No. 1, Jan. 1981, pp. 46-54.

5. Johnson, W., "Influence of Unsteady Aerodynamics on Hingeless Rotor Ground Resonance, Journal of Aircraft, Vol. 19, No. 8, Aug. 1982, pp. 668-673.

6. Johnson, W., Helicopter Theory, Princeton University Press, Princeton, New Jersey, 1980.

7. Johnson, W., "A Comprehensive Analytical Model of Rotorcraft Aerodynamics and Dynamics", NASA TM 81182, June 1980.

8. Greenberg, J.M., "Airfoil in Sinusoidal Motion in a Pulsating Flow, NACA TN 1326, 1947.

Appendix A: Equations Used in this Study

The equations of blade equilibrium, the linearized perturbational blade equation in multiblade coordinates, together with the perturbational equations in the pitch and roll degrees of freedom are given below.

Equilibrium Equations

Flap:

$$\begin{aligned}
&\beta_0\{\bar{\omega}_F^2 + (\bar{\omega}_L^2 - \bar{\omega}_F^2)\sin^2\theta_c + \frac{\bar{\ell}^3}{3} + \frac{\bar{\ell}^2}{2}\bar{e}\} \\
&\quad + \zeta_0\{(\bar{\omega}_L^2 - \bar{\omega}_F^2)\sin\theta_c\cos\theta_c + \nu\frac{\bar{\ell}^4}{4}\beta_p\} \\
&\quad + \beta_0\zeta_0\{\nu\frac{\bar{\ell}^4}{4}\} \\
&\quad + \beta_p\{\frac{\bar{\ell}^3}{3} + \frac{\bar{\ell}^2}{2}\bar{e}\} - \nu\{\frac{\bar{\ell}^4}{4}\theta_0 + \\
&\quad + \frac{\bar{\ell}^3}{3}(-\lambda + 2\bar{e}\theta_0) - \frac{\bar{\ell}^2}{2}\bar{e}\lambda\} = 0 \qquad (A.1)
\end{aligned}$$

Lead-Lag

$$\begin{aligned}
&\beta_0\{-(\bar{\omega}_L^2 - \bar{\omega}_F^2)\sin\theta_c\cos\theta_c\} \\
&\quad + \zeta_0\{-\bar{\omega}_L^2 + (\bar{\omega}_L^2 - \bar{\omega}_F^2)\sin^2\theta_c - \frac{\bar{\ell}^2}{2}\bar{e} + \\
&\quad + \nu(-\frac{\bar{\ell}^4}{4}\beta_p\theta_0 - \frac{\bar{\ell}^3}{3}2\lambda\beta_p)\} + \beta_0\zeta_0\{\nu\frac{\bar{\ell}^3}{3}\lambda\} \\
&\quad + \nu\{-\frac{c_{d0}}{a}(\frac{\bar{\ell}^4}{4} + 2\frac{\bar{\ell}^3}{3}\bar{e}) - \frac{\bar{\ell}^3}{3}\lambda\theta_0 + \\
&\quad + \frac{\bar{\ell}^2}{2}\lambda(\lambda - \bar{e}\theta_0)\} = 0 \qquad (A.2)
\end{aligned}$$

where

$$\bar{\omega}_F^2 = \frac{K_\beta}{m\ell^2R^3}$$

$$\bar{\omega}_L^2 = \frac{K_\zeta}{m\Omega^2R^3}$$

$$\nu = \frac{\rho_A abR}{m}\ ;\ \bar{e} = \frac{e}{R}\ ;\ \bar{\ell} = 1 - \bar{e}$$

When there is no structural flap-lag coupling, the terms containing $\sin\theta_c$ and $\cos\theta_c$ must be deleted from the above equations as well as in the stability equations given below.

$$\theta_0 = \theta_c - \theta_{ZL}$$

where θ_0 is the effective angle of attack

θ_c is the collective pitch setting of the blade

θ_{ZL} is the zero lift angle of attack

Linearized Stability Equations

n-cosine Flap

$$\beta_{nc}F_{nc}(1) + \beta_{ns}F_{nc}(2) + \zeta_{nc}F_{nc}(3) + \zeta_{ns}F_{nc}(4) + \dot{\beta}_{nc}F_{nc}(5) + \dot{\beta}_{ns}F_{nc}(6) + \dot{\zeta}_{nc}F_{nc}(7) + \ddot{\beta}_{nc}F_{nc}(8) + \ddot{\theta}F_{nc}(9) + \dot{\theta}F_{nc}(10) + \dot{\phi}F_{nc}(11) = 0 \qquad (A.3)$$

where

$$F_{nc}(1) = \bar{\omega}_F^2 + (\bar{\omega}_L^2 - \bar{\omega}_F^2)\sin^2\theta_c + \nu\frac{\bar{\ell}^4}{4}\zeta_0 + \frac{\bar{\ell}^3}{3} + \frac{\bar{\ell}^2}{2}\bar{e} - n^2\frac{\bar{\ell}^3}{3} - n^2\frac{1}{2}\nu\bar{b}\frac{\bar{\ell}^3}{3}\cos\theta_0$$

$$F_{nc}(2) = n(\nu\frac{\bar{\ell}^4}{4} + \nu\frac{\bar{\ell}^3}{3}\bar{e} + \bar{g}_{SF})$$

$$F_{nc}(3) = (\bar{\omega}_L^2 - \bar{\omega}_F^2)\sin\theta_c\cos\theta_c + \nu\frac{\bar{\ell}^4}{4}(\beta_p + \beta_0)$$

$$F_{nc}(4) = (2\frac{\bar{\ell}^3}{3}(\beta_0 + \beta_p) - 2\nu\frac{\bar{\ell}^4}{4}\theta_0 + \nu\frac{\bar{\ell}^3}{3}\lambda)n$$

$$F_{nc}(5) = \nu\frac{\bar{\ell}^4}{4} + \nu\frac{\bar{\ell}^3}{3}\bar{e} + \bar{g}_{SF}$$

$$F_{nc}(6) = n\{2\frac{\bar{\ell}^3}{3} + 2\frac{1}{2}\nu\frac{\bar{\ell}^3}{3}\bar{b}\cos\theta_0\}$$

$$F_{nc}(7) = 2\frac{\bar{\ell}^3}{3}(\beta_0 + \beta_p) - 2\nu\frac{\bar{\ell}^4}{4}\theta_0 + \nu\frac{\bar{\ell}^3}{3}\lambda$$

$$F_{nc}(8) = \frac{\bar{\ell}^3}{3} + \frac{1}{2}\nu\bar{b}\frac{\bar{\ell}^3}{3}\cos\theta_0$$

$$F_{nc}(9) = -\frac{\bar{\ell}^3}{3}\delta_n$$

$$F_{nc}(10) = -\delta_n\nu\frac{\bar{\ell}^4}{4}$$

$$F_{nc}(11) = \delta_n\{2\frac{\bar{\ell}^3}{3} + \bar{h}_2(2\nu\frac{\bar{\ell}^3}{3}\theta_0 - \nu\frac{\bar{\ell}^2}{2}\lambda)\}$$

where $\delta_n = 1$ when $n = 1$
$= 0$ $n \neq 1$

$\bar{g}_{SF} = \dfrac{g_{SF}}{m\Omega R^3}$; g_{SF} = damping in flap

b = semichord

n-Sine Flap

$$\beta_{ns}F_{ns}(1) + \beta_{nc}F_{ns}(2) + \zeta_{ns}F_{ns}(3) + \zeta_{nc}F_{ns}(4) + \dot{\beta}_{ns}F_{ns}(5) + \dot{\beta}_{nc}F_{ns}(6) + \dot{\zeta}_{ns}F_{ns}(7) + \ddot{\beta}_{ns}F_{ns}(8) + \ddot{\phi}F_{ns}(9) + \dot{\phi}F_{ns}(10) + \dot{\theta}F_{ns}(11) = 0 \qquad (A.4)$$

where

$$F_{ns}(1) = \bar{\omega}_F^2 + (\bar{\omega}_L^2 - \bar{\omega}_F^2)\sin^2\theta_c + \nu\frac{\bar{\ell}^4}{4}\zeta_0 + \frac{\bar{\ell}^3}{3} + \frac{\bar{\ell}^2}{2}\bar{e} - n^2\frac{\bar{\ell}^3}{3} - \frac{1}{2}\nu\bar{b}\frac{\bar{\ell}^3}{3}n^2\cos\theta_0$$

$$F_{ns}(2) = n\{-\nu\frac{\bar{\ell}^4}{4} - \nu\frac{\bar{\ell}^3}{3}\bar{e} - \bar{g}_{SF}\}$$

$$F_{ns}(3) = (\bar{\omega}_L^2 - \bar{\omega}_F^2)\sin\theta_c\cos\theta_c + \nu\frac{\bar{\ell}^4}{4}(\beta_0 + \beta_p)$$

$$F_{ns}(4) = n\{-2\frac{\bar{\ell}^3}{3}(\beta_0 + \beta_p) + 2\nu\frac{\bar{\ell}^4}{4}\theta_0 - \nu\frac{\bar{\ell}^3}{3}\lambda\}$$

$$F_{ns}(5) = \nu\frac{\bar{\ell}^4}{4} + \nu\frac{\bar{\ell}^3}{3}\bar{e} + \bar{g}_{SF}$$

$$F_{ns}(6) = n\{-2\frac{\bar{\ell}^3}{3} - 2\frac{1}{2}\nu\frac{\bar{\ell}^3}{3}\bar{b}\cos\theta_0\}$$

$$F_{ns}(7) = 2\frac{\bar{\ell}^3}{3}(\beta_0 + \beta_p) - 2\nu\frac{\bar{\ell}^4}{4}\theta_0 + \nu\frac{\bar{\ell}^3}{3}\lambda$$

$$F_{ns}(8) = \frac{\bar{\ell}^3}{3} + \frac{1}{2}\nu\bar{b}\frac{\bar{\ell}^3}{3}\cos\theta_0$$

$$F_{ns}(9) = \delta_n\frac{\bar{\ell}^3}{3}$$

$$F_{ns}(10) = \delta_n\nu\frac{\bar{\ell}^4}{4}$$

$$F_{ns}(11) = \delta_n\{2\frac{\bar{\ell}^3}{3} + 2\nu\frac{\bar{\ell}^3}{3}\theta_0\bar{h}_2 - \bar{h}_2\nu\frac{\bar{\ell}^2}{2}\lambda\}$$

n - Cosine lead-lag

$$\zeta_{nc}L_{nc}(1) + \zeta_{ns}L_{nc}(2) + \beta_{nc}L_{nc}(3) + \beta_{ns}L_{nc}(4) + \dot{\zeta}_{nc}L_{nc}(5) + \dot{\zeta}_{ns}L_{nc}(6) + \dot{\beta}_{nc}L_{nc}(7) + \dot{\beta}_{ns}L_{nc}(8) + \ddot{\zeta}_{nc}L_{nc}(9) + \ddot{\beta}_{nc}L_{nc}(10) + \ddot{\phi}L_{nc}(11) + \ddot{\theta}L_{nc}(12) + \dot{\vartheta}L_{nc}(13) = 0 \qquad (A.5)$$

where

$$L_{nc}(1) = -\bar{\omega}_L^2 + (\bar{\omega}_L^2 - \bar{\omega}_F^2)\sin^2\theta_c - \frac{\bar{\ell}^2}{2}\bar{e} + n^2\frac{\bar{\ell}^3}{3} - \nu\frac{\bar{\ell}^4}{4}\beta_p\theta_0$$

$$L_{nc}(2) = -n\{2\nu\frac{c_{d0}}{a}\frac{\bar{\ell}^4}{4} + \nu\frac{\bar{\ell}^3}{3}\theta_0\lambda + \bar{g}_{SL}\}$$

$$L_{nc}(3) = -(\bar{\omega}_L^2 - \bar{\omega}_F^2)\sin\theta_c\cos\theta_c - n^2\frac{1}{2}\nu\bar{b}\frac{\bar{\ell}^3}{3}\sin\theta_0$$

$$L_{nc}(4) = n\{2\frac{\bar{\ell}^3}{3}(\beta_0 + \beta_p) - \nu\frac{\bar{\ell}^4}{4}\theta_0 - \nu\frac{\bar{\ell}^3}{3}(-2\lambda + \bar{e}\,\theta_0)\}$$

$$L_{nc}(5) = -2\nu \frac{c_{d0}}{a} \frac{\bar{\ell}^4}{4} - \nu \frac{\bar{\ell}^3}{3} \theta_0 \lambda - \bar{g}_{SL}$$

$$L_{nc}(6) = -n\, 2 \frac{\bar{\ell}^3}{3}$$

$$L_{nc}(7) = 2 \frac{\bar{\ell}^3}{3} (\beta_0+\beta_p) - \nu \frac{\bar{\ell}^4}{4} \theta_0$$

$$- \nu \frac{\bar{\ell}^3}{3} (-2\lambda + \bar{e}\theta_0)$$

$$L_{nc}(8) = 2n \frac{1}{2} \nu \bar{b} \frac{\bar{\ell}^3}{3} \sin\theta_0$$

$$L_{nc}(9) = - \frac{\bar{\ell}^3}{3}$$

$$L_{nc}(10) = \frac{1}{2} \nu \bar{b} \frac{\bar{\ell}^3}{3} \sin\theta_0$$

$$L_{nc}(11) = \delta_n \{ \frac{\bar{\ell}^3}{3} (\beta_p+\beta_0) + \bar{h}_2 \frac{\bar{\ell}^2}{2} \}$$

$$L_{nc}(12) = \delta_n \bar{h}_2 \frac{\bar{\ell}^2}{2} \zeta_0$$

$$L_{nc}(13) = \delta_n \{\nu \frac{\bar{\ell}^4}{4} \theta_0 - \frac{\bar{\ell}^3}{3} 2\lambda\nu\}$$

where $\bar{g}_{SL} = g_{SL}/m\Omega R^3$; g_{SL} = damping in lag

n-Sine lead-lag

$$\zeta_{ns}L_{ns}(1) + \zeta_{nc}L_{ns}(2) + \beta_{ns}L_{ns}(3) + \beta_{nc}L_{ns}(4)$$
$$+ \dot{\zeta}_{ns}L_{ns}(5) + \dot{\zeta}_{nc}L_{ns}(6) + \dot{\beta}_{ns}L_{ns}(7)$$
$$+ \dot{\beta}_{nc}L_{ns}(8) + \ddot{\zeta}_{ns}L_{ns}(9) + \ddot{\beta}_{ns}L_{ns}(10)$$
$$+ \ddot{\theta}\, L_{ns}(11) + \ddot{\phi}\, L_{ns}(12) + \dot{\phi}\, L_{ns}(13) = 0 \qquad (A.6)$$

where

$$L_{ns}(1) = - \bar{\omega}_L^2 + (\bar{\omega}_L^2 - \bar{\omega}_F^2)\sin^2\theta_c - \frac{\bar{\ell}^2}{2} \bar{e}$$
$$+ n^2 \frac{\bar{\ell}^3}{3} - \nu \frac{\bar{\ell}^4}{4} \beta_p\theta_o$$

$$L_{ns}(2) = n\{2\nu \frac{c_{d0}}{a} \frac{\bar{\ell}^4}{4} + \nu \frac{\bar{\ell}^3}{3} \lambda\, \theta_0 + \bar{g}_{SL}\}$$

$$L_{ns}(3) = -(\bar{\omega}_L^2 - \bar{\omega}_P^2)\sin\theta_c\cos\theta_c$$
$$- n^2 \frac{1}{2} \nu\bar{b} \frac{\bar{\ell}^3}{3} \sin\theta_0$$

$$L_{ns}(4) = n\{-2 \frac{\bar{\ell}^3}{3} (\beta_0+ \beta_p) + \nu \frac{\bar{\ell}^4}{4} \theta_0$$
$$+ \nu \frac{\bar{\ell}^3}{3} (-2\lambda + \bar{e}\theta_0)\}$$

$$L_{ns}(5) = -2\nu \frac{c_{d0}}{a} \frac{\bar{\ell}^4}{4} - \nu \frac{\bar{\ell}^3}{3} \lambda\, \theta_0 - \bar{g}_{SL}$$

$$L_{ns}(6) = 2n \frac{\bar{\ell}^3}{3}$$

$$L_{ns}(7) = 2 \frac{\bar{\ell}^3}{3} (\beta_p+\beta_0) - \nu \frac{\bar{\ell}^4}{4} \theta_0$$
$$- \nu \frac{\bar{\ell}^3}{3} (-2\lambda + \bar{e}\theta_0)$$

$$L_{ns}(8) = -2n \frac{1}{2} \nu \bar{b} \frac{\bar{\ell}^3}{3} \sin\theta_0$$

$$L_{ns}(9) = - \frac{\bar{\ell}^3}{3}$$

$$L_{ns}(10) = \frac{1}{2} \nu \bar{b} \frac{\bar{\ell}^3}{3} \sin\theta_0$$

$$L_{ns}(11) = \delta_n \frac{\bar{\ell}^3}{3} (\beta_p+ \beta_0) + \frac{\bar{\ell}^2}{2} \bar{h}_2\}$$

$$L_{ns}(12) = -\delta_n \bar{h}_2 \frac{\bar{\ell}^2}{2} \zeta_0$$

$$L_{ns}(13) = \delta_n\{-\nu \frac{\bar{\ell}^4}{4} \theta_0 + \frac{\bar{\ell}^3}{3} 2\lambda\nu\}$$

Roll

$$\frac{N}{2} m\Omega^2R^3\{\beta_{1c} < \nu \frac{c_{d0}}{a} \frac{\bar{\ell}^4}{4} + \nu \frac{\bar{\ell}^3}{3} \lambda\theta_0 + \bar{g}_{SF}$$
$$+ \nu \frac{\bar{\ell}^4}{4} + 2\nu \frac{\bar{\ell}^3}{3} \bar{e} + \bar{h}_2(\nu \frac{\bar{\ell}^3}{3} (\beta_p+\beta_0)$$
$$+ \nu \frac{\bar{\ell}^3}{3} \theta_o\zeta_o + \frac{1}{2} \nu \bar{b} \frac{\bar{\ell}^2}{2} \sin\theta_0) >$$
$$+ \beta_{1s} < -2\nu \frac{\bar{\ell}^4}{4} \zeta_0 + \nu\frac{\bar{\ell}^4}{4} (\beta_p+ 3\beta_0)\theta_0$$
$$+ \frac{1}{2} \nu \bar{b} \frac{\bar{\ell}^3}{3} \cos\theta_0 + \bar{h}_2 (2\nu \frac{\bar{\ell}^3}{3} \theta_0 - \frac{\bar{\ell}^2}{2} \beta_p - \bar{\ell}^2 \beta_0$$
$$+ \nu \frac{\bar{\ell}^2}{2} (-3\lambda + \bar{e}\theta_0)) > + \zeta_{1c} < -\nu \frac{\bar{\ell}^4}{4} \theta_0$$
$$+ \bar{h}_2\nu \frac{\bar{\ell}^3}{3} \theta_0(-\beta_p + \beta_0) > + \zeta_{1s} < \nu \frac{\bar{\ell}^4}{4} \zeta_0\, 2\theta_0$$
$$- \nu \frac{\bar{\ell}^4}{4} (\beta_p+ \beta_0) + \beta_p\bar{g}_{SL} - \bar{h}_2 (\bar{\ell}^2\zeta_0$$
$$- 2\nu \frac{c_{d0}}{a} \frac{\bar{\ell}^3}{3} - \nu \frac{\bar{\ell}^2}{2} \lambda\theta_0) > + \dot{\beta}_{1c} < -\nu \frac{\bar{\ell}^4}{4} \zeta_0$$
$$+ \nu \frac{\bar{\ell}^4}{4} (\beta_0+\beta_p)\theta_0 + 2 \frac{\bar{\ell}^3}{3}$$
$$+ 2 \frac{\bar{\ell}^2}{2} \bar{e} + 2 \frac{1}{2} \nu \bar{b} \frac{\bar{\ell}^3}{3} \cos\theta_0 - \bar{h}_2(\bar{\ell}^2\beta_0$$
$$- \nu \frac{\bar{\ell}^3}{3} \theta_0 - \nu \frac{\bar{\ell}^2}{2} (-2\lambda+\bar{e}\theta_0))>$$
$$+ \dot{\beta}_{1s} < -2 \frac{\bar{\ell}^3}{3} \zeta_0 - \bar{g}_{SF} - \nu \frac{\bar{\ell}^4}{4} - 2\nu \frac{\bar{\ell}^3}{3} \bar{e}$$
$$- \bar{h}_2 (\nu \frac{\bar{\ell}^3}{3} (\beta_p+ \beta_0) + 2 \frac{1}{2} \nu\bar{b} \frac{\bar{\ell}^2}{2} \sin\theta_0) >$$
$$+ \dot{\zeta}_{1c} < \nu \frac{\bar{\ell}^4}{4} \zeta_0 2\theta_0 + \beta_p\bar{g}_{SL}$$
$$- \bar{h}_2(\bar{\ell}^2\zeta_0 - 2 \nu \frac{c_{d0}}{a} \frac{\bar{\ell}^3}{3} - \nu \frac{\bar{\ell}^2}{2} \lambda\theta_0) >$$
$$+ \dot{\zeta}_{1s} < 2 \nu \frac{\bar{\ell}^4}{4} \theta_0 - \nu \frac{\bar{\ell}^3}{3} \lambda + 2\nu \frac{\bar{\ell}^3}{3} \bar{e}\theta_0$$
$$+ \bar{h}_2 \nu\beta_p \frac{\bar{\ell}^3}{3} 2 \theta_0 >$$
$$+ \ddot{\beta}_{1c} < - \frac{\bar{\ell}^3}{3} \zeta_0 - \bar{h}_2 \frac{1}{2} \nu\bar{b} \frac{\bar{\ell}^2}{2} \sin\theta_0 >$$

$$+ \ddot{\beta}_{1s} < -\frac{\bar{\ell}^3}{3} - \frac{1}{2}\nu\bar{b}\frac{\bar{\ell}^3}{3}\cos\theta_0 - \frac{\bar{\ell}^2}{2}\bar{e}$$
$$- \bar{h}_2\beta_p\frac{\bar{\ell}^2}{2} >$$
$$+ \ddot{\zeta}_{1c} < \frac{\bar{\ell}^3}{3}(\beta_p + \beta_0) + \bar{h}_2\frac{\bar{\ell}^2}{2} >$$
$$+ \ddot{\phi} < -\frac{\bar{\ell}^3}{3} - \frac{\bar{\ell}^2}{2}\bar{e} - \bar{h}_2\beta_p\frac{\bar{\ell}^2}{2} - \bar{h}_2\frac{\bar{\ell}^2}{2}(\beta_p + \beta_0)$$
$$- \bar{h}_2\left(\frac{\bar{\ell}^2}{2}(\beta_p + \beta_0) + 2\bar{h}_2\bar{\ell}\right) >$$
$$+ \dot{\phi} < -\frac{\bar{\ell}^3}{3}2\zeta_0 - \nu\frac{\bar{\ell}^3}{3}\bar{e} - \nu\frac{\bar{\ell}^4}{4} - \bar{h}_2\beta_p\nu\frac{\bar{\ell}^3}{3}$$
$$- \bar{h}_2\beta_0\nu\frac{\bar{\ell}^3}{3} > + \ddot{\theta} < \frac{\bar{\ell}^3}{3}\zeta_0 >$$
$$+ \dot{\theta} < \nu\frac{\bar{\ell}^4}{4}\zeta_0 - 2\frac{\bar{\ell}^3}{3} - \frac{\bar{\ell}^2}{2}2\bar{e} - 2\bar{h}_2\beta_p\frac{\bar{\ell}^2}{2}$$
$$- \bar{h}_2\nu\frac{\bar{\ell}^3}{3}\theta_0 + \nu\frac{\bar{\ell}^2}{2}\lambda 2\bar{h}_2 + \bar{h}_2\nu\frac{\bar{\ell}^2}{2}\lambda$$
$$- \bar{h}_2\nu\frac{\bar{\ell}^3}{3}2\upsilon_0 > \}$$
$$- I_{xx}\Omega^2\ddot{\phi} + I_{xy}\Omega^2\ddot{\theta} = 0 \qquad (A.7)$$

Pitch

$$\frac{N}{2}m\Omega^2R^3\{\beta_{1c} \quad 2\nu\frac{\bar{\ell}^4}{4}\zeta_0 - \nu\frac{\bar{\ell}^4}{4}(\beta_p + 3\beta_0)\theta_0$$
$$- \frac{1}{2}\nu\bar{b}\frac{\bar{\ell}^3}{3}\cos\theta_0$$
$$- \bar{h}_2\left(\nu\frac{\bar{\ell}^3}{3}2\theta_0 - \frac{\bar{\ell}^2}{2}\beta_p - \bar{\ell}^2\beta_0\right.$$
$$\left. + \nu\frac{\bar{\ell}^2}{2}(-3\lambda + \bar{e}\theta_0)\right) >$$
$$+ \beta_{1s} < \nu\frac{c_{d0}}{a}\frac{\bar{\ell}^4}{4} + \nu\frac{\bar{\ell}^3}{3}\lambda\theta_0 + \bar{g}_{SF} + \nu\frac{\bar{\ell}^4}{4}$$
$$+ 2\nu\frac{\bar{\ell}^3}{3}\bar{e} + \bar{h}_2\left(\beta_p\nu\frac{\bar{\ell}^3}{3} + \beta_0\nu\frac{\bar{\ell}^3}{3}\right.$$
$$\left. + \nu\frac{\bar{\ell}^3}{3}\zeta_0\theta_0 + \frac{1}{2}\nu\bar{b}\frac{\bar{\ell}^2}{2}\sin\theta_0\right) >$$
$$+ \zeta_{1c} < -\nu\frac{\bar{\ell}^4}{4}\zeta_0 2\theta_0 - \beta_p\bar{g}_{SL} + \nu\frac{\bar{\ell}^4}{4}(\beta_p + \beta_0)$$
$$+ \bar{h}_2\left(\bar{\ell}^2\zeta_0 - 2\nu\frac{c_{d0}}{a}\frac{\bar{\ell}^3}{3} - \nu\frac{\bar{\ell}^2}{2}\lambda\theta_0\right) >$$
$$+ \zeta_{1s} < -\nu\frac{\bar{\ell}^4}{4}\theta_0 + \bar{h}_2\nu\frac{\bar{\ell}^3}{3}(-\beta_p + \beta_0)\theta_0 >$$
$$+ \dot{\beta}_{1c} < 2\frac{\bar{\ell}^3}{3}\zeta_0 + \bar{g}_{SF} + \nu\frac{\bar{\ell}^4}{4} + 2\nu\frac{\bar{\ell}^3}{3}\bar{e}$$
$$+ \bar{h}_2\left(\nu\frac{\bar{\ell}^3}{3}(\beta_p + \beta_0) + 2\frac{1}{2}\nu\bar{b}\frac{\bar{\ell}^2}{2}\sin\theta_0\right)$$
$$+ \dot{\beta}_{1s} < -\nu\frac{\bar{\ell}^4}{4}\zeta_0 + \nu\frac{\bar{\ell}^4}{4}\theta_0(\beta_p + \beta_0) + 2\frac{\bar{\ell}^3}{3}$$
$$+ 2\frac{\bar{\ell}^2}{2}\bar{e} + 2\frac{1}{2}\nu\bar{b}\frac{\bar{\ell}^3}{3}\cos\theta_0$$
$$- \bar{h}_2\left(\bar{\ell}^2\beta_0 - \nu\frac{\bar{\ell}^3}{3}\theta_0 - \nu\frac{\bar{\ell}^2}{2}(-2\lambda + \bar{e}\theta_0)\right) >$$
$$+ \dot{\zeta}_{1c} < -2\nu\frac{\bar{\ell}^4}{4}\theta_0 + \nu\frac{\bar{\ell}^3}{3}\lambda - \nu\frac{\bar{\ell}^3}{3}\bar{e}\,2\theta_0$$
$$- \bar{h}_2\beta_p\nu\frac{\bar{\ell}^3}{3}2\theta_0 >$$
$$+ \dot{\zeta}_{1s} < \nu\frac{\bar{\ell}^4}{4}\zeta_0 2\theta_0 + \beta_p\bar{g}_{SL} - \bar{h}_2\bar{\ell}^2\zeta_0$$
$$+ \bar{h}_2\nu\frac{c_{d0}}{a}2\frac{\bar{\ell}^3}{3} + \bar{h}_2\nu\frac{\bar{\ell}^2}{2}\lambda\theta_0 >$$
$$+ \ddot{\beta}_{1c} < \frac{\bar{\ell}^3}{3} + \frac{1}{2}\nu\bar{b}\frac{\bar{\ell}^3}{3}\cos\theta_0 + \frac{\bar{\ell}^2}{2}\bar{e} + \bar{h}_2\beta_p\frac{\bar{\ell}^2}{2} >$$
$$+ \ddot{\beta}_{1s} < -\frac{\bar{\ell}^3}{3}\zeta_0 - \bar{h}_2\frac{1}{2}\nu\bar{b}\frac{\bar{\ell}^2}{2}\sin\theta_0 >$$
$$+ \ddot{\zeta}_{1s} < \frac{\bar{\ell}^3}{3}(\beta_0 + \beta_p) + \bar{h}_2\frac{\bar{\ell}^2}{2} >$$
$$+ \ddot{\phi} < -\frac{\bar{\ell}^3}{3}\zeta_0 >$$
$$+ \dot{\phi} < -\nu\frac{\bar{\ell}^4}{4}\zeta_0 + 2\frac{\bar{\ell}^3}{3} + \frac{\bar{\ell}^2}{2}2\bar{e} + 2\bar{h}_2\beta_p\frac{\bar{\ell}^2}{2}$$
$$+ \bar{h}_2\nu\frac{\bar{\ell}^3}{3}\theta_0 - \nu\frac{\bar{\ell}^2}{2}2\lambda\bar{h}_2 + \bar{h}_2\nu\frac{\bar{\ell}^3}{3}2\theta_0$$
$$- \bar{h}_2\nu\frac{\bar{\ell}^2}{2}\lambda >$$
$$+ \ddot{\theta} < -\frac{\bar{\ell}^3}{3} - \frac{\bar{\ell}^2}{2}\bar{e} - \bar{h}_2\frac{\bar{\ell}^2}{2}(\beta_p + \beta_0)$$
$$- \bar{h}_2\beta_p\frac{\bar{\ell}^2}{2} + \bar{h}_2\left(-\frac{\bar{\ell}^2}{2}(\beta_p + \beta_0) - 2\bar{\ell}\bar{h}_2\right) >$$
$$+ \dot{\theta} < -\frac{\bar{\ell}^3}{3}2\zeta_0 - \nu\frac{\bar{\ell}^4}{4} - \nu\frac{\bar{\ell}^3}{3}\bar{e} - \nu\frac{\bar{\ell}^3}{3}\beta_p\bar{h}_2$$
$$- \nu\frac{\bar{\ell}^3}{3}\beta_0\bar{h}_2 > \} - I_{yy}\Omega^2\ddot{\theta} + I_{yx}\Omega^2\ddot{\phi} = 0$$
$$(A.8)$$

Appendix B: Rotor, Blade and Body Properties

Rotor Geometry

Number of blades	3
Radius, cm	81.1
Chord, cm	4.19
Hinge offset, cm	8.51
Blade airfoil	NACA 23012
Profile drag coefficient	0.0079
Lock number	7.73
Solidity ratio	0.0494
Lift curve slope	2π
Height of rotor hub above gimbal, cm	24.1

Blade Mass Properties

Blade mass (to flap flexure), gm	209
Blade mass centroid (Ref. flexure centerline), cm	18.6
Blade flap inertia (Ref. flexure centerline), gm m^2	17.3

Blade Frequency and Damping

	Conf. 1	Conf.4
Nonrotating flap freq. Hz	3.13	6.63
Nonrotating lead-lag freq. Hz	6.70	6.73
Damping in lead-lag (% critical)	0.52%	0.53%

Body Mass Properties

Rotary inertia in pitch, gm m^2	633
Rotary inertia in roll, gm m^2	183

Body Frequency and Damping

Pitch frequency, Hz	2
Roll frequency, Hz	4
Damping in roll (% critical)	0.929%
Damping in pitch (% critical)	3.20%

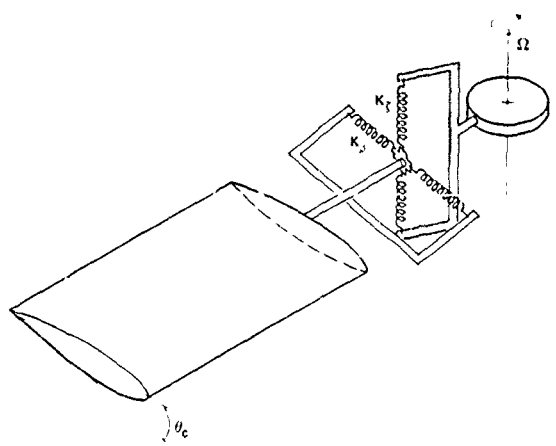


Figure 1. Equivalent Spring Restrained Blade Model.

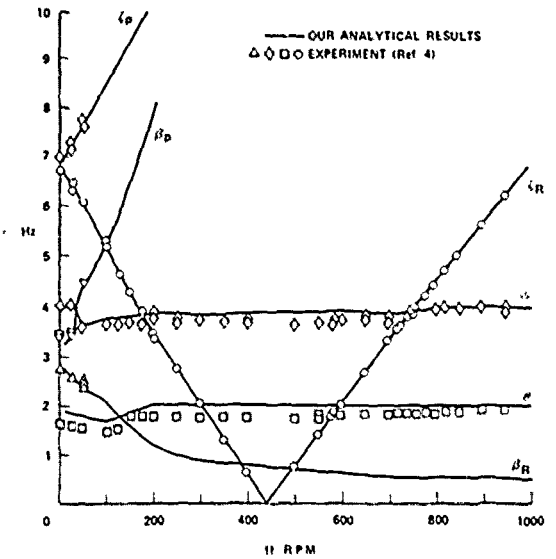


Figure 2. Modal Frequencies as a Function of Ω, θ_c = 0 (Configuration 1).

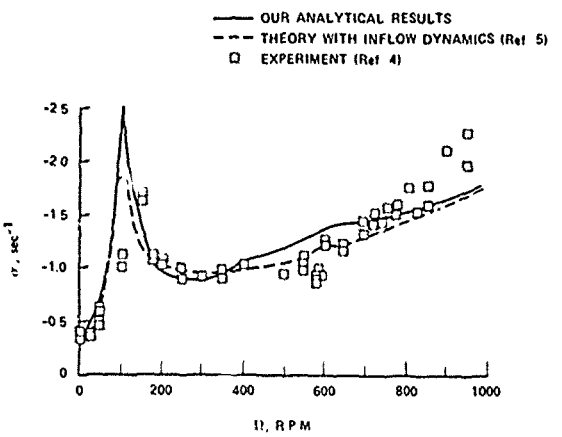


Figure 3. Body Pitch Mode Damping as a Function of Ω, θ_c = 0 (Configuration 1).

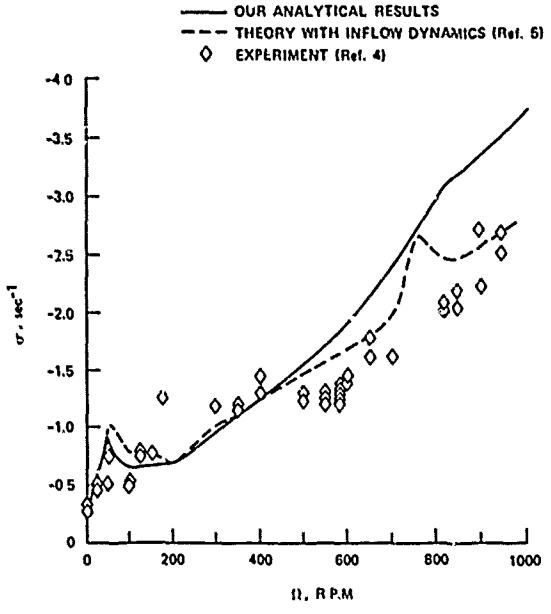


Figure 4. Body Roll Mode Damping as a Function of Ω, θ_c = 0 (Configuration 1).

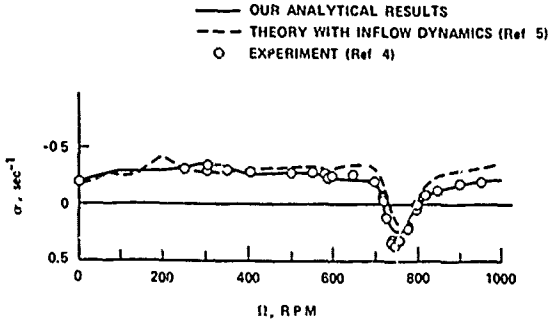
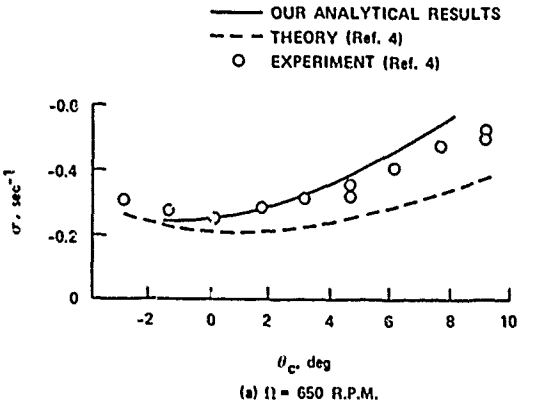


Figure 5. Regressing Lag Mode Damping as a Function of Ω, θ_c = 0 (Configuration 1).



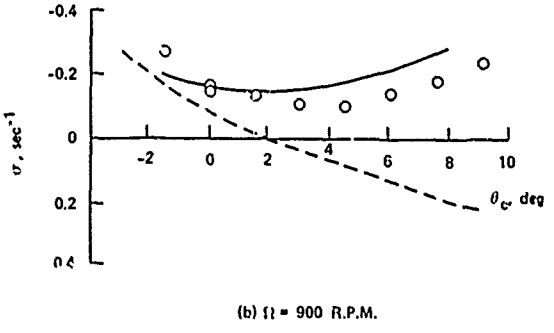


Figure 6. Lead Lag Regressing Mode Damping as a Function of θ_c at (a) 650 R.P.M. and (b) 900 R.P.M. (Configuration 1).

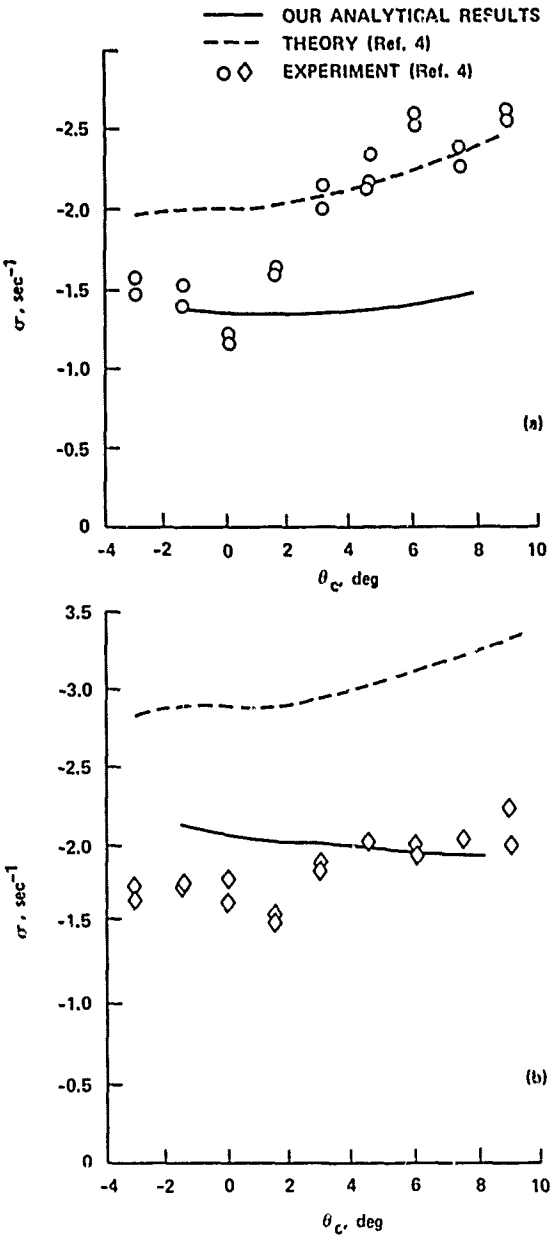


Figure 7. Variation of Damping in (a) Pitch and (b) Roll with θ_c at Ω = 650 R.P.M. (Configuracion 1).

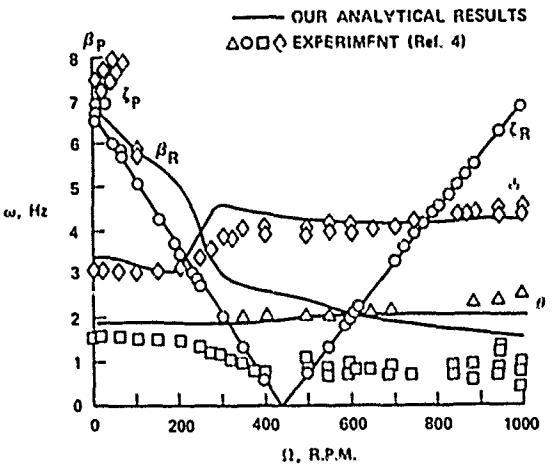


Figure 8. Variation of Modal Frequencies with Ω, θ_c = 0 (Configuration 4).

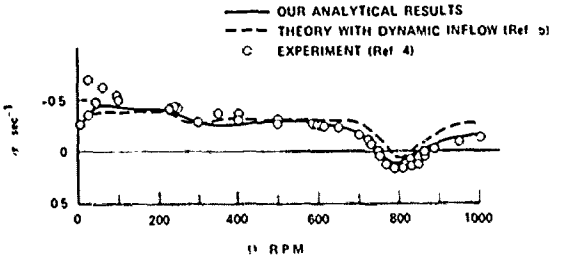


Figure 9. Variation of Damping in Lag Regressing Mode with Ω, θ_c = 0 (Configuration 4).

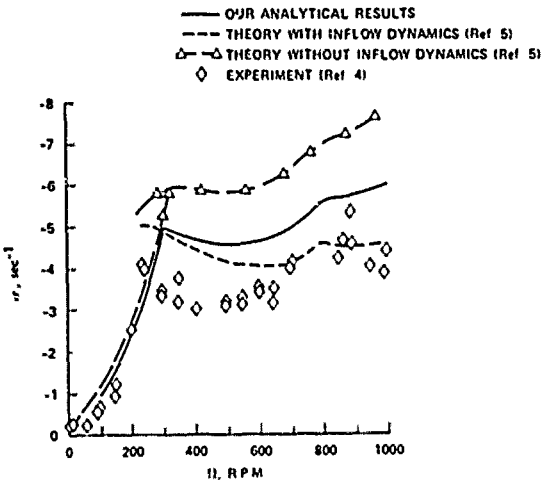


Figure 10. Variation of Damping in Roll with Ω, $\theta_c = 0$ (Configuration 4).

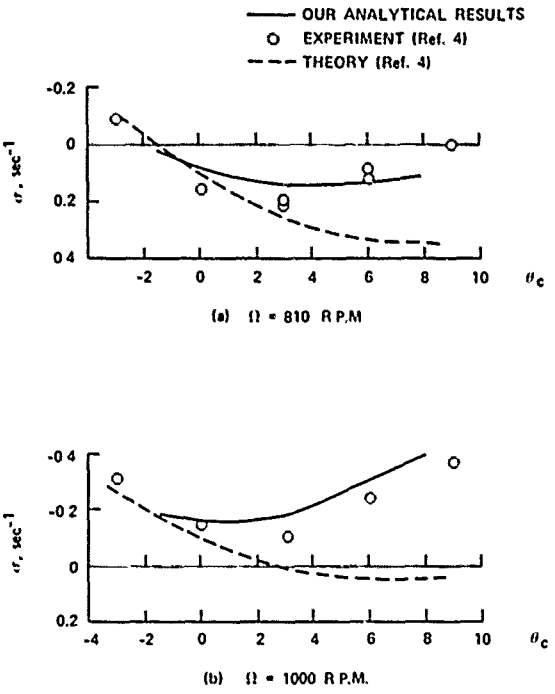


Figure 12. Variation of Damping in Lag Regressing Mode with θ_c at (a) 810 R.P.M. and (b) 1000 R.P.M. (Configuration 4).

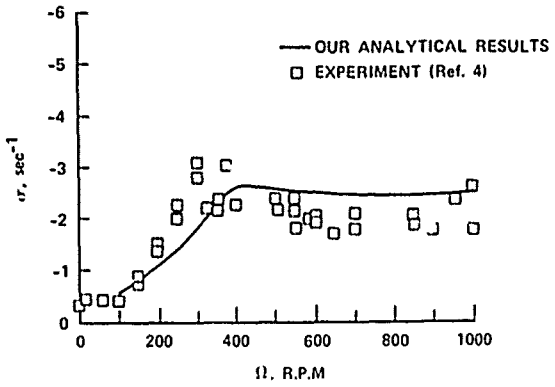


Figure 11. Variation of Damping in Pitch with Ω, $\theta_c = 0$ (Configuration 4).

DISCUSSION

COMPARISON OF EXPERIMENTAL COUPLED HELICOPTER ROTOR/BODY STABILITY RESULTS WITH A SIMPLE ANALYTICAL MODEL

P. P. Friedmann
C. Venkatesan

Jing Yen, Bell Helicopter Textron: It would be interesting to compare your "F = ma" terms with whatever Johnson has, and Bell has, and whoever else has, to see where the differences are. Because if you leave the dynamic inflow out...you don't have dynamic inflow in your analysis.

Friedmann: That's right.

Yen: You also show some other curves without dynamic inflow; however, your theory and their theories don't come close. My question is, are you going to compare your "F = ma" terms with theirs?

Friedmann: I don't see exactly what you mean by "F = ma" terms but let me try to answer your question, but based on the recommendations I've received from Wayne and Bill Bousman, I'm going to put dynamic inflow in these equations and see what happens.

Yen: That's a new program. I'm talking about the documentation of these equations.

Friedmann: The documentation of these equations is available in a document, and these equations are fully documented.

Yen: I'm saying you should compare your equations with their documented equations to see....

Friedmann: I don't like to compare equations with equations, if I can compare solutions with solutions.

Wayne Johnson, Session Chairman: What you're saying, Jing, is the same remark that could have been made yesterday in the presentation of these results.

Yen: Yes, exactly.

Johnson: Peretz didn't have a copy of the ITR stuff so he was doing this without that information. I've actually laid his calculations alongside what the rest of us did and it's all within the same band, okay? His is sort of on the bottom end, but I wouldn't consider it radically different from any of the other six. Between any two of those analyses that we've done, the differences are roughly equal in magnitude. This is a fairly straightforward situation so that's why at least everybody got the same trends, but there still are differences.

Bob Ormiston, Aeromechanics Laboratory: Can I make a couple of comments here? First of all, based on my look at the data, working with the analysis and the experimental results, and your finding that the variation of the regressing-mode lead-lag damping as a function of pitch angle, some of the curves you showed there where you compared the FLAIR results against your results without any consideration of dynamic inflow, shows a major difference between the two analyses which is really significant. We never understood why we got such poor coorelation in that area, and going back to "F = ma" or whatever the terms are would be very interesting; we should do that. I want to acknowledge that I think there has been a major improvement or whatever in the correlation there, but the business about the regressing lead-lag mode damping as a function of rpm, where the effect of dynamic inflow shows a slight improvement is a much fuzzier situation. However, I'll take issue with you a little bit because of the way you presented the data: your result without inflow, Wayne's result with inflow, and you show roughly the same level of predicted damping. Now people who have done the apples-to-apples comparison, like Gaonkar, have shown that the increment due to dynamic inflow is precisely in the direction to improve the correlation with the data. It's small for that mode, but it's in the right direction.

Friedmann: As I indicated, I'm going to put in the dynamic inflow based on Wayne's recommendation. Now regarding the equations, they are documented.

Ormiston: That's not a more fundamental problem than the "F = ma," or the elastics or the lift curve slope, which is pretty important as you've pointed out. So that really ought to be traced down when you've shown such a major improvement in the correlation.

Friedmann: The equations are very straightforward and very simple.

Ormiston: Well, they're not really simple.

Dewey Hodges, Aeromechanics Laboratory: I'd like to take issue with one conclusion, and that is that in your case you have ζ set equal to $\zeta_o + \Delta\zeta$ and $\beta = \beta_o + \Delta\beta$, you also obviously, somewhere along the line, said $\phi = \phi_o + \Delta\phi$, and $\theta = \theta_o + \Delta\theta$, and then linearized.... [Friedmann: No.] You had to. Then linearized in $\Delta\theta$ and $\Delta\phi$, but now ϕ_o and θ_o have to be zero, so in essence you're just simply linearizing the equations in ϕ and θ. So [regarding] your assertion about the ordering scheme, you have no way of validating that kind of a conclusion because you're linearizing the equations in ϕ and θ anyway, as I do and everybody else does. For this problem it has to be a linear problem so your ordering scheme hasn't even been exercised.

Friedmann: I agree with you that the ordering scheme has not been exercised as far as the nonlinear terms in pitch and roll are concerned. No disagreement, your point is well taken and I should have mentioned it. However, what I wanted to point out is that by this slightly smaller order of magnitude you don't lose anything because it does not kick out of the equations any of the linear terms or anything else important. This happens because you get products of the various types of

pitch-and-roll motions multiplying the blade degrees of freedom, so the ordering scheme does not cause any fatal flaws, because otherwise....

Hodges: If your equations are linear anyway then the ordering scheme has nothing to do with it.

Friedmann: The equations are not linear.

Hodges: They are in ϕ and θ.

Friedmann: They are linear in ϕ and θ, as have been everybody's results because [in] this particular problem, the fuselage degrees of freedom are totally perturbational quanities.

Hodges: The only way you can exercise your ordering scheme is in forward flight.

Friedmann: Absolutely, no disagreement.

AEROMECHANICAL STABILITY ANALYSIS OF COPTER

Sheng K. Yin
Engineering Specialist

and

Jing G. Yen
Manager of Flight Technology

Bell Helicopter Textron
Fort Worth, Texas

Abstract

A plan has been formed for developing a comprehensive, second-generation system with analytical capabilities for predicting performance, loads and vibration, handling qualities, aeromechanical stability, and acoustics. This second-generation system named COPTER (COmprehensive Program for Theoretical Evaluation of Rotorcraft) is designed for operational efficiency, user friendliness, coding readability, maintainability, transportability, modularity, and expandability for future growth. The system is divided into an executive, a data deck validator, and a technology complex. At present a simple executive, the data deck validator, and the aeromechanical stability module of the technology complex have been implemented. This paper describes briefly the system, discusses the implementation of the technology module, and presents correlation data. The correlation includes hingeless-rotor isolated stability, hingeless-rotor ground-resonance stability, and air-resonance stability of an advanced bearingless-rotor in forward flight.

Introduction

Each helicopter manufacturer has employed several analytical methods of varying complexity to determine loads and vibrations, aeroelastic stability, stability and control, performance, and acoustics. It was the consensus of the U.S. Army and the U.S. helicopter industry that these first-generation methods had limited capability, since they were not generally applicable to all types and sizes of helicopters, were difficult to maintain and improve, and were not truly comprehensive. In 1976, a decision was made by USAAMRDL at Fort Eustis to develop the Second-Generation Comprehensive Helicopter Analysis System (2GCHAS) using modern software design techniques and modules for the technology complex. In order to maintain its competitive position in the technical community and assist the government in the development of 2GCHAS, Bell Helicopter Textron Inc. (BHTI) initiated the COmprehensive Program for Theoretical Evaluation of Rotorcraft (COPTER).

The COPTER System

The COPTER system is designed for operational efficiency, user friendliness, coding readability, maintainability, transportability, modularity, and expandability for future growth. The system is divided into an executive, a data deck validator, and a technology complex. The source is coded in VS FORTRAN to take advantage of the structured programming features. Each subprogram has a prologue to explain its function, inputs and outputs, computational method and sequence, creation/modification dates, and authors. Various built-in diagnostic options are available throughout the program.

A user can invoke the executive of the system at a TSO (IBM's Time Sharing Option) terminal by typing the command "COPTER." The executive then presents a menu on the screen with options available to the user. These options include editing input data, running programs interactively, browsing outputs, and submitting batch jobs. The executive can also prompt the user for inputs and interface interactively with the user.

The executive takes advantage of the System Productivity Facility (SPF), an IBM product, to invoke the editing and browsing options. This allows full-screen editing and scrolling of the input data and browsing the output immediately after running the programs. Any error messages will be displayed on the terminal screen.

Presented at the ITR Methodology Assessment Workshop, NASA Ames, June 21-22, 1983.

The executive drives two programs. The first program is the Data Deck Validator (DDV), which reads inputs, interprets key words, checks for errors, and generates error messages wherever appropriate. It also retrieves block data from the master data base, creates the run data base, and generates an annotated echo of the input data. The second program contains the technology modules of the COPTER system. It reads the run data base as its input, executes the user-specified technology modules, and generates engineering data that can be printed or plotted. The flow chart in Figure 1 summarizes the COPTER system.

Aeromechanical Stability

In recent years, the helicopter community has been challenged by the development of hingeless and bearingless rotors. The area of greatest challenge has been predicting aeroelastic stability characteristics for such rotors. As a result, the U.S. Army awarded several methodology assessment contracts to helicopter companies in 1981. The results were encouraging, but inconclusive (References 1 and 2).

Bell has been working toward the development of viable hingeless and bearingless rotor systems for over a decade. The effort has led to an experimental hingeless rotor (Reference 3), two production hingeless rotors (e.g., Reference 4), and a successful advanced bearingless rotor (Reference 5).

Recognition of Bell's in-house design requirements and the lack of a comprehensive capability in analyzing stability characteristics of hingeless and bearingless rotors resulted in the decision that the aeromechanical stability module should be the first technology module to be implemented in the COPTER system.

Analytical Model

Modal representations are used for the rotor and the airframe dynamics. A two-dimensional, strip, quasi-steady theory is employed for the blade aerodynamics. The effects of compressibility, reverse flow, and stall are modeled using the aerodynamic table look-up technique. A dynamic inflow model similar to the one discussed in Reference 6 is included as an option. Dynamic coupling between the rotor and the airframe is achieved by using time-invariant mass matrix methodol-

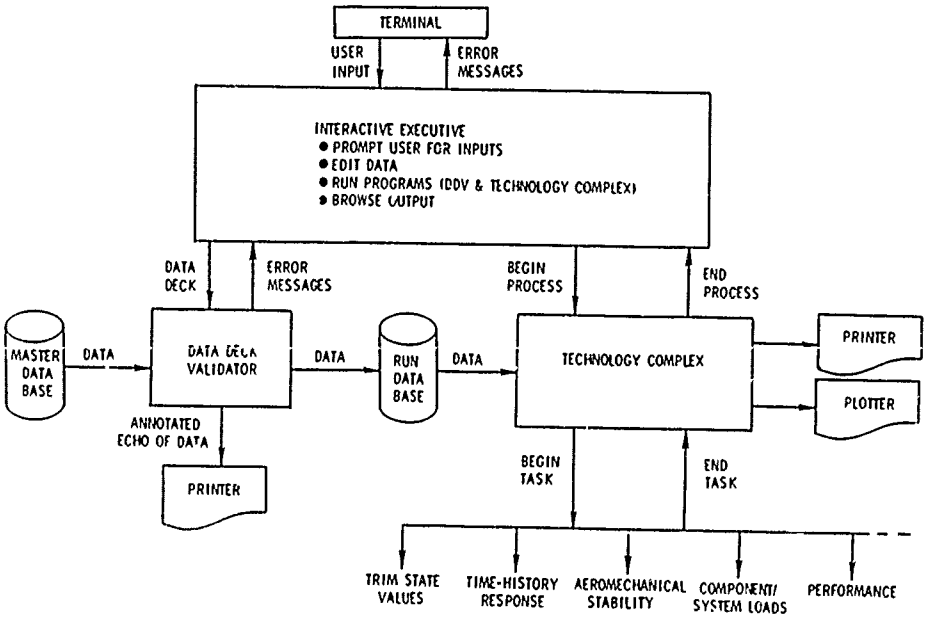


Figure 1. The COPTER system.

ogy (Reference 7). The time-invariant mass matrix capability also facilitates the modeling of various hub types, such as bearingless, hingeless, gimbaled, and teetering rotors. Hub loads are calculated by either the mode-deflection or the force-integration method. At present, the analysis interfaces with the C81 computer program to obtain trim values.

Two methods of solution are available to the analysis: multiblade coordinate transformation and Floquet transition matrix. The multiblade coordinate transformation is used for multibladed rotors in hover, while the Floquet method is used for two-bladed rotors and all forward-flight conditions. The solution is presented in eigenvalue and eigenvector forms.

Correlations

Validation is one of the most important phases in the development of any analytical design tool. The aeromechanical stability analysis has been validated by comparing the results with those of established computer programs and by correlating with measured model data. The correlations shown in this paper include a hingeless-rotor isolated stability, a hingeless-rotor ground resonance, and stability of an advanced bearingless rotor with simulated body degrees-of-freedom in forward flight.

The hovering data of a hingeless-rotor isolated stability were obtained from cases A/2 and A/4 of the Army Integrated Technology Rotor (ITR) methodology assessment contract. A complete description of the two-bladed rotor model is presented in Reference 1. Case A/2 was for a uniform blade with a soft feathering flexure, but with no precone or droop. Case A/4 was for the same blade as case A/2, but with a 5° hub precone. Measured and computed blade lead-lag damping values vs blade pitch angles were plotted at a rotor speed of 1000 rpm and are shown in Figures 2 and 3 for case A/2 and case A/4, respectively. For both cases, it was found that the effect of the dynamic inflow on the blade inplane damping was small. Analytical data shown in Figures 2 and 3 were obtained without employing the dynamic inflow model.

A correlation with ground-resonance data measured on a model-scale, three-bladed hingeless rotor, coupled with body pitch and roll degrees-of-freedom, was performed. Descriptions of the experimental model, experimental results, and analytical representation of the model hardware can be found in Reference 1. This was case C/1 of the ITR methodology assessment contract. System frequencies,

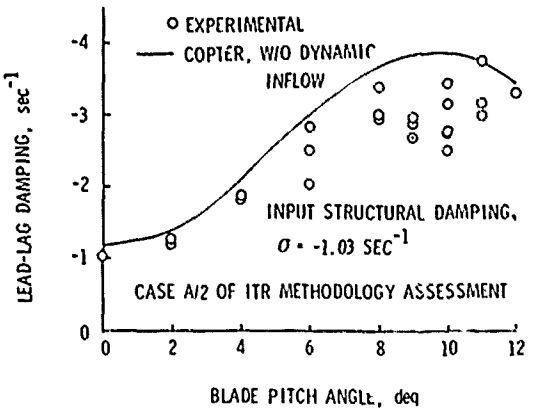


Figure 2. Lead-lag damping vs blade pitch angle, no precone or droop, soft feathering flexure, 1000 rpm, isolated two-bladed hingeless rotor.

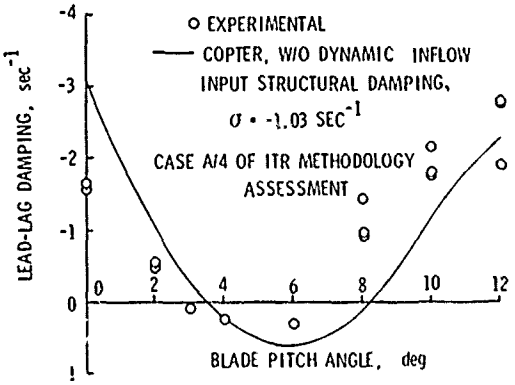


Figure 3. Lead-lag damping vs blade pitch angle, 5° precone, soft feathering flexure, 1000 rpm, isolated two-bladed hingeless rotor.

damping values of lead-lag regressing mode, and body pitch and body roll modes were plotted as rotor speeds varied from 0 to 1000 rpm. The blade was untwisted with 0° blade pitch angle. The analysis was conducted with and without the dynamic inflow. For this case (coupled rotor/body), including the dynamic inflow in the analysis improved the correlation.

Data in Figures 4 through 7 show correlations of system frequencies, lead-lag regressing mode damping, body pitch mode damping, and body roll mode damping, respectively. Analytical results, with and without the dynamic inflow, are presented in Figures 5 through 7. Computed system frequencies depicted in Figure 4 were obtained with the dynamic inflow included in the computation; those calculations without the dynamic inflow were not as good. To avoid further cluttering of the data in Figure 4, computed frequencies without the dynamic inflow were deleted from this figure.

It should be pointed out here that the analytical data shown in these figures were obtained by using the force-integration technique in the calculation of hub forces and moments. The results showed distinct frequency shifts in the body/lead-lag crossings when the mode-deflection method was used. The difference in the results between the mode-deflection method and the force-integration method was attributed to the fact that the mode-deflection method did not include the complete dynamic coupling terms.

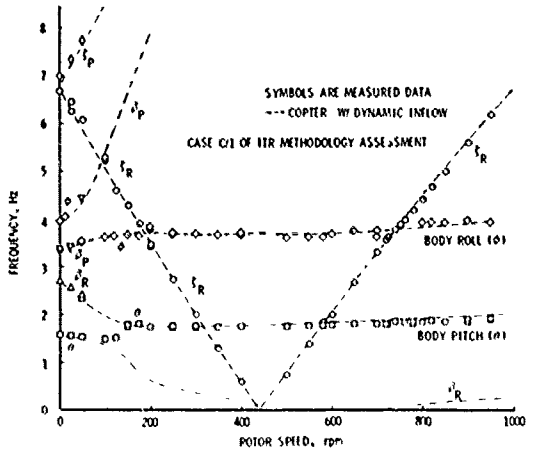


Figure 4. Correlation of ground resonance frequencies, flat pitch.

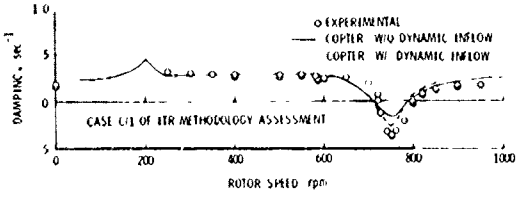


Figure 5. Correlation of lead-lag regressing mode damping, flat pitch.

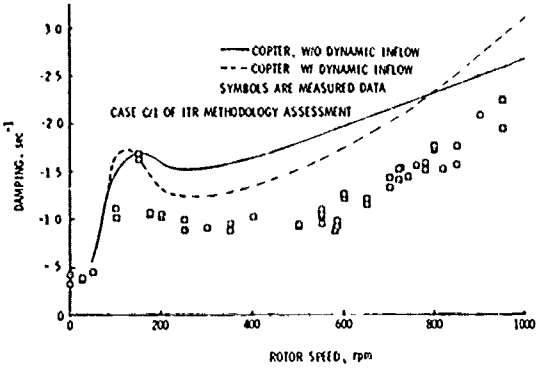


Figure 6. Correlation of body pitch damping, flat pitch.

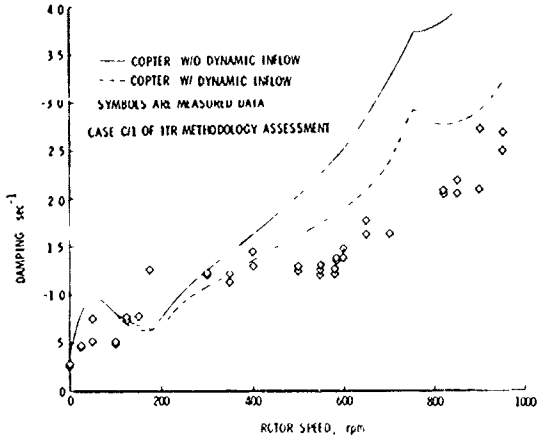


Figure 7. Correlation of body roll damping, flat pitch.

A correlation of aeromechanical stability in forward flight was made by using experimental data measured on a one-fifth scale model rotor with an advanced bearingless hub. Descriptions of the experimental apparatus and procedures are presented in Reference 8. The particular rotor and body used for this correlation effort were the baseline rotor and the baseline fuselage configurations identified as R-1 and F-2, respectively, in Reference 8. The rotor had a hub precone of 2.75° with no blade droop or sweep.

Correlation of blade regressing inplane frequency (fixed system) and lead-lag damping (rotating system) vs rotor speed at a tunnel speed of 27.7 kn and 1g rotor thrust is shown in Figure 8. Measured data for body pitch and roll mode frequencies were not available. However, computed body pitch and roll frequencies are included in Figure 8 to indicate the rotor speeds where the regressing inplane mode crosses the body modes.

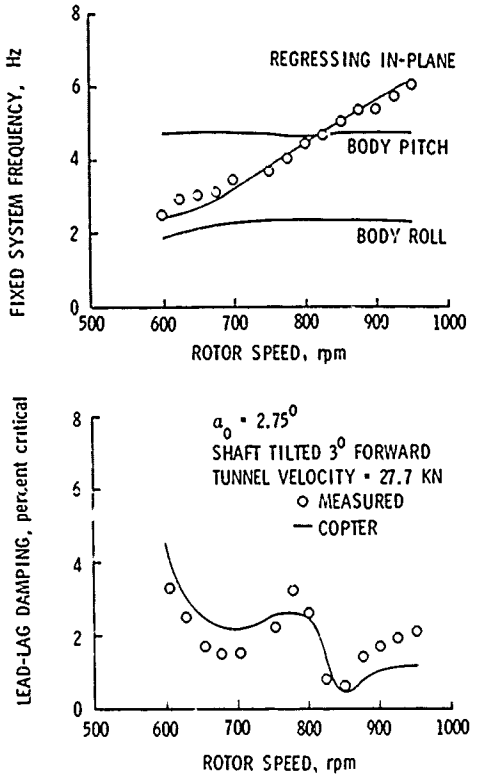


Figure 8. Correlation of frequency and damping vs rotor speed in forward flight, 1g thrust.

A correlation of regressing inplane frequency (fixed system) and blade lead-lag damping (rotating system) vs rotor thrust at 750 rpm and a 27.7-kn tunnel speed is presented in Figure 9.

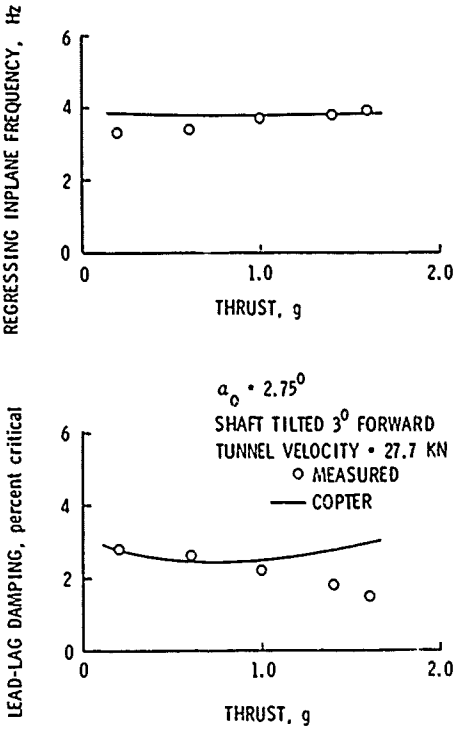


Figure 9. Correlation of inplane frequency and damping vs rotor thrust in forward flight, 750 rpm.

Concluding Remarks

A second-generation comprehensive aeromechanical stability analysis has been developed as part of the overall technology capabilities of the COPTER system. The technology complex of the system is modularized. The system, therefore, has great potential for growth and improvement, and new physics can be incorporated at any point of the COPTER life cycle.

The use of dynamic inflow improves the ground-resonance correlation.

The mode-deflection method usually does not include the complete dynamic coupling terms, as does the force-i. e-

gration method. Its application to the ground-resonance analysis may lead to erroneous rotor/body crossing and incorrect damping.

Application of the Floquet transition matrix to aeromechanical stability in forward flight produces eigenvalue and eigenvector solutions. This eliminates most of the shortcomings associated with a time history solution.

Acknowledgement

The authors would like to acknowledge the contribution of Mr. P. Y. Hsieh and Dr. Tom Waak in the Scientific and Technical Computing Department and Dr. Gene Sadler in the Rotor Dynamics Group at Bell to the planning and design of the COPTER system and implementation of the aeromechanical stability analysis.

References

1. Yen, J. G., "Integrated Technology Rotor Methodology Assessment," Final letter report by Bell Helicopter Textron Inc. to Contract No. NAS2-10872, 11 December 1981.

2. Anonymous, "ITR Methodology Assessment Workshop," NASA Ames, 21-22 June 1983.

3. Cresap, W. L., Myers, A. W., and Viswanathan, S. P., "Design and Development Tests of a Four-Bladed Light Helicopter Rotor System," Journal of the American Helicopter Society, January 1979.

4. Cresap, W. L., and Myers, A. W., "Design and Development of the Model 412 Helicopter," Preprint No. 80-56, American Helicopter Society, May 1980.

5. Alsmiller, G. R., Sonneborn, W. G. O., and Metzger, R. W., "The All-Composite Rotorcraft," Preprint No. A-83-39-61-1000, American Helicopter Society, 9-11 May 1983.

6. Peters, D. A., "Hingeless Rotor Frequency Response with Unsteady Inflow," NASA SP-352, February 1974.

7. Sadler, S. G., Corrigan, J., and Yen, J. G., "Component Coupling with Time-invariant Mass Matrix for Non-isotropic Rotating and Nonrotating Systems," Preprint No. 82-0731, AIAA SDM Conference, May 1982.

8. Weiler, W. H., "Correlation and Evaluation of Inplane Stability Characteristics for an Advanced Beaingless Main Rotor," NASA CR-166448, May 1983.

DISCUSSION

AEROMECHANIC STABILITY ANALYSIS OF COPTER

Sheng K. Yin
Jing G. Yen

Jerry Miao, Sikorsky Aircraft: What is the difference between this COPTER aeromechanical stability module and DRAV21?

Yen: Well, they're basically the same. COPTER, as I said, is a second generation analysis. The aeromechanical stability analysis happens to be one of the technology modules. One of the primary differences between them is that now we transport all of those C81 trims into here; in DRAV21 all those trims were done internally, so that's one of the differences. I consider it to be a very important one.

Bill White, U.S. Army AVRADCOM: In COPTER, do you have an internal blade modal-generation program?

Yen: No, our Myklestad [program] provides the modes.

White: How do you typically handle nonlinear blade dampers, such as you design in your current rotor systems?

Yen: Well, I have not really applied these linear or eigenvalue analyses for that. The thing I have done for a nonlinear lead-lag damper, say, is I do it at each value. How should I say this? You know the motion as a function of the rpm or whatever, and you change input values versus rpm.

Bill Warmbrodt, NASA Ames: Your correlation with this five degrees of precone, that's a remarkable improvement over what DRAV21 showed.

Yen: Okay, I'd like to make a point here. The reason I show this is not to make any comment about whether the correlation is good or poor or whatever. This is one of the correlations we used to validate the math model and I want to make the point that more correlations are certainly required before we can make use of this analysis as a design tool. To answer your question, the major difference here is the trim. For this analysis all the trim values were obtained from C81. For the DRAV21 data which we gave to the government as a result of the methodology contract, all those trims were done inside the program DRAV21.

White: Using C81 as your trim program, is that a temporary thing or is it long term part of COPTER?

Yen: It's a temporary thing. I had a chart here earlier [Fig. 1] and I did not really address that point. The program COPTER itself will provide trim values, but for the time being we've only completed a very small portion of it. So yes, that is one of our goals.

AEROELASTIC CHARACTERISTICS OF THE AH-64 BEARINGLESS TAIL ROTOR

D. Banerjee
Chief, Aeromechanics R&D
Hughes Helicopters, Inc.
Culver City, CA 90230

Abstract

A Composite Flexbeam Tail Rotor (CFTR) with a structurall, and aeroelastically unique hub design has been developed at Hughes Helicopters, Inc. (HHI) for the AH-64, Advanced Attack Helicopter. The full scale rotor has been successfully tested in the wind tunnel over the full steady sideslip envelope of the AH-64. The test program has defined the performance, loads, and dynamic characteristics of the CFTR for rotor speeds up to 1.0 N_R and airspeeds up to 197 knots. Uniqueness of the design is reflected in its patented hub design. The elastomeric shear attachment of the flexbeam to the hub results in a soft-inplane S-mode and a stiff-inplane C-mode configuration. The properties of the elastomer have been chosen for proper frequency placement and stable damping of the inplane S-mode. Both frequencies are well separated from the 1-flap frequency. The stress-critical pitch case/blade interface has been carefully designed to minimize loads. The flexbeam spanwise thickness and width distribution have been tailored for near-uniform corner stresses. The 1/rev chordwise load is maintained within the flexbeam and is not transferred to the hub. The 2/rev chordwise loads are transferred to the hub after significant attenuation due to hub shear pad damping and separation of the reactionless 1-chord frequency from 2/rev. The carry-through design of the flexbeam across the rotor hub allows the flexbeam to deform within the hub to reduce the hub loads to a minimum. Kinematic pitch-lag coupling is introduced to improve the first cyclic inplane C-mode damping at high collective pitch.

Presented at the Integrated Technology Rotor (ITR) Methodology Workshop, NASA Ames Research Center, Moffett Field, CA, June 20-21, 1983.

1.0 Introduction

Hughes Helicopters, Inc. (HHI) has designed, fabricated and successfully wind tunnel tested a Composite Flexbeam Tail Rotor (CFTR) for the AH-64 Advanced Attack Helicopter.

Over the past several years, a variety of bearingless tail rotors have been developed. The CFTR is a bearingless rotor whose design features have benefited from recent advances in composites technology and lessons learned from research into the basic characteristics of bearingless rotors that have to be addressed to achieve a successful design. Reference 1 describes the experimental development of a bearingless rotor and shows that a rotor system whose coupling effects are not well understood can run into fundamental dynamic instability problems. Instabilities encountered in the design were:

1) Inplane C-mode instability.
2) Inplane S-mode instability.
3) Stall flutter in the third flexible mode (torsion).
4) Stall flutter in the fourth flexible mode (second flap).

This reference also provides valuable information on the effect of key parameters such as blade sweep, tip weight, kinematic pitch-flap coupling, flexbeam width, etc., on the dynamic and aeroelastic behavior of the rotor. The choice of flexbeam geometry was found to be crucial to the level of flexbeam loads, and hence, the permissible amount of the kinematic pitch-flap coupling, which influences the flexbeam fatigue loads. In Reference 2, a hingeless rotor had a carefully designed flexbeam and was inherently stable. A closer look at this concept raised several questions regarding the "optimality" of the load path in the rotor. In Reference 3, the

rotor system encountered an instability involving the first flap/chord mode at moderate collective pitch. The rotor described in Reference 4 encountered flap-lag frequency coalescence and resultant instability which was eliminated by changing the pitch-flap coupling (δ_3) from a conventional value of -35 to -45 degrees (flap up induces pitch down), to +35 degrees, thus reducing the first flap frequency to below 1/rev. However care had to be exercised in the use of such pitch/flap coupling since it can lead to static divergence in flap/pitch. The rotor loads and performance characteristics resulting from the varying δ_3 were not addressed.

These rotors can be generally categorized as stiff-inplane or soft-inplane rotors. Typical problems associated with stiff-inplane rotors have been:

1) Inadequate structural stiffness in the flexbeam to ensure adequate separation of 1-chord and 1-flap frequencies. This generally results in coupled flap-lag instability (Reference 1).

2) Since the hub and drive system torsional stiffness lower the frequency of the 1-chord reactionless and collective modes, they have to be taken into account in sizing the flexbeam chordwise stiffness characteristics to avoid coalescence of the 1-chord and 1-flap modes.

3) In ensuring good separation of the 1-chord and 1-flap modes, the 1-chord frequency is generally placed high (between 1.5/rev and 1.7/rev). Dynamic amplification of 1/rev and 2/rev Coriolis bending moments result in high 1/rev and 2/rev chordwise fatigue loads in the flexbeam.

4) In order to accommodate the high loads of a stiff inplane rotor, a relatively stiffer flexbeam is required. This also increases the torsional stiffness of the flexbeam resulting in higher torsional loads on the control system.

Soft-inplane rotors have potential problems of:

1) Dynamic coupling of the rotor and support structure resulting in "ground resonance" type problems.

2) Structural loads in the flexbeam of a bearingless rotor could determine a lower bound on the flexbeam stiffness, and hence, the 1-chord frequency of the rotor blade.

With the above concerns in mind, the Composite Flexbeam Tail Rotor (CFTR) has been developed at Hughes Helicopters, Inc. It has a structurally tailored flexbeam chordwise stiffness distribution to locate the cyclic 1-chord frequency above 1/rev, and the flexbeam is mounted to the hub between elastomeric "soft" supports whose stiffness and damping are tailored to locate the collective and reactionless 1-chord frequencies below 1/rev. A description of the rotor design and dynamic characteristics are presented in Sections 2 and 3, respectively.

2.0 CFTR - Description

An exploded view of the CFTR is shown in Fig. 1. This shows that the axes of the blade-pair assembly are perpendicular to each other, and are separated axially so one flexbeam may cross over the other. The CFTR has upper and lower hub plates which sandwich the blade-pair assembly. The hub assembly is bolted to the tail rotor drive shaft. The flexbeam extends from the tip of one blade, across the hub, to the tip of the opposite blade. Bending and twisting motion of the flexbeam, between the edge of the hub and the inboard end of the blade, provides the fundamental flap, lag, and torsional motions of the rotor blades. The flexbeams are attached to the hub plates through elastomeric shear (inplane) pads. The laminated elastomeric pitch shear support aligns the pitch case with respect to the flexbeam. The pitch horn is bolted to the trailing edge of the pitch case. The spanwise location of the pitch link attachment is adjusted for an effective pitch-flap coupling (δ_3) of -35 degrees (pitch down with flap up). The pitch link is inclined to provide negative pitch-lag coupling (δ_4 positive, pitch up with blade lag) to augment inplane damping at high collective pitch and rotor speed. A brief description of each component follows.

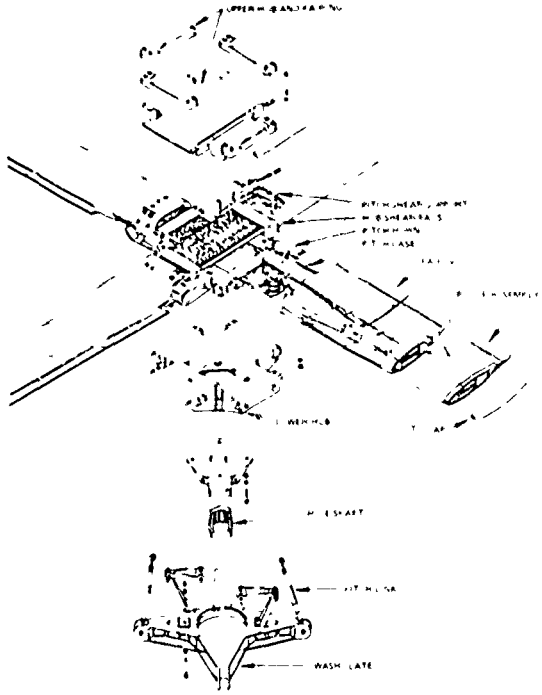


Fig. 1 CFTR assembly

2.1 Flexbeam

The heart of the CFTR is the fiberglass/epoxy flexbeam that carries across the full span of each blade-pair assembly and attaches the two blade sections of each blade-pair assembly to each other and to the hub. The flexbeam, which is of rectangular cross-section is built of layers of S-glass/epoxy with the filaments oriented ±5 degrees to the spanwise axis. S-glass was selected for its good fatigue strength, relatively high elongation, and low modulus of elasticity. Fiber orientation of ±5 degrees was selected as having a good fatigue strength and low torsional stiffness combined with the inplane shear strength to carry the driving torque and inplane blade loads. The spanwise distribution of flexbeam width and thickness is configured for near uniform spanwise distribution of combined corner stresses while maintaining a low structural torsional stiffness.

The flexbeam is formed as a flat beam that operates in the untwisted condition when the blade is producing design lift at $\theta 3/4 \approx 8$ degrees so that the torsional stress within the flexbeam is minimized.

2.2 Hub

The hub, as shown in Figs. 1 and 2, consists of upper and lower hub plates which sandwich the flexbeams between elastomeric inplane shear pads. Each set of pads is clamped between two load carrying beamlike structures, an upper hub plate "cross beam" and the "cross beam" stiffener of the lower hub plate. These beams carry shear loads due to preloading and reaction loading of the pads to support points on their ends. The pads themselves consist of an elastomeric section bonded to a thin aluminum plate which in turn is bonded to the flexbeam. Four anchor bolts (two on each end of each shear pad) attach the pads to the lower hub plate which carries all the reaction loads to the drive shaft. The elastomeric pads provide a soft mount between the flexbeam and hub and are designed to allow the flexbeam to bend with respect to the rigid hub and to keep the primary bending moments within the flexbeam where the filaments are oriented to accommodate them. In addition, the hub, which is of hollow construction, is designed to minimize the load path. These features are shown schematically in Fig. 3.

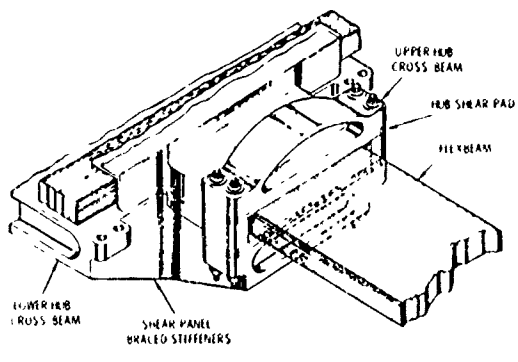


Fig. 2 Hub design

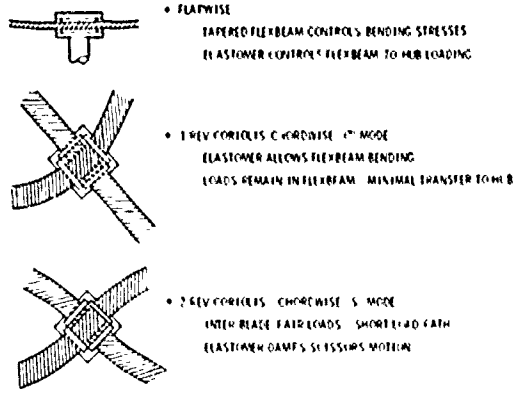


Fig. 3 Hub design criteria

In the flapwise direction, the flexbeam is designed for transfer of minimal bending moment loads into the hub as a result of the flexbeam taper and bending within the hub. The elastomer is clamped to preload it and ensure that it always has a net compression load. All flap bending loads are transferred between the flexbeam and hub through compression in the elastomer. The loads are transmitted by the upper hub plate "cross beam" and the lower hub plate "cross beam" stiffeners to the shear panel braced stiffeners (Fig. 2). These stiffeners are very deep and, therefore, are structurally very efficient for carrying the loads. The bolts for attaching the shaft flange to the lower hub plate are anchored at the intersection of these stiffeners with the central pocket. This results in the shortest possible load path.

Three predominant chordwise loads are encountered. The first is the steady driving torque which is reacted by the elastomer in shear. The other two result from Coriolis forces. The hollow hub allows the 1/rev Coriolis bending moment loads to be carried in the flexbeam instead of being transferred into the hub. The 2-rev Coriolis moments result in the inplane scissors S-type motion in which the adjacent blades work against each other as shown in the

lower sketch of Fig. 3. In this case, the loads are taken in shear through the elastomers and through short load paths across the rugged corners of the hub.

2.3 Pitch Case

The pitch case is a wet-filament wound fiberglass epoxy hollow structure that fits around, and is bonded to the flexbeam and blade root where these three components intersect. Inboard of the blade root, the pitch case enlarges to give the flexbeam room in which to twist as the blade feathers (Fig. 4). The pitch case tapers in the spanwise direction (Fig. 4) to reduce the flapwise stiffness (without sacrificing torsional rigidity). This minimizes the bending moment in the pitch case/blade root attachment induced by the pitch shear support and, hence, the resultant bending stresses. Near the inboard end of the pitch case, a hoop-wound stiffening ring provides the strength required to support the pitch horn and the elastomeric shear support loads.

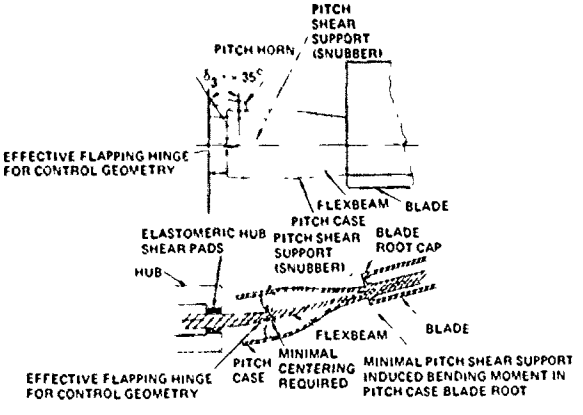


Fig. 4 CFTR blade root geometry

2.4 Pitch Shear Support ("Snubber")

The elastomeric pitch shear support is a laminated metal/elastomer device that is stiff with respect to radial loading, but soft in torsion and inplane shear. It centers the pitch case with respect to the flexbeam. Its spanwise location is kept well outboard, beyond the region of maximum flap bending curvature in the flexbeam. This minimizes the rotational deflection of the pitch case relative to the flexbeam as seen in the lower view of Fig. 4, and so minimizes pitch shear support-induced bending moments at the point where the pitch case, flexbeam, and blade join at the blade root station.

2.5 Blade

The primary material for the wet filament wound blade structure is Kevlar-49/epoxy.

Unidirectional fibers with maximum tensile strength and modulus are used for leading edge obstacle strike protection, and for the trailing edge longo that carries high axial loads and has high stiffness. The airfoil-shaped blade section is a multi-tubular Kevlar/epoxy structure that is bonded around the flexbeam (Fig. 5). A C-shaped channel is added in the aft airfoil region to stiffen the outer skin. The leading edge balance weight is a multiple-rod molded construction. The small diameter rods easily conform to twisted contour of the leading edge. The portion of the leading edge cavity between the leading edge balance weight and Kevlar spar tubes is filled with syntactic foam.

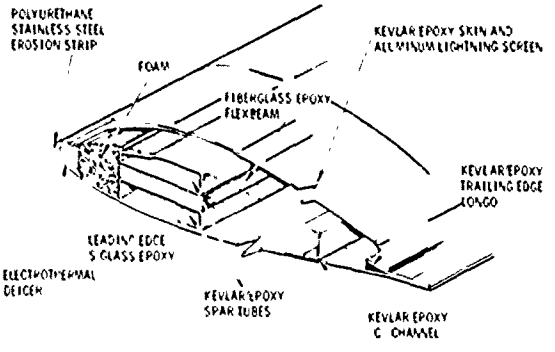


Fig. 5 CFTR blade cross-section

The blade has a -9 degree twist, and is positioned about the flexbeam so that when the flexbeam is untwisted, the blade pitch angle at 3/4-radius is 8 degrees. The orientation of the flexbeam with respect to the blade chord at different radial stations is shown in Fig. 6.

3.0 CFTR - Dynamics

The fundamental mode of instability for bearingless rotors has been shown both analytically and experimentally to be associated with the coupling between the first flap and the first inplane (reactionless and cyclic) modes (References 1, 3, 4, 5, 6 and 7). For bearingless tail rotor designs (References 1, 2 and 4), the inplane frequency generally lies between 1 and 2/rev, with the reactionless (S) mode frequency slightly

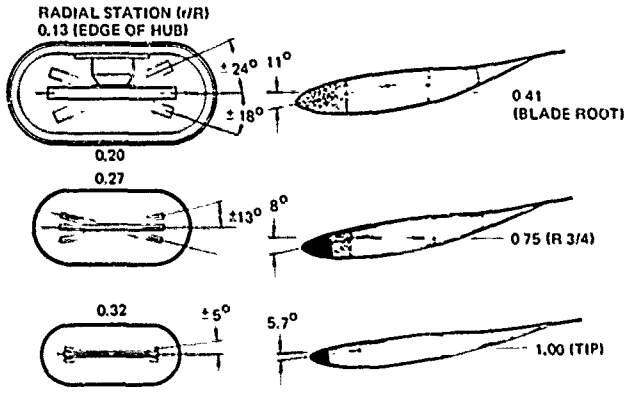


Fig. 6 Blade/pitch case/flexbeam cross-sections

lower than the cyclic (C) mode frequency - the difference depending on the hub configuration and the rotor pylon structural properties. Both an increase in collective pitch and (conventional) negative pitch flap coupling tend to bring the first flap and the first inplane frequencies closer together, by increasing the first flap frequency and lowering the first inplane frequency. This often results in the lightly damped first inplane modes (both the reactionless and cyclic) becoming unstable. Typical solutions to the above problem have been the stiffening of the flexbeam in the chordwise direction (Reference 1) and the use of positive pitch flap coupling (References 4 and 6) to separate the modes. These solutions have been applied with limited success because first, structural design considerations put a limit on the chordwise stiffness of the flexbeam, and second, even though a stable rotor system was presented in Reference 4 (with positive pitch-flap coupling), similar experimental effort in Reference 1 showed the presence of a stall-induced flap-lag-torsion large amplitude limit cycle instability.

At HHI, the above dynamic problems have been solved for the CFTR by lowering the S-mode inplane frequency below 1/rev (soft inplane) while maintaining the C-mode inplane frequency above 1/rev (stiff inplane) and well separated from the first flap frequency. Some of the design parameters that resulted in this dynamically unique bearingless tail rotor design are discussed below.

3.1 Flexbeam to Hub Support

By supporting the flexbeam to the hub through elastomeric hub shear pads with no restraint within the hub, the S-mode inplane shear and bending moments are reacted through the elastomeric hub shear pad. The stiffness of the shear pad has been tuned to accurately place the first S-inplane frequency below 1/rev (this frequency for the current design is at approximately 0.6/rev) and well separated from the first flap frequency at all operating conditions. The damping in the shear pad elastomer provides a high level of damping in the first S-inplane motion. This, along with its large separation from the 2/rev resonance condition ensures a low level of blade dynamic loading for the 2/rev Coriolis forces. In the C-mode inplane configuration, the hollow construction of the hub and the influence of the elastomeric shear pads allows the flexbeam to bend within the hub. This ensures that the bending moment loads are carried across the hub within the flexbeam. Since the inplane loads are not reacted by the shear pads in this configuration, the first C-inplane frequency stays well above 1/rev. The location of this frequency and its damping can be optimized by proper choice of flexbeam width, tip weight, pitch-flap coupling and other parameters.

3.2 Flexbeam Geometry

A rectangular flexbeam configuration was chosen. However, the spanwise distribution of width and thickness were tailored for optimum placement of fundamental 1-flap and 1-chord frequencies as well as acceptable combined corner stresses. The "soft" hub mount of the flexbeam and root-end kinematic pitch-lag coupling ensured high damping of the rotor chord modes. Hence no attempt was made to sandwich elastomeric material into the flexbeam design. The chordwise stiffness was designed for adequate separation of 1-chord and 1-flap frequencies. The spanwise distribution of flexbeam width and thickness has been configured for near uniform spanwise distribution of combined corner stresses while maintaining a low structural torsional stiffness. This is vitally important as can be seen in Fig. 7, which shows a comparison of flapwise bending stresses for different flexbeam configurations for a blade flapping of $\hat{\beta}$ = 15 degrees. Detailed calculations show that a flexbeam with a uniform width and thickness is totally unacceptable for fatigue loads at high forward speeds.

3.3 Tip Weight

The tip balance weight has been eliminated for the CFTR. This results in a simpler tip design without a tip weight attachment fitting. Since the fundamental dynamic effect is an increased first C-mode chordwise frequency, the removal of the tip weight is beneficial in separating the first flap and the first chord frequencies. The spanwise balance weight is located on the top and bottom of the pitch case at its root end (Station 10.0). This location results in reduced

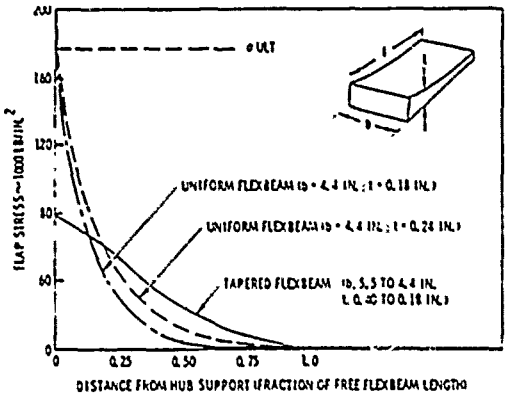


Fig. 7 Flapwise flexbeam stress (blade flap = 15 degrees)

feathering control loads due to reduced "tennis racquet" effect.

3.4 Pitch Link Attachment

The pitch link is attached to the trailing edge of the pitch case. For the design value of negative pitch-flap coupling (δ_3 = -35 degrees), the blade spanwise pitch horn attachment point is well inboard, resulting in a small swashplate and a compact design. In addition, the direction of the pitch link load is the same as that of the rotor thrust, thus reducing the flexbeam flap shear load. Dynamically, because of the inboard attachment of a trailing edge pitch link, the second flap frequency is much higher than it would be for a leading edge attachment. This is very important in raising the second flap frequency above and maintaining good separation from 3/rev. As shown in Fig. 1, the pitch link is inclined radially inwards from the swashplate to the pitch horn at an angle of 70 degrees to the hub plane. This induces kinematic pitch-flap-lag coupling to improve the first inplane (C-mode) damping at high collective pitch settings. The coupling results in positive pitch-lag motion, i.e., nose down with blade lag motion. This is in general agreement with the requirement for stiff-inplane rotors.

3.5 Chordwise Blade Balance

As in the existing AH-64 metal tail rotor the chordwise c.g. of the CFTR blade has been located at 35 percent chord to reduce the weight of the blade and the "tennis racquet" loads on the control system. Ballistic damage considerations, however, require the rotor to be stable with a failed pitch link. This condition is satisfied by stabilizing the coupled pitch-flap mode with a leading edge weight in the outboard portion of the blade between 70 and 90 percent radius.

4.0 Wind Tunnel Test Procedure

4.1 General Description

The Composite Flexbeam Tail Rotor (CFTR) was evaluated through extensive wind tunnel tests to determine rotor performance, loads, and dynamic characteristics in hover and in low and high speed forward flight, and in sideslip conditions that are representative of the production AH-64 flight spectrum.

Testing was conducted in the Boeing Vertol V/STOL wind tunnel located at Philadelphia, Pennsylvania. The essential objectives of the wind tunnel tests were:

1) Define dynamic and aeroelastic stability characteristics of the CFTR over the sideslip flight envelope of the AH-64.
2) Define rotor loads, and blade load and stress characteristics.
3) Define performance characteristics.
4) Define start/stop response characteristics.

A fully instrumented blade pair assembly was mounted on the Dynamic Rotor Test Stand (DRTS). The DRTS assembly provided support, control, and drive for the CFTR. A typical installation with the rotor positioned for forward flight with sideslip is shown in Fig. 8. Sideslip was simulated by presetting the sting inclination, and remotely controlling the DRTS pitch angle. Twenty-six rotating gages were monitored. This included flap, lag and torsion gages on the flexbeam and the blade, pitch link, rotor hub, output shaft, etc. Additional rotating and non-rotating measurements include shaft torque balance thrust, pitching and rolling moments, shaft angle, RPM indicator, control system load, etc.

4.2 Control System and Rotor Support System

A close-up view of the drive and support system is seen in Fig. 9. The test stand drive shaft is coupled to the output drive shaft of the rotor with adapting hardware. The "scissors" drive the rotating swashplate from the output shaft.

The control system consists of the pitch link attached to the pitch horn at one end and to the rotating swashplate at the other. The non-rotating swashplate is mounted on two hydraulic actuators (Fig. 9) spaced apart azimuthally by 180 degrees.

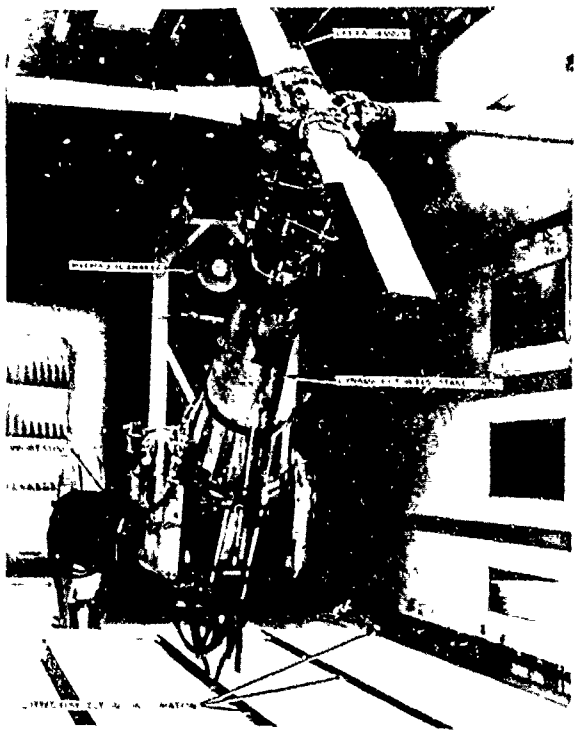


Fig. 8 Composite flexbeam tail rotor in the wind tunnel test section

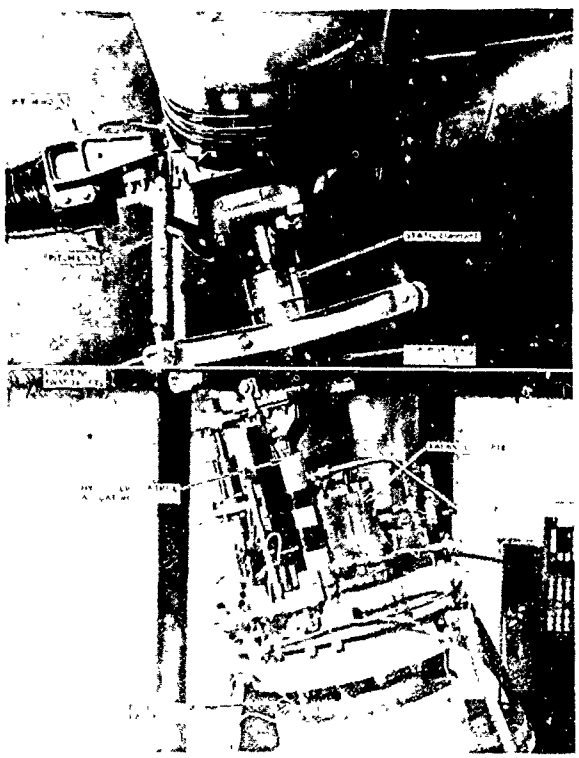


Fig. 9 CFTR drive and support system assembly

The static mast is mounted on the DRTS with an interface hardware called the balance adapter that is in turn supported to the test stand with a dynamic balance. The dynamic balance (Fig. 9) is strain-gaged to measure the CFTR thrust, rolling and pitching moments.

A description of the test rotor components is provided in Reference 9.

4.3 Collective and Cyclic Excitation

In preparation for wind tunnel tests, provision was made to excite the rotor using collective and cyclic shakers. These were available to excite lowly damped fundamental rotor modes in order to measure their damping characteristics.

Cyclic modes were driven by a 300 lbf, 0-200 Hz, shaker mounted on the sting as shown in Fig. 8. The shaker excitation was applied to the Dynamic Rotor Test Stand (DRTS) below the stand balance.

Collective excitation was provided through the collective pitch hydraulic drive system. The collective pitch excitation was used with an amplitude of ±0.5 degree blade pitch change over a frequency range 0 - 35 Hz.

4.4 Test Precautions

Procedures that were established to ensure the integrity of the CFTR through the complete test envelope included:

Non-rotating rap tests were done at the start of each day's testing. The response of the blade in the flap, lag and torsion degrees of freedom were observed on the spectrum analyzer. In addition to visual inspection, this test provided confidence in the structural integrity of the CFTR.

Selected rotor response gages were continuously monitored for all test conditions on twelve on-line monitors and the spectrum analyzer. Certain critical gages, in addition to performance parameters, were also observed on the on-line flatbed plotters.

Additional test protection was observed by introducing the collective pitch dump capability that was designed to automatically drop the collective pitch to a previously tested safe level when any one of selected critical gage response exceeded a prespecified value. Spectral analyzers were also used to continuously monitor the non-harmonic content of selected responses.

This procedure for on-line data monitoring and automatic collective pitch dump, safety of the CFTR wind tunnel test was assured.

4.5 Test Stand Shake Test

Prior to mounting the CFTR on the Dynamic Rotor Test Stand (DRTS), a shake test was conducted to determine dynamic characteristics of the test stand. The purpose of this investigation was to:

1) Identify and isolate CFTR response characteristics that were essentially the influence of test stand dynamics.

2) Determine any distabilizing influence of the test stand on the rotor dynamics.

This was done by determining the test stand frequencies, generalized masses, generalized dampings, and mode shapes of all modes in the frequency range 0 - 100 Hz. The hub modal data was incorporated in a fully coupled CFTR/DRTS aeroelastic stability analysis to verify that the integrated systems are free from adverse dynamic or aeroelastic coupling.

The influence of the test stand on the CFTR modal characteristics were found not to be significant.

4.6 Data Reduction Facility

Test data was processed for on-line or off-line reduction and presentation. Off-line digitized data was available in four formats.

1) Low Speed Calculated Data presents steady state static data of wind tunnel test configuration. This data includes rotor advance ratio, RPM. shaft angle, collective pitch, C_T, C_p, velocity of wind tunnel, balance steady thrust pitching and rolling moments, velocity of sound, etc.

2) High Speed Calculated Data essentially calculates the steady and alternating values of the different interaction equations (combined stresses).

3) Stress Analysis Data presents the steady and alternating values of 29 channels of data being monitored for each test point.

4) Harmonic Analysis Data presents the magnitude and phase of the first 10 harmonics of all 29 channels of data recorded.

Six on-line flatbed plotters were used to plot any combination of dimensional or nondimensional parameters in their final corrected forms. Also available was on-line spectral analysis of any selected data channel and corresponding hard copies.

The wind tunnel control console offered on-line monitoring of many key control parameters. These were viewed in alphanumeric or analog form on digital displays, oscilloscopes, or oscillographs. A safety-of-flight monitor was also provided. This data was continuously recorded from a number of preselected data channels whenever the rotor or tunnel was activated. The parameters that triggered the rotor blade pitch dump were monitored in analog form on oscilloscopes.

5.0 Evaluation of Results

The test program determined the performance, loads, and dynamic characteristics of the CFTR for rotor speeds up to 1.0 N_R and airspeeds up to 197 knots. The complete impressed pitch range, as limited by test stand capabilities or rotor structural requirements was investigated in hover, low and high speed forward flight and sideslip conditions. Static sideslip limits as defined in the AH-64 System Specification (Reference 10) were investigated at airspeeds of 139, 164, and 197 knots. The stop/start characteristics of the rotor in wind velocities up to 45 knots were defined. The test explored the full steady state sideslip envelope of the AH-64 as seen in Fig. 10 where test points are superimposed on the helicopters sideslip envelope.

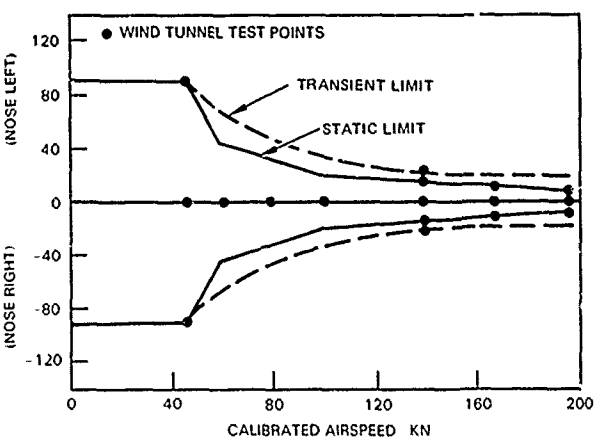


Fig. 10 AH-64A sideslip envelope

For hover tests, the rotor speed was varied from 0 to 1.0 N_R (1403 RPM) in steps of 0.2 N_R (420 RPM). Collective pitch was varied over the full range that was available at 0.8 N_R, 0.9 N_R and 1.0 N_R within the limits of the test stand capability.

Fig. 11 presents a comparison of the CFTR power versus thrust coefficient as measured in the wind tunnel at zero wind tunnel speed. Fig. 12 is the corresponding plot of rotor thrust coefficient versus impressed blade pitch setting.

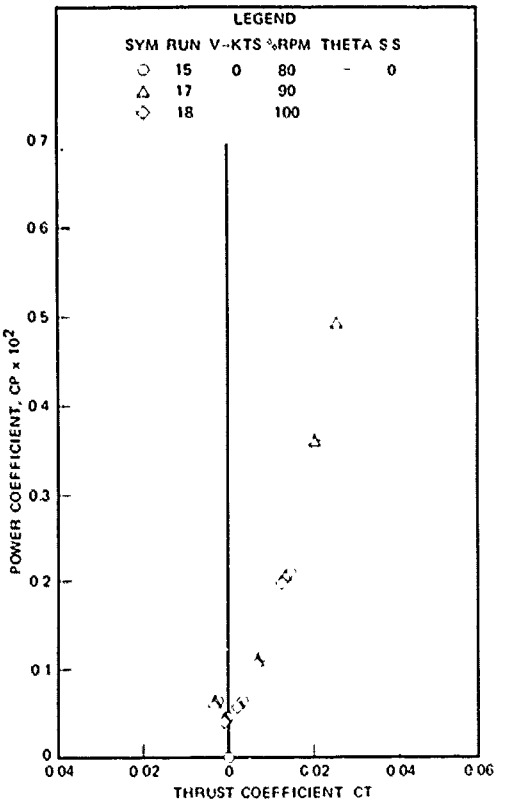


Fig. 11 Hover test, baseline blade performance data

Forward flight tests were conducted for the conditions shown in Fig. 10. Sideslip angles at V = 138 knots, 164 knots and 197 knots were essentially restricted to the steady sideslip limits. Attempts to test at higher left and right sideslip angles resulted in autorotation of the rotor for zero collective pitch. This, of course, is a test stand limitation and will not be encountered in actual flight.

Typical spanwise distribution of flexbeam and blade loads at V = 164 knots and β_{SS} = +6 degrees is shown in Figs. 13 through 18. Pitch case loads (station 4.2 to 25.0 inches) are not shown in these figures since it was not instrumented. Flexbeam loads for various pitch angles are shown between station 6.2 inches and 25.0 inches and the blade loads between station 25.0 inches and 56.0 inches. The pitch case,

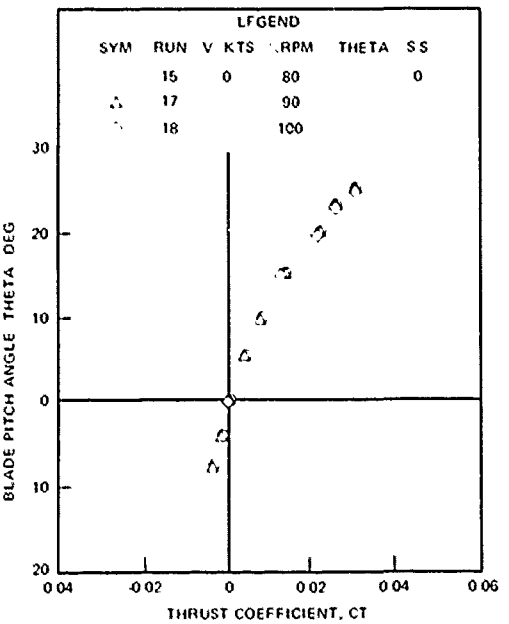


Fig. 12 Hover test, baseline blade performance data

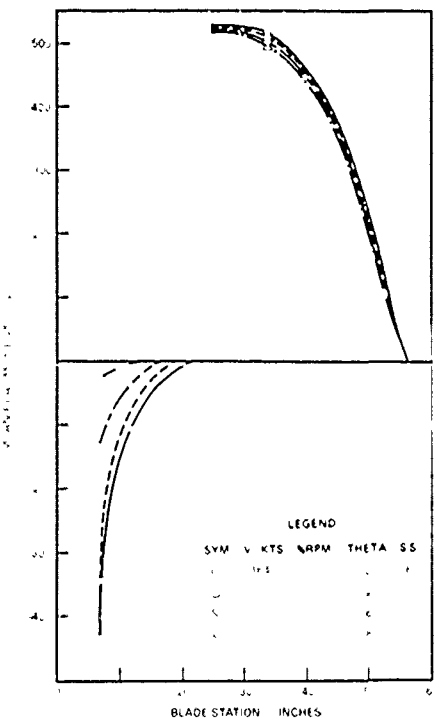


Fig. 13 CFTR wind tunnel test - mean flap moment distribution

flexbeam, and blade junction is at station 25.0. These stations are important in understanding the discontinuities and inflections in the bending moment plots.

The steady loads between the pitch case, flexbeam and blade should balance at the junction, station 25.0. However, because of phase differences between the loads in the pitch case, flexbeam, and blade, the plots of the oscillatory loads do not necessarily add up at the junction.

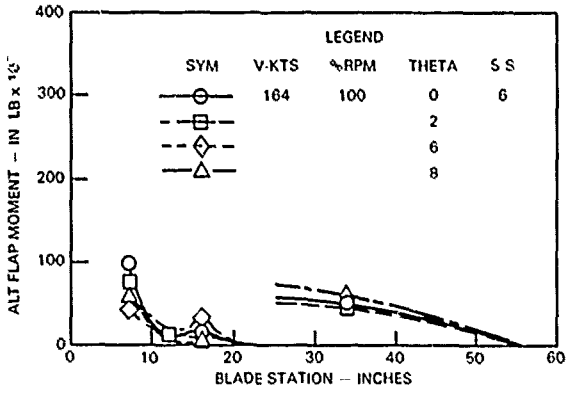


Fig. 14 CFTR wind tunnel test - alternating flap moment distribution

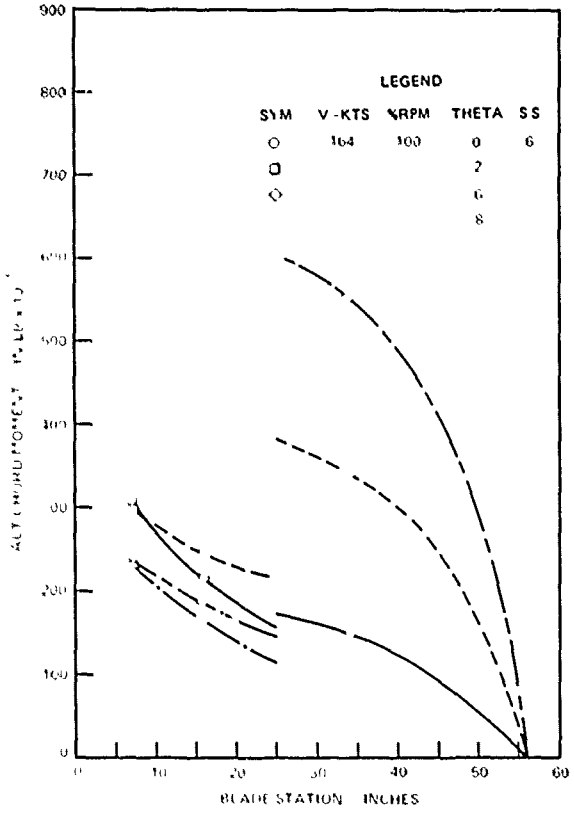


Fig. 16 CFTR wind tunnel test - alternating chord moment distribution

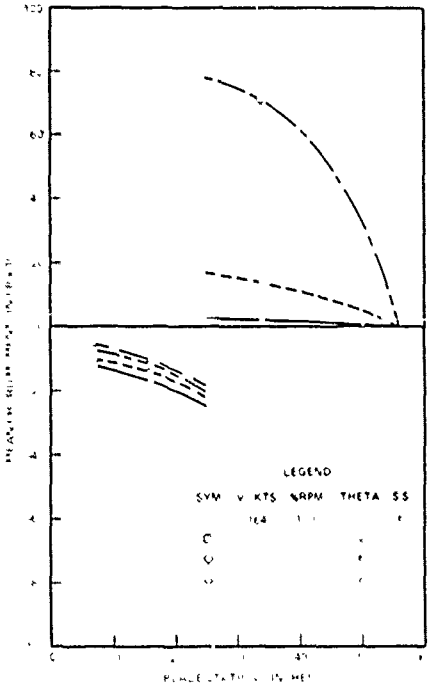


Fig. 15 CFTR wind tunnel test - mean chord moment distribution

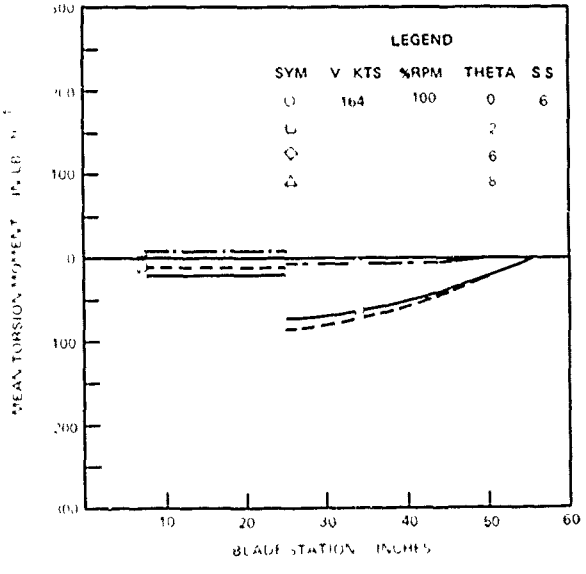


Fig. 17 CFTR wind tunnel test - mean torsion moment distribution

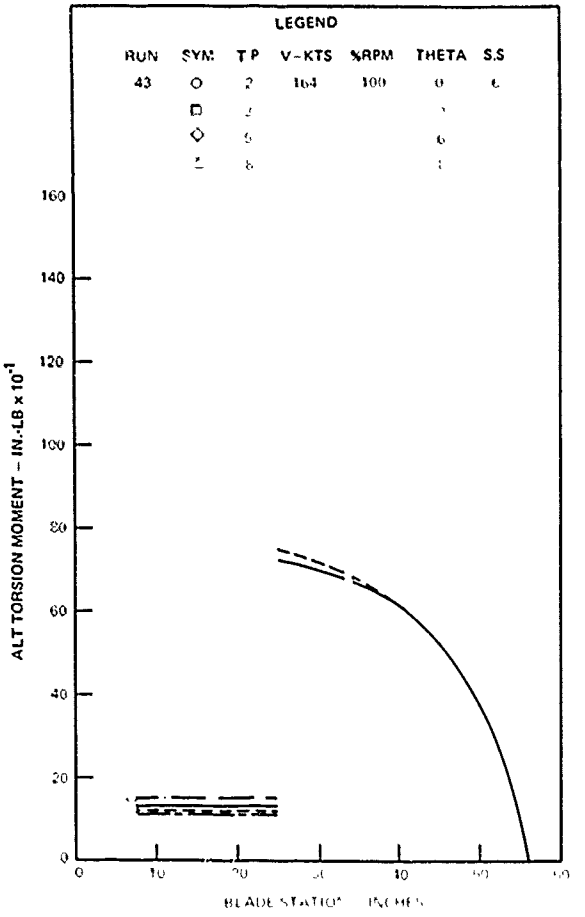


Fig. 18 CFTR wind tunnel test - alternating torsion moment distribution

Steady and alternating flapwise bending moments are shown in Figs. 13 and 14. Both show a steep drop in flexbeam bending moment from the edge of the hub to approximately station 10.0 inches. As per design, the flexbeam flap bending moment tapers to practically zero between station 20.0 inches and 25.0 inches. The jump discontinuity in the bending moment between the flexbeam and blade at station 25.0 is the bending moment in the pitch case. The flapwise bending moment in the pitch case would reduce to zero at the pitch link/pitch horn attachment. Similarly, the bending moment distribution is drawn such that the value at the blade tip (station 56.0 inches) is zero. Chordwise bending moments are seen in Figs. 15 and 16. The discontinuity at station 25.0 inches reflects the chordwise loads in the pitch case. The component of pitch link compression load in the chordwise direction produces this bending moment. The chordwise load in the pitch case is essentially the result of the pitch link inclination. Unlike the flap bending moment distribution, the chordwise moment in the flexbeam has a more gradual distribution. The torsion bending moments are shown in Figs. 17 and 18. The steady flexbeam torsion load is due to the steady wind-up of the flexbeam. Measured flexbeam torsional load for $\theta_{3/4} = 8$ degrees is approximately zero since the flexbeam is untwisted at this pitch setting. The difference between the blade and flexbeam torsion bending moment at station 25.0 inches is the torsion load in the pitch case reacted by the pitch link. Fig. 17 also shows the relative magnitude of the flexbeam torsion load to the pitch link load. Alternating torsion load in the flexbeam is a result of flexbeam feathering with blade flapping with the root-end pitch flap (δ_3) coupling.

5.1 Dynamic Results

As discussed in Section 4.3, collective and cyclic shakers were available to excite lowly damped fundamental rotor modes in order to measure their damping characteristics.

The collective pitch excitation had an amplitude of ±0.5 degrees blade pitch change over a frequency range of 0 - 35 Hz. The cyclic excitation was input as non-rotating test stand force with the 300 lbf shaker. Shaker forces of 50 lbf and 100 lbf were used from 0 - 70 Hz.

Accordingly, collective and cyclic excitation were attempted to excite the rotor modes at each point in hover in the test envelope. However, after many attempts it was determined that the rotor fundamental modes were heavily damped and, hence, could not be excited with either of the two shakers. It was decided at this point that envelope expansion of CFTR wind tunnel test would be based on the magnitude of non harmonic flap, lag or torsion response as seen on the on-line spectrum analyzer.

Dynamic analysis research tool (DART) analysis program was used to define the CFTR dynamic and aeroelastic characteristics and blade loads of the CFTR. This program is described in Reference 11.

Two basic types of analysis were used to substantiate the dynamic and aeroelastic characteristics of the CFTR. First, an eigenvalue analysis was used for configurations in hover to establish freedom from aeroelastic instability throughout the complete blade pitch and rotor speed ranges of the CFTR. This also established the blade modal characteristics. Second, forward flight stability was established by trimming the rotor at

different points of the flight envelope. Since the analysis included nonlinear structural couplings and aerodynamics (including dynamic stall), rotor trim without nonharmonic response indicated positive stability margins.

The resonance diagrams generated by DART for reactionless, cyclic and collective boundary conditions are shown in Figs. 19, 20 and 21, respectively. Test frequencies obtained at zero and operating RPM are superimposed on the resonance diagrams.

Tabulated results of the non-rotating rap tests are shown in Table 1. The fundamental 1-flap, 2-flap, 1-chord and 1-torsion modes show good correlation with analytical data. Spectral plots of non-rotating rap tests for flexbeam chord and flap gages are shown in Figs. 22 and 23, respectively.

Results of cumulative spectrum plots for different forward flight tests are shown in Table 2. Spectral plots for one flexbeam chord gage for V = 139 knots and 197 knots are shown in Figs. 24 and 25, respectively.

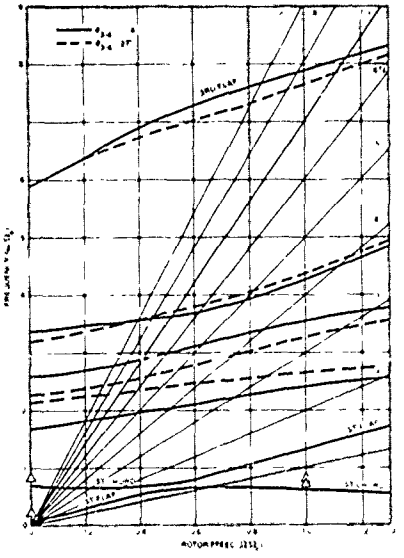


Fig. 19 CFTR resonance diagram - reactionless modes

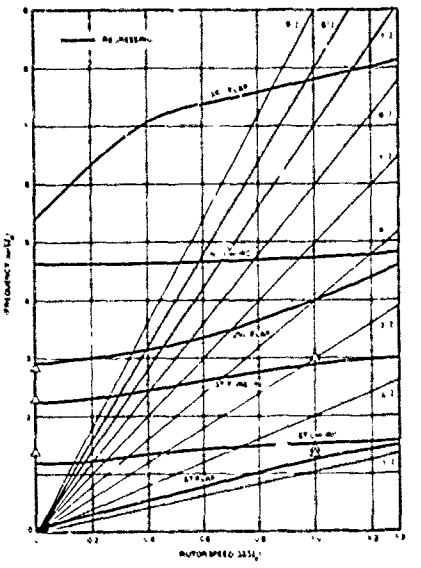


Fig. 20 CFTR resonance diagram - cyclic modes, $\theta_{3/4} = 0$

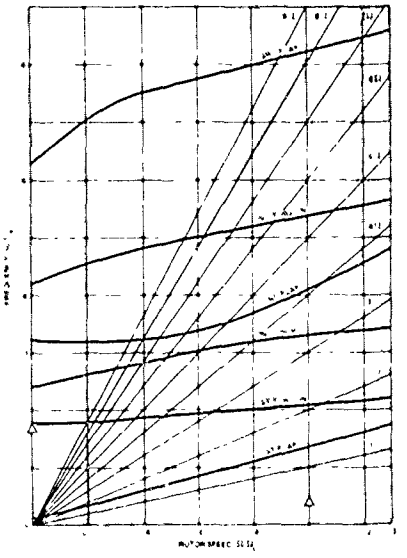


Fig. 21 CFTR resonance diagram - collective modes, $\theta_{3/4} = 0$

Table 1. Nonrotating Modal Frequencies - Correlation of Test Results with Analysis

Configuration	Mode	Frequency - Hz (/Rev) Analysis	Test
Reactionless Boundary Condition	1-Flap	3.5 (0.15)	4.4 (0.19)
	1-Chord	16.4 (0.7)	18.2 (0.78)
Cyclic Boundary Condition	1-Chord	30.4 (1.3)	32.3 (1.38)
	1-Torsion	51.4 (2.2)	53.8 (2.3)
	2-Flap	69.0 (2.95)	70.2,(3.0, 66.4 2.84)
Collective Boundary Condition	1-Torsion	40.9 (1.75)	40.0 (1.71)
	2-Flap	57.3 (2.45)	58.0 (2.48)

Table 2. Inplane Modal Frequencies for Various Test Conditions

Figure No.	Test Condition V(KTS)	β_{ss} (Deg.)	Collective Pitch	Flexbeam Chord Gage Resonant Frequencies Hz (/Rev)
–	25	-90	Sweep	8.4 (0.36/Rev); 17.8 (0.76 Rev); 33.0 (1.41 Rev)
24	139	+15	Sweep	6.8 (0.29/Rev); 16.8 (0.72/Rev); 29.0 (1.24/Rev); 70.0 (3/Rev)
25	197	-8	Sweep	7.5 (0.32/Rev); 15.2 (0.65/Rev); 29.7 (1.27/Rev), 70.0 (3/Rev)
–	197	-2	Sweep	7.5 (0.32/Rev); 15.7 (0.67/Rev); 29.5 (1.26/Rev), 70.0 (3/Rev)
–	0-164 Sweep	0	0	7.7 (0.33/Rev), 16.8 (0.72/Rev); 30.5 (1.30/Rev); 70.0 (3/Rev)

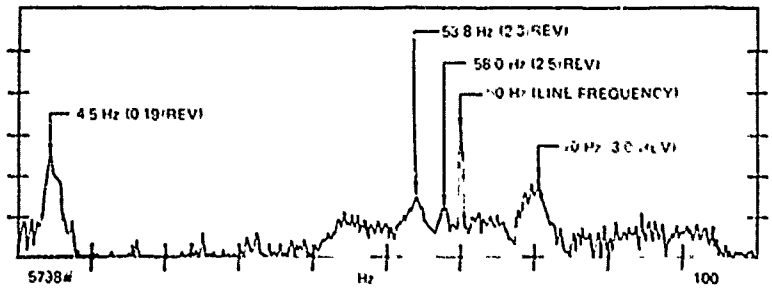


Fig. 22 Frequency spectrum of flap response - nonrotating rap test

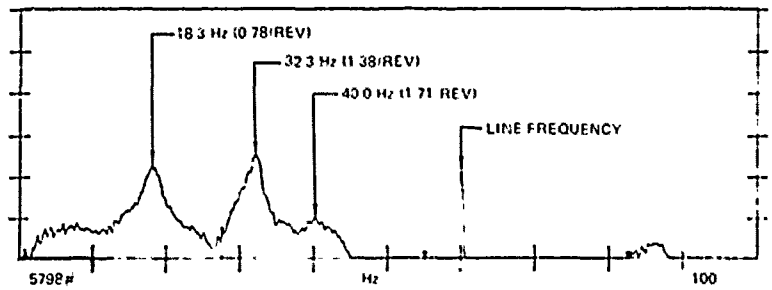


Fig. 23 Frequency spectrum of chord response - nonrotating rap test

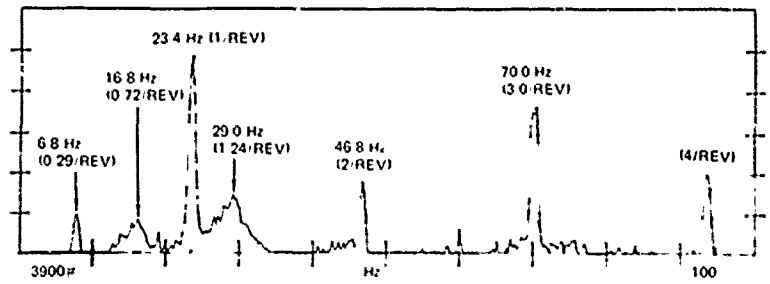


Fig. 24 Frequency spectrum of flexbeam chord response - V = 139 knots, β_{SS} = +15 degrees, θ sweep, Ω = 1403 rpm

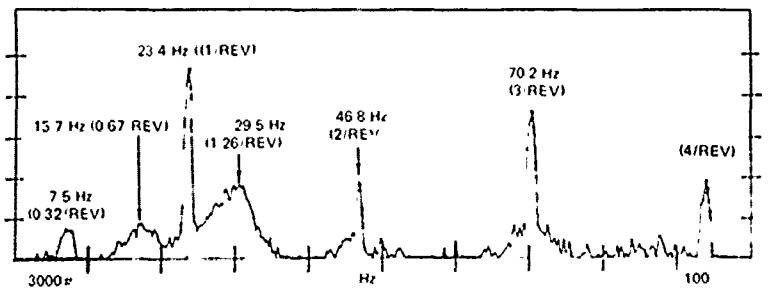


Fig. 25 Frequency spectrum of flexbeam chord response - V = 197 knots, β_{SS} = -8 degrees, θ sweep, Ω = 1403 rpm.

5.1.1 Reactionless Boundary Condition

The reactionless boundary condition corresponds to an isolated rotor. The reactionless modes resonance diagram for the collective pitch extremes of -14 degrees and +27 degrees is shown in Fig. 19. In the reactionless or "scissors" (S-mode) inplane boundary condition, the steady and 2/rev inplane shear and bending moments are reacted through the elastomeric hub shear pads. The stiffness and damping of the shear pads provide the hub restraint for blade chordwise motion. The first chord frequency is primarily dependent on the stiffness and spanwise offset of the hub shear pad. Its frequency is located at approximately 0.6/rev which provides good separation from the first flap frequency and 2/rev Coriolis excitation. The first flap frequency is governed by the effective hinge offset (approximately 10 inches) and the value of kinematic pitch-flap coupling. The first flap is generally highly damped. The high damping of the first chord mode is a reflection of hub shear pad damping characteristics. This is evidenced by the results of shake tests using the collective and fixed system shakers. Since the hub shear pads do not feather with pitch change, the first chord frequency and damping remain essentially unchanged with change in blade collective pitch. The first flap frequency and damping are generally unchanged with collective pitch.

The higher modes have been shown analytically (Reference 11) to be well damped with minimal change with collective pitch.

The coupled mode shapes corresponding to the fundamental modes are shown in Figs. 26 and 27. The first chord mode, Fig. 26, shows very little coupling with the flap and torsion motion of the blade. The elastic deflection in the chordwise direction is essentially in the hub shear pad with the blade moving as a rigid body. The first flap mode, Fig. 27, shows the coupling between the blade flap and torsion motion (pitch/flap coupling).

In contrast to conventional rotors, the first torsion mode reflects feathering motion about the pitch link/pitch horn attachment. The shear stiffness of the snubber in flap and chord and the chordwise stiffness of flexbeam between station 15.0 inches and 25.0 inches, in addition to the control system stiffness, have significant influence on the frequency of this mode. This is determined from the strain energy data corresponding to the first torsion mode.

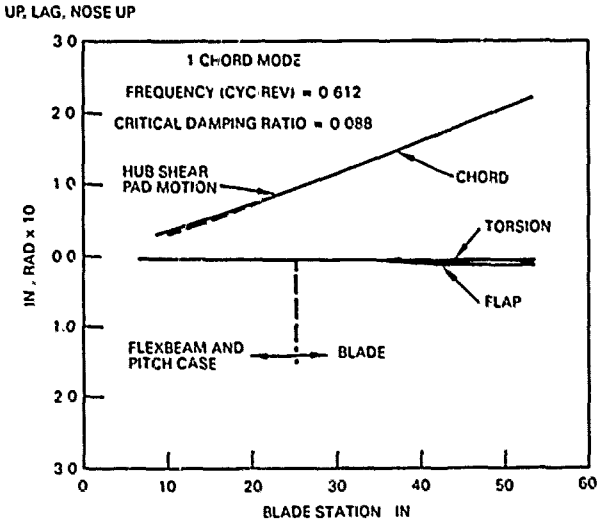


Fig. 26 Reactionless B.C., mode shape plots – 1-chord mode

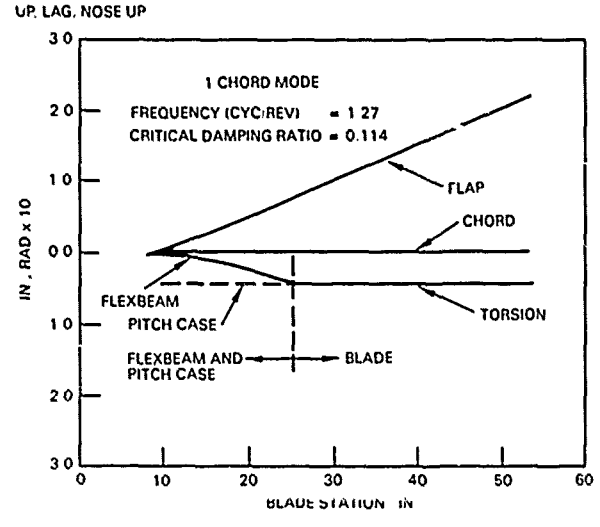


Fig. 27 Reactionless B.C., mode shape plots -- 1-flap mode

5.1.2 Cyclic Boundary Condition

In the cyclic or C-mode boundary condition, the 1/rev inplane bending moments are contained within the flexbeam in the carry-through hub construction and are not reacted through the hub shear pads and the hub. The hub support flexibility is modeled. The coupling between the hub

motion and blade feathering due to swashplate motion is included. The kinematic flap-lag-torsion coupling due to pitch link/pitch horn spanwise and chordwise location and pitch link inclination is also included in the analysis.

The regressing frequencies for zero collective pitch are shown in Fig. 20. The first chord frequency, which reflects the stiffness of the flexbeam and the inertia of the blade, is well separated from the first flap frequency and from 1/rev resonance.

Fig. 28 shows the influence of collective pitch on blade frequencies. The first flap frequency remains practically unchanged with collective pitch. The pitch orientation of the flexbeam with respect to the blade chord ensures minimal variation of the first chord frequency over the collective pitch range of the rotor. The first torsion mode shows a drop in frequency with collective pitch thus further separating it from 3/rev. As expected, the second flap frequency increases and the second chord frequency decreases with changes in collective pitch from zero.

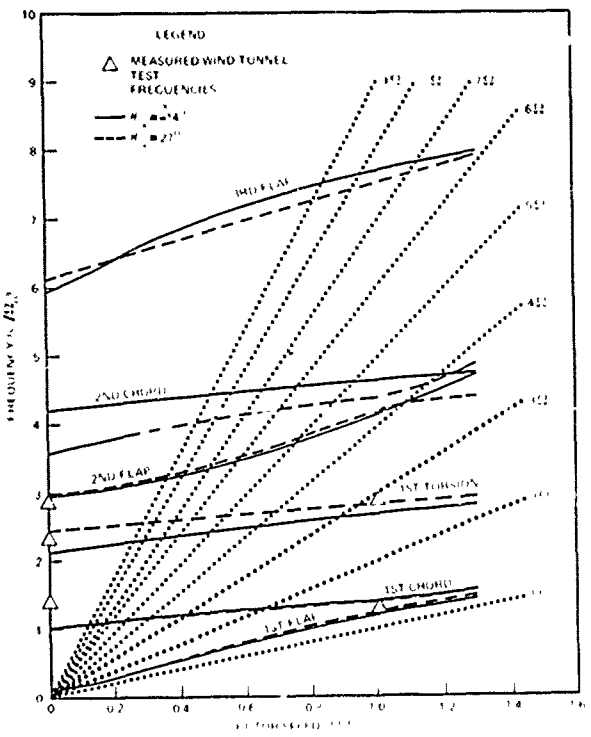


Fig. 28 CFTR resonance diagram, cyclic modes $\theta_{3/4}$ = -14 and 27 degrees

Figs. 29 through 31 show the fundamental coupled mode shapes for the cyclic boundary condition. The first flap mode, Fig. 29, shows the pitch/flap coupling for cyclic boundary condition. The first chord mode shows the amount of kinematic pitch/lag coupling induced by the inclined pitch link. The first torsion mode, Fig. 31, shows the extent of flap coupling.

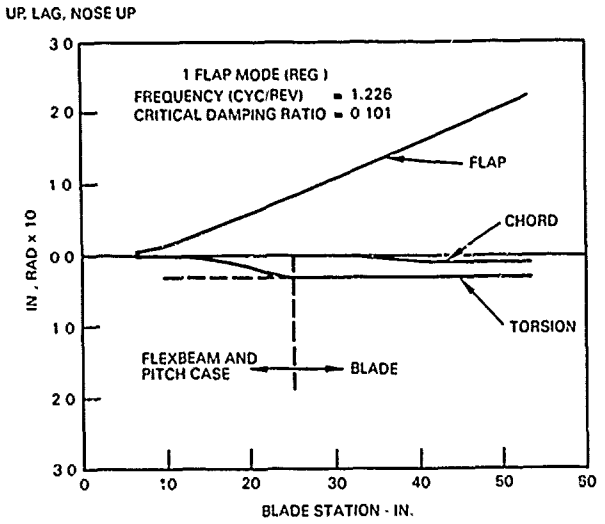


Fig. 29 Cyclic B.C., mode shape plots – 1-flap mode

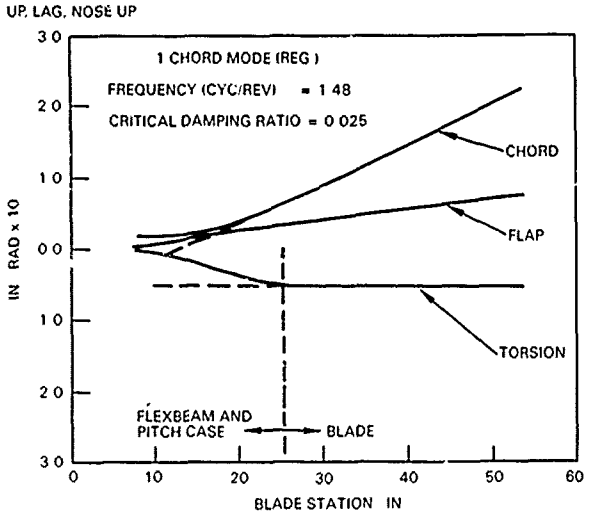


Fig. 30 Cyclic B.C., mode shape plots – 1-chord mode

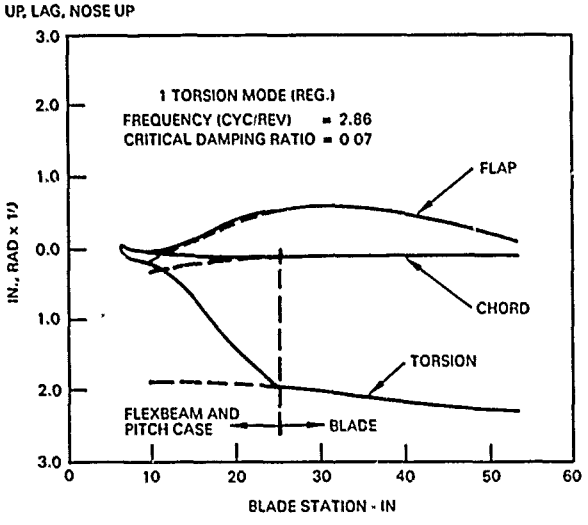


Fig. 31 Cyclic B.C., mode shape plots – 1-torsion mode

This was achieved through placement of the reactionless 1-chord frequency below 1/rev. Comparisons of harmonic loads between the CFTR and a similar size rotor (Reference 12) based on test data are seen in Figs 32 through 35. Figs. 32 and 33 are flight test loads of the YUH-60A tail rotor. Figs. 34 and 35 are wind tunnel test loads for the CFTR. This comparison is a study of the relative magnitudes of the harmonic loads for geometrically similar rotors with different dynamic characteristics. Absolute magnitudes of the loads should not be compared. The spanwise distribution and relative harmonic content of flapwise flexbeam loads are similar between the two rotors (Figs. 32 and 34). However harmonic contents of chordwise loads between the two rotors are quite different. In Fig. 33 (stiff inplane rotor), chordwise 2/rev loads are higher than the 1/rev loads. The CFTR (Fig. 35, soft inplane rotor) chordwise 2/rev loads are an order of magnitude lower than the 1/rev loads. This trend has been found for all test conditions.

5.1.3 Collective Boundary Condition

The difference between the collective and reactionless boundary conditions are in the model for the control system and drive system. The drive system torsional flexibility is represented by its flexibility in the blade inplane structural model at the hub. The control system stiffness is reflected by the structure from the tail rotor actuators to the pitch horn. The effective mass of the swashplate assembly has a significant influence on the first torsion frequency.

The resonance diagram for the collective boundary condition is shown in Fig. 21 for zero collective pitch. The predicted first chord modal frequency, which is essentially the drive system torsion mode, is omitted in the plot. This is because the frequency and damping of the first chord mode is more accurately predicted in the stability analysis of the tail rotor drive system rather than from the rotor model. The drop in the frequency of the first torsion mode (from those of the reactionless boundary condition) is a reflection of the reduction of control system stiffness and the inclusion of swashplate assembly inertia for the collective boundary condition. The second chord frequency is also reduced as a result of torsional flexibility of the drive system. Experimentally determined 1-chord frequency is included for comparison.

5.2 Harmonic Loads

As discussed in Section 3.0, the CFTR was designed for low chordwise 2/rev Coriolis load.

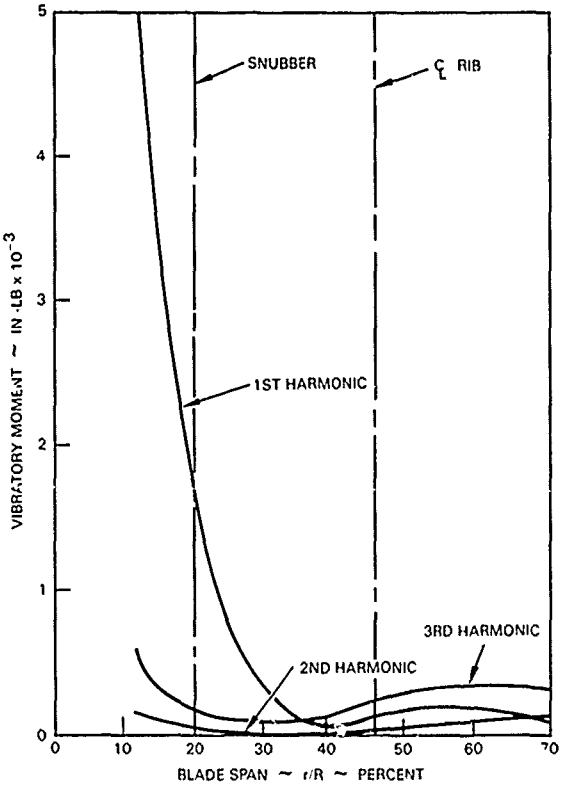


Fig. 32 YUH-60A tail rotor blade harmonic analysis flatwise (V = 143 KTS)

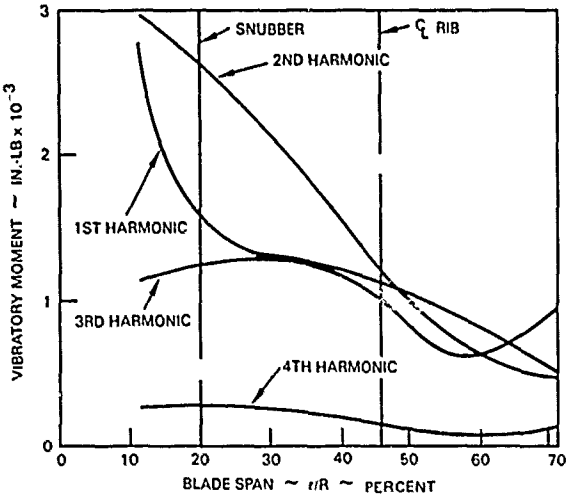


Fig. 33 YUH-60A tail rotor blade harmonic analysis edgewise (V = 143 KTS)

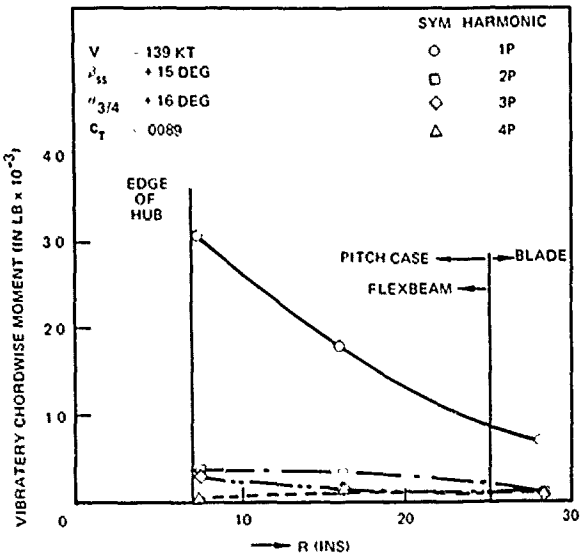


Fig. 35 CFTR - flexbeam harmonic loads

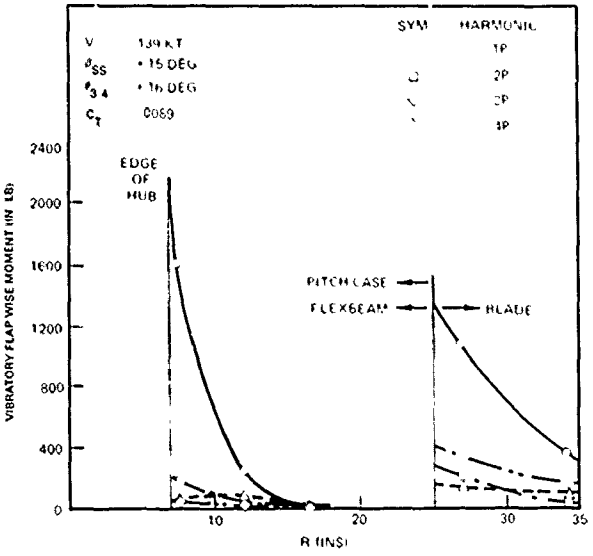


Fig. 34 CFTR - flexbeam harmonic loads

6.0 Concluding Remarks

As discussed in the preceding sections, the HHI Composite Flexbeam Tail Rotor has a dynamically unique design. This rotor has been demonstrated, through wind tunnel tests, over the full sideslip envelope of the AH-64, Advanced Attack Helicopter. The wind tunnel tests have validated that the CFTR:

1) Is aeroelastically stable throughout the complete collective pitch range and up to operational rotor speed of 1403 RPM.

2) Is aeroelastically stable for forward flight speeds up to 197 knots and sideslip flight representative of the AH-64 flight envelope.

3) Has excellent dynamic characteristics at all pitch angles, rotor speeds and test conditions.

4) Exhibits low flexbeam flapwise and chordwise steady and alternating stresses. Loads were well below endurance limit for all conditions tested in the wind tunnel.

5) Does not require a complicated flexbeam cross-section design with elastomeric material sandwiched in the flexbeam to provide damping.

These excellent characteristics have been achieved through judicious choice of design innovations which are the result of industry experience with bearingless rotors. Some of these innovations are discussed below:

1) In order to avoid stability problem characteristics of bearingless tail rotors, the first inplane reactionless (S-mode) frequency was tuned below 1/rev while maintaining the first inplane cyclic (C-mode) frequency above 1/rev. Both frequencies are well separated from the first flap frequency. This was accomplished through the design of the chordwise stiffness of the flexbeam, and by elastomerically mounting the flexbeam to the hub.

2) By allowing the flexbeam to freely flex within the hub, the load transfer to the hub is minimized. The 1/rev chordwise load is maintained within the flexbeam and not transferred to the hub. The 2/rev chordwise loads are transferred to the hub after significant attenuation due

to hub shear pad damping and separation of the first chord reactionless frequency from 2/rev.

3) The trailing edge pitch link attachment was found to be advantageous over a leading edge configuration (for a bearingless rotor of the "pusher" type).

a) For the required kinematic pitch-flap coupling of -35 degrees, the trailing edge pitch link attachment permits a smaller swash-plate and a compact control system design.

b) The trailing edge pitch link attachment raises the second flap frequency, thus providing good separation from 3/rev.

c) The nominal pitch link load (compression) for a trailing edge pitch link attachment is in the same direction as the rotor thrust, thus reducing considerably the flap shear load in the flexbeam, inboard of the pitch shear support.

4) The inclination of the pitch link introduces positive pitch-lag coupling (nose down with blade lag). This coupling adds damping to the first chord cyclic mode through pitch coupling, especially at high collective pitch settings.

5) The relative pitch orientation of the flexbeam chord with respect to the blade chord causes the cyclic first chord frequency to first increase and then decrease through the collective pitch range of the rotor. This ensures minimum decrease of the cyclic first chord frequency and prevents coalescence with the first flap frequency.

6) The above means of introducing damping and of preventing dynamic instabilities involving the lowly damped 1-chord mode, eliminates the need for introducing structural damping through elastomeric inserts in the flexbeam.

7) The leading edge balance weight between station 39 and 51 was introduced to move the blade dynamic center of gravity forward and eliminate blade flutter due to structural failure of the feathering control system.

8) The blade spanwise balance weight is located at station 9.7 (on top and bottom of pitch case) rather than at blade tip. Elimination of tip balance weight increases the cyclic first chord frequency and avoids coalescence with the first flap frequency. The balance weights on the top and bottom surfaces of the pitch case act as "Chinese" weights, thus reducing feathering control loads.

7.0 References

1. Edwards, W.T. and Miao, W., "Bearingless Tail Rotor Loads and Stability", Boeing-Vertol Company, prepared for Applied Technology Laboratory, Research and Technology Laboratories (AVRADCOM), Fort Eustis, VA 23604, USAAMRDL TR 76-16, November 1977.

2. Fenaughty, R.R. and Noehren, W.L., 'Composite Bearingless Tail Rotor for UTTAS", Journal of the American Helicopter Society, July 1977.

3. Cook, C.V., A Review of Tail Rotor Design and Performance, Vertica, Vol. 2, pp. 163-181, 1979.

4. Hughes, C.W., "Design and Testing of a New Generation Tail Rotor", Bell Helicopter Textron, presented to the AHS Technical Council for consideration of the Robert L. Lichten Award, February 1978.

5. Maloney, P.F. and Porterfield, J.D., Elastic Pitch Beam Tail Rotor, Kaman Aerospace Corporation, USAAMRDL TR 76-35, U.S. Army Air Mobility Research and Development Laboratory, Fort Eustis, VA 23604, December 1976.

6. Gaffey, T.M., "The Effect of Positive Pitch-Flap Coupling (Negative δ_3) on Rotor Blade Motion Stability and Flapping", Journal of American Helicopter Society, April 1969.

7. Ormiston, R.A. and Hodges, D.H., "Linear Flap-Lag Dynamics of Hingeless Rotor Blades in Hover", Journal of American Helicopter Society 17 (2), April 1972.

8. Head, R.F. and Banerjee, D., "Helicopter Tail Rotor of the Elastomerically-Mounted Composite Flexbeam Type', Patent No. 4,381,902, May 1983.

9. Banerjee, D., "Composite Flexbeam Tail Rotor for the AH-64 Advanced Attack Helicopter Wind Tunnel Test Report", Hughes Helicopters, Inc., Report No. 150-V-2003, HHI 82-362, December 1982.

10. Systems Specification for Advanced Attack Helicopter, AMC-SS-AAH-H10000A.

11. Banerjee, D., "Composite Flexbeam Tail Rotor for the YAH-64 Advanced Attack Helicopter, Aeroelasticity and Rotor Blade Loads Report", Hughes Helicopters, Inc., Report No. 150-V-2001, HHI 82-184, June 1982.

12. YUH-60A - Structural Load Survey, Sikorsky Aircraft Report No. SER-70406.

13. Huber H., Frommlet, H., and Buchs, W., "Development of a Bearingless Helicopter Tail Rotor", Sixth European Rotorcraft and Powered Lift Aircraft Forum, Paper No. 16, September 16-18, 1980, Bristol, England.

DISCUSSION

AEROELASTIC CHARACTERISTICS OF THE AH-64 BEARINGLESS TAIL ROTOR

D. Banerjee

Dick Bielawa, United Technologies Research Center: I think that this rotor demonstrates a truism that I hold; that the analyst is always running to catch up with the designer. As soon as we feel we've got everything in that we could imagine, the designer says "I've got something new for you." Specifically, were you able to validate the excellent stability characteristics that you demonstrated experimentally with an analysis?

Banerjee: Well, we did very accurately determine the frequencies of these different inplane modes, both the reactionless and collective, as well as the cyclic, as where they are. For instance experimentally, we got the first inplane frequency from the spectrum analyzer to be about 1.4 per rev around zero collective pitch and the inplane frequencies for the collective and the reactionless modes were below 1 per rev. Those were quite accurately determined. However, we spent one full day trying to excite these modes so we could get some reading of the damping of these modes and hence verify with analytical predictions, but we just could not excite these modes even though we knew what the frequencies were and we used a 300-pound shaker. Using that 300-pound shaker, we used a shaking force of up to 150 pounds at the cyclic inplane frequency but we just couldn't see the in-plane mode being excited. It would be nice to have some kind of a correlation but we couldn't excite it.

Bielawa: You didn't use the DART analysis or anything like that, did you?

Banerjee: We did use the DART analysis for prediction for all our design purposes and for predicting the damping characteristics, but we could not validate [it] with test data. The only thing we could validate were the frequencies.

Dave Sharpe, Aeromechanics Laboratory: What were the magnitudes of the damping predictions, were they highly damped?

Banerjee: For the cyclic inplane frequencies the inplane damping was predicted to be between four and five percent. The reactionless, because of the elastomer, was predicted to be between seven and eight percent at all collective pitch settings.

Jing Yen, Bell Helicopter Textron: I heard you say you moved your chordwise CG from 35 percent forward. To where?

Banerjee: With a failed pitchlink configuration, we essentially had to move it to an effective dynamic CG of around 29 percent, I'd have to go back and look.

Yen: Which airfoil was used?

Banerjee: The airfoil that was used is an HH02 airfoil.

Bill Warmbrodt, NASA Ames: Do you have plans to fly this tail rotor?

Banerjee: I think right now it's under consideration. I have no idea what the next step of the actual qualification tests would be for this rotor.

Pete Arcidiacono, Sikorsky Aircraft: It looks like a lot of good work. Do you have any trouble transmitting steady torques to the blades or do you anticipate any fatigue problems in accommodating the vibratory torques through the elastomer?

Banerjee: Of course we had to take that into account to determine the gap between the flexbeam and the shims in the chordwise direction on either side of the flexbeam. We didn't see that as a problem and we didn't have any interference problems either.

Arcidiacono: How much windup did you get under steady torque loads? Or, I guess, how much is the gap, is a better question.

Banerjee: Two tenths of an inch at the most.

PANEL SESSION TWO

THE PROBLEM OF MATH MODEL VALIDATION

Panel Chairman: William G. Bousman
U.S. Army Aeromechanics Laboratory

Panel Members: Peter J. Arcidiacono
Sikorsky Aircraft

Robert A. Ormiston
U.S. Army Aeromechanics Laboratory

Jing G. Yen
Bell Helicopter Textron

W. Euan Hooper
Boeing Vertol

E. Roberts Wood
Hughes Helicopters

Donald J. Merkley
U.S. Army Applied Technology Laboratory

Peretz P. Friedmann
University of California, Los Angeles

William J. McCroskey
U.S. Army Aeromechanics Laboratory

INTRODUCTION

William G. Bousman

Good afternoon. The panel this afternoon is on the problem of math model validation. I would like to start by introducing the panel members. Starting from my left we have Jing Yen from Bell, Euan Hooper from Boeing Vertol, Bob Wood from Hughes Helicopters, Pete Arcidiacono from Sikorsky, and then some government and academic representatives; Jim McCroskey from the Aeromechanics Laboratory, Don Merkley from the Applied Technology Laboratory, Peretz Friedmann from UCLA, and Bob Ormiston from the Aeromechanics Laboratory: What I'm going to do will be a little bit more like a standard panel today. I'm going to make some remarks and then I've given some questions to the panel members. I'm going to ask them to spend roughly ten minutes discussing particular issues. The purpose of this panel really is to step back a little bit from what we've been doing in the last day in looking at the

PRECEDING PAGE BLANK

very detailed correlation effort. In that process we've raised a number of questions which I think are continuing and ongoing questions in the field. I think this panel's main purpose is to look at some of these general questions and perhaps, although we won't solve anything today, we'll add a little light to the way we should do things to do perhaps better in the future.

I think that a very natural place to start is the rotor loads comparison that was done at the rotorcraft dynamic specialist meeting here in 1974 [Slide 1]. It's one of the few previous major correlation efforts that we've had and it's sort of a benchmark we all look to. There are some similarities with what we've done at this workshop and there are some differences. In '74 we looked at just one rotor; that made it quite a bit less expensive, and here we've had six experimental configurations. In '74 we compared analyses only--we didn't have the experiments--and with this comparison we've been able to do both. The bigger differences are that in '74 we were looking at rotor loads and in this comparison we've looked at stability. In that effort we looked primarily at the aerodynamic modeling in forward flight; that was what was dominating the differences between configurations and was having the predominant effect in stretching the capabilities of the analyses. I think in what we've been doing here it's really structural modeling, between hingeless and bearingless rotors, rotor/body coupling, these sorts of things that have been dominant. The advance ratio was the primary variable for that rotor loads effort and here it's structural configuration. But in both cases we've used the primary company codes for analysis, it's a best-effort thing. That effort was unfunded back then. I shouldn't say unfunded; it was supported by the companies, whereas the present effort was funded by the government.

SIMILARITIES AND DISSIMILARITIES

1974 ROTOR LOADS COMPARISON	ITR METHODOLOGY ASSESSMENT
o SINGLE HYPOTHETICAL ROTOR	o SIX EXPERIMENTAL CONFIGURATIONS
o ANALYTICAL COMPARISONS ONLY	o ANALYTICAL COMPARISONS AND COMPARISON TO EXPERIMENTAL DATA
o ROTOR LOADS BASIS OF COMPARISON	o ROTOR STABILITY BASIS OF COMPARISON
o AERODYNAMIC MODELLING IN FORWARD FLIGHT IS DOMINANT INFLUENCE	o STRUCTURAL MODELLING IN HOVER IS DOMINANT INFLUENCE
o ADVANCE RATIO IS PRIMARY INDEPENDENT VARIABLE	o STRUCTURAL CONFIGURATION IS PRIMARY INDEPENDENT VARIABLE
o PRIMARY COMPANY CODE USED FOR ANALYSIS	o PRIMARY COMPANY CODE USED FOR ANALYSIS
o EFFORT UNFUNDED	o EFFORT FUNDED

Slide 1

But I'd like to go back to some of the results of that study. Just to do a little recollection, the 1974 comparison made some recommendations [Slide 2]. There were four recommendations from that study and there was a fifth implicit recommendation, which was not stated. (1) The first recommendation was just to continue doing these comparisons, so we've done one now nine years later. (2) The second recommendation was to do detailed computer experiments, i.e., experimentation with large computer models, to look at what was happening. (3) The third recommendation identified what was felt were the biggest unknowns in the aerodynamic models; dynamic stall, blade/vortex interaction, and three-dimensional (3-D) flow effects at the tip. (4) The fourth and last recommendation was that we should do a large-scale rotor test and that our large-scale rotor test would be the basis for another comparison. The implicit recommendation was that the industry could not fund this level of correlation simply on their own funds; there needed to be a central sponsor for that work.

I'd like to go on and look at what has happened in these recommendations and I'm going to group the first and second together [Slide 3]. These are, of course, my opinions; but just for talking purposes I'll be very opinionated. There's essentially been no progress since 1974, in either the comparisons or in doing the computer experiments that were recommended. There are a number of reasons. One of them is that to do a comparison across the industry you need a government sponsor; it will not occur spontaneously through the professional societies or anything like that. That costs money and takes time on someone's part. I think that any sort of experiment with these very, very large and not always well-documented programs takes very well-qualified people; very clever, very knowledgeable people, to get through the arcane programs that exist. The people who are that well qualified do not want to spend the best years of their lives upgrading computer codes. We don't like to be probed by sociologists, but I think that if you look at the sociology of research, the people who are the most competent are always going to want to challenge the new problems. They want to do the things that are low on an exponential curve; they don't want to be working up at the 75% and 80% point of the exponential curve, polishing and working on the problem where there's not a lot of recognition. There's not a lot of reward to get a code just working slightly better, or

RECOMMENDATIONS OF 1974 ROTOR LOADS COMPARISON

1. CONTINUE STANDARD COMPARISONS.
2. DETAILED COMPUTER EXPERIMENTS SHOULD BE PURSUED TO UNDERSTAND DIFFERENCES UNCOVERED IN THE COMPARISONS.
3. FUNDAMENTAL EXPERIMENTS SHOULD BE PURSUED TO UNDERSTAND DYNAMIC STALL, BLADE/VORTEX INTERACTION AND THREE-DIMENSIONAL FLOW EFFECTS.
4. DETAILED WIND TUNNEL TESTS OF A LARGE SCALE ROTOR SHOULD BE MADE TO SUPPORT FUTURE COMPARISONS.
5. FUTURE COMPARISONS SHOULD BE FUNDED BY THE GOVERNMENT (IMPLICIT RECOMMENDATION).

Slide 2

STANDARD COMPARISONS AND COMPUTER EXPERIMENTS (NO. 1 AND 2)

- o NO PROGRESS SINCE 1974
- o REASONS:
  - COMPARISONS REQUIRE GOVERNMENT SPONSOR, THEY WILL NOT OCCUR SPONTANEOUSLY.
  - EXPERIMENTS REQUIRE CAREFUL, COMPETENT WORK. ONLY EXTREMELY WELL QUALIFIED PEOPLE CAN DEAL WITH THE MYSTERIES OF THE LARGE ANALYSIS PROGRAMS.
  - EXTREMELY WELL QUALIFIED PEOPLE DO NOT WANT TO WASTE THE BEST YEARS OF THEIR LIVES UPGRADING COMPUTER CODES.
  - COST

Slide 3

significantly better even, because even if you do get it significantly better you probably can't prove it. And then, it's costly.

I go to the next slide [Slide 4] and look at the third recommendation, and that's the only bright spot we really have from those recommendations. We've had significant progress since 1974 in looking at some of the fundamental areas. Last May there was an AGARD meeting in London, I believe, on rotor loads and it looked at what had happened in the past eight years. Of the 19 papers, one was on dynamic stall, three were on blade/vortex interaction, and three were on 3-D effects; so a lot has been done, a lot is being reported. I'd say that since '74 we've seen very good, very detailed experiments on dynamic stall, and very good detailed experiments on 3-D effects on airfoils, largely nonlifting. The blade/vortex interactions are starting to occur now; we're starting to see some efforts that way. That sounds very good but I would inject a very personal comment; it is interesting to me that

PURSUE FUNDAMENTAL EXPERIMENTAL RESEARCH ON AERODYNAMIC EFFECTS (NO. 3)

- o SIGNIFICANT PROGRESS SINCE 1974
- o AS EXAMPLE, OF 19 PAPERS IN 1982 AGARD MEETING ON ROTOR LOADS:
  - 1 PAPER ON DYNAMIC STALL
  - 3 PAPERS ON BLADE/VORTEX INTERACTION
  - 3 PAPERS ON 3-D EFFECTS
- o GOOD, DETAILED EXPERIMENTS ON DYNAMIC STALL AND 3-D EFFECTS HAVE BEEN DONE
- o BLADE/VORTEX INTERACTION EXPERIMENTS ARE STARTING

Slide 4

by and large the push in all these experiments has not been from the rotor-loads or dynamics community; rather, it has been the aerodynamicists who are looking at these fundamental problems. The blade/vortex interactions are almost uniformly the acousticians', it seems to me, at least in this country. Dynamic stall: mostly it has been the fluid mechanicians although some of that work has been going into the rotor loads calculations. I don't want to put down any of this work in any respect, but I think that some of the fundamental experiments could benefit from the dynamics community's input, and I'm not sure that that's occurring.

Now the fourth recommendation [Slide 5] was that we should do a big wind tunnel experiment, a full-scale rotor or nearly full-scale, and there's been no progress since '74 on that. And I'll put at the top [of the reasons] cost because it is an extremely expensive process. But there are some other reasons which we, I think, have to address first before we go to that costly experiment. I don't think we really understand the limitations of the current data sets that exist right now. I'm not sure we've used them enough, certainly not in the published literature, to understand their limitations so that we do not repeat past errors. I'm not sure that we understand enough about how to efficiently access these large data sets. There's no question that the next full-scale rotor experiment will have a tremendously larger amount of data then what was taken in the early 60s at Langley. It's going to be very difficult to access. It's already a very expensive process to validate codes with these data--we may have to do pilot work before we do the full scale experiment just to see that the correlation part can be done.

The last implicit recommendation was cost [Slide 6], and I'd like to point out that we have said that Government should fund future comparisons, and indeed we have funded this one, but there are some reasons why we haven't seen more of it. One is that it just costs a lot; it doesn't matter who does it. This program here: just to run the codes, set up the model properties, and have someone sit down and go over the data, even for some of the simple experiments, costs us $275,000. Numbers don't always mean something, but from my perspective of our Division here at Ames, that represents 1 to 2 yr of our contract budget if we funded it in a normal fashion. And I just put that in to show you that certain groups that are interested in this

WIND TUNNEL TEST OF FULL SCALE ROTOR (NO. 4)

- o NO PROGRESS SINCE 1974
- o REASONS:
  - COST
  - INSUFFICIENT UNDERSTANDING OF LIMITATIONS OF CURRENT DATA SETS
  - INSUFFICIENT UNDERSTANDING OF HOW TO EFFICIENTLY ACCESS LARGE DATA SETS

Slide 5

GOVERNMENT MUST FUND FUTURE COMPARISONS (NO. 5)

- o LIMITED PROGRESS SINCE 1974, I.E. ITR METHODOLOGY ASSESSMENT
- o REASONS:
  - COST (ITR ASSESSMENT WAS $275,000 JUST TO SET UP MODEL PROPERTIES AND RUN PROGRAMS).
  - THERE IS ONE CHANCE IN TWO THAT A PROGRAM WILL OVERRUN COSTS BY 30% (AUGUSTINE'S LAW III).
  - ALL PROGRAMS TAKE 1.33 MORE TIME TO COMPLETE THAN ESTIMATED (AUGUSTINE'S LAW XXII).
  - WHEN COST OR SCHEDULE PROBLEMS ARISE THE VALIDATION EFFORT IS CUT OUT (BOUSMAN'S LAW).

    THIS HAPPENS FOR BOTH ANALYTICAL PROGRAMS AND EXPERIMENTAL PROGRAMS.

Slide 6

work simply do not have the funds within the Government. The only way we were able to fund this thing was by tying it in to a 6.3 development program, the ITR program.

There are also some reasons why the validation, even a limited validation, doesn't occur and these are a consequence of Augustine's laws. The first is that when you start a program the chances are that there is going to be a cost overrun. Augustine's third law is that there's one chance in two that programs will overrun cost by 30%, and he also has his law number 22, that all programs take a factor of 1.33 more time to complete than estimated--that's his fantasy factor. It doesn't matter then whether it's an experimental program where you plan to take the data and compare with theory at the and or it's an analytical program where you're going to develop a theory and at the end compare it with experimental data. When you reach the end, there are going to be cost or schedule problems and the thing that is going to be cut is the validation effort. That's Bousman's law, I'm not going to give you a number, but you can have the law. This happens for both experimental and analytical programs. No one is to blame, it is nobody's fault, it is just the sociology of how we do our business and how things work out.

I'd like to move on then, hoping to raise some issues, and give the questions that I've given to the panel. There are eight; they are all related and many of them have come up already in our discussions of the last day and a half [Slide 7]. But how do we go about validation? How much correlation is enough? We started touching on that yesterday just before we stopped and it was getting very interesting because it is a very gray area. And why do we use math models without validation? How are experimental data bases developed and qualified, because we have to have some confidence in their accuracy, and how are they managed? I've asked Don Merkley to address that one specifically. Why are some data bases never used, or only used to a limited degree? What can we do in the future to reduce the cost; are there other things we can do in computer networking that will have some potential here? Will 2GCHAS change the framework of our validation requirements? Maybe we have too many codes already and if we go to one big comprehensive code with a

QUESTIONS TO PANEL

1. HOW ARE MATH MODELS VALIDATED?
2. HOW MUCH CORRELATION IS ENOUGH?
3. WHY IS IT THAT MATH MODELS ARE USED WITHOUT VALIDATION?
4. HOW ARE EXPERIMENTAL DATA BASES DEVELOPED, QUALIFIED, AND MANAGED?
5. WHY ARE SOME DATA BASES NEVER USED OR ONLY TO A LIMITED DEGREE?
6. WHAT CAN BE DONE TO REDUCE COST OF FUTURE VALIDATION EFFORTS?
7. WILL 2GCHAS CHANGE THE FRAMEWORK OF OUR VALIDATION REQUIREMENTS?
8. WHAT ROLE DOES THE SIMPLE MODEL OR LIMITED EXPERIMENT PLAY IN THE VALIDATION OF COMPLEX MODELS?

Slide 7

limited number of technology modules we can reduce the cost in that sense; Bob Ormiston, who is the 2GCHAS manager, will address that. Then what role does the simple model or limited experiment play in the validation of complex models? I think we've seen, particularly from the data set A, that a simple experiment can look at some very fundamental elements of a very complex model. There is room in there, I think, for work to be done in academia as well as in the government laboratories, and I've asked Peretz to address that question. But for the questions in general, I'd like to start out the panel with Jing Yen from Bell Helicopter.

PREPARED REMARKS BY JING YEN

The item I'm going to address here today is Item 3 on Mr. Bousman's list which reads: "Why is it that math models are used without validation or with validation only in limited areas" [Slide 8]? Logically, the very first thought which comes to my mind to answer this question is the cost. We all know that math-model validation is very costly and at most times it does not seem to be cost-effective either. For instance C81 was audited extensively in 1974 and 1975 under Bell IP&D funding. My recollection for that effort was that the cost was nearly 7000 hr. As a result of that audit several errors were found and fixed, yet C81 still has undefined problems; otherwise the U.S. Army would not have made the decision to go ahead with 2GCHAS. The second reason I could think of is the lack of qualified experimental data. Again we all realize, or recognize, the fact that qualified data doesn't come easily. For instance, recently I tried to correlate some rotor loads data using the C81 analysis. I started with ground-run data of rotor loads measured versus cyclic stick position at a given collective. Such a simple task resulted in a major project. The reason is that to have a very valid rotor-loads correlation, one needs to have very good definitions of items like the feathering spring rate, the mast bending stiffness, the pylon-mounting spring rate, the rotor properties, the C_l, C_d,

WHY IS IT THAT MATH MODELS ARE USED WITHOUT VALIDATION OR VALIDATION ONLY IN LIMITED AREAS?

- COST
- LACK OF QUALIFIED EXPERIMENTAL DATA
- HELICOPTER MANUFACTURERS' DESIGN TRADITION
- PROPRIETARY DATA

Slide 8

and C_m properties, how the environment was controlled, and you also need error free instrumentation. So it's a big, big task to qualify experimental data. It doesn't come that easily

The third point I have here is that each helicopter manufacturer has its own unique design tradition, for instance Bell Helicopter has been producing teetering rotors and hingeless rotors. I'm just wondering how many analyses at Boeing Vertol, Sikorsky, or Hughes have been validated for teetering rotors. The helicopter manufacturers then develop their design tools mostly in support of their own production line, to be cost effective.

Surely the last but not the least item on the list is proprietary data. Should I decide to correlate one of Bell's analyses with the S76 type of helicopter, where could I get the qualified data on the S76 from? Would they share it with me?

The other question is, what can we do [Slide 9]? First, I would like to suggest that the Government create and manage a data bank. The most important customer of the U.S. helicopter manufacturers is still the Government. It has the best opportunity to collect data from the various helicopter manufacturers and, in view of the 2GCHAS needs, obviously the 2GCHAS project office may be ideal to assume that responsibility. Then all the qualified experimental data should be documented

WHAT CAN BE DONE?

- GOVERNMENT MANAGED DATA BANK
- ADS-10 AND QUALIFIED EXPERIMENTAL DATA
- VALIDATED ANALYSIS

"GOVERNMENT MUST LEAD"

Slide 9

properly and the aircraft or the hardware used to produce those qualified data should be clearly defined according to an established standard, such as the Aeronautical Design Standard, ADS-10. Incidentally the ADS-10 requirement has been around now for nearly 10 yr, as far as I know. From the Army's most important major helicopter-development programs, I would like to ask how many ADS-10 documentations have been made available with qualified experimental data that we can take advantage of? Then I would say that the U.S. Government should promote the concept of validation by demanding a substantiation of any correlation presented in any major proposals. They could also request the author to provide all the input data necessary to provide their correlation and to provide evidence of that math model's validation. We all know that Bob Ormiston had a rotor loads workshop back in 1974. At that time I was 9 yr younger and I was there. Can you imagine if we take another 9 yr, it will be the year 1992. Therefore obviously the bottom line here is that the U.S. Government must lead for the reasons I have said and the time is right now.

PREPARED REMARKS BY EUAN HOOPER

I expect each of us is going to find that our ground is gradually being covered as we move down the table, so I'm quite glad to be among the first. To me it's no surprise that we do not do an adequate job of validating math models. I think there are so many frustrations, like what's shown on my viewgraph [Slide 10]. That's just a partial list of the difficulties that we run into that everybody's experienced. The math model doesn't quite match the test that you're trying to work with, because of uncertainty about test conditions, particularly if we're going back into history. We've all experienced these things, critical calibrations lost and so on. There's also a psychological factor, the last one, "Poor correlation tends to discredit the analyst," that's enough to put off many people. You get into analysis and you know your reputation is on the line if it doesn't agree. It leads to some overoptimistic claims for correlation which we've all seen in the literature and, no doubt about it, analysts tend to take it personally when the correlation isn't good and that's a discouragement. The cost of course (Bill Bousman has referred to it) is excessive and analysis is time-consuming.

I was prompted to recall, myself, that there's a superb data base available in the literature over the last 20 yr of dynamic airloads testing on all those

WHY ARE MATH MODELS INADEQUATELY VALIDATED?

- NO FUN
  - MATH MODEL DOESN'T QUITE MATCH TEST HARDWARE
  - UNCERTAINTY ABOUT TEST CONDITIONS
  - IMPRECISE PHYSICAL PROPERTIES
  - FLIGHT DATA UNREPEATABLE - HIGH SCATTER
  - CRITICAL CALIBRATIONS LOST
  - CRITICAL DATA CHANNELS DEFECTIVE
  - POOR CORRELATION TENDS TO DISCREDIT ANALYST
- EXPENSIVE
  - ITR METHODOLOGY ASSESSMENT CONTRACTS COST $275,000
  - PRECISE PHYSICAL PROPERTIES NEEDED
- TIME CONSUMING

Slide 10

aircraft, both wind tunnel and flight testing [Slide 11]. It's a data base that I've taken a personal interest in. At the moment, I'm putting together a paper comparing them all on a common basis. At Vertol we've tried to correlate using some of these data bases with our own analyses. It's probably worth recalling that we submitted a proposal a couple of years ago. I must admit I winced when I saw that it came to close to a couple of hundred thousand dollars to go through that big data base and apply analyses to it, not only our analyses but other analyses as well. This was done just to validate them, to see how they came out in great depth, in the higher frequency components as well as the steady state. Wayne [Johnson] decided not to accept it. I'm sure he had good reasons--it's very expensive and time-consuming. I thought it was a surefire proposal for success. I don't think that great big data base has been exercised a fraction of the amount that it should have been. Each one of those aircraft has got maybe 40 or 50 pressure channels on the blades; there's a wealth of high frequency data on them and only very spotty validation exercises have been done.

I've got another point here, the second point about in-depth validations. You know we've spent the best part of a couple of days discussing validations using damping as the criterion for success; but you really have to, and I'm sure Dick Bielawa has done this, go into greater detail in each of these cases because the damping alone [illegible] the only criterion. You really need a knowledge of the mode shape of the [illegible]ility. In many cases I find that a weakness of that validation process is th[illegible] the analyst will look only at a single end-product number rather

MUCH DATA AVAILABLE FOR VALIDATION - MORE NEEDED

- E.G., DYNAMIC AIRLOADS TESTS
  - H-34 FLIGHT TEST
  - H-34 WIND TUNNEL TEST
  - UH-1 FLIGHT TEST
  - CH-47 FLIGHT TEST
  - XH-51A FLIGHT TEST
  - NH-3A FLIGHT TEST
  - CH-53A FLIGHT TEST
  - AH-1G FLIGHT TEST
- IN-DEPTH VALIDATIONS REQUIRED
- TESTS MUST BE PLANNED WITH RESPECT TO METHODS VALIDATION REQUIREMENTS

Slide 11

than dig down into the depths to understand why the validation is poor, and I think that's something that we all have to accept.

What can we do to improve? There really are some things that we can do [Slide 12]. I'm sure you're all familiar with these Independent Research and Development (IR&D) evaluation sheets [Slides 13 & 14]; we all go through the IR&D exercise when the Government comes in every other year and evaluates our progress. I would like to see, and I looked around to find if there was some guidance for the governmnent people who are involved in these evaluations, if there's some guidance to give weight to the use of validation when methodology is developed. I'm suggesting that a very practical thing the Government could do is to really put some teeth into that process, since reams of [methodology] have been developed under government funding and under IR&D, and insist that IR&D methodology be validated and in such a way that the contractors will realize that the points that they accumulate will be affected by the quality of the validation.

The next point is that I don't know how many contractors actively use IMPD funds. This is something that we've only been exposed to at Boeing in engineering for the last year or two, but Internal Methods & Process Development (IMPD) is another form of overhead, like IR&D, and at the moment we've got a team of lawyers in Philadelphia and lawyers in Seattle working on just how you can use IMPD funds

DETAILED VALIDATION OF METHODS MUST BECOME WIDELY ACCEPTED AS AN INTEGRAL PART OF METHODOLOGY DEVELOPMENT

WHAT CAN BE DONE?

- IR&D EVALUATION SCORE SHEETS COULD GIVE QUANTIFIABLE CREDIT FOR VALIDATION STUDIES CONDUCTED IN CONJUNCTION WITH METHODOLOGY DEVELOPMENT.
- CLARIFY AND ENCOURAGE USE OF IMPD FUNDS FOR VALIDATION OF METHODS - IMPD IS PRESENTLY USED FOR IMPROVING MANUFACTURING METHODS ONLY.
- NASA/ARMY CONTINUE TO MAKE COMPREHENSIVE DATA BANKS AVAILABLE FOR USE IN VALIDATION STUDIES (DATAMAP).
- RFP'S COULD PLACE INCREASED IMPORTANCE ON VALIDATION OF ANALYTICAL METHODS PROPOSED FOR USE. (EVALUATION & AWARD FACTORS SECTION COULD DEFINE SPECIFIC DATA BANKS THAT MUST BE USED FOR CORRELATION.)
- DCAA CONFERS 'VALIDATION' STATUS ON COST & SCHEDULE METHODOLOGY. SHOULD A SIMILAR APPROACH BE USED FOR THE VALIDATION OF ANALYTICAL METHODOLOGY?

Slide 12

INDEPENDENT RESEARCH AND DEVELOPMENT PROJECT TECHNICAL EVALUATION

DATE

1 COMPANY NAME AND FISCAL YEAR	2 PROJECT NO	3 PROJECT TITLE

4 EVALUATOR (Name and Organization)

5 EVALUATOR INTEREST — I WOULD BE INTERESTED IN

a RECEIVING INFORMATION ON PROGRESS OF THIS PROJECT [ ] YES [ ] NO

b ATTENDING A FUTURE ON SITE REVIEW ON THIS PROJECT [ ] YES [ ] NO

6 EVALUATION BASIS

a TECHNICAL PLAN (Brochure) [ ] YES [ ] NO

b ON SITE REVIEW [ ] YES [ ] NO

c PERSONAL FAMILIARITY [ ] YES [ ] NO

7 EVALUATOR QUALIFICATIONS (For This) — I HAVE

a [ ] MINIMAL QUALIFICATIONS TO EVALUATE THIS PROJECT

b [ ] GENERAL KNOWLEDGE OR PAST EXPERIENCE IN THIS TECHNICAL AREA

c [ ] SPECIFIC KNOWLEDGE OF CURRENT WORK IN THIS TECHNICAL AREA

d [ ] SPECIFIC KNOWLEDGE OF CURRENT WORK ON SIMILAR PROJECTS

8 EVALUATION (For each category circle the single most applicable code. If a standard code does not apply enter a comment in item 9 identifying the category recommended code and finding. For continuing projects, projects funded in the current and past year evaluate all categories. For new projects, do not evaluate the PROGRESS category. For projects completed or terminated in the past year do not evaluate OBJECTIVE, APPROACH, and RESOURCES. Consider personnel, facilities, equipment, and funding in evaluating RESOURCES.)

CATEGORY	RATING (Score)	CODE	EVALUATION FINDING
OBJECTIVE	UNSATISFACTORY (0)	a	VAGUE/NOT SPECIFIED/TOO BROAD (If selected do not evaluate further)
	SATISFACTORY (1)	b	CLEARLY DEFINED
APPROACH	UNSATISFACTORY (0)	a	INSUFFICIENT INFORMATION FOR EVALUATION/UNREASONABLE
	POOR (1)	b	INADEQUATELY PLANNED/UNNECESSARILY DUPLICATES KNOWN WORK (Cite examples in item 9)
	SATISFACTORY (2)	c	ADEQUATELY PLANNED/REASONABLE
	GOOD (3)	d	NOVEL/BETTER THAN COMPETITIVE APPROACHES
		e	VERY WELL PLANNED/HIGHLY PROFESSIONAL
	EXCELLENT (4)	f	EXPLORES AREA(S) OF VITAL IMPORTANCE
		g	OUTSTANDING/MAY LEAD TO A BREAKTHROUGH
RESOURCES	UNSATISFACTORY (0)	a	INSUFFICIENT TO ACCOMPLISH OBJECTIVE (Explain in item 9)
		b	EXCESSIVE RELATIVE TO STATED OBJECTIVE (Explain in item 9)
	SATISFACTORY (1)	c	REASONABLE TO ACCOMPLISH OBJECTIVE

FUNDING (Fill in amount(s) in $K)			CURRENT YEAR	PAST YEAR
PROGRESS	UNSATISFACTORY (0)	a	INSUFFICIENT INFORMATION FOR EVALUATION	
	POOR (1)	b	RESULTS NOT COMMENSURATE WITH RESOURCES EXPENDED	
	SATISFACTORY (2)	c	RESULTS LIMITED BY A REDUCTION IN RESOURCES	
		d	PROJECT TERMINATED DUE TO NEGATIVE RESULTS	
		e	REASONABLE RESULTS CONSIDERING RESOURCES EXPENDED	
	GOOD (3)	f	RESULTS ACCEPTED BY RECOGNIZED TECHNICAL JOURNALS OR SOCIETIES	
		g	RESULTS ADVANCE TECHNOLOGY	
	EXCELLENT (4)	h	RESULTS INCORPORATED IN A GOVERNMENT OR COMMERCIAL CONTRACT	
		i	OUTSTANDING RESULTS/BREAKTHROUGH	

9 COMMENTS (In addition to comments relating to above categories, provide suggestions to improve the project or its written description. Concerning the written project description, check to insure that Key Words listed relate to the subject covered. If additional space is required, comments may be continued on the back of this form.)

10	11 a	b	(COMPLETE ON BACK OF THIS FORM AND RECORD RESULTS HERE)

DD FORM 1855

S/N 0102-083-4000

Slide 13

9 COMMENTS *(Continued)*

10 DESIGNATION *(From the terms below, circle the code that most closely describes the project and record the results in item 10 on the front of this form. Items a through d describe IR&D effort. Items e through n are not IR&D effort.)*

CODE	TERMS *(See ASPR references for complete definitions.)*
a	BASIC RESEARCH is that research which is directed toward increase of knowledge in science. The primary aim is a fuller knowledge or understanding of the subject under study, rather than any practical application thereof *(see ASPR 15-205.35)*
b	APPLIED RESEARCH is that effort which *(a)* normally follows basic research, but may not be severable from the related basic research, *(b)* attempts to determine and exploit the potential of scientific discoveries or improvements in technology, materials, processes, methods, devices, or techniques, and *(c)* attempts to advance the state-of-the art. Applied research does not include efforts whose principal aim is design, development, or test of specific items or services to be considered for sale; these efforts are within the definition of the term "development," defined below *(see ASPR 15-205.35)*
c	DEVELOPMENT is the systematic use, under whatever name, of scientific and technical knowledge in the design, development, test, or evaluation of a potential new product or service *(or of an improvement in an existing product or service)* for the purpose of meeting specific performance requirements or objectives. Development shall include the functions of design engineering, prototyping, and engineering testing *(see ASPR 15-205.35)*
d	SYSTEMS AND OTHER CONCEPT FORMULATION STUDIES are analyses and study efforts either related to specific IR&D efforts or directed toward the identification of desirable new systems, equipments or components, or desirable modifications and improvements to existing systems, equipments, or components *(see ASPR 15-205.35)*
e	B & P EFFORT. The major characteristic of B & P is the presence of intent to use the results directly for preparing a specific bid or proposal. If the effort is long range and intended to lead to as-yet-unspecified future business, it is more properly considered to be IR&D *(see ASPR 15-205.3)*
f	EFFORT IN SUPPORT OF A CONTRACT OR GRANT. If it is necessary to conduct a research and development task in order to fulfill the requirements of a contract, then the effort is not independent R&D and is considered to be in direct support of the contract whether or not it is specifically set forth in the contract work statement. To validate the claim of duplication of a contract or grant, the contracting agency, dates and identifying numbers should be shown under COMMENTS *(Item 9)*. The foregoing does not preclude *(a)* an IR&D project from terminating in a contract or grant, *(b)* continuing an effort after a contract is terminated, or *(c)* exploring areas closely related to a contract *(see ASPR 15-205.19)*.
g	MANUFACTURING AND PRODUCTION ENGINEERING EFFORT. Manufacturing and production engineering effort includes engineering activities conducted in connection with current manufacturing processes and current production problems and is not considered to be IR&D. This does not exclude consideration of the manufacturing or production effort during IR&D development of an item *(see ASPR 15-205.21)*
h	UNPLANNED EFFORT. Funds may not be set aside for some, as yet undefined, future requirement. If it is obvious by lack of description of a proposed effort that no specific planned approach has been formulated, then the funds allotted to such effort must be considered as contingency funds and the effort not to be IR&D in nature *(see ASPR 15-205.7)*
i	FACILITY DESIGN AND CHECKOUT EFFORT. The effort directly associated with the design and checkout of new facilities and equipment installed therein is not considered to be IR&D even though the installation may be used at some future time for IR&D effort.
j	MARKET ANALYSIS SURVEY, OR STUDY. This effort consists of determining the demand for various types of products to see whether it is worthwhile to develop and produce them. It is not IR&D.
k	LITERATURE SEARCHES. Pure literature searches do not strictly conform to ASPR definitions of research and development. However, if a literature search is succeeded by further efforts to advance the contractor's state-of-the-art, then the effort should be considered IR&D.
l	CONSULTING EFFORT. It may be necessary for a contractor to hire a consultant to provide support for an IR&D project. Such effort should be considered IR&D. However, if that effort is totally conducted by a consultant, it is not considered to be IR&D effort performed by the contractor.
m	VENDOR PRODUCT SURVEY. Inspection or test of a vendor's products to determine or verify the intended use will not be classified as IR&D. This includes tests to verify conformance with the vendor's specifications.
n	TRAINING EFFORT. Some training is inherent in many IR&D efforts, however, if a technical program is established by a contractor to train his personnel and no advancement of the contractor state-of-the-art is attempted, then it must be considered to be strictly training and not IR&D *(see ASPR 15-205.44)*

11 POTENTIAL RELEVANCE *(Check appropriate block and record the results in item 11 on the front of this form)* THIS PROJECT HAS A POTENTIAL RELATIONSHIP TO THE FUNCTIONS OR OPERATIONS OF THE

a. DOD ☐ YES ☐ NO

b. NASA ☐ YES ☐ NO

Slide 14

for engineering methodology development. It's very complex. We thought we had it all set up this year to do a lot of methodology improvement using IMPD funds, but just a few months ago it all collapsed and now we don't have it. I gather that it's a very uncertain, ill-defined process. This next chart [Slide 15] isn't going to help you a bit, but this is the official definition of the difference between IR&D and IMPD. I'll leave it just to let you read those two definitions for a moment; if anybody understands them I'd like to see them after the panel. I believe IMPD can be used, this is my personal belief, for the validation of methodology. It's something [where] you're not developing new techniques; you're validating existing technology, and I think that's a legitimate charge, but I'd appreciate somebody else's comment on that subject. I think it's a great source of funding, internal funding within companies, for further validation.

The next item on the list [of Slide 12] is that NASA/Army continue to make comprehensive data banks. These data banks that exist are superb and I think nobody's going to disagree that we're hoping that the government will continue.

Next, requests for proposal (RFPs), I think, could place increased emphasis on validation studies. I went back and looked at the ITR RFP [Slide 16] and in the evaluation-award-factor section there really is a statement (I've underlined it there, "This evaluation will be based on the substantiation provided for the analysis techniques, including consideration of the adequacy of the substantiation." So

INDEPENDENT RESEARCH & DEVELOPMENT (IR&D)
AND
INTERNAL METHODS & PROCESS DEVELOPMENT (IMPD)

IR&D

INDEPENDENT RESEARCH AND DEVELOPMENT (IR&D) IS DEFINED AS BASIC RESEARCH, APPLIED RESEARCH, DEVELOPMENT, AND SYSTEMS AND OTHER CONCEPT FORMULATION STUDIES INTENDING TO DISCOVER AND APPLY NEW FACTS, TECHNOLOGY, IDEAS, AND CONCEPTS TO A PRODUCT OR SERVICE FOR SALE INCLUDING ELEMENTS, COMPONENTS, SYSTEMS AND MATERIALS THEREOF.

IMPD

INTERNAL METHODS AND PROCESS DEVELOPMENT (IMPD) IS DEFINED AS INQUIRY, EXAMINATION, INVESTIGATION AND EXPERIMENTATION LEADING TO THE DISCOVERY OF NEW FACTS OR THE PRACTICAL APPLICATION OF EXISTING KNOWLEDGE FOR THE DEVELOPMENT OF NEW OR IMPROVED PROCESSES, SYSTEMS, METHODS, TOOLS, MATERIALS OR SPECIAL EQUIPMENT WHEN REQUIRED FOR IN-HOUSE USE IN THE RESEARCH, DESIGN, DEVELOPMENT AND PRODUCTION OF PRODUCTS OR SERVICES INTENDED FOR SALE.

Slide 15

CONTINUATION SHEET	REF NO OF DOCUMENT BEING CONTINUED	PAGE	OF
NAME OF OFFEROR OR CONTRACTOR			

SECTION M - EVALUATION AND AWARD FACTORS (Continued)

2 Analysis Techniques - The offeror's capability to analyze technologies relevant to preliminary design of the ITR will be evaluated. This evaluation will be based on the substantiation provided for the analysis techniques, including consideration of the adequacy of the substantiation. Evaluation of the offeror's analysis techniques will be weighted in favor of those analysis areas that have the greatest potential for insuring success of the project or minimizing risk of failure.

Slide 16

there is a statement that says that any analysis techniques that you propose to use in your response must be validated. So I went back and looked at our own to see how well did we validate the analyses that we proposed to use, and really, the bottom line is, not very impressively. I would say 80% to 90% of the discussion was describing all the features of the analysis and maybe 10% was describing the validation of the analysis. This was not very good, but we were one of the winners so it can't have counted too much against us. I don't quite know how to do it but I think the government could well put some more teeth into that requirement with RFPs, and insist that validation quality be improved.

Now I think this is the last point I've got; really I'm not too serious about this one; but if you think of it, the Defense Contract Audit Agency (DCAA) confers validation status on cost and schedule methodology. This is very serious; we have been through a process of being devalidated for the Cost/Schedule Status Report (C/SSR) system that we have in use for the CH-47D program. Believe me, it gets the company's attention when that happens because if you lose your validation status, you are not allowed to bid on the next major contract. If we had lost this we would not have been allowed to bid on the JVX program. So it got a lot of attention, we were reexamined, and we passed. Now I'm not really suggesting that something as serious as that should be applied to air resonance analysis, that we're not allowed to bid on it if we can't match up, but I think there's some middle ground there where I tnink you can be subject to some examination by the contracting authorities, the Government, to see whether your methodology is acceptable. That's all I have. Thank you.

PREPARED REMARKS BY BOB WOOD

I'd like to continue along with the same theme as my colleagues. At the same time I'd like to perhaps digress in one manner and that is to try to put part of this in a very positive light. I'll give a couple of examples and then I'll conclude with a recommendation that I'd like the panel and the audience, perhaps, to consider. Some of what I have on the first viewgraph [Slide 17] has already been covered. We often think of validation as a means to simply validate a model and at that point we close the door on it and we use it, as a validated and approved model. In truth though, I think what we have is that the correlation studies that accompany that validation have many payoffs, both to the government as a user and to industry. I've listed four of those on the first viewgraph, and some of these have been touched on as I think, the participants in the ITR methodology study have tried to understand the reasons for the lack of correlation in one area or another.

The first one, reading from top down, is elimination of errors in modeling. This comes from careful study and careful comparison. Sometimes we find that as result of our correlation effort we don't change the model at all but it does unfold a better understanding of the problem. In addition to that we find by careful comparison at times (and this has come up frequently at this meeting) that there are areas, I think dynamic inflow is one that's been discussed numerous times here, where development of an improved math model results. And finally, in the

PANEL ON MATH MODEL VALIDATION

6/22/83

CORRELATION STUDIES HAVE IMPORTANT BENEFITS IN ADDITION TO VALIDATION. AMONG THESE ARE:

- ELIMINATION OF ERRORS IN MODELLING
- BETTER UNDERSTANDING OF PROBLEM
- DEVELOPMENT OF IMPROVED MATH MODEL
- IDENTIFICATION OF MISSING ANALYSIS PARAMETERS

Slide 17

correlation process, from time to time we find ourselves identifying what I call missing analysis parameters. That is we suddenly uncover, say, "Wow, we left out an entire effect," or an entire part of a math model just was not put in it.

So you might say "Well, Bob, that all sounds very general," so I thought what I'd do is simply give some examples. They're not meant to be any better than any other studies anyone else has done, and where possible I'll identify the data base. These all result from validation efforts that I've been involved in at one time or another.

This first one [Slide 18] I call an error in math modeling. It was related to correlation efforts one time with [what I think is] a very fine data base that was listed in an earlier viewgraph, the H-34 data of Scheiman's. There the goal of the analysis was correlation of time histories of blade flapwise moments (that was the major goal) and it seemed relatively easy in that analysis to get good agreement with cyclic or half peak-to-peak values, but to match that time-history signature was something else. Whereas, as all of you would probably agree, we haven't solved the blade-airloads problem, certainly, since 1974, we did find in that correlation activity that a very major parameter was the three-dimensional (3-D) airloads at the blade tip.

PANEL ON MATH MODEL VALIDATION (CONT'D)

6/22/83

EXAMPLE - ERROR IN MATH MODELLING

- A GOAL OF ANALYSIS WAS CORRELATION OF TIME HISTORY OF BLADE FLAPWISE MOMENTS
- COMPARISON SHOWED GOOD AGREEMENT OF CYCLIC OR 1/2 PEAK-TO-PEAK VALUES
- COMPARISON SHOWED POOR AGREEMENT OF MOMENT TIME HISTORY SIGNATURE
- STUDY REVEALED TREATMENT OF 3-D AIRLOADS AT BLADE TIP IN ERROR

Slide 18

In terms of better understanding of the problem, this one [Slide 19] we stumbled on last year that I could identify. It relates to some work we were doing in dynamic NASTRAN. We had earlier run, for the attack helicopter, the dynamic NASTRAN model and we had obtained what we considered to be fairly good correlation with the attack helicopter data. Then we wanted to do some work on getting airframe forced response at N per rev. We have on the attack helicopter a second vertical-bending mode that is very near N per rev. So we expected in this work that using this normal-mode response method, which is built into NASTRAN, that obviously this second bending mode would turn up as a primary contributor to any forcing function at the rotor hub. Much to our surprise that mode, which is only a half a hertz removed from the excitation, ranked third in the modal priorities. Also the primary mode contributing to the response at the pilot's station was a wing-symmetric bending mode that was four hertz removed. When you compare our experience to, say 15 yr ago, when it was just an unwritten rule in the helicopter industry [that] if you have a mode near your primary excitation and you have a vibration problem, then that's the mode you go to work on. It would have been a waste of money for us to have chased after that second bending mode when indeed it was a mode off. So I would classify that as an example of one of those things one uncovers in validation or correlation that leads to sort of a surprise or improved understanding.

EXAMPLE - BETTER UNDERSTANDING OF PROBLEM

- A GOAL OF ANALYSIS WAS OBTAINING AIRFRAME FORCED RESPONSE AT N/REV
- A NORMAL MODE FORCED RESPONSE ANALYSIS WAS OBTAINED USING DYNAMIC NASTRAN
- PREVIOUSLY GOOD CORRELATION HAD BEEN FOUND BETWEEN TEST AND NASTRAN MODES
- AN UNEXPECTED RESULT OF FORCED RESPONSE ANALYSIS WAS THAT FREQUENCY PLACEMENT WAS OF SECONDARY IMPORTANCE

Slide 19

Another example is what many of you have talked on today, and there have been some excellent discussions on it. Today and yesterday Dick Bielawa and Frank Tarzanin spoke on areas where they would like to improve their models based on what they'd already seen in the ITR methodology, and this is simply another example of that. Again this particular one [Slide 20] made use of the Scheiman data. In the validation process we found a drastic difference in steady chordwise bending between the math model and the test data. At that time I was at Sikorsky. It turned out to be a very simple effect that we had not recognized. The leading edge weights are not an integral part of the blade; they transfer their CF to the blade tip cap and we had not properly accounted for that. When we put that in, it was very pleasant to see that in our chordwise moments, that steady shift did come in, so again the validation was a rewarding process; we learned more; and the model was improved one step.

Finally, in this identification of missing parameters [Slide 21], this was the classic example I can recall here. It was with regard to the noise program, the RAP or TRAMP program developed for NASA. We were correlating with Wallops Island data taken on a UH-1B and we got good agreement with the pressure time-histories at an observer, but the acoustic spectra just didn't look right at all. A study of those data revealed that what we'd left out was the very important effect of ground

EXAMPLE - DEVELOPMENT OF IMPROVED MATH MODEL

- A GOAL OF ANALYSIS WAS CORRELATION OF TIME HISTORY OF BLADE CHORDWISE MOMENTS
- COMPARISON SHOWED POOR AGREEMENT OF STEADY CHORDWISE BENDING
- STUDY SHOWED CAUSE OF DISCREPANCY WAS TREATMENT OF BLADE BALANCE WEIGHTS
- GOOD AGREEMENT ACHIEVED WITH IMPROVED BLADE EQUATIONS THAT PROPERLY MODELLED WEIGHTS

Slide 20

EXAMPLE - IDENTIFICATION OF MISSING PARAMETERS

- A GOAL OF ANALYSIS WAS CORRELATION OF ACOUSTIC SPECTRA FOR HELICOPTER FLY-BY
- COMPARISON SHOWED POOR AGREEMENT BETWEEN MEASURED AND CALCULATED NOISE SPECTRA
- STUDY REVEALED MISSING ANALYSIS PARAMETERS WERE GROUND REFLECTION AND MICROPHONE HEIGHT
- ONCE ADDED, GOOD AGREEMENT WAS ACHIEVED

Slide 21

reflection, and when we called NASA and asked for the height of the microphone, they were unable to give it to us. It was a nice problem to be able to solve because we found we had enough acoustic data so we could solve backwards and calculate the height of the microphone. As I recall, about two months later, Bob Pegg did call us and give us the height of the microphone. It was one of those pleasant experiences of solving the problem backwards where we found out we had been using the right height.

That really concludes the main points. Next I want to simplify what I've said in one recommendation which I though the panel and perhaps the audience might want to consider. This goes right back to where we started at the 1974 dynamics specialists meeting where Bob Ormiston looked at the blade loads for a hypothetical rotor. This meeting has moved another step along that path because at this particular conference, we have reviewed a comparison of analyses of various manufacturers and government agencies, but we have a new element--it was not a hypothetical rotor; these were actual test rotors and these were actual test data. I think what's come out of this workshop that's been of great interest to me has been the tremendous interest each of the analysts has shown. I almost have the feeling he can't wait to get back to [improve] areas where he sees his model has fallen short. There seemed to me a possibility for a followup meeting to the one we're currently attending. Maybe there's somebody at the end of the table who has this already prepared for their talk, but a possibility might be simply to reconvene this type of meeting with the same data and give the participants a chance to refine their analyses. Then someone might say "Well but if we do, just think, they'll go back and turn all those knobs." Well maybe we ought to allow them to turn the knobs but if they turn the knobs, I think they ought to be required, if they show improved validation, to come up with a specific listing of what it is, what changes they've made, to obtain that validation. That's all I have.

PREPARED REMARKS BY PETER ARCIDIACONO

Bill Bousman, in his opening remarks, indicated that he had posed a series of questions to the panel members, and I plan to comment briefly on most of the questions that he posed rather than discuss any one of them in depth. However, before I proceed I personally would like to compliment the government personnel for (and I'll use the word wisdom, because I really do think it was a good thing to do) their wisdom in sponsoring this methodology assessment effort. Certainly if I look at what's going on at Sikorsky right now, many of the activities that we have in progress are the direct result of this methodology assessment and the detailed scrutiny that the existing analyses were forced to go through. I think that probably has resulted from the fact that this analysis exercise, as Bob Wood pointed out, did have some real data with which we were correlating our analyses. We couldn't hide from the correlation and each analyst certainly wanted to look good. So I point out that in a certain sense a key government objective was achieved, which is to force, if you will, industry to develop improvements to their analyses. I don't mean to imply that Sikorsky is not also interested in that objective; however, I think most of the industry members here will agree that left to our own devices, the objective of improved analyses may take very much longer to achieve because of the unique operating environment in which we find ourselves. This operating environment requires at times that analytic developments be stretched out, or even stopped, in any particular area because of higher priority needs and/or because of the perception that a particular analysis is good enough for the foreseeable short-term applications. So I too believe that the Government has a unique role to play to stimulate more in-depth studies of our analytic capabilities than might otherwise occur. I would strongly endorse, therefore, that more frequent efforts of this type be undertaken.

If I would turn to the questions now, I'll try to avoid belaboring some of the points that were already made; the first question was "how are math models validated?" What I have here [Slide 22] is what might be construed to be an ideal listing of activities that would take place, not to say that all of these activities actually do take place. We start at the beginning; (1) we have a set of equations. Certainly there ought to be a check of the derivation of the equations. There is usually a lot of algebraic manipulation and calculus involved, and it's not always obvious exactly how best to check those equations. (2) Once you have a set of equations, you can look for familiar terms and properties of the equations. (3) The third item is, program the code and check out the code. This is the one that I think is a major stumbling block. It's probably a sign of old age but I like to think in the old days we did a lot more hand checking of a major loops of codes than perhaps gets done today. Obviously, then, you can degenerate the analysis to compare with known results for simpler cases. That's done to a reasonable degree. Next, there ought to be more limited parametric studies done to examine what the analysis is saying from the standpoint of reasonableness. (4) Ideally, I think you need some small-scale specialized parametric models. We've tried this in the past, sometimes with mixed success because the scale of the model sometimes introduces problems which are uniquely associated with scale. I recall one, for example, where

HOW ARE MATH MODELS VALIDATED?

- CHECK DERIVATION OF EQUATIONS
- LOOK FOR FAMILIAR TERMS, PROPERTIES (E.G. SYMMETRY)
- CHECK PROGRAMMING CODE
  - HAND CHECKS OF MAJOR LOOPS
  - COMPARE WITH KNOWN VALID RESULTS FROM OTHER SIMPLER ANALYSES
  - EXAMINE LIMITED PARAMETRIC TRENDS FOR REASONABLENESS
- CORRELATE WITH SMALL SCALE SPECIALIZED PARAMETRIC MODELS
- CORRELATE WITH LARGE SCALE WIND TUNNEL MODELS
- CORRELATE WITH FLIGHT TEST (USUALLY LACKING IN SOME DATA ELEMENTS)
- UNDERSTAND THE REASONS FOR LACK OF CORRELATION AND IMPROVE THE ANALYSIS IF TECHNOLOGY AND FUNDS PERMIT (AND DETAIL DATA EXISTS)
- USE THE ANALYSIS WITH JUDGEMENT

Slide 22

we had a bearingless rotor with a snubbed-torque tube, and we couldn't scale down the full-scale snubber. We ended up representing it with some sort of rubber device. We found the damping of each individual blade was different by quite a bit and it presented a few problems. It's at that point where the 30%-or-more overrun starts to come in. I think there should be an optimum scale at which to do the test. (5) I call the next point "large scale," but perhaps more properly it should be stated as "larger scale" wind tunnel models that incorporate some degree of parametric capability. That's very important, I believe. (6) Then, of course, there is the flight test. Usually you find that the flight-test data is lacking some areas which then influences the next item which is, (7) if you don't like your correlation, to try and understand the reasons for the lack of correlation and improve the analysis if the technology exists and if the detailed data exists, to help you probe into the reasons for the lack of correlation. (8) Finally, having gone through the iteration loop once, you'll still find that the analysis does not agree and must be used with judgment.

How is it decided how much correlation is needed [Slide 23]? I don't think there's any one pat answer, although someday a standard may be developed. It depends on any one of these factors or a combination of the factors that we end up with. The schedule may be very urgent. From past experience, the design may depart by a little or a lot. What are the safety consequences of an error? Is the design forgiving? If you need an auxiliary damper, have you anticipated that and made provisions for its installation? Most importantly, can you conduct safe build-up testing? Last, but perhaps not least, is that the availability of funding helps to determine how much correlation is done.

HOW IS IT DECIDED HOW MUCH CORRELATION NEEDED?

DEPENDS ON:

- o URGENCY OF SCHEDULE
- o DEGREE OF DEPARTURE OF DESIGN FROM PAST EXPERIENCE
- o SAFETY CONSEQUENCES OF ERROR
- o DEGREE OF FORGIVENESS IN CONFIGURATION
- o ABILITY TO CONDUCT SAFE BUILD-UP OF TESTING
- o AVAILABILITY OF FUNDING

Slide 23

Why are the math models used without full validation [Slide 24]? We probably need a definition of what constitutes full validation. I might offer one--that the analysis shows no anomalies when you examine the design parameters that are thought to be important for a generic configuration to which you're planning to apply the analysis. If that's our definition, then I think the first line on the slide is correct, "that fully validated analyses are never available in time"; they are certainly not available for the first version of a new configuration. I think then

WHY IS IT THAT MATH MODELS ARE USED WITHOUT FULL VALIDATION?

- o FULLY VALIDATED ANALYSES ARE NEVER AVAILABLE IN TIME.
- o ANALYSIS DEVELOPMENT, THEREFORE, IS OUT OF MAIN STREAM PROGRAM EFFORTS AND SHORT-TERM PAYOFF IS NOT THERE.
- o AS A RESULT, AVAILABLE ANALYSES THAT HAVE SHOWN PROMISE ARE OFTEN USED COUPLED WITH JUDGEMENT AND EARLY DESIGN CONFIRMATION/DEVELOPMENT TESTS.
- o WHY SHOULD THIS BE?
  - o TECHNOLOGY FOR IMPROVING ANALYSIS ACCURACY NOT ALWAYS AVAILABLE
  - o PARAMETRIC DATA BASE FOR CORRELATION NOT ALWAYS AVAILABLE
  - o FUNDING NOT ALWAYS AVAILABLE

Slide 24

a certain perception of the value of analysis is developed by management. Since the analysis development tends to be out of the mainstream-aircraft-program efforts and short term payoffs are usually not there, sometimes when priority decisions are made, analysis developement tends to suffer. As a result I think we're always in a position where we are trying to use available analyses that have shown some degree of promise in certain areas. Hopefully we couple that with good engineering judgment and early design-confirmation or risk-reduction testing. Why should this be? I think some of these points have been made before. You may have the best reasons in the world for improving the analysis but the technology for improving it may not be available. You might want to do more correlation, but the data base is not always available. The data base that was used in the ITR methodology assessment was certainly the product of many man-years of effort. If you tried to consider corresponding data bases that would be required for other specialized applications then you just get a reinforcement of the conclusion that correlation and validation efforts are very expensive. I finally mentioned funding.

How are experimental data bases developed, qualified and managed [Slide 25]? I don't have too much to say here, but I think I would endorse the government primarily working in this area. I think what they have going for them is a lot of time available for doing a bang-up good job of getting the data and keeping it under control. I think in industry if we had to do it that we would do it only with very great difficulty because of time and budget constraints and all the things that I've mentioned.

Why don't we use certain data bases [Slide 26]? I think these are fairly obvious: funding limits, the data's late, maybe there is incomplete documentation of the data, there's usually a concern for some degree of nonrepresentativeness of the model, or we may just be unaware of the availability.

HOW ARE EXPERIMENTAL DATA BASES DEVELOPED, QUALIFIED AND MANAGED?

BY GOVERNMENT: WITH A LOT OF TIME AVAILABLE

BY INDUSTRY:
- WITH GREAT DIFFICULTY BECAUSE OF TIME AND BUDGET CONSTRAINTS, EVOLVING DESIGN, LACK OF ANALYSIS UPDATE AND MINIMAL DOCUMENTATION
- BEST DONE UNDER CONTRACT

Slide 25

WHY ARE SOME DATA BASES NOT
FULLY USED FOR VALIDATION?

- o FUNDING LIMITS
- o DATA USUALLY LATE
- o INCOMPLETE DOCUMENTATION
- o CONCERN FOR REPRESENTATIVENESS OF MODEL
- o UNAWARE OF AVAILABILITY

Slide 26

Simple models, I think, are very important [Slide 27]. I'm high on parametric analyses and tests. I think they do serve two purposes; 1) they can provide a data base for the design engineer to use in the event that the correlation with analysis is not all that one would hope it to be, and 2) they certainly provide a guide for the researcher. The second point on this slide ties in with something that Dick Bielawa brought up on force-phasing matrices. I personnaly find that I often wish that there was more attention paid in reports to explaining in some detail the physical mechanism, the underlying physical phenomena, behind certain trends that are either measured or predicted. This certainly would help to instill a sense of confidence and help provide some sort of a logical validation of either the data base or the analysis on the part of the user.

How to improve cost effectiveness [Slide 28]? My first point has been made a couple of times--I think the government ought to establish an approved data base.

WHAT ROLE DOES THE "SIMPLE" MODEL/EXPERIMENT
PLAY IN THE VALIDATION OF COMPLEX MODELS?

- o PARAMETRIC ANALYSES AND TESTS ARE VERY IMPORTANT, ESPECIALLY FOR STABILITY
  - o DATA BASE FOR DESIGN
  - o GUIDE FOR RESEARCHER
- o EQUALLY IMPORTANT IS THE EXPLANATION OF THE PHYSICAL PHENOMENA PRODUCING THE INDIVIDUAL PARAMETER TRENDS OBSERVED. THIS FOSTERS UNDERSTANDING AND HOPEFULLY A "LOGICAL" VALIDATION ON THE PART OF THE USER.

Slide 27

WHAT CAN BE DONE TO IMPROVE COST-EFFECTIVENESS OF CORRELATIONS?

- ESTABLISH APPROVED GOVERNMENT DATA BASE
- PROVIDE CONTINUOUS (MATCHING) FUNDING SO THAT ANALYSIS AND CORRELATION CAN BE IMPROVED, KEPT UP TO DATE AND WELL DOCUMENTED. THIS IS AS OPPOSED TO MAJOR EFFORTS DONE EVERY X NUMBER OF YEARS.

Slide 28

With respect to funding, I think that Bill Bousman mentioned that the ITR methodology assessment was funded by the government. I think because of the fact that, if you will, that we were showing our best wares in a fishbowl that were considerable matching dollars put in under IR&D. So there are couple of points here, one is that I think that we should provide more or less continuous finding so that we can keep a steady effort going on the analysis and the correlation and so maintain the efficiency that's associated with a minimum of interruptions. So I would suggest a more or less continuous effort as opposed to major efforts done every X number of years. Somebody mentioned that 9 yr ago, we did some sort of a limited exercise. It really should be done every year to keep everyone current. Next as I mentioned are the matching funds. I think to interest management and perhaps to interest government, some sort of a cooperative effort could be established whereby IR&D funds would be put up to match government infusion of money.

Finally 2GCHAS, what will be its impact [Slide 29]? I think ideally it will impact the situation. I'd like to think it will provide a higher standard for the

WILL 2GCHAS CHANGE THE FRAMEWORK OF VALIDATION REQUIREMENTS?

- YES, PRESUMABLY VERIFICATION OF SOFTWARE ITSELF WILL BE MORE STRINGENT.
- ATTENTION CAN THEN FOCUS ON TECHNICAL ASPECTS OF THE CORRELATION PROBLEM.
- TECHNOLOGY UPDATES WILL HOPEFULLY BE EASIER AND LESS COSTLY.

Slide 29

software verification so that we aren't continually faced with trying to understand a potential reason for lack of correlation and then wondering whether or not the blooming equations are coded properly or did someone change the computer system and it's no longer giving the right answers. Every six months we go through a calibration of our physical instruments and the government won't let us use the instruments if they don't have a calibration stamp on it. There's no reason why we shouldn't have a six-month calibration of analysis to make sure that something hasn't gotten out of whack. If we have good software then presumably the attention can be focused in the fundamental area, on the technical aspects of the correlation problem, and if shortcomings are identified presumably 2GCHAS will allow us to update the technology in a much less costly manner.

PREPARED REMARKS BY JIM McCROSKEY

Bill thought he asked me to make some comments on validation methodology and so I decided that he'd asked me to make some comments on how the aerodynamics community goes about validating some of the large aerodynamic codes. What I'm going to talk about basically is the fixed wing community, how it validates large aerodynamic codes. I'd like to make several prefatory remarks. There has been a lot of progress since 1974 in predicting fixed wing airloads. I'd also like to say that the general feeling, one general theme I'll try to develop, is that it's not enough just to compare with experiment. Finally I'm going to emphasize this building block approach [Slide 30].

I realize that we're always impatient, we want to leap ahead, but there also is a case to be made for taking one step at a time and I want to show you how some of the things are built up that have led to some pretty spectacular successes in computational aerodynamics. Some of this stuff is a motherhood-type thing and yet I think it bears reemphasizing. When you start on developing a large code you really have to start small and simple, first validate the pieces and then progress in steps. Now this has been done in a couple of examples in which the added complexity in one case was carried over to the equations but the configuration remained very simple. That goes in the jargon of the field [by the name of] Large Eddy Simulation for the calculation of basic turbulence, and there are very large codes that are run for enormous lengths of time that have produced information about the very difficult problem of turbulence pretty much from first principles, but only for very simple

VALIDATING LARGE AERODYNAMIC CODES

- BUILDING BLOCK APPROACH
  - START SMALL AND SIMPLE
  - VALIDATE PIECES
  - PROGRESS IN STEPS
    - ADD COMPLEXITY TO EQUATIONS FOR SIMPLE CONFIGURATIONS (LES)
    - ADD COMPLEXITY TO CONFIGURATIONS FOR SIMPLE EQUATIONS (PANAIR)
- INVOLVE OTHER QUALIFIED PARTIES
  - PILOT CODES TO SELECT USERS
  - INDEPENDENT EVALUATION
  - SPECIAL WORKING GROUPS
- SOME EXAMPLES

Slide 30

configurations, like flow in a channel. Well, that's a bit away from the real world but nevertheless that investigation has been very successful. It has given a lot of basic information that the whole engineering community will benefit from in the future. Now there's been a development over a few years of a thing called PANAIR, a large panel code, in which a considerable amount of complexity has been added to the configuration but the equations are based on simple linear theory. That code has gone through a lot of growing pains, a lot of development, a lot of validating, and a lot of iterative feedback. It's a big code, but people have been using it and they pretty much have confidence in it now.

One thing that people at Ames have found in the applied computational area is that it's very important for the code developers to involve other qualified parties, and I emphasize the word qualified. You don't release these research codes to just anyone, but you can go beyond a research code into a pilot code, give it to select users, and really benefit a lot from what you learn from them. Now another thing that's done from time to time I put down under the heading of "independent evaluation," I'll say more on this later, but that is when you basically let somebody else go work with the code and see what happens. Then there has been a great deal of good work and progress that's come out of some special working groups and I'll mention these as we go along.

Well, continuing to preach to you a little bit about the building block approach [Slide 31], one thing that the computational fluid dynamics (CFD) community here at Ames has recognized and has tried to separate out is a distinction between what they call "math" modeling and what they call "physics" modeling. I have the impression from what little I've heard about the efforts here that you're tending to lump both of those together in what you call a math model for rotor airloads predictions. But if you think along the lines of the math modeling, first of all, I think

THE BUILDING BLOCK APPROACH

- "MATH" MODELING
  - COMPARISON WITH "KNOWN" OR EXACT SOLUTIONS
  - INCREMENTAL CHECKOUT
- "PHYSICS" MODELING
  - COMPARISON WITH SPECIAL-PURPOSE EXPERIMENTS
  - COMPARISON WITH REAL LIFE
    - EXPERIMENTS
    - ESTABLISHED RULES OF THUMB
  - INCREMENTAL CHECKOUT

Slide 31

it's important to recognize that comparison with experiment is not necessarily math validation, it's not even code checkout, you may just be twiddling. When you do separate out the math modeling [you can] try to compare with "known" or exact solutions. An exact solution is fairly obvious. In aerodynamics you have linear theory that's used to check out lots of codes, incompressible airfoils, elliptical wings, but then they go to other equations where there are some exact solutions. Burger's equation is a simplification, a viscous equation, that's used. A lot of code checkout is done on 1-D nozzles, which seems kind of funny but there's an awful lot to be learned about the math modeling of the various codes from this. Now, you don't always have exact solutions available to you that are sufficiently close to the problem that you're interested in [to] really represent a decent validation. I'd like to point out an example of a working group that's in progress at the present time [and is sponsored] by AGARD in which they are trying to develop a series of solutions to the Euler equations (that's an inviscid set of fluid dynamic equations) and what they're striving for here is a solution, or series of solutions, for validating and checking codes for which you don't have an experiment at all because you don't have experimental airfoils or experimental wings without the viscous effects that are always there. And in a sense what they're developing is a "known" solution, an exact solution being developed by committee. A number of people are running their codes and doing some standard cases and comparing the solutions, and the intent is that from these we will see a number of solutions that are pretty close in agreement. Even though these are solutions for which you don't have any other check, you eventually will find a consensus that you've got a known solution which can then be used for checking out future codes, either of this type, or simpler or more complicated.

Then the incremental checkout, I think, is very important. Obviously these aerodynamicists start with a code, which is a big code, and they check it with an airfoil. Then they move on to a wing, and then to wings plus bodies. Then maybe they get bold and move to, as in this PANAIR case, a wing/body/tail/nacelle combination, maybe with an inlet and an exhaust, and then maybe add some structure to it. But this is done in the best cases, in increments.

That's just what that particular community thinks of as the math modeling. Then there's the physics modeling. Do the equations that you're working with really meet the physics? And there's where you begin to look at special-purpose experiments. I separate that out from comparison with real life because in these special-purpose experiments you're looking at things that are relatively simple but well defined, and they do a couple of things for you. One is they check the codes, and secondly they help you to define the empiricism. For example turbulence models or in computational chemistry, shock-tube reaction rates and disassociation rates, things of that sort. You do it on a simple but special-purpose basis; there've been some examples of this in the helicopter community too. At ONERA (Office National d'Etudes et de Recherches Aerospatiales) there was a special-purpose rotor experiment done at high tip speed and moderately-high forward flight [speed] for a straight untwisted rotor blade that didn't have the dynamic properties of any other, and it was run at zero lift. That's pretty unrealistic and yet it allowed us to do

a lot of direct correlation with a transonic numerical code that at that particular moment had exactly those limitations. There was no suitable set of data from the regular body of helicopter experiments, but this special purpose experiment was extremely valuable in finding little things about the code that could be improved and in giving us the confidence to move ahead.

But of course you want to go beyond that, and that's what I call comparison with real life. Wherever possible you want to have experiments but sometimes you simply have to go by established rules of thumb You don't have the data set that you really want, but you know whether or not a certain trend should go in a certain direction. Here's really where you begin to learn and where you iterate, but hopefully you're not just twiddling constants.

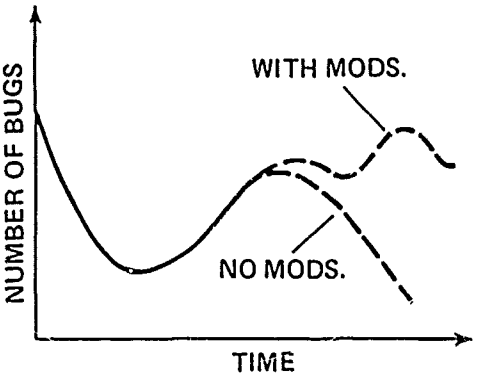
Again I emphasize the incremental checkout--step by step. I had an example here of stratospheric modeling by computational chemistry in which the problem was to determine the ozone depletion in the atmosphere. That's really a very complicated problem because strictly speaking you should be solving the Schrodinger wave equation; you've got the fluid mechanics of the atmosphere--very complex chemistry, and you don't really know for sure what is going on. Without going through the details of that let me just say that the approach was not to either jump into a large code and start turning the crank, or to send up a fleet of aircraft to continuously sample over two or three years and by the experimental approach determine the ozone depletion rates versus time. Instead a series of steps was done in which little pieces of the problem were studied one at a time, and things were identified that needed to be done that could be answered in shock tube experiments. Along the way a tremendous amount of useful, what we would think of as design information, came out from these simple steps. Eventually they did lead to running a series of large calculations.

As I said the CFD people here at Ames have found a tremendous benefit in involving other users in the use of the codes [Slide 32]. There have been a number of variations on this theme but typically it means taking a research code, making some sort of a pilot code out of it, and then other users work with it. Sometimes they come here--there are memorandums of understanding (MOUs) with industry where the user community sends someone here to learn how to use a code over a six-month period or something like that. That investment although it's hard to sell in the beginning, always turns out to be a very fruitful one for the company in the long run. Sometimes the codes are taken back to the companies or other government laboratories and universities. But typically these are researcher-type people who begin to work with the codes, and they're sort of in the gap between the day-to-day designers and the researchers here at Ames. As they start making validations and comparisons of their own, they learn a lot of things that come back here. Also they invariably try the codes on things that were never considered by the people here at Ames, so the extensions become very, very valuable.

Now for these independent evaluations. There've been some instances, in particular there's a 3-D wing code here developed in the early 70s called the Bailey-Ballhaus small disturbance code. Now the Air Force, on competitive contract, allowed one of the aircraft companies, who won the competition on this contract, to

INVOLVING OTHER USERS

- USE OF PILOT CODES
  - VALIDATIONS AND COMPARISONS
  - EXTENSIONS
  - FEEDBACK
- INDEPENDENT EVALUATIONS
- SPECIAL WORKING GROUPS
  - GAMM
  - AGARD
  - STANFORD CONF. ON TURBULENCE MODELING



Slide 32

take the code, run it for a few months, try it out, just basically evaluate it, and then report back. That was done virtually independently of the Ames people; it was an outside independent evaluation. I understand that Langley has done that sort of thing from time to time on some of their large codes, probably the aeroelastic codes (I wouldn't know for sure).

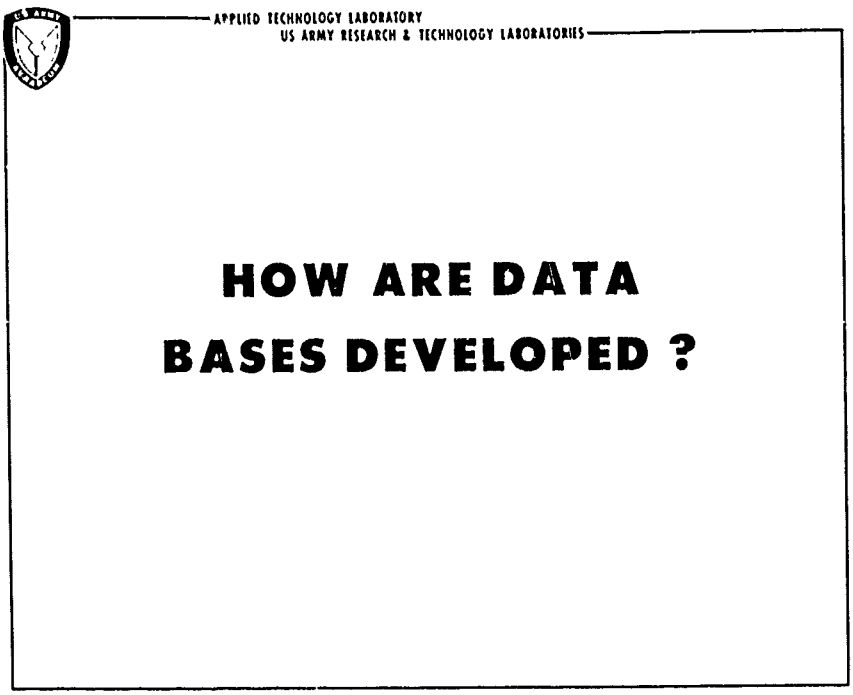
Finally, these special working groups can be very valuable. I think workshops like these are time well spent and money well spent. The European community often finds that they don't have the luxury to go it alone; Country H, Country B, Country S can't afford to go it alone so they cooperate; they have workshops. One organization is called GAMM; it escapes me for the moment what it is, but it certainly does a lot of good work--that just goes to show what's important and what's not. As most of you know, AGARD has panels which engage from time to time in special projects that usually result in some standard cases of more or less certifiable experimental data being offered to the user community with comments about it. But there are also these special projects like the one I described on the solutions to the Euler equations. In fluid mechanics one can't fail to mention the problem, again, of turbulence; the extreme importance and the extreme difficulty of that. One must also point to a very fruitful series of conferences, in fact, at Stanford in which many many people pooled their ideas, first on getting certifiable data sets, and then trying to compute a whole batch of special problems and comparing the results.

I should say that a lot of this information that I've presented is more or less self-evident. Some may or may not apply to the way you want to go at things. But

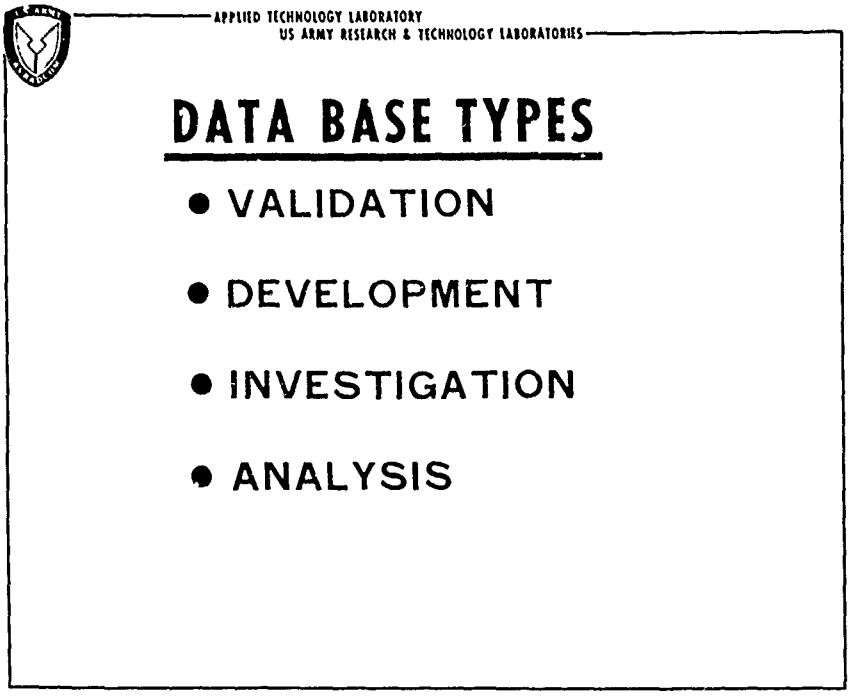
in conclusion let me say that I think it's important to recognize there's really no quick and easy way to beauty, but it can approached systematically, and when it is, more often than not it really pays off.

PREPARED REMARKS BY DON MERKLEY

The first couple of questions that we have here, I'll go through rather quickly because I think they are fairly obvious to everyone here. One is how data bases are developed [Slide 33]. There are several types of data bases and for each type I think we have a different way that we may go about developing them. The first one is for validation purposes [Slide 34]. The thing I really want to emphasize in just about any of the data bases, and especially in validation, is the need for good documentation. I think that's been brought out several times this afternoon. You must pay very close attention to details and provide answers to all possible questions that might arise in the future in using this data. If it's a test data-base, [information] with respect to the method and locations of all the measurements, calibration procedures, calibration data, whether filtering was used, conversions, test conditions, and test article descriptions are very important. For developing new flight vehicles or systems, they usually have a common goal in the industry--and that's quick answers, Unfortunately this does not lend itself to providing very good documentation, if any documentation results at all. These tests are usually designed by fate and fortune. Small experiments for investigating specific phenomena exist. The comments about documentation are equally important there. These experiments also are good for validating certain aspects, or modules or components, of large analysis systems. Then we have the analytic data base. When we think of



Slide 33

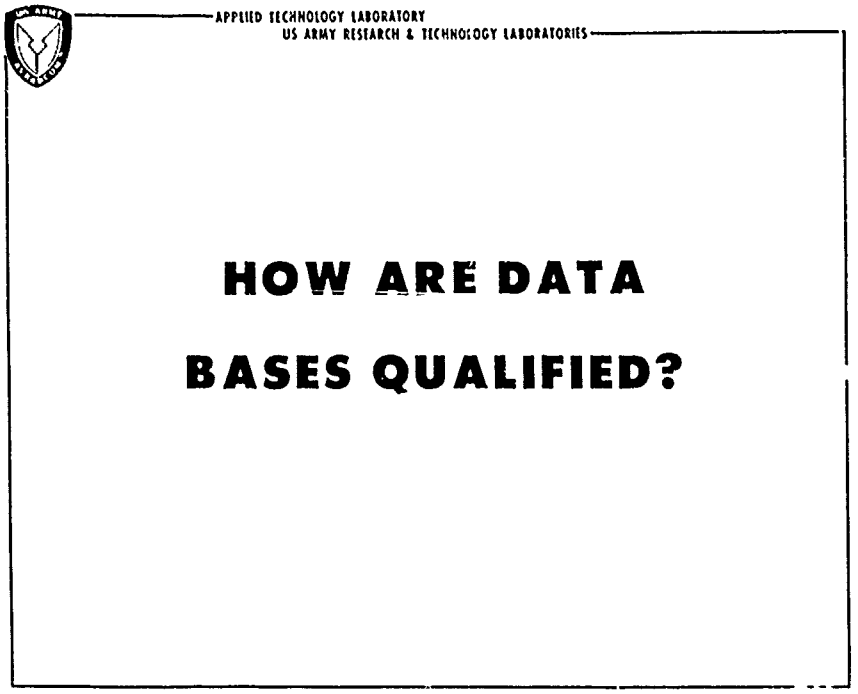


Slide 34

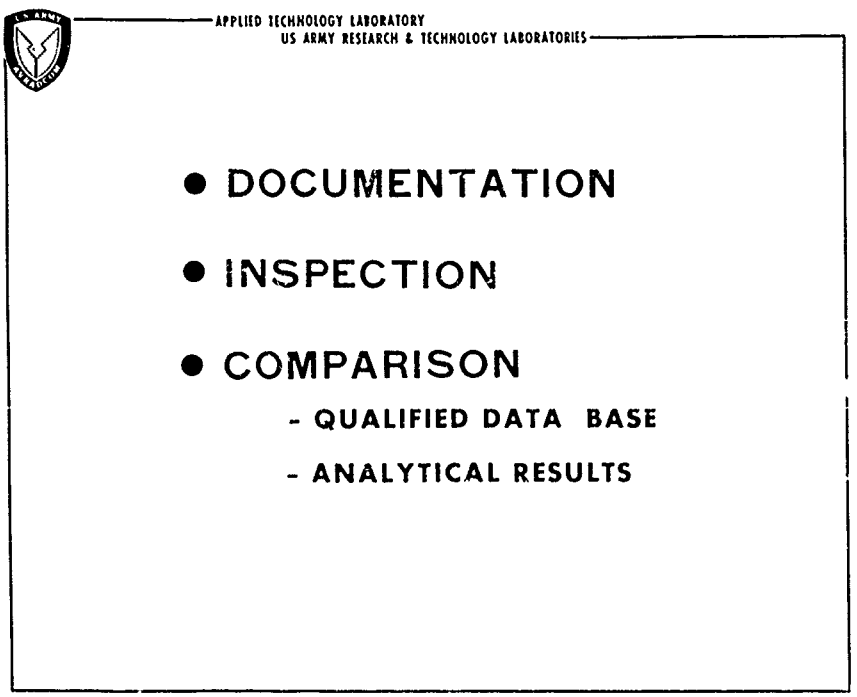
data bases we normally think of test data bases, but analytic data could be very voluminous, and also provides problems with respect to qualifying it and managing it.

The next question is how data bases are qualified [Slide 35]. This again brings emphasis to documentation [Slide 36]. The qualification of the data base could actually start before the tests begin, with proper documentation. For any data base to be of any use it must be well documented; I can't emphasize that too much. The best time to do that is before and during and the test while everything is ready at hand, and not trying to find the answers after the fact. Then the first quality check of a new data base is normally done, I would say, by inspection by someone who is knowledgeable of the type of expected magnitudes and trends of the data. Then more extensive qualification of the data base can be accomplished by comparisons with other qualified data bases and analytical results from analysis with known characteristics.

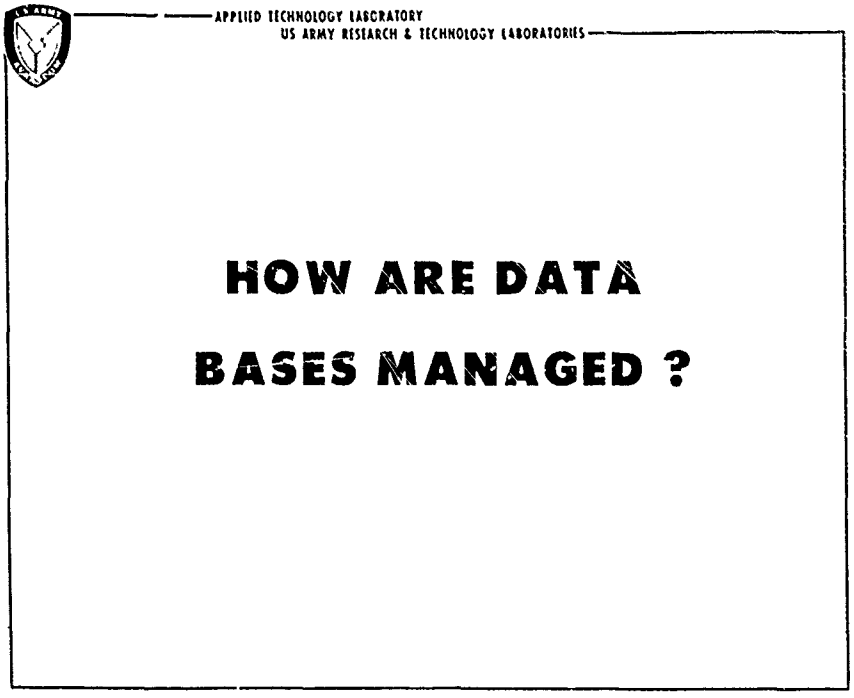
How are data bases managed [Slide 37]? Some of the modern test data-bases are very large. For example the Army's Operational Load Survey (OLS) has over 72,000 functions of time and the [Tip Aeroacoustic Test] data that was done out here at Ames is over twice that much. We're talking about data that resides on magnetic tape where there's over 350 data tapes just for the TAAT data alone. Without proper software tools this data is very difficult to access and manage It would be impractical to do otherwise.



Slide 35



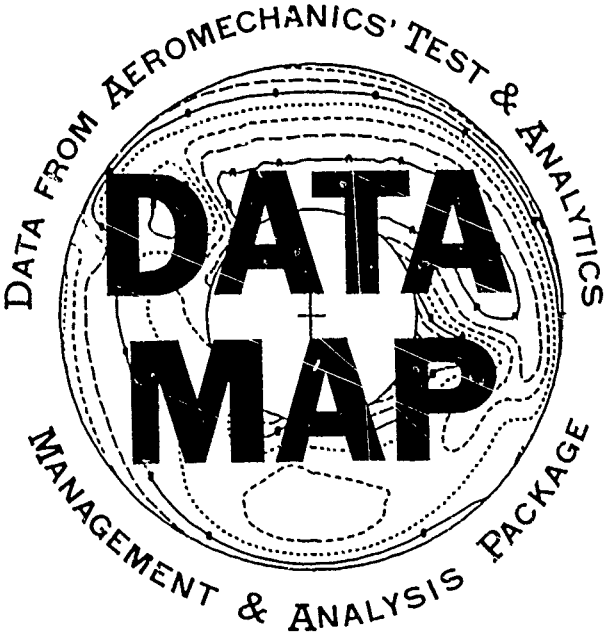
Slide 36



Slide 37

DATAMAP [Slide 38] is an interactive computer software system that was developed by the Army to manage such data bases by providing direct access to the data with the ability to analyze and derive certain parameters and display the data in various formats. This is a chart [Slide 39] that gives the numbers of analyses and derivations that are available to the user and here [Slide 40] are some examples of various output formats that are available to the user. It is an interactive system [Slide 41] that can be invoked in various combinations; either totally interactive at a terminal which can then provide hard copies through a hard copy device or generate plot files for output onto an incremental plotter, or the system can be invoked through a batch operation for a producing very large outputs. One of the very versatile features of DATAMAP is its ability to provide access to more than one data base simultaneously, and this is where it can lend itself very well to validation exercises. For example [Slide 42] you can have the files of test data and analysis data, then access those and put them up interactively on the screen in the various plot formats.

DATAMAP has been gaining very good acceptance [Slide 43]. We have it installed at a number of facilities. Most of the helicopter manufacturers have it installed. Sikorsky is shown in parentheses on the slide because they are in the process of receiving it right now. We're preparing the tapes for them. Kaman is talking about it. We've been talking with the Kaman people; they're waiting to get their new computer system that it will fit on. We've also been talking to a number of people at NASA Langley, at various facilities over there--three groups in particular: the impact dynamics group, the VSTOL wind tunnel people, and the acoustics


DATA FROM AEROMECHANICS' TEST & ANALYTICS
DATA
MAP
MANAGEMENT & ANALYSIS PACKAGE

Slide 38

DATA-MAP
PROCESSING CAPABILITIES

ANALYSES

AMPLITUDE SPECTRA
HARMONIC ANALYSIS
DIGITAL FILTERING
MOVING BLOCK DAMPING
CYCLE AVERAGING
MIN/MAX ANALYSIS
ACOUSTIC ANALYSES:
- NARROW BAND ANALYSIS
- OCTAVE ANALYSIS
- THIRD OCTAVE ANALYSIS
- PERCEIVED NOISE LEVEL CALCULATION
- NETWORK WEIGHTED INTEGRATION

NUMERIC INTEGRATION
NUMERIC DIFFERENTIATION
LINEAR ADJUSTMENT

STOCHASTIC PROCESS ANALYSES:
- FREQUENCY RESPONSE FUNCTION
- COHERENCE FUNCTION
- AUTO-SPECTRAL DENSITY
- CROSS-SPECTRAL DENSITY
- AUTO-CORRELATION
- CROSS-CORRELATION

BASIC STATISTICAL ANALYSES:
- MEAN
- VARIANCE
- STANDARD DEVIATION
- TEST FOR NORMAL DISTRIBUTION

DERIVATIONS

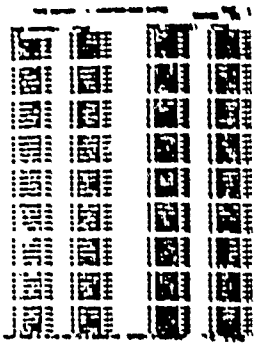
TRUE AIRSPEED
ROTOR AZIMUTH
ROTOR RPM
SHAFT HORSEPOWER
SHAFT THRUST COEFFICIENT
SHAFT TORQUE COEFFICIENT
DENSITY ALTITUDE
F A FLAPPING
LATERAL FLAPPING
F/A CYCLIC FEATHERING
LATERAL CYCLIC FEATHERING

COLLECTIVE FEATHERING
MACH NUMBER
C_p
C_n
C_c
C_m
BLADE DISPLACEMENT
BLADE SLOPE
FLOW MAGNITUDE
FLOW DIRECTION

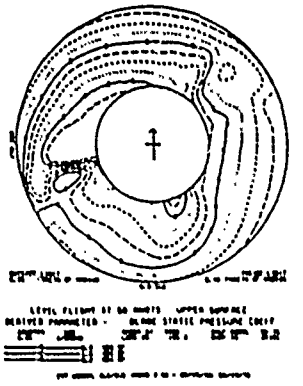
Slide 39

DATA-MAP OUTPUT OPTIONS

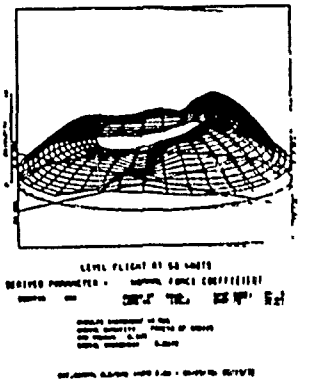
PRINTOUT



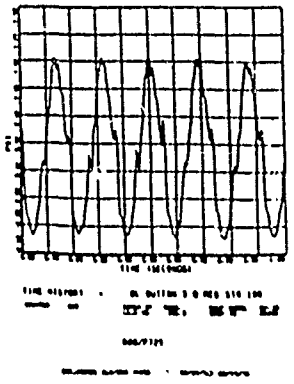
CONTOUR PLOT



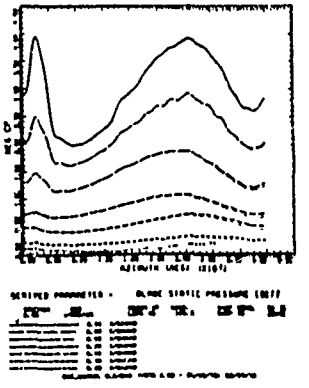
SURFACE PLOT



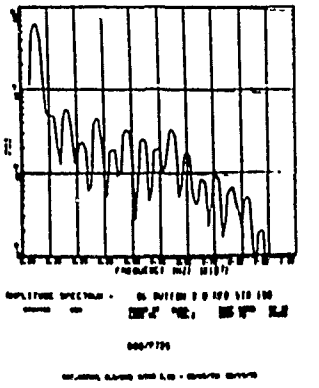
TIME HISTORY
X-Y PLOT



MULTIPLE CURVE
X-Y PLOT

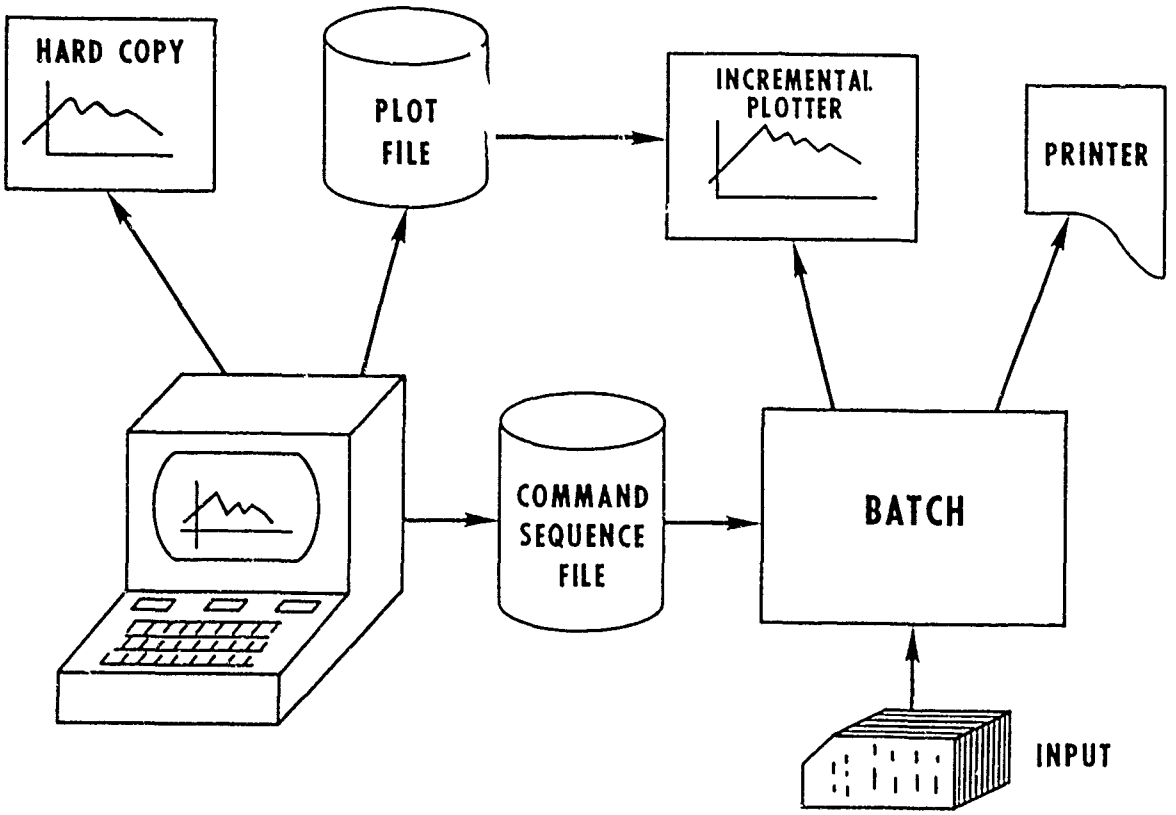


LOG-LOG or SEMI-LOG
X-Y PLOT



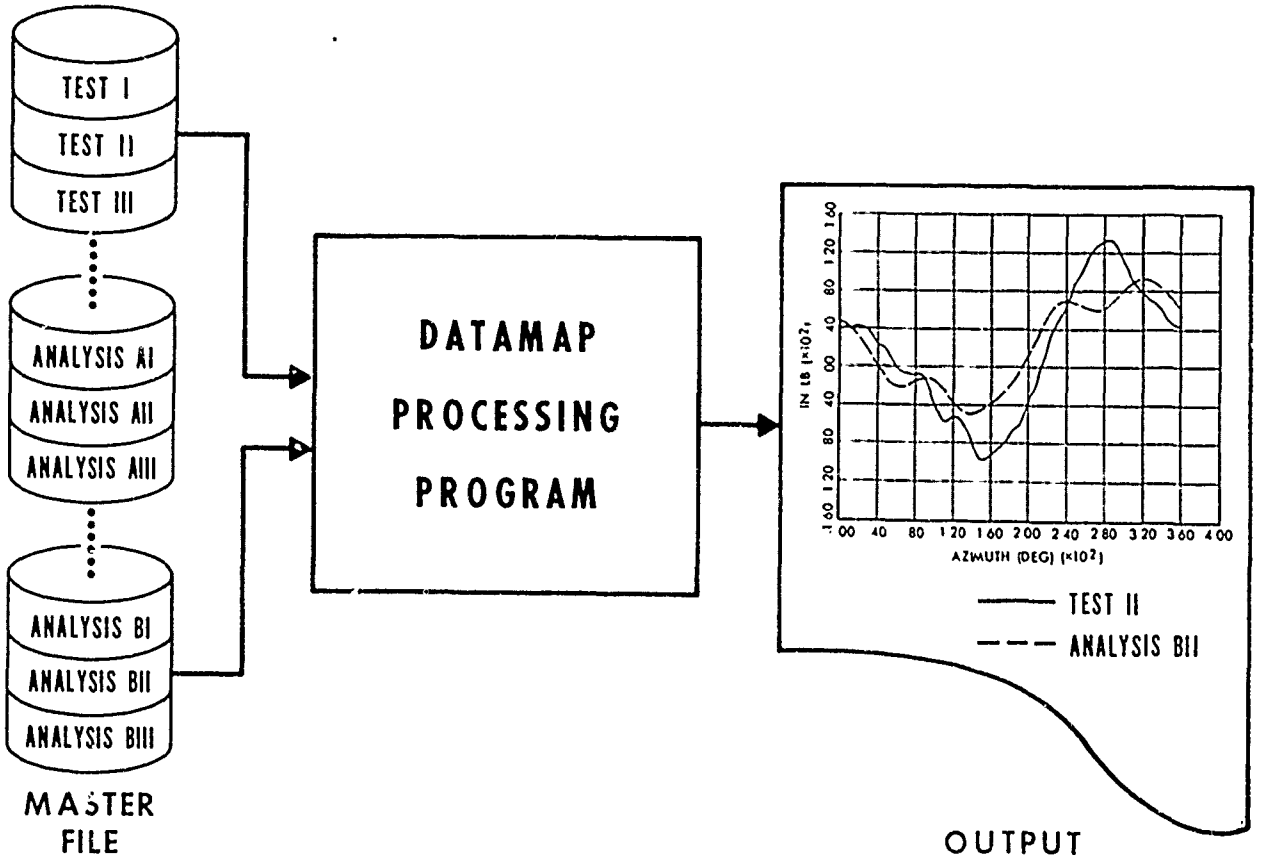
Slide 40

DATAMAP MODES OF OPERATION



Slide 41

DATAMAP CORRELATION ABILITY



Slide 42



APPLIED TECHNOLOGY LABORATORY
US ARMY RESEARCH & TECHNOLOGY LABORATORIES

DATAMAP FACILITIES

- APPLIED TECHNOLOGY LABORATORY
- AEROMECHANICS LABORATORY
- NASA AMES
- PAX RIVER NAVAL AIR TEST CENTER
- RAE FARNBOROUGH
- RAE BEDFORD
- BELL HELICOPTER TEXTRON
- BOEING VERTOL
- HUGHES HELICOPTERS
- (SIKORSKY AIRCRAFT)

Slide 43

people. After this slide was made, Georgia Tech requested a copy of the program. Calspan and UTRC are also [interested]; I've spoken to them recently.

There are a number of data bases that are up on the system [Slide 44]. It was originally designed for the OLS to access that data; however, provisions were made for general characteristics so that we could interface with any data base, whether analytical or test. This is actually only a partial list of data that is up on the system. I'm just providing several plots here [Slide 45] as an illustration of some of the plot features useful in correlating test data with analysis. This case [Slide 46] is a C81 analysis with individual points or test points and the line is a radial distribution of beam bending moments. This [Slide 47] is another example with the 3-D plots and it gives more of a qualitative comparison than quantitative.

I think DATAMAP has been shown to be a versatile system, is user friendly and is gaining acceptance in the government and industry as a data base analysis and management tool. I think we've heard comments from just about every speaker previous to me this afternoon that I think this system here provides an answer to; providing a standard for interfacing analysis and test data for use in validating and maintaining data bases.

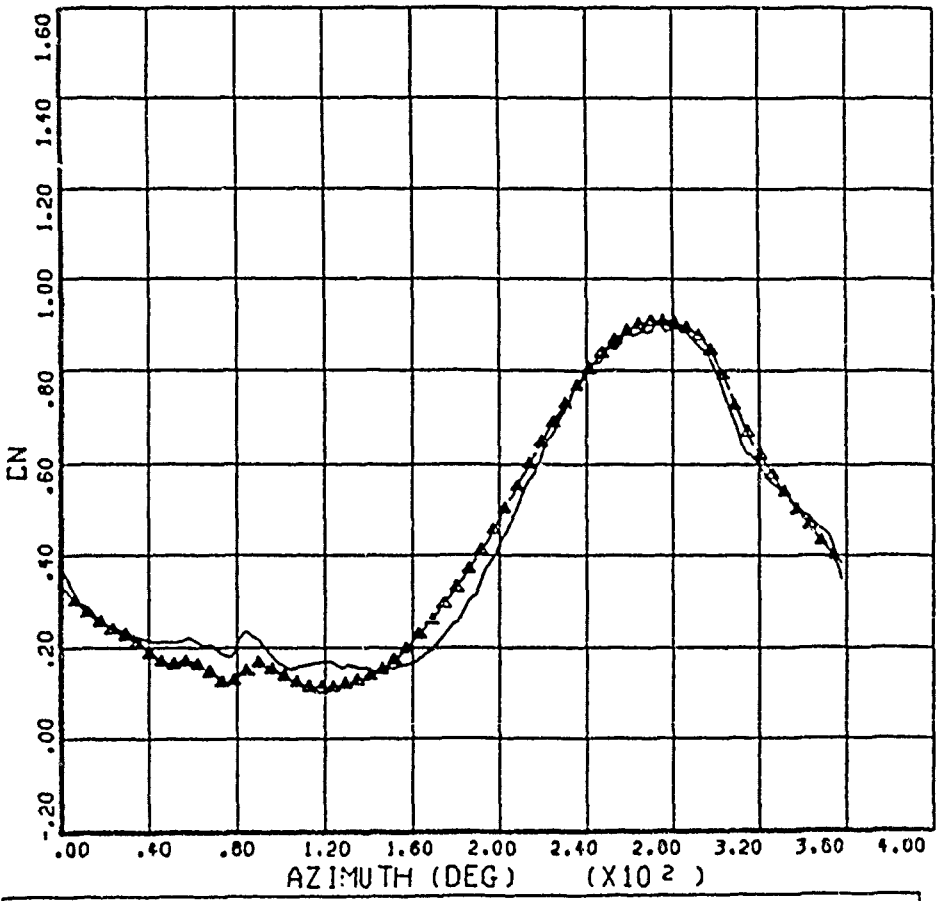


APPLIED TECHNOLOGY LABORATORY
US ARMY RESEARCH & TECHNOLOGY LABORATORIES

DATAMAP DATA BASES

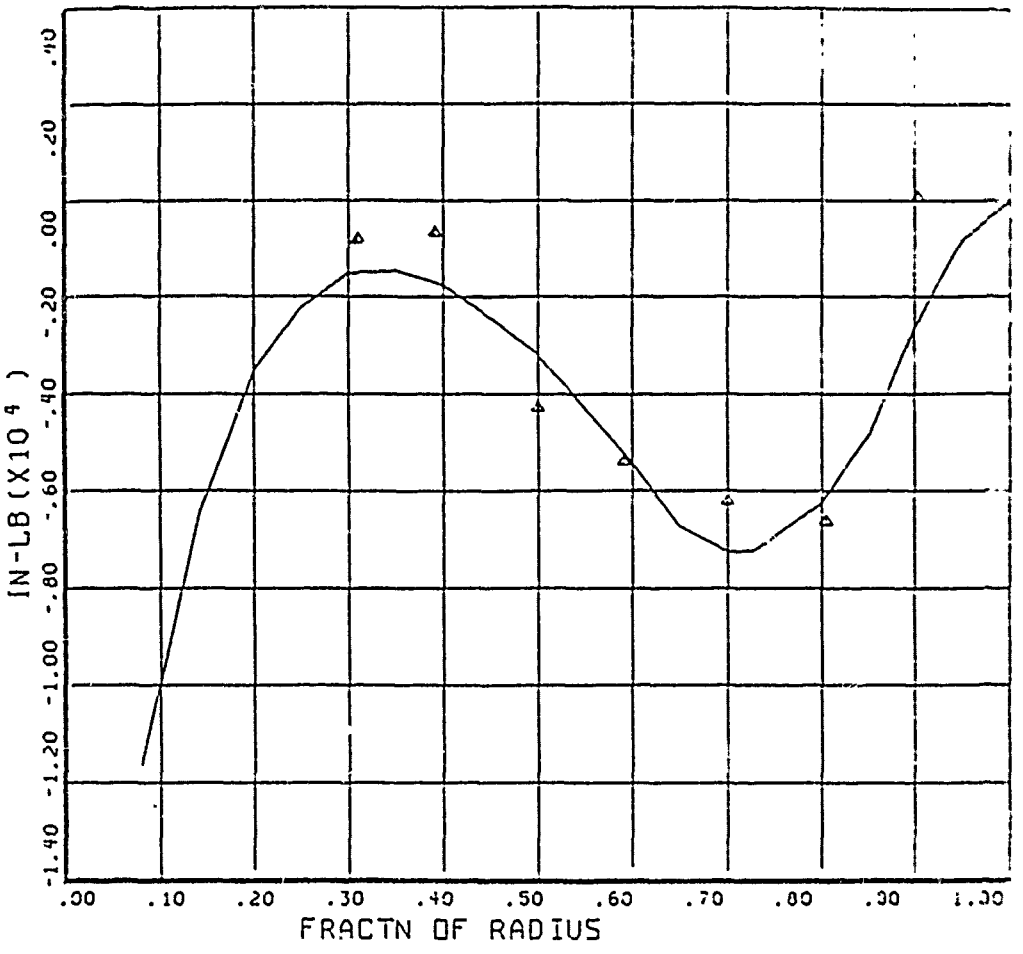
- ARMY OPERATIONAL LOADS SURVEY (OLS)
- NASA TIP AERO-ACOUSTIC TEST (TAAT)
- RAE WESSEX TEST DATA
- RAE PUMA TEST DATA
- ARMY YAH-63 CRASH TEST (T41)
- KRASH ANALYSIS PROGRAM
- ROTORCRAFT FLIGHT SIMULATION COMPUTER PROGRAM, C81
- MANEUVER CRITERIA EVALUATION PROGRAM (MCEP)
- RAE YOUNG'S PERFORMANCE ANALYSIS
- YUH-61A EXTENDED MAIN ROTOR MAST FLIGHT TEST
- AIR-TO-AIR COMBAT TESTS (AACT)

Slide 44



BMT.USARTL DATAMAP (VERS 3.07 · 03/02/81) 19APR'83 RAE FARNBOROUGH

Slide 45



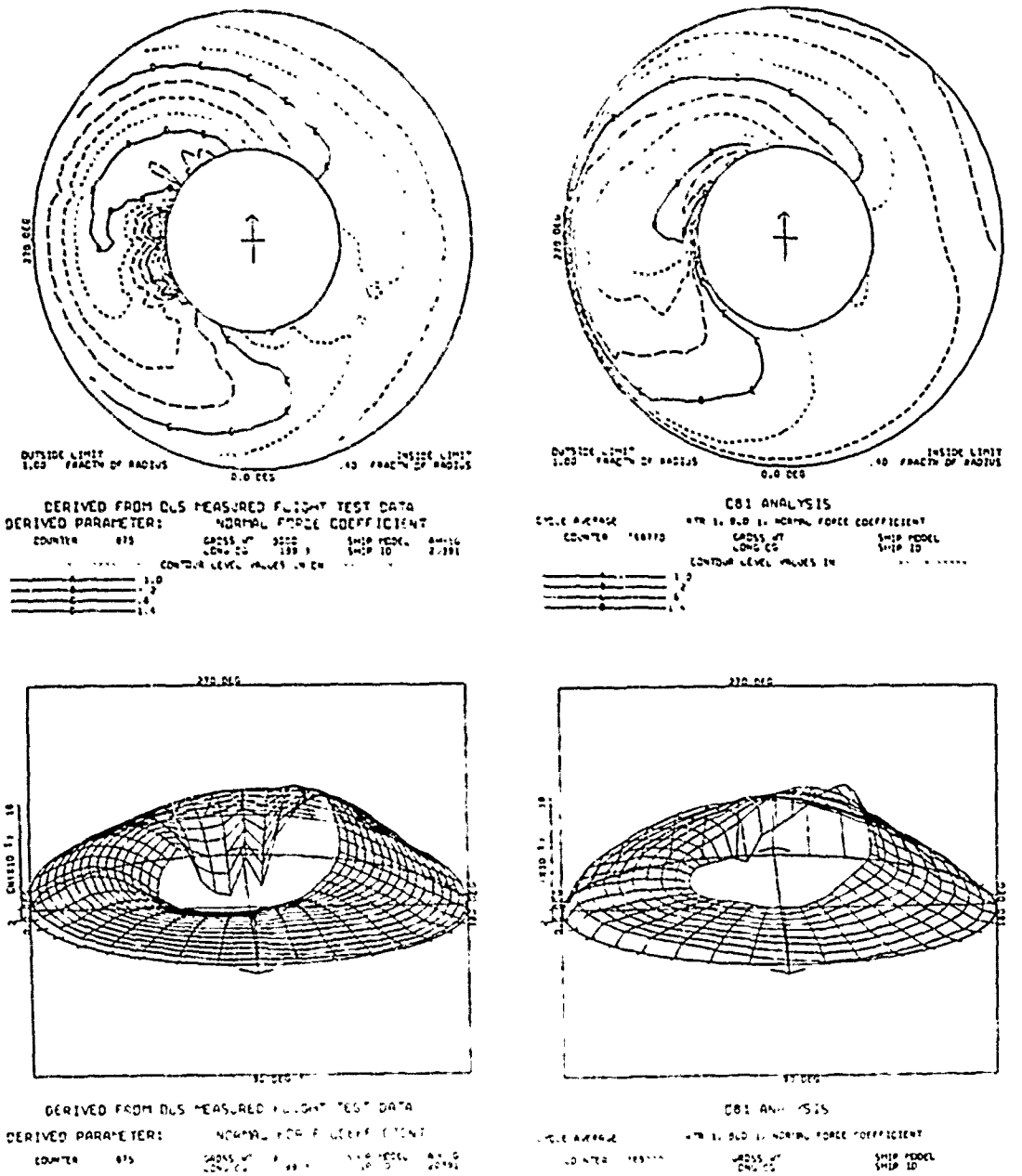
COMPARISON OF TEST DATA AND C81 ANALYSIS

CYCLE AVERAGE: RTR 1, BLD 1, BEAM BENDING MOMENTS

COUNTER 768770 GROSS WT SHIP MODEL
LONG CG SHIP ID

———— 30.00 DEG
△ △ △ △ △ 80.00 DEG

Slide 46


DERIVED FROM DLS MEASURED FLIGHT TEST DATA
DERIVED PARAMETER: NORMAL FORCE COEFFICIENT
C81 ANALYSIS

Slide 47

PREPARED REMARKS BY PERETZ FRIEDMANN

I'd like to echo what other members of the panel have said, that in my opinion this is one of the really productive meetings I have attended, and I hope we won't have to wait 9 yr until we have another one because I probably won't be alive then.

Our Chairman gave me a homework problem: what role does the simple model or limited experiment play in the validation of complex models [Slide 48]? I decided that it's probably reasonable to try and identify precisely what we mean by each word in the question, so that we know what we are talking about. I would like to define certain things which are associated with simple models and complex models and limited experiments in rotor dynamics or aeroelasticity. It is difficult to talk precisely about general things so I would like to talk about the hingeless rotor, which is a convenient example to use, but with certain modifications this applies equally well to bearingless rotors, coupled rotor/fuselage problems, or forward flight. So let's see first what is the complex model. Well, I define it to be a mathematical model which is capable of simulating the behavior of real, whatever "real" means, hingeless rotor blades with all pertinent detail. This basically means that you simulate the inboard elements, the outboard element, mass and stiffness distributions, and various other properties. In case some of you have forgotten what a hingeless rotor looks like, I just quickly would like to show it to you

I. SOME PRELIMINARY CONSIDERATIONS

DEFINITION AND DESCRIPTION OF COMPLEX MODELS, SIMPLE MODELS AND LIMITED EXPERIMENTS, IN ROTOR-DYNAMICS, AEROELASTICITY (RW) AND AEROMECHANICS

CONSIDER FIRST A HINGELESS ROTOR BLADE IN HOVER. WITH CERTAIN MODIFICATIONS THESE COMMENTS ARE ALSO APPLICABLE TO BEARINGLESS ROTORS, COUPLED ROTOR/FUSELAGE SYSTEMS, AND FORWARD FLIGHT

A. THE COMPLEX MODEL

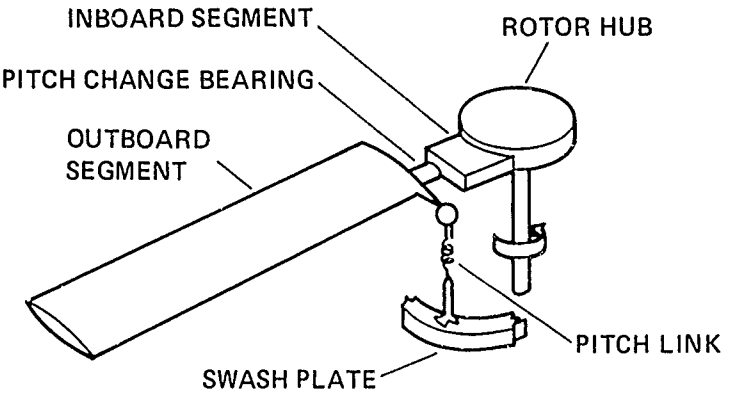
DEFINED TO BE A MATHEMATICAL MODEL CAPABLE OF SIMULATING THE BEHAVIOR OF A REAL HINGELESS ROTOR BLADE WITH ALL PERTINENT DETAIL. PROPERTIES ONE MIGHT INCLUDE:

- INBOARD ELEMENT STIFFNESS DISTRIBUTION
- OUTBOARD ELEMENT STIFFNESS DISTRIBUTION
- MASS DISTRIBUTION FOR BOTH SEGMENTS

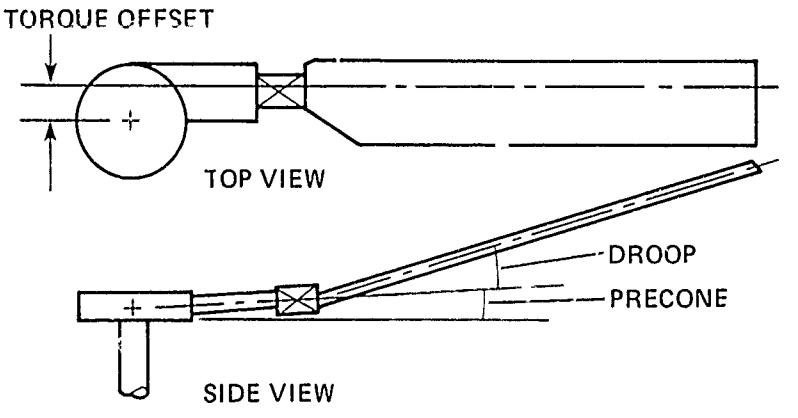
Slide 48

again [Slide 49]. The various other properties you might want to include in such a complex model are root offset, pitch link flexibility, swashplate flexibility, torque offset, precone, droop, sweep, variable built-in twist, variable elastic axis locations for each cross-section of the undeformed blade, variable center of mass, variable center of tension, and finally you have to remember it's a composite-material-type blade, so anisotropy and associated structure effects should be there in a complex model.

So then you would like to do dynamic stability prediction and this basically means that for this hingeless blade you should do a fully coupled flap-lag-torsional analysis and you should retain your geometrically nonlinear terms which are, as you all know, painful. In doing that you have to state your assumptions very carefully. That is, I think, something which is quite important and people are not very careful about really stating the assumptions which limit the analysis very, very clearly so that everybody can look at it and figure out what's in there. So if you



(a)



(b)

Slide 4

have an ordering scheme, you can say what it is, [describe] all possible aerodynamics, and finally [describe] how nonlinearities are treated and how solutions are obtained.

Now, if you want to do all of these things, then it quickly becomes apparent that it's very difficult to do. Since this is the end of a long day, I have a quotation for you from a very reputable source, Sherlock Holmes, and he says, "Like all other arts, the science of deduction and analysis is one which can only be acquired by long and patient study, nor is life long enough to allow any mortal to obtain the highest possible perfection in it. Before turning to those moral and mental aspects of the matter which present the greatest difficulties let the inquirer begin by mastering more elementary problems." That's where the restricted model can be useful.

This brings us to the simple model. If you want to talk about simple models, then essentially I would recognize two such simple models. One is the offset-hinge-spring restrained model of the hingeless blade where you can either have flap-lag or flap-lag-torsion; Bob Ormiston and Dewey Hodges have used that model very effectively. Another model is the distributed model but with some restrictions introduced, such as no sweep or no droop; isotropic material; and for restricted aerodynamics, quasi-steady or unsteady 2-D strip theory, dynamic inflow or maybe some static or dynamic approximation to stall effects.

We have now seen what the complex model is and what the simplest model is and we have to define the limited experiment. My interpretation is that the simple experiment [is one] in which uncertainties associated with modeling are reduced to a minimum. Typical examples would be the flap-lag model which has been used by Bob Ormiston and Bill Bousman to investigate the stall induced flap-lag instability, or the small-scale rotor dynamic model for coupled rotor-body aeromechanical investigations which has been used by Bousman.

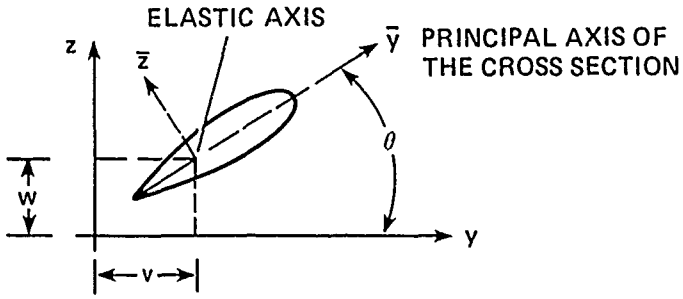
And now we go to the last part of the question, which is the role of the simple model or limited experiment in validation of the complex model. And here I again turn to the same source for inspiration let's go back to Sherlock Holmes and he claims that "when you follow two separate chains of thought, Watson, you will find some point of intersection which should approximate the truth." That's where the simple model comes in, because it is, in my opinion, the intersection between the complex and the simple model which should approximate the truth. So in order to be able to have an intersection there are a number of things which are demanded, both of the simple model and the complex model. The complex model should have in it the required flexibility to enable the user to simulate the limited experiment and the simple model. You can't have a complicated model which can only do complicated problems. The simple model can be used to generate theoretical test cases for the complex model when limited test results are not available. Such comparisons indicate whether the complex model is basically sound by showing its ability to reproduce fundamental blade behavior. And in fundamental blade behavior I would like to mention a few cases. One is, for example, the flap-lag instability in hover and its sensitivity to partial elastic coupling including, maybe, the second lag-mode type of instability. That's a good test: to see whether a program can do those

things. Another good test is the stall induced flap-lag instability which has been both theoretically and experimentally simulated by Ormiston and Bousman. Another one is the test which has been used in this comparison study which I like to call the precone-induced, bubble-like unstable region in coupled flap-lag-torsional analysis. In order to be able to reproduce such limited experiments or test cases, it obviously implies that the complex model should have the capability for simulating the restricted aerodynamics which are used in the simple model. For this exercise of trying to figure out whether the fundamentals are right in a complex code, [the code] should have the capability for producing stability boundaries, which are sometimes the physical indicators of the soundness of the code.

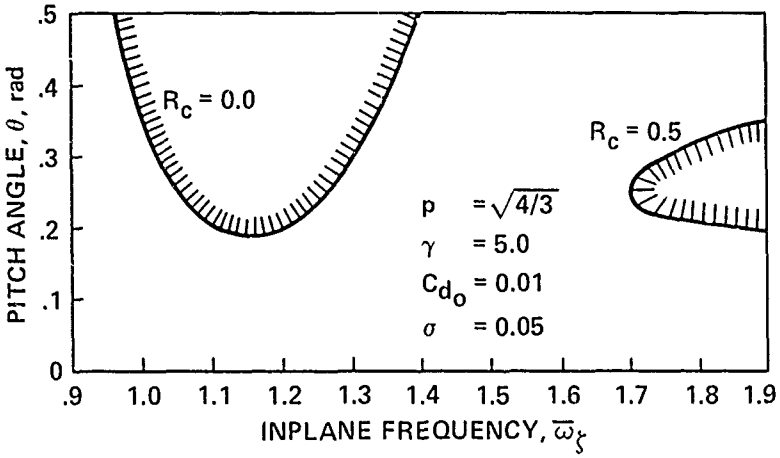
Since I mentioned these few test cases I just wanted to show you more or less what I mean [Slide 50]. This is the flap-lag instability; if your code doesn't produce such a thing with no elastic coupling and then move it out with partial elastic coupling, there is something wrong with your code. Another example is what came out from a simple finite element analysis, which essentially uses a finite model of a beam [Slide 51] in which it turned out that, at least based on very carefully done calculations, the second lag mode has a whole region of instability [Slide 52]. This was also found by Dewey Hodges and Inderjit Chopra. It's a good test case, because if it doesn't happen, then maybe something is wrong in the analysis.

Finally, the last two items which I wanted to show again are very good test cases for these complex codes. First is the stall-induced flap-lag instability as a function of angle of attack which is both experimentally and theoretically validated by Ormiston and Bousman [Slide 53]. And finally, another very simple test case which is typical is this bubble-like unstable region [Slide 54], which is a precone, induced flap-lag instability, and its sensitivity to maybe torsional stiffness and structural damping. So, these simple test cases and limited experiments are very useful to validate more complicated codes.

In concluding I would like to make a few additional comments. In forward flight, again, simple analysis can be used to validate complex analysis; however, in forward flight it's very important that 1) the code should have a capability for generating stability boundaries, and 2) the intimate relation between trim and the aeroelastic problem is again very crucial. If you do wind tunnel tests, I have recently seen one of the Professor Ashley's students who has found that the wind tunnel wall has significant effects on the unsteady aerodynamic loading and maybe wind tunnel effects in forward flight could be important when somebody does limited experiments, so that's something which I just wanted to mention. Also since the problem is nonlinear, both linear and nonlinear system identification techniques should be used since it's very rare that all the parameters are completely specified. Finally, I wanted to mention that in my mind there is a basic difference between model validation and curve fitting, and I hope people are aware of the difference.



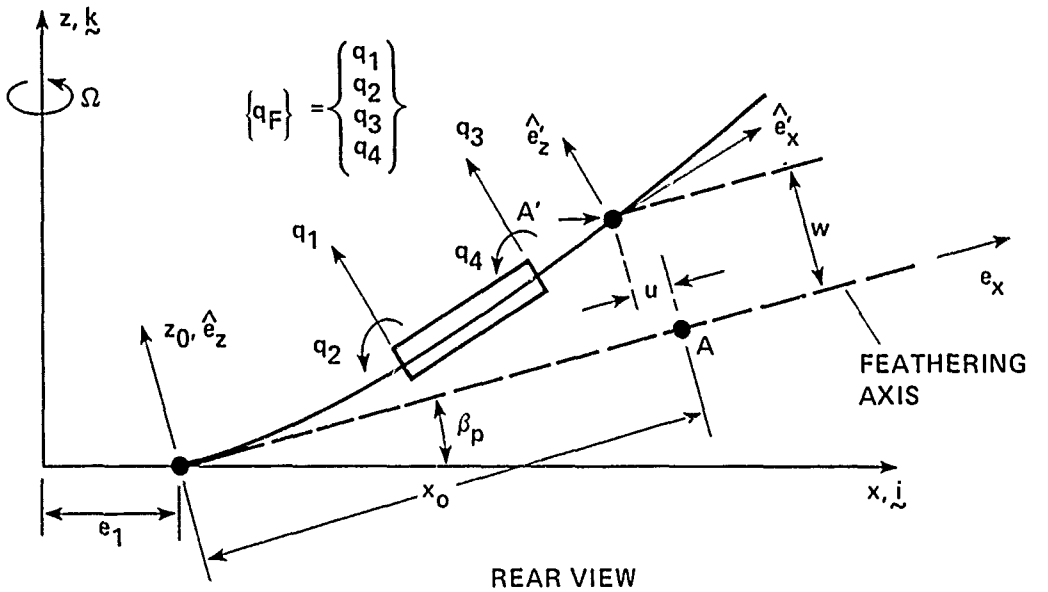
$$E_{C_1} = [(EI)_{\bar{z}} - (EI)_{\bar{y}}] \sin^2\theta_G$$
$$E_{C_2} = [(EI)_{\bar{z}} - (EI)_{\bar{y}}] \sin\theta_G \cos\theta_G$$



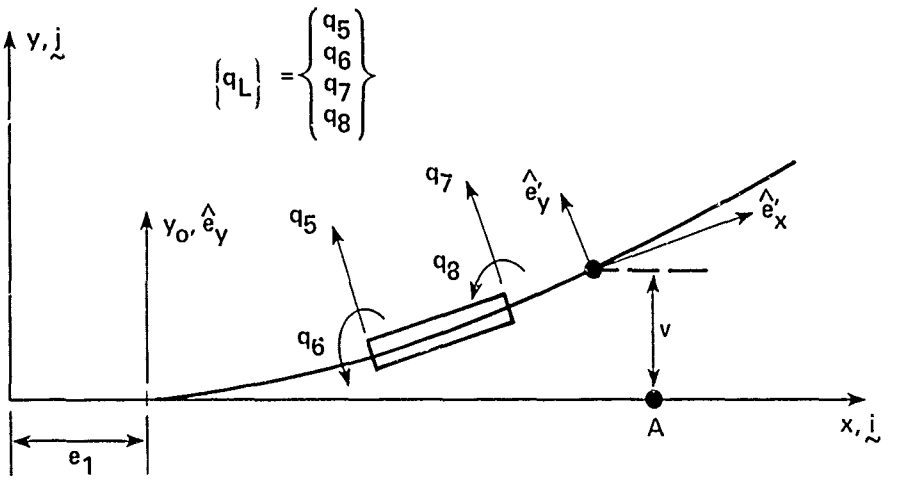
EFFECT OF ELASTIC COUPLING ON FLAP-LAG INSTABILITY IN HOVER

- SOURCE OF ELASTIC COUPLING
- MECHANISM OF FLAP-LAG INSTABILITY

Slide 50



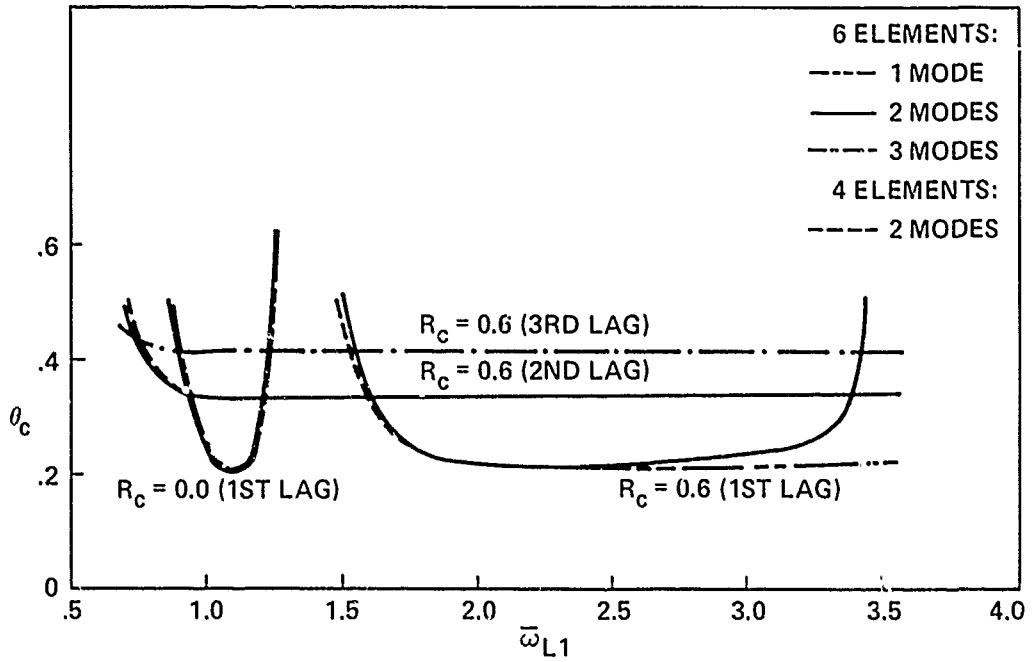
REAR VIEW



TOP VIEW

GEOMETRY ILLUSTRATING APPLICATION OF FINITE ELEMENT METHOD TO COUPLED FLAP-LAG PROBLEM IN HOVER (TAKEN FROM REF. 3)

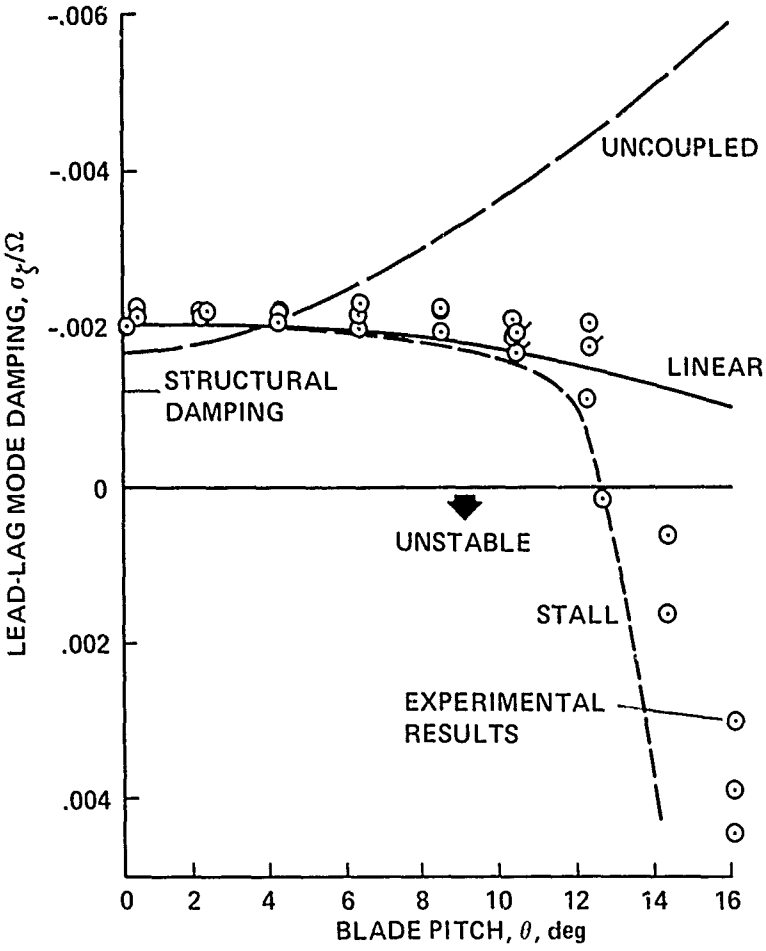
Slide 51



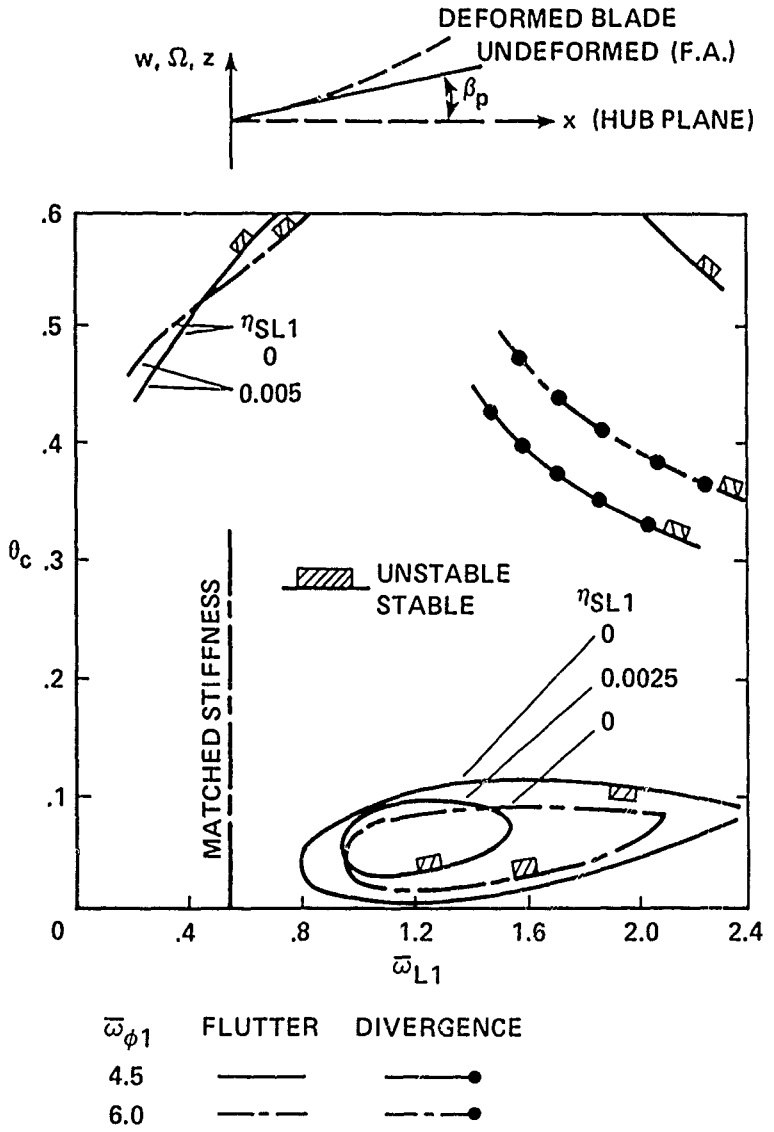
SECOND LAG MODE INSTABILITY IN PRESENCE OF PARTIAL ELASTIC COUPLING, $R_c = 0.60$

$\sigma = 0.10$, $\gamma = 5.0$, $\bar{\omega}_{F1} = 1.15$

Slide 52


-.006
-.004
-.002
0
.002
.004
LEAD-LAG MODE DAMPING, σ_ζ/Ω
UNCOUPLED
LINEAR
STRUCTURAL
DAMPING
UNSTABLE
STALL
EXPERIMENTAL
RESULTS
0
2
4
6
8
10
12
14
16
BLADE PITCH, θ, deg

Slide 53



PRECONE INDUCED FLAP-LAG INSTABILITY

$\beta_p = 3°$, $\bar{x}_A = 0$, $\sigma = 0.08$, $\bar{\omega}_{F1} = 1.14$, $\gamma = 8.0$, $R_c = 1.0$

Slide 54

PREPARED REMARKS BY BOB ORMISTON

[Bill Bousman] didn't tell me I had to limit myself when he have me the assignment, but he did say I should talk about 2GCHAS. I'd like to start off on a tangent though and refer back to a couple of years ago when the methodology contracts were just getting under way and Bill [Bousman], myself, and, I think, Bob Powell were coming out of one of the first contractors after having looked at some of their results in comparison with the task we gave them, and going back to the airport we were saying, "by golly, that really was interesting, this was super fascinating, just can't wait to see what the other folks are going to get," and the idea hatched then that as a fallout to the ITR project maybe we should have some kind of workshop. I haven't had an awful lot more to do with it since then and the reason I bring that up is that before this is all over I want to throw my commendation on to Bill Bousman in particular, and to Dave Sharpe, who I know did an awful lot of work on this, for what I think has turned out to be a great success. About all I've had to do with it was sign a few PR's and I'm afraid to go back and add those up. At any rate, as somebody said before, probably everything that I'm going to say has been said in many areas as far as the correlation or validation goes. I was checking down my list as we went down the table and there was one area that hadn't been covered and I thought "boy, I just might luck out," but Peretz caught that with his presentation, so you've probably heard all this before.

I'd like to talk just a little bit about correlation before I touch base on 2GCHAS [Slide 55]. This is obviously not very profound anymore, after all that's been said, but I felt that it really did need to be said; correlation of theory with experimental data is not a trivial enterprise, and I emphasize the last word. This comes from our experience in this area over a number of years plus the results of ....s particular workshop and activity. We use the words correlation, validation, certification, and all kinds of terms rather loosely, and I'm not going to try to define them all precisely for you, I just want to make a few remarks about some points. Basically I look at correlation as comparing two things, whether it's an

BASIC MESSAGE

CORRELATION OF THEORY WITH EXPERIMENTAL DATA IS NOT A TRIVIAL ENTERPRISE



Slide 55

analysis or a theory or a code; you can correlate any of those with experimental data, and that's the main focus here. There is correlation with other data sets that may not be experimental. The main thing is looking at how those two things come together.

Continuing in the this vein I'll try to classify a couple of different aspects of this talk about validation [Slide 56]. There are really two things you can think about. (1) How do you determine if the analysis is valid, and here I could mean theory, or code or whatever, but I'll use the term analysis, and (2) how do you get a valid analysis? These are really two different things, but the second one involves the first one. How do you determine if the analysis is valid? [You can] correlate the code results with other results, then assess the adequacy and you have to make a judgment, is that or is that not adequate. It could be valid, invalid, or have some range of validity. I'd like to also make the point that you may not want to validate an analysis, say, for design purposes precisely. Any analysis has limitations but you often are very interested in not using a code exactly for what it was intended, but seeing how good it is "off design," so to speak. That's sometimes an important thing to determine, how valid is it? For what range of parameters? How do you get a valid analysis? Either you've got an old one that you're trying to fix up or you've got a new one that you're trying to develop so that it will be valid. You've got to go through a process of checking to see if it is valid; if it isn't, fix it and check it again.

This [Slide 57] is a fairly crude attempt to identify some of the aspects involved in correlation and validation. The two lines are supposed to come together at correlation. We have the experiment on top and the analysis on the bottom. The

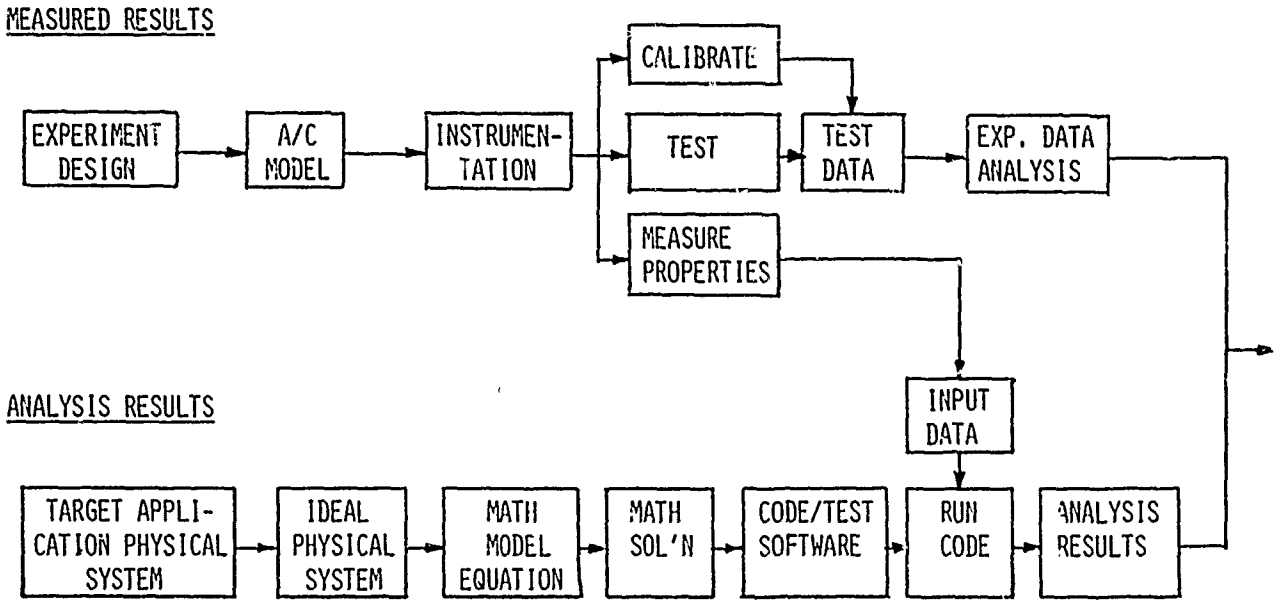
VALIDATION

TWO BASIC ISSUES

- HOW TO DETERMINE IF ANALYSIS IS VALID
  - CORRELATE CODE RESULTS WITH OTHER RESULTS
  - ASSESS ADEQUACY OF CORRELATION
  - VALID, INVALID, RANGE OF VALIDITY
- HOW TO GET A VALID ANALYSIS
  - FIX OLD ANALYSIS/DEVELOP NEW ANALYSIS
  - CHECK IF VALID/CHANGE/CHECK AGAIN

Slide 56

THE CORRELATION PROCESS



Slide 57

point to be made here is that there are really a lot of places in these two processes where the question of validation or correlation comes up. Take the experimental one on the top. You usually have an experimental design, you've got an experimental model, instrumentation, then other things like calibration and the actual test of the model itself. There are also some other "mini-experiments," if you will, to measure the [model] properties. You get the test data and then you've got to analyze it. All of these things have to do with the ultimate accuracy or the success of the validation/correlation enterprise. On the bottom, you want analytical results. That usually starts with the notion to develop a computer program which involves certain choices, like what kind of system are you developing it for in the beginning, then an ideal physical system or math model, a math solution, coding, actually running the code and getting results, and then the comparison. I'd like to go through a couple of these boxes. A lot has been said that covers most of them, but I'd like to make a few points. Up at the top for the experiment results is that the experimental design can be crucial. This involves all kinds of things, like what particular cases are you going to compare? If you're going to design an experiment, what particular range of parameters are you going to investigate? What kind of model do you want to design? Where are your potential errors going to be? What are the sources of errors? How can you best minimize those in the interest of getting the best possible correlation or learning the most about the weak areas of the analysis or whatever else? What it says is that if you do your thinking ahead

of time you're a lot better off, and a lot of thinking needs to be done in this process if you are serious about it. With respect to the aircraft and the model, that was really meant to be two diffent physical systems. Oftentimes a model, as has been said, is very specialized for certain purposes, or it may be a complete aircraft. In that case it is very, very complicated in terms of using that physical system and that data to correlate. That gets down to the bottom (the analysis) where when you developed your computer program you had to make a judgment on how elaborate it was going to be, what particular problem or how complex a configuration you were going to tackle.

Moving on to the next one, even if you've identified a real physical system, even a simple one, when you attempt to model it you usually make certain assumptions and you have in your mind an idealization of that physical system: if it's the airmass it's usually assumed to be perfect fluid for most of the things that we do--you forget the viscous effect. So you've got an ideal physical system and you've got to know what the relationship of that is to the model that you designed for your experiment, or the model that you assumed for your [theory]. If you have made a mistake in your judgment or an incorrect assumption there, the rest of the process almost doesn't matter and you're not going to get good correlation. Moving up to the test again, I'd like to make a few comments about the measured properties. We usually think of a test as you turn on the rotor, you spin it up, you shake it or do something else, and you measure the pressures, or the vibrations, or the stability, or whatever else. Measuring the properties or determining the properties of the hardware itself is just as important as measuring the damping on the model, or the frequency on the model or something else. If the results don't correlate because you didn't know what the collective pitch angle was or because you didn't know what the inflow dynamics were, there's just no way to tell. So almost every one of those parameters is equally important. We tend to focus on the most complicated part and that's oftentimes a mistake and the answer is somewhere else, it's more mundane. But speaking from experience, some of those simpler tests to measure the elastic axis of a blade can be a lot more complicated than measuring the damping of the transient motion. [You can even ask] why should we be measuring where the elastic axis is anyway, it's not really a beam, that was an assumption. If it turns out that it acts more like a plate, then the concept of an elastic axis goes out, so there are a lot of concerns here. On the experimental data analysis, I don't think I need to say anything more after Bill Warmbrodt did a great job this morning in opening our eyes or showing us what we thought was there anyway.

There are a couple of other things about the bottom of the figure. When you're doing all kinds of approximations and assumptions, errors and problems can crop up in all those steps I've shown on the bottom. In going from the ideal physical system to the math modeling, there may be some assumptions in the math modeling. [For example], I'm going to use an Euler-Bernoulli beam theory but I've got to throw out some higher order terms; that might be an approximation in the math modeling. [There may be] other things in the mathematical solution procedures; convergence, accuracy and whatnot. Many of these you may not even know about or suspect unless you've taken a lot of time to go out and investigate that particular problem area all by itself. The coding of the analysis and testing the code, the whole software

problem, is a whole other discipline and I think Pete Arcidiacono touched on that. That's a major issue for the 2GCHAS project, obviously. Placing it at that point in the analysis-and-results scheme of things isn't meant to imply that you wait that far along until you're going to think about that. You think about all of these things in the appropriate place. Then you run the code, get analytical results and so forth, and then you've got correlation to look at, judge, and figure out how you're actually going to decide whether it's valid code or not. I just have the point on the bottom part that there are other ways to check your analysis: other analyses, closed form solutions, and lots of other very intelligent, logical things to do and I think Jim's discussion was very apropos in this regard. A lot of internal things can be done, particularly in the math model area, within these blocks back and forth to check and validate certain of those elements, which has already been said.

I'm getting ahead of myself here, but I just would like to make a couple of comments about the need for a 2GCHAS type of system [Slide 58]. I think it's well understood and a lot of people agree that there are an awful lot of reasons for doing the 2GCHAS system. There are a few specific ones which have to do with the validation process and the difficulties that it presents to us that we've seen for all the analyses we've looked at today. Those alone would tend to give you the idea that you ought to come up with something like 2GCHAS. We all know it's expensive.

HOW 2GCHAS CAN HELP VALIDATION PROCESS

EFFICIENT USER INTERFACE

DATA BASE MANAGER

GRAPHICS

MODELING FLEXIBILITY

CHECK AND CORRELATE AT INTERMEDIATE STEPS, ANALYZE AND CORRELATE AT MODULE LEVEL

CONSISTENCY CHECK ON PHYSICAL DATA SET

COMPARATIVE CROSS CHECKS OF THEORY

SOFTWARE QUALITY ASSURANCE

EASIER/FASTER/CHEAPER/MORE RIGOROUS

Slide 58

We all know it's data intensive. It needs to be done rigorously. It needs to be done on lots of data sets. A point that was brought out here and we've seen over and over and over again [is that an analysis] looks good on one data set but there's another data set which is physically or mathematically in concept no different, but the correlation is out the window, and that just means that you were lucky the first time. So [you need] a lot of data sets. The point comes up, looking at the cost and the number of analyses that we have looked at here, why go through all the trouble, effort, and expense to validate all of those if they ostensibly are aimed at analyzing the same problem. That's the argument to do a 2GCHAS system.

Okay, as you know it's something that is in process now. What is it going to do; what could it do, can it do to help the validation process? First of all, one of the objectives of the system is to provide an efficient user interface and that's really important. You've got to manipulate data sets and do analyses--do lots of things, and watching people carry around data sets manually [you realize] that it just tremendously impedes the process timewise and effortwise. Next is database management; I think Don Merkley covered the rationale for that and a need for that as far as the correlation/validation process is concerned. The graphics that will be incorporated in 2GCHAS; obviously for the real-time interactive activity of the person who's doing the work, the graphics, no question, could be valuable. There is also modeling flexibility: suppose I forgot that I had a certain effect in the experiment, and I've got to go back and fix that, or suppose I want to compare one analysis against another or one approach against another because that data set needs to be checked that way. The business of checking intermediate steps; that could be checking at the module level in the 2GCHAS framework or it could be intermediate steps of some other aspect of the characterization of the system. It's very important to know whether you really have good correlation or, if it's not satisfactory, how do you go back and pick the process apart in an attempt to solve the problem. There is a possibility there will be some capability to check the input data, or the data set defining the models, for consistency--validating that data set if you will. I think I mentioned comparative cross-checks of theory. There's nothing like having two separate analyses that model the same physical system, the identical ideal physical system, but maybe have a different theoretical formulation, have a completely different set of code, and are intended to calculate the same result. We've used this technique in the past to validate some of our codes. Somebody said correlation wasn't fun, but it's a lot of fun to see the two codes which are totally different come out with the same answer down at nine decimal places; you're pretty sure that just didn't happen by coincidence, that both of them are wrong and they both got the same wrong answer. Ideally that should be a very effective tool available in the 2GCHAS framework. Software quality assurance is one aspect that I'm going to make a few remarks about. Our product assurance with 2GCHAS allows you to check that area of potential problems. The bottom line is that it should be easier, faster, cheaper and more rigorous. All we have to do now is get it and we'll be on our way.

Bill Bousman, Session Chairman: We've had an opportunity to listen to the panel members give their opinions on a very difficult subject and it's your turn now to address specific question to the panel or if you have general comments or whatever else. Any questions?

Dick Bielawa, United Technologies Research Center: I've got one question I'd like to throw out just in general is that the data set that we used served its purpose admirably; the question that comes up is where do we go from here? My own recommendation is that any future data sets should not address the same problems that we've already looked at. We should be looking at new problems, let us say problems that are attendant to special configurations, and probably more important we should be addressing the problems we expect for the ITR itself. So far we've been talking about rather basic issues but are we really covering all of the problems we would expect with the ITR?

Bousman: Perhaps that gets into the question of the difference between "known unknowns" and "unknown unknowns."

Bielawa: Well for one example, I know that more than one manufacturer is talking about gimbaled rotors. Are there data sets that pertain to gimbaled rotors? There are special problems associated with gimbaled rotors.

Jing Yen, Bell Helicopter Textron: Yes, we do, the Army XV-15 program, Bell's model 301. We have loads data, vibration data, and performance data.

Bob Ormiston, Aeromechanics Laboratory: I just want to make a comment. This may be a little bit risky, but the fact that you've added one hinge or one gimbal to the configuration doesn't necessarily mean that some other data sets which may have a hinge or a bearing or a gimbal somewhere else in the configuration, such as a flap hinge or a lag hinge; it doesn't necessarily mean that that data set is invalid for the gimbaled configuration. If all rotors were built out of aluminum and you now had a rotor built out of a composite material and there was a fundamental change in, say, the mechanical properties or the constitutive laws or whatever defining that, then that would probably be a totally different ball game. That's a little bit risky for me to say because I know that sometimes going to a slightly different configuration which has different behavior can oftentimes surprise you even though the domain of the physics was not changed. You just have to make a judgment on how many different data sets are you going to provide, and you can't do as many as you want. But I would like to see a gimbaled rotor set of test data.

Bousman: Let me ask a question for the audience. We have a number of people from universities here; do they see small experiments, perhaps even smaller than those done at the government research laboratories, or small analyses that could be used as check cases? Is this something that they see in their research program? Does anybody want to take that? Or for that matter do the companies see that? Do you

see that in some of your programs that you have going with the universities? Do you see the potential for that, doing some check cases like Peretz has suggested or some small experiments?

Euan Hooper, Boeing Vertol: Yes. I think that that's very reasonable. In the break I was discussing it with Inderjit Chopra, representing the University of Maryland, and I'm sure that there are activities that can be carried on by the academic community which would complement the contractual work. The difficulty is always one of timing since the academic community tends to be slower.

Bousman: Another question that I might throw out to the panel or some of the audience (we started to talk about this yesterday) is having some standards for data sets or for documentation because there are potential improvements, through either something like DATAMAP or [perhaps] we can do things with computer networks. I could see some potential there. Whether you call it cost-sharing or reducing costs, I don't know; but obviously if you have standardized data sets and computers, the government then has the potential to allow access to computer time to industry who can then access a standard data set where they know which preprocessor whey need and then do computations. The tradeoff is that if the industry uses the government's computers to compute some test cases then they need to provide those results, but you don't have to go through a contract so the turnaround is fast. Is that a potential there? Wayne?

Wayne Johnson, NASA Ames: I'm not sure it answers your question but I'd like to say that I don't really believe that just having a data base manager constitues having a documented data base. It's a prerequisite to handling the data that we're able to produce in experiments these days, but having data accessible does not give the person trying to use the data any information about the airplane it came from or the instrumentation. It does not give him a road map to the test. All these things have to be done, really, before the casual user can come in and pull out the few numbers that he wants. I feel that that has to be done by the people who run the test as well, because there has to be something that was learned by the person who was actually running the test. Unless he actually goes to the trouble of trying to pass that information on to us, it will be lost very soon and the quality of the data will suffer as a consequence. So I think that's something that seems to be lacking. We publish papers and we put data on mag tape, but I think this experience has shown us that in order to document the data for the ITR correlation, it was necessary to do an awful lot of work to produce parameters even though all the data had been published before. It was necessary to do an awful lot of work to get it to the point where you could actually use it. It seems to be a step that is missing in a lot of what we do.

Mike Watts, NASA Ames: Your question [about computer networks], Bill. As a matter of fact, I've already talked to Hughes about demonstrating DATAMAP and opening up the tip aero data by phone modem link to our computer for general industry use, and I've been talking to several other industries around about setting up a tour, with myself demonstrating DATAMAP. I know Don has done similar things with [Patuxent River] and several other people. So if there's anybody in industry interested that

I haven't contacted yet, have them contact us, Gerry Shockey or myself, because this is being set up right now.

Don Merkley, U.S. Army Applied Technology Laboratory: I think that really opens up a lot of logistic problems.

Watts: Yes it does. We've been talking about it for the last month and we fairly well have it worked out how we're going to handle the phone links and calling into our computer and other things.

Merkley: Well, it's not only that setup, where you have phone links where they're calling up your computer and using your data base. You've got to make sure that the data they're interested in is on your master file. That's still a big problem, I think, especially when you start talking about having many data bases on file.

Watts: Yes. It's a problem we've already addressed and we've got it pretty well worked out how we're going to handle it.

Merkley: It'll be really interesting when you get eight or nine people trying to call you at once.

Watts: It will have to be fairly limited scheduled use, but the scheduling we will be able to do.

Merkley: The other aspect is providing contractors with portions of the data base that they're interested in on mag tape to install on their own system in-house, which also provides logistics problems with their requests for data and providing them copies of that data.

Andy Kerr, U.S. Army Research & Technology Laboratories: I guess as I look around the room I see a lot of analyst-type people and I see a sprinkling of tester kind of people and we all know that these aren't necessarily always the same kind of people, and we're beginning to see, perhaps, the third kind of person we're going to need if we're going to have this and that's the human data-manager kind of person. Don has come up against it and we've been looking at ways to see whether we can put our data base with COSMIC or something like that and let them take care of handling all the interface with the people who want to use that data.

How do you get the data out there? You need to have somebody who's knowledgeable about the strengths and weaknesses and where the problems are with those data bases when they hand it out. Just putting a data base on the airwaves is not doing anybody a favor unless they can ask a question about it. I know for a fact that it is very difficult to find anybody who comes under the classification of a researcher of any type, tester or analyst who wants to be a data keeper, because it's a full-time job. It's a full-time-plus job if we're going to be able to let that data base go out and be used. I'd be interested if anybody has any suggestions or if there is a general feeling that we're going to have to, finally if the government's going to have these data bases to staff it with a . . . It's more than a librarian, it has be

a technically competent person, or people, or group to be able to make that data base useful.

Hooper: While I wish every success for DATAMAP I have an uneasy feeling that it's getting off to a rather slow start. Weren't the data for the Tip Aero Acoustic Test taken about 3 yr ago? Is that right, Mike? That you said summer of '80?

Mike Watts: Was it summer of '80 or summer of '81? I think '81.

Hooper: '81, then, two years ago. Okay, and I gather there's a report just coming out which will give an introduction to the scope of the testing; it doesn't give the data, just an introduction to the scope of the testing. The data's all going to be stored on DATAMAP and accessible. But it's now two years after the data were taken and it strikes me as a long gap. I don't know whether it's the first time and it's slow getting off its feet or not, but there's another aspect and that's at the other end of the scale, say 20 yr after the data were taken. I commented on that large data base that exists on air load testing, [it's] superbly documented, you can go back to the Scheiman test and it's magnificently detailed and accessible. DATAMAP has to be responsive to that as well; in 20 yr time, it's got to be accessible. But it seems to be slow getting off the ground, is that right, Don? Is that fair?

Merkley: That's a loaded question. Yes, I think that's a fair assessment, but you've got to consider what we're dealing with too. The data base is there and I think it's not really a matter of how old the data is. As you say, you refer to the Scheiman data which is much more than 20 yr old, and it's just as good today.

Watts: For DATAMP, Don and Dick did a really good job of documenting that. With the tip aero test, yes, we have been a little slow on the report, but we have had several reports already out on the use of the data. But it's just the overall report that has not come out yet.

Bob Wood, Hughes Helicopters: I'd like to raise a point if I could, Bill. It's just something that occurred to me and might be very controversial but the question relates to data bases and what type of data bases we want, or what type of data, what type of analysis we want to favor, or perhaps prioritize in terms of correlation. The analogy I'm going to use is to refer to what the acousticians did. I think about 10 yr ago they were doing most of their correlation based on octave band and third octave [band] predictions, and they finally came to the conclusion that this is not the way to go. The way to go really is to [decide] that until you can match the pressure time-history at an observer's ear, you really haven't solved the problem. also, if you do the pressure time-history you have a means by which you can go back. It gives you a very nice handle for looking at the analysis and finding out where it isn't matching the test. I noticed today, for instance, on the ITR study that (I think that) Dick Bielawa pointed out that he used a time-history approach and everyone else used an eigenvalue approach and when you validate an eigenvalue approach it seems to me, when we look at a plot, what we're really looking at basically at each rpm, at each collective, is simply one point. You either hit it or you don't hit it. But if you try to match a time history, as Dick was

trying to do, I think perhaps you have a better handle at how to go back to your initial analysis and find out what's wrong. In that regard I think that that was a time history that Bob had in his 1974 loads prediction method and I'm simply opening up the question, should we direct ourselves along the lines that the acousticians did and aim for validation on time histories in favor perhaps of other parameters.

Peretz Friedmann, UCLA: I just wanted to correct the potential for misinterpretation of what Bob Wood said. The time-history solutions do not provide any physical insight to the phenomenon because it's very difficult to figure out which modes are interacting and in what manner.

Wood: I guess I would differ with you there, Peretz, because I think really in a time history in a 360° plot you basically have a total trace of what's happening both on the advancing and retreating side of the blade so you can, if it's a blade loads program, you can look at the blade at 90°, which is a very-high-Mach-number situation, or on the stall side and there's a fair amount of information there if you want to take the time to dig it out.

Bousman: I think there's a potential with a time history to make a lot of progress over what we do today but I think that what we do today isn't that good. For instance you see in forward-flight loads that the dominant effect is the once-per-rev flapping which everybody is getting fine. That's not the problem. You look at two time-histories, the analytical and the experimental, and you say, yes, they've got one per rev and you look at the Coriolis in the lead-lag and you say, yes, that's okay too. What you should be doing is doing a harmonic analysis; take out once per rev and look at the N per revs for the correlation comparison. But I think until you start doing some more specialized techniques, I don't think just the pure time-history is that much better.

Wood: But I guess it seems to me that this many years after the helicopter has evolved we still don't see papers (they're conspicous by their absence) that show radial, azimuthal comparisons of blade loads vs. test and show them all around the azimuth and then break it into harmonics to show a comparison. We'll see cyclic values and we'll see good correlation there. We'll see flapping, as you pointed out, but the nub of the problem is ultimately, hidden in there, we ought to be able to match that signature.

Bousman: There's a lot more information in there, that's true.

Wood: But the acousticians themselves, like the RAP program, depend on our ability to calculate airloads around the azimuth so they can get the pressure time-history. So it's interrelated and the aerodynamicist with the inflow problem is tied right into it. I'm just throwing it out and I knew it wouldn't be popular; I knew it might be controversial.

Dick Bielawa, United Technologies Research Center: I'd just like to comment on that. I think a good way of looking at it is along the lines that Jim [McCroskey]

mentioned, where he made the distinction between physics modeling and math modeling. My preoccupation with time history shouldn't be construed that that's all I want to do. I think that dealing with the time history in as much depth as I did fall into the category of physics modeling. At this point I am more assured that the equations are right, so the next thing is to say, let's get an efficient solution to those equations. I don't think the time-history is an efficient solution to the equations, an eigensolution is. But I'm in a better position now to say that my eigensolution will be more correct because it is based upon a physics modeling that I have more confidence in.

Bob Ormiston, U.S. Army Aeromechanics Laboratory: Just a couple of comments. It depends on the type of problem you're trying to solve. For the bread-and-butter-type stability problems like this, you'd agree an eigenanalysis, a linear stability analysis, is the way to go. It occurred to me that there's an issue here that maybe we're not addressing. It has to do with the kinds of things we do, or the balance of which ones we do, in validating an analysis or a code. We've all seen how expensive it is to [correlate] with experimental data, although that's the most satisfying in the end, from front to back. But it would seem to me that if one had to think what's the most logical way to validate a code or an analysis or whatever else, and we try to come up with an optimum approach, or at least a better approach, one would have to say maybe 99% of your effort, maybe 95%, should go into those preliminary steps: checking the software, running test cases, checking your solution techniques, the internal checks of the assumptions on a math model and so forth. Then the experimental correlation and validation, even though it's extremely important, ought to be the last step, the last judgment, and you should design that in the beginning so you know just what you have to do with the experimental validation.

Bill Warmbrodt, NASA Ames: After considering the correlation that was shown yesterday and in the discussion of the past two days, I'd like to have the members of the panel that were from the industry say whether or not they feel confident in their current in-house capability to analyze aeroelastic stability for the preliminary, detail, and final designs for what they're considering for the next-generaltion ITR. Are they happy with their in-house analyses after going through this correlation effort? Are they confident that they can predict aeroelastic stability for an ITR, be able to build one?

Pete Arcidiacono, Sikorsky Aircraft: The answer to your second question, are we happy? No. Are we confident? Yes. There is no other answer, is there? There will be an ITR rotor designed and developed and successfully checked out despite all of the analytic deficiencies. That's been the name of the game for 50 years.

Wood: To amplify on what Pete just said, [an example is] the work that Dev Banerjee described this morning on the CFTR. The first CFTR that we built was not funded by the government--it had to be internally funded. Basically what we had to convince our management of was that the analysis was sufficiently correlated such that they were willing to put up a half a million dollars to build one and let us put it through the rpm and collective range that we wanted to do. I think that that really

puts the analyst to the test because the only option we had if it didn't work was we would have gone back to the president of our company with a handful of pieces. Fortunately Dev's analysis worked well and we moved on to bigger and better things.

Hooper: I think it's rare that at the outset of a program anybody's going to be satisfied with the methodology they've got. The short answer is, in our case, no. I'm not satisfied.

Yen: Well, Bill, to answer your question, for the kind of design concepts which we've been doing, the type or rotor, the type of pylon, the type of gear, and so forth; and with the math model for ground and air resonance which we have right now, we feel comfortable to design those same types. I made the comment earlier that the helicopter manufacturers' analyses are mostly tailored to their own needs. For those types of unique features which we are doing, yes. The answer is yes. But if you want me then to correlate with Hughes or some other companies, then maybe no.

Paul Mirick, U.S. Army Applied Technology Laboratory: I think another answer to the question is seen in the way the preliminary design for the ITR is being done. One of the important features of that program is the model test because we saw, I think, from the correlation effort as it was going along that we did not have confidence, enough confidence, in the analyses. Therefore there is a model test as part of the ITR program to help assure that we are going to have an aeroelastically stable ITR.

Bousman: I'd like to give Don [Merkley] a question, sort of like Wayne Johnson's. I'm just ignorant of DATAMAP's capabilities and what you do there but if some guy comes in with a new data base and says hey, this is really great, everyone will like it, could you put it on DATAMAP? What kind of documentation do you require? Is there a document that he must fill out that is then provided to the users so that they can then figure out what the data-base basis is? Or is it more ad hoc, or what?

Merkely: To be fair to your question, we haven't been in that position yet. So no, there is no required documentation, minimum documentation, or something like that required to put data up on DATAMAP. There are things that must be known about the data in order to put it into DATAMAP in a useful manner, but I think what you are really getting at is, are there minimum requirements that the government is imposing on people that have data bases that they want to put up? At this time nothing exists like that.

Bousman: Are there any more questions? Marcelo?

Marcelo Crespo da Silva, University of Cincinnati: Just a comment and perhaps a question. The way I see it, there seems to be a gap here that perhaps should be bridged. I'm still perplexed to see six different companies getting six different results supposedly for analyzing the same problem, and they all differ from the result of experimentation. Now perhaps we have a duplication of effort without everybody talking to [each other], that is, the companies and the people outside the

companies. Maybe there is a reason for that; perhaps I can't blame them if they are are trying to protect their own codes. Maybe there should be more talking among the people involved in this effort. I know that at Stanford, for example, they have started a center for very large integrated systems, electronics, perhaps that may not be a bad idea. A center for rotorcraft dynamics is to be eventually created. If I were a Howard Hughes with a lot of money I would certainly donate the money for that, but maybe the companies, the six companies, could participate with some amount of money and come up with some kind of support for a center like that where they would contribute people that would talk and try to solve these problems and all of them would pool [their resources] and would benefit from these contributions. So I myself, I wish I could contribute toward an explanation of some of that discrepancy. There's no way I can because I don't know what you're talking about. You talk about the analyses but I haven't seen the analyses; I haven't seen any equations so I can't point my fingers and say, "you have dropped this term here," or "you're doing that incorrectly," or perhaps the discrepancy is in the aerodynamic modeling. Or maybe, as someone mentioned yesterday, in getting the equilibrium solutions, your company felt that you should drop all quadratic terms, and then you did that for some time and eventually if you allow me to analyze it, that quadratic term should be put back in and then you did that. Perhaps that's part of the result. That's a part of the problem why you don't have very close results. So to that question can you, the presidents of your companies, can they, perhaps with 10% of their salaries, donate money for a center like that. That would be a lot of money.

Arcidiacono: I think very valid questions are being raised there. There are a million and one questions you can ask. If you want to do the job and do it right it's going to be a massive investment in effort and money, and I think we've talked about it and we're kind of skirting around the issue now. Are we going to come up with the money to do the job right, or are we just going to get together every five years and sit around and compare superficially, or what? As I pointed out before, I think we need a more continuous flow of support. Otherwise there is going to be business as usual and five years from now we'll be sitting here, just with more grey hairs.

Crespo da Silva: But why don't you provide support yourselves? You sell a lot of helicopters, a lot of rotorcraft, and part of that profit perhaps could be turned back into your own work?

Arcidiacono: Sure. But it's an investment over the long term and there are other demands on the money that are higher priority, that's all. I think every one of us faces that, and until you recognize that as a fact of life, we just won't be able to communicate with one another.

Wood: I think when Pete answered Bill Warmbrodt's question he said, "we have confidence in the analysis but we're not satisifed with it." I think that was basically the bottom line. As long as the manufacturer has confidence that he can build a safe design that's ready to fly, or at least ready for wind tunnel testing, then he is probably not going to want to pay the money to go any further. That's where

those of us who are analysts have problems convincing our management to go further and put more dollars in. We were joking about this at the break, and I think the comment was made that perhaps it would be nice if someone in the group here were promoted to president of one of these companies. Then we could see if they would still stay in the same line of reasoning.

Ormiston: I'd just like to make a comment because Marcelo kind of hit a nerve that's been open in me for a long time. Now we've sat here and we've looked at the correlations and they're not as good as we all would like. There's something there that we still haven't figured out and we've discussed this term and that term until we're blue in the face and we can talk about it and talk about it and talk about it. You've got to go in there and dig into the equations. And Pete's right, you know. If you want to take the time and the effort to go and do it, it's money and it's time and maybe we should put that in something else. Maybe the answer is, is there some single thing we can do, some specific thing we can do, is there some clever way we can maybe make some progress in cracking that nut. I'll just throw out an example maybe, if you've got your handout and you turn to [Figure 9 of Dave Sharpe's paper] there's a plot there that shows a number of curve that for no apparent reason show a very wide variation in damping. In that case it isn't because it's stall because you're at low angles, it isn't because its rotor/body coupling because it's an isolated rotor. There're so many things you can rule out but it is just sitting there staring you in the face. Maybe we could let one teeny-weeny little contract to the people who did those calculations to specifically go in and trot out their terms, and come and meet for two days, bash their heads together and say which term did [each] leave out. You may find something out from that, may be you won't, but I think those guys may go back and they'll be able to scratch their heads about some very specific things that really get to the meat of their equations, their damping, their results, and they're talking apples and apples or hard facts. I think the answer is that if there is some single clever thing we can think of as a group we ought to do that, rather than go home and say "well, it was a great effort," and "boy, we learned a lot," but still know in the back of our minds that for that simple case they just were totally all over the place.

Yen: To continue what you have said, Bob, Peretz showed some correlations there, his computer code produced a certain line wich did not agree with Dr. Johnson's curve. Peretz' work, I understand, was done under government contract, so it would be much easier for you to give him another contract to compare his code with Dr. Johnson's code. Wouldn't that be much easier than to ask four [helicopter companies] to compare all our codes with each other?

Ormiston: Wayne and Peretz aren't going to be designing these helicopters. I'm sort of thinking of a quick and dirty way to may be get you a major increment in your capability by removing some of the uncertainty. Most of those analyses which were compared, I think, were the companies' analyses in that particular case. I want to corral Peretz to somehow find out why that one case I was interested in that he compared with the FLAIR analysis, and the same thing goes for Wayne's analysis, why those are so far apart. Maybe we'll try to do that.

Alex Berman, Kaman: Along those same lines, I think the objective which we call validation is really inappropriate because validation is either a yes or no answer, and if you had to apply that to all the data which was presented here today, it would all be no. I think a broader objective should be that we should use test data not to validate a model, but use the test data to improve our analyses because in every case they will require improvement. No analysis compared to any test is going to be completely satisfactory. I think that projects like we have here really should have a continuing phase in which you seek to find methods of improving your analyses rather than just stopping at this point.

Jim McCroskey, U.S. Army Aeromechanics Laboratory: If you think that a few of these calculations spread all over the map, you should see some of the results that have happened when fluid dynamicists have tried to calculate pretty simple turbulent flows with a variety of different turbulent model--I go back to this Stanford conference. I'm not sure that I can, off the top of my head, give you a clear set of guidelines on how to go about this but a lot of effort by a lot of people both in the planning and in the implementation and in the actual dog work that was involved in it went into a succession of two conferences. First of all, trying to assess the validity of various data sets to see whether it was worth the effort of trying to correlate with them, because, let's face it, there are some problems where you can probably calculate more accurately than you can measure the particular phenomena. Those tend to be special cases but those kinds of things exist where the measurement difficulties are so great that you just really can't get it. So anyway, this group went to a lot of effort to produce some certified data sets and then they issued very specific rules for what the "computors" should try to do, and the format in which they should present it, and then the means by which they got together and evaluated it. A lot of new information emerged from those two meetings and a lot of paths that have turned out to not be very fruitful have now been turned off and other paths have opened up. So if you are considering ongoing correlation/validation exercises of this type, you might look into just some of the actual mechanics and methodology that these two conferences employed to maximize the gain from the amount of effort that went into it.

Larry Lehman, Neilsen Engineering and Research: I think probably for about the last 30 minutes we have been discussing a very interesting issue. But it's really away from the technology issues and it's really one of a communications problem as much as anything else. In a number of other areas of engineering endeavor, of course, I've sat in on some meetings where this has occurred before. There are some conflicting interests; there are a lot of different industry groups, part of which have proprietary information, but some of their information is not proprietary and the question is how can they conveniently share that? We're even lucky here because a lot of our work is not really that classified. There are lot of areas of engineering research where they're doing very classified research and they can't even let the data out, yet they somehow have to share that data. Again there, one potential answer that has been posed, and I say potential because it's not clear whether it is the answer or not, maybe it's a partial answer, is this data base question because it's sort of an area of focus and one way that might facilitate that transfer of data. But again it has its own attendant problems but it's a very good potential

way of doing that. If you look at just the trends in technology in general, clearly society is evolving towards that state where we'll have a more rapid transfer of information which means possibly data bases or something similar. So I think it is very important that the issue has been brought up and discussed. It's not a quick answer but I think in all of those cases that it will take some independent party that doesn't necessarily have that proprietary interest to promote that properly. It's not necessarily inexpensive but it's not probably any more expensive than other ways that you might go in the long haul.

Bousman: If we have no more questions, I think I'd like to finish up. I would like to just thank some people that were instrumental for this meeting: Bob Canfield who did so well on the vugraphs, Mike McNulty on the tape transcriptions and many of you will hear from him again because he will be editing this volume, and especially I'd like to thank Dave Sharpe who arranged simply every detail for this whole meeting from beginning to end. He is a Jack of all trades; doughnuts, rooms, projection, and everything else. And for that I'd like to thank him, and of course all the speakers too.

LIST OF ATTENDEES

ANALYTICAL METHODS, INC.
David R. Clark

U.S. ARMY APPLIED TECHNOLOGY LABORATORY
Charles E. Hammond
Donald Merkley
Paul Mirick
Robert Powell

BOEING VERTOL COMPANY
Peter Dixon
Euan Hooper
Frank J. Tarzanin, Jr.

BELL HELICOPTER TEXTRON
James Harse
Gene Sadler
Jing G. Yen

DAVID TAYLOR NAVAL SHIP RESEARCH AND DEVELOPMENT CENTER
James Biggers

GEORGIA INSTITUTE OF TECHNOLOGY
G. Alvin Pierce

HUGHES HELICOPTER, INC.
Debashis Banerjee
E. Roberts Wood
Friedrich Straub

KAMAN AEROSPACE CORP.
Nicholas Giansante
Henry Howes
Robert Jones

MCINTOSH STRUCTURAL DYNAMICS, INC.
Samuel C. McIntosh, Jr.

McNEAL-SCHWENDLER CORP.
Michael Gockel
Richard H. McNeal

NASA AMES RESEARCH CENTER
J. A. Albers
Fred Baker
Mark Betzina
Jeff Cross
David Few
Steve Haff
Leonard Haslim
John Jinkerson
Wayne Johnson
Bob Kufeld
John Madden
Norman Michaud
Hirokazu Miura
Randy Peterson
Ray Piziali
Ed Seto
Gerry Shockey
Charles Smith
Peter Talbot
Bill Warmbrodt
Gloria Yamauchi

NEILSEN ENGINEERING AND APPLIED RESEARCH
Larry Lehman

SIKORSKY AIRCRAFT
Peter J. Arcidiacono
Raymond G. Carlson
Wen Liu Miao
John Plonsky
Robert Sopher

UNITED TECHNOLOGIES RESEARCH CENTER
Richard Bielawa
Anton Landgrebe

STANFORD UNIVERSITY
Holt Ashley

UNIVERSITY OF CALIFORNIA, LOS ANGELES
Peretz Friedmann

PRECEDING PAGE BLANK

U.S. ARMY AEROMECHANICS LABORATORY
William Bousman
Don Boxwell
Bob Canfield
Frank Caradonna
Marcelo Crespo Da Silva
John Davis
Seth Dawson
Dewey Hodges
Don Kunz
Jim McCroskey
Mike McNulty
Robert A. Ormiston
Mike Rutkowski
Dave Sharpe
Wendell B. Stephens
Yung Yu

U.S. ARMY AVIATION SYSTEMS COMMAND
Sam T. Crews
William White

U.S. ARMY RESEARCH & TECHNOLOGY LABORATORIES
Andrew W. Kerr
Mike Scully

U.S. ARMY RESEARCH OFFICE
Edward Saibel

UNIVERSITY OF MARYLAND
Inderjit Chopra
Everett Jones

ADVANCED ROTORCRAFT TECHNOLOGY
Ronald DuVal

NASA National Aeronautics and Space Administration

Report Documentation Page

1. Report No.	2. Government Accession No.	3. Recipient's Catalog No.
NASA CP-10007 USAAVSCOM CP 88-A-001		

4. Title and Subtitle

Integrated Technology Rotor Methodology Assessment Workshop

5. Report Date

June 1988

6. Performing Organization Code

7. Author(s)

Michael I. McNulty and William G. Bousman (editors)

8. Performing Organization Report No.

A-86381

10. Work Unit No.

992-21-01

9. Performing Organization Name and Address

Ames Research Center, Moffett Field, CA 94035 and *Aeroflightdynamics Directorate, U.S. Army Aviation Research and Technology Activity, Ames Research Center, Moffett Field, CA 94035-1099

11. Contract or Grant No.

12. Sponsoring Agency Name and Address

National Aeronautics and Space Administration Washington, DC 20546-0001 and U.S. Army Aviation Systems Command, St. Louis, MO 63120-1798

13. Type of Report and Period Covered

Conference Publication
June 21-22, 1983

14. Sponsoring Agency Code

15. Supplementary Notes

Point of Contact: William G. Bousman, Ames Research Center, MS 215-1
Moffett Field, CA 94035 (415) 694-5890 or FTS 464-5890

16. Abstract

This conference proceedings contains the formal papers presented at the Integrated Technology Rotor (ITR) Methodology Assessment Workshop held at Ames Research Center on June 21-22, 1983. This workshop was cosponsored by the U.S. Army Research and Technology Laboratory (AVRADCOM) and the National Aeronautics and Space Administration.

The conference proceedings contains 14 formal papers and the results of two panel discussions. In addition, a transcript of discussion that followed the paper presentations and panels is included. The papers are of two kinds. The first seven papers were directed specifically to the correlation of industry and government mathematical models with data for rotorcraft stability from six experiments. The remaining 7 papers dealt with related topics in the prediction of rotor aerolastic or aeromechanical stability. The first of the panels provided an evaluation of the correlation that was shown between the mathematical models and the experimental data. The second panel addressed the general problems of the validation of mathematical models.

17. Key Words (Suggested by Author(s))	18 Distribution Statement
Aeroelastic stability Aeromechanical stability Rotor stability Rotorcraft dynamics	Unclassified-Unlimited Subject Category - 01

19. Security Classif (of this report)	20. Security Classif (of this page)	21 No of pages	22 Price
Unclassified	Unclassified	380	A13

NASA FORM 1626 OCT 86
GPO 588-154/99181

END